

2006

Electrocoagulation technology as a process for defluoridation in water treatment

Mohammad Mahdi Emamjomeh

University of Wollongong

Recommended Citation

Emamjomeh, Mohammad Mahdi, Electrocoagulation technology as a process for defluoridation in water treatment, Doctor of Philosophy thesis, School of Civil, Mining and Environmental Engineering, University of Wollongong, 2006. <http://ro.uow.edu.au/theses/1923>

NOTE

This online version of the thesis may have different page formatting and pagination from the paper copy held in the University of Wollongong Library.

UNIVERSITY OF WOLLONGONG

COPYRIGHT WARNING

You may print or download ONE copy of this document for the purpose of your own research or study. The University does not authorise you to copy, communicate or otherwise make available electronically to any other person any copyright material contained on this site. You are reminded of the following:

Copyright owners are entitled to take legal action against persons who infringe their copyright. A reproduction of material that is protected by copyright may be a copyright infringement. A court may impose penalties and award damages in relation to offences and infringements relating to copyright material. Higher penalties may apply, and higher damages may be awarded, for offences and infringements involving the conversion of material into digital or electronic form.

ELECTROCOAGULATION TECHNOLOGY AS A PROCESS FOR DEFLUORIDATION IN WATER TREATMENT

A thesis submitted in fulfilment of the
requirements for the award of the degree

DOCTOR OF PHILOSOPHY

from

UNIVERSITY OF WOLLONGONG



by

MOHAMMAD MAHDI EMAMJOMEH

B.Sc., M.Sc. Environmental Health Engineering

School of Civil, Mining and Environmental Engineering

February 2006

**IN THE NAME OF ALLAH,
THE MOST GRACIOUS, THE MOST MERCIFUL**

This thesis is especially dedicated to my family. To my parents, for their unfailing support and long patience, I am extremely grateful. To my wife, **Fereshteh Sadraie**, for her support, understanding and sacrifice over these years and also to my beautiful daughters, **Bahareh** and **Fahimeh Emamjomeh**, who were eagerly waiting for me every night to come back home, although I could not spend as much time as I wished with them, I am truly grateful.

AFFIRMATION

I, Mohammad Mahdi Emamjomeh, declare that this thesis, submitted in fulfilment of the requirements for the award of Doctor of Philosophy, in the School of Civil, Mining and Environmental Engineering, Faculty of Engineering, University of Wollongong, is wholly my own work unless otherwise referenced or acknowledged. The thesis was completed under the supervision of A/Prof. M. Sivakumar and has not been submitted for qualification at any other academic institution.

Mohammad Mahdi Emamjomeh

February 2006

The following publications are the result of this thesis project:

1. **Emamjomeh, M. M.**, Sivakumar, M. and Schafer, A. I. (2003), "Fluoride removal by using a batch electrocoagulation reactor", *7th Annual Environmental Engineering Research Event (EERE) Conference*, 1st- 4th December, Marysville, Victoria, Australia, PP. 143-152
2. **Emamjomeh, M. M.** and Sivakumar, M. (2004), "Effects of calcium ion on enhanced defluoridation by Electrocoagulation/flotation (ECF) process". *8th Annual Environmental Engineering Research Event (EERE) Conference*, 6th – 9th December, Wollongong, New South Wales, Australia, PP. 263-274
3. Sivakumar, M., **Emamjomeh, M. M.** & Chen, M. (2004), "Use of electrocoagulation (EC) as an alternative method to chemical coagulation in water treatment". *8th Annual Environmental Engineering Research Event (EERE) Conference*, 6th – 9th December, Wollongong, New South Wales, Australia, PP. 320-332
4. **Emamjomeh, M. M.** & Sivakumar, M. (2005), "An empirical model for defluoridation by batch monopolar electrocoagulation/flotation (ECF) process", *Journal of Hazardous Materials*, In Press, Corrected Proof
5. **Emamjomeh, M. M.** and Sivakumar, M.(2005), "Defluoridation using a continuous electrocoagulation (EC) reactor", *47th Annual New Zealand Water and Wastewater Association (NZWWA) Conference and Expo (EnviroNZ05-Water matters)*, 28th -30th September, Aotea Centre, Auckland, New Zealand, Published in the Conference proceeding

6. **Emamjomeh, M. M.** and Sivakumar, M. (2005), "Electrocoagulation technology for nitrate removal", *9th Annual Environmental Research Event (ERE) Conference*, 29th November - 2nd December, Hobart, Tasmania, Australia, Published in the Conference proceeding
7. Sivakumar, M. and **Emamjomeh, M. M** (2005), "Electrochemical method for fluoride removal: Measurement, Speciation and Mechanisms". *9th Annual Environmental Research Event (ERE) Conference*, 29th November - 2nd December, Hobart, Tasmania, Australia, Published in the Conference proceeding
8. Sivakumar, M. and **Emamjomeh, M. M** (2006), "Speciation and Mechanisms of defluoridation by an Electrochemical method" *The second International Association of Science and Technology for Development (IASTED) Conference on Advanced Technology in the Environmental Field (ATEF)*, February 6-8, Lanzarote, Canary Islands, Spain (Full paper accepted and in press)
9. Sivakumar, M. and **Emamjomeh, M. M** (2006), "Electrochemical generation of aluminium coagulant for fluoride removal by a continuous flow electrocoagulation reactor", *Journal of Science of the Total Environment*, Submitted
10. **Emamjomeh, M. M.** and Sivakumar, M. (2006), " Review of pollutants removed by Electrocoagulation and Electrocoagulation/flotation processes", *Journal of Hazardous Materials*, Under preparation

ACKNOWLEDGMENTS

The author would like to express his sincere gratitude to **A/ Prof. M. Sivakumar** for his supervision, encouragement, invaluable guidance and inspiration provided during the course of this research and providing the necessary facilities for this research.

I am grateful to the Ministry of Health and Medical Education (MHME) of the Islamic Republic of Iran and the Qazvin University of medical sciences for awarding me a research scholarship through which the complete financial support for this research was provided.

I also would like to thank the laboratory senior technical staff in the faculty of Engineering and the University of Wollongong's Sustainable Water and Energy Research Group (SWERG), especially Joanne George, Norm Gal, Ian Kirby, Nick Mackie and Greg Tillman for their laboratory assistance.

The author wishes to thank Mrs. Leonie McIntyre, Mr. Des Jemison and Mr. Peter Turner of the ITS staff for their contributions. The assistance provided by the Faculty of Engineering, University of Wollongong is also appreciated.

I wish to express my appreciation to Mr. Mohammad Mahdi Farhoudi, Mr. Saeid Hesami and Mrs Lorelle Pollard for their helpful comments and assistance.

Most importantly, I would like to express my deepest thanks to my brothers, sister and members of my family in Iran who have provided continued support throughout this study and indeed for my entire life.

This study would not have been finished without support and encouragement from all my fellow Iranians at the University of Wollongong and their families. In particular, the author is indebted to Mr. Vahid Mottaghtalab, Mr. Mehrdad Bahrami Samani, Mr. Mahdi Ahmadian, Mr. Hossein Jalalifar, Mr. Behzad Fatahi and Dr. Faramarz Doulati together with their respective families

ABSTRACT

Excess fluoride ion in drinking water is a serious public health problem because it has beneficial and harmful effects. When an optimum amount of 1 mg/L is present in drinking water it helps prevent decay in teeth, but long term consumption of water containing excessive fluoride (≥ 1.5 mg/L) can lead to fluorosis of the teeth and bones. There are several methods for removing fluoride, and one method that has recently received attention is electrocoagulation (EC) technology. The word “electrocoagulation” will be sometimes used with “electroflotation” and can be considered as the electrocoagulation/flotation (ECF) process. Through the process of electrolysis, coagulating agents such as metal hydroxides are produced. When aluminium electrodes are used, the aluminium dissolves at the anode and hydrogen gas is released at the cathode. The coagulating agent combines with the pollutants to form large size flocs. As the bubbles rise to the top of the tank they adhere to particles suspended in the water and float them to the surface. In fact, a conceptual framework of the overall electrocoagulation process is linked to coagulant generation, pollutant aggregation, and pollutant removal by flotation and settling.

Batch experiments were designed and conducted to study the different operational parameters such as current density, electrolysis time, pH of solution, distance between electrodes, initial fluoride concentration, electrolyte conductivity, particle size, zeta potential, mass ratio of aluminium and fluoride in solution ($\text{Al}^{3+}/\text{F}^-$ mass ratio), and ions effects (specially Ca^{2+} effect) on the defluoridation by EC process. In the EC process the amount of aluminium ion produced is proportional to the charge which is a product of the current supplied and electrolysis time. The charge affects

fluoride removal significantly, however to avoid excessive energy consumption one must limit the charge applied. In this batch ECF process, the minimum electrolysis time required to reduce the fluoride concentration to the desirable concentration ($F^- = 1$ mg/L), is defined as the optimum detention time (d_{to}). The results of batch experiments showed that the residual fluoride concentration reduced from 10 to 1 mg/L when d_{to} was 55, 45, and 35 min at a 1.5, 2 and 2.5 A current range, respectively. The optimum charge values were found between 5000 -5400 C and 9500-10500 C respectively for the initial fluoride concentrations of 10 and 25 mg/L. It has been confirmed that the rate of F^- removal follows a simple first order process. The batch experimental results showed that the Al^{3+}/F^- mass ratio was between 13 and 17.5 and the defluoridation process is found to be more efficient when pH is kept constant between 6 and 8. Based on the effects of ion competition, the presence of Ca^{2+} ion enhances the defluoridation process.

Continuous flow experiments were also designed and conducted to investigate the effects of different parameters including current input, initial concentration of fluoride, initial pH, and flow rate on the efficient removal of fluoride. The most efficient treatment was obtained from the highest rate of charge as observed in the batch reactor. An XRD analysis of the composition of dried sludge obtained by electrocoagulation shows the formation of aluminium fluoride hydroxide complexes $[Al_nF_m(OH)_{3n-m}]$ and confirms the main mechanism for removing fluoride in both the batch and continuous flow reactors. To reduce F^- concentration from 5 to 1 mg/L, it was found that the total operational cost of the current ECF process is less than 40 % of the Nalgonda (NA) process.

The experimental results further showed that the rate constant (K_{exp}) depends on the independent variables or critical parameters such as the current concentration (I/V), the effect of Ca^{2+} concentration, distance between the electrodes (d), pH of the solution, and the initial concentration of fluoride (C_0). An empirical model is developed to predict both the optimum detention time and optimum flow rate for fluoride removal. The results show good agreement between the experimental data and the predictive equation. Overall, the electrocoagulation technology using aluminium electrodes is an effective process for defluoridation of water that contains excess fluoride.

TABLE OF CONTENTS

Title	Page
AFFIRMATION	i
LIST OF PUBLICATIONS	ii
ACKNOWLEDGMENTS	iv
ABSTRACT	v
TABLE OF CONTENTS	xiii
LIST OF FIGURES	xv
LIST OF TABLES	xxv
LIST OF SYMBOLS AND ABBREVIATION	xxvii

CHAPTERS

CHAPTER 1:

INTRODUCTION

1.1	Introduction	1
1.1.1	Fluoride health problems.....	2
1.1.2	Defluoridation process	4
1.1.3	Electrocoagulation technology.....	5
1.2	Aims and objectives	7
1.3	Scope of the study	8
1.4	Research approach	10

CHAPTER 2:

EC FUNDAMENTALS AND DEFLUORIDATION PROCESS – A REVIEW

2.1	Introduction	17
-----	--------------------	----

2.2 EC fundamentals 18

2.2.1 Definition of electrocoagulation (EC)..... 18

2.2.2 Definition of electroflotation (EF) 18

2.2.3 Electrocoagulation-flotation (ECF)..... 19

2.2.4 History..... 21

2.2.5 Principles of the ECF process 22

2.2.5.1 Electrochemistry 22

2.2.5.2 Coagulation 28

2.2.5.3 Flotation 29

2.2.6 Advantages of ECF process 30

2.2.7 Disadvantages of ECF process..... 31

2.2.8 Cell configuration..... 32

2.2.9 Energy consumption..... 33

2.2.10 Coagulant dose..... 34

2.2.11 Removal process 35

2.3 Defluoridation methods..... 36

2.4 Summary 47

CHAPTER 3:

REVIEW OF POLLUTANTS REMOVED BY

ELECTROCOAGULATION

3.1 Introduction 48

3.2 Application on EC and ECF process..... 49

3.2.1 Oily wastewater treatment..... 49

3.2.2 Dye treatment..... 52

3.2.3 Organic removal..... 55

3.2.3.1 Recovery of phenolic compounds..... 55

3.2.3.2 Municipal wastewater treatment 56

3.2.3.3 Industrial wastewater treatment 58

3.2.4 Heavy metals removal..... 61

3.2.5	Potable water treatment by EC.....	63
3.2.6	Nitrate, nitrite and ammonia removal	71
3.2.7	Fluoride removal	72
3.3	Summary	80

CHAPTER 4:

THEORETICAL CONSIDERATIONS

4.1	Introduction.....	91
4.2	Theoretical background.....	91
4.2.1	Hydrolysis reaction (electrode oxidation).....	93
4.2.1.1	Charge loading	94
4.2.1.2	Operational cell potential of EC reactor.....	95
4.2.2	Coagulation-flotation process (removal process).....	96
4.2.3	Representative equations for reactors	99
4.2.3.1	Batch reactor	99
4.2.3.2	Continuous flow reactor.....	102
4.2.4	Solution scheme	104
4.3	Empirical model	105
4.4	Summary	106

CHAPTER 5:

FLUORIDE REMOVAL BY A BATCH MONOPOLAR ELECTROCOAGULATION REACTOR

5.1	Introduction.....	108
5.2	Materials and methodes.....	108
5.2.1	Bench scale batch ECF design	108
5.2.2	Experimental procedures.....	112
5.2.2.1	Solution chemistry	112

5.2.2.2 Analytical techniques	114
5.2.3 Experimental set-up	120
5.3 Results and discussion	124
5.3.1 Effects of electrolysis time.....	124
5.3.2 Effect of current values	129
5.3.2.1 Effect of current density.....	129
5.3.2.2 Effect of current concentration.....	131
5.3.3 Effect of pH.....	133
5.3.4 Effect of electrolytic conductivity (as Cl^-).....	135
5.3.5 Effect of initial fluoride concentration.....	138
5.3.5.1 Ground water sample from Alice Spring	143
5.3.6 Effect of distance between electrodes	146
5.3.7 Competition ions effects	149
5.3.7.1 Effect of anions (Cl^- , NO_3^- , SO_4^{2-}):	149
5.3.7.2 Effect of cations (Mg^{2+} and Fe^{3+}):.....	150
5.3.7.3 Effect of Ca^{2+}	151
5.3.8 Particles size effects	155
5.3.8.1 Effect of the charge on the aggregate size	160
5.3.9 Zeta potential for electrocoagulation	162
5.3.10 Sludge production in ECF process.....	164
5.4 Summary:	170

CHAPTER 6:

FLUORIDE REMOVAL BY A CONTINUOUS FLOW EC REACTOR

6.1 Introduction.....	173
6.2 Materials and methodes.....	173
6.2.1 Continuous flow ECF design	173
6.2.2 Experimental procedures.....	181
6.2.3 Experimental set up.....	184

6.3	Results and discussion	187
6.3.1	Effects of surface charge density	187
6.3.2	Effect of flow rate	190
6.3.3	Effect of initial fluoride concentration	192
6.3.4	Effect of pH.....	195
6.3.5	Effect of total detention time.....	196
6.3.6	Sludge quantity	207
6.3.7	Total operational costs	211
6.4	Summary	215

CHAPTER 7

SOLUTION SPECIATION AND REMOVAL MECHANISMS

7.1	Introduction	217
7.2	Basic principles	218
7.2.1	Chemical speciation	218
7.2.2	A chemical equilibrium modelling system	218
7.3	Speciation results	221
7.3.1	Speciation of Al in water.....	221
7.3.1.1	Dependence of aluminium solubility on the pH	222
7.3.2	Speciation of Al-F complexes.....	226
7.3.2.1	Effect of pH on speciation of Al-F complexes.....	227
7.3.2.2	Effect of fluoride concentration on speciation of Al-F complexes	231
7.3.3	Aluminium hydroxide precipitation.....	234
7.3.4	Calcium precipitation.....	237
7.4	Removal mechanisms.....	240
7.4.1	Mechanism and speciation	241
7.4.2	Characterisation of sludge.....	243
7.5	Summary:	247

CHAPTER 8

EC MODELLING

8.1	Introduction	248
8.2	Results: determination of experimental rate constants.....	249
8.3	Discussion of results: (data modelling and analysis)	250
8.3.1	The multiple regression analysis.....	250
8.3.1.1	Estimating parameters using the method of least squares:.....	253
8.3.1.2	The precision of estimated parameters.....	254
8.3.1.3	Precision of the estimated model	256
8.3.1.4	Searching for residuals and linearity.....	258
8.3.2	Empirical model	261
8.3.3	Monopolar and bipolar processes.....	265
8.3.4	Model verification.....	266
8.3.5	Empirical model and continuous flow data.....	269
8.4	Summary	275

CHAPTER 9:

CONCLUSIONS AND RECOMMENDATIONS FOR FURTHER RESEARCH

9.1	Conclusions.....	277
9.1.1	Electrocoagulation fundamental.....	277
9.1.2	Batch and continuous flow EC reactor experiments	278
9.1.3	Solution speciation and removal mechanisms	280
9.1.4	EC modelling of design.....	281
9.2	Recommendations for further research	283

REFERENCES.....	287
-----------------	-----

APPENDIX A

Summary of results for defluoridation by batch EC process at the different operational parameters..... A.A-1

APPENDIX B

Determination of the kinetic constants for the defluoridation by electrocoagulation process at the different operational parameters.....A.B-1

APPENDIX C

Data for particle size analysis.....A.C-1

APPENDIX D

Summary of results for the defluoridation by continuous flow EC reactor..... A.D-1

APPENDIX E

Total operational cost estimation for the pilot -scale continuous flow EC reactor.....A.E-1

APPENDIX F

How pH and F^- concentration will influence the solubility of aluminium hydroxide (MINEQL⁺ model)A.F-1

APPENDIX G

Summary of the results for the determined the experimental rate constants (K_{exp}) by batch EC process at the different operational parametersA.G-1

APPENDIX H

Summary of the statistical results for comparison between the experimental and predicted rate constants.....A.H-1

APPENDIX I

Summary of the statistical output results between predicted and experimental dataA.I-1

LIST OF FIGURES

Figure 1-1	Countries with endemic fluorosis due to excess fluoride in drinking water (Qian et al., 1999).....	3
Figure 1-2	Interactions occurring within an ECF process	6
Figure 1-3	Structure of the chapters in the thesis	11
Figure 1-4	Flow diagram of the whole research programme undertaken.....	16
Figure 2-1	Schematic of an electroflotation system (adapted from Lesney, 2002)19	
Figure 2-2	Processes in an electrocoagulation reactor (adapted from Holt et al., 2003)	20
Figure 2-3	Schematic of main processes relating to ECF.....	23
Figure 2-4	Variables affecting the rate of an electrode reaction (after Bard and Faulkner, 2001)	26
Figure 2-5	Pathway of a general electrode reaction (based on Figure 1.3.6, Bard and Faulkner, 2001)	27
Figure 2-6	Monopolar and bipolar electrode connections in the EC reactor (adapted from Jiang et al., 2002).....	32
Figure 2-7	Bench scale EC reactor with two electrodes connection: (a) bipolar, and (b) monopolar.....	33
Figure 3-1	Flow diagram of a hybrid process including electrocoagulation, flotation by aeration, and microfiltration processes for the municipal wastewater permeates removal (adapted from Pouet and Grasmick, 1995)	57
Figure 3-2	Laboratory scale processes: (a) EF process, (b) EC and EF processes (adapted from Dimoglo et al., 2004).....	59
Figure 3-3	Summary of EC performance for removal of the pollutants in different current densities and various electrolysis times[a] Fe electrode, [b] Al electrode (quoted in Dimoglo et al., 2004)	60
Figure 3-4	Schematics of EC process [a] Up-flow electrocoagulation reactor and [b] horizontal-flow electrocoagulation reactor (adapted from Jiang et al., 2002).....	65

Figure 3-5	Experimental set up for EC and CC processes (after Sivakumar et al., 2004).	70
Figure 3-6	Influence of initial fluoride concentration on the EC process. (after Mameri et al., 1998).....	75
Figure 3-7	Residual fluoride for different charge loadings at different initial concentrations: pH = 6 ± 0.5 , time = 32 min (after Shen et al., 2003)..	77
Figure 4-1	Summary of ECF processes	92
Figure 4-2	Measured E_{cell} for the batch monopolar EC reactor, ($E_c=12$ mS/m, $C_o = 10$ mg/L).....	96
Figure 4-3	Simplified schematic depicting the electrode oxidation and the possible reactions occurring between the electrode and the bulk of the liquid..	98
Figure 4-4	Completely mixed batch reactor (CMBR) schematics.....	99
Figure 4-5	Plug flow reactor schematic.....	102
Figure 4-6	A flowchart of the empirical modelling approach	106
Figure 5-1	Schematic diagram of an electrocoagulation reactor	110
Figure 5-2	(a) Image of the aluminium electrode used in ECF process, and (b) Schematic of electrode dimensions.....	111
Figure 5-3	Plan views of the electrocoagulation box	111
Figure 5-4	Schematic of electrodes parallel connection (monopolar arrangement)	112
Figure 5-5	[a] Atomic Absorption Spectrophotometer (AAS), [b] UV-Visible spectrophotometer	115
Figure 5-6	Fluoride ion selective electrode (ISE 6.0502.150, Switzerland).....	116
Figure 5-7	[a] the particle size measurement apparatus (Galai CIS-1), [b] Zeta potential measurement apparatus (Malvern Zetasizer 1000/3000) ...	117
Figure 5-8	[a] XRD measurement apparatus (Philips no RN 1730), [b] Light microscopy apparatus together digital colour camera and display server (Nikon 256763, Japan)	118
Figure 5-9	Scanning electron microscopy apparatus (Leica Cambridge Stereoscan -S440).....	120

Figure 5-10	Experimental electrocoagulation/flotation (ECF) reactor.....	121
Figure 5-11	Influence of electrolysis time on fluoride removal and production of total aluminium concentrations ($I=1.5$ A, $d=5$ mm, $pH=6$, $C_o=10$ mg/L, $d=5$ mm)	125
Figure 5-12	Relationship between theoretical and experimental Al^{3+} concentration with electrolysis time ($I=1.5$ A, $C_o=10$ mg/L, $T=25$ °C, $pH=6$, $d=5$ mm)	125
Figure 5-1	Relationship between theoretical and experimental Al^{3+} concentration for removal of fluoride at this ECF process ($C_o=5-25$ mg/L, $Ec_{in}=10-50$ mS/m, $T=25$ °C, $pH=6-8$, $d=5$ mm).....	126
Figure 5-14	Images of (a) small bubbles generation and (b) floc flotation in ECF process.....	127
Figure 5-15	Effect of released aluminium dosage on the residual fluoride concentration ($C_o=10$ mg/L, $Ec_{in}=10$ mS/cm, $T=25$ °C, $pH=6-8$, $d=5$ mm)	128
Figure 5-16	Relationship between charge and total aluminium released to the EC rector ($i=1-2.5$ A, $t=5-60$ min)	129
Figure 5-17	Variation of residual fluoride concentration with time at different current densities on ECF process ($d=5$ mm, $C_o=10$ mg/L, $Ec_{in}=10$ mS/m, $pH=6$).....	130
Figure 5-18	Determination of the kinetic constants of defluoridation at different current densities on ECF process ($Ec_{in}=10$ mS/m, $C_o=10$ mg/L, $d=5$ mm, $pH=6$)	131
Figure 5-19	Determination of the kinetic constants for defluoridation by ECF process at different current concentrations ($C_o=10$ mg/l, $T=25$ °C, $d=5$ mm, and $Ec_i=10$ mS/m)	132
Figure 5-20	Effect of initial pH on defluoridation ($i=18.75$ A/m ² , $d=5$ mm, $Ec_{in}=10$ mS/m, $C_o=10$ mg/L, and $t=60$ min).....	133
Figure 5-21	Effect of constant pH on fluoride removal ($i=18.75$ A/m ² , $d=5$ mm, $Ec_{in}=10$ mS/m, $C_o=10$ mg/L, and $t=60$ min)	134
Figure 5-22	Variation of fluoride concentration with time at different current densities on ECF process ($d=5$ mm, $C_o=10$ mg/L, $Ec_{in}=1000$ mS/m, $pH=6$)	136

Figure 5-23	Effects of electrical conductivity on defluoridation by ECF process at different current densities ($d=5$ mm, $C_o=10$ mg/L, $t=60$ min, $pH=6$)	136
Figure 5-24	Effects of conductivity on the energy consumption at different current densities ($d=5$ mm, $C_o=10$ mg/L, $pH=6$)	137
Figure 5-25	Effects of different initial fluoride concentration on defluoridation by ECF process ($i=18.75$ A/m ² , $d=5$ mm, $pH=6$, $Ec_{in}=10-50$ mS/m)....	138
Figure 5-26	Variation of residual fluoride concentration with time at different current densities and initial fluoride concentrations on ECF process, [a] $C_o=10$ mg/L, [b] $C_o=15$ mg/L, [c] $C_o=25$ mg/L ($d=5$ mm, $Ec_{in}=10-25$ mS/m, $pH=6$).....	140
Figure 5-27	Determination of the kinetic constants of defluoridation at different current densities and initial fluoride concentrations on ECF process [a] $C_o=10$ mg/L, [b] $C_o=15$	141
Figure 5-28	Effects of different initial fluoride concentration on defluoridation by ECF process for the various samples ($I=1$ A, $d=5$ mm, $pH_{in}=6$, $Ec_{in}=422$ mS/m).....	143
Figure 5-29	Determination of the kinetic constants for the defluoridation of Alice Springs sample by ECF process at different current concentrations ($C_o=13$ mg/L, $d=5$ mm, $pH_{in}=6$, $Ec_{in}=422$ mS/m).....	144
Figure 5-30	Variation of fluoride concentration with time at different current values and initial fluoride concentrations on the various samples by ECF process ($d=5$ mm, $pH_{in}=6$), [a] $I=1.5$ A, [b] $I=2$ A, [c] $I=2.5$ A	145
Figure 5-31	Determination of the kinetic constants of defluoridation at different current densities and electrodes distancing on ECF process [a] $d=5$ mm, [b] $d=10$ mm, [c] $d=15$ mm ($C_o=10$ mg/L, $Ec_{in}=10$ mS/m, $pH=6-8$)	147
Figure 5-32	Effect of electrode gap on the electrocoagulation of fluoride at two different currents 0.5 and 1 A ($A/V=22$ m ⁻¹ , $pH=6$, $Ec_{in}=10$ mS/m, $C_o=10$ mg/L, $t=60$ min).....	148
Figure 5-33	Effect of anions on defluoridation by ECF process	149
Figure 5-34	Effect of cations on defluoridation by ECF process	150
Figure 5-35	Effect of different Ca^{2+} ion concentrations on defluoridation by ECF ($C_o=15$ mg/L, $pH=7$, $I=1$ A, $t=60$ min, $d=5$ mm, and $T=25$ °C)..	151

Figure 5-36	Effect of electrolysis time on defluoridation by ECF at different Ca^{2+} ion concentrations ($C_0=15$ mg/L, pH = 7, I= 1 A, d=5 mm, and T=25 °C)	152
Figure 5-37	Effect of electrolysis time on defluoridation by ECF at different Ca^{2+} ion concentrations ($C_0=25$ mg/L, pH = 7, I= 1.5 A, d=5 mm, and T=25 °C)	152
Figure 5-38	Determination of the kinetic constants of defluoridation process at different calcium concentrations on ECF process ($C_0=25$ mg/L, pH= 7, I= 1.5 A, d=5 mm, and T=25 °C).....	153
Figure 5-39	Effect of initial Ca^{2+} ion concentrations on defluoridation by ECF and residual calcium concentration in the solution ($C_0=15$ mg/L, pH = 7, I= 1 A, t = 60 min, d=5 mm, and T=25 °C).....	154
Figure 5-40	Definitions of the most popular values in a distribution curve (Adapted from Allen, 1997).....	158
Figure 5-41	Effect of electrolysis time on the floc size in the ECF process (I=1.5A, $C_0=10$ mg/L, pH=6, d=5mm, and T=25°C)	160
Figure 5-42	Effect of current value and electrolysis time on the floc size in the ECF process ($C_0=10$ mg/L, pH =6, d=5mm, t= 5-60 min, I=1.5-2.5A, and T=25°C).....	161
Figure 5-43	Effect on Electrocoagulation reactor's zeta potential and residual fluoride concentration with electrolysis time on defluoridation (I=2.5A, pH = 8, $C_0=10$ mg/L)	163
Figure 5-44	SEM images of the anode surface (a) before and (b) after ECF process	165
Figure 5-45	Images of the sludge formation on the defluoridation by ECF process (a) flotation of sludge, (b) sedimentation of sludge.	166
Figure 5-46	Effect of electrolysis time and current values on the ratio of total produced sludge volume/ sample volume (V_s/V) for defluoridation by ECF process ($C_0=10$ mg/L, pH = 8, d=5 mm, and T=25 °C)	167
Figure 5-47	Collected total sludge mass versus electrolysis time in different current values for defluoridation by ECF process, [a] I=1A, [a] I=1.5A, [a] I=2A, [a] I=2.5A, ($C_0=10$ mg/L, pH = 8, d=5mm, and T=25 °C)	168
Figure 5-48	Collected total sludge volume versus charge value for defluoridation by ECF process ($C_0=10$ mg/L, pH = 8, d=5 mm, and T=25 °C)	169

Figure 5-49	Collected total sludge mass charge value for defluoridation by ECF process ($C_o=10$ mg/L, $pH = 8$, $d=5$ mm, and $T=25$ °C).....	169
Figure 6-1	[a] Schematic and [b] image of a continuous flow EC reactor	174
Figure 6-2	Schematic of an electrocoagulator used in continuous EC process including its dimension	175
Figure 6-3	[a] Schematic and [b] image of the aluminium electrodes used in continuous EC process together its dimensions	176
Figure 6-4	Schematic of sedimentation tank and surface sludge collector.....	178
Figure 6- 5	Plan views of the electrocoagulation box	178
Figure 6-6	Image of a V-shape weir conducted in the sedimentation tank	179
Figure 6-7	End view of the V-shape weir, EC box, and sedimentation and flotation sections.....	180
Figure 6-8	End view of flow out of the V-shape weir at sedimentation tank.....	180
Figure 6-9	Schematic diagram of a continuous flow electrocoagulation reactor	181
Figure 6-10	Experimental set up of a continuous flow electrocoagulation reactor	186
Figure 6-11	Effect of total aluminium concentration on residual fluoride concentration in ECF process ($C_o= 10$ mg/L, $pH_{in} = 6$, $E_c=50$ mS/m, $Q=150$ mL/min, $i =12.5 -50$ A/m ²)	187
Figure 6-12	Effete of surface charge density on the final fluoride concentration for defluoridation by ECF process ($C_o= 10$ mg/L, $pH_{in} = 6$, $E_c=50$ mS/m, $Q=150-400$ mL/min, $i =12.5 -50$ A/m ²)	188
Figure 6-13	Effect of surface charge density on the residual fluoride concentration at different initial fluoride concentration in a continuous flow electrocoagulation	189
Figure 6-14	Effect of flow rate on the defluoridation efficiency at different current densities from 12.5 to 50 A/m ² in a continuous flow electrocoagulation ($C_o= 15$ mg/L, $pH_{in} = 6$, $E_c=50$ mS/m).....	190
Figure 6-15	Effect of flow rate on the residual fluoride concentration at the different current densities in a continuous flow electrocoagulation ($pH_{in} =6$, $E_c =50$ mS/m, $C_o=25$ mg/L).....	191

Figure 6-16	Effect of initial fluoride concentration on the residual fluoride concentration at the different current densities in a continuous flow EC reactor.....	193
Figure 6-17	Effete of surface charge density on the final fluoride concentration for defluoridation by ECF process ($C_o= 25$ mg/L, $pH_{in} = 6$, $Ec=50$ mS/m, $Q=150-400$ mL/min, $i =12.5 -50$ A/m ²).....	194
Figure 6-18	Effect of influent pH on the fluoride removal in a continuous flow electrocoagulation ($C_o = 10$ mg/L, $i = 18.75$ A/m ² , $Q = 150$ mL/min, $Ec = 50$ mS/m).....	196
Figure 6-19	Effect of detention time on the residual fluoride concentration at different flow rate values and current densities in a continuous flow electrocoagulation reactor ($C_o= 10$ mg/L, $pH_{in} = 6$, $Ec=50$ mS/m) ..	197
Figure 6-20	Effect of detention time on the residual fluoride concentration at different flow rate values and current densities in a continuous flow electrocoagulation reactor ($C_o= 15$ mg/L, $pH_{in} = 6$, $Ec=50$ mS/m) ..	200
Figure 6-21	Effect of detention time on the residual fluoride concentration at different flow rate values and current densities in a continuous flow electrocoagulation reactor ($C_o= 25$ mg/L, $pH_{in} = 6$, $Ec=50$ mS/m) ..	203
Figure 6-22	Images of the (a) settled sludge and (b) floated sludge in a continuous flow electrocoagulation system.....	208
Figure 6-23	Total sludge volume versus flow rate in different current density and flow rates in a continuous flow electrocoagulation reactor ($C_o=10$ mg/L, $pH_{in} = 6$, $d=5$ mm, operational time = 8 h).....	208
Figure 6-24	Total sludge volume versus flow rate in different surface charge density in a continuous flow electrocoagulation reactor ($C_o=10$ mg/L, $i=12.5 -50$ A/m ² , $pH_{in} = 6$, $d=5$ mm, operational time = 8 h)	209
Figure 6-25	Total sludge mass versus flow rate in different surface charge density in a continuous flow electrocoagulation reactor ($C_o=10$ mg/L, $i=12.5 -50$ A/m ² , $pH_{in} = 6$, $d=5$ mm, operational time =8 h).....	210
Figure 6-26	Effect of current density on the total operating, energy and the Al materials costs at the different initial fluoride concentration in the continuous flow EC reactor ($pH_{in}= 6$, $Ec=50$ mS/m, $d=5$ mm)	212
Figure 6-27	Effect of current density on the different operating costs at the different initial fluoride concentration in the continuous flow EC reactor ($pH_{in}= 6$, $Ec=50$ mS/m, $d=5$ mm).....	213

Figure 6-28	Cost comparison on the aluminium electrode consumption for ECF process and the coagulant consumption for CC process.....	214
Figure 7-1	Chemical equilibrium problem solving process (from Environmental Research Software, 1996)	220
Figure 7-2	Distribution diagram of mononuclear species for Al-H ₂ O as a function of pH (Al _T = 1 × 10 ⁻⁶ M, T=25°C; Ionic strength = 0.001 M).....	223
Figure 7-3	Solubility of aluminium hydroxide at various pH values by using MINEQL ⁺ software.....	226
Figure 7-4	Distribution diagram of chemical species formed from 1 × 10 ⁻⁶ M aquo Al ³⁺ ion; 1 × 10 ⁻⁵ M fluoride ion as a function of pH	228
Figure 7-5	Solubility of aluminium hydroxide as a function of pH at various concentrations of total F ⁻	232
Figure 7-6	Distribution diagram of Al-F complex species formed in a solution with 0.52 mM F ⁻ as a function of pH (T=25°C).....	232
Figure 7-7	Equilibrium concentrations of Al-F complexes in a solution with 0.01 mM F ⁻ at various pH values (T=25°C).....	235
Figure 7-8	Equilibrium concentrations of Al-F complexes in a solution with 0.52 mM F ⁻ at various pH values (T=25°C).....	236
Figure 7-9	Solubility of fluorite in the presence of different Ca ²⁺ ions and without aluminium concentration in the solution at different pH by using MINEQL ⁺ software (C ₀ =15 mg/L, and T=25 °C).....	238
Figure 7-10	Solubility of aluminium hydroxide at different Ca ²⁺ ions at different pH by using MINEQL ⁺ software (C ₀ =15 mg/L, and T=25 °C)	238
Figure 7-11	Composition of dried sludge analysed by XRD spectrum on defluoridation by ECF process (C ₀ =15 mg/L, Ca _{in} =100 mg/L, t =60 min, I=1.5A, d= 5 mm, pH =7, and T=25 °C)	239
Figure 7-12	Aluminium oxidation process and complexing reactions	240
Figure 7-13	Composition of dried settled sludge in batch reactor analysed by XRD spectrum (C ₀ = 10 mg/L, i = 25 A/m ² , t =60 min, pH _{in} =6, Ec _{in} =15 mS/m).....	243
Figure 7-14	Composition of dried settled sludge for continuous flow reactor analysed by XRD spectrum (C ₀ = 10 mg/L, i = 25 A/m ² , Q= 200mL/min, pH _{in} =6, Ec _{in} =15 mS/m)	244

Figure 7-15	Composition of dried collected sludge from surface of the electrodes analysed by XRD spectrum ($C_o = 10 \text{ mg/L}$, $i = 18.75 \text{ A/m}^2$, $t = 60 \text{ min}$, $\text{pH}_{in} = 6$, $E_{c,in} = 15 \text{ mS/m}$)	244
Figure 7-16	Composition of dried settled sludge analysed by XRD spectrum ($C_o = 10 \text{ mg/L}$, $i = 25 \text{ A/m}^2$, $t = 60 \text{ min}$, $\text{pH}_{in} = 6$, $E_{c,in} = 15 \text{ mS/m}$)	245
Figure 7-17	Composition of dried settled sludge analysed by XRD spectrum ($C_o = 25 \text{ mg/L}$, $i = 31.25 \text{ A/m}^2$, $t = 60 \text{ min}$, $\text{pH}_{in} = 6$, $E_{c,in} = 15 \text{ mS/m}$)	246
Figure 7-18	Composition of dried floating sludge analysed by XRD spectrum ($C_o = 10 \text{ mg/L}$, $i = 25 \text{ A/m}^2$, $t = 60 \text{ min}$, $\text{pH}_{in} = 6$, $E_{c,in} = 15 \text{ mS/m}$)	246
Figure 8-1	Randomly distributed residuals (a) non- standardised (b) standardised	259
Figure 8-2	Normal probability plot between expected and observed cumulative data with interval confidential of 95 %	261
Figure 8-3	Relationship between the experimental and predicted rate constants for the ECF process at different operational parameters ($I = 1\text{-}2.5 \text{ A}$, $V = 3.66 \text{ L}$, $C_o = 10\text{-}25 \text{ mg/L}$, $d = 5\text{-}15 \text{ mm}$, $E_{c,in} = 10\text{-}50 \text{ mS/m}$, $\text{Ca}^{2+} = 50\text{-}300 \text{ mg/L}$, $\text{pH} = 6\text{-}8$, and $T = 25 \text{ }^\circ\text{C}$)	262
Figure 8-4	Relationship between theoretical fluoride removal efficiency and the experimental defluoridation efficiency by ECF process at different operational parameters ($I = 1\text{-}2.5 \text{ A}$, $V = 3.66 \text{ L}$, $C_o = 10\text{-}25 \text{ mg/L}$, $d = 5\text{-}15 \text{ mm}$, $\text{Ca}^{2+} = 50\text{-}300 \text{ mg/L}$, $E_{c,in} = 10\text{-}50 \text{ mS/m}$, $\text{pH} = 6\text{-}8$, and $T = 25 \text{ }^\circ\text{C}$).	264
Figure 8-5	Comparison between monopolar and bipolar systems for defluoridation by ECF process for the same concentration of Ca^{2+} and the same operational parameters ($i = 10.2 \text{ A/m}^2$, $C_o = 10 \text{ mg/l}$, $d = 20 \text{ mm}$, and $\text{pH} = 6\text{-}8$)	265
Figure 8-6	Comparison between predicted and experimental residual fluoride concentrations with electrolysis time for bore water data ($I = 1.3 \text{ A}$, $V = 3.66 \text{ L}$, $C_o = 13 \text{ mg/L}$, $d = 7 \text{ mm}$, $\text{pH} = 7.8$)	266
Figure 8-7	Comparison between predicted and experimental residual fluoride concentrations with electrolysis time for Mameri's data ($I/V = 353 \text{ A/m}^3$, $C_o = 10 \text{ mg/L}$, $d = 20 \text{ mm}$, $\text{pH} = 6$, $\text{Ca}^{2+} = 280 \text{ mg/L}$)	267
Figure 8-8	Comparison between predicted and experimental final fluoride concentrations with initial fluoride concentration for Shen's data ($I/V = 278 \text{ A/m}^3$, $d = 4 \text{ mm}$, $\text{pH} = 6$, $\text{Ca}^{2+} = 0 \text{ mg/L}$)	268
Figure 8-9	Relationship between the experimental and predicted flow rate for defluoridation by the continuous flow EC reactor at different	

operational parameters ($I/V=380-1000 \text{ A/m}^3$, $C_o=10-25 \text{ mg/L}$, $t_{ro}=26-53 \text{ min}$, $d=5 \text{ mm}$, $Ec_{in}=10-50 \text{ mS/m}$, $Ca^{2+}=15 \text{ mg/L}$, final $pH=6-8$, and $T=25 \text{ }^\circ\text{C}$) 271

- Figure 8-10 Relationship between the experimental and predicted optimum residence time for defluoridation by the continuous flow EC reactor at different operational parameters ($I/V=380-1000 \text{ A/m}^3$, $Q=150-300 \text{ mL/min}$, $C_o=10-25 \text{ mg/L}$, $d=5 \text{ mm}$, $Ec_{in}=10-50 \text{ mS/m}$, $Ca^{2+}=15 \text{ mg/L}$, final $pH=6-8$, and $T=25 \text{ }^\circ\text{C}$)..... 272

- Figure 8-11 Comparison between the predicted and experimental optimum flow rates with the different current concentrations at the different initial fluoride concentrations for defluoridation by the continuous flow EC reactor ($d=5 \text{ mm}$, $pH_{in}=6$, $Ca^{2+}=15 \text{ mg/L}$, $Ec_{in}=20-35 \text{ mS/m}$)..... 273

- Figure 8-12 Comparison between the predicted and experimental optimum flow rates with the different current concentrations for defluoridation by continuous flow EC restore ($d=5 \text{ mm}$, $pH_{in}=6$, $Ca^{2+}=15 \text{ mg/L}$, $Ec_{in}=10 \text{ mS/m}$)..... 274

LIST OF TABLES

Table 1-1	Health impacts from long term use of high fluoride concentration in drinking water (WHO, 2004; NHMRC and ARMCANZ, 2004)	3
Table 1-2	Research activities.....	8
Table 2-1	Summery of different defluoridation methods in water and wastewater treatment.....	41
Table 3-1	Effect of the hybrid process on the removal of COD, SS, and turbidity (adapted from Pouet and Grasmick, 1995)	57
Table 3-2	Sludge Produced by EC and CC Process (after Sivakumar et al., 2004)	70
Table 3-3	Summary of pollutants removed by electrocoagulation in water and wastewater sources.....	83
Table 5-1	Electrode area to reactor volume ratio (A/V) and current density 109	
Table 5-2	Micron bar sizer for video pro images used for 3.2 magnification factor in Nikon light microscopy.....	119
Table 5-3	Relationship between operating current value, current density, and current concentration in the ECF reactor	122
Table 5-4	Important experimental variables in ECF reactor	123
Table 5-5	Optimum detention time and optimum charge for defluoridation by ECF process at the different initial fluoride concentrations (d=5 mm, $E_{c_{in}}=10-25$ mS/m, pH=6-8)	142
Table 5-6	Characteristics of water quality Alice Spring sample used for defluoridation	143
Table 5-7	Definitions of mean diameters of particles (Allen, 1997).....	159
Table 5-8	Calculated values of mean diameters for selection of particles in the different electrolysis time by EC process ($I=1.5A$, $C_o=10$ mg/L, pH=6, d=5mm, and $T=25^{\circ}C$)	159
Table 6-1	Relationship between current operating value, current density and concentration in the continuous flow EC reactor.....	182

Table 6-2	Water quality characteristics of test water used for synthetic samples	183
Table 6-3	Important experimental variables measured in the continuous flow EC reactor.....	183
Table 6-4	Summarised design parameters for continuous flow EC reactor	184
Table 6-5	The experimentally determined optimum residence time and optimum surface charge density to achieve the desirable fluoride concentration range in the electrocoagulator for different flow rates, current densities, and initial fluoride concentrations.....	207
Table 6-6	Estimated total operational cost for defluoridation using a pilot-scale continuous flow EC reactor ($Q = 200 \text{ mL/min}$, $i = 12.5 \text{ A/m}^2$, $U = 4.27 \text{ V}$, $C_0 = 5 \text{ mg/L}$, and surface charge density = 30000 C/m^2).....	211
Table 7-1	Predominant aluminium species in drinking water (Sposito, 1996) .	222
Table 7-2	Total molar concentration of the mononuclear Al ion species at different pH ($Al_T = 1 \times 10^{-6} \text{ M}$, $T=25^\circ\text{C}$; Ionic strength = 0.001 M)	225
Table 7-3	Predominant aluminium-fluoride species in aqueous solution (Sposito, 1996; and from MINEQL ⁺ data base, 1996)	227
Table 7-4	Total molar concentrations of aluminium speciation in the presence of 0.01 mM F (from MINEQL ⁺ model).....	230
Table 7-5	Total molar concentrations of aluminium speciation in the presence of 0.52 mM F (from MINEQL ⁺ model).....	233
Table 8-1	Descriptive statistics of sampled data	251
Table 8-2	Correlation between all the variables included in the SPSS statistical tool	252
Table 8-3	Summary of statistical results for the predictive equation	253
Table 8-4	Summary of analysis of variance (ANOVA) results	257
Table 8-5	Prediction of the optimal flow rate and residence time for various current concentrations and initial fluoride concentrations in the continuous flow EC reactor ($pH_{in}=6$, $Ca^{2+}=15 \text{ mg/L}$, and $d=5\text{mm}$) .	270

LIST OF SYMBOLS AND ABBREVIATIONS

SYMBOLS

A	Area of electrode (m^2)
Al^{3+}/F^-	Aluminium to fluoride mass ratio
[Al-F]	Aluminium fluoro-complexes (mol)
[Al-OH]	Aluminium hydroxy-complexes (mol)
A_p	Plan area of the settling zone (m^2)
A/V	Electrode area to cell volume ratio (m^2/m^3)
AW	Atomic weight (gr/mol)
B	Least squared coefficients
B_1	Regression coefficient
b_0	Constant
b_1, b_2, b_p	Multi-regression coefficients
C	Coulomb
C_0	Initial pollutant concentration at time $t = 0$, (mg/L)
$C_{Al} = [Al_T]$	Total concentration of aluminium (mg/L or gr/m^3)
$C_{Al(E)}$	Experimental Al^{3+} concentration (gr/m^3)
$C_{Al(T)}$	theoretical Al^{3+} concentration (gr/m^3)
C_e	Concentration of pollutant in effluent (mg/L)
C_F	Total concentration of the fluoride component (gr/m^3)
CI	Confidence interval (%)
C_i	Concentration of specie i
C_{ox}	Oxidised species
C_{Re}	Reduced species
C_t	Concentration of pollutant at any time (mg/L)
C_w	Weir coefficient
$C'_{Al(T)}$	Concentration of Al^{3+} dissolving to volume of cell per unit area of electrode ($gr/m^2 \cdot m^3$)
d	Distance between electrodes (mm)
d_p	Particle diameter (μm)

d_s	Diameter of a sphere having the same surface as the particle (μm)
d_{sv}	Diameter of a sphere having the same external surface to volume ratio
d_v	Diameter of a sphere having the same volume as the particle (μm)
E	Equilibrium potential (V)
E_{an}	Anodic potential (V)
E_c	Electrical conductivity (mS/m)
$E_{c\text{ in}}$	Initial conductivity (mS/m)
E_{ca}	Cathodic potential (V)
E_{cell}	Overall potential (V)
E_{lo}	Loss potential (V)
E_{so}	Solution potential (V)
$E^{\circ} = E^{\circ}_{\text{Cell}}$	Standard cell potential (V)
E°_{A}	Standard anodic potential (V)
E°_{C}	Standard cathodic potential (V)
e^-	Electron
e_i	Residuals
F	Faraday's constant ($F = 96500 \text{ C/mol}$)
g	Gravitational constant (9.81 m/s^2)
h	Height of reactor (mm)
H	Height of the sedimentation tank (mm)
H	Height of liquid above the bottom of the V-notch (mm)
$[\text{H}^+]_0$	Initial acidity
i	Current density (A/m^2)
I	Current input (A)
I_1	Current pass across each electrode (A)
I_T	Total current input (A)
I/V	Current concentration (A/m^3)
K	Rate constant of the process (min^{-1})
K_{exp}	Experimental kinetic constant (min^{-1})
K_{pre}	Predicted kinetic constant (min^{-1})
$K_{\text{so}}, K_{\text{s1}}, K_{\text{s2}}$	Solubility product constant
K°	Thermodynamic equilibrium constant

L	Length of the sedimentation tank (mm)
$M_{(Al)}$	Molecular weight of Al ($M = 27 \text{ g/mol}$)
MS	Mean square
MW	Molecular weight (g/mol)
N	Number of electrodes in the electrocoagulator
N	Number of samples
n	Number of electrons consumed in the electrode reaction
$N-1 = d_f$	Degree of freedom for a sample or number of independent variables
N_e	Quantity of mol electrolysed in the electrode reaction
O	Oxidant
O_{bulk}	Oxidant in the bulk solution
$[OH^-]_0$	Initial alkalinity
O_{oxid}	Oxidised species
O_{surf}	Oxidant in the surface region
O'	Intermediate oxidant specie
O'_{ads}	Oxidant adsorbed on electrode's surface
P	Number of values estimated
pH_{in}	Initial pH
pH_f	Final pH
Q	Flow rate (mL/min)
Q_o	Optimal flow rate (mL/min)
Q_e	Quantity of electricity (C)
R	Reynolds Number
R	Reductant
R	Correlation coefficient
R	Gas constant ($R = 8.314 \text{ Jmol}^{-1}\text{K}^{-1}$)
R^2	R squared
$r_{Al^{3+}}$	Coagulant generation rate (gr Al^{3+} /s)
R_{bulk}	Reductant in the bulk solution
Re	Reynolds number
R_{ef}	Removal efficiency (%)
r_H^+	Bubble generation rate (gr H^+ /s)

R_{surf}	Reductant in the surface region
R'	Intermediate reductant
R'_{ads}	Intermediate adsorbed on electrode's surface
S	Surface area of a sphere
SE	Standard error
$SE_{\hat{Y}}$	Standard error of the estimate
SS	Sum of the squared residuals
S_v	Surface to volume ratio
S_x	Standard deviations of the two independents variables
S_y	Standard deviations of the two dependent variables
T	Temperature ($^{\circ}\text{C}$ or $^{\circ}\text{K}$)
t	Time (electrolysis or treatment time) (min)
t_d	Detention time (min)
t_{do}	Optimum detention time (min)
t_r	Residence time (min)
t_{ro}	Optimum residence time (min)
U	Cell voltage (V)
U_0	Cell voltage is applied between two feeder electrodes (V)
U_T	Total cell voltage (V)
V	Volume of reactor (m^3)
V_h	Horizontal velocity (m/s)
V_0	Surface overflow rate ($\text{m}^3/\text{m}^2.\text{min}$)
V_s	Stokes' settling velocity (m/s)
V_{se}	Sludge volume (mL)
V_{sp}	Volume of a sphere
W	Width of the sedimentation tank (mm)
W	Weber number
X_1, X_2, X_p	Independent variables
\bar{X}	Mean of values of X
X_A	Total conversion of substance "A" after treatment time
X_i	Value of the variable for i^{th} case
X_{NL}	Mean diameters of particles by definition of Number, Length

X_{NS}	Mean diameters of particles by definition of Number, Surface
X_{NV}	Mean diameters of particles by definition of Number, Volume
X_{LS}	Mean diameters of particles by definition of Length, Surface
X_{LV}	Mean diameters of particles by definition of Length, Volume
X_{SV}	Mean diameters of particles by definition of Surface, Volume
X_{VM}	Mean diameters of particles by definition of Volume, Moment
Y_i	Observed values of Y
\hat{Y}_i	Predicted values of Y
Z	Number of electrons involved in the oxidation/ reduction reaction
Δ	Change or difference
ΔG^0	Standard Gibbs free energy change in a chemical process (J/mol)
ΔG	Free energy of reaction at any moment in time
α	Kinetic order of the process
ε_c	Current efficiency (%)
σ	Surface charge density (C/m ²)
θ	Inside weir angle
γ	Activity coefficient
γ_{OH}	molar ratio of hydroxide to Al ³⁺
ρ_s	Density of particle (kg/m ³)
ρ_w	Density of water (kg/m ³)
σ^2	Variance
μ	Viscosity of water (Pa.s)

ABBREVIATIONS

AA	Activated alumina
AAS	Atomic absorption spectroscopy
ANOVA	Analysis of variance
ARMCANZ	Agriculture and Resource Management Council of Australia and New Zealand
AWWA	American Water Works Association
AUD	Australian Dollar
BAT	Best available technology

BSE	Back scattered electron
CC	Chemical coagulation
COD	Chemical oxygen demand
CMP	Chemical mechanical polishing
CMBR	Completely mixed batch reactor
DAF	Dissolved air flotation
DC	Direct current
DOC	Dissolved organic carbon
EC	Electrocoagulation
EDS	Energy dispersive spectroscopy
EF	Electroflotation
EFC	Electrocoagulation/flotation
HRT	Hydraulic retention time
ICCD	International Centre for Diffraction Data
ISE	Ion selective electrode
LDV	Laser Doppler Velocimetry
NA	Nalgonda process
NEERI	National Environmental Engineering Research Institute
NHMRC	National Health and Medical Research Council
pH	Negative logarithm of the hydrogen ion concentration in a solution
PFR	Plug flow reactor
PRB	Population Reference Bureau
RO	Reverse osmosis
SEEC	Specific electrical energy consumption
SEM	Scanning electron microscopy
SHE	Saturated hydrogen electrode
SI	System International
Sig T	Significant t-test
Sig F	Significant F-test
SPSS	Statistical Package for the Social Sciences
SOR	Surface overflow rate
SS	Suspended solids

STP	Standard Temperature and Pressure
Surf	Surface
TDS	Total dissolved solids
TOF-SIMS	Time-of-flight secondary ion mass spectroscopy
UNESCO	United Nations Educational, Scientific and Cultural Organization
UNICEF	United Nations Children’s Fund
U.S	United State
USEPA	United State Environmental Protection Agency
UV	Ultraviolet
WEF	Water Environment Federation
WHO	World Health Organization
XPS	X-ray photoelectron spectroscopy
XRD	X-ray diffraction

CHAPTER 1

INTRODUCTION

1.1 INTRODUCTION

We are aware that water is essential for life, for drinking, for producing food, for washing, and for maintaining our health. In addition, water is needed for ensuring the reliability and sustainability of the earth's ecosystem. In 2002, 83 % of the world's population of around 5.2 billion used improved sources of drinking water. Of the 1.1 billion using water from unimproved sources, which represented 17 % of the global population, nearly two thirds live in Asia (WHO, 2002). The world's population in 2005 was reported to be 6.47 billion when 94 % of the urban population and 71 % of the rural population were using drinking water from improved sources (PRB, 2005). As the human population will increase to about 9.3 billion by 2050 (UNESCO, 2003), providing drinking water will be a critical problem in the future, especially in developing countries with limited water treatment processes and strategies for sustainable water management. The right of all people to access safe drinking water is a challenge for attention to water treatment methods now and in future.

Better management of water resources and improvement of proper treatment processes can limit environmental pollution. There is broad range of treatment processes that can be used for water treatment. The quality of raw water can be considered as an important parameter when selecting the actual treatment process. Inorganic constituents, which may be present in natural or contaminated water sources, become a major public health problem in drinking water. Excessive

presence of fluoride concentration, as an inorganic element, in community water supplies can cause dental and skeletal fluorosis. Removing Fluoride in drinking water and wastewater has been the subject of many publications and studies that have progressively developed the aspects of toxicity on man and the environment. Fluoride can also be found in industrial wastewaters such as glass manufacturing (Sujana et al., 1998), and in high concentrations in the semiconductor industries (Toyoda & Taira, 2000). The discharge of these wastewaters without treatment into the natural environment would contaminate groundwater and other sources.

1.1.1 Fluoride Health problems

Fluoride ion in water has beneficial and harmful effects on the environment and the human. When an optimum amount of 1 mg/L is present in the drinking water fluoride helps prevent teeth decay but long term consumption of water containing excess fluoride can lead to fluorosis of the teeth and bones (WHO, 2004; NHMRC and ARMCANZ, 2004). Artificial fluoridation of drinking water by municipalities at 1 ppm of fluoride ion probably does not reduce tooth decay, except for a slight benefits for the deciduous teeth of 5-year-old children (Kauffman, 2005). Long term consumption of water containing 1.5 mg/L of fluoride leads to dental fluorosis (WHO, 2005). Glistening white and yellow patches appear on the teeth which may eventually turn brown. Skeletal fluorosis is a bone disease caused by excessive consumption of fluoride. Health impacts from long term use of high fluoride concentration in drinking water have been summarised in Table 1-1.

Table 1-1 Health impacts from long term use of high fluoride concentration in drinking water (WHO, 2004; NHMRC and ARMCANZ, 2004)

Fluoride concentration (mg/L)	Effects
<0.5	Dental caries
0.5 - 1.5	Promotes dental health
1.5 - 4	Dental fluorosis
>4	skeletal fluorosis

In groundwater, the natural concentration of fluoride depends on the geological, chemical, and physical characteristics of the aquifer, the porosity and acidity of the soil and rocks, temperature, the action of other chemical elements, and the depth of wells. Water with high fluoride content is usually found at the foot of high mountains and in areas with geological deposits of marine origin. Due to these variables, the fluoride concentrations in groundwater can range from less than 1 mg/L to more than 35 mg/L (WHO, 2005). A study by UNICEF, as shown in Figure 1-1, illustrates that fluorosis is endemic in at least 27 countries across the globe (Qian et al., 1999).



Figure 1-1 Countries with endemic fluorosis due to excess fluoride in drinking water (Qian et al., 1999)

These countries are: Algeria, Argentina, Australia, Bangladesh, China, Egypt, Ethiopia, India, Iran, Iraq, Japan, Jordan, Kenya, Libya, Mexico, Morocco, New Zealand, Palestine, Pakistan, Senegal, Sri Lanka, Syria, Tanzania, Thailand, Turkey, Uganda, and United Arab Emirates.

The fluorosis problem is most severe in the two most populated countries of the world, China and India. WHO has recently estimated that 2.7 million people in China have a crippling form of skeletal fluorosis (WHO, 2002). An estimated 62 million people in India in 17 out of the 32 states are affected with dental, skeletal, and/or non-skeletal fluorosis. The extent of fluoride contamination varies from 1.0 to 48.0 mg/L (Qian, 1999). In Kenya, concentrations up to 25 mg/L have been reported. The total number of people affected is not known but an estimated number would be in the tens of millions (WHO, 2002). The fluoride concentration was recorded at 13 mg/L in a bore near the Indulkana region in central Australia. This bore is not used for human consumption (Fitzgerald et al., 1999). Fluoride also can be found in industrial wastewaters, such as in glass manufacturing industries (Sujana et al., 1998) and in semiconductor industries (Toyoda and Taira, 2000). The discharge of these wastewaters without treatment into the natural environment would contaminate ground and surface waters. To reduce major public health problems, high fluoride concentrations in drinking water need to be removed.

1.1.2 Defluoridation process

There are several defluoridation processes that have been tested globally, such as adsorption (Lounici et al., 1997), chemical precipitation (Parthasarathy et al., 1986; Sujana et al., 1998; Toyoda & Taira, 2000), electrodialysis (Amor et al., 2001), and

the electrochemical method (Ming et al., 1983; Li-Cheng, 1985; Mameri et al., 1998). The important defluoridation technologies for drinking water have been considered by Nalgonda technique (alum and lime) and Prasanthi technology (activated alumina) in India (Susheela, 1992). In precipitation technology, alum or a combination of alum and lime are respectively added to water with a high and low concentration of fluoride, which is then removed by flocculation, sedimentation, and filtration. Using chemical coagulants for precipitation is one of the essential processes used to treat conventional water and waste water. But chemical coagulation is less acceptable than other processes (Rajeshwar and Ibanez, 1997) because it generates large volumes of sludge, is costly, and requires the hazardous waste categorisation of metal hydroxides. If a new process can replace conventional chemical coagulation the process would be more efficient with little modification to present water treatment plants and many of the problems caused by chemical coagulation would be solved. Electrocoagulation (EC) is a new electrochemical technique with many applications, which has been suggested as an alternative to conventional coagulation process (Mills, 2000).

1.1.3 Electrocoagulation technology

Electrocoagulation is an alternative technique for removing pollutants from water and waste water. This process involves applying an electric current to sacrificial electrodes, usually aluminium, inside a processing tank. The electrodes are arranged at the bottom of a tank filled with water containing dispersed solids (Lesley, 2002). The word “electrocoagulation” will be used with “electroflotation” and can be expressed as the electrocoagulation/flotation (ECF) process. Through this process coagulating agents such as metal hydroxides are produced. The coagulating agents

can adsorb pollutants from the waste water and consolidate the small suspended particles to larger ones that can be removed by sedimentation. Indeed, in the ECF process, the coagulant is generated in situ by the electrolytic oxidation of an appropriate anode material (aluminium or iron). The removal mechanism can be considered similar to coagulation with chemical coagulants. Interactions occurring within an ECF process are shown in Figure 1-2.

EC: Electrocoagulation
EF: Electroflotation
ECF: Electrocoagulation/flotation

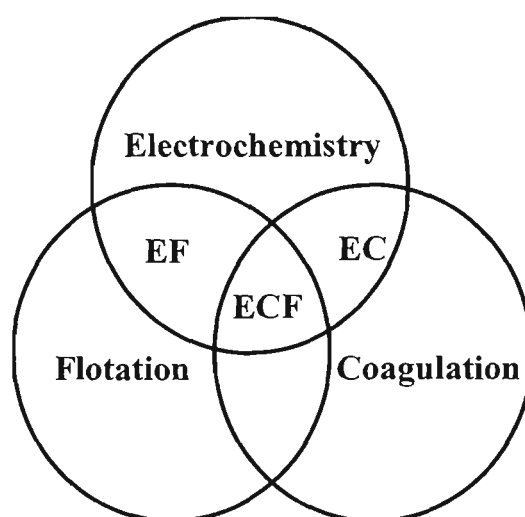


Figure 1-2 Interactions occurring within an ECF process

Electrocoagulation has been practiced sporadically for most of the 20th century with varying popularity, as its history, application, and limitation will be discussed in the next chapters (2 and 3). In this research, an electrocoagulation technology using aluminium anode is used for defluoridation in water treatment. To understand how the EC process works, it is important to discuss the mechanism of water electrolysis and other related chemical reactions. So, understanding of EC fundamentals together pollutant removal mechanisms and the speciation of Al-F complexes are vitally important which were shortly considered in the literatures. The previous research studies on the batch and continuous flow experiments using Al electrode in

monopolar and bipolar configuration showed that EC method is an effective process for defluoridation, yet more investigation needs to be done. A number of studies have been also performed to describe the effects of the different operational parameters; however, no empirical model has been developed using critical parameters for fluoride removal by monopolar ECF process. The main aims of this thesis together research programme undertaken are considered in the following of this chapter.

1.2 AIMS AND OBJECTIVES:

The aim of this study is firstly to understand the fundamental characteristics of electrocoagulation and then to make an attempt to apply it for fluoride removal through batch and continuous experiments in order to verify its applicability. The specific objectives are:

- To review the literature for information and data on pollutant (especially fluoride) removals by electrocoagulation and the fundamentals of the electrocoagulation process.
- To design and construct a batch electro-coagulator and assess the removal efficiency and select the appropriate EC technology for removing Fluoride.
- To design and construct a continuous flow electrocoagulator based on results from the batch experiments.
- To determine how various operating parameters affect the efficiency of removing fluoride with a view to optimize operating condition.
- To discover the mechanisms for removing fluoride in the electrocoagulator based on the solution speciation and floc particle characteristics.

- To develop an empirical mathematical model for correlating the experimental rates of removing fluoride with a predetermined set of electrocoagulation reactor operational parameters.
- To predict the efficient removal of fluoride using an empirical model and compare the results from the model with the experimental laboratory data, independent data, and continuous flow data.

1.3 SCOPE OF THE STUDY

To achieve the presented research objectives, the overall project was separated into eight primary phases as shown in Table 1-2.

Table 1-2 Research activities

TASK
Phase 1: Literature survey on the fundamentals of the EC process and a review of pollutant (especially fluoride) removal by EC technology
Phase 2: Presentation of the general theoretical consideration of the EC process.
Phase 3: Designing and constructing a batch electrocoagulator to assess the removal and appropriate EC technology for treating fluoride
Phase 4: Finding out the effects of various operating parameters on the efficient removal of fluoride
Phase 5: Designing and constructing a continuous flow electrocoagulator and evaluate the efficient removal of fluoride.
Phase 6: Investigation of the mechanisms for removing fluoride in the EC process, based on solution speciation and dried sludge characteristics
Phase 7: Development of an empirical model using critical parameters such as current concentration, distance between electrodes, pH of the solution, ion competition effect (Ca^{2+}) and initial fluoride concentration
Phase 8: Prediction of the fluoride removal efficiency, calibration and verification of the empirical model with dependent , independent and continuous flow data

In the first phase of this research a literature survey on the fundamental of electrocoagulation and a review of pollutant removal (especially fluoride) by electrocoagulation technology was carried out. The second phase dealt with the general theoretical consideration of the EC process. A fundamental understanding of electrocoagulation was applied for removing pollutions in water and waste water treatment plants. Three different mechanisms including, electrode oxidation, gas bubble generation, sedimentation and flotation of flocs formed in the electrocoagulation/flotation processes were included in this stage. The third phase involved designing and constructing a batch electrocoagulator and then assessing the removal of and use of appropriate EC technology for clarifying pollutants, especially excess of F^- in water and waste water supplies. The fourth phase was to elucidate the effects of some operational parameters including, current density, electrolysis time, current concentration, pH of the solutions, distance between electrodes, initial concentration of fluoride, electrolyte conductivity, particle size, zeta potentiometer, Al^{3+}/F^- mass ratio, cations effects (especially Ca^{2+}) on the efficient removal of fluoride by the ECF batch process. At phase five, a continuous flow electrocoagulator was designed and constructed based on the results obtained from batch experiments, The effects of current inputs, initial concentration of fluoride, initial pH, flow rate, and detention time have been investigated. At phase six, the fluoride removal mechanisms were investigated in the electrocoagulator based on the solution speciation and dried sludge characteristics. The compositions of dried sludge were studied in two steps, first by X-Ray Diffraction (XRD) spectroscopy, and then soft analysis by relevant software. MINEQL⁺ software (Environmental Research Software, 1999) was utilised to show how different pH would influence the solubility

of aluminium hydroxide $[\text{Al}(\text{OH})_3]$. The seventh phase was performed to develop an empirical model using critical parameters such as current concentration, electrode distance, pH of the solution, ion competition effect (Ca^{2+}) and initial concentration of fluoride. The theory of chemical batch reactor was used as the basis for developing the semi empirical model. The eighth phase was carried out to predict the fluoride removal efficiency using the empirical model and compare the results with the experimental laboratory data and other data from the literature. It was also achieved to provide a statistically good linear fit and present the agreement between the independent data and predictive equation. The SPSS package was used as a statistical tool to approximate the multiple correlations of all data by analysing the regression.

1.4 RESEARCH APPROACH

This thesis is presented in 9 chapters, with the flowchart showing how they are arranged, illustrated in Figure 1-3.

- Chapter 1 presents a general overview of the research objectives together with a background of the electrocoagulation technology basis for the removal of fluoride. It is divided into four main topics, the introduction, the objectives, the scope, and a summary of the tasks performed while completing this research. The first section considers three aspects including fluoride health problems, defluoridation process and electrocoagulation technology.

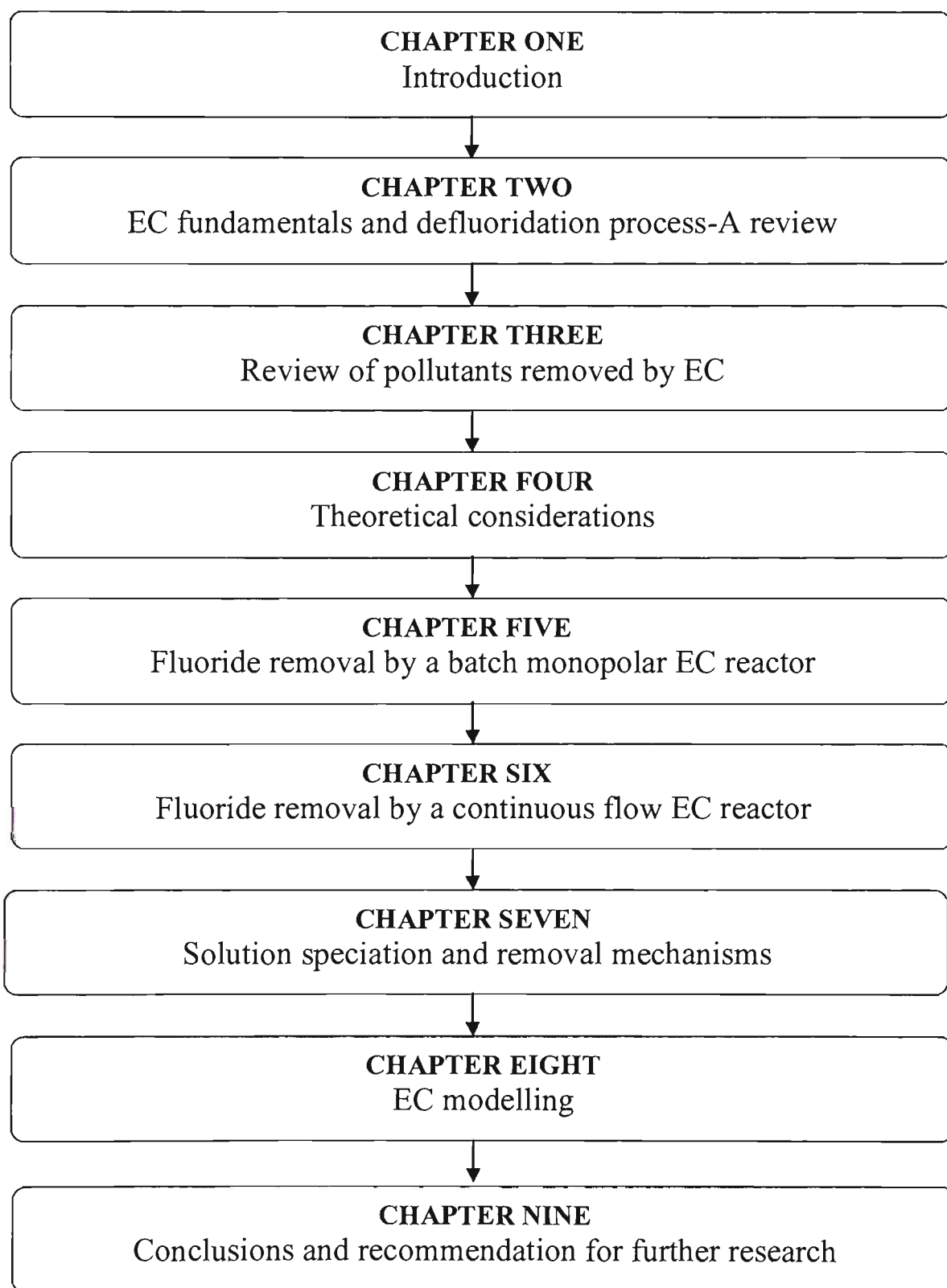


Figure 1-3 Structure of the chapters in the thesis

- Chapter 2 includes a review on the fundamentals of electrocoagulation. During the early stages of this chapter a definition of electrocoagulation (EC),

electroflotation (EF) and electrocoagulation/flotation (ECF) are presented. Several sections contain information on the background of electrocoagulation, the principles of electrocoagulation based on three important sciences including electrochemistry, coagulation, and flotation, and the advantages and disadvantages of EC, cell configuration, energy consumption, and coagulant dosage. Towards the end a review of the different defluoridation methods including, precipitation, adsorption/ion exchange, membrane, and electrochemical or electrocoagulation methods is included.

- Chapter 3 includes a review of the removal of pollutants, especially fluoride, by electrocoagulation in water and waste water treatment plants. The main aim is to present bench scale and field scale research studies of electrocoagulation technology for the different pollutants removed via water and waste water processes. Although this chapter emphasises more concepts related to defluoridation by electrocoagulation, a summary at the end presents the different pollutants removed by electrocoagulation and associated references.
- Chapter 4 contains a general theoretical consideration of the electrocoagulation process with information on the electrochemical mechanism occurring in the reactor. The main aim is to understand fundamentals of electrocoagulation as applied to the removal of pollution in water and waste water. Towards the end information regarding the mechanism of contaminants removed by EC, especially when aluminium

electrodes are used by EC, is included. This is to present a theoretical model based on three different mechanisms including, oxidation of the electrode, gas bubble generation, and sedimentation and flotation of flocs formed in the electrocoagulation/flotation processes. The basic equations are included to present a theoretical as well as empirical model for predicting the efficient removal of fluoride by the ECF process.

- Chapter 5 deals with a laboratory batch monopolar electrocoagulation reactor is designed and constructed for removing fluoride. The effects of some operational parameters such as, electrolysis time, current density, current concentration, pH of the solution, distance between electrodes, initial concentration of fluoride, electrolyte conductivity, particle size, zeta potentiometer, aluminium concentration ($\text{Al}^{3+}/\text{F}^-$ mass ratio), mass balance, and the ionic competition effects (specially Ca^{2+} effect) are elucidated on the efficient removal of fluoride in a batch scale. Towards the end of the chapter information regarding the considerable amount of sludge produced in the base and surface of the electrobox is included to explain the general mechanisms controlling the efficient defluoridation by the electrocoagulation/flotation process.
- Chapter 6 shows the design and construction of a continuous flow electrocoagulator based on the results of batch experiments. The effects of some operational parameters including, current inputs, detention time, pH of the solution, the volume of sludge produced, initial concentration of fluoride, and flow rate on the efficient removal of fluoride in the continuous flow

electrocoagulator are investigated. The optimum flow rate to achieve a desirable concentration of fluoride is based on the time spent in the continuous flow reactor. Towards to the end of this chapter information regarding the specific electrical energy consumed (SEEC), including the total operational cost of removing fluoride by the EC system.

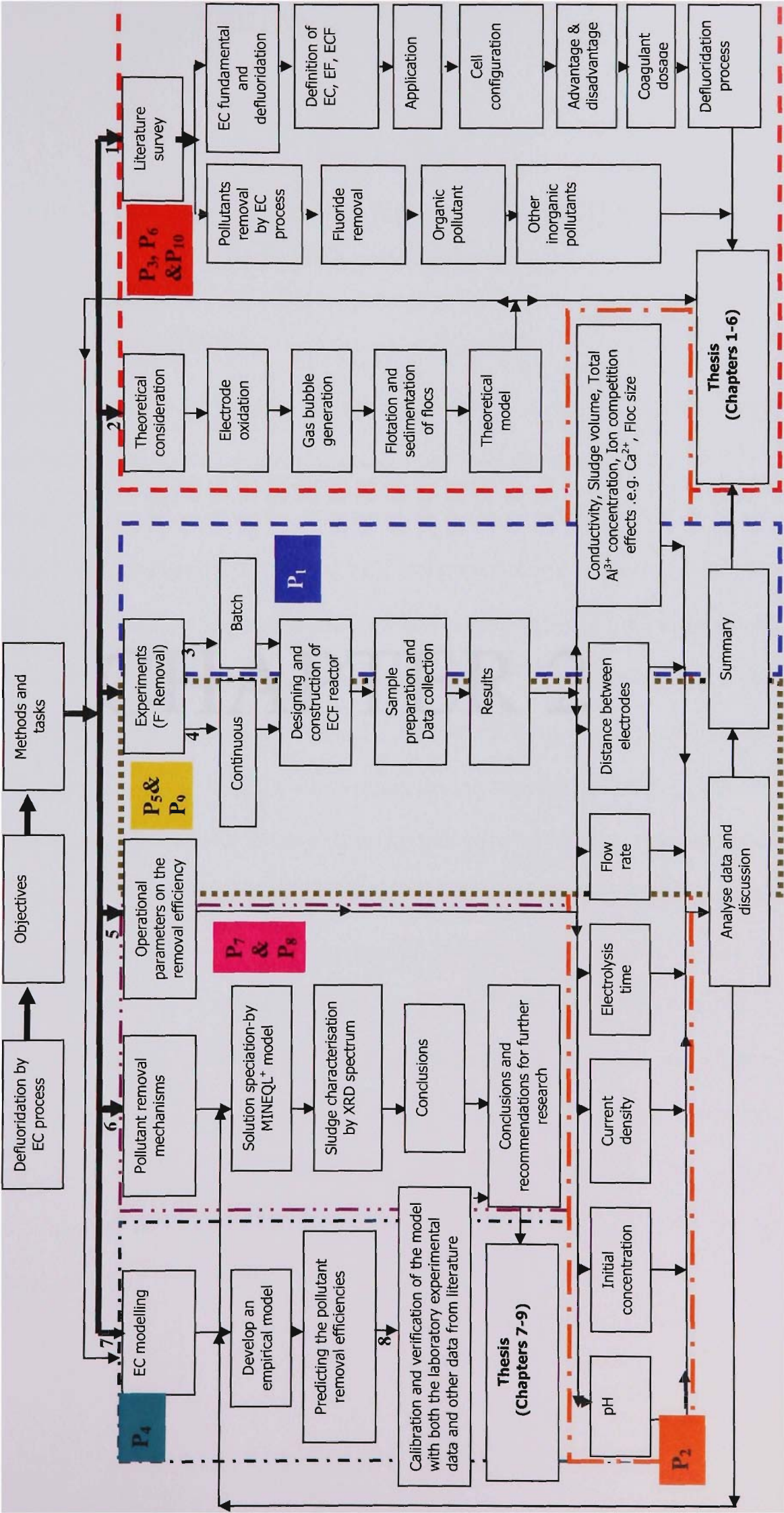
- Chapter 7 gives general information about the speciation solution in the presence of fluoride and aluminium ions. A geochemical speciation package (MINEQL⁺) is used to characterise the electrolyte systems used in these experiments. The results are shown as a function of pH for the solubility of gibbsite [Al(OH)₃]. As between pH 5 and 6, the predominant hydrolysis products are Al(OH)²⁺ and Al(OH)₂⁺. The solid Al(OH)₃ is most prevalent between pH 6 and 8.5 when the soluble species Al(OH)₄⁻ is the predominant species above pH 9. The equilibrium concentrations of the soluble complexes and the speciation are calculated by MINEQL⁺ software. The fluoride removal mechanisms are investigated in the electrocoagulator based on the solution speciation and dried sludge characteristics. The composition of the dried sludge is studied by XRD spectroscopy.
- Chapter 8 shows the evaluation of the developed empirical model with predictions of the efficient removal of fluoride. This chapter presents the results of plotted experimental data as predicted by the model. The empirical model is developed by a statistical tool known as “SPSS package”. The main aim of this chapter is first to present an empirical model using critical parameters including current concentration (I/V), distance between electrodes

(d), effects of ion competition (Ca^{2+}), pH of the solution, and initial concentration of fluoride (C_o) on evaluating the rate constant (K) for removing fluoride using a monopolar ECF process. Second, to determine the optimal detention time required to achieve a desirable concentration of fluoride. In this chapter the empirical model is calibrated with experimental data gathered during this research and then the independent data set is used for its verification.

- Chapter 9 summarises the results and principal conclusions of the research work in this thesis, together with suggestions and recommendations for further research.

A summarized flow diagram that the author developed during this research is shown in Figure 1-4.

Figure 1-4 Flow diagram of the whole research programme undertaken



CHAPTER 2

CHAPTER 2

EC FUNDAMENTALS AND DEFLUORIDATION PROCESS – A REVIEW

2.1 INTRODUCTION

This chapter presents information regarding the basics of electrocoagulation and electroflotation processes used in water and waste water treatment plants. The first section presents a definition of electrocoagulation (EC), electroflotation (EF) and electrocoagulation/flotation (ECF). The ECF process is defined as the sum of EC and EF processes because electrocoagulation is found to generate coagulant at the anode area when the electroflotation process generates bubbles to float the pollutants to the surface at the cathode. In this process the aluminium dissolves at the anode and hydrogen gas is released at the cathode when aluminium electrode is used. Several sections in this chapter discuss information related to background and application of the electrocoagulation process, the advantages and disadvantages of EC process, cell configuration, energy consumption, coagulant dosage, removal process, and its principles based on three important sciences including electrochemistry, coagulation, and flotation. Towards the end of this chapter information regarding the different defluoridation methods including precipitation, adsorption/ion exchange, membrane, and electrochemical or electrocoagulation methods are included. The general information for different defluoridation methods have been summarised in the chapter summary.

2.2 EC FUNDAMENTALS

2.2.1 Definition of electrocoagulation (EC)

Electrocoagulation is the process of destabilising suspended, emulsified, or dissolved contaminants in an aqueous medium by introducing an electric current into the medium. In its simplest form, an electrocoagulation reactor may be made up of an electrolytic cell with one anode and one cathode. The conductive metal plates are commonly known as ‘sacrificial electrodes’ and may be made of the same or different materials as the anode (Mollah et al., 2001). Electrocoagulation is the electrochemical production of destabilisation agents (such as Al, Fe) that brings about neutralisation charge for removing pollutant. Once charged, the particles bond together like small magnets to form a mass. This process has proven very effective in removing contaminants from water and is characterised by reduced sludge production, no requirement for chemical use, and ease of operation (Rajeshwar and Ibanez, 1997). Colloid – destabilising agents that effect on-charge neutralisation are produced by electrolysis in the EC process. For example, aluminium anodes are used to produce aluminium cations which have the same effect as the addition of Al-based coagulants in conventional treatment systems.

2.2.2 Definition of electroflotation (EF)

The electroflotation (EF) process is a separation technology for removing pollutants by electrolytic gas generation. It is similar to the dissolved air flotation process (DAF) except that gas bubbles are produced by electrolysis of water in the EF process (Chen et al., 2002b).

Electroflotation is a process for removing dispersed particles from liquid by gas bubbles (Figure 2-1). By passing a steady electric current through a liquid, the aluminium dissolves at the anode, hydrogen gas is released at the cathode, and dissolution of Al anodes produces an aqueous aluminium species. The bubbles also float to the top of the tank, collide with suspended particles on the way up, adhere to them, and float them to the surface of the water (Lesney, 2002).

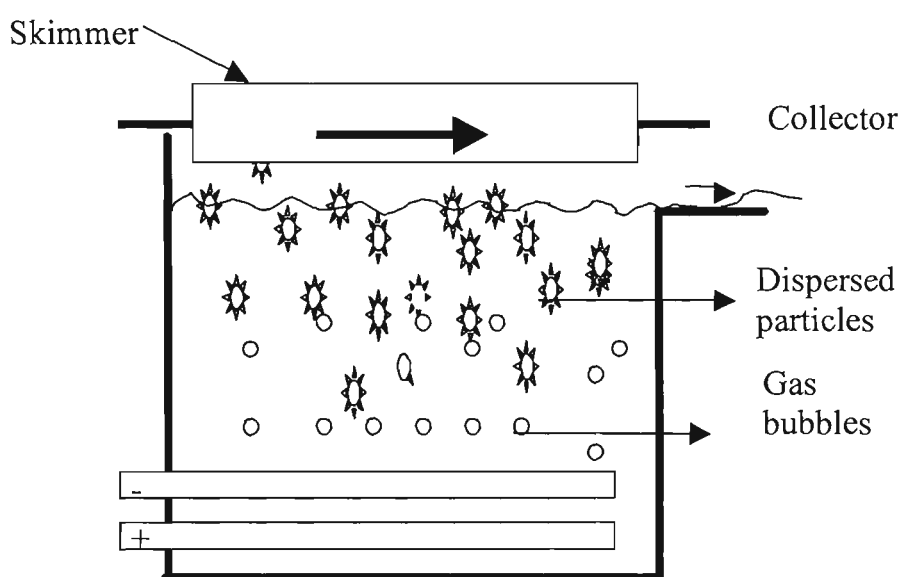


Figure 2- 1 Schematic of an electroflotation system (adapted from Lesney, 2002)

2.2.3 Electrocoagulation-flotation (ECF)

The electrocoagulation-flotation process provides an alternative technique for removing pollutants from water and waste water. This process involves applying an electric current to sacrificial electrodes inside a reactor tank where the current generates a coagulating agent and gas bubbles. In addition, electrocoagulation-flotation is a technique involving the electrolytic addition of coagulating metal ions

directly from sacrificial electrodes. These ions coagulate with pollutants in the water, similar to the addition of coagulating chemicals such as alum and ferric chloride, and allow for easier removal of the pollutants by sedimentation and flotation. Interactions occurring within an ECF reactor have been shown in Figure 2-2.

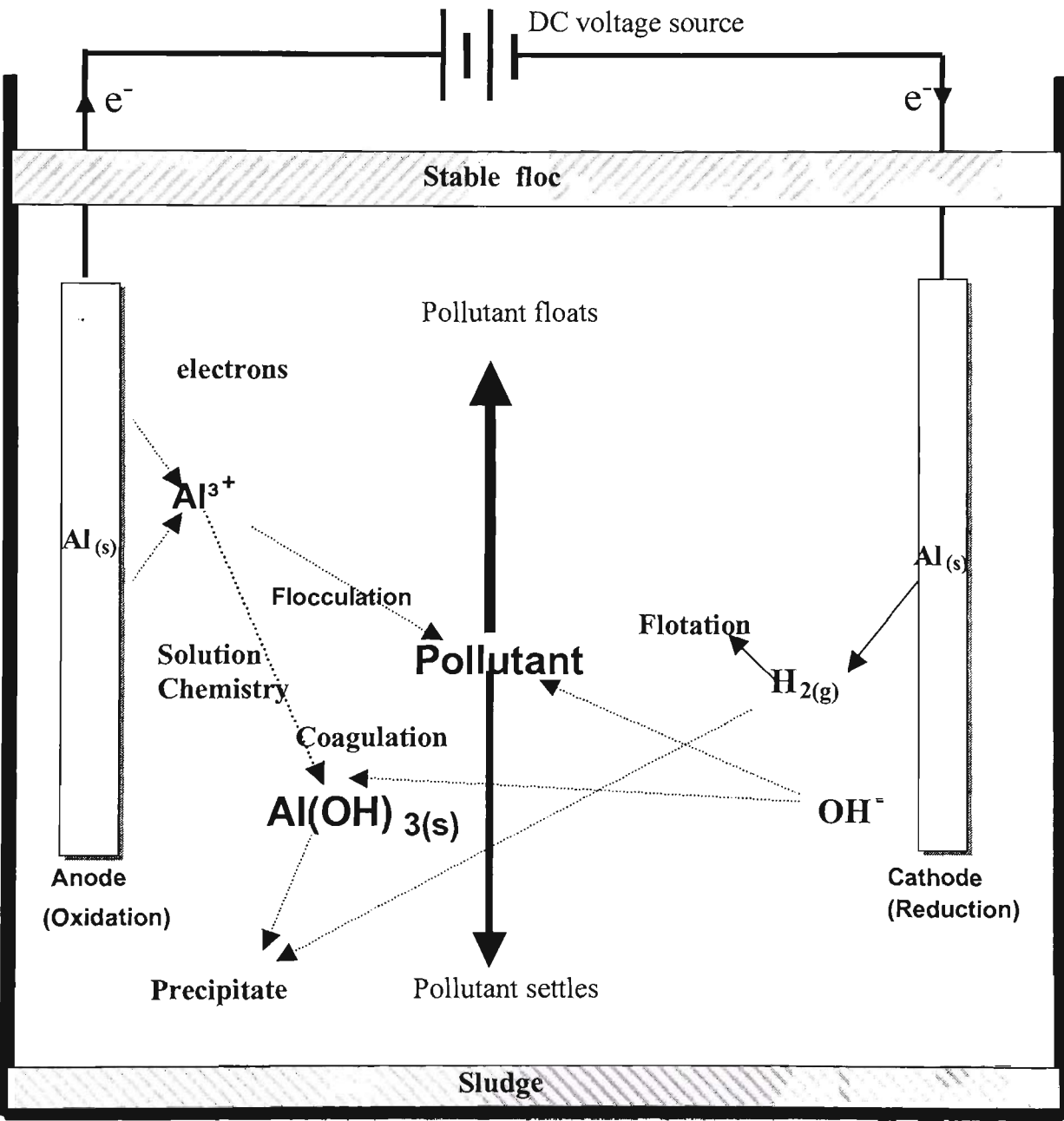


Figure 2-2 Processes in an electrocoagulation reactor (adapted from Holt et al., 2003)

2.2.4 History

At the turn of the nineteenth century, the EC system was seen as a promising technology when used for a water treatment plant in London. Electrocoagulation has been practiced for most of the 20th century with sporadic popularity. In the United States, a patent for purification of wastewater by electrolysis of aluminium and iron electrodes was received in 1909 (Vik et al., 1984). In the following decades, the process was used to treat water and waste water in the U.S. A method for purifying drinking water by electrocoagulation was first applied in the U.S in 1946 (Stuart, 1946; Bonilla, 1947). Aluminium electrodes were used to produce aluminium hydroxide flocs by hydrolysis and reaction at the electrode for removing colour from drinking water. Moreover, investigations in 1946 and 1956 showed that EC technology was not developed for other industrial purposes because low level environmental awareness and insufficient financial incentives were probably responsible for abandoning this technology (Vik et al., 1984).

Since 1970, the concept has become increasingly popular in Europe, South America, and Russia, where electrocoagulation technologies have been primarily used to treat waste water from metal finishing and metal processing industries and to purify water supplies. In North America, electrocoagulation has been successfully used for pulp and paper, mining, and metal processing industries. In the 1980, there was an array of study on EC technology by Russian scientists on the treatment of waste water. Nikolaev et al. (1982) showed the possibility of treating natural water in small systems by two-stage filtration under the influence of aluminium ions which produced electrolytic dissolution. In the first stage, removal of suspended solids was 90-92 %, which reached 98-99 % in the second stage. Removing colour reached 85-

90 % using the EC process. In 1987, an investigation using electrocoagulation technology for water treatment showed that aluminium ions and hydrogen gas are released at the anode and cathode electrodes, respectively (Przhegorlinskii et al., 1987). An ECF process was conducted by Zolotukhin (1989) to remove suspended solids from mine water. After 15 min electrolysis time, the results showed that they decreased from 1500 mg/L to less than 50 mg/L when the consumption of electrical energy did not exceed 0.5 kWh/m³.

In the 1980s and in recent years, smaller scale electrocoagulation processes have been effective processes for treating water and waste water (Chen et al., 2002). This process is very effective for removing a wide range of pollutants because they have all been considered separately in chapter three.

2.2.5 Principles of the ECF process

The various foundations used in the ECF process considered here may be conveniently classified according to the contribution of three basic sciences, electrochemistry, coagulation, and flotation (as is shown in Figure 2-3). Each of these areas have been summarised in this section:

2.2.5.1 Electrochemistry

Electrochemistry is a branch of chemistry concerned with the interrelation of electrical and chemical effects. In a general case, EC and ECF technologies based on the concept of electrochemical cells known as “electrolytic cells”.

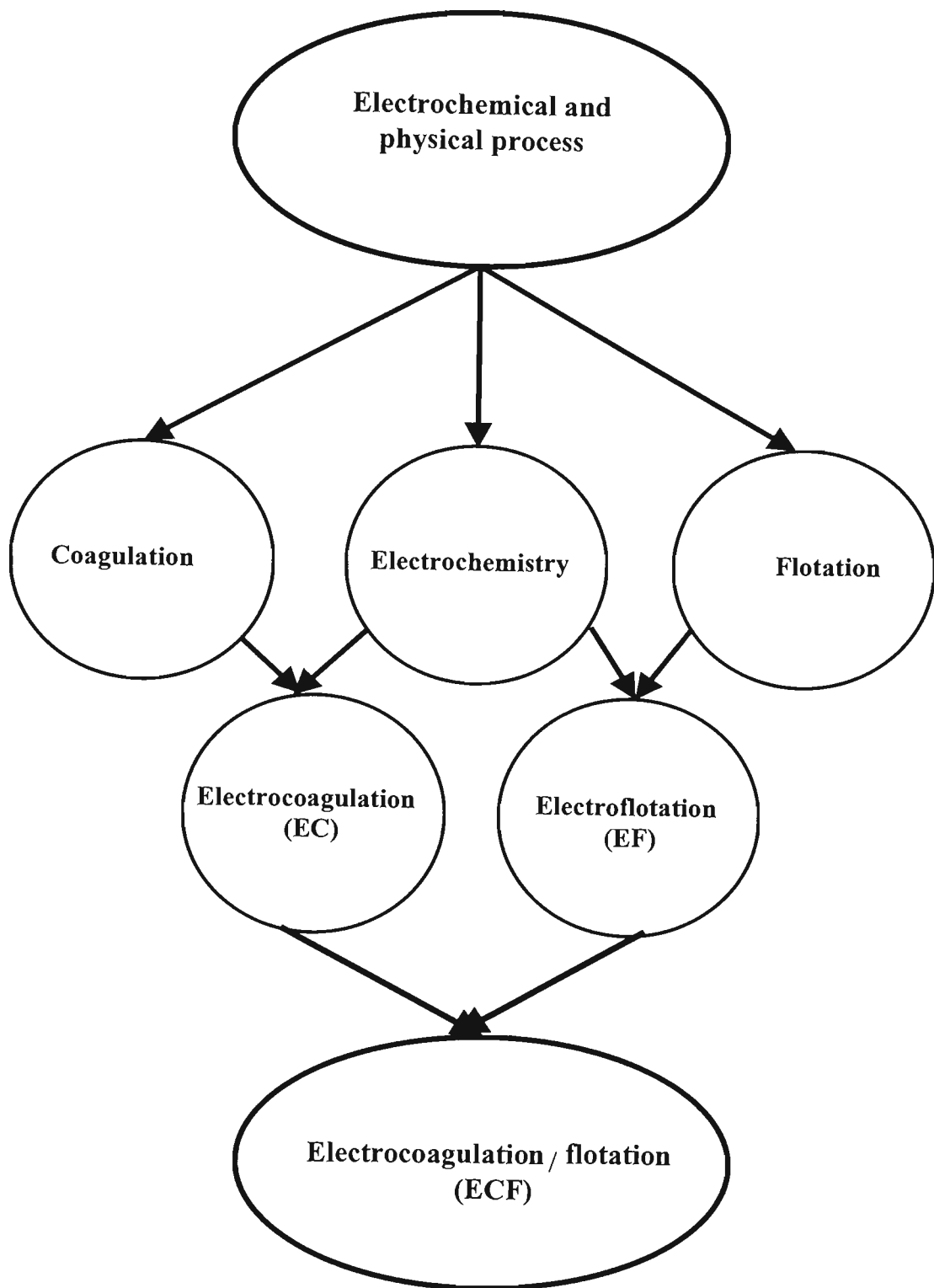


Figure 2-3 Schematic of main processes relating to ECF

In an electrocoagulator, electrolysis is based on applying an electric current through the solution to be treated by electrodes. The anode is a sacrificial metal (usually aluminium or iron) that withdraws electrons from the electrode which releases

aluminium or iron ions to the bulk solution, and precipitation of $\text{Al}(\text{OH})_3$ or $\text{Fe}(\text{OH})_3$ at the electrocoagulator. When electrodes are immersed into a solution to allow a direct current to flow through the solution, a chemical change occurs at the electrodes. The fundamentals of the chemical change depend on the type of electrodes, the applied potential difference or electromotive force, and characterisation of the solution (Sawyer and McCarty, 1994).

The material used at the anode determines the type of coagulant released into the solution, depending on the type of electrode. Different electrode materials, including aluminium (Vik et al., 1984; Ming et al., 1987; Mameri et al., 1998; Hu et al., 2003), iron (Drondina et al., 1985; Larue and Vorobiev, 2003), stainless steel (Matteson et al., 1995; Abuziad et al., 1998), and platinum (Poon, 1997), have been reported by other researchers. To pass current to each electrode and release the coagulant, a potential difference and current flow is required. The potential difference can be assumed from the electro-chemical half cell reactions occurring at each electrode, which differ depending on the pH and species present in the solution. A half cell is an electro-chemical reaction from an electrode containing an oxidised and reduced species. For example, electrolytic dissolution of Al anodes in water produces aqueous Al^{3+} species:



where E^0_{A} is standard anode potential. The Nernst equation is used to calculate the equilibrium potential (E) for any half cell reaction (Rieger, 1994).

$$E = -\frac{\Delta G^0}{nF} - \frac{RT}{nF} \ln \frac{C_{\text{ox}}}{C_{\text{Re}}} \quad (2-2)$$

where C_{ox} and C_{Re} are the product of concentrations of oxidised and reduced species, respectively. ΔG^0 is a standard Gibbs free energy change in a chemical process. F , n , T , and R are Faraday numbers, number of electrons consumed in the electrode reaction, temperature ($^{\circ}\text{K}$), and the gas constant ($8.314 \text{ Jmol}^{-1}\text{K}^{-1}$) respectively. The potential of an electrochemical cell is a measure of how far an oxidation-reduction reaction is from equilibrium. The Nernst equation describes the relationship between the free energy of reaction at any moment in time (ΔG) and the standard-state free energy of a reaction.

$$\Delta G = \Delta G^0 + RT \ln C_i \quad (2-3)$$

where C_i is concentration of specie i . The sign of ΔG shows the direction of the reaction has to shift to reach equilibrium. The magnitude of ΔG tells us how far the reaction is from equilibrium at that moment. Thermodynamics are used to determine the concentration of stable aqueous species that will be discussed in chapter 7 (solution speciation section).

Providing a minimum cell potential for the electrocoagulation reactor is necessary. The overall potential (E_{cell}) for a reactor is calculated as the sum of the anodic (E_{an}), cathodic (E_{ca}), solution (E_{so}), and loss (E_{lo}) potentials, as follows:

$$E_{cell} = E_{ca} - E_{an} - E_{so} - E_{lo} \quad (2-4)$$

The loss potential (E_{lo}) is included to account for potential losses such as the energy required to overcome the passivating layer. The solution potential (E_s) is a function of its conductivity (E_c), the distance between electrodes (d), and the current density (i) (Bard and Faulkner, 2001), as follows:

$$E_s = \frac{d.i}{E_c} \quad (2-5)$$

The electrical conductivity is an important parameter for carrying current through a solution. It depends on the presence and concentration of ions in a solution and has a significant effect on its potential. It will be discussed in chapters 4 and 5.

A study on the behaviour of electrochemical cells shows which parameters on the rate of an electrode reaction are important (Bard and Faulkner, 2001). Some of these parameters, including current value, electrolysis time, electrode material, pH solution, and bulk concentration of species, are shown schematically in Figure 2-4.

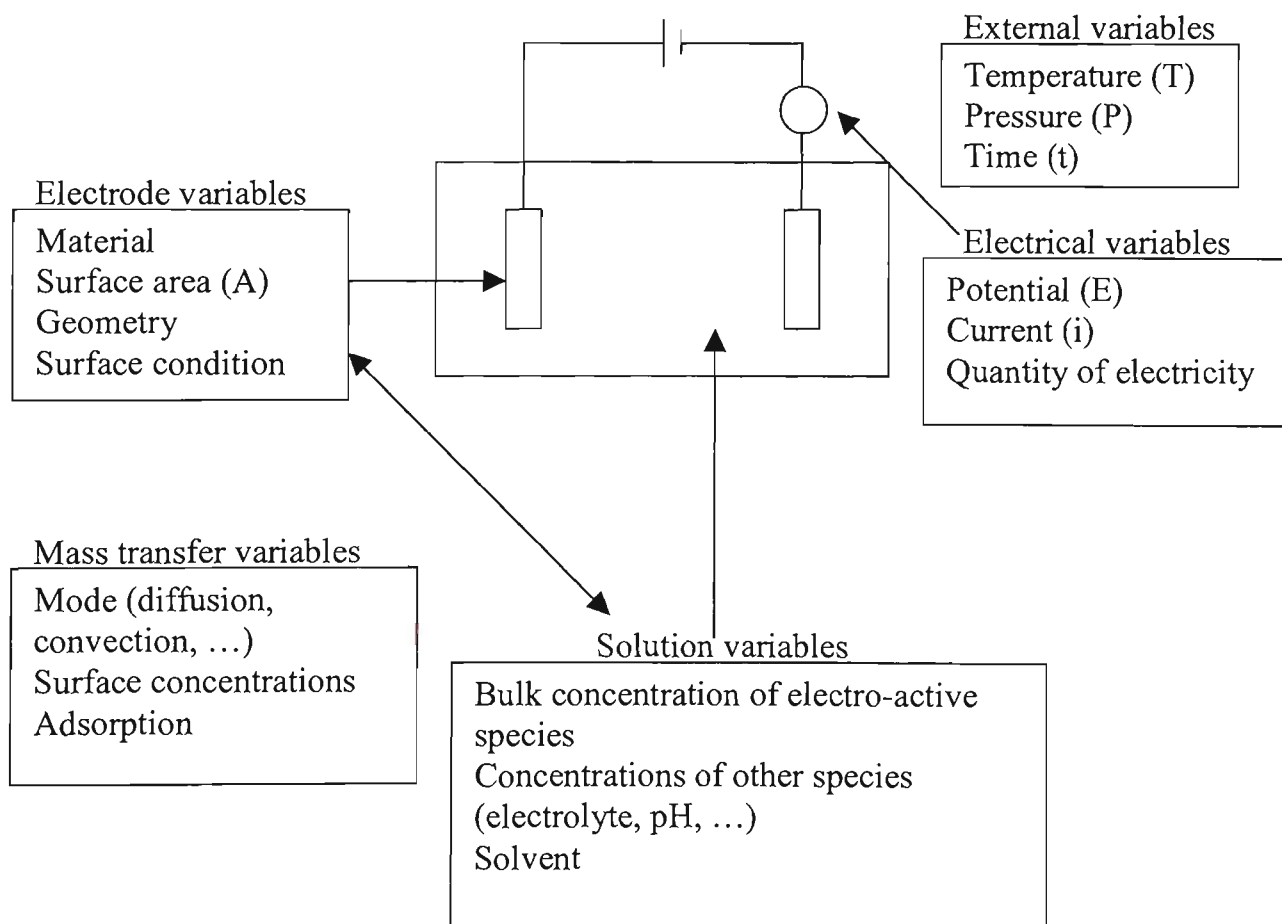


Figure 2- 4 Variables affecting the rate of an electrode reaction (after Bard and Faulkner, 2001)

The effects of these operational parameters on removing pollutant (e.g. fluoride) by the ECF process will be discussed in chapter 5. In the electrocoagulation reactor the coagulant addition rate is determined by the relevant electrode kinetics. An electrode reaction occurs in the interfacial area between electrode and solution. As shown in Figure 2-5, the oxidant (O_{bulk}) distributed from bulk solution to the electrode surface area (O_{surf}). To make this process more understandable, Eq. 2-6 is expanded schematically in Figure 2-5 to consider a series of steps that cause a change in the oxidised species (O) to reduce from (R) in an electrode reaction (Bard and Faulkner, 2001), as follows:

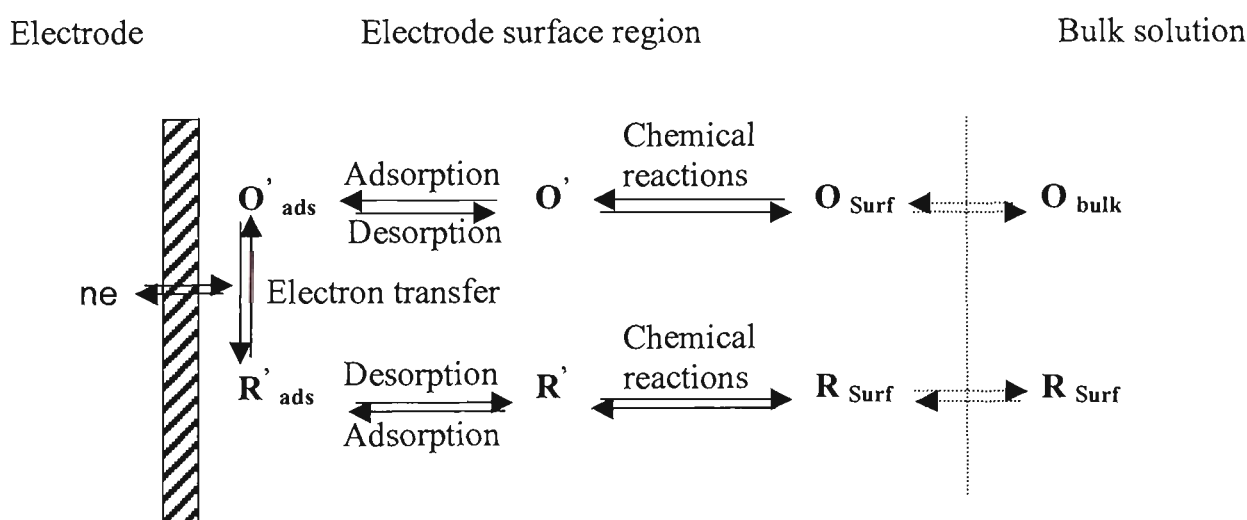


Figure 2-5 Pathway of a general electrode reaction (based on Figure 1.3.6, Bard and Faulkner, 2001)

An intermediate labelled O' is formed before adsorption onto the electrode surface (O'_{ads}). Electron transfer appeared at the surface and the specie is reduced to form R'_{ads} . A similar process, in reverse order, the reductant (R_{surf}) dispersed from the

electrode surface region to the bulk solution (R_{bulk}). The processes limiting the rate may be the charge transfer at each electrode when its relationship to the operating current density in the electrocoagulation process will be considered in the next chapters (chapters 5 and 6).

2.2.5.2 Coagulation

Using chemical coagulants for coagulation is one of the most essential processes in conventional drinking water treatment. Coagulation and flocculation are both used for treating pollutants in water treatment processes. Coagulation means a process used to cause the destabilisation and initial coalescing of colloidal particles where flocculation is an aggregation of smaller particles into large particles. In order to overcome the stability of particles in treated water, a coagulant is added. The coagulant can be added either chemically or electrically in the solution. For chemical coagulation, destabilisation is induced by the addition of a suitable coagulant, and particle contact is ensured through appropriate mixing devices. The most common metals used in coagulation are aluminium and iron (III), as they both form insoluble metal hydroxides at low concentrations. These metals are usually added as sulphates or chloride species, for example, FeCl_3 , $\text{Fe}_2(\text{SO}_4)_3$, AlCl_3 , and alum [$\text{Al}_2(\text{SO}_4)_3 \cdot 14 \text{H}_2\text{O}$]. The coagulants cause the aggregate in the particles to form into larger heavier masses (known as flocs) which can be more easily removed by settling and filtration. Precipitation pathways describe the interaction of the pollutant with the metal hydroxide precipitate. These metal hydroxides are known as "sweep flocs". When the coagulant precipitates it can react with particles of pollutant binding them to the precipitate. Also, by continuous addition of more coagulants to a solution, the

attracting force between the primary charges and other trivalent Al^{3+} or Fe^{3+} ions increases, causing the double layer to minimise when the van der Waals forces exceed the forces of repulsion. The required coagulant dose is a function of the chemistry of the treatment water, particularly the pH, alkalinity, hardness, ionic strength, and temperature (Binnie et al., 2002).

2.2.5.3 Flotation

The flotation process works by the attachment of fine bubbles to the particles concerned. Since the overall density of the bubble-particle complex is significantly less than the liquid, it then rises to the surface where the floated material (scum) is skimmed off (King, 1982). The various processes used in flotation may be conveniently classified according to the method of generating the bubbles. There are three main methods including, Air flotation, dissolved air flotation, and electroflotation (Matis and Zouboulis 1995).

The main difference between electroflotation and more conventional flotation methods is the method of producing bubbles. The basis of electrolytic or electroflotation is the generation of hydrogen bubbles in a dilute aqueous solution by passing a direct current between two electrodes (Chen et al., 2002b). One of the advantages of electroflotation is the small bubbles generated (less than 50 μm in diameter). Fukui and Yuu, (1984) reported that the diameter of an electrolysed gas bubble is about 20 μm . The effectiveness of the flotation process for removing pollutants depends on the type of electrodes and current values because the current affects mixing within the reactor and also possible contact between individual pollutant particles, coagulant, and bubbles. Thus, the pollutant removal rate by

flotation was expected to increase accordingly when the current in the EF process increased.

In the electroflotation process the gases raise particles and coagulant aggregates to the surface by flotation. The process consists of the following basic steps: (Koren and Syversen, 1995; Matis and Mavros, 1991)

- Gas bubble generation.
- Contact between gas bubble and other liquid pollutant drops.
- Gas bubble adsorption on the surface of the particle.
- The gas bubbles and liquid drops rising to the surface

In the EF process a layer of foam will be created at the surface which consists of gas bubbles and floated particles that can be removed by skimming. The rate of flotation depends on parameters such as the size of the particle, the water residence time in the electrolytic cell and the flotation tank, the particle zeta potential, temperature and pH value of solution (Rubio et al., 2002).

2.2.6 Advantages of ECF process

The advantages of ECF technology have been summarised by Mollah et al. (2001) as follows:

1. ECF requires simple equipment and is easy to operate with sufficient operational latitude to handle most problems encountered.
2. Waste water treated by ECF gives palatable, clear, colourless, and odourless water.

3. Sludge formed by ECF tends to be readily settleable and easy to dewater because it is mainly composed of metallic oxides/hydroxides.
4. Flocs formed by ECF are similar to chemical floc except that EC floc tends to be much larger, contains less bound water, is more stable, and therefore can be separated faster by filtration.
5. ECF produces effluent with less dissolved solid (TDS) content compared with chemical treatments. If this water is reused the low TDS level helps lower the water recovery cost.
6. The ECF process has the advantage of removing the smallest colloidal particles because the applied electric field sets them in fast motion, thereby facilitating coagulation.
7. The ECF process avoids using chemicals so there is no problem with neutralising excess chemicals and no possibility of secondary pollution caused by chemical substances added at high concentration, as when chemical coagulation of waste water is used.
8. The gas bubbles produced during electrolysis can carry the pollutant to the top of the solution where it can be easily concentrated, collected, and removed.
9. It needs less maintenance.

2.2.7 Disadvantages of ECF Process

The disadvantages of ECF technology have been summarised by Mollah et al. (2001) as follows:

1. The 'sacrificial electrodes' are dissolved into solution as a result of oxidation and need to be replaced regularly.

- 2. The use of electricity may be expensive in many places. Unless, is supplied by renewable energy sources.
- 3. An impermeable oxide film may be formed on the cathode leading to loss of efficiency.
- 4. High conductivity of the waste water suspension is required.

2.2.8 Cell configuration

The electrode connections in an electrocoagulation reactor (Figure 2-6) are monopolar and bipolar. With monopolar connections an electric potential is connected between n pairs of anodes and cathodes (Mollah et al., 2004a; Jiang et al., 2002). Parallel connections to each electrode cause current (I_0) to pass across each electrode and solution but if an electrical potential (U_0) is applied between two feeder electrodes, a series connections to bipolar electrodes cause the same current to pass through “n” electrode pairs.

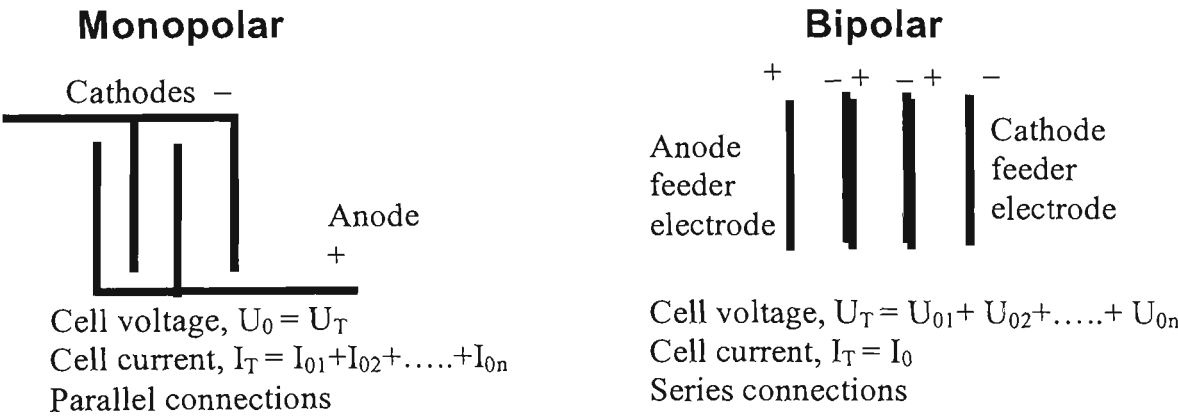
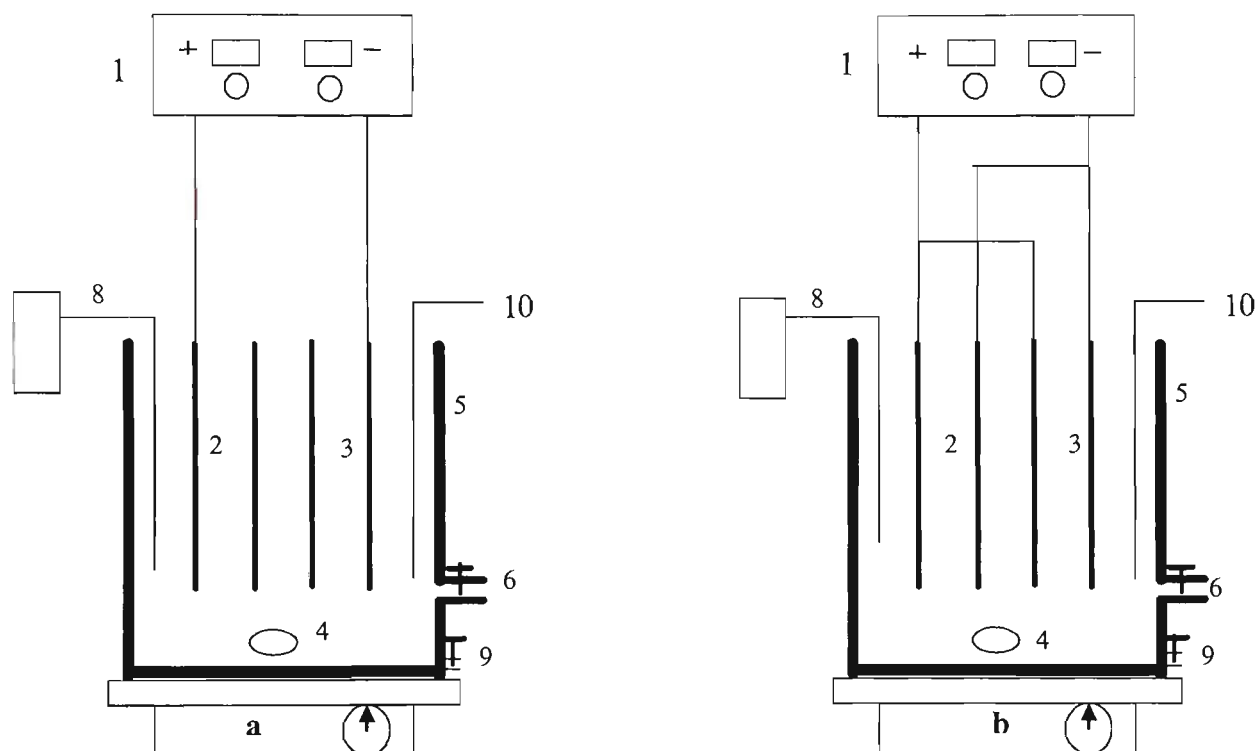


Figure 2-6 Monopolar and bipolar electrode connections in the EC reactor (adapted from Jiang et al., 2002)

A simple arrangement of an EC cell is shown in Figures 2-7 (a, and b) where the electrodes are monopolar and bipolar connections in the electrocoagulation reactor. Cell voltage and current are measured as digital and need to be controlled in all these experiments.



1. DC power supply
2. Electrode (Anode)
3. Electrode (Cathode)
4. Magnetic bar-stirring
5. Electrolytic cell
6. Sampling valve
7. Digital magnetic stirring controller
8. PH meter
9. Drain tube
10. Temperature control

Figure 2-7 Bench scale EC reactor with two electrodes connection: (a) bipolar, and (b) monopolar

2.2.9 Energy consumption

The energy required for the ECF process depends largely on the conductivity of the liquid and distance between the electrodes. The conductivity of a suspension can be adjusted by varying the salinity concentration. Higher concentrations result in higher mobility of ions and lower resistance between the cells. As noted above the EC process depends on the amount of current passing through the water so power and energy requirements for an EC cell depend on the voltage and current which pass through the cell. The power and energy used were calculated with Eq. 2-7 and Eq. 2-8, respectively.

$$Power = I.E_{cell} (Watts) \quad (2-7)$$

$$Energy = \frac{I.E_{cell} .t}{1000} (kWh) \quad (2-8)$$

2.2.10 Coagulant dose

Contaminant removal and the feasibility of EC depend on the concentration of coagulant after electrolysis. Indeed, the electrolysis time determines the coagulant dosage rate because it depends on the current range. The current in an electrochemical process is the most important parameter for controlling the reaction in a reactor. Because current not only determines the coagulant dosage rate but also the mixing rate within electrocoagulation. The current range determines the rate of dissolution of Al^{3+} concentration. The lower the current the less aluminium is released from the anode and hence the pollutant reduction is low.

In electrocoagulation Faraday's law can be used to describe the relationship between the current, volume of the reactor, and the amount of aluminium which goes into solution (g Al m^{-3}).

$$C_{Al(T)} = \frac{I \cdot t \cdot M_{(Al)}}{Z \cdot F \cdot V} \quad (2-9)$$

where

$C_{Al(T)}$ Theoretical concentration of Al^{3+} dissolving to volume of cell (g Al m^{-3})

I Total current (A)

V Volume of cell (m^3)

t Time (min)

$M_{(Al)}$ Molecular weight of Al ($M = 27 \text{ g mol}^{-1}$)

Z Number of electrons involved in the oxidation/ reduction reaction ($Z = 3$)

F Faraday's constant ($F = 96500 \text{ C mol}^{-1}$)

From Eq. 2-9, when t is the mean hydraulic retention time (min), using flow rate (Q) in mL/min and current density (I/A) in continuous reactor, Eq. 2-10 can be rearranged to give:

$$C'_{Al(T)} = \frac{i \cdot M_{(Al)}}{Z \cdot F \cdot Q} \quad (2-10)$$

where $C'_{Al(T)}$ and i are the amount of aluminium concentration goes into volume of solution per unit area of electrode and current density, respectively. More information will be discussed in chapters 5 and 6.

2.2.11 Removal process

The factors affected by removing pollutants in electrocoagulation have been investigated in many studies. In terms of operating conditions it can be affected by charge loading (Chen et al., 2000), the applied current range (Koparal and Ogutveren, 2002; Tsai et al., 1997), initial concentration of pollutants (Koparal and Ogutveren, 2002), current density (Mameri et al., 1998; Chen et al., 2000; Jiang et al., 2002), type of electrode (Tsai et al., 1997; Koparal and Ogutveren, 2002), and the distance between electrodes (Mameri et al., 1998). In addition it is affected by the characteristics of raw water such as pH (Mameri et al., 1998), conductivity (Chen et al., 2000), temperature of the influent (Mameri et al., 1998), and the target material for removal (Chen et al., 2000; Mills, 2000).

In the electrocoagulation reaction the destabilisation mechanisms of the contaminants and particulate suspension have been described by Mollah et al. (2001), as follows:

- Double-layer compression which is achieved electrically by producing ions at the anode during oxidation.
- Charge neutralisation of the ionic species present in waste water, which is caused by the counter ions produced by electrochemical dissolution of the sacrificial electrode.
- Floc formation and floc formed as a result of coagulation create a sludge blanket that entraps the colloidal particles.

Depending on the physical and chemical properties of the solution, type and concentration of the pollutants, pH solution, and concentration of coagulant, the

dominant species will differ in an electrocoagulation reactor. It will be discussed for more speciation in chapter 7.

2.3 DEFLUORIDATION METHODS

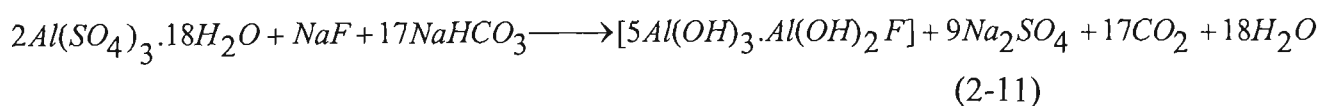
Fluoride removal in drinking water and waste water has been the subject of many publications and studies. Fluoride removal methods can be divided into the following categories, each with their own advantages and limitations (Daw, 2004 and Rao, 2003):

- Chemical addition/precipitation
- Adsorption/ion exchange
- Membrane
- Electrocoagulation/ electrochemical

USEPA lists the best available technology (BAT) fluoride treatment methods as activated alumina (AA) and reverse osmosis (RO). The Water Quality Association lists AA and RO as well as electro-dialysis, bone char, and distillation as additional methods of fluoride removal (Angers, 1998). Reardon and Wang (2000) reported that defluoridation can be divided into precipitation and sorption. Adding lime is the most common technology of the first group and is used for high concentrations of fluoride. Lime is used to form CaF_2 precipitate and reduce the fluoride. In laboratory experiments a two column limestone reactor has been designed to reduce fluoride from 109 mg/L to 4 mg/L. The second group (sorption methods) needs regular column regeneration and are not cost effective for treating waste waters with high fluoride (usually greater than 10mg/L). However, lime is the cheapest chemical used

to remove fluoride from waste water but reducing fluoride to 1 mg/L using lime only is impossible (Choi and Chen, 1979).

The important defluoridation technologies for drinking water have been considered by the Nalgonda technique and the activated alumina process in India (Susheela, 1992). The National Environmental Engineering Research Institute (NEERI), Nagpur, has been involved in defluoridation research since the early 1960s. One of the technologies was Nalgonda technology (named after the village in India where the method was established). Here raw water was mixed with enough alum and lime. It is a combination of different processes, including rapid mixing, chemical interaction, flocculation, sedimentation, filtration, disinfection, and sludge production. Alum is used as a coagulant to flocculate fluoride ions in water. Lime is added because it removes more fluoride under alkaline conditions. In this technique turbidity, colour, odour, and bacterial pollution are also decreased significantly. The reaction occurs through the following equation:



Some of advantages of the Nalgonda technique are summarised as follows (Nawlakhe and Paramasivam, 1993):

- Cost effective
- Adaptable for domestic and small community levels
- Do not need the regeneration of media
- Simplicity of design, operation, and maintenance

There is concern that the sludge produced by the Nalgonda process may be an environmental health issue because it is toxic (WHO, 2005). A new method for fluoride removal has been developed at the Indian Institute of Science using magnesium oxide. The main advantages of this method were reported, as follows (Rao & Mamatha, 2004; Mamatha & Rao, 2005):

- All chemical used are non-toxic
- Does not involve any recharge process
- Environmentally safe re-use of fluoride bearing magnesium oxide sludge

The Prasanthi technology (using activated alumina) is another important method for defluoridation in Indian villages (Susheela, 1992). Alumina, which is aluminium oxide, is insoluble in water. The activated alumina (AA) is permeable and the surface area per unit of weight is quite high. The fluoride ion is adsorbed to the surface of AA as optimum adsorption occurs when the pH of the water is 5–6. However, alumina needs to be activated by regeneration and costs more. The cost of each plant was estimated to be RS 35,000 (Susheela, 1992).

Toyoda and Taira (2000) proposed two stage method for treating high fluoride concentration (100 mg/L). The main process of this method were reported the formation of CaF_2 by adding Ca salt such as $\text{Ca}(\text{OH})_2$ and the adsorption of residual fluorine by $\text{Al}(\text{OH})_3$ by addition of an Al salt. Step one of the conventional treatment reduced fluoride from 100 mg/L to 20 mg/L which can be further reduced to 2.5 mg/L by adding Al salt and neutralising in step two. The advantages of this method were reported to be reducing sludge and running costs.

Electrocoagulation process is used as another method for defluoridation which will be explained in the next chapter (chapter 3). A summary of different methods for removing fluoride from water and waste water are summarised in Table 2-1. It is observed that the electrodialysis and reverse osmosis processes tend to be more efficient and cost more, and are therefore less suitable for many applications in developing countries. Lime is the cheapest chemical used to remove fluoride from waste water but large dosage and alkaline pH of the treated water make it unsuitable for its application. The activated alumina has become an efficient process for fluoride removal. However, the AA bed needs to be regenerated by the caustic soda and acid solutions which involving more cost and handling of hazardous chemicals. Removal of fluoride by adsorption on to low-cost materials like kaolinite clay, Gypsum, clay pot, red soil, charcoal, fly-ash, brick, and serpentine were investigated. However, low adsorption capacity and low fluoride removal efficiency were found some disadvantages of these materials. It was observed that reduced sludge production, no requirement for chemical handling, high treatment efficiency, and ease of operation are some advantages of the electrocoagulation technology for fluoride removal which will be explicated in the next chapter.

Table 2-1 Summary of different defluoridation methods in water and wastewater treatment

<i>Reference</i>	<i>Fluoride removal method</i>	<i>Results</i>	<i>Advantages</i>	<i>Disadvantages</i>	<i>Relative Cost</i>
Precipitation					
Solsona (1985); Heidweiller (1990)	Alum +lime (Nalgonda)	150 mg/alum + 7 mg lime/mg F	Established process	Sludge produced, high chemical dose	Med-high
	Alum	150 mg/mg F	Established process	Sludge produced, residual Al present	Med-high
	Lime	30 mg/mg F	Established process	Sludge produced, alkaline pH of the treated water	Med-high
	Gypsum & Fluorite	5 mg/gypsum + <2 mg fluorite /mg F	Simple	Low efficiency, high residual Ca	Low-med
Parthasarathy et al. (1986)	Addition of calcium salts and polymeric aluminium hydroxide	The addition of calcium fluoride greatly accelerates the precipitation reaction. The presence of sulphate reduces the precipitation efficiency	Less concentration of the coagulant is required- Effective removal efficiency	-	-
Saha (1993)	Chemical treatment	Fluoride reduction by aluminium chloride in the presence of CaCl ₂ has been very useful	Higher removal efficiency, Save a huge quantity of fresh water for dilution	-	-
Huang & Liu (1999)	Addition of calcium chloride to generate precipitate and then its removal by gas bubble generation using DAF	Effective fluoride removal efficiency by precipitation- flotation from the semiconductor manufacturer wastewater	Significant treatment efficiency	Need many different apparatus for precipitation and flotation process	--

¹ Note- dash indicates information is not available

<i>Reference</i>	<i>Fluoride removal method</i>	<i>Results</i>	<i>Advantages</i>	<i>Disadvantages</i>	<i>Relative Cost</i>
Toyoda & Taira (2000)	Addition of CaF ₂ and Al salt [Al ₂ (SO ₄) ₃]	The CaF ₂ granule is aggregated by gel-state Al(OH) ₃ floc	Significant contribution to environmental preservation, low cost other than conventional systems	-	Reduce the total cost to one-tenth those of a conventional system
Veressinina et al. (2001)	Precipitation by alum	80 mg alum per 1 mg fluoride removal is needed	Great potential removal	-	-
Miramontes et al. (2003)	Precipitation with cake alum and a polymeric anionic flocculent	Optimum pH = 7.1, formation of fluoro- aluminium hydroxide solids	Cheaper than AA and RO methods	-	0.32-0.38 US \$/m ³ , or (0.42-0.5 AU \$/m ³) ²
Rao & Mamatha (2004); Mamatha & Rao (2005)	Treatment by magnesium oxide	This method is an efficient, cost-effective, and environment friendly process	All chemical used are non-toxic, avoids generation of corrosive wastes, and simple operation	-	7 Paisa/ 1 litre of removed fluoride (F ⁻ = 2-5 mg/L), or (2.1 AU \$/m ³) ³
Adsorption/ion exchange					
Choi and Chen. (1979)	Adsorption by activated carbon (AC), activated bauxite (AB), and activated alumina (AA)	AC are not effective on solution with high salinity, AA is more effective than AB	More than 90% removal efficiency for (AA & AB) in pH range of 5-8	-	Using AB is low cost
Simonsson (1979)	Reaction with limestone particles in a fixed bed	Removal efficiency (99%)	Cheap, save energy, large reduction of the sludge quantity,	Drainage of the bed is needed	Low cost

² 1 USD = 1.327 AUD

³ 100 Paisa = 1 INR = 0.03 AUD

<i>Reference</i>	<i>Fluoride removal method</i>	<i>Results</i>	<i>Advantages</i>	<i>Disadvantages</i>	<i>Relative Cost</i>
Solsona (1985); Heidweiller (1990)	Plant carbon	300 mg F/kg	Locally available	Requires soaking in potassium hydroxide	Low-med
	Clay pots	80 mg F/kg	Locally available	Low capacity, slow	Low
	Activated alumina	Variable	Effective, well established	Needs trained operators	Medium
	Bone	900 g F/m ³	Locally available	Not universally accepted	Low
	Bone char	1000 g F/m ³	Locally available	Not universally accepted	Low
Hao and Huang (1986)	Adsorption by hydrous alumina	Optimum pH = 5	Established process, Great removal efficiency	-	-
Jinadasa et al. (1988)	Adsorption by kaolinitic clay	Fluoride Adsorption conformed to both Langmuir and Freundlich isotherms, optimum pH between 5-6	Suitable for village level, Simple	Low capacity	Low cost
Wasay et al. (1996)	Adsorption by lanthanum-impregnated silica gel	High removal efficiency (99.9%), First-order adsorption rate	Good adsorption capacity,	The column needs to be regenerated	Low cost
Meeussen et al. (1996)	Adsorption by goethite-silica sand system	Good prediction of the transport of acidity and fluoride in a goethite-coated sand column	High efficiency at acidic pH values (4-6)	-	-
Sujana et al. (1998)	Adsorption by alum sludge	The optimum pH was found to be 6, the adsorption followed first order rate kinetics	Simple, fast, and promising treatment method,	Raw sludge is highly acidic	Low cost

Reference	Fluoride removal method	Results	Advantages	Disadvantages	Relative Cost
Sivasamy et al. (2001)	Adsorption by coal-based	First-order adsorption rate	High efficiency at acidic pH values, simple operation	Low capacities of the coal-based sorbent	Low cost
Raichur & Basu (2001)	Adsorption by mixed rare earth oxides	Kinetics of adsorption was much faster compared to activated alumina, optimum pH = 6.5	Simple, great potential removal,	-	-
Ku & Chiou (2002)	Adsorption by activated alumina	The optimum pH was found to be 5-7, The presence of sulfate ion inhibited the adsorption process	-	-	-
Agarwal et al. (2003)	Fluoride sorption by kaolinite & montmorillonite	Kaolinite is less effective than montmorillonite in sorbing fluoride – the best pH for removal is between 5-7	Enhanced degree of mineral decomposition)	-	-
Fang et al. (2003)	Adsorption by lanthanum (III)	The optimum pH was found to be 6	High efficiency at acidic pH values,	The column needs to be regenerated	Low cost
Chidambaram et al. (2003)	Adsorption by natural materials such as: red soil, charcoal, fly-ash, brick, serpentine	Red lateritic soil has the highest removal capacity because of presence oxide of aluminium and iron onto its components	Low cost, locally available natural material especially for the rural population in Asian and other developing countries	Low adsorption capacity	Low cost
Coetzee et al. (2003)	Adsorption by clays	Not many useful South Africa clays, Bauxitic clays have the best overall adsorption fluoride potential	Cost effectiveness, simple operation,	Low adsorption capacity	Low cost

<i>Reference</i>	<i>Fluoride removal method</i>	<i>Results</i>	<i>Advantages</i>	<i>Disadvantages</i>	<i>Relative Cost</i>
Sinha et al. (2003)	Fluoride sorption by Eichhornia crassipes and activated carbon	Carbonized E. crassipes showed better removal efficiency than the noncarbonized plant	Reuse of regenerated carbons , basic for designing a fixed –bed	-	Low cost
Daw (2004)	Adsorption by activated alumina	Development of domestic defluoridation units-DDUS	Regeneration of exhausted AA and its reuse for multiple cycles	-	-
Membrane					
Solsona (1985); Heidweiller (1990)	Electrodialysis and reverse osmosis	High removal efficiency	Can remove other ions used for high salinity	Skilled operators, high cost, not much used	Very high
Amor et al. (2001)	Electrodialysis	High removal efficiency	A reasonable process for removing fluoride from brackish water	Need many apparatuses and skilled operators, not simple	High cost-expensive operation
Ndiaye et al. (2005)	Reverse osmosis	The rejection of fluoride ion is typically higher than 98%	Great feasibility for applying in industrial influents, high removal efficiency	Not simple, High cost	The cost of the designed separation plant (€76,000), or (AU\$ 122360) ⁴
	Electrocoagulation or electrochemical				
Li-Cheng (1985)	Electrocoagulation/flotation with Al electrodes, and then sedimentation	The Al ³⁺ consumption is 15.1 gram / gram F ⁻	Take bubble flotation method as post-treatment	-	-

⁴ 1 EUR = 1.61 AUD

<i>Reference</i>	<i>Fluoride removal method</i>	<i>Results</i>	<i>Advantages</i>	<i>Disadvantages</i>	<i>Relative Cost</i>
Ming et al. (1987)	Electrocoagulation with Al electrodes and then sedimentation	F ⁻ concentration decreased from 4-5 mg/L to 0.5 -1 mg/L at current value of 0.1 – 3A	Is easier, and safer than use of activated alumina method	-	Less low cost than activated alumina method
Drondina and Darko (1994)	Electrocoagulation and electroflotation process in separate cells	Al electrodes for EC, Stainless steel & titanium electrode coated with manganese oxides for EF processes were effective	Simple, Low sludge produced, effective process	-	-
Mameri et al. (1998)	Electrocoagulation using bipolar Al electrodes	The Al ³⁺ /F ⁻ weight ratio attained 17/1, first order removal rate,	Effective process	-	-
Yang and Dluhy (2002)	Electrochemical generation of Al-sorbent	Freshly Al-sorbent reduce F ⁻ concentration from 16-2 mg/L in 2 min	Effective and fast treatment	pH need to be adjusted	-
Shen et al. (2003)	Electrocoagulation and electroflotation process	F ⁻ can be reduced from 15 to less than 2 mg/L by charge loading of 5 Faradays/m ³ , and optimum pH around 6	Simple, effective process	-	-
Hu et al. (2003) Hu et al. (2005)	Adsorption and sedimentation	Co-existing anions are effective on defluoridation process, Ca ²⁺ is helpful in reducing F ⁻	Effective process in low current	--	-

2.4 SUMMARY

In its simplest form, an ECF reactor may consist of an electrolytic cell with one anode and one cathode where current is passed through the electrodes, electrolysing the water and producing bubbles of hydrogen gas. Consumable metal plates (sacrificial anode electrodes) such as Al, continuously produce ions in the system. The electrolytic dissolution of Al cathode by reduction in water produces bubbles of hydrogen gas that float some of the flocs formed between water contaminants and a range of coagulant species and metal hydroxides formed by hydrolysis. The EC process involves three successive stages including: formation of coagulants by electrolytic oxidation of the 'sacrificial electrode', destabilisation of the contaminants, and aggregation of the destabilised phases to form flocs. This chapter has focused on the key foundation sciences including electrochemistry, coagulation and flotation for all electrocoagulation processes. The EC technology has a wide range of application for treatment of water containing oil waste, dyes, suspended particles, organic matter, heavy metals, fluoride and etc. Several methods were globally studied for defluoridation namely, adsorption, chemical precipitation, electrodialysis, and electrochemical methods. The EC process has fundamentally eliminated the disadvantages of the chemical coagulation. The precipitation method with aluminium salt and calcium hydroxide was found to be not cost effective. Discharging of the sludge produced from Nalgonda process was found to be an environmental health problem. The EC process has fundamentally eliminated the disadvantages of the chemical coagulation. Reduced sludge production, larger flocs formation, no requirement for chemical handling, and ease of operation are some advantages of EC over chemical coagulation.

CHAPTER 3

CHAPTER 3

REVIEW OF POLLUTANTS REMOVED BY ELECTROCOAGULATION

3.1 INTRODUCTION

This chapter presents information pertaining to the removal pollutants, especially fluoride, by electrocoagulation in water and waste water. Fluoride can be found from wastewaters derived from semiconductor, metal processing, fertilizers, and glass-manufacturing industries. The discharge of these wastewaters without treatment into the natural environment may also contribute to groundwater contamination when long-term drinking of water containing high fluoride content can result in mottling of teeth and softening of bones. Therefore, an effective process (EC technology) that produces less waste sludge and that could replace the conventional chemical coagulation, increase the wastewater treatment efficiency and that can be retrofitted to existing facilities would be highly desirable. Electrocoagulation can be applied to a broad range of water and wastewater treatment systems and is most effective in removing inorganic contaminants and pathogens. Because of its broad applicability, it has been used for ground water and surface water remediation at several sites (Joffe & Knieper, 2000). This process is characterised by ease of operation, reduced production of sludge, and no need to handle chemicals. It has been applied efficiently to various water treatment problems. Therefore if EC can replace conventional chemical coagulation (CC), very little modification is required to make the present treatment plants more efficient and resolve the many problems caused by CC process (Rajeshwar and Ibanez, 1997). Overall, electrocoagulation is an electrochemical

technique with many applications, in which a variety of unwanted dissolved particles and suspended matter can be effectively removed from an aqueous solution by electrolysis. The main aim of this chapter is to present bench and field scale research studies for the EC and ECF technology to remove different pollutants from water treatment plants. Although this chapter emphasises more concepts related to defluoridation by electrocoagulation it also discusses other pollutants removed by EC and ECF process. At the end of this chapter a summary of some selected pollutants removed by electrocoagulation and associated references are presented.

3.2 APPLICATION ON EC AND ECF PROCESS

Electrocoagulation is an electrochemical technique with many applications for water and wastewater treatment when each application has been considered separately in this section.

3.2.1 Oily wastewater treatment

Electrocoagulation/flotation process to treat refinery waste waters and remove emulsified oils was studied by Kaliniichuk et al. (1976). Their results showed that waste water treated with aluminium hydroxide formed by dissolution of aluminium anodes when hydrogen evolved at the cathode floats, the hydroxide floc adsorbed the oil. An electrolytic process to treat oily waste water was considered by Weintraub et al. (1983). A pilot plant with iron electrodes was designed to treat between 300-7000 mg/L of emulsified oil at flow rate of 4 L/min. The results illustrated that ferric ion destabilises the emulsion by neutralising the charge on the droplets and then precipitates as ferric hydroxide, while the oil is adsorbed onto the flocculent precipitate. It was found that the effluent oil could be reduced to 10 mg/L or less when the dissolution rate of iron was increased in this process.

An electroflocculation-electroflotation system was used by Balmer and Foulds (1986) to separate oil from oil-in-water emulsions. They described how a particularly effective separation could be achieved by electrochemical dissolution of a sacrificial iron anode. The main conclusions of their investigation are summarised as follows:

- Electroflocculation can be combined with electroflotation to separate dispersed oil from aqueous emulsions.
- The production rate of a generated reagent is controlled by the electrical current rate.
- Several different anode materials are effective for electrocoagulation.
- The electrical energy consumption is optimised by using high conductivity electrolytes (i.e. high salt content) with small electrode spacing in a low current.
- The consumption rate of the sacrificial anode depends on the current applied.

Ibanez et al. (1995) also described a simple laboratory experiment based on an electrolytic process for treating oily waste water. The results showed that an oil layer is formed at the top of the solution after a few minutes of electrolysis. The solution became clear at the bottom after almost half an hour and the top layer of oil can be skimmed off. Free oil can generally be removed from water by skimming.

Using chemical coagulation with ferric chloride and lime is one of the most successful methods for destabilising oil water emulsions. An attempt was made by Ogutveren and Koparal (1997) to remove oil from synthetic and oily wastes through an electrochemical method using iron or aluminium electrodes. These experiments were performed with initial oil concentrations of 50, 200, and 500 mg/L. The effects

of applied potential, initial oil concentration, and supporting electrolyte concentration on the rate of efficient removal of oil have been investigated. The experimental results showed that aluminium electrodes are more efficient than iron electrodes. It may be because of high adsorption capacity of hydrous aluminium oxides.

A combined process of electrocoagulation and electroflotation in a continuous flow reactor was used by Chen et al. (2000) to treat waste water from restaurants in Hong Kong with a high oil and grease content. Here, electrocoagulation destabilised and aggregated the fine particles while electroflotation was responsible for floating the flocs produced in the electrocoagulation unit. The effects of operational variables on the system, including electrocoagulation and electroflotation charge loading ($C_L = \frac{I.t}{F.V}$), detention time, influent pH, conductivity, sludge production, characterisation of restaurant wastewater, and energy consumption, were investigated. The results showed that the electrocoagulation-electroflotation system was a feasible process for this treatment. Electrical conductivity had no significant effect on the efficient removal of pollutant when the water product pH was kept constant between 6 and 7. The loading charge and detention time were the most important operational variables for efficient treatment in either the electrocoagulation or electroflotation process.

The results on the investigation of the electrocoagulation process for treatment of oily wastewater indicated that using an EC reactor successfully destabilises oil in water emulsions. Dispersed gas bubbles formed from electrolysis are extremely fine and uniform. The effect of the most important operating parameters such as current inputs, electrolysis time, and initial oil concentration were investigated upon the

performance of the EC and EF processes. Several different anode materials are effective for electrocoagulation. However, the results showed that aluminium electrodes have better treatment performance than iron electrodes.

3.2.2 Dye treatment

Decolourization of dye solution by electrocoagulation has become an attractive method in recent years. A bipolar packed bed electrochemical reactor consisting of soluble electrodes was used in the batch mode to remove dye by Ogutveren et al. (1992). The effects of pH, current rate, electrolysis time, initial concentration of dye, and applied potential on the removal rate of dye have been investigated. Dye removal rate of 100% was achieved in a very short time (3-5 min) while the maximum power consumption was found to be 2.24 kWh/m³.

An electrocoagulation-electroflotation process was developed to remove colour from waste water by Ibanez et al. (1998). The gas bubbles can carry the pollutant to the top of the solution where it can be more easily concentrated, collected, and removed. The metallic ions can be reacted with the OH⁻ ions which are produced at the cathode. Insoluble hydroxides adsorb pollutants and are then removed by precipitation and flotation.

Decolourisation of a strongly coloured solution containing reactive textile dyes using the electrocoagulation process was investigated by Gurses et al. (2002). The 4 × 4 cm iron and aluminium plates, and cylindrical graphite, were applied in the electrocoagulator. Cell voltage and current rate were digitally measured. The experimental results showed that effective parameters on the decolourisation process were found to be cell voltage, electrolysis time, and current density. They also

reported that several interactive mechanisms are possible between the dye molecules and hydrolysis products when the rate of these interactions depends on the pH of the solution. Two main mechanisms were being considered in the research: precipitation and adsorption. Each was being proposed for a separate pH range, as follows:

Precipitation:



Adsorption:



Under experimental conditions, the negatively charged dye molecules were neutralised. The positive charge of the aggregates may be attributed to the adsorption of dye-monomeric and dye-polymeric colloidal particles on the Al(OH)_3 precipitates.

An electrocoagulation process for the decolourisation of reactive dyes was developed in Korea (Kim et al., 2002). They investigated the effects of different operating parameters including current density, number of electrodes, electrolyte concentration, electrode gap, dye concentration, pH of solution, and the inlet flow rate on decolourisation using the continuous electrocoagulation process. However, the removal mechanism has not been considered in the study by the authors. The results showed that removing dye using Al electrodes was more efficient than Fe electrodes. It is because of low absorption capacity of ferrous ions which is caused by the iron sacrificial anode. Also, the power consumption for electrocoagulation increased

proportionally when the current density, electrode gap, and concentration of electrolyte in the solution were increased. The dye removal efficiency was reported to be between 60 -98.5 %.

An electrocoagulation technology using aluminium electrodes has been proposed by Can et al. (2003) for decolourising reactive dye solution. The removal of a reactive textile dye (Remazol Red RB 133) to investigate the effects of waste water conductivity, initial pH, current density, dye concentration, treatment time, and energy consumption in batch electrocoagulation reactor was carried out. The results showed that decolourisation decreased steadily when the conductivity in the solution was increased. The experimental results showed that the colour removal decreased when the initial pH increased from 5 to 9. Decolourisation decreased from 90% to 70% when the initial concentration of dye was increased from 100 to 1000 mg/L. This means that removal is a function of the initial concentration of dye. Aluminium hydroxy-polymeric species remove dye molecules by precipitation and flotation. The results showed that electrocoagulation is an efficient process for removing dye from waste water.

In 2004, the use of batch and continuous electrocoagulation reactors were investigated for decolourising dye solution (Daneshvar et al., 2004; Mollah et al., 2004; Fan et al., 2004, and Den & Huang, 2005). The researchers focused on the technical performance of this process while the effects of various parameters including wastewater conductivity, pH solution, current density, and operating time have been discussed. Daneshvar et al. (2004) showed that more colour was removed in the EC cell with monopolar electrode connections than those with bipolar

electrode connections. However, there was missing information for its reason in this paper. To increase the removal of dye the optimum conditions for operating the EC process were experimentally determined by Mollah et al. (2004), ever since an EC process using sacrificial iron electrodes was used to treat a solution of orange II dye. It was found that 98.5% of dye was removed under parameters including, current value of 4 A, voltage value of 42 V, initial pH of 7.3, conductivity of 381 mS/m, flow rate of 350 mL/min, an initial 10 mg/L concentration of dye, and solution with a temperature of 25 °C.

Dyeing is the most important process usually applied in almost all textile-manufacturing industries. In the developed countries these wastewaters are treated by traditional methods like, physical and chemical processes. The biological methods are cheap and simple to apply, but can not be applied to most textile wastewaters because most commercial dyes are toxic to the organisms used in the process. The electrocoagulation technology is considered to be potentially an effective tool for treatment of textile wastewaters with high removal efficiency. The removal efficiency was found to be dependent on the initial pH, the dye concentration, the applied current density, the electrolysis time in batch model, and the flow rate in continuous flow reactor. It was found that maximum 98.5% of the dye was removed from the solution by EC technology.

3.2.3 Organic removal

3.2.3.1 Recovery of phenolic compounds

In Thailand two aluminium plates placed inside in an electrocoagulation reactor acting as reactors were applied to recover phenolic compounds by Phutdhawong et

al. (2000). Sodium chloride (2 g) was added as an electrolyte and current (0.5 A, 22 V) from a DC power supplier was passed through the solution. It was previously proposed that main reactions produce aluminium ions at the sacrificial anode, and hydroxide ions and hydrogen at the cathode. The aluminium ion liberated from the anode may also interact directly with an anion or a phenol which then precipitates out of the solution in the form of an insoluble salt, e.g. aluminium triphenolate $[\text{Al}(\text{OAr})_3]$. The experimental results showed that this method can also be applied to some phenolic compounds and can eliminate unwanted particles or chemical species from an aqueous solution.

3.2.3.2 Municipal wastewater treatment

In France an electrocoagulation and flotation system was joined to study the membrane process (microfiltration) on the flux of municipal waste water permeates (Pouet et al., 1992; Pouet and Grasmick, 1995). The experiments were conducted in a continuous mode with a 71 L electrolytic cell and 15 aluminium electrodes, as is shown schematically in Figure 3-1. The experimental results for removal of COD, SS, and turbidity from the municipal wastewater permeate using the hybrid process has been summarised in Table 3-1. This study showed that a combination (hybrid process) of an electrocoagulation-flotation system with microfiltration could increase the removal efficiency. As seen, due to combination of electrocoagulation, flotation and microfiltration, it possible to increase by more than 30 % the turbidity removal yield, by more than 20 % that of the COD and by more than 65 % that of the SS in comparison with electrocoagulation alone. So the association of theses three processes seems to be a good alternative to an extensive treatment because of its effectiveness.

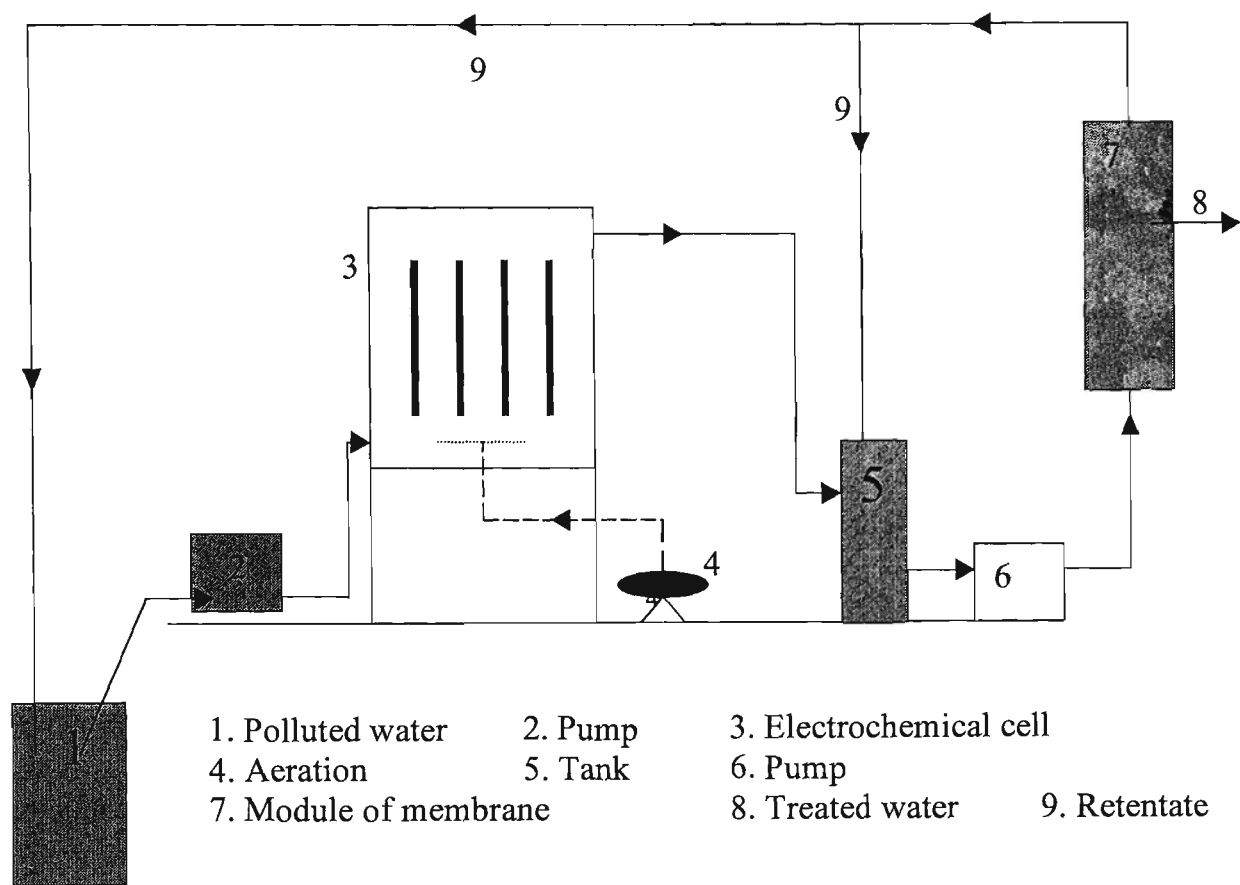


Figure 3-1 Flow diagram of a hybrid process including electrocoagulation, flotation by aeration, and microfiltration processes for the municipal wastewater permeates removal (adapted from Pouet and Grasmick, 1995)

Table 3-1 Effect of the hybrid process on the removal of COD, SS, and turbidity (adapted from Pouet and Grasmick, 1995)

Removal efficiency (%)	Flotation Only	Electrocoagulation without flotation	Electrocoagulation with flotation	Electrocoagulation, flotation, and microfiltration
Turbidity	25	67	89	99
COD	26	54	70	77
SS	10	32	60	98

Traditional methods for treating of laundry wastewater consist of various combinations of biological, physical and chemical methods. Due to the large

variability of the composition of this kind of wastewater, most of these traditional methods are becoming inadequate for the simultaneous removal of high content of pollutants. A new bipolar EC and EF process was developed to treat laundry waste water (Ge et al., 2004). The operating parameters including initial pH, hydraulic residence time (HRT), and current density were investigated. The laboratory results showed that the COD removal was greater than 70 %. The removal of phosphate, surfactant, and turbidity could be above 90 % in a wide pH range of 5-9.

These studies showed that The ECF technique can be effectively used for organic removal from wastewater. The pollutant removal processes were reported to be to neutralize pollutant charge, generate ultra-fine bubbles and separate the coagulated flocs from water or wastewater.

3.2.3.3 Industrial Wastewater Treatment

An electrocoagulation process was conducted for treatment of different soluble oily wastes with very high COD by Calvo et al. (2003). Electrocoagulation tests were conducted initially in a continuously operated laboratory scale unit to reduce COD from 70 to 90 %. For different concentrations of soluble oils, removing of the COD was between 49.5 %-77.8 % when the current rate was a constant 7 A. However, the removal of COD increased to 90 % when the current rate was increased to 10 A. As seen, the removal efficiency is increased when the current input increases. The capacity and efficiency of an electrocoagulation process depends on the nature of the liquid waste.

The removal of COD, turbidity, phenol, hydrocarbon, and grease from petrochemical wastewater was studied by Dimoglo et al. (2004) using the electrocoagulation (EC) and electroflotation (EF) process. Two laboratory scale reactors were used for the EF, EC, and EF processes, as shown schematically in Figure 3-2 (a, and b).

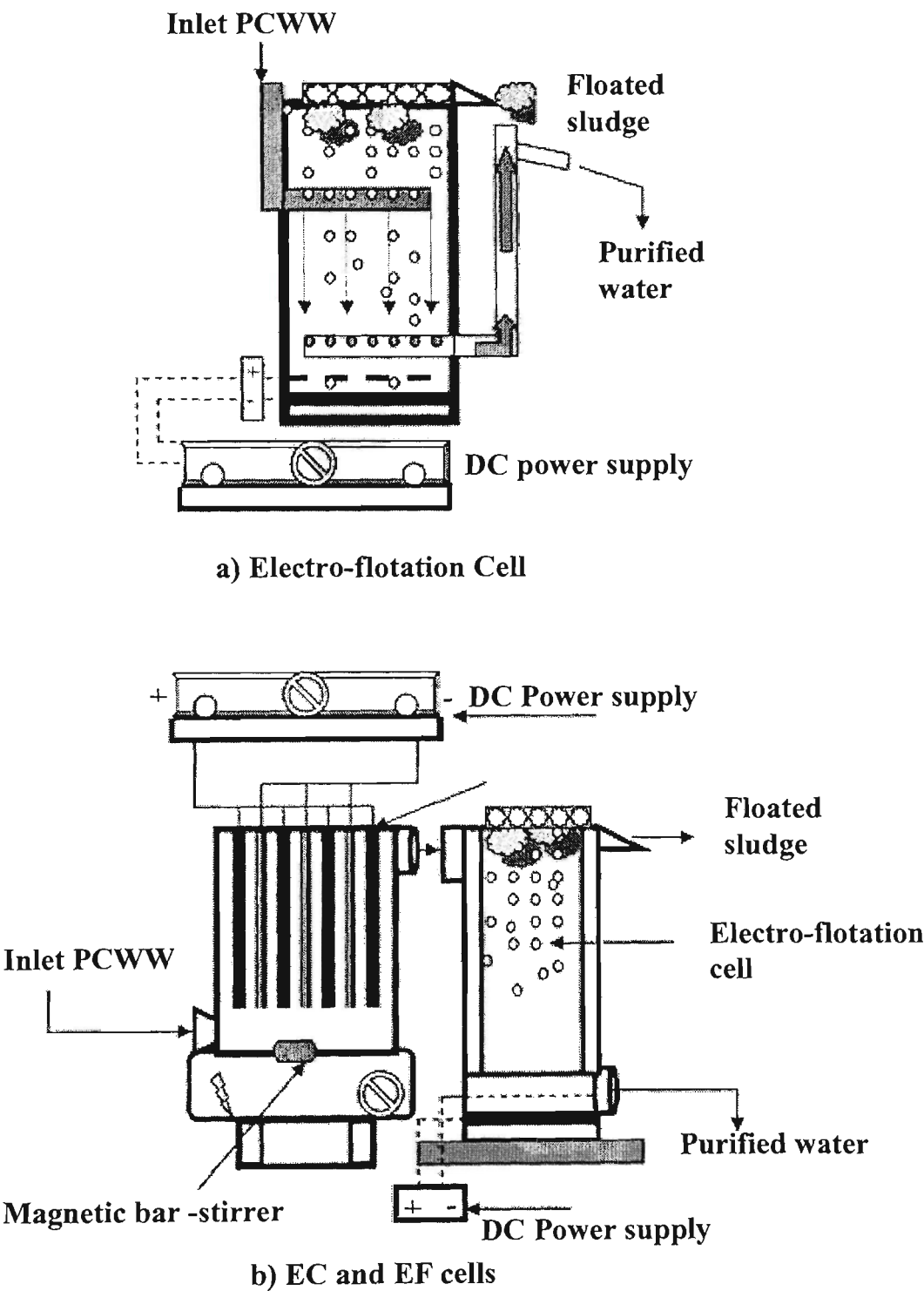


Figure 3-2 Laboratory scale processes: (a) EF process, (b) EC and EF processes (adapted from Dimoglo et al., 2004)

Iron and aluminium electrodes were used in the EC unit because a graphite anode and stainless steel electrode were used in the EF unit. The experimental results showed that using Al and Fe electrodes in EC process affectively treats wastewater. A comparison between Al and Fe electrodes at different electrolysis times was used in the EC process to remove pollutants, and the results are shown in Figure 3-3 (a, and b). The results showed that more phenol and hydrocarbons were removed with Al electrodes and more turbidity and grease was removed with Fe electrodes. It may be because of low adsorption capacity of hydrous ferric oxides. There is no significant different between Al and Fe electrodes for COD removal.

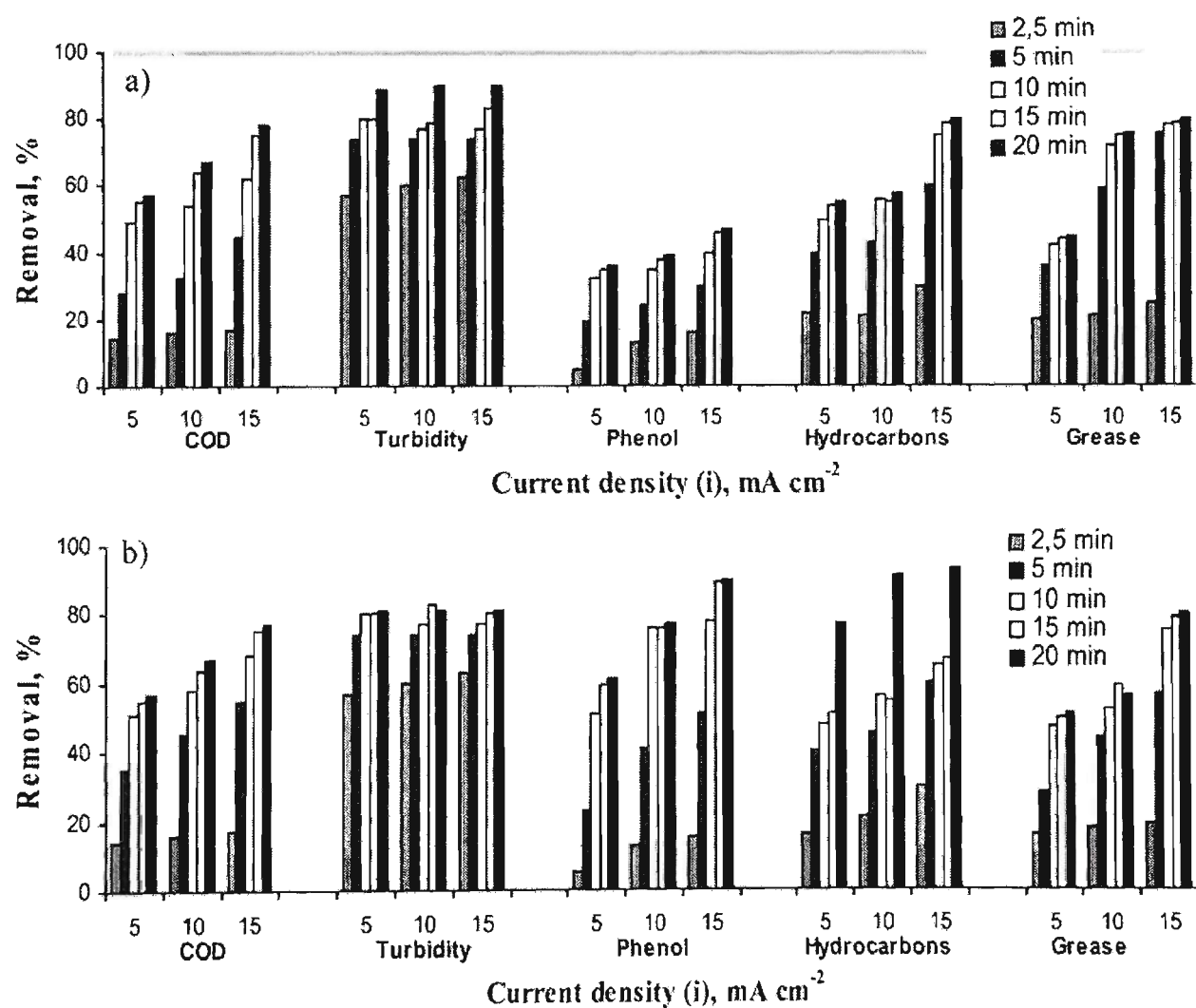


Figure 3-3 Summary of EC performance for removal of the pollutants in different current densities and various electrolysis times[a] Fe electrode, [b] Al electrode (quoted in Dimoglo et al., 2004)

Treatment of chemical mechanical polishing (CMP) waste water from a semiconductor plant by electrocoagulation was investigated by Lai and Lin (2004); and Belongia et al. (1999). The experimental results under different operating conditions showed that the rate aluminium dissolved into the aqueous solution was calculated as 10.4 mg/min when the potential and electrolysis time respectively were found to be 20 V and 30 min in the electrocoagulator (Lai and Lin, 2004). The experimental results showed that electrocoagulation of the CMP waste water with an Al/Fe electrode removed 96.5 % of turbidity and 88.7 % of COD in less than 30 min of electrolysis time in the electrocoagulator (Belongia et al., 1999).

The research studies showed that electrocoagulation is an efficient technology for treatment of industrial wastewaters. However, the capacity and efficiency of an electrocoagulation process depends on the nature of the liquid waste and initial pollutant concentrations.

3.2.4 Heavy metals removal

Removing arsenic from industrial effluent using an EC batch reactor was investigated by Balasubramanian and Madhavan (2001). It was found that the rate of removal depends on the different operational parameters including initial concentration of arsenic, current density, the influence of pH, and electrolysis time. The generation of ferric ions can easily be controlled during electrocoagulation by adjusting the operating conditions. The results showed that arsenic can be removed through electrocoagulation. However, the arsenic removal mechanism was not considered by the authors in the study.

Studies on removing arsenic by the EC process indicated that hydrous metal oxides such as ferric or aluminium hydroxides adsorb arsenic strongly. Laboratory scale experiments to remove arsenic by the EC process were conducted with three types of electrodes, namely iron, aluminium, and titanium by Kumar et al. (2004). The highest removal of arsenic (99 %) was obtained by using iron electrodes at a pH range of 6-8. It may be because of high adsorption capacity of hydrous ferric oxides for arsenic removal. It was noted that As (III) removal mechanism in EC process seems to be oxidation of As (III) to As (V) and subsequent adsorption on to hydrous ferric oxides.

A comparison between a bench scale electroflotation (EF) system and dissolved air flotation (DAF) from soil washing water was undertaken by Park et al. (2002) to remove cadmium ions. The results showed that much more cadmium (100 %) was removed by electroflotation using aluminium electrodes. The results also showed an unsatisfactory removal of cadmium by the DAF process. It can be concluded that electroflotation was considered to be an effective technology to treat cadmium from contaminated soil washing water.

The results on the investigation of the electrocoagulation process for treatment of heavy metals indicated that using an EC reactor successfully removes arsenic and cadmium from water or wastewater. The highest removal of arsenic was obtained by using iron electrodes when the removal mechanism was considered to be adsorption of arsenic on hydrous ferric oxides. However, no evidence was reported to support the mechanism.

3.2.5 Potable water treatment by EC

Coagulation using chemical coagulants is one of the most essential processes in the conventional treatment of drinking water. However chemical coagulation (CC) has some inherent problems in cost, maintenance, and sludge production. Thus electrocoagulation (EC) has recently been suggested as an alternative to conventional coagulation. Several reports have been published in scientific journals on electrocoagulation combined with electroflotation for treating potable water (Nikolaev et al., 1982; Musquere and Ellingsen, 1983; Vik et al., 1984; Mills, 1992; Ciorba et al., 2000; Pulido et al. 2001; Jiang et al., 2002; Holt et al., 2002; Han et al., 2002; and Abuzaid et al., 2002).

An electrocoagulation process for potable water treatment was studied in USA by Vik et al. (1984). Some laboratory experiments including a DC power supply (6-12 V), resistance box to regulate current intensity, and a multi-meter to read the values were performed. In the electro-chemical cell four plate aluminium anodes and cathodes (dimension 14×20×0.25 cm) were used as electrodes, at a flow rate of 0.171 L/min. This process was compared with a conventional water treatment process and was an effective process for use in small water treatment plants because of the following:

- The amount of chemicals having to be transported to the solution is lower than for chemical treatment (approx. 1/10 of the amount).
- The electrocoagulator unit will be made with enough electrodes for at least one year of treatment (long lifetime).
- The maintenance and operation of the EC system will be simple.

- A lesser amount of sludge is formed in an EC system.

An innovative electrocoagulation process has been shown to affectively treat raw water sources to produce potable water by Mills (1992). In this process coagulant formation and particle destabilisation occurred through electrolytic cells in the turbulent flow in which iron or ferric hydroxide was continuously produced. Aggregation occurred in the flocculation stage with the formation of large particles that could readily be separated from the water. The experimental results on the capability of the EC process for removing heavy metals from contaminated streams, leachate from mining, and land fill sites showed that the molybdenum was reduced from 9.95 to 0.006 mg/L in leachate at a mining site, and iron was reduced from 130 to 0.015 mg/L in leachate from a land fill site (Mills, 1992).

An electrocoagulation-flotation process has been developed by Jiang et al. (2002) in the UK for treating water. An electrocoagulator reactor with a 500 W DC power supply, a peristaltic pump, a flow meter, a reservoir for raw water and an outlet reservoir, a separation/flotation tank, and plate aluminium (maximum Al 97 %, minimum Al 95 %) anodes and cathodes was used in this research. The electrocoagulator operated under the following conditions:

- Water flow rate of $0.01 \text{ m}^3\text{h}^{-1}$
- Two electrode arrangements, bipolar electrodes connected in series via the water and monopolar electrodes connected in parallel.
- The quality of the treated water was measured in terms of dissolved organic carbon (DOC), ultra-violet absorbance at 420 nm, pH and conductivity.

- Operating electrical current densities of $3\text{-}25\text{ Am}^{-2}$, which produced Al (III) concentrations of $2.4\text{-}14\text{ gm}^{-3}$, determined as the sum of the concentrations in the treated effluent and floc sludge.
- pH values of 6.5 and 7.8 ± 0.2

Electrocoagulation experiments were performed by two laboratory arrangements, up-flow electrocoagulator configuration and horizontal flow configuration, as shown schematically in Figure 3-4 (a, and b).

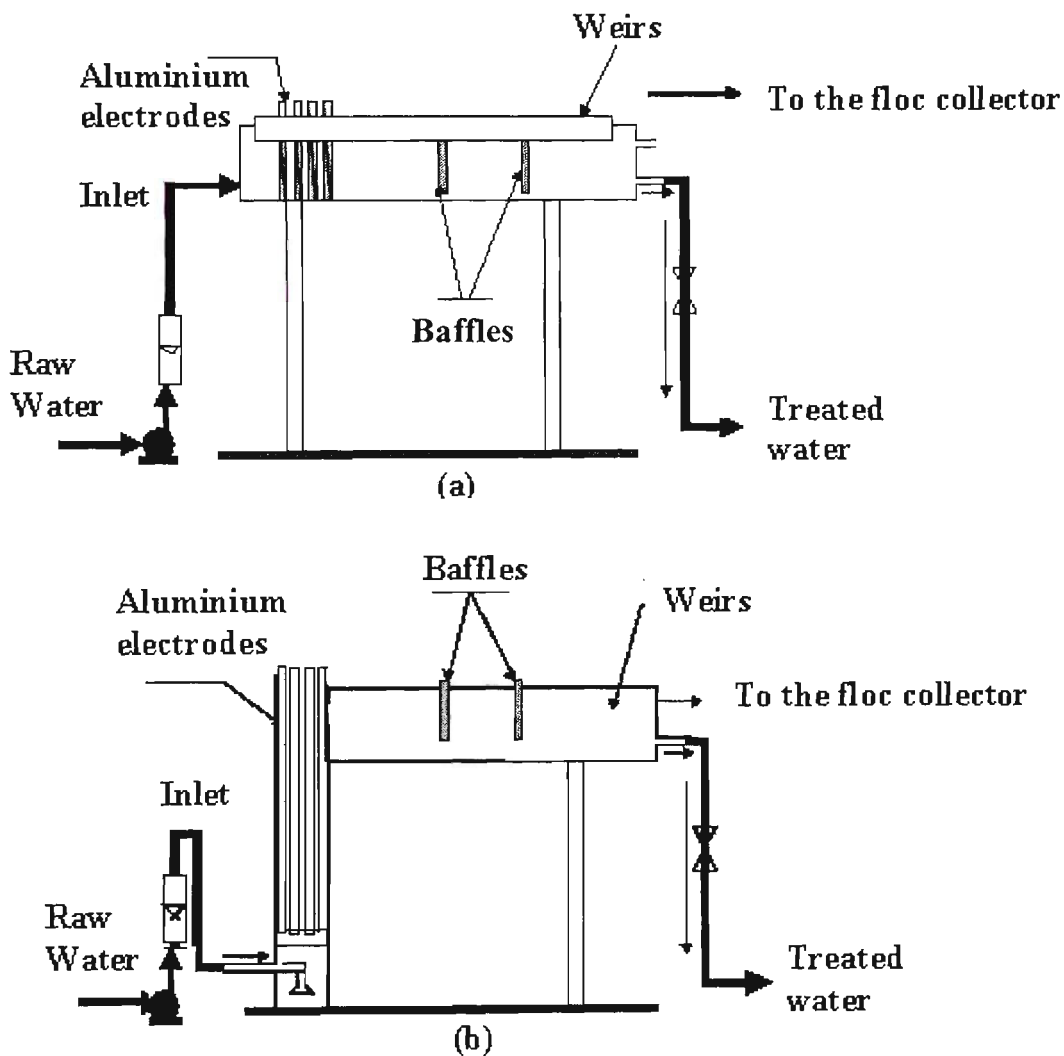


Figure 3-4 Schematics of EC process [a] Up-flow electrocoagulation reactor and [b] horizontal-flow electrocoagulation reactor (adapted from Jiang et al., 2002)

Regarding the specific electrical energy consumed using monopolar and bipolar connections (different electrode arrangements); the experimental results showed that the energy consumed by electrocoagulation was very low. For example at current densities of 10-20 Am^{-2} it was 20 and 20-30 kWh (kg Al)^{-1} for the monopolar and bipolar electrode arrangements. Over wider current densities of 10-60 Am^{-2} the electrical energy consumed was 20-80 kWh (kg Al)^{-1} . The results showed that an up-flow electrocoagulator configuration performed better than a horizontal flow configuration when both bipolar and monopolar electrode arrangements were used. In an up-flow reactor, an average of 5-8 % more DOC, colour, and UV 254 removal were achieved than in a horizontal flow reactor. The up-flow reactor arrangement allows more collisions to occur between the gas bubbles and the resulting Al-contaminant flocs which enhance the overall flotation performance.

A laboratory batch electrocoagulation reactor on removing turbidity was performed by Han et al. (2002) to compare with conventional chemical coagulation (CC). The experimental results showed that current efficiency (ε_c), which is defined as a fraction of the current passing through an electrolytic cell, was more than 100 % for the batch EC system. Based on the initial pH of removing turbidity in the electrocoagulation process, the experimental results showed that the highest efficiency was obtained between pH 6- 8 during experiments. It may be because of minimum solubility of aluminium hydroxide in this pH ranges. It is clear that most of the particles are negatively charged in water while similar charges prevent aggregation through electrostatic repulsion. Thus, the characteristics of particles and zeta potential, which represents the electric condition of particles, are important factors in the EC operating process. It was recommended that the particle charge

should be maintained in the range of -10 mV to $+10$ mV for providing proper conditions for coagulation (Han et al., 2002). For the same removal a lower dosage of aluminium was needed for the EC process than the CC process. In addition the EC process was less sensitive to pH than the CC process. The experimental results showed that the EC process was more efficient than the CC process at removing turbidity.

A relationship between electrolysis voltage and other operational parameters on the electrocoagulation process was analysed by Chen et al. (2002a). The electrolysis voltage is strongly dependent on the current density, the conductivity of water and waste water, the inter-electrode distance, and the state of the electrode surface. One of the objectives was to find theoretical models for the voltage of electrolysis required in the electrocoagulation process. Regarding any theoretical analysis, when current passes through an electro-chemical reactor it must overcome the potential equilibrium difference, anode over-potential, cathode over-potential, and ohmic potential drop of solution (Scott, 1995). The total electrolysis voltage (U_T) of the monopolar connection was the same as the electrolysis voltage between electrodes, as follows:

$$U_T = U_0 \quad (3-1)$$

The total electrolysis voltage for the bipolar connection can be expressed as follows:

$$U_T = (N - 1)U_0 \quad (3-2)$$

where N is the number of electrodes. A quantitative comparison between chemical dosing and electrocoagulation was investigated by Holt et al. (2002). Chemical coagulation was evaluated using an adaptation of the standard jar testing technique,

with aluminium sulphate as the chemical coagulant. Sodium hydroxide and hydrochloric acid solution were added for final pH adjustment. The pollutant used was “potter clay” comprising kaolinite (67%), quartz (25%), illite/micas (3%), feldspar (3%), and other trace elements (2%), as characterised by X-ray diffraction analysis. A batch electrocoagulation reactor was conducted for a quantitative comparison on experiments such as turbidity, zeta potential, and pH solution. Four aluminium anodes with five stainless steel cathodes were used in the electrocoagulator. Current over a 0.25- 2A range was investigated when it held constant for each run. The results showed that the mechanism for delivering coagulant was a key difference between chemical dosing and electrocoagulation performance. In chemical coagulation, coagulant addition is a discrete (shot-fed) event with equilibrium determining aluminium speciation and pH. By contrast, in electrocoagulation the continuous addition of aluminium and hydroxyl ions results in a non- equilibrium state and is a function of current and time (Holt et al., 2002). Another search by the same authors (Holt et al., 2005) showed that three operating stages (lag, reactive and stable) were identified in a batch electrocoagulation reactor. Little or no turbidity change is observed in the lag stage with the majority (95 %) of turbidity removal occurring during the reactive stage. All experiments had an initial lag stage in their turbidity response, before a rapid decrease. At the reactive stage, the greatest reduction in turbidity occurred which showed aggregation by an adsorption mechanism. Continued precipitation of aluminium hydroxide during the stable stage, and a decrease in turbidity, indicated a sweep coagulation mechanism. In this stage the highest current (2 A) reduced the pollutant level in the short term.

A laboratory batch electrocoagulation reactor was designed and constructed in Australia by Sivakumar et al. (2004) to remove turbidity. This research was directed towards comparing the efficient removal of turbidity and colour, the size of flocs formed, and volume of sludge generated by the electrocoagulation (EC) and chemical coagulation (CC) processes. The operational parameters, including pH, electrolysis time, and total concentration of aluminium were investigated in this research. In the electrochemical cell, five plate aluminium (purity of Al 95-97% Ullrich Aluminium Company Ltd, Sydney) anodes and cathodes (dimensions 250×100×3 mm) were used as electrodes. The electrodes were connected in a monopolar configuration, as shown schematically in Figure 3-5. The experimental results showed that the concentration of aluminium required in EC process was much less than the CC process to achieve the same performance. When turbidity could be removed at a rate of 87 % the concentration of aluminium needed by the EC process was only 2.2 mg/L but around 6 mg/L was needed in CC process. The results obtained also showed that floc formed by the EC process was larger than by the CC process. It was reported that more turbidity was removed and much better treatment could be achieved in the EC process. The volumes of sludge produced on the EC process were much less than the CC process at two detention times of 90 and 180 min. At an operating value of 1 A and 1 min electrolysis time, the volumes of sludge were 2.6 and 3.8 mL/L in EC process when the detention time increased from 90 to 180 min in the sedimentation tank. As shown in Table 3-2, the volume of sludge in the sedimentation tank increased from 8.7 to 10.6 mL/L in the CC process when the detention time increased from 90 to 180 min. Because more sludge is settled when the detention time increases in the sedimentation tank.

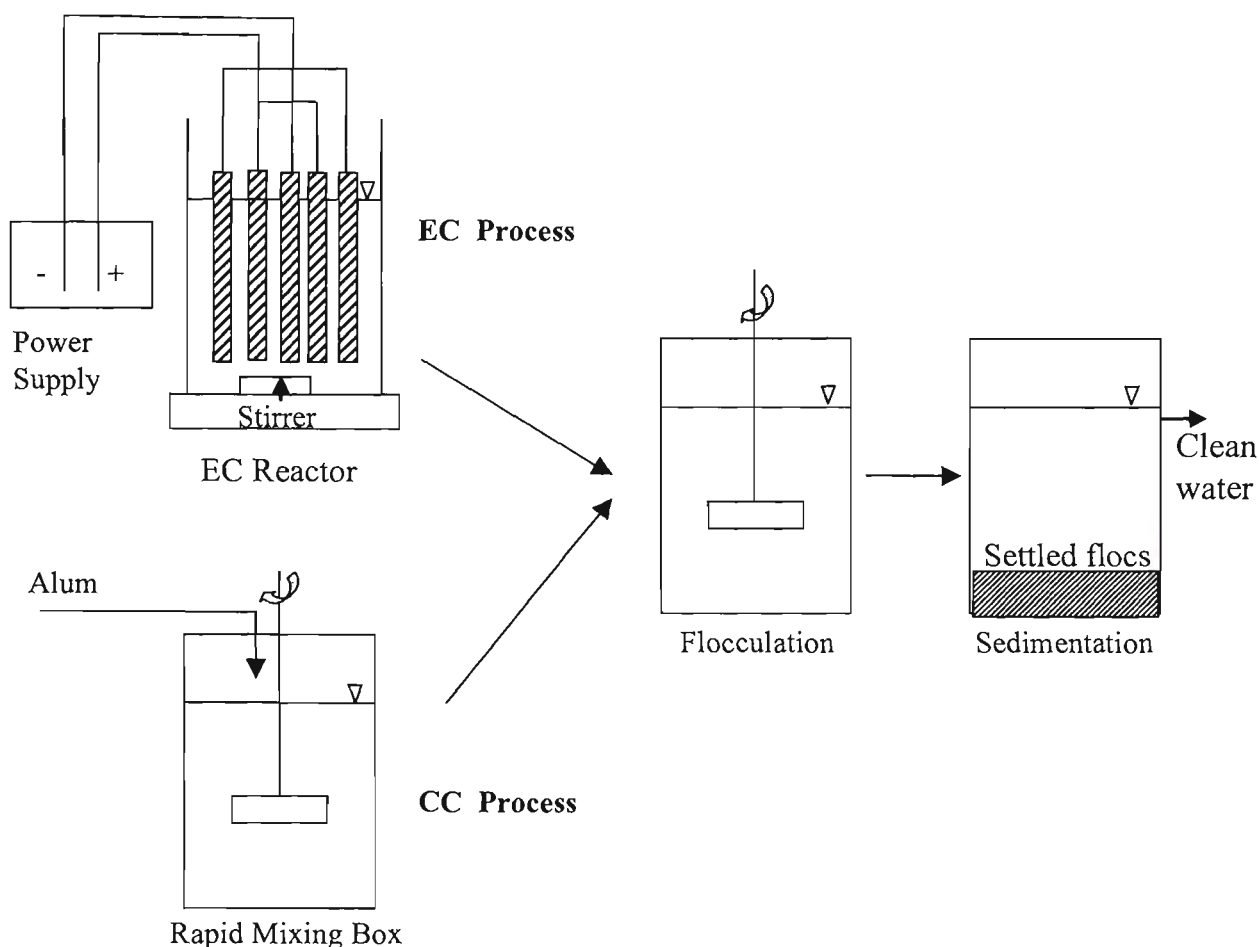


Figure 3-5 Experimental set up for EC and CC processes (after Sivakumar et al., 2004).

Table 3-2 Sludge Produced by EC and CC Process (after Sivakumar et al., 2004)

Treatment Process	Initial pH	EC Conductivity (mS/m)	Turbidity Removal (%)	Sludge volume (at 90min) (mL/L)	Sludge volume (at 180min) (mL/L)
EC	6.5	15	88	2.6	3.8
CC	6.5	15	88	8.7	10.6

The research studies showed that electrocoagulation process is more efficient than coagulation process for potable water treatment. Less aluminium dosage was needed to get the same removal efficiency in EC process, which is related to chemical cost and sludge production.

3.2.6 Nitrate, nitrite and ammonia removal

The electrochemical method was used by Lin and Wu (1996) to investigate nitrite and ammonia removal from aqueous solution. The results showed that removal was improved when electrolysis time in the cell was extended. The pH effect on nitrite removal was less significant than conductivity and current input. The iron electrode was unsuitable for removing nitrite due to its low removal efficiency. However insoluble electrodes such as a graphite anode and titanium dioxide cathode were appropriate for removing nitrite and ammonia by electrochemical cells. It was thought there are two possible mechanisms involved in the process, electro-flotation and electro-oxidation. More investigations need to be done.

Electrochemical reduction of nitrate ions was studied in synthetic solutions after ion exchange column regeneration by Paidar et al. (1999). A copper cathode could remove nitrate ions from the solution. At a current density of 38 A/m^2 , the concentration of nitrate was reduced from 600 to 50 mg/L. The mechanism of denitrification was related to an electro-reduction process, as nitrate ions were reduced to nitrite, ammonia, and nitrogen gas. However, no evidence was noted to present the removal mechanism in the paper.

A comparison of electrocoagulation (EC) and electro-reduction for removing nitrate from water was investigated by Koparal and Ogutvern (2002). A batch reactor (160 cm^3) consisting of a graphite rod anode and carbon cathode was used for electro-reduction. Electrocoagulation experiments have been also carried out by a bipolar packed bed reactor filled with iron rings. The optimum pH was between 9 and 11. The reduction of nitrate to N_2 gas can also be possible in this process and nitrate

removal has been accomplished with the precipitation of $\text{Fe}(\text{OH})_3$. However, no evidence was presented to support it by the authors.

The removal of some inorganic compounds such as nitrate, nitrite, and ammonium ions from paper mill effluents by electrocoagulation was studied by Ugurlu (2004). In these experiments iron and aluminium plates were used as electrodes. Nitrate removal at same electrolysis time (7.5 min) reached 95 and 65 % when Fe and Al electrodes were used. It was found that 40 - 80 mA current value was sufficient to remove some inorganic compounds by electrocoagulation on the large scale, from paper mill effluents. The removal mechanisms were not considered by the author.

The results on the investigation of the electrocoagulation process for treatment of nitrate, nitrite, and ammonia indicated that using an EC reactor removes the pollutants from aqueous solution. However, further investigations need to be done when the removal mechanisms were not considered in the literatures.

3.2.7 Fluoride removal

An electro-chemical method to remove fluorine from drinking water was studied by Li-Cheng (1985). The main aim was to describe a mechanism for removing fluorine by electric coagulation. The experiments were conducted at a 4 L/hour flow rate with an initial F^- concentration 4.5 mg/L. When aluminium electrodes are used as electrodes for removing fluoride the following processes are summarised:

1. Electrochemical process:

It contains the reaction on the anode (reduction of aluminium) and cathode electrode, and formation of aluminium hydroxide. As a side reaction on the cathode, hydrogen gas can be taken as minute bubbles and floc floating up together.

2. Adsorption of $\text{Al}(\text{OH})_3$ towards fluorine:

After electrolysing the formation of $\text{Al}(\text{OH})_3$ flocs is possible. The fluorine can be adsorbed by these flocs and then the aluminium fluoride complex will be settled.

3. Moving process of fluorine in the electric field:

In the electrocoagulation process the fluoride ions move towards the anode. The following reactions may occur by a combination of F^- with Al^{3+} , Na^+ and subsequent precipitation of Cryolite (Na_3AlF_6).

The experimental results showed that the removal of fluoride reached 78% when the initial concentration of fluoride and current density 4.5 mg/L and 21 A/m². The consumption of aluminium in the electrocoagulator was 15.1 gram for every gram of fluoride ion removed. The experimental results indicated that not only can the concentrations of fluoride ion be reduced by electrocoagulation process but also the total hardness, ammonia (as N), chloride, and ferrous contents. However, the effects of two important parameters including electrolysis time and initial pH on the fluoride removal were not considered by the author.

An electrocoagulation technique was applied by Ming et al. (1987) to remove excess fluoride in potable water. Different parameters were investigated in this study by the EC process including pH, current density, and stirring rate on defluoridation. It was found that fluoride can be reduced from 5 to 1 mg/L by precipitation at a pH range of 5.5 -7. In the electrocoagulation process, hydrogen is released at the cathode and micro bubbles that are adsorbed into flocs produced by electrolysis are floated up to the surface. The experimental results showed that when the speed of stirring is increased in the electrocoagulation reactor defluoridation decreased in the EC

process. This is because some micro-bubble cut off the adsorption layer between the fluoride and colloids and a shearing stress will be produced on the colloidal clots. In this study, the $\text{Al}^{3+}/\text{F}^-$ ratio was found to be between 10 -15 to ensure a satisfactory result. In summary, the results indicated that the electrocoagulation method is an efficient fluoride treatment for potable water. However, the mechanism of fluoride removal was not considered by the authors in the paper.

Removal of fluorine and chromium from industrial waste waters and underground sources using electrochemical technology was investigated by Drondia and Drako (1994). The process consisted of two stages. First iron (II) and calcium hydroxide solutions were added and the sediment was separated. In the second stage, electrocoagulation and electroflotation processes were applied after acidification. Electrocoagulation and electroflotation processes were conducted with different electrode types, including aluminium (D-16), and an insoluble anode (titanium coated with manganese oxides) or a soluble anode (grid of stainless steel). The experiments were conducted at initial concentration of F^- from 8-14 mg/L. The main aims of this research are as follows:

- To study the effect of the initial pH on purification by EC process.
- To study the efficiency of applying aluminium hydroxide. This is produced by dissolution of the aluminium anode under current values.
- To review the possibility of using electroflotation for separation

The experimental results of applying aluminium hydroxide generated by hydrolysis showed that electrocoagulation is an efficient process for removing fluoride because of its higher adsorption capability. The results showed that defluoridation was more

efficient for a pH ranging from 6.35-6.65 when the initial fluoride concentration decreased from 14 to 1 mg/L. In this research, the effects of the important parameters including current and electrolysis time were not considered.

An efficient EC process for defluoridation of Sahara water (Ain Boukhial region) at North Africa that does not require a large investment was investigated by Mameri et al. (1998). The influence of some experimental parameters including electrolysis time, initial concentration of fluoride, distance between electrodes, current density, temperature solution, initial pH, electrode area to cell volume ratio (A/V), were investigated on the defluoridation using bipolar aluminium electrodes. Effect of the initial fluoride concentration on the EC process is shown in Figure 3-6.

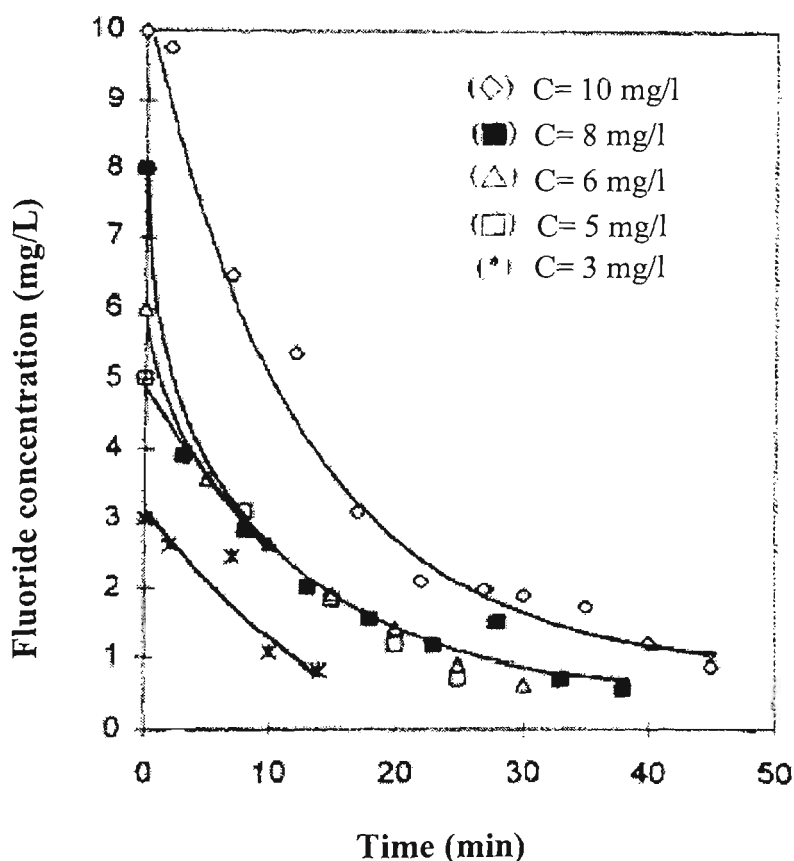


Figure 3- 6 Influence of initial fluoride concentration on the EC process. (after Mameri et al., 1998)

The results presented in Figure 3-6 showed that the treatment time is needed to increase when initial concentration in the solution is increased. The kinetic of defluoridation of the drinking water followed an exponential law with electrolysis time. The results showed that defluoridation is more efficient for a pH ranging from 5 to 7.6, where strong fluoro-aluminium complexes such as: AlF_3 , $AlOHF_3^-$ and $Al(OH)_2F_2^-$ are present, inducing an efficient aluminium complexation by fluoride. In this process the experimental Al^{3+}/F^- mass ratio was found to be 16 -17.5. The experimental results showed when the distance between electrodes is increased; the less fluoride is removed due to an increasing ohmic resistance between electrodes. The determination of the characteristics of water before and after the treatment has confirmed no contamination of the natural water by aluminium during experiments was observed. The results obtained showed that the aluminium bipolar electrodes system is an effective process for the defluoridation. However, no evidence was presented in this paper to support the mechanism of defluoridation.

Defluoridation by aluminium sorbent (Al-sorbent), which was produced in a parallel-plate electrochemical reactor by anodic dissolution of aluminium electrodes in a dilute sodium chloride (NaCl) aqueous solution, was studied by Yang and Dluhy (2002). A trace amount of chloride ions in the solution is enough to penetrate the oxide film on the aluminium electrodes for dissolving to continue. Tap water was used as the experimental design parameters for defluoridation. Based on the aluminium hydroxide solubility diagram, the principal soluble specie is the monomeric anion of $Al(OH)_4^-$ when $pH > 8$. At lower pH, $pH < 6$, the dominant soluble species are cationic monomers such as Al^{3+} . The experimental results indicated that

the freshly generated Al-sorbent is able to reduce fluoride from 16 to 2 mg/L in 6 min. However, the effluent from the reactor also needs a pH adjustment. The review shows that measurement of fluoride concentration was done by SPADNS method. A buffer must be added to the samples to prevent the interference of the Al^{3+} ions, which was not considered by the authors.

The combined EC and EF process was successfully used to remove fluoride ions from industrial wastewater (Shen et al., 2003). In this combined process the EC unit was used to produce aluminium hydroxide flocs. The EF unit was used to separate the flocs formed from water, by floating them to the surface of the cell. The research investigated that aluminium hydroxide floc is believed to strongly adsorb fluoride ions. The experimental result, which is schematically shown in Figure 3-7, illustrated that the residual fluoride decreased when charge loading was increased in the EC reactor.

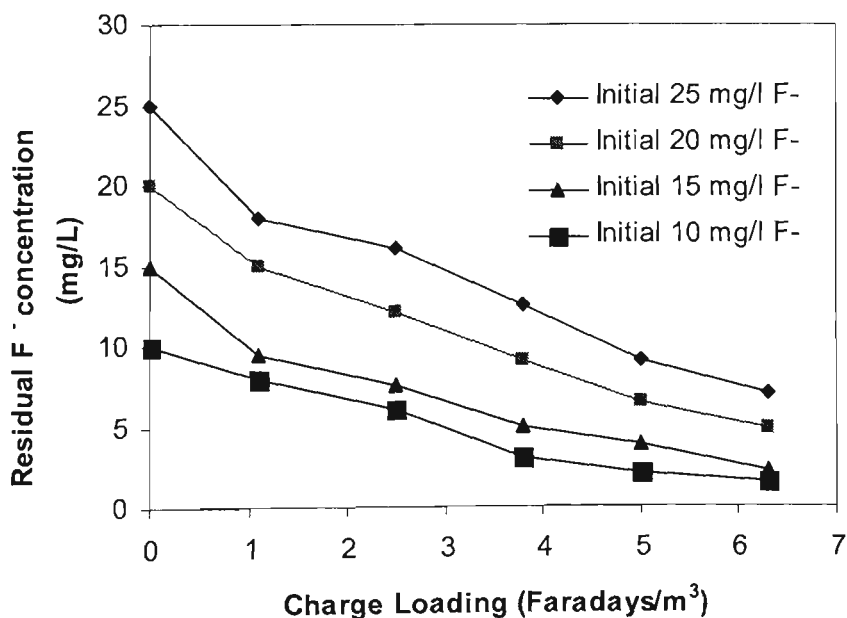


Figure 3-7 Residual fluoride for different charge loadings at different initial concentrations: $\text{pH} = 6 \pm 0.5$, time = 32 min (after Shen et al., 2003).

As seen, at the same charge loading, the residual fluoride decreased when the initial concentration decreased. The experimental results also showed that the presence of Ca^{2+} helps precipitate the fluoride ions and reduce residual concentration. This is probably because of the formation of CaF_2 . The defluoridation process was found to be efficient at pH 6 for this process. In order to explain the mechanism for removing fluoride, the composition of the sludge was investigated using X-ray Photoelectron Spectroscopy (XPS). The results indicated that defluoridation is a chemical adsorption process with F^- replacing the $-\text{OH}$ group from $\text{Al}_n(\text{OH})_{3n}$ floc. At high initial concentration, according to the equilibrium, more fluoride was found in the sludge. However, no information regarding the sludge volume measurement was presented for EC process.

A laboratory batch EC reactor was used to investigate the effect of some anions including Cl^- , NO_3^- , and SO_4^{2-} on defluoridation by the ECF system (Hu et al., 2003). Defluoridation in solutions containing F^- , SO_4^- and Cl^- ions was higher than in solutions containing F^- , SO_4^- and NO_3^- ions because the lyotropic¹ series of anions for Al^{3+} are $\text{F}^- > \text{SO}_4^- > \text{Cl}^- > \text{NO}_3^-$. The experimental results showed that defluoridation did not change very much with concentrations of Cl^- and NO_3^- but decreased when the concentration of SO_4^- ions is increased. It may be due to competition effect stated by Hu et al. (2003) that increase of the concentration of sulphate and other anions, which have a strong affinity with Al^{3+} , decreases the adsorption capacity of fluoride onto hydrous alumina. Further research is needed to

¹ Materials in which liquid crystalline properties appear induced by the presence of a solvent, with mesophases depending on solvent concentration, as well as temperature

yield a more complete understanding of the mechanism of the EC process. The effect of pH was not considered by the authors.

A laboratory batch electrocoagulation-flotation reactor was used for defluoridation and SS removal of wastewater from semiconductor manufacturers that contains large amounts of fluoride by Hu et al. (2005b). Experiments for the ECF process with seven aluminium electrodes were undertaken in a bipolar batch reactor. An anodic surfactant, sodium dodecyl sulphate (SDS), was also applied to improve the flotation performance of the ECF process to remove the dissolved fluoride ions and CaF_2 particles in the semiconductor wastewater following calcium precipitation. The semiconductor wastewater was first treated by the conventional precipitation process with calcium salts and then removed by the proposed ECF process. The dissolved fluoride ions after calcium precipitation were effectively removed (more than 90 %) in the ECF process. The defluoridation process was found to be efficient for a pH ranging from 6.5 to 7.5 during experiments. The experimental results showed that the dosage of SDS in ECF process is much lower than in the dissolved air flotation (DAF) or dispersed air flotation (DiAF) processes, because the CaF_2 particles can be collected by hydro-fluoro-aluminium flocs in ECF process. However, no information regarding cost estimation was presented for the ECF and DAF processes.

The previous research studies on the batch and continuous flow experiments using Al electrode in monopolar and bipolar configuration showed that electrocoagulation technology is an effective process for defluoridation, but more investigation needs to be done. Diverse range explanations have been presented in the literatures for the optimization of operating condition in batch and continuous flow reactor. A number

of studies have been also performed to describe the effects of the different operational parameters, yet no attempt has been made to present an empirical model for fluoride removal using monopolar ECF process. Using critical parameters, an empirical equation is given to calculate the optimal detention time for fluoride removal in batch and the optimum flow rate for continuous flow reactor. The speciation of Al and Al-F complexes were not considered by the previous researchers. This thesis aims to better understanding of the electrocoagulation fundamentals and investigation on the fluoride removal mechanisms in the EC process based on the solution speciation and dried sludge characteristics. Information regarding the specific electrical energy consumption (SEEC) and the total operational costs are also included to provide an estimation of the cost of fluoride removal by the EC process.

3.3 SUMMARY

Electrocoagulation is an electrochemical technique with many applications. Oily wastes can be removed from aqueous solution by EC process. The experimental results showed that aluminium electrodes are more efficient than iron electrodes. It may be because of high adsorption capacity of hydrous aluminium oxides for oil removal. The electrocoagulation technology is also considered to be potentially an effective tool for treatment of colour from textile wastewaters with high removal efficiency. The removal efficiency was found to be dependent on the initial pH, the dye concentration, the applied current density, and the electrolysis time in batch model. It was found that maximum 98.5% of the dye was removed from the solution by EC technology. The capacity and efficiency of the EC process for treatment of

industrial wastewaters was found to be dependent on the nature of the liquid waste and initial pollutant concentrations. The results on the investigation of the EC process for treatment of heavy metals indicated that using an EC reactor successfully removes arsenic and cadmium from water or wastewater. The highest removal of arsenic was obtained by using iron electrodes when the removal mechanism was considered to be adsorption of arsenic on hydrous ferric oxides. However, no evidence was reported to support it. Other research studies showed that EC process is more efficient than coagulation process for potable water treatment. Less aluminium dosage was needed to get the same removal efficiency in EC process, which is related to chemical cost and sludge production. The results on the investigation of the electrocoagulation process for treatment of nitrate, nitrite, and ammonia indicated that the pollutants can be removed from aqueous solution. However, further investigations need to be done when the removal mechanisms were not considered in the literatures. The previous research studies on the batch and continuous flow experiments using Al electrode in monopolar and bipolar configuration showed that EC method is an effective process for defluoridation, yet more investigation needs to be done. A number of studies have been also performed to describe the effects of the different operational parameters; however, no empirical model has been developed using critical parameters for fluoride removal by monopolar ECF process. The speciation of Al and Al-F complexes were not more considered in the literatures. The fluoride removal mechanisms are investigated in the electrocoagulator based on the solution speciation and dried sludge characteristics. In summary, Table 3-3 presents pollutants removed by EC in water and waste water sources and also associated references.

Table 3-3 Summary of pollutants removed by electrocoagulation in water and wastewater sources

Reference	Pollutants	Current or current density	cell voltage (V)	Electrode materials & electrode Connections	Removal path	Flow rates	Treatment efficiency (%)	Reactor
OIL & GREASE								
Kaliniichuk et al. (1976)	Oil- refinery	20-35 A/m ²	1.2-1.7	Al- Packed sheets	Floated and settled	-	60-99.5	Batch
Clemens (1981)	Oil- wastewater	300 -2500 A	8-12	-	Floated and settled	-	-	²
Weintraub et al. (1983)	Oil	100 A/m ²	5-30	Fe-mesh	Flotation in separate cell	50-300 mL/min	70-99	Continuous
Balmer and Foulds (1986)	Oil	200-781 mA	3-39	Fe/Pt- mesh	Flotation then filtration	-	70-100	Continuous
Ibanez et al. (1995)	Oil -wastewater	-	1.5	Fe/stainless steel	Floated and settled	-	60-99	A 250 mL beaker
Hosny (1996)	Oil	1.2A, 100 A/m ²	8	A lead anode and stainless steel cathode	Floated	10-50 mL/min	65- 92	Batch and continuous
Rubach and Saur (1997)	Oil	40-220A	4-45	Corrugated Al plate	Floated	0.25-1.5 m ³ /h	95-99	Continuous
Chen et al. (2000)	Restaurant oil, COD	0.2-0.6 A, 30-80 A/m ²	1.3-15.5	Fe and Al- Bipolar	Floated and settled	6-9 L/h	95-99	Continuous
Mostefa and Tir (2004)	Oil	60-140 A/m ²	-	Flat sheets of steel/stainless steel	Flotation in separate cell	-	85-99	Batch
Carmona et al. (2006)	Oil suspension from water	100-300 A/m ²	-	Al electrodes- Monopolar	Floated and settled	370 mL/min	80-99	Continuous

² Note- blank indicates information was not available

Reference	Pollutants	Current or current density	cell voltage (V)	Electrode materials & electrode Connections	Removal path	Flow rates	Treatment efficiency (%)	Reactor
COLOUR								
Ogutveren and Koparal (1992)	Dye	10-17.5 mA	0.86-1.3	Graphite rods- Bipolar packed bed	Settled	-	98-100	Batch
Lin and Peng (1994)	Textile wastewater-Dye	1-3.5A	-	Fe- Monopolar	Floated and settled	0.75 L/min	50-61	Batch and continuous
Ibanez et al. (1998)	Dye	-	9	Fe/Steel	Settled	-	-	A 10 mL beaker
Gurses et al. (2002)	Dye	1-5 mA/cm ²	5-15	Fe and Al plates, and cylindrical graphite	Settled	-	85-99	Batch
Kim et al. (2002)	Dye	1- 4.5 A/m ²	-	Al, Fe, and stainless steel-Monopolar	Settled	50-200 mL/min	95-99.6	Continuous
Can et al. (2003)	Dye	2.5-25 mA/cm ²	30	Al/Al- Monopolar	Floated and settled	-	70-92.5	batch
Daneshvar et al. (2004)	Dye	60-80 A/m ²	-	Iron (ST 37-2) and steel (grade 304)- Monopolar	Settled	-	32-95	Batch
Mollah et al. (2004b)	Dye	4A	42	Carbon steel plates- Bipolar	Settled	350-600 mL/min	97-99	Continuous
Bayramglu et al. (2004)	Textile wastewater-Dye-COD	45-200 A/m ² , 6A	30	Al/Fe- Monopolar	Settled	-	85-99	Batch
Fan et al. (2004)	Dye	-	25-150	Graphite plate- Bipolar packed bed	Settled	1-5 L/h	90-96	Continuous
Kobya et al. (2005)	Dye	25-250 A/m ²	4-12	Al/Al -Monopolar	Settled	-	60-95	Batch

Reference	Pollutants	Current or current density	cell voltage (V)	Electrode materials & electrode Connections	Removal path	Flow rates	Treatment efficiency (%)	Reactor
Golder et al. (2005)	Dye, COD	1-30 mA/cm ²	-	Mild Steel electrode pair	Settled	-	Dye 80-99, COD 74-89	Batch
Can et al. (2006)	Textile wastewater-Dye	100 A/m ²	<30	Al/Al- Monopolar	Floated and settled	-	70-80	Batch
HEAVY METALS								
Osipenko and Pogorelyi (1977)	Cr ⁶⁺	8.33 A/m ²	-	Fe - Monopolar	Settled	-	70-85	Continuous
Gnusin et al. (1985)	Cd ²⁺	10-30A/m ²	-	Steel- Monopolar	Settled	-	65-91	Continuous
Drondina et al.(1985)	Se and St	10-20 A/m ²	-	Fe/Fe	Floated	-	55-83	Continuous
Pozhidaeva et al. (1989)	Ni, Cr	2000 A/m ²	-	Steel	Settled	-	60-85	Continuous
Poon (1997)	Groundwater contaminants: Ni, Zn, Pb, Cu, CN	110 – 220 A/m ²	3-5	A platinum-clad columbium screen/ a stainless steel screen cathode	Floated and settled	19 L/min	75-96	Batch and continuous
Balasubramanian and Madhavan (2001)	Arsenic	50 –125 A/m ²	-	Two Fe/ stainless steel electrodes	Settled	-	75-95	Glass beaker of 500ml (Batch)
Park et al. (2002)	Cadmium	420 mA	24	Al/Al - Monopolar	Floated and settled	-	80-90	Batch
Ninova (2003)	Cu , Zn	100- 500A/m ²	-	Two Fe electrodes	Settled	-	65-88	Batch

Reference	Pollutants	Current or current density	cell voltage (V)	Electrode materials & electrode Connections	Removal path	Flow rates	Treatment efficiency (%)	Reactor
Kumar et al. (2004)	Arsenic	15-22 A/m ²	5-15	Two Fe, or Al or Titanium electrodes	Settled	-	Max 99	Batch
Hansen et al. (2005)	Arsenic	0.8-1.2 A/dm ²	-	Two Fe electrodes	Floated and settled	3 L/h	80-98	Continuous
Gao et al. (2005)	Chromium(VI)	0.1 A, 2.5 F/m ³	-	Fe/ Fe electrodes- Monopolar	Floated and settled	50 mL/min	80-97	Continuous
Den and Haung. (2005)	Silica nano-particles	0-3 A, 1-25 A/m ²	0-200	Fe/ Fe electrodes- Monopolar	Floated and settled	80-380 mL/min	75- 95	Continuous
Parga et al. (2005)	Arsenic	4-5 A	20-40	Seven parallel plates of Fe and Carbon steel	Sedimentation and flotation by air	600 mL/min	60- 99	Continuous
Urban and industrial Wastewaters								
Novikova et al. (1982)	Detergents	100 A/m ²	-	Fe vertical plate electrodes	Flotation in cell then filtration	-	65-78	Continuous
Grechko et al. (1982)	Pesticides	150A/m ²	-	Al/Al Sheets	Settled then filtered	-	-	Continuous
Vik et al. (1984)	Aquatic humus, TOC	0-2000 C	6-12	Al/Al Monopolar	Floated	170 mL/min	40- 70	Continuous
Pouet et al. (1992)	Urban wastewater: COD	5A	40	Al/Al -	Floated and settled and microfiltration	350 L/h	69-77	Continuous
Pouet and Grasmick (1995)	Municipal wastewater: COD	0-40A	0-80	Al/Al- Plate	Settled and floated with DAF	350 L/h	70-80	Continuous

Reference	Pollutants	Current or current density	cell voltage (V)	Electrode materials & electrode Connections	Removal path	Flow rates	Treatment efficiency (%)	Reactor
Baklan and Kolesnikova (1996)	Organic compounds	120 A/m ²	3.5	Fe and Al plates	Settled	-	65-90	Batch
Hernlem and Tsai (2000)	E- coli	0.8 A	9-20	An electrode pack from Sanilec 6 electrolyzer	Chlorine generation and disinfection by electroflotation	42 mL/min	-	Continuous
Phutdhawong et al.(2000)	Phenolic compounds	0.5 A	22	Two Al plates	Settled	-	60-92	Batch
Shin et al.(2001)	Livestock wastewater	0.6-1.9 A	24-48	Al/Al- Monopolar	Floated	-	SS -90, BOD- 41	Batch
Ciorba et al.(2002)	Nonylphenol ethoxylates	0.02 A	2	Two Al/Fe	Adsorption on floc and settled	-	30-50	Batch
Larue et al.(2003)	Latex particles	110-880 A/m ²	2.1 -18.7	Two Fe electrodes	Settled and filtered	-	-	Batch
Jiang et al.(2002)	DOC, colour	2.5-10 A/m ²	-	Al/Al Monopolar	Floated and settled	170 mL/min	DOC -51 Colour 70-76	Continuous
Kobya et al.(2003)	Textile wastewater COD	5-20 mA/cm ²	<30	Fe/Al- Monopolar	Floated and settled	-	90- 99.5	Batch
Ge et al.(2004)	COD, SS Laundry wastewater	30 A	32	Al/titanium - Bipolar	Floated and settled	1.5 m ³ /h	70-90	Continuous (Field test)
Kobya et al. (2005)	COD	25-200 A/m ²	<30	Al and Fe- Monopolar	Floated and settled	-	65-93	Batch

Reference	Pollutants	Current or current density	cell voltage (V)	Electrode materials & electrode Connections	Removal path	Flow rates	Treatment efficiency (%)	Reactor
Hutnan et al. (2005)	Municipal wastewater- COD	30-80 A/m ²	3-18	Fe/ Al electrodes- Monopolar	Floated and settled	1 m ³ /h	50-80	Continuous
Zhu et al. (2005)	Virus- wastewater	0.1-0.3 A	-	Fe/steel rod -shaped electrodes	Settled	-	99.99	Batch
	SS							
	&TURBIDITY							
Stuart (1946)	Turbidity, hardness colour	5.8A-28A	2.1-5.1	Two Al sheet	Settled	-	55-74	Batch
Bonilla (1947)	Turbidity, hardness colour	2-7.3 A	8.8 – 28	Parallel Al sheet (Monopolar)	Settled	-	50-70	Batch
Sandbank et al.(1973)	Suspended solids	0.14 -3.2A 22 – 500 A/m ²	9.5 – 11.5	Graphite and iron	Electrofloitation	-	80-83	Batch and continuous (Field test)
Przhegorlinskii et al.(1987)	Suspended Solids	5 – 50A/m ²	-	Al and Fe-Plates	Settled	-	75-80	Continuous
Zolotukhin (1989)	Mine water: SS	-	9-20	Al/Fe plate	Floated and settled	0.015 m ³ /h	90-94	Continuous
Mills (1992)	Raw water and bacteria, E. coli	11-62.5 A/m ²	3	Fe and steel plate	Settled	4.5-23 L/min	90-99	Continuous
Matteson et al.(1995)	SS, Kaolinite	0.01 A/m ²	15-50	Two flat steel wire mesh	Settled	-	90-95	Batch
Abuziad et al. (2002)	turbidity	0.2-1A	-	Fe/ Stainless steel	Settled	-	80- 95	4L reactor
Holt et al. (1999); Holt et al. (2002)	Potter's clay	0.25 – 2 A	3-24	Al/Stainless steel Monopolar	Floated and settled	-	90-95	Batch

Reference	Pollutants	Current or current density	cell voltage (V)	Electrode materials & electrode Connections	Removal path	Flow rates	Treatment efficiency (%)	Reactor
Han et al.(2003)	Turbidity	-	-	Al/Al Monopolar	Settled	-	90	Batch
Larue and Vorobiev (2003)	Turbidity	1A		Two Fe electrodes	Settled	-	90-93	Batch
Holt et al. (2004); Holt et al. (2005)	Turbidity Potter's clay	0.25 – 2 A	3-24	Al/Stainless steel Monopolar	Floated and settled	-	90-95	Batch
Sivakumar et al.(2004)	Turbidity	0.5-2.5A 6.25-31.25 A/m ²	6-25	Al/Al Monopolar	Settled	-	60- 88	Batch
IONS								
Gnusin et al.(1986)	Natural water	10-500 A/m ²		Steel/Al - Monopolar	Settled			Continuous
Sanfan and Qinlai (1987)	Brackish water: hardness, SO ₄ ²⁻ , Cl ⁻	2-30 A/m ²	1.3-3.6	Al/Fe plate	Settled and filtered	10 L/h	60-80	Continuous
Sanfan (1991)	Brackish water	1-22 A/m ²	1.1-3.1	Al/Fe plate	Floated and settled	18 L/h	40-76	Continuous
Daneshvar et al.(2002)	Brackish water: hardness, SO ₄ ²⁻ , Cl ⁻	22 A/m ²	-	Fe and steel plate	Floated and settled	10-18 L/h	40-90	Continuous
Alfafara et al.(2002)	P & Algae from eutrophied lake water	80- 430 A/m ²	-	Al/ titanium alloy or carbon anode	Electroflocculation and electroflotation	-	40-50	Batch and continuous
Bektas et al.(2004)	Boron	0-5A, 100-300 A/m ²	0-30	Al/Al-Monopolar	Settled	-	92-96	Continuous
Yilmaz et al.(2005)	Boron	0-5 A	0-30	Al/Al-Monopolar	Settled	-	55- 97	Continuous

Reference	Pollutants	Current or current density	cell voltage (V)	Electrode materials & electrode Connections	Removal path	Flow rates	Treatment efficiency (%)	Reactor
Lin and Wu (1996)	Nitrite and ammonia	1-2.5 A	-	Graphite/ Titanium dioxide, Monopolar	Electro-oxidation and electroflotation	-	60-99	Batch
Paidar et al.(1999)	Nitrate	28-76 A/m ²	-	Ti/Pt anode and Cu cathode	Electrochemical reduction	-	60- 91	Batch
Koparal and Ogutvern (2002)	Nitrate	-	2.9 , 20 –80	Graphite rod anode and carbon cloth cathode for Electro-reduction, Fe packed bed for EC, Bipolar	Electro-reduction and electrocoagulation	-	80-90	Batch
Ugurlu (2004)	Nitrite, nitrate, and ammonia	40-80 mA	12	Al and Fe electrodes	Electro-reduction and electrocoagulation	-	65-95	Batch
Emamjomeh and Sivakumar (2005)	Nitrate	0.5-2.5 A, 6.2-31.2 A/m ²	6-25	Al/Al Monopolar	Floated and settled	-	70-90	Batch
Li-cheng (1985)	Fluoride	0.1 – 3A 2.2 – 66.7 A/m ²	2.5 – 17	Al/Al plates	Adsorption, flotation, and sedimentation	4 L/h	15-92	Continuous
Ming et al.(1987)	Fluoride	14 A/m ²	-	Al/Al Monopolar	Adsorption, and sedimentation	-	80-88	Batch
Drondina and Darko (1994)	Fluoride	-	-	Al electrodes for EC, Stainless steel & titanium electrode for EF	Floated and settled in separate cells	-	85-90	-

Reference	Pollutants	Current or current density	cell voltage (V)	Electrode materials & electrode Connections	Removal path	Flow rates	Treatment efficiency (%)	Reactor
Mameri et al.(1998)	Fluoride	3.12-289 A/m ²	1-2.4	Al//Al Bipolar	Settled	-	70-92	Batch
Yang and Dluhy (2002)	Fluoride	1 A	14	Al/ Al plates, Parallel	Adsorption and Sedimentation	-	55- 88	Continuous
Shen et al.(2003)	Fluoride	0-5 F/m ³	-	Al//Al Bipolar	Adsorption and Sedimentation	-	67- 90	Continuous
Hu et al.(2003)	Fluoride	0.4 A	-	Al//Al Bipolar	Adsorption and Sedimentation	-	20-100	Batch
Hu et al.(2005a)	Fluoride	0.6A	35	Al//Al Bipolar	First calcium precipitation and then Sedimentation	-	70-95	Batch

CHAPTER 4

CHAPTER 4

THEORETICAL CONSIDERATIONS

4.1 INTRODUCTION

This chapter presents a general theoretical consideration of the electrocoagulation process with an electrochemical mechanism occurring in the reactor. To understand how the EC process works it is important to discuss the mechanism of water electrolysis and other related chemical reactions. The first section presents a synthesis of the EC technology and mechanism associated with water electrolysis. Several sections discuss information regarding the chemistry and kinetics of removing fluoride when three different mechanisms including, electrode oxidation, gas bubble generation, and flotation and sedimentation of flocs formed, interact in the ECF processes. From the literature review it was found that the kinetics of defluoridation follows the exponential law with time (Mameri et al., 1998). Towards the end of this chapter, information regarding the basic equations is included to present a theoretical, as well as empirical model for prediction fluoride removal by the ECF process. The chemical theory of batch reactor is used as the basis for development of the empirical model in the following pages.

4.2 THEORETICAL BACKGROUND

As noted in chapter 2, the ECF process is an electrochemical technique in which a variety of unwanted dissolved particles and suspended matter can be effectively removed from an aqueous solution by electrolysis of the electrodes. In a general sense, electrocoagulation or electroflotation are technologies based on the concepts

of electrochemical cells, specifically known as “electrolytic cells”. In an electrolytic process a source of direct current is connected to a pair of electrodes immersed in a liquid that serves as the electrolyte. To understand the electrochemical behaviour of the system, it is important to describe the general electrolytic reactions. The basis of electrocoagulation is the in situ formation of a coagulant species that can remove various pollutants from the water and wastewater being treated. There are three main mechanisms in the whole of electrocoagulation-flotation process:

- Electrode oxidation
- Gas bubble generation
- Flotation and sedimentation of flocs formed

The total processes in ECF can be summarised in Figure 4-1.

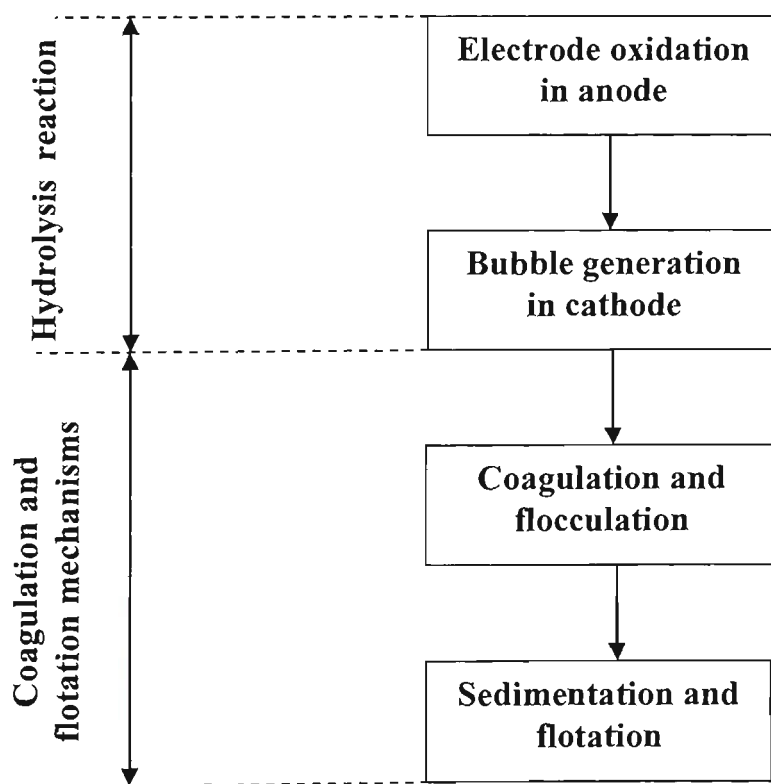


Figure 4-1 Summary of ECF processes

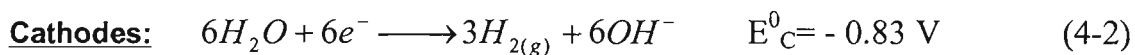
The mechanism for removing pollutants is based on hydrolysis reaction and the coagulation-flotation mechanism in the ECF reactor. Application of direct electric current through electrodes induces electrolysis reactions, as presented in the following pages.

4.2.1 Hydrolysis reaction (Electrode oxidation)

Electrolytic dissolution of the metal anode (M) in water produces aqueous M^{n+} species:



Reduction takes place at the cathodes which results in hydrogen bubbles being produced by the following reaction:



where E^0_C is standard cathode potential. A significant factor for operating EC technology and its field of application depends in many cases on the right choice of electrode material, especially the anodes. An anode must be easily treated, and also cheap and long lasting. Electrodes must have adequate mechanical strength and an extended operating life. The choice of material is limited to dissolved and undissolved materials. Iron and aluminium electrodes will dissolve and are suitable for many applications but materials such as platinum, carbon, and graphite are used as sources of undissolved anodes. Aluminium is the most commonly used material and is used in this research. The effluent with aluminium electrodes was very clear and stable but appear greenish with iron electrodes and then turn yellow and turbid because of formation of Fe (II) and Fe (III) ions into solution (Chen et al., 2000).

4.2.1.1 Charge loading

In order to use Faraday's law, the relationship between current value, electrolysis time, and the amount of electric charge that flows through a circuit must be recognised. By definition one coulomb of charge transferred when a 1-amp current flows for 1 second ($1\text{ C} = 1\text{ A.s}$), the following relations demonstrate the direct proportionality between current (I) and electrolysis rate:

$$I = dQ_e / dt \quad (4-3)$$

$$Q_e / zF = N_e \quad (4-4)$$

where Q_e and N_e are quantity of electricity and mol electrolysed in the electrode reaction, respectively. From Eq. 4-3 and 4-4, Eq. 4-5 can be expressed as:

$$Rate(mol / s) = dN_e / dt = I / zF \quad (4-5)$$

An electrode process is a heterogenous reaction which occurs in the interfacial area between electrode and solution. A heterogeneous charge-transfer reaction means a charge-transfer reaction, with the charge transferred across a phase boundary, typically between a solid and liquid phase. Since electrode reactions are heterogenous, their reaction rates are usually described in units of mol/s per unit area. From Eq. 4-5, Eq. 4-6 can be expressed as (Bard and Faulkner, 2001):

$$Rate(mol / s.m^2) = I / zFA = i / zF \quad (4-6)$$

where i is the current density (A/m^2). In most electrochemical processes the current density is the most important parameter for controlling the reaction rate, as the process at constant current density a steady dissolution of aluminium and hydrogen generation rate are certified. Faraday's law has been experimentally shown to explain

the dissolution of aluminium in an electrocoagulator (Vik et al., 1984). Thus, Faraday's law describes the coagulant and hydrogen generation rate as follows:

$$r_{Al^{3+}} (g Al^{3+} s^{-1}) = \frac{I(AW)}{ZF} \quad (4-7)$$

$$r_{H^+} (g H^+ s^{-1}) = \frac{I(MW)}{ZF} \quad (4-8)$$

where AW and MW are the atomic weight and molecular weight respectively. Thus, operation at constant current density a constant dissolution of aluminium and hydrogen generation rates is ensured.

4.2.1.2 Operational cell potential of EC reactor

Based on the primary half-cell equations (Eq. 2-1 and Eq. 4-2) for the EC system, the standard equilibrium potential (Eq. 4-9) was +0.83 V (at 298.15 °K, 1 atm, and 1 molar solution). Note that these values were relative to the standard hydrogen electrode (SHE).

$$E_{Cell}^0 = E_C^0 - E_A^0 \quad (4-9)$$

where E_{Cell}^0 is standard cell potential. This provides a minimum cell potential for the EC reactor and variations in solution conditions including pH and total concentration of aluminium. In an electrolytic cell the energy source is provided by a direct current power supply. As for the EC process, the actual cell potential was measured at constant currents. Figure 4-2 shows the resultant potential difference for the batch electrocoagulation reactor in the range of loading different pollutants in this research.

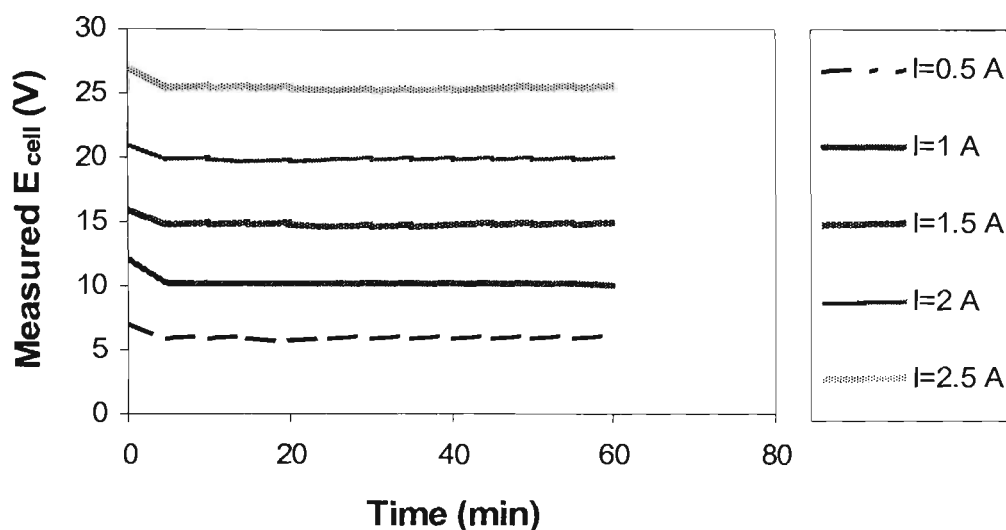


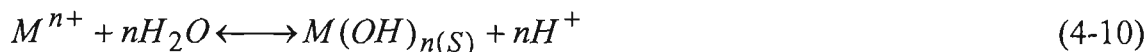
Figure 4-2 Measured E_{cell} for the batch monopolar EC reactor, ($E_c=12$ mS/cm, $C_o = 10$ mg/L)

As seen, the cell potential increased as the current increased. A potential cell range was observed for each current. A higher potential was detected in all cases. This high potential overcomes a range of resistances including electrode spacing, conductivity, and surface resistance. The cell potential stabilised within one minute after operation under a wide range of operational conditions including pH, conductivity, and the initial pollutant concentrations.

4.2.2 Coagulation-flotation process (removal process)

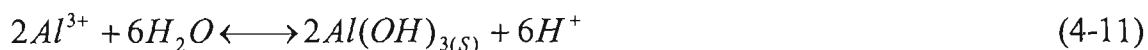
Three basic sciences in the ECF process including electrochemistry, coagulation, and flotation may interact to make it work. As described in section 2.2.5 in chapter 2, these contributions were conceptualised in as a diagram in the ECF process (Figure 2-4). The fundamental electrocoagulation reactions at the anodes and cathodes were given in equations 4-1 and 4-2. The dissolution of the metal anode allows floc formation, while the H_2 bubbles float and drive the flotation process. The bubbles

float to the top of the tank, collide with suspended particles on the way up, adhere to them, and float them to the surface of the water. The M^{n+} ions further react as shown in Eq. 4-10 to form solid $M(OH)_n$ precipitate.



The metal hydroxides $[M(OH)_n]$ react as coagulants, destabilise and aggregate suspended particles or precipitate, and adsorb dissolved contaminants.

The electrode material determines the coagulant type. By passing a steady electric current through a solution and aluminium electrodes, the dissolution of the aluminium anodes allow floc formation, while the production of hydrogen bubbles at the cathode traps flocs and other suspended matter, bringing them to the surface as a float. From Eq 4-10, the formation of a floc by electrocoagulation (using sacrificial aluminium electrodes) is given in the following equation:



In this research, a laboratory batch electrocoagulation reactor was designed with the intention of presenting a kinetic model for removing fluoride using aluminium electrodes. Some of the possible reactions and mechanisms occurring in the boundary layer between the electrode and bulk of the liquid have been summarised in Figure 4-3. To oxidise a soluble electrode (e.g. aluminium) in the electrochemical cell, current value and potential differences across the electrodes are required.

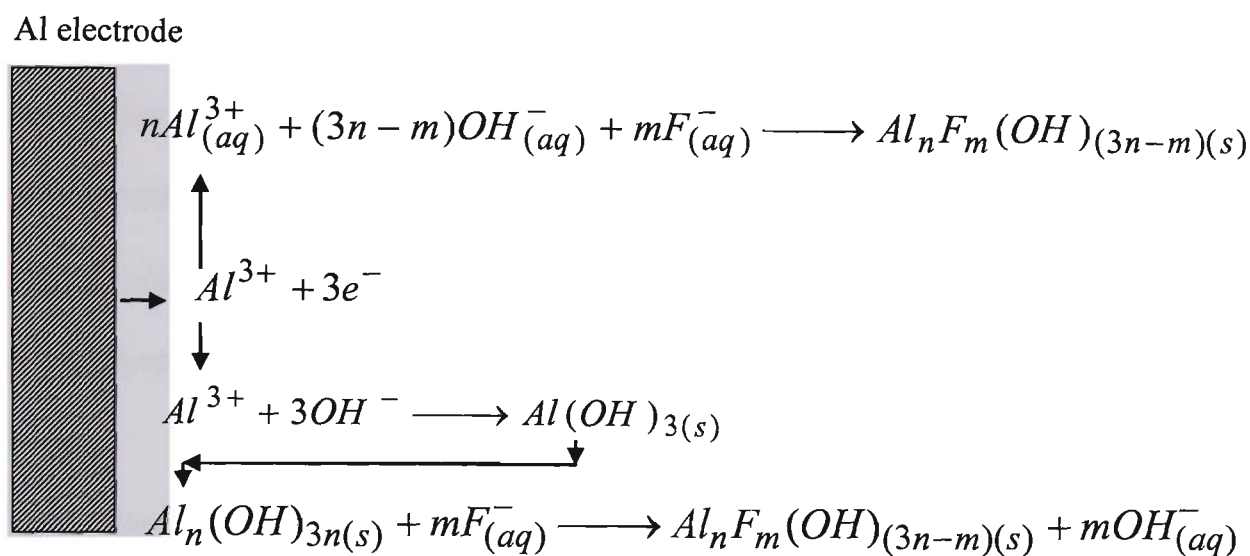


Figure 4-3 Simplified schematic depicting the electrode oxidation and the possible reactions occurring between the electrode and the bulk of the liquid

It is believed that precipitation or adsorption reaction may occur when aluminium electrode is used for fluoride removal by ECF process. To understand the chemical speciation of Al and other species with fluoride ions, the mechanism for removing fluoride will be explained in more detail in chapter 7. The only mathematical model of electroflotation was reported by Matis and Zouboulis (1995), who used a macroscopic approach to evaluate the overall kinetic for removing paint in an electro-flotation cell. They removed pollutant to the surface using a first order kinetic expression to describe flotation. Various kinetic approaches are available that could describe the electrocoagulation-flotation mechanism. Also, Mameri et al. (1998) derived a first-order kinetic model for removing fluoride from water by electrocoagulation. Therefore, the chemical batch reactor theory, material balances, and reaction kinetics concepts involving the coagulation-flotation mechanisms are used as a basis for developing the empirical modelling efforts in the following pages.

4.2.3 Representative Equations for reactors

The model presented in this manuscript was based on the concept of kinetics for conservative substances reacting in the reactors. The fundamental approach to show the change occurring in a vessel or some type of container, such as a tank, is the mass balance analysis. The mass balance in both reactors may be modelled following this expression:

$$[Accumulation] = [Input] - [Decrease due to reaction] - [Output] \quad (4-12)$$

Reactors may be operated in either batch or continuous flow manner.

4.2.3.1 Batch reactor

If the component is increasing because of the reaction, the reaction term in Eq. 4-12 will have the sign opposite to that shown. In completely mixed batch reactor (CMBR), which is schematically shown in Figure 4-4, the reactor is first charged with reactants, and the products are discharged after completion of the reaction.

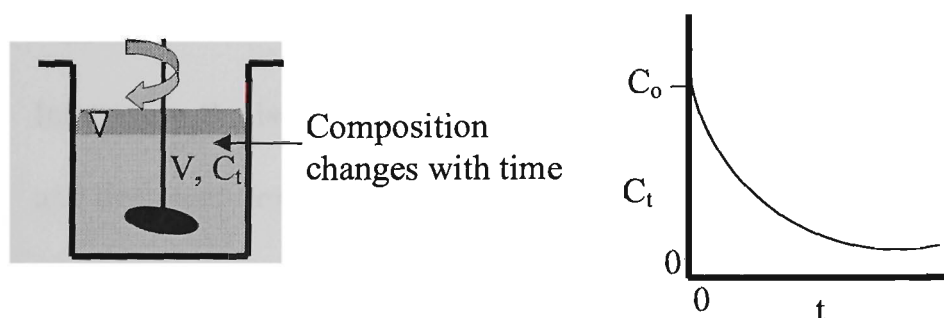


Figure 4-4 Completely mixed batch reactor (CMBR) schematics

During the reaction, the volume of reactor is constant when the reaction rate is varied with time. Thus the total net masses going in and out are zero for a batch reactor. From Eq. 4-12, the generalized mass equation for a CMBR during the reaction may be presented by the following expression:

$$[Accumulation] = - [Decrease due to reaction] \quad (4-13)$$

The fundamental equation for the design of the reactors is the rate equation and the equation for the law of conservation of mass (Reynolds, 1996). Starting at an initial pollutant concentration of C_o , the rate equation for the various reaction orders is given (Nirmalakhandan, 2002):

$$\left(\frac{dC_t}{dt}\right)V = -rV = -(KC_t^n)V \quad (4-14)$$

where “n” is the reaction order, “r” is the rate of removal of the pollutant by reaction ($ML^{-3}T^{-1}$), and K is the reaction rate constant ($M^{1-n} T^{-1}$). C_t is the concentration of the pollutant at any time, t, during the reaction and V is the reactor volume that remains constant in CMBR reactor. Chemical kinetics is concerned with the rate at which reactions occur. Consider a batch reactor with a first order reaction ($n=1$), the accumulation term is dC_t/dt and the reaction term is KC_t ; thus the mass balance equation, Eq. 4-14, becomes

$$\frac{dC_t}{dt} = -KC_t \quad (4-15)$$

Integrating the last equation (Eq. 4-15) between the initial and final concentrations, and treatment time, leads to the following expression:

$$\int_{C_o}^{C_t} \frac{dC_t}{C_t} = -K \int_0^t dt \quad (4-16)$$

which gives

$$\ln\left(\frac{C_t}{C_o}\right) = -Kt \quad \text{or} \quad \ln\left(\frac{C_o}{C_t}\right) = Kt \quad (4-17)$$

Eq. 4-17 can be rewritten to Eq. 4-18, as follows:

$$C_t = C_o \cdot e^{-K \cdot t} \quad (4-18)$$

As noted in section 4.2, the highest current (2.5A) removed fluoride quickest due to the ready availability of Al^{3+} ions in the solution. However at higher currents more coagulant (aluminium) is available per unit time, which may be unnecessary, because not only is excess residual aluminium unsafe for drinking water, high current is also uneconomic in terms of energy consumption. In this batch ECF the minimum electrolysis time required to reduce the fluorine concentration to the NHMRC and ARMCANZ (2004); and WHO (2004) drinking water guidelines ($0.5 < F^- \leq 1.5$ mg/L) is defined as the detention time (t_d). The detention time was experimentally determined to achieve the desirable fluoride concentration range in the electrocoagulator. From Eq. 4-18, the detention time can be expressed as:

$$t_d = \frac{1}{K} \ln\left(\frac{C_o}{C_t}\right) \quad (4-19)$$

When the fluoride concentration (C_t) reaches to 1 mg/L, the optimal detention time (t_{do}) can be expressed as Eq. 4-20:

$$t_{do} = \frac{1}{K} \ln(C_o) \quad (4-20)$$

The overall fluoride removal efficiency (R_{ef}) in batch reactor may be obtained using the following expression:

$$R_{ef} = (C_o - C_t) / C_o = 1 - C_t / C_o \quad (4-21)$$

From Eq. 4-18, Eq. 4-21 can be rearranged to Eq. 4-22, as follows:

$$R_{ef} = 1 - e^{-K.t} \quad (4-22)$$

4.2.3.2 Continuous flow reactor

Continuous reactors can be classified according to the mixing regime. Mixing in a continuous system is determined by the residence time (t_r) and flow rate (Q). Residence time is a function of reactor volume and flow rate ($t_r = V/Q$). A plug flow reactor (PFR) is one type of continuous reactor which behaves mathematically like a batch reactor. Plug flow reaction time is theoretically equivalent to a batch reaction system (Huck & Averill, 1983). In perfect plug flow there is no mixing and they have the same residence time. A plug flow reactor operated at steady state is shown in Figure 4-5, the feed and its composition, the discharge and its composition, and the composition at any point in the reactor are constant with respect to time.

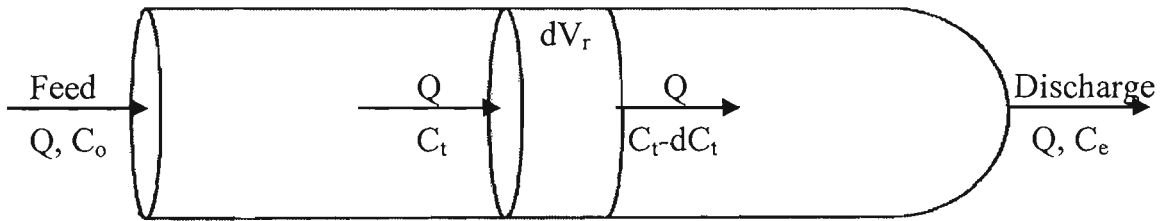


Figure 4-5 Plug flow reactor schematic

In the plug flow reactor, the concentration within the reactor is a function of the distance along the reactor, thus the composition of the fluid varies from point to point along the flow path. Therefore, the mass balance for a reaction component must be made for a differential volume, dV_r , as was shown in Figure 4-5. From Eq. 4-12, the mass balance equation for PFR in steady state, there is no accumulation, is given (Nirmalakhandan, 2002):

$$[Input] = [Decrease\ due\ to\ reaction] + [Output] \quad (4-23)$$

The mass balance in the differential reactor volume, dV_r , becomes:

$$QC_t = Q(C_t - dC_t) + rdV_r \quad (4-24)$$

which gives

$$QdC_t = rdV_r \quad (4-25)$$

Since a plug flow reactor with a first order reaction is considered, substituting of the reaction rate ($r = -KC_t$) in Eq. 4-25 gives

$$QdC_t = -(KC_t)dV_r \quad (4-26)$$

Integrating the Eq. 4-26, leads to the following expression:

$$\int_{C_o}^{C_e} \frac{dC_t}{C_t} = -\frac{K}{Q} \int_0^{V_r} dV_r \quad (4-27)$$

which gives:

$$\ln\left(\frac{C_e}{C_o}\right) = -\frac{K}{Q} V_r \quad (4-28)$$

where C_e is the effluent or final concentration. Since $V_r = Q.t_r$, substituting of V_r in Eq. 4-28 provides Eq. 4-29

$$\ln\left(\frac{C_e}{C_o}\right) = -K.t_r \quad (4-29)$$

or

$$C_e = C_o.e^{-K.t_r} \quad (4-30)$$

where t_r is mean residence time of the fluid. Eq. 4-30 can be rewritten to Eq. 4-31, as follows:

$$t_r = \frac{1}{K} \ln\left(\frac{C_o}{C_e}\right) \quad (4-31)$$

When the final fluoride concentration (C_e) reaches to 1 mg/L, Eq. 4-31 can be rearranged to Eq. 4-32:

$$t_{ro} = \frac{1}{K} \ln(C_o) \quad (4-32)$$

where t_{ro} is optimum residence time. The overall fluoride removal efficiency (R_{ef}) in continuous flow reactor may be obtained using the following expression:

$$R_{ef} = 1 - e^{-K.t_r} \quad (4-33)$$

Since Eq. 4-32 for a plug flow reactor is the same as Eq. 4-20 for a batch reactor, a plug flow reactor will have the same performance as a batch reactor if the detention and residence times are the same. More information will be explained in chapter 8.

4.2.4 Solution scheme

A solution and application of Eq. 4-18 will be presented here for modelling purposes. The initial analysis of the solution procedure is based on showing how Eq. 4-18 fits with the experimental data collected. Thus, the first step is to plot the experimental data by calculating the $-\ln(C_t/C_o)$ versus electrolysis time. Based on the plotted data, which will be explained in chapter 8 (EC modelling), it appears that the points may be fitted by a linear regression. A first order behaviour for the process is appeared. In the procedure, the slope of each line represents an experimentally determined rate constant (K_{exp}) for the process. Concerning the approach and data analysis, the

experimentally determined constant results are attached to independent variables, including current concentration (I/V), initial pollutant concentration (C_o), pH of the solution, distance between electrodes (d), and ion competition effects specially Ca^{2+} concentration. The K_{exp} can be expressed as a function of I/V , C_o , d , pH, and Ca^{2+} concentration, as follows:

$$K_{exp} = f(I/V, C_o, d, pH, Ca^{2+}) \quad (4-34)$$

where current concentration (I/V) is the ratio between the current flowing through a compartment of an electrochemical cell and the volume of that compartment. The appropriate correlations between an experimentally determined constant with different corresponding independent values need to be found separately, and that will be clarified in chapter dealing with EC modelling (chapter 8).

4.3 EMPIRICAL MODEL

A schematic diagram of the empirical modelling approach is presented in Figure 4-6. The chemical batch reactor theory was used as the basis for developing the empirical model, including statistical scheduling of the experimental data gathered. Based on the theoretical background and experimental fluoride removal rate (K_{exp}), an empirical rate constant is developed for the process. A primary analytical tool for correlating the experimental data is used by the SPSS package. A multiple regression analysis is used by SPSS package to estimate the coefficients of the linear equation, involving one or more independent variables. In fact the model is developed to predict the removal of fluoride. Development of the empirical model will be presented in chapter 8.

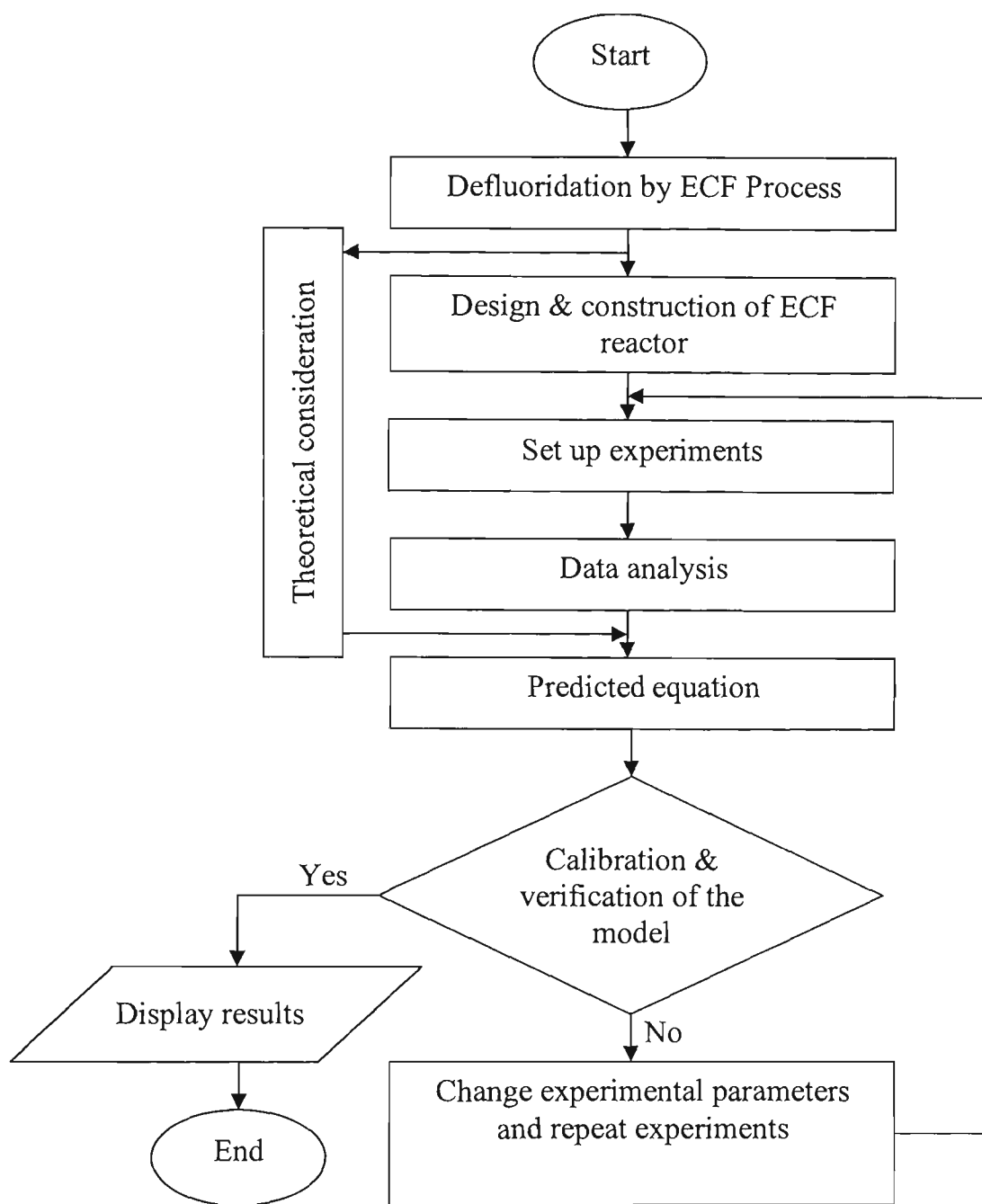


Figure 4-6 A flowchart of the empirical modelling approach

4.4 SUMMARY

The total process of removing pollutants is based on three mechanisms in the whole ECF process including electrode oxidation, gas bubble generation, and the coagulation-flotation mechanism. Application of direct electric current through electrodes induces electrolysis reactions. The metal hydroxides $[M(OH)_n]$ react as

coagulants, destabilise and aggregate suspended particles or precipitate, and adsorb dissolved contaminants. The chemical batch reactor theory, material balances, and reaction kinetic concepts were used as a basis for developing the empirical modelling efforts. The model presented in this manuscript was based on the concept of kinetics for conservative substances reacting in the reactors. In the process, not only mass balance and flow models are important, but also the rate at which the process occurs determines the size of the treatment facilities that must be provided. The overall rate constant for the entire ECF process is determined experimentally (K_{exp}) and included in a model. A multiple regression analysis is used by SPSS package to estimate the coefficients of the linear equation, involving one or more independent variables. An empirical model using critical parameters is developed for the process, when the experimental rate constant depends on some operating parameters including current concentration (I/V), initial pollutant concentration (C_o), distance between electrodes (d), pH of the solution, and ion competition effects specially Ca^{2+} concentration.

CHAPTER 5

CHAPTER 5

FLUORIDE REMOVAL BY A BATCH MONOPOLAR ELECTROCOAGULATION REACTOR

5.1 INTRODUCTION

This chapter presents the design and construction of a batch electrocoagulator and assesses the removal and appropriate EC technology for clarifying excess F^- in water and waste water sources. Several sections of this chapter discuss information related to the effects of operating parameters such as, electrolysis time, current density, current concentration, pH of the solution, distance between electrodes, initial fluoride concentration, electrolyte conductivity, particle size, zeta potential, mass ratio of aluminium and fluoride in solution (Al^{3+}/F^- mass ratio), and the affect of ion competition (especially Ca^{2+}) on removing fluoride in a batch scale. Batch reactors are usually well mixed and have a constant volume. Towards the end of this chapter information regarding the amount of sludge produced on the top and bottom of the electro-box was included.

5.2 MATERIALS AND METHODES

5.2.1 Bench scale batch ECF design

Batch reactors are usually well mixed and have a fixed volume. The initial concentrations of pollutants are changed with electrolysis time as the reactions proceed. The literature does not disclose any regular approach to EC reactor design and operation.

Chapter 5- Fluoride removal by a batch monopolar electrocoagulation reactor

However, in the literature, the ratio of the surface area of electrode to volume ranges from 6 to 41 m² /m³, as is shown in Table 5-1. In this research the electrodes were designed with a ratio of surface area to reactor volume (A/V) of 22 m² /m³, which is agree with the cited range from the literature.

Table 5-1 Electrode area to reactor volume ratio (A/V) and current density

Reference	A/V (m ² /m ³)	Current density (A/m ²)	Pollutant
Holt at al. (2005)	10.5	3.4-27	Turbidity- clay solution
Mameri et al. (1998)	6.4 -34.6	3.12-289	Fluoride- water
Ming et al. (1983)	6-8	14	Fluoride- water
Hu et al. (2003)	40.9	55	Fluoride- Water
Can et al. (2003)	16.78	25-250	Colour- dye solution
Chen et al. (2000)	18.6	30-80	Oil-restaurant wastewater

A laboratory batch electrocoagulation reactor was designed and constructed with coagulation, flotation, and pollutant removal in situ. This batch reactor was constructed from Perspex (as shown in Figure 5-1) with internal dimensions: 132 mm length by 120 mm width by 300 mm hight.

The maximum fluid height and total dead volume in the reactor reach 250 mm and 3.96 L, respectively. Five plate aluminium (purity of Al 95–97%, Ullrich Aluminium Company Ltd, Sydney) anodes and cathodes (dimension 250×100×3 mm) were used as

Chapter 5- Fluoride removal by a batch monopolar electrocoagulation reactor

electrodes and the flat surface area was lowered 200 mm into the box containing an aqueous solution.

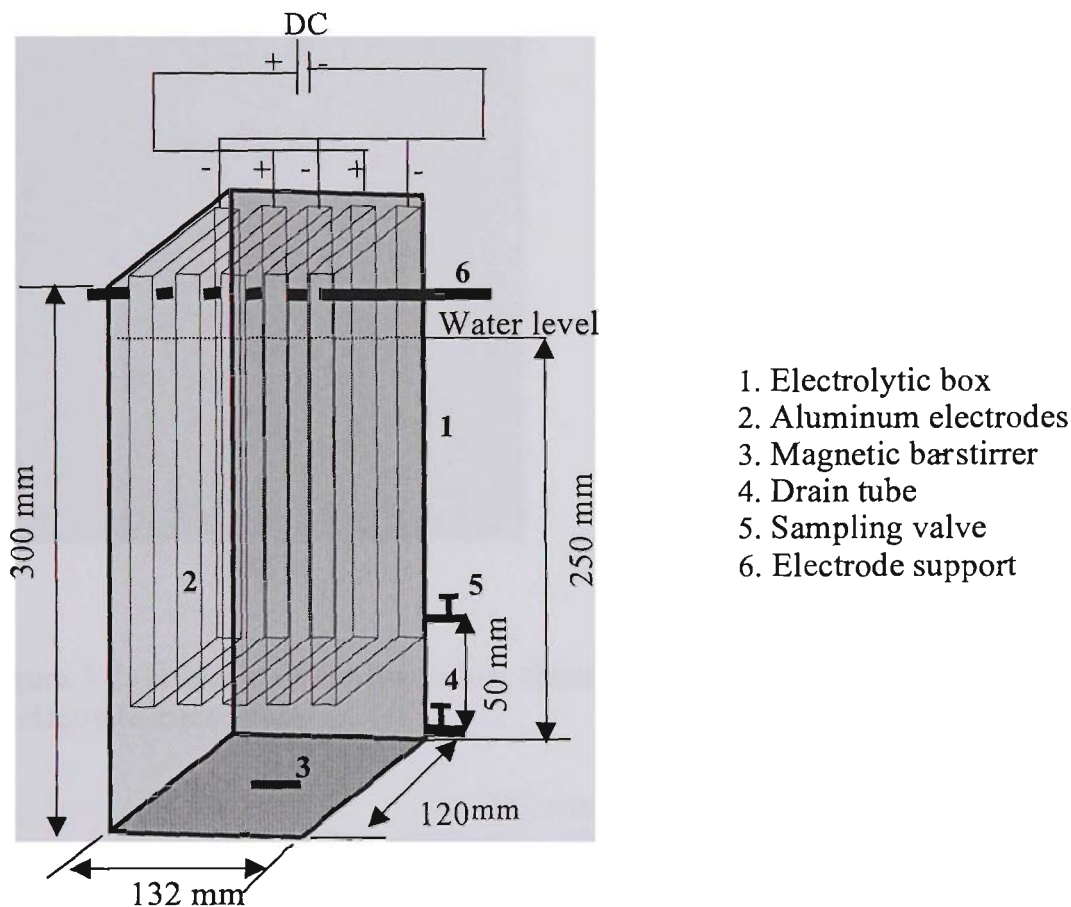


Figure 5-1 Schematic diagram of an electrocoagulation reactor

An image of the aluminium electrodes together with its dimensions are shown in Figure 5-2 (a, and b). The net capacity of the batch electrocoagulation reactor reaches to 3.66 L when the total volume of electrodes is $3 \times 10^{-4} \text{ m}^3$. The total anode active area is 0.08 m^2 . The maximum current density, which is the current divided by the active electrode area is 31.25 A/m^2 when current is held at 2.5 A. A plan view of the electrocoagulation box is shown in Figure 5-3.

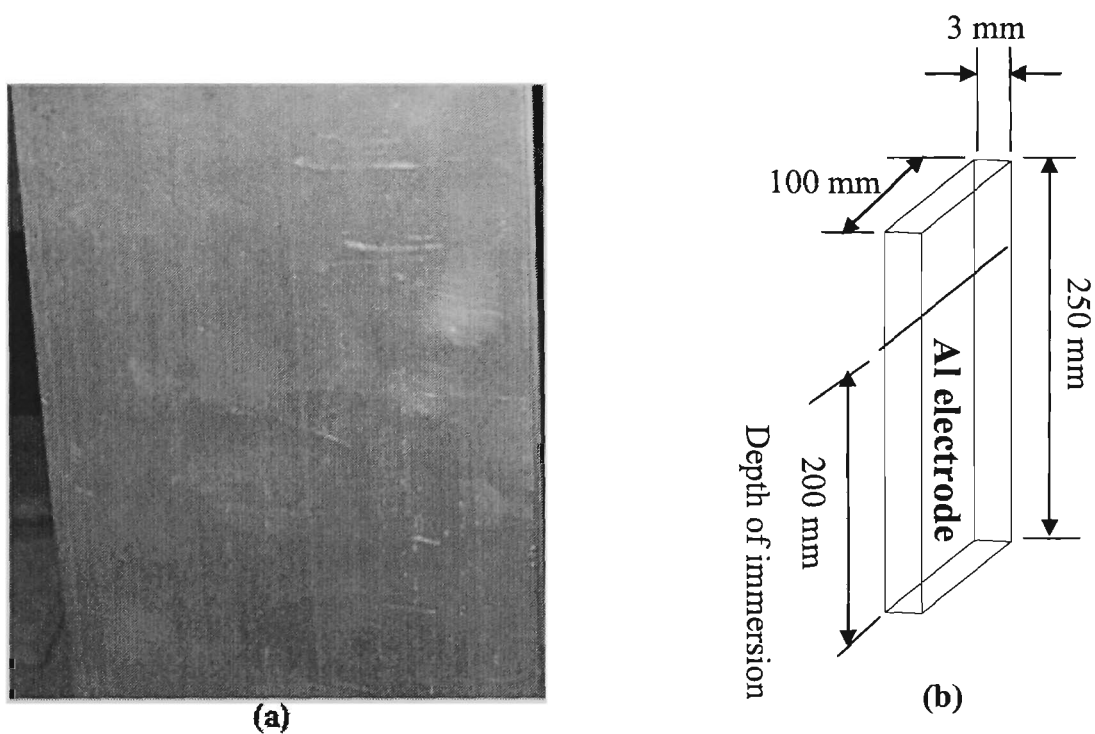


Figure 5-2 (a) Image of the aluminium electrode used in ECF process, and (b) Schematic of electrode dimensions

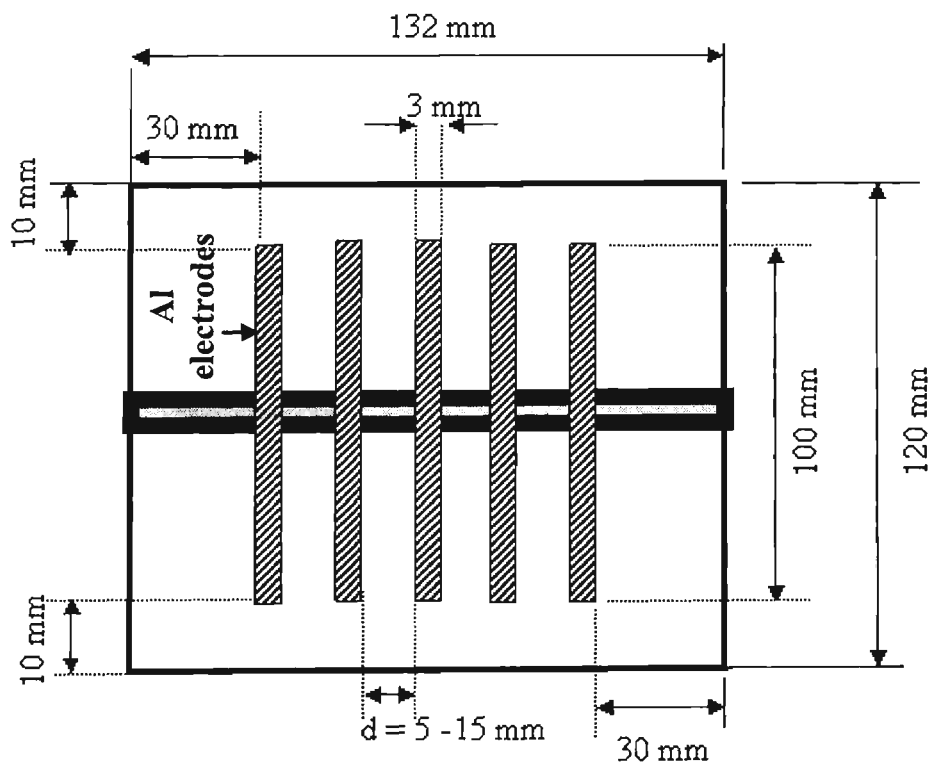


Figure 5-3 Plan views of the electrocoagulation box

Chapter 5- Fluoride removal by a batch monopolar electrocoagulation reactor

The electrodes were connected in a monopolar configuration (Figure 5-4) where stirring was achieved by a magnetic bar placed between the bottom of the electrodes and the reactor. A draining tube was installed at the bottom of the box for cleaning. Samples of treated water were collected from a valve located 50 mm from the bottom of the reactor. The gaps between the two neighbouring electrode plates were kept between 5 and 15 mm.

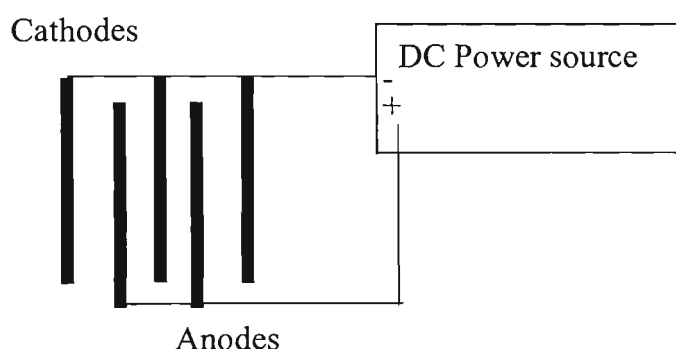


Figure 5-4 Schematic of electrodes parallel connection (monopolar arrangement)

5.2.2 Experimental Procedures

Different experimental methods were used in the electrocoagulator to characterise the EC process and its response are given in the following sections.

5.2.2.1 Solution chemistry

The influence of various experimental methods on defluoridation was achieved in a batch reactor using synthetic water (distilled water + NaF salt), and ground water sample from Alice Springs (case study). In synthetic or spiked samples, initial concentrations of fluoride (from 10 to 25 mg/L as F⁻) were prepared by mixing sodium fluoride in de-

Chapter 5- Fluoride removal by a batch monopolar electrocoagulation reactor

ionised water. Sodium bicarbonate (1 mM) was only added in synthetic samples to maintain alkalinity. The alkalinity acts to buffer the water in a pH range where the coagulant can be effective. Alkalinity must be present in excess of that destroyed by the acid released by the coagulant for effective and complete coagulation to occur. 1 M Sodium hydroxide and 1:5 hydrochloric acid solutions were added for pH adjustment. Sodium chloride (0.1 M) was occasionally added to the aqueous solution to promote conductivity in some samples. To prevent interference from the Al^{3+} ion, TISAB buffer [58 g of NaCl, 57 mL of glacial acetic acid, 4 g 1,2 cyclohexylene-diamine-tetraacetic (CDTA), 125 mL 6N NaOH were dissolved in 1000 mL distilled water and stirred until a pH 5.3 – 5.5 was reached] was added to the samples (AWWA and WEF, 1998). Total concentration of aluminium was determined by the Standard Methods (AWWA and WEF, 1998) by acidifying the sample with concentrated nitric acid (HNO_3) to $\text{pH} < 2$. The samples were transferred to a beaker where 5 mL of concentrated acid HNO_3 was added, and then boiled without allowing the sample to dry. The samples were cooled, filtered, and then transferred to a 100 ml volumetric flask where distilled water was added to make up to the mark. Once the samples are prepared, the total concentration of aluminium was determined using the Atomic Absorption Spectrophotometer. Dissolved aluminium concentration was determined based on the Standard Methods (AWWA and WEF, 1998) by the Eriochrome cyanin R method. It provides a means for estimating aluminium with low concentration (less than 0.5 mg/L). After preparing a calibration curve the absorbent rate of filtered samples was read on a spectrophotometer using a wavelength of 535 nm.

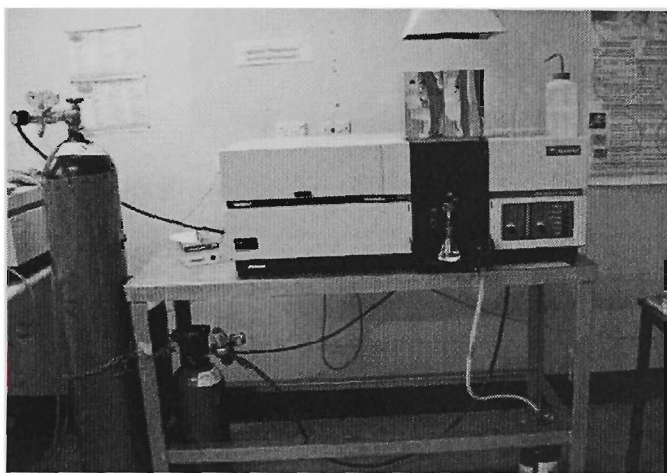
5.2.2.2 Analytical techniques

Based on the Standard Methods (AWWA and WEF, 1998), the pollutant was characterised by a combination of experiments, fluoride measurement, current and voltage measurement, aluminium and calcium measurement, particle size distribution, zeta potential measurement, X-ray diffraction, photomicrography, pH meter, and conductivity meter. Direct current from a DC power supply (0–18 V, 0–20 A, ISO-TECH, IPS-1820D) was passed through the solution via the five electrodes. Cell voltage and current were readily monitored to an accuracy of \pm (0.5% of reading +2 digits) using a digital power display. All of the following experiments were conducted by the Standard Methods (AWWA and WEF, 1998):

Total aluminium and calcium analysis: Total Al^{3+} and Ca^{2+} concentrations were measured to an accuracy of ± 0.01 mg/L using Atomic Absorption Spectrophotometer (AAS), which is shown in Figure 5-5 (a). It was calibrated with standard aluminium solutions from 5–400 mg/L. After adjusting wavelength (309 nm) and extinguish flame, aspirate the standard metal solutions into the flame and record absorbance. The instrument is adjusted to zero absorbance with the standard containing no aluminium concentration. Concentration is determined by comparing the absorbance of unknown samples with that of known solutions on a calibration curve of absorbance against concentration. This procedure was duplicated to present the calcium calibration curve, except that the wavelength was 422 nm. Also, the dissolved aluminium concentration was measured to an accuracy of ± 0.01 mg/L by a spectrophotometer, Model UV-1700 UV-Visible, using a wavelength of 535 nm, see Figure 5-5 (b). It was calibrated with

Chapter 5- Fluoride removal by a batch monopolar electrocoagulation reactor

standard aluminium solutions from 0-0.3 mg/L by accurately measuring the calculated volumes of standards into volumetric flasks, and then reading absorbance on a spectrophotometer. After adjusting instrument to zero absorbance with the standard containing no aluminium concentration, the concentration of the standard aluminium solutions against absorbance was plotted to present a calibration curve.



(a)



(b)

Figure 5-5 [a] Atomic Absorption Spectrophotometer (AAS), [b] UV-Visible spectrophotometer

Fluoride measurement: Fluoride was determined to an accuracy of ± 0.004 mg/L using the ionometric standard method (AWWA and WEF, 1998) with a selective fluoride electrode (Metrohm ion analysis, Fluoride ISE 6.0502.150, Switzerland), see Figure 5-6. It was calibrated before using with standard solutions of 0.5, 2.5, 5, 25, and 50 mg/L F⁻. Electrodes were rinsed thoroughly with distilled water before being immersed in the samples, then washed again and re-immersed to confirm the reading.

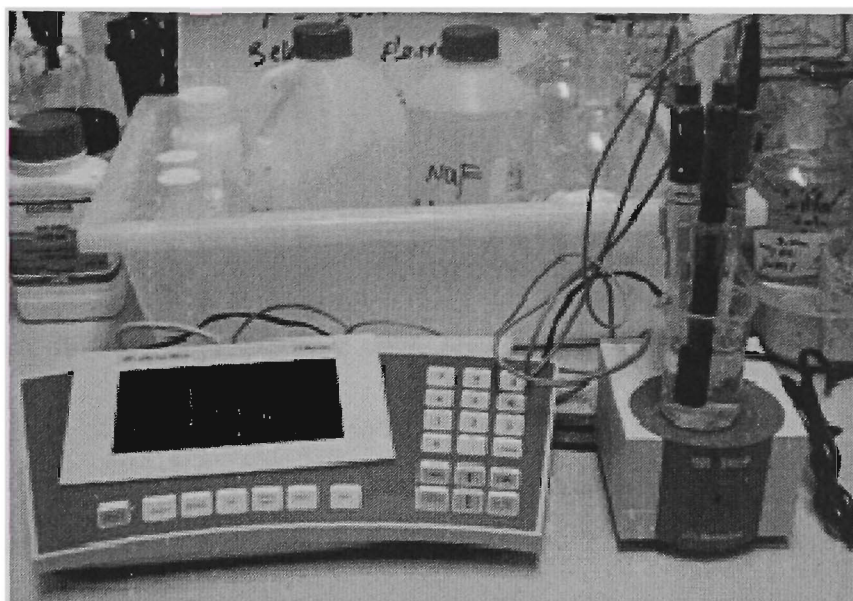


Figure 5-6 Fluoride ion selective electrode (ISE 6.0502.150, Switzerland)

Conductivity meter: Electrical conductivity is a numerical expression of the ability of an aqueous solution to carry an electric current. It was determined to an accuracy of $\pm 0.1 \mu\text{S}/\text{cm}$ by using an Alpha 800 laboratory conductivity meter, which was calibrated using a standard solution of $141.3 \text{ mS}/\text{m}$.

pH meter: The pH was determined to an accuracy of ± 0.01 pH units using the Mocro-2 pH meter, which was calibrated before each use with standard pH solution of 4, 7, and 10. Electrodes were rinsed thoroughly with distilled water before being immersed in the sample, then washed again and re-immersed to confirm the reading.

Particles size measurement: The particle size distribution was measured by the Galai CIS-100 Model 2010 particle analyser and scanning instrument, as is shown in Figure 5-7 (a). The instrument operates between 0.5 to $150 \mu\text{m}$. The sample was poured into a

Chapter 5- Fluoride removal by a batch monopolar electrocoagulation reactor

cuvette with a small magnetic stirrer to ensure adequate mixing of the sample throughout the analysis. Since the main menu appears on the PC monitor, the unit test is initiated and system electronics are checked via-100 automatic electronics diagnostics program. When the unit test was successfully done, the next stages in the sequence are performed and acquisition runs at an acceptable rate. The cuvette was then placed in the particle size analyser and various properties recorded.

Zeta potential measurement:

Zeta potential was measured using a Malvern Zetasizer 1000/3000, as is shown in Figure 5-7 (b). It uses a Laser Doppler Velocimetry (LDV) which is a well established engineering technique for measuring the velocity of particles moving through a fluid in an electrophoresis experiments. It was calibrated with a Malvern zeta potential standard (AZ55). This latex is used to check the correct operation of the instrument. When prepared according to the instructions it will give a value of $-55 \text{ mV} \pm 5 \text{ mV}$.



(a)



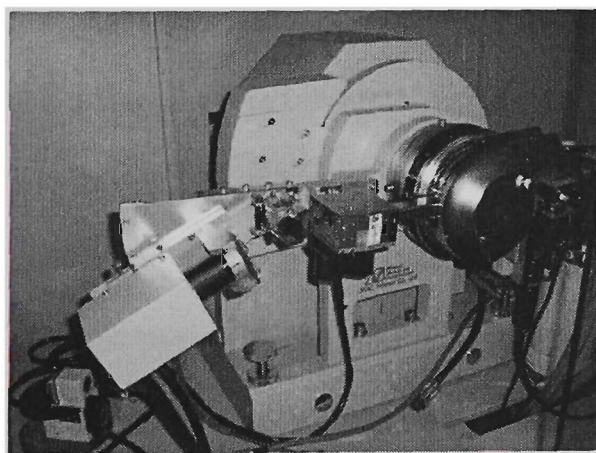
(b)

Figure 5-7 [a] the particle size measurement apparatus (Galai CIS-1), [b] Zeta potential measurement apparatus (Malvern Zetasizer 1000/3000)

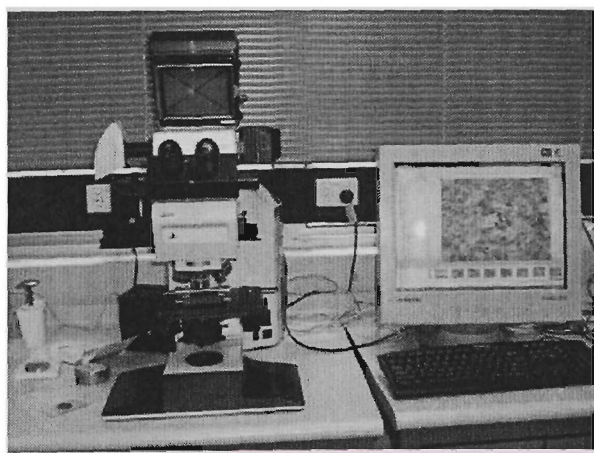
X-ray diffraction (XRD):

To determine the composition and structure of the sludge, it was analysed by X-ray diffraction (XRD) technique. The XRD measurements were carried out by the Philips no RN 1730 with CuK_α source [see Figure 5-8 (a)]. The analysers were fitted by ICCD standard patterns and Trace 5 software. A 40 kV pass voltage and 20mA current were used for its spectra. In order to do XRD on the sludge, it was dried at 108-110°C for 12-18 hours and then crushed to fine powder to use in XRD spectrum. The US national Institute of Standard and Technology (NIST) offers a certified α -quartz standard. The crystalline quartz content is suitable for calibration when analysing by X-ray diffraction.

Light microscopy: Photomicrography was used to show the floc shape after aggregation. A Nikon (256763, Japan) light microscopy with a digital colour camera attached was used to an accuracy of $\pm 0.1\mu\text{m}$ [Figure 5-8 (b)]. A pipette was used to extract solution, particles, and aggregates from each sample and place them onto a glass slide.



(a)



(b)

Figure 5-8 [a] XRD measurement apparatus (Philips no RN 1730), [b] Light microscopy apparatus together digital colour camera and display server (Nikon 256763, Japan)

Chapter 5- Fluoride removal by a batch monopolar electrocoagulation reactor

The light microscope was focused using objective lens of 5X and 10X with magnification of 3.2. The micron bar sizer for video pro images is defined in Table 5-2.

Table 5-2 Micron bar sizer for video pro images used for 3.2 magnification factor in Nikon light microscopy

Objective lens	Size (μm)
5	150
10	75
20	38
50	15

Scanning electron microscopy (SEM):

Scanning electron microscopy (SEM) was performed using a Leica Cambridge Stereoscan S440 instrument with an Oxford Link beryllium (Be) window detector for energy dispersive spectroscopy (EDS) operating at accelerating voltage of 20 kV (Figure 5-9). SEM was performed using a secondary electron detector for investigating porosity and a back scattered electron (BSE) detector to examine the composition, homogeneity, distribution, and grains size of microstructure, abraded surfaces of worn specimens, and fractured surfaces. It was calibrated with voltage of 20 KV, current probe of 600 PA, filament current of 2.4 μA, and filament of tungsten. The samples were prepared by coating with gold (Au) to ensure conductivity.

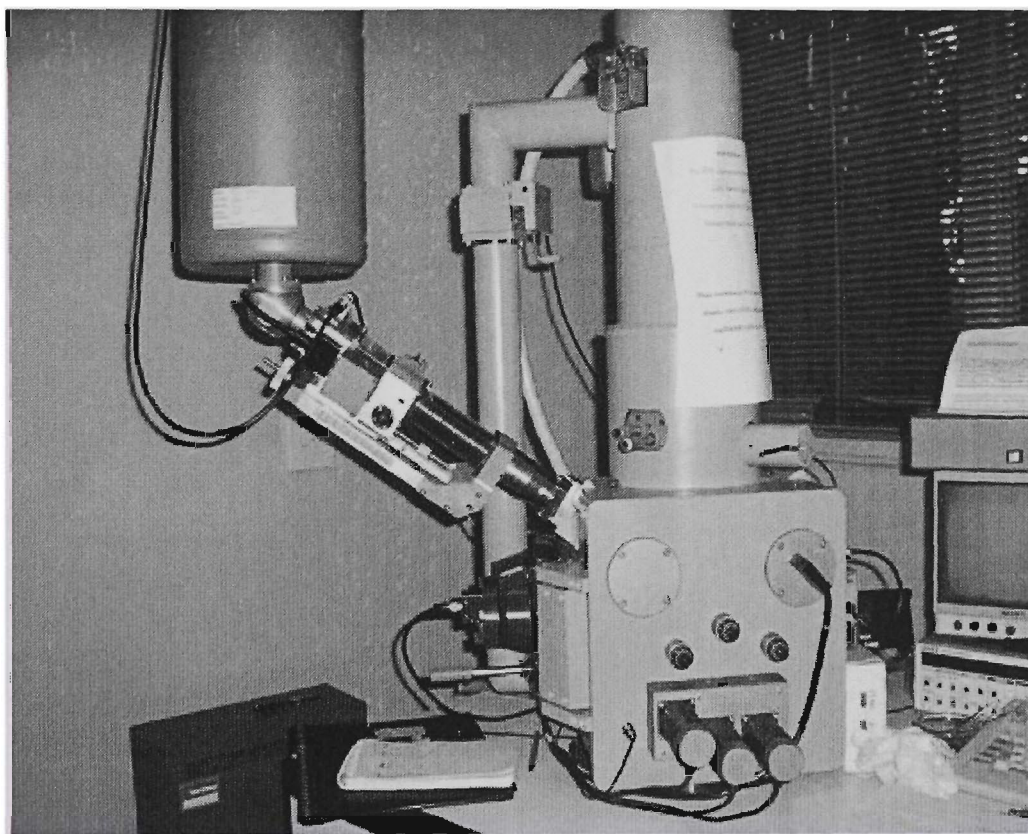


Figure 5-9 Scanning electron microscopy apparatus (Leica Cambridge Stereoscan -S440)

5.2.3 Experimental set-up

Electrocoagulation batch experiments were performed for 60 min in each run and samples were taken every 5 minutes from the drain in the electrocoagulator (Figure 5-10). All experiments were conducted at temperature of $25 \pm 1^\circ\text{C}$ with different initial concentrations of F ranging from 10 to 25 mg/L. For example, Fluoride solutions 10 mg/L as F^- were prepared by mixing sodium fluoride ($5.2 \times 10^{-4} \text{ M}$) and Sodium bicarbonate ($5 \times 10^{-4} \text{ M}$) in de-ionised water. The pH of the feed and product water was measured for each experiment because it was kept constant by adding sodium hydroxide or hydrochloric acid during the experiments.

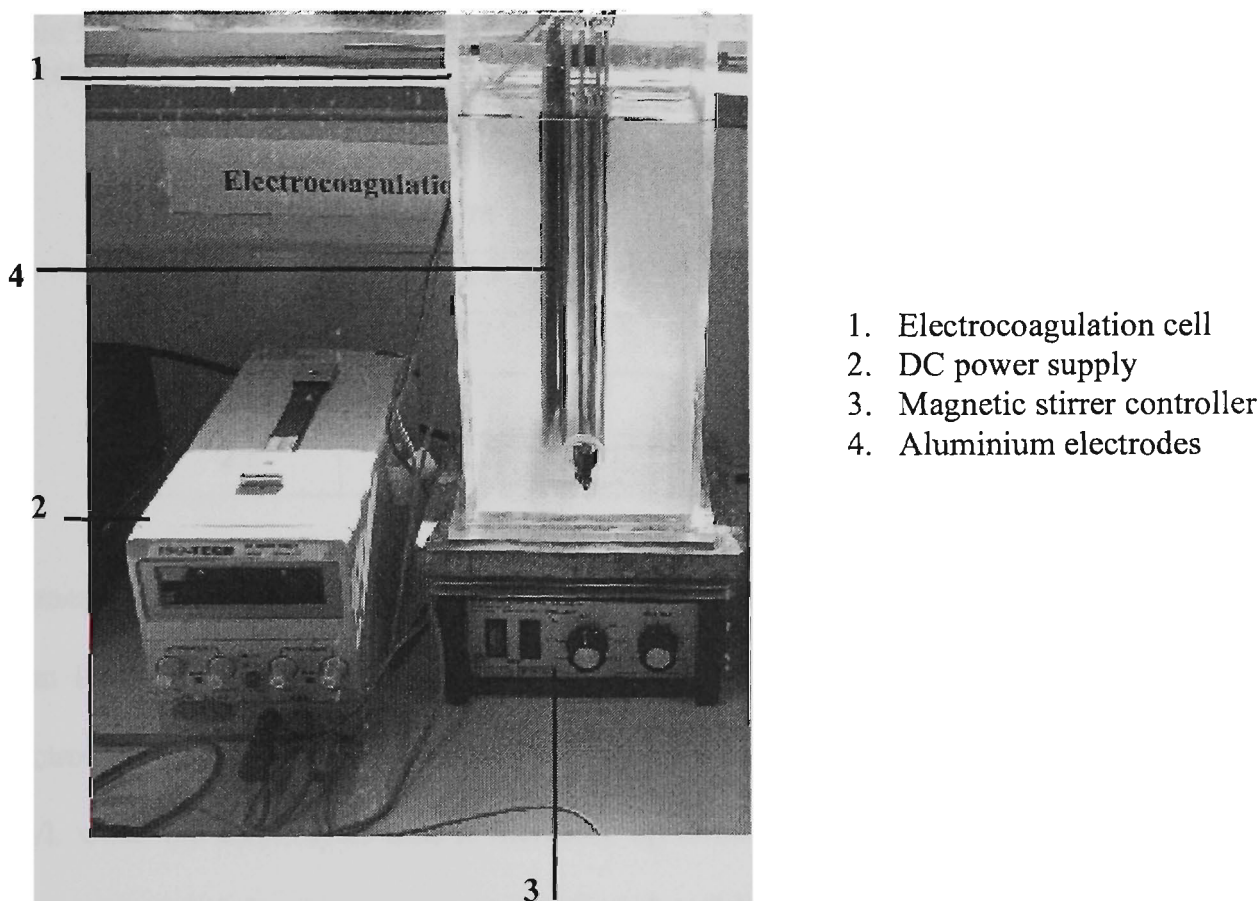


Figure 5-10 Experimental electrocoagulation/floatation (ECF) reactor

The conductivity of the solution was between 10-1000 mS/m when the electrode distance and initial fluoride concentration was 5 mm and 10 mg/L, respectively. Power was from a DC power supply. The ECF reactor operated in a galvanostatic mode which means that the current was held constant while the cell potential varied to maintain the required current. Current varied from 1 – 2.5 A, but it was kept constant for each run. Based on total anode active area (0.08 m^2), the relationship between operating current and current density in the ECF reactor is shown in Table 5-3.

Chapter 5- Fluoride removal by a batch monopolar electrocoagulation reactor

Table 5-3 Relationship between operating current value, current density, and current concentration in the ECF reactor

Current (A)	Current density (A/m ²)	Current concentration (A/m ³)
1	12.5	273
1.5	18.75	410
2	25	546
2.5	31.25	683

Mameri et al. (1998) reported that the residual fluoride concentration is not reduced from 10 to less than 1 mg/L when the current density is less than 10 A/m² in 45 min electrolysis time. In this research, the initial fluoride concentration ranges between 10-25 mg/L when the electrolysis time is increased up to 60 min. Thus, the minimum current value and current density are presented to be 1 A and 12.5 A/m², respectively.

In this chapter the following experimental parameters were identified to quantify the performance of electrocoagulation for defluoridation in the synthetic water samples:

- Initial fluoride concentration
- Current requirement, current density (based on the electrodes area), and current concentration (based on volume of the electrocoagulator)
- Distance between electrodes
- Coagulant (aluminium) concentration requirements
- pH of solution
- Ca²⁺ effect (ion competition effects)
- Conductivity of solution

Chapter 5- Fluoride removal by a batch monopolar electrocoagulation reactor

- Electrolysis time
- Particle size analysis
- Zeta potential
- Sludge production and characteristics

The important experimental variables in ECF reactor are summarised in Table 5-4.

Table 5-4 Important experimental variables in ECF reactor

Operational parameters		Electrode distancing (mm)	Initial pH	Initial fluoride concentration (mg/L)	Ca ²⁺ concentration (mg/L)
Current density (A/m ²)	Current concentration (A/m ³)				
12.5	273	5-15	2 – 10	10-25	50-300
18.75	410	5-15	2 – 10	10-25	50-300
25	546	5-15	2– 10	10-25	50-300
31.25	683	5-15	2 – 10	10-25	50-300

The effects of the various operating parameters, as previously mentioned in the chapters 3 and 4, were proposed to be investigated in different ranges. The fluoride concentration in groundwater exceeds from 1.5 mg/L in some regions, as previously noted in Figure 1-1 in chapter 1, and sometimes reaches to more than 20 mg/L (WHO, 2005). The fluoride concentration was recorded at 13 mg/L in a bore near the Indulkana region in central Australia (Fitzgerald et al., 1999). Thus, the initial fluoride concentration ranges between 10 -25 mg/L in this research. Concerning to the different initial fluoride concentrations, the expected values for current density, which were previously mentioned, are represented. The inter electrode distance was chosen in the range of 5 to

15 mm corresponding to the values used in the electrochemical industry and other literatures (Mameri et al., 1998; and Hu et al., 2003). The initial pH is one of important solution chemistry factors in terms of raw water when it will affect the speciation of Al. The solubility of aluminium in equilibrium with solid phase $\text{Al}(\text{OH})_3$ depends on the surrounding pH when it is investigated in the various ranges from 2 to 10 during experiments. Previous research by the authors (Mameri et al., 1998; Shen et al., 2003; Toyoda and Taira, 2000) showed that the Ca^{2+} ion competition effect on defluoridation process is very significant when it was used in different range of 50-300 mg/L.

5.3 RESULTS AND DISCUSSION

5.3.1 Effects of electrolysis time

Electrolysis time or treatment time is one of the important parameters of defluoridation in batch electrocoagulation runs. The electrolysis time and current value are significant parameters in the more electrochemical process. The electrolysis time and current value determines the coagulant dosage (Al^{3+} concentration) and rate of generating bubble. Figure 5-11 shows the influence of electrocoagulation time and production of total aluminium concentrations on removal of the fluoride by the ECF process when current value is kept constant 1.5 A. Theoretically, based on Faraday's law (Eq. 2-9), current and duration of electrolysis should affect the quantity of aluminium released to a system using aluminium electrodes. The relationship between theoretical $[\text{Al}_T]$ and experimental $[\text{Al}_E]$ aluminium concentration with electrolysis time is shown in Figure 5-12.

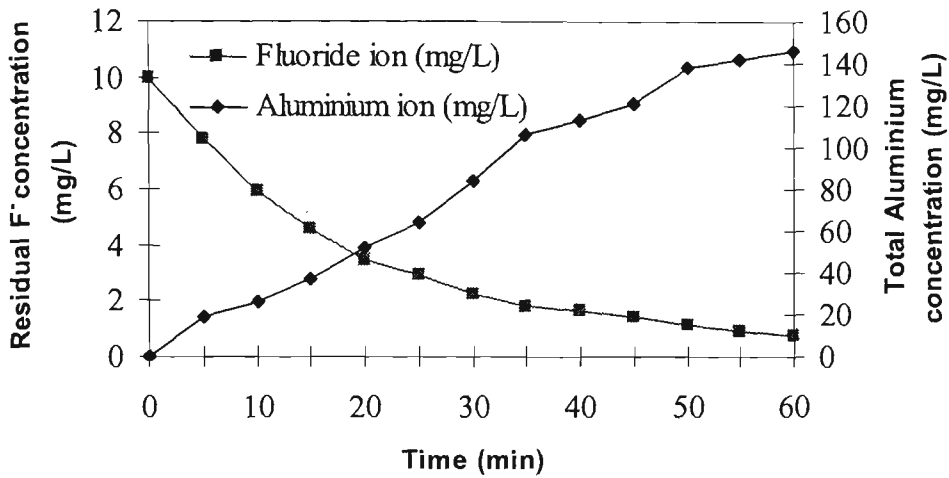


Figure 5-11 Influence of electrolysis time on fluoride removal and production of total aluminium concentrations ($I=1.5$ A, $d=5$ mm, $pH=6$, $C_o = 10$ mg/L, $d=5$ mm)

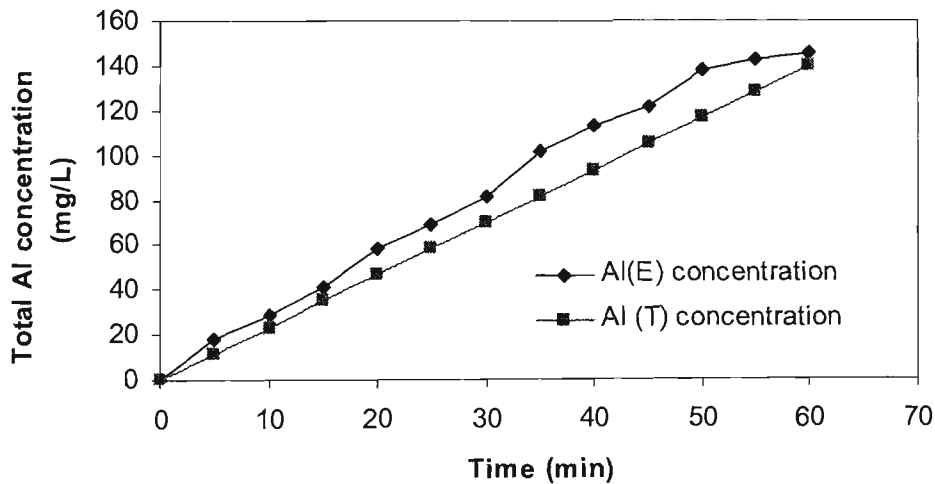


Figure 5-12 Relationship between theoretical and experimental Al^{3+} concentration with electrolysis time ($I=1.5$ A, $C_o=10$ mg/L, $T=25$ °C, $pH=6$, $d=5$ mm)

The results shown in Figure 5-11 indicate that the residual fluoride concentration is decreased from 10 mg/L to less than 1 mg/L by increasing the electrolysis time from 5 to

60 min at a constant current of 1.5 A when the total Al^{3+} concentration is respectively increased from 18 to 145 mg/L. As seen in Figure 5-12, the amount of Al^{3+} that is produced in the cell is higher than the value predicted by Faraday's law. This may be explained by the dissolution of aluminium as a result of pitting corrosion caused by some ions. It means that the presence some ions catalysis the aluminium corrosion and this corrosion can produce more aluminium. Eq. 5-1 defines current efficiency as a ratio of the concentration of Al^{3+} dissolution $[C_{\text{Al(E)}}]$, over the theoretical concentration of Al^{3+} dissolution $[C_{\text{Al(T)}}]$.

$$\varepsilon_c = C_{\text{Al(E)}} / C_{\text{Al(T)}} \quad (5-1)$$

The results, presented in Figure 5-13, obtained from different current densities show that current efficiency (ε_c), which is defined as a fraction of the current passing through an electrolytic cell (or an electrode), is more than 100 % for the batch system.

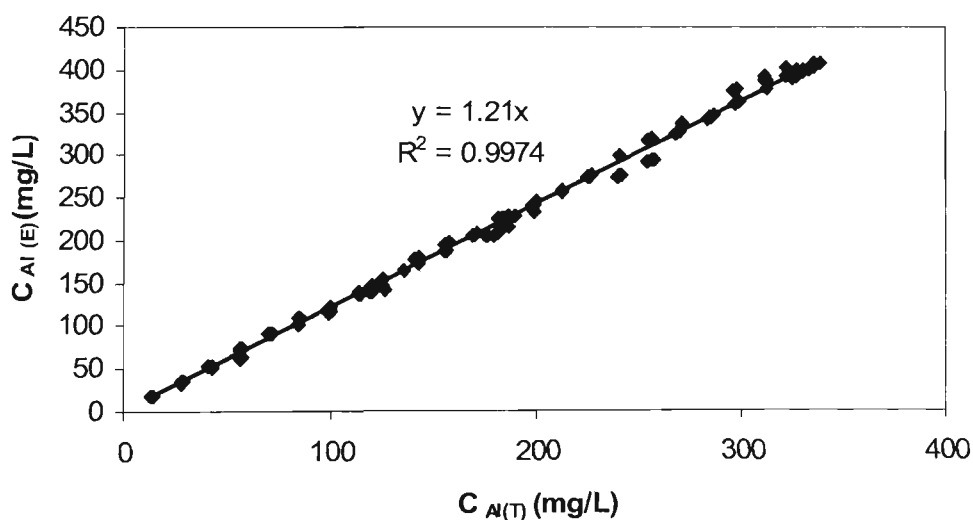


Figure 5-13 Relationship between theoretical and experimental Al^{3+} concentration for removal of fluoride at this ECF process ($C_0=5\text{-}25$ mg/L, $E_{c_{in}}=10\text{-}50$ mS/m, $T=25$ °C, $\text{pH}=6\text{-}8$, $d=5$ mm)

Chapter 5- Fluoride removal by a batch monopolar electrocoagulation reactor

This result showed that the value (ϵ_c) was 121 %. Other authors also reported this result with values ranging from 100–130 % in a bipolar electrocoagulation process (Li-Cheng, 1985; Ming et al., 1983; and Mameri et al., 1998).

The duration of electrocoagulation (electrolysis time) based on its theory, may be divided into electrolysis time and flocculation time. When current passed through the cells the electromagnetic forces first overcome the attractive forces between polar molecules and colloidal particles in suspension and then shear the molecules. The anode then releases Al^{3+} ions into the solution and hydrogen ions are reduced to hydrogen gas, thus valence states of any dissolved metals were reduced and allowed them to complex. The aggregates formed can then be removed by decantation and flotation. Thus, Electrocoagulation time affects not only the production of metallic ions at an anode, but also the production of hydrogen bubbles in a cathode. The small bubbles are used to capture contaminant particles in water or waste water and float them to the surface for removal, as shown in Figure 5-14 (a, and b).

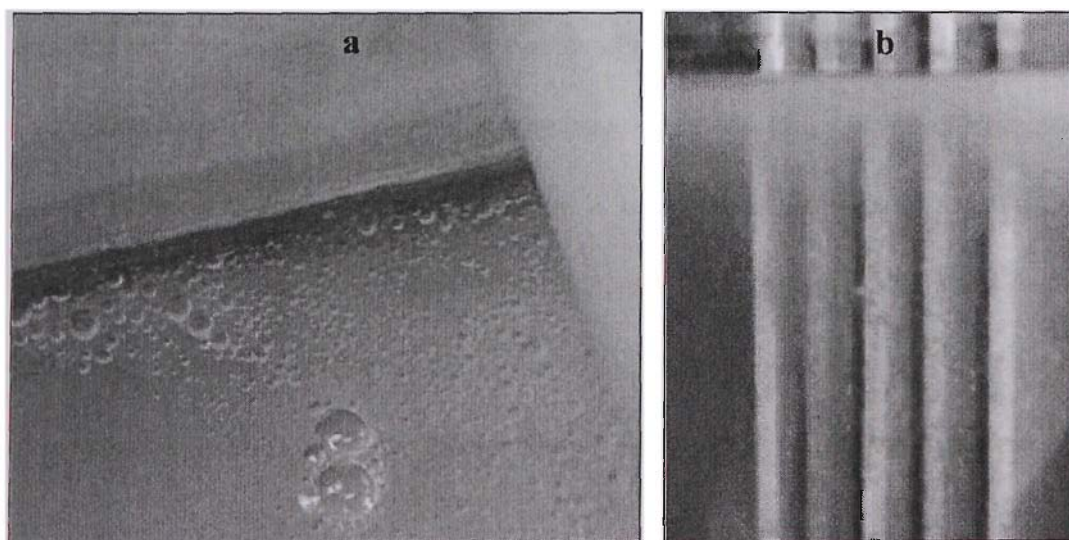


Figure 5-14 Images of (a) small bubbles generation and (b) floc flotation in ECF process

Chapter 5- Fluoride removal by a batch monopolar electrocoagulation reactor

At initial fluoride concentration 10 mg/L, the amount of experimental aluminium released during the electrolysis time at different current densities from 12.5 to 31.75 A/m² (or 1-2.5 A) is shown in Figure 5-15.

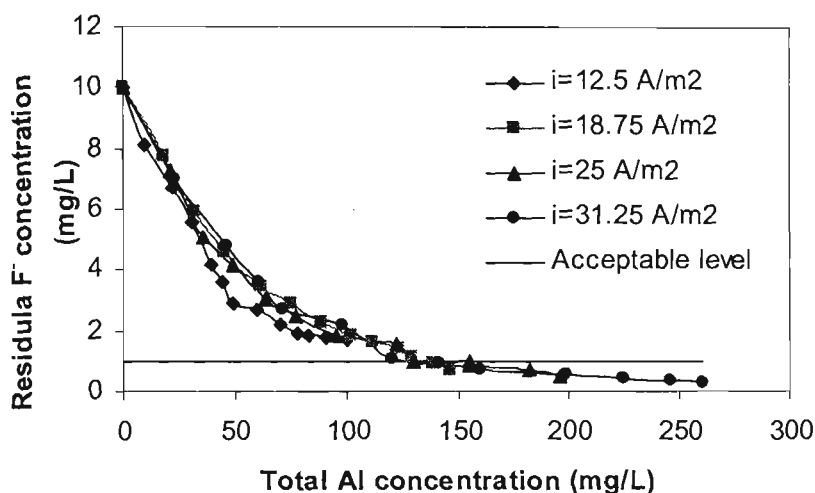


Figure 5-15 Effect of released aluminium dosage on the residual fluoride concentration ($C_o=10$ mg/L, $E_{c_{in}}=10$ mS/m, $T=25$ °C, $pH=6-8$, $d=5$ mm)

As shown in Figure 5-15, the residual fluoride concentration reaches to 1 mg/L when the total aluminium concentration is between 120-155 mg/L. This emphasizes that the amount of aluminium released to the system by electrocoagulation is affected by the current and electrolysis time in the electrocoagulation cell. The experimental mass ratio Al^{3+}/F^- was found between 13-17.5 in a monopolar ECF process when the residual aluminium concentrations on the effluent were found to be less than 0.2 mg/L which is desirable based on NHMRC and ARMCANZ (2004) guidelines. This result agrees with the results obtained by Mameri et al. (1998) observation in the bipolar electrocoagulation process.

The experimental results, as shown in Figure 5-16, showed that combination of the current and electrolysis time (or charge) will lead to an increase in aluminium released to the system.

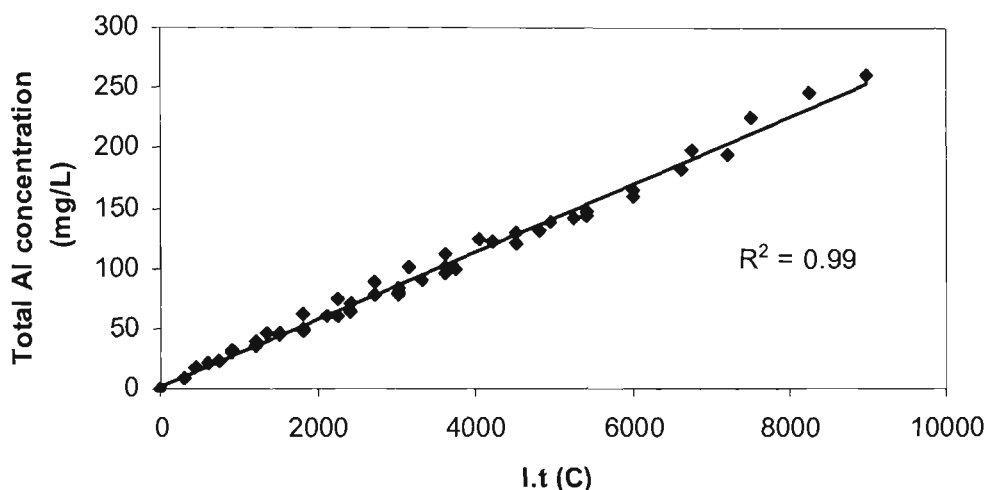


Figure 5-16 Relationship between charge and total aluminium released to the EC reactor ($i=1-2.5A$, $t=5-60$ min)

As seen, there is linear relationship between charge and total aluminium concentration. Thus the total aluminium was used as a basis, which combines current and time for comparison in the proceeding. The residual and total concentrations of aluminium together the different current values, electrolysis time, and removal efficiency are summarised in Appendix A when initial fluoride concentration is 10 mg/L.

5.3.2 Effect of current values

5.3.2.1 Effect of current density

Variation of residual fluoride concentration with electrolysis time at different current density is shown in this section. In most electrochemical processes current density is the

Chapter 5- Fluoride removal by a batch monopolar electrocoagulation reactor

most important parameter for controlling the reaction rate in the reactor. Based on the experimental parameters previously noted in Table 5-4, the influence of current density on defluoridation experiments was studied with monopolar electrodes. Figure 5-17 shows fluoride removal when the current density varied from 12.5 to 31.25 A/m² and pH was kept constant at 6.

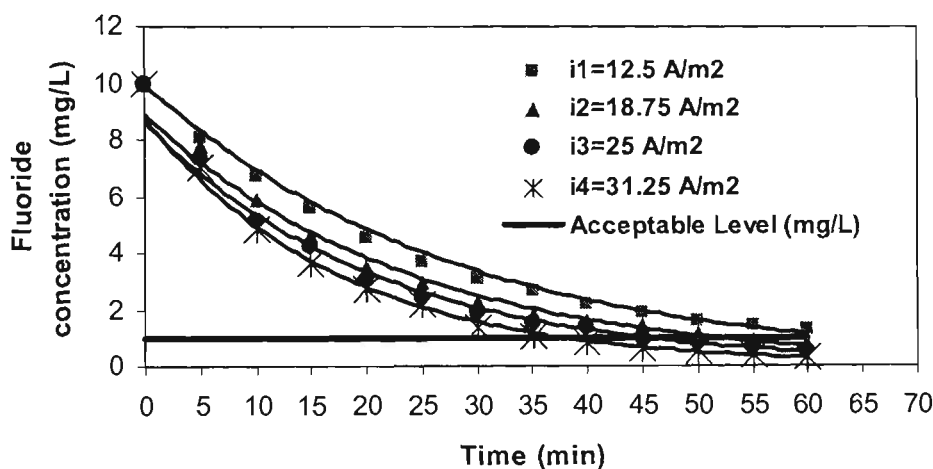


Figure 5-17 Variation of residual fluoride concentration with time at different current densities on ECF process ($d=5$ mm, $C_o=10$ mg/L, $E_{c_{in}}=10$ mS/m, pH =6)

Residual fluoride decreases with increasing current density because the current range determines the rate of dissolution of Al^{3+} concentration. The lower the current, the less aluminium is released from the anode and fluoride reduction is low. The results shown in Figure 5-17 indicate that the highest current (2.5 A) removed fluoride the quickest because of the ready availability of Al^{3+} ions for coagulation. This result agrees with the results obtained by Li-Cheng (1985), Ming et al., (1983), and Mameri et al., (1998). The rate of change of F^- in the ECF process has already been expressed in Eq. 4-24. From

this equation, a plot of $-\ln(C_t/C_0)$ with time is shown in Figure 5-18 for various current densities at a conductivity of 10 mS/m.

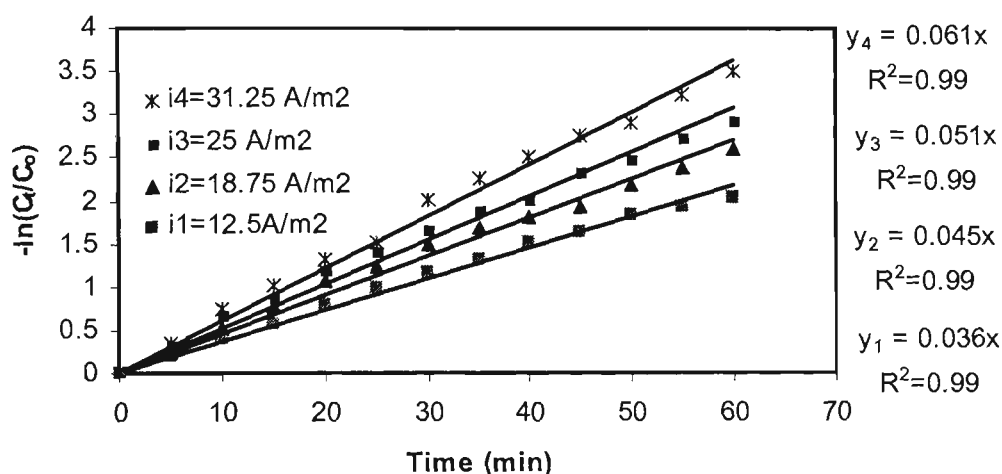


Figure 5-18 Determination of the kinetic constants of defluoridation at different current densities on ECF process ($Ec_{in} = 10$ mS/m, $C_0 = 10$ mg/L, $d = 5$ mm, $pH = 6$)

The linear relation between $-\ln(C_t/C_0)$ with time confirms the fact that the kinetics of defluoridation follows the exponential law. It appears that the reaction rate increases from 0.36 to 0.061 $(\text{min})^{-1}$ when current density is increased from 12.5 to 31.25 A/m^2 in the solution, respectively.

5.3.2.2 Effect of Current concentration

Current concentration is the ratio between the current flowing through a compartment of an electrochemical cell and the volume of that compartment. The total net volume was constant in the batch model during all experiments. The influence of electrolysis time on defluoridation at different current concentrations is shown in Figure 5-19. It appears that

the lower the current concentration the less aluminium is released from the anode and the fluoride reduction is low.

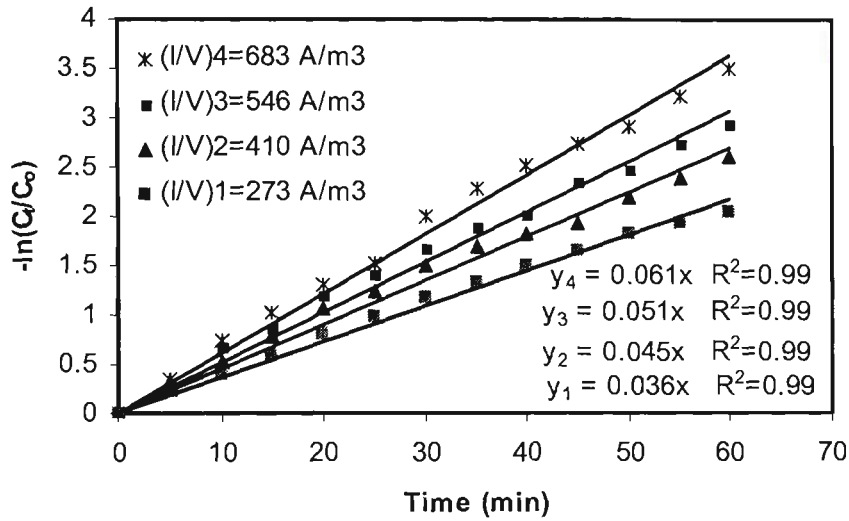


Figure 5-19 Determination of the kinetic constants for defluoridation by ECF process at different current concentrations ($C_0 = 10$ mg/L, $T = 25^\circ\text{C}$, $d = 5$ mm, and $E_c = 10$ mS/m)

As seen, the linear relation for each current concentration confirms the fact that kinetics of defluoridation follows the exponential law with electrolysis time. The rate of change of F^- concentration is found as a first order kinetic model. Plots of $-\ln(C_t/C_0)$ with time for various current concentrations on defluoridation at the different operational parameters including the initial concentration of fluoride from 10 to 25 mg/L, the electrode distance from 5 to 15 mm, the constant pH range from 6 to 9, and the Ca^{2+} concentration from 0 to 300 mg/L, are shown in Appendix B. Details will be explained in chapter 8.

5.3.3 Effect of pH

The coagulation process depends on the pH of a solution. Coagulation with Al salts occurs at a wide range of pH due to different mechanisms, and amorphous aluminium hydroxide is least soluble at pH between 6 and 8 (Sposito, 1996). The effect of initial pH in buffered and non-buffered cases was investigated. Its effect on defluoridation in a non-buffered case when the pH was from 2-10 is shown in Figure 5-20.

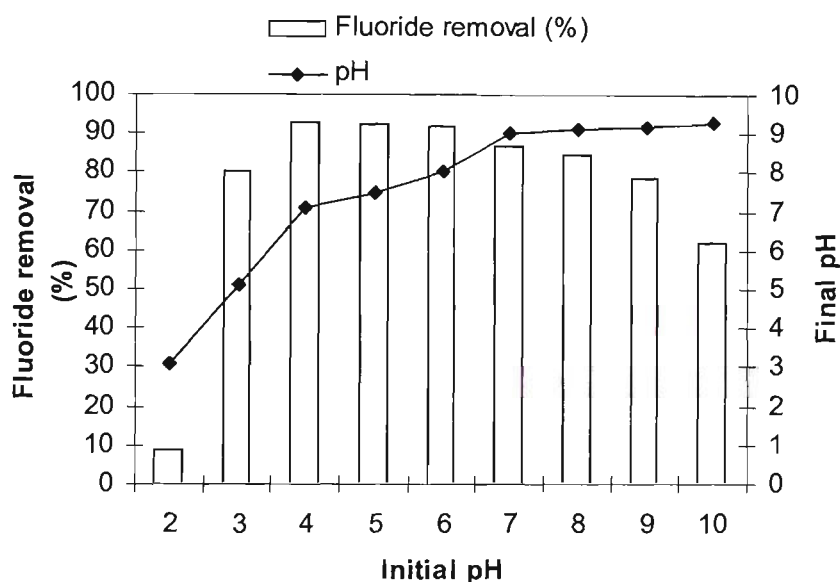


Figure 5-20 Effect of initial pH on defluoridation ($i=18.75 \text{ A/m}^2$, $d=5 \text{ mm}$, $E_{c,in}=10 \text{ mS/m}$, $C_o=10 \text{ mg/L}$, and $t=60 \text{ min}$)

By increasing the initial pH from 2 to 3 in a non-buffered case the final pH increases from 3.1 to 5.1, because of hydrolysis reaction on the cathode electrode (Eq. 4-2). When the influent pH was 2, no $\text{Al}(\text{OH})_3$ floc was formed and less fluoride was removed in the EC treatment system. There is a significant difference in the removal of fluoride between an initial pH 2 and 3 because different Al-F speciation is produced. That will be discussed in detail in chapter 7 (Solution speciation). As seen in Figure 5-20 there is no

Chapter 5- Fluoride removal by a batch monopolar electrocoagulation reactor

significant effect on defluoridation by an EC system when initial pH values are between 4 and 6. In this initial pH range the final pH is increased from 6 to 8 and the residual fluoride concentration reached a constant value of 0.74 mg/L. By increasing the initial pH range from 6 to 10, the residual fluoride concentration increased from 0.74 to 3.8 mg/L when the final pH increased from 8 to 9.3. The fluoride removal efficiency decreased when the final pH is more than 9. It is because of formation of $Al(OH)_4^-$ and AlO_2^- that are soluble and useless for defluoridation. No $Al(OH)_3$ floc was observed when the pH is beyond 10.

The experiments were also carried out at a constant (buffered case) pH within the range of 4-10 when the initial fluoride concentration was 10 mg/L. The current density was maintained at 18.75 A/m^2 during the experiments. Fluoride removal as a function of the constant pH is shown in Figure 5-21.

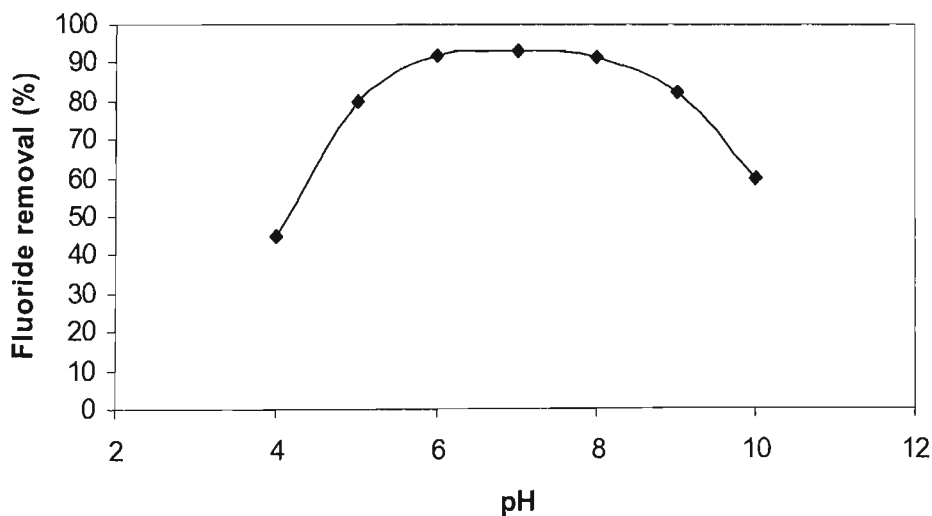


Figure 5-21 Effect of constant pH on fluoride removal ($i=18.75 \text{ A/m}^2$, $d=5 \text{ mm}$, $Ec_{in}=10 \text{ mS/m}$, $C_o=10 \text{ mg/L}$, and $t=60 \text{ min}$)

Chapter 5- Fluoride removal by a batch monopolar electrocoagulation reactor

As seen, fluoride removal increases slowly, with the pH increasing from 5 to 6. It remains unchanged between the pH range of 6 –8 and then decreases when the pH is increased further. These results mean that defluoridation is more efficient when the pH is constant between 6 and 8 during experiments. It may be also explained by the strong presence of aluminium hydroxide in this pH range which maximized the fluoro-hydroxide aluminium complex formation. Since aluminium hydroxide is an amphoteric hydroxide, pH is a sensitive factor for the formation of $\text{Al}(\text{OH})_3$ flocs. The solubility of aluminium in equilibrium with solid phase $\text{Al}(\text{OH})_3$ depends on the surrounding pH, as the solid $\text{Al}(\text{OH})_3$ is most prevalent between pH 6 and 8. The soluble species $\text{Al}(\text{OH})_4^-$ is the predominant species at above pH 9. That will be explained in detail in chapter 7.

5.3.4 Effect of electrolytic conductivity (as Cl⁻)

Fluoride removals of samples with 10, 100 and 1000 mS/m conductivity were investigated. The conductivity of a suspension can be adjusted by varying its salinity. The conductivity of the solution was increased from 100 to 1000 mS/m by increasing sodium chloride from 0.01 and 0.1 M, respectively. Figure 5-22 shows fluoride removal when the current densities are increased from 12.5 to 31.25 A/m^2 in a constant conductivity 1000 mS/m. With 1.5, 2, and 2.5A operating current, the minimum electrolysis time required to reduce fluoride to the desirable concentration ($\text{F}^- = 1 \text{ mg/L}$), is found to be 55, 45, and 35 min, respectively. Figure 5-23 also shows variation of residual fluoride with the different current densities between 12.5 and 31.25 A/m^2 at conductivity of 10- 1000 mS/m.

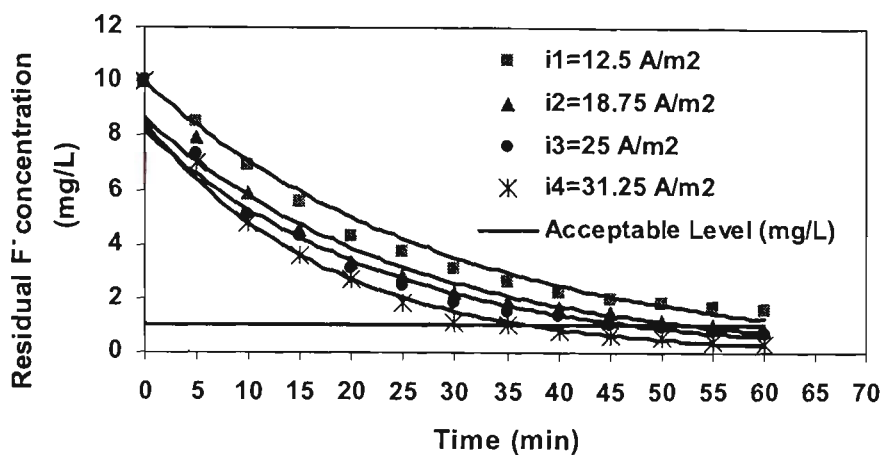


Figure 5-22 Variation of fluoride concentration with time at different current densities on ECF process ($d=5$ mm, $C_o=10$ mg/L, $E_{c_{in}}=1000$ mS/m, $pH=6$)

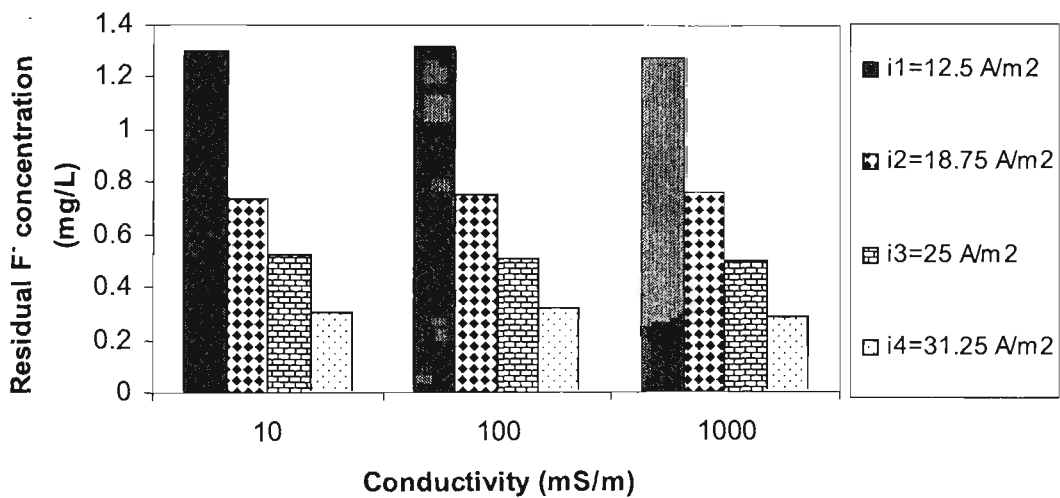


Figure 5-23 Effects of electrical conductivity on defluoridation by ECF process at different current densities ($d=5$ mm, $C_o=10$ mg/L, $t=60$ min, $pH=6$)

From results obtained in Figure 5-23, it can be concluded that there is no significant effect on fluoride removal by the EC process when conductivity (by adding chloride concentration) is increased in the solution. As seen, the concentration of Cl⁻ had no

significant effect on defluoridation by the EC process. It may be explained that increase of the concentration of Cl^- , which is not considered as a strong affinity with Al^{3+} , has no significant effect on the adsorption capacity of fluoride onto hydrous alumina. The affinities of Cl^- ion with Al^{3+} is too small to replace F^- ions that were combined with Al^{3+} (Hu et al., 2003).

Figure 5-24 shows the effects of conductivity on the energy consumption at different current densities. At 18.75 A/m^2 , the energy consumption decreased from 5.5 to 0.75 kWh/m^3 when the conductivity was increased from 10 to 1000 mS/m , respectively.

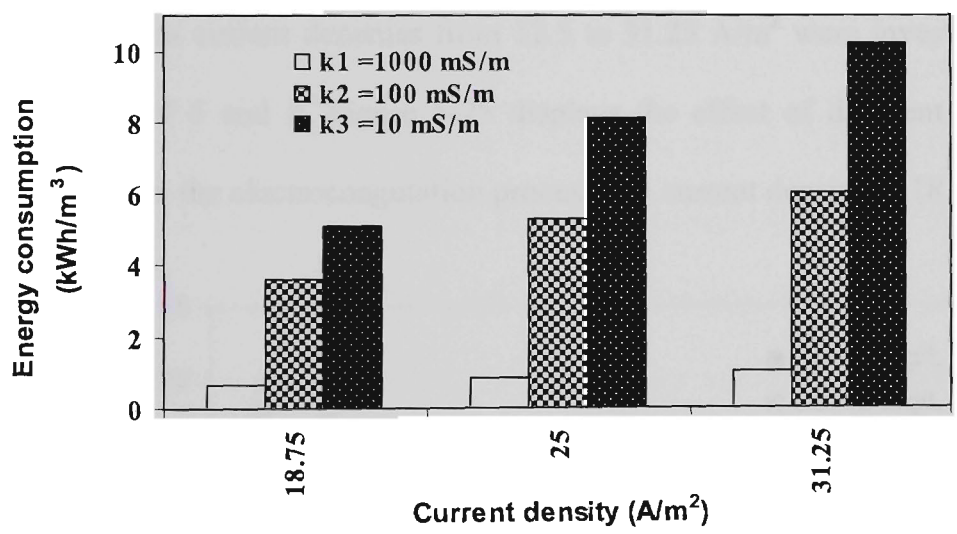


Figure 5-24 Effects of conductivity on the energy consumption at different current densities ($d=5 \text{ mm}$, $C_0=10 \text{ mg/L}$, $\text{pH}=6$)

Electrical power requirements depend on the concentration of aluminum needed to reduce high fluoride concentration to a desirable concentration (1 mg/L), on the configuration of the electrochemical cell, and on the conductivity of the wastewater. Increasing conductivity (by adding salt) to the sample does not increase the removal of

pollutants, as shown in Figure 5-23, but power consumption can be saved significantly. However it is important to keep in mind that increasing conductivity by adding salt will decrease the quality of the treated effluent. The added chloride ion in the aqueous solution will be increased the total dissolved solid (TDS) concentration and hardness in the solution.

5.3.5 Effect of initial fluoride concentration

As explained in section 5.3.3, defluoridation process is more efficient for a pH ranging from 6 to 8 during experiments. Thus, the effects of initial fluoride concentrations from 10 to 25 mg/L at current densities from 12.5 to 31.25 A/m² were investigated between the pH range of 6 and 8. Figure 5-25 displays the effect of different initial fluoride concentration on the electrocoagulation process at a current density of 18.75 A/m².

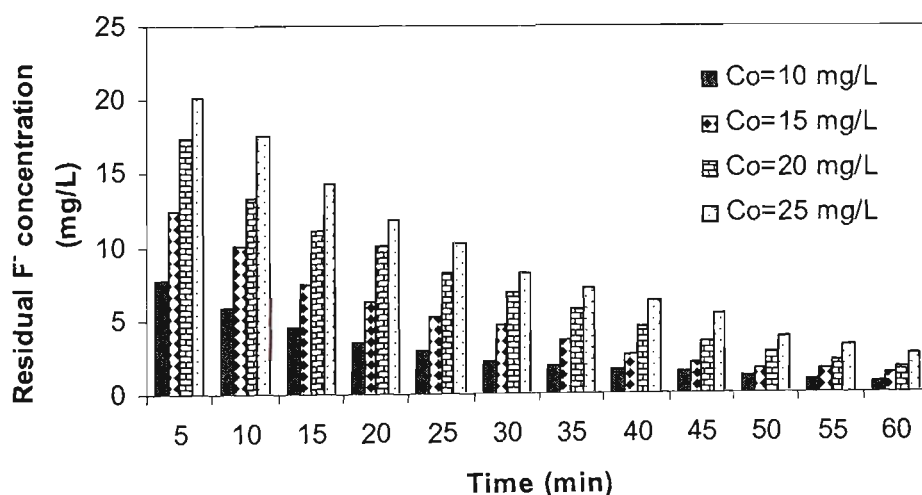


Figure 5-25 Effects of different initial fluoride concentration on defluoridation by ECF process ($i=18.75$ A/m², $d=5$ mm, $pH=6$, $Ec_{in}= 10-50$ mS/m)

Chapter 5- Fluoride removal by a batch monopolar electrocoagulation reactor

As seen, the values of residual fluoride concentrations increase when the initial fluoride concentrations increase at a constant electrolysis time and current density, because the highest pollutant loading (25 mg/L) needs to a higher current or longer electrolysis time for more treatment. Thus high current values produce more coagulant in the ECF cell which helps improve defluoridation. Considering of Figure 5-25, suggests that the high initial fluoride concentration (25 mg/L) can not be reduced to the desirable fluoride concentration (1 mg/L) in the effluent at 60 min electrolysis time by electrocoagulation when the current density is low (18.75 A/m^2).

In the EC process the amount of aluminium ion produced is proportional to the charge which is a product of the current supplied and electrolysis time. The charge affects fluoride removal significantly. Figures 5-26 (a, b, and c) show fluoride removal at different current densities when initial fluoride is increased from 10 to 25 mg/L. As seen in Figure 5-26, a drop in residual fluoride is expected when the current density increases. It also appears that the reaction rate decreases when initial concentration of F^- in the solution is increased, because higher fluoride concentration needs more coagulant. At a current density of 25 A/m^2 the residual fluoride reaches from 10 mg/L to less than 1 mg/L after 55 minutes of electrolysis times. The results show that the current density values of less than 25 A/m^2 are not sufficient to reduce fluoride from 15 to 1 mg/L even at 60 min electrolysis time. In Figures 5-27 (a, b, and c), plots of $-\ln(C_t/C_0)$ with time are shown for various current densities and different initial fluoride concentrations. From results obtained in Figure 5-27 (a, b, and c), in every experiment the logarithm linear

relation for each current density confirms the fact that the kinetics of defluoridation follows the exponential law with time.

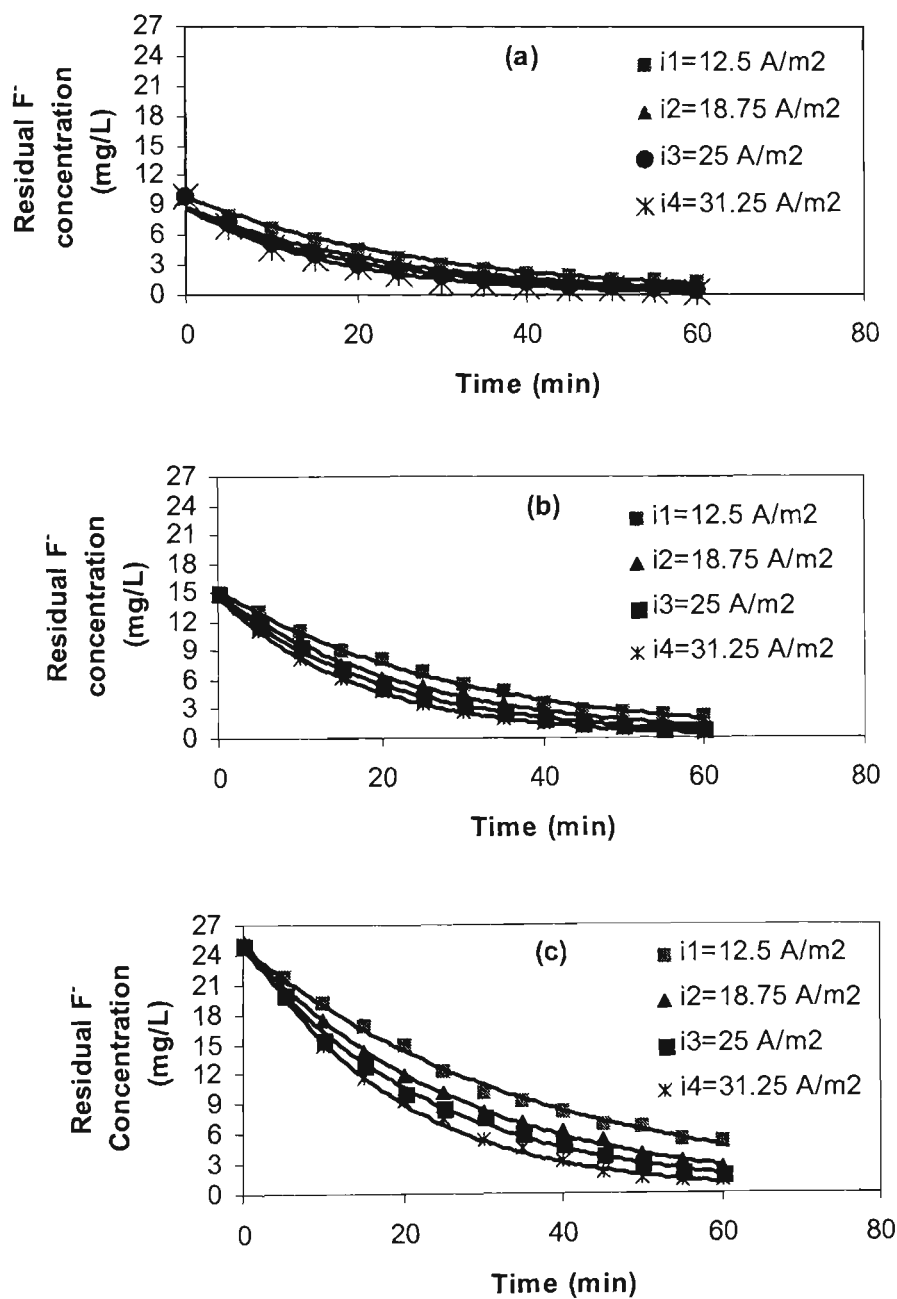


Figure 5-26 Variation of residual fluoride concentration with time at different current densities and initial fluoride concentrations on ECF process, [a] $C_0=10 \text{ mg/L}$, [b] $C_0=15 \text{ mg/L}$, [c] $C_0=25 \text{ mg/L}$ ($d=5 \text{ mm}$, $E_{c_{in}}=10\text{-}25 \text{ mS/m}$, $\text{pH}=6$)

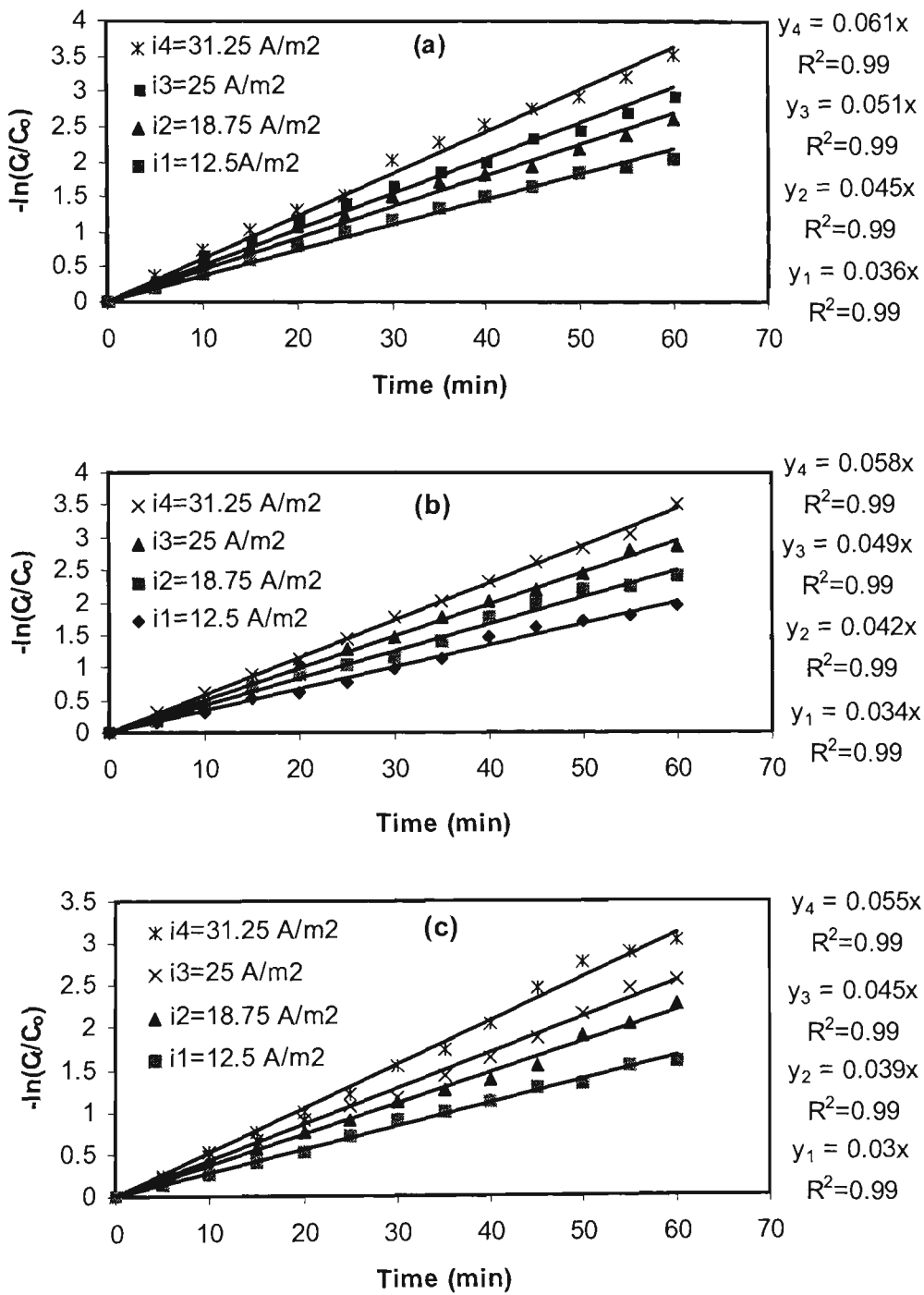


Figure 5-27 Determination of the kinetic constants of defluoridation at different current densities and initial fluoride concentrations on ECF process [a] $C_0 = 10 \text{ mg/L}$, [b] $C_0 = 15 \text{ mg/L}$, [c] $C_0 = 25 \text{ mg/L}$ ($d = 5 \text{ mm}$, $E_{cin} = 10\text{-}25 \text{ mS/m}$, $\text{pH} = 6$)

Chapter 5- Fluoride removal by a batch monopolar electrocoagulation reactor

The results from the batch experiments showed that the highest current improved the removal of fluoride. However at higher currents more coagulant (aluminium) is available per unit time, which may be unnecessary, because not only is excess residual aluminium unsafe for drinking water, high current is uneconomic in terms of energy consumption. In batch ECF a minimum electrolysis time is required to reduce fluorine to the desirable concentration ($F^- = 1$ mg/L) (NHMRC and ARMCANZ, 2004) and is called the optimum detention time (t_{do}). As noted in section 5.3.1, the combination of current and time (charge) determine the pollutant removal. Thus it is advisable to limit charge to avoid excessive energy consumption. This has been summarised in Table 5-5.

Table 5-5 Optimum detention time and optimum charge for defluoridation by ECF process at the different initial fluoride concentrations ($d=5$ mm, $E_{c,in} = 10-25$ mS/m, $pH=6-8$)

Current value (A)	$I_1=1$ A	$I_2=1.5$ A	$I_3=2$ A	$I_4=2.5$ A	$q=It$
Initial fluoride concentration (mg/L)	t_{do} (min)	t_{do} (min)	t_{do} (min)	t_{do} (min)	Optimum charge (C)
10	>60	55	45	35	5000-5400
15	>60	>60	55	45	6600-6800
20	>60	>60	$70 > t_{do} > 60$	55	8250-8400
25	>60	>60	>60	$70 > t_{do} > 60$	9500-10500

The results showed that residual fluoride reduced from 10 to 1 mg/L when the optimum detention times were respectively 55, 45 and 35 min at 1.5, 2 and 2.5 A. At a higher current, the electrolysis time was shorter. It can be concluded that electrolysis time must also be considered with operating current for evaluating removal (optimum charge). The residual aluminium concentrations on the effluent were found to be less than 0.2 mg/L which is desirable concentration based on NHMRC and ARMCANZ (2004) guideline.

5.3.5.1 Ground water sample from Alice Spring

Defluoridation experiments were also conducted using samples of bore water taken from Central Australia (Alice Springs). However, this bore is not used for human consumption. The main characteristics of this water, presented in Table 5-6, shows a high concentration of Cl^- and low concentrations of Ca^{2+} , Mg^{2+} , and K^+ . The defluoridation process by electrocoagulation process at the different initial fluoride concentrations of 10 and 15 mg/L was studied with synthetic solution having an average characteristic of the ground water sample from Alice Spring, as shown in Figure 5-28. The synthetic samples were prepared by using NaF (F^-), NaCl (Cl^- and conductivity), CaCl_2 (Ca^{2+}), MgCl_2 (mg^{2+}), KCl (K^+) salts dissolved in distilled water.

Table 5-6 Characteristics of water quality Alice Spring sample used for defluoridation

Sample	Concentration (mg/L)							
	Ca^{2+}	Mg^{2+}	K^+	Cl^-	pH	F^-	Alkalinity mg/L (CaCO_3)	Ec (mS/m)
Alice Spring sample	8	6	11	628	7.8	13	100	422

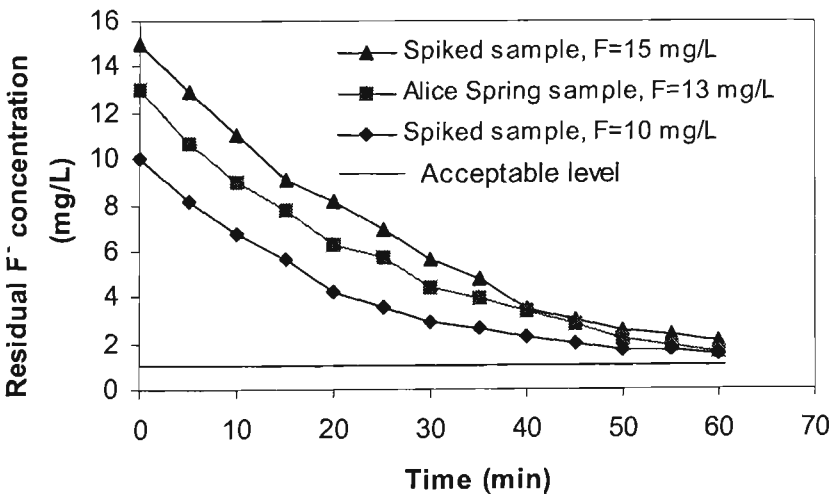


Figure 5-28 Effects of different initial fluoride concentration on defluoridation by ECF process for the various samples ($I=1\text{A}$, $d=5\text{ mm}$, $\text{pH}_{\text{in}}=6$, $\text{Ec}_{\text{in}}=422\text{ mS/m}$)

Chapter 5- Fluoride removal by a batch monopolar electrocoagulation reactor

As seen, current values $\leq 1\text{A}$ will not reduce the fluoride from 13 to 1 mg/L even after 60 min of electrolysis time on the samples from Alice Springs, because the higher initial fluoride concentration needs more coagulant. Higher current leads to a higher aluminium concentration (coagulant). The rate of change of F⁻ in Alice Springs sample is shown in Figure 5-29. Residual fluoride decreases with increasing current concentration because the current range determines the rate of dissolution of Al^{3+} concentration.

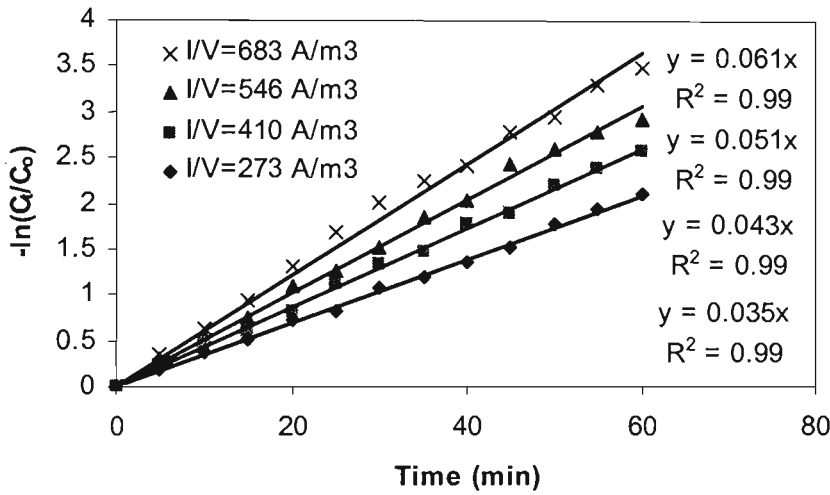


Figure 5-29 Determination of the kinetic constants for the defluoridation of Alice Springs sample by ECF process at different current concentrations ($C_0 = 13 \text{ mg/L}$, $d = 5 \text{ mm}$, $\text{pH}_{\text{in}} = 6$, $E_{\text{c,in}} = 422 \text{ mS/m}$)

The linear relation between $-\ln(C_t/C_0)$ with time confirms the fact that the kinetics of defluoridation follows the exponential law. More details will be explained in chapter 8 when these experimental results are used to verify the analytical model.

Figures 5-30 (a, b, and c) show that when the fluoride removal at currents from 1.5 - 2.5A where the fluoride concentrations in the synthetic samples were compared with those from Alice Springs.

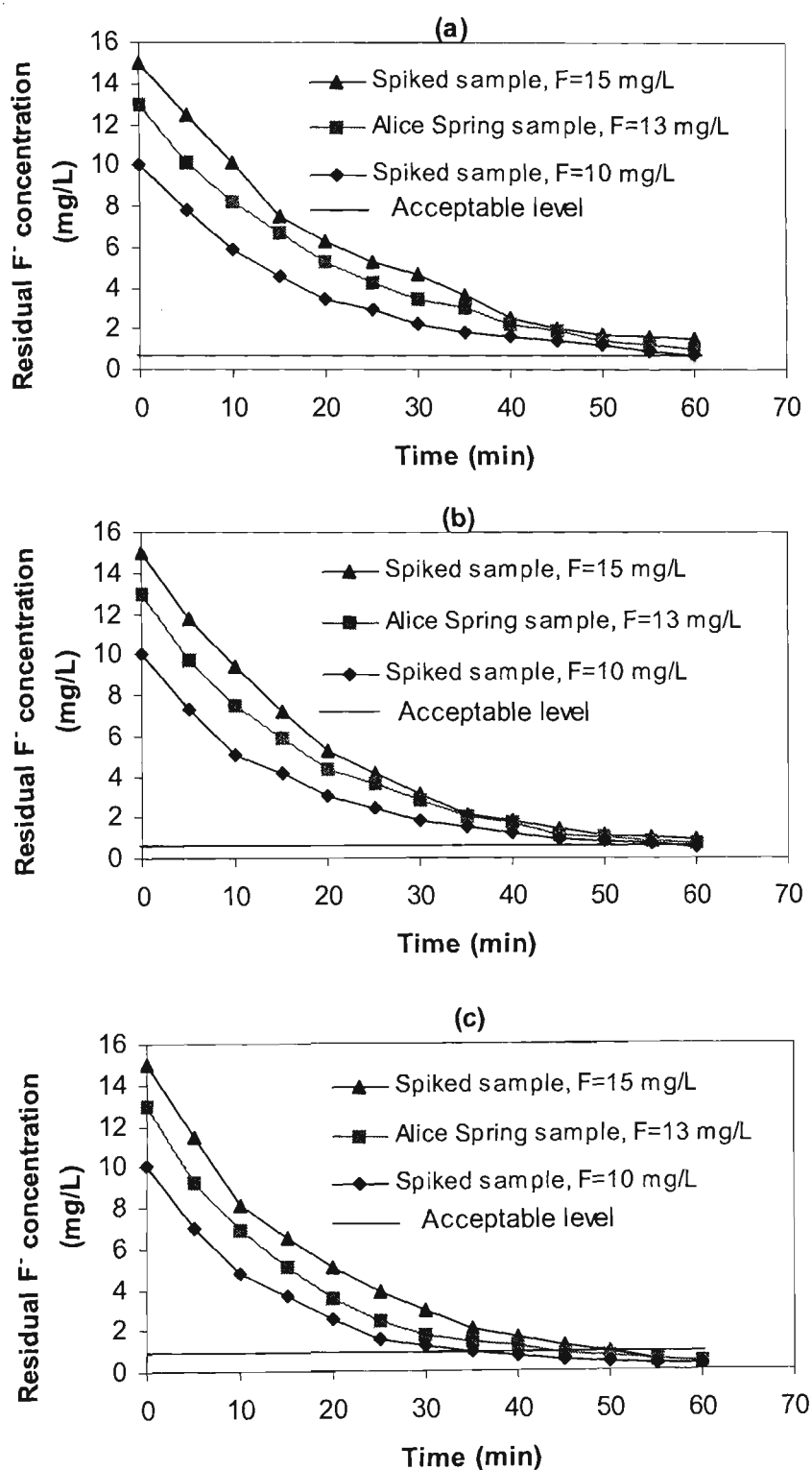


Figure 5-30 Variation of fluoride concentration with time at different current values and initial fluoride concentrations on the various samples by ECF process ($d=5$ mm, $pH_{in}=6$), [a] $I=1.5$ A, [b] $I=2$ A, [c] $I=2.5$ A

Chapter 5- Fluoride removal by a batch monopolar electrocoagulation reactor

The fluoride removal behaviour is found to be similar at spiked samples and bore water sample. The same results were obtained for a similar concentration on the synthetic samples. It was previously explained in section 5.3.4 that the concentration of Cl^- had no significant effect on defluoridation by the EC process. The concentrations of all three co-existing cations (Ca^{2+} , Mg^{2+} , and K^+) in synthetic solutions, which was shown in Table 5-6, were found to be low when the competition effect of these cations at this range of concentration had no significant effect on the residual fluoride concentration. The competition effect of co-existing cations such as Ca^{2+} , Mg^{2+} in the aqueous solution will be separately explained in the following this chapter.

5.3.6 Effect of distance between electrodes

The distance between the electrodes (d) was changed from 5 to 15 mm, which corresponds to the values used by other authors (Ming et al., 1983; and Li-Cheng, 1985). When the distance between the cathodes and the anodes is increased from 5 to 15 mm so too is resistance between the electrodes. The highest inter- electrode distance needs the higher potential. This high potential overcomes a range of resistances including electrode spacing, conductivity, and surface resistance. However, for short inter-electrode distances the current density may become too high and can cause short circuit. Therefore, the experiments have been done with inter- electrode distance of 5, 10, and 15 mm distance between electrodes and various current densities. Plots of $-\ln(C_t/C_0)$ with time are shown schematically in Figures 5-31 (a, b, and c).

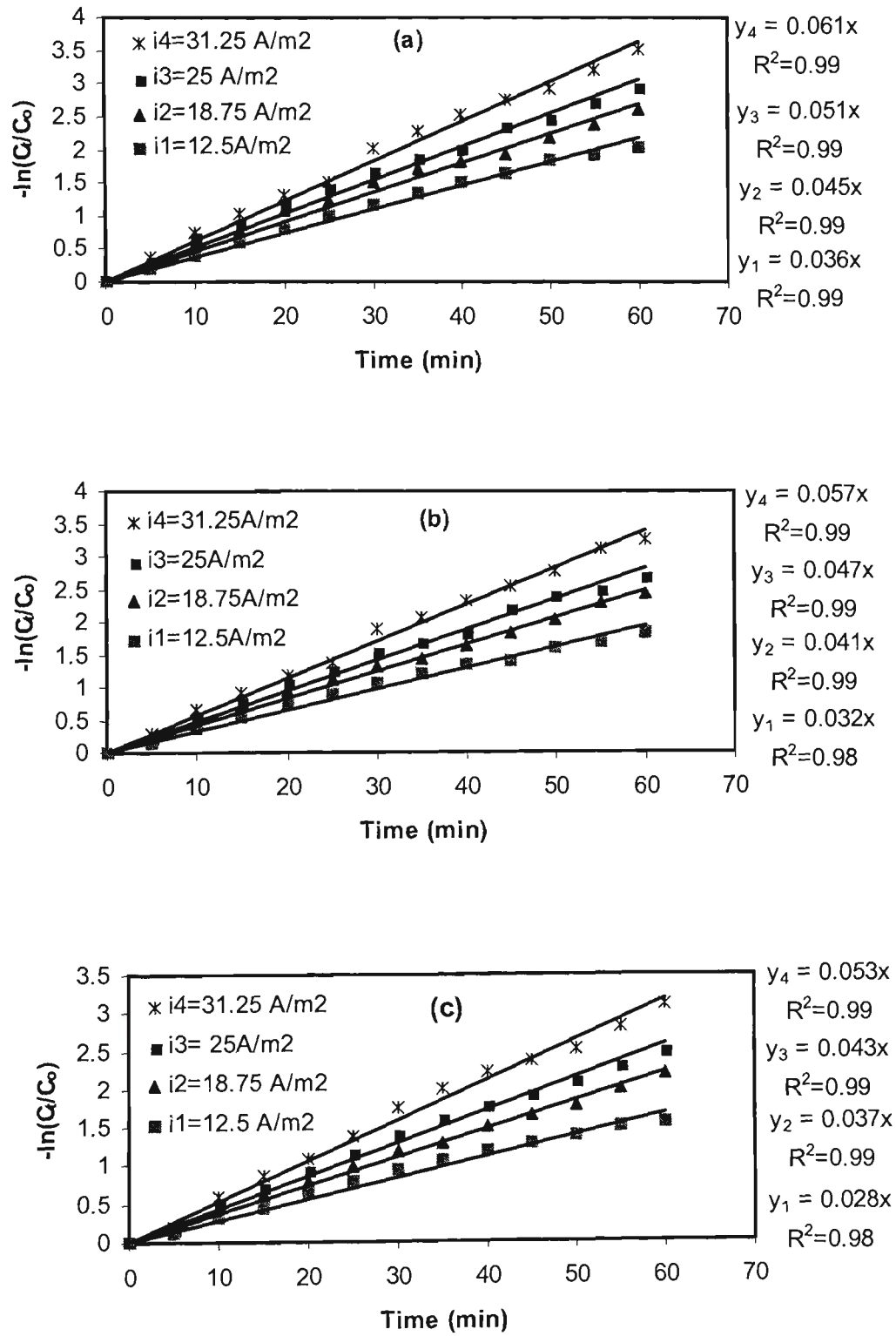


Figure 5-31 Determination of the kinetic constants of defluoridation at different current densities and electrodes distancing on ECF process [a] d=5 mm, [b] d=10 mm, [c] d=15 mm ($C_0=10 \text{ mg/L}$, $E_{cin} = 10 \text{ mS/m}$, pH = 6-8)

Chapter 5- Fluoride removal by a batch monopolar electrocoagulation reactor

From results obtained in Figure 5-31 (a, b, and c), in every experiment the logarithm linear relation for each current density confirms the fact that the kinetics of defluoridation follows the exponential law with time. At the different current densities, it appears that the reaction rate decreases when the distance between electrodes is increased in the solution. This effect is due to the higher formation rates of aluminium hydroxide for shorter inter –electrode distance in electrocoagulator. Figure 5-32 shows that fluoride removal efficiency decreased when the inter electrode distance is increased from 5 to 15 mm.

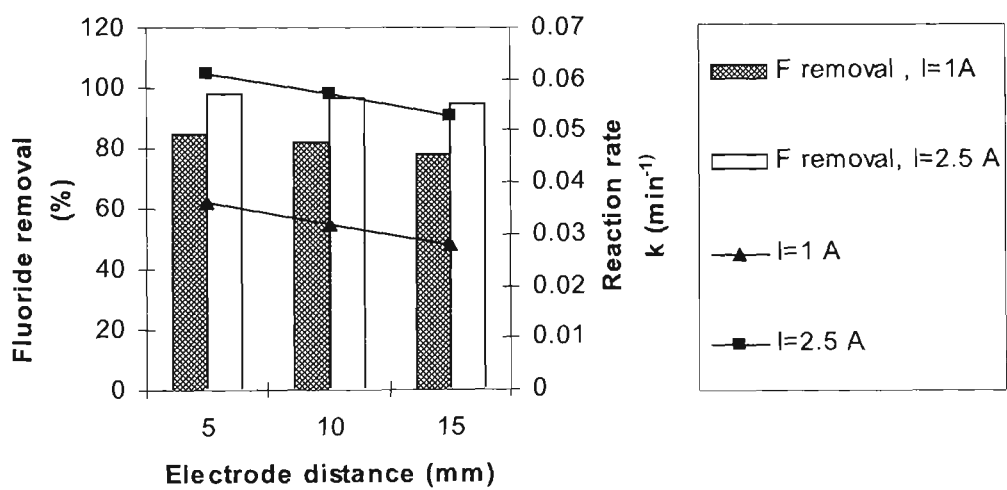


Figure 5-32 Effect of electrode gap on the electrocoagulation of fluoride at two different currents 0.5 and 1 A ($A/V=22 \text{ m}^{-1}$, $\text{pH}=6$, $E_{c_{in}}=10 \text{ mS/m}$, $C_o=10 \text{ mg/L}$, $t=60 \text{ min}$)

At 1 A operating current, the fluoride removal efficiency decreases from 85% to 75% when the distance between the electrodes is increased from 5 to 15 mm. It could be due to breaking of the fluoro-aluminium complexes formed on the anode when there is more space. The rate constants are using for the predictive equation that will be discussed in chapter 8.

5.3.7 Competition ions effects

5.3.7.1 Effect of anions (Cl^- , NO_3^- , SO_4^{2-}):

The defluoridation process by electrocoagulation process at the different anion concentrations was separately studied with using synthetic solutions. The synthetic samples were individually prepared by using NaCl (Cl^-), NaNO_3 (NO_3^-), and Na_2SO_4 (SO_4^{2-}) salts dissolved into the F^- containing solution (NaF + distilled water). The effect of some anions such as Cl^- , NO_3^- , and SO_4^{2-} on fluoride removal by the EC system is shown in Figure 5-33.

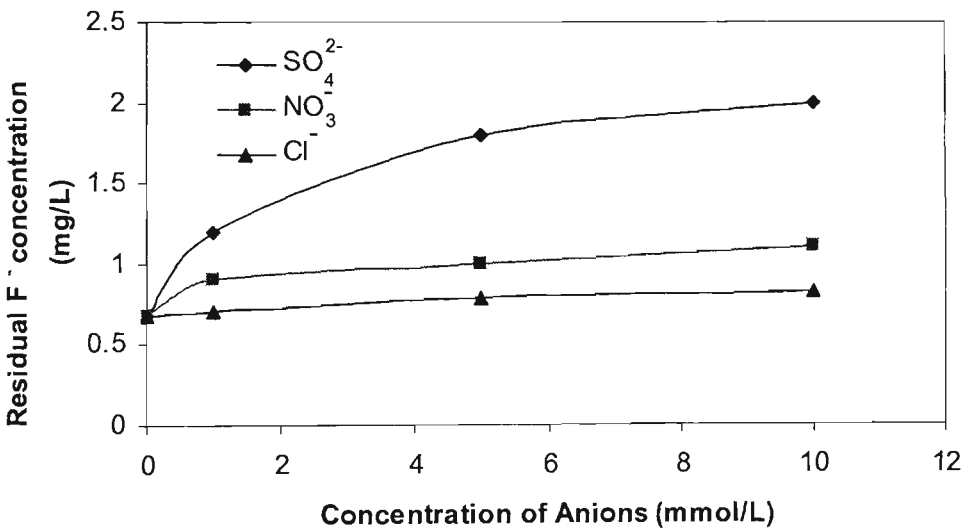


Figure 5-33 Effect of anions on defluoridation by ECF process ($C_0=15$ mg/L, pH =7, I=2 A, t=60 min, T=25 °C, and d=5 mm)

It appears that the concentrations of Cl^- and NO_3^- have no effect on defluoridation, because the affinities of Cl^- and NO_3^- ions with Al^{3+} are too small to replace F^- ions that were combined with Al^{3+} . As seen, the residual fluoride removal increases in EC process when the concentration of SO_4^{2-} ions in the solution is increased. It might be due to

competition effect stated by Hu et al. (2003). This means that increase of the concentration of sulphate anion, which has a strong affinity with Al^{3+} , decreases the adsorption capacity of fluoride onto hydrous alumina. Sulphate ion, the only possible species, is able to replace F^- ions coordinating with aluminium in the solution. The affinity of different anions with Al^{3+} are $\text{F}^- > \text{SO}_4^{2-} > \text{Cl}^- > \text{NO}_3^-$ (Hu et al., 2003).

5.3.7.2 Effect of cations (Mg^{2+} and Fe^{3+}):

To explain the effect of cation on defluoridation by the EC process, various concentrations of Mg^{2+} and Fe^{2+} cations were separately added to the synthetic sample (see Figure 5-34). The synthetic samples were individually prepared by using FeCl_3 (Fe^{3+}), and MgCl_2 (Mg^{2+}) salts dissolved into the F^- containing solution (NaF + distilled water).

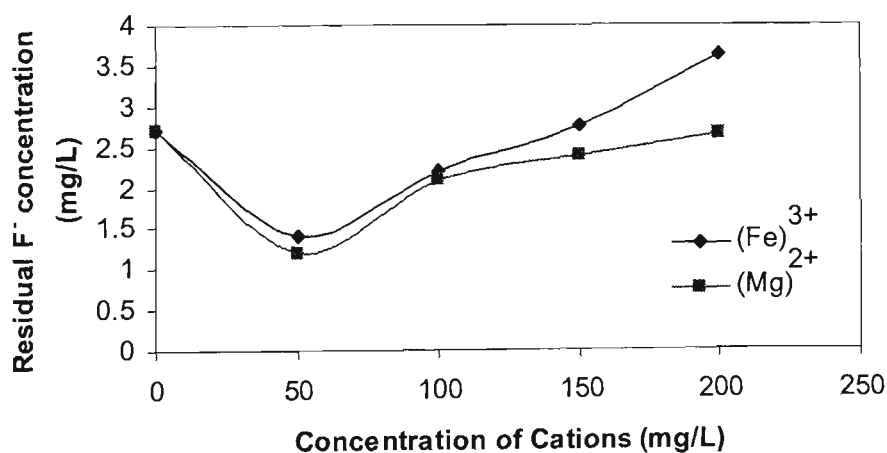


Figure 5-34 Effect of cations on defluoridation by ECF process ($C_0=15$ mg/L, pH =7, $I=1$ A, $t=60$ min, $T=25$ °C, and $d=5$ mm)

Chapter 5- Fluoride removal by a batch monopolar electrocoagulation reactor

Both Fe^{3+} and Mg^{2+} are good coagulants when they are used as a co-coagulant with aluminium salt. As seen, the residual fluoride concentration decreased when the concentrations of Mg^{2+} and Fe^{2+} cations were less than 50 mg/L and then it increased with increasing of concentration of the cations. It might be due to competition effect that means high Fe^{3+} and Mg^{2+} may lead to the precipitation of $\text{Fe}(\text{OH})_3$ and $\text{Mg}(\text{OH})_2$ onto the surface of the $\text{Al}(\text{OH})_3$ flocs, because the affinity between fluoride and $\text{Fe}(\text{OH})_3$ or $\text{Mg}(\text{OH})_2$ is much smaller than $\text{Al}(\text{OH})_3$ (Shen et al., 2003; and Hicyilmaz et al., 1997).

5.3.7.3 Effect of Ca^{2+}

The Ca^{2+} ion competition effect on defluoridation process by EC process was investigated when it was used in different range of 50-300 mg/L. Figure 5-35 shows that defluoridation is efficient when Ca^{2+} concentration in the solution is increased.

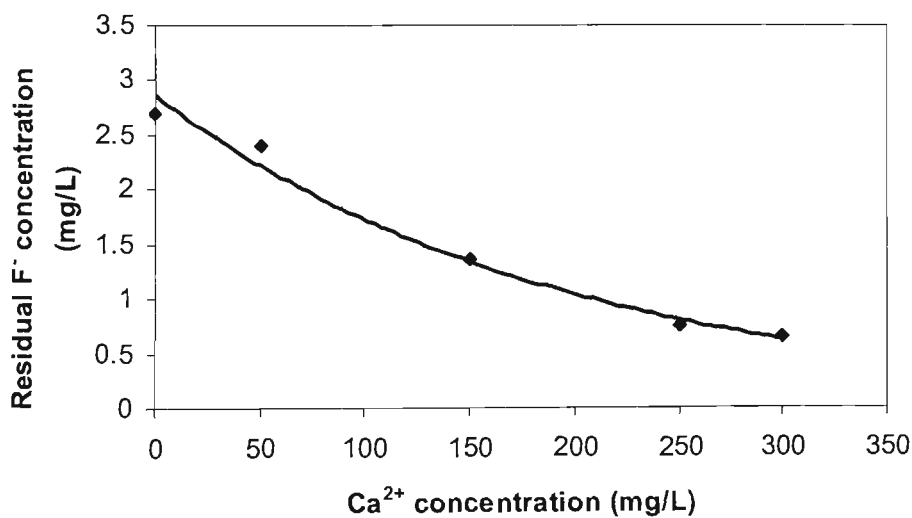


Figure 5-35 Effect of different Ca^{2+} ion concentrations on defluoridation by ECF ($C_0=15$ mg/L, pH = 7, $I=1$ A, $t=60$ min, $d=5$ mm, and $T=25$ °C)

Chapter 5- Fluoride removal by a batch monopolar electrocoagulation reactor

This is because the CaF_2 granule is aggregated by a small amount of $\text{Al}(\text{OH})_3$ floc that is formed by aluminium anode (electrode) oxidation, and then the sediment consisting of CaF_2 and small amount of $\text{Al}(\text{OH})_3$ settle at the bottom of the electrobox. The effect of the Ca^{2+} concentration on the fluoride removal during the EC process are shown in Figures 5-36 and 5-37 at different current inputs.

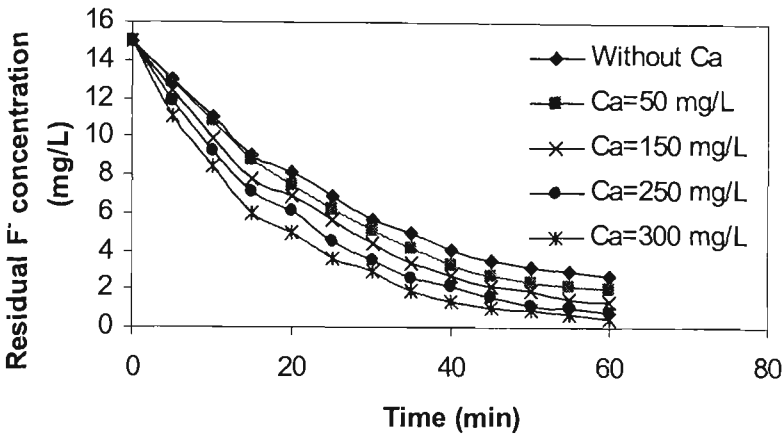


Figure 5-36 Effect of electrolysis time on defluoridation by ECF at different Ca^{2+} ion concentrations ($C_o=15$ mg/L, $\text{pH} = 7$, $I= 1$ A, $d=5$ mm, and $T=25$ °C)

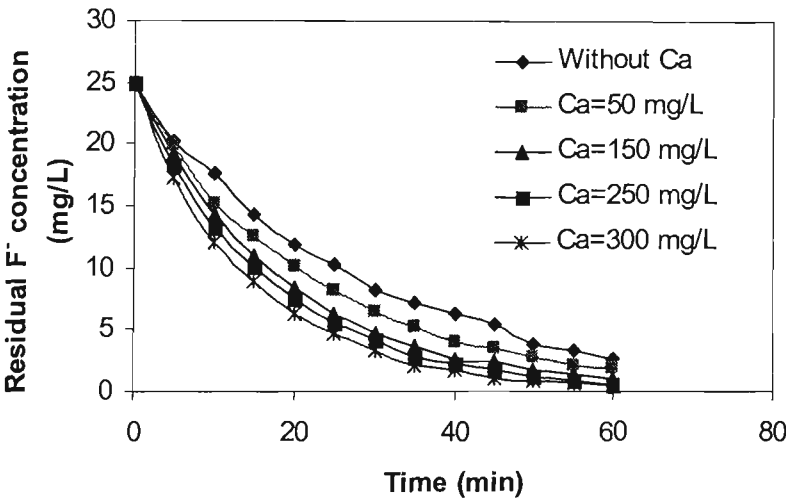


Figure 5-37 Effect of electrolysis time on defluoridation by ECF at different Ca^{2+} ion concentrations ($C_o=25$ mg/L, $\text{pH} = 7$, $I= 1.5$ A, $d=5$ mm, and $T=25$ °C)

Chapter 5- Fluoride removal by a batch monopolar electrocoagulation reactor

As seen in Figures 5-36 and 5-37, the residual fluoride concentration is decreased when the initial concentration of calcium is increased. From results obtained in Figure 5-37, the residual fluoride is decreased from 1.85 to 0.54 mg/L when initial concentration of calcium is increased from 50 to 300 mg/L at a constant current value of 1.5A and 60 min electrolysis time. This can be explained by the fact that most fluoride is treated in the precipitation process by formation of CaF_2 and the addition of Al ions.

Plots of $-\ln(C_t/C_0)$ with time for various calcium concentrations is shown in Figure 5-38 when the initial fluoride and current value are 25 mg/L and 1.5A respectively.

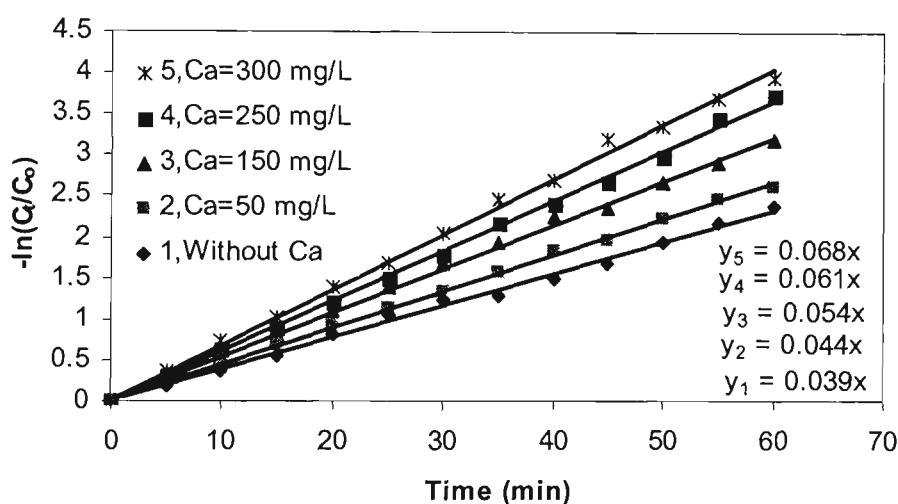


Figure 5-38 Determination of the kinetic constants of defluoridation process at different calcium concentrations on ECF process ($C_0=25$ mg/L, pH= 7, $I= 1.5$ A, $d=5$ mm, and $T=25$ °C)

It can be seen that rate of defluoridation increases from 0.039 to 0.068 min^{-1} when calcium is increased from 0 to 300 mg/L in the solution. However it is important to keep in mind that at higher initial calcium where more fluoride is removed, excess residual

calcium will be more available in the effluent (see Figure 5-39). Increasing Ca^{2+} in the solution will increase hardness in drinking water.

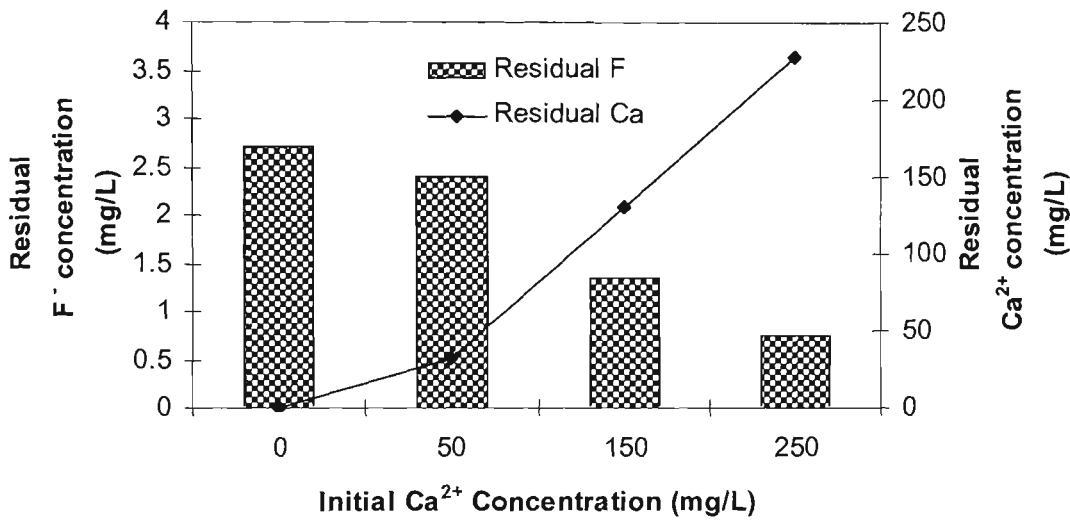


Figure 5-39 Effect of initial Ca^{2+} ion concentrations on defluoridation by ECF and residual calcium concentration in the solution ($C_o=15$ mg/L, $\text{pH} = 7$, $I= 1$ A, $t = 60$ min, $d=5$ mm, and $T=25$ °C)

By adding 250 mg/L of Ca^{2+} ions to the solution, defluoridation increased by approximately 13%. As shown in Figure 5-39 the residual calcium is increased when higher initial calcium is used. By increasing calcium to 250 mg/L, residual fluoride is decreased to 0.75 mg/L when the residual calcium reaches 228 mg/L. Consequently the Ca^{2+} ion is effective in defluoridation by ECF process but its concentration in drinking water must be controlled. The maximum acceptable level for hardness in drinking water is 200 mg/L (CaCO_3) which is caused by calcium and magnesium salt (NHMRC and ARMCANZ, 2004).

5.3.8 Particles size effects

Particle size is a characteristic dimension which is determined by its geometry. Spherical particles are described by their diameter but this does not apply for non-spherical particles. For example, a flake or fibre has different dimensions in different directions. Particles of identical shape can be composed of different chemical substances and have different densities. The differences in shape and density cause considerable confusion in defining particle size. The size of a homogeneous spherical particle is uniquely defined by its diameter. Derived diameters are determined by measuring a size-dependent property of the particle and relating it to a single linear dimension. The most widely used of these are the equivalent spherical diameters.

The surface to volume ratio is of fundamental importance since it controls the rate at which the particle reacts with its surroundings (Allen, 1997). This is given by:

$$\frac{S}{V_{sp}} = \frac{\pi d_s^2}{\frac{\pi}{6} d_v^3} = \frac{6 d_s^2}{d_v^3} \quad (5-2)$$

$$S_v = \frac{6}{d_{sv}} \quad (5-3)$$

where,

S Surface area of a sphere;

V_{sp} Volume of a sphere;

d_v Diameter of a sphere having the same volume as the particle;

d_s Diameter of a sphere having the same surface as the particle;

Chapter 5- Fluoride removal by a batch monopolar electrocoagulation reactor

S_v Surface to volume ratio;

d_{sv} Diameter of a sphere having the same external surface to volume ratio as the particle

Particle size was determined using the Galai CIS-100 particle counter. The system consists of a laser based analyser. A beam of laser starting from the generator is filtered, enlarged, and collimated until it becomes parallel. When particles are placed homogeneously in the parallel beam in some special way, diffraction and scattering occur and part of beam will diffuse outwardly at some angle to light axle. The Galai CIS-100 system contains a cuvette with a magnetic stirrer that disperses the particles equally in a liquid medium in order to maintain a uniform suspension of particles. This instrument was connected to a PC, and the analysed results were displayed on the PC monitor. The instrument operates in the size ranges 0.7 to 150, 2 to 300, 5 to 600 and 12 to 1200 μm . The product sample after ECF process was injected to a cuvette with a very small magnetic bar-stirrer, and then put into the analyser. The particle counter had an acquisition range of 0.5 to 150 μm particle diameter. The measurement style was normally set to 'Regular' and stirring speed was 'Speed 2'. After processing, all the tables and figures could be seen on the PC monitor. When certain physical characteristic of a particle are the same as or approximately the same as a spherical particle of the same constitution, the diameter of this particle is represented by the diameter of a sphere. The diameter of a particle is normally expressed by micrometer. The median of a particle size distribution is the size of which we can find 50% of the volume of all particles. The median divides the distribution into two equal parts, i.e. 50% of the

Chapter 5- Fluoride removal by a batch monopolar electrocoagulation reactor

cumulative distribution curve. The mean is an “average” particle size. There is no unique mean. We can average all particle diameters, weighting them according to their volumes, surface areas, numbers or any other physical characteristic. The mean (\bar{X}) is the centre of gravity of the distribution. For the mean, the moment of the sums of the elementary areas of the relative distribution, of width dx , about the ordinate, equals the sum of the moments of the elements about the ordinate (Allen, 1997):

$$\bar{X} = \frac{\sum x d\phi}{\sum d\phi} \quad (5-4)$$

where ϕ can be number, mass or volume distribution, as for a number distribution $d\phi = dN$ and:

$$\bar{X} = \frac{\sum x dN}{\sum dN} = x_{NL} \quad (5-5)$$

where N is the number of particles. For a mass (volume) distribution $d\phi = dV = x^3 dN$ giving:

$$\bar{X} = \frac{\sum x dV}{\sum dV} \quad (5-6)$$

$$\bar{X} = \frac{\sum x(x^3 dN)}{\sum x^3 dN} \quad (5-7)$$

$$\bar{X} = \frac{\sum x^4 dN}{\sum x^3 dN} = x_{VM} \quad (5-8)$$

The mode is the most commonly occurring (most popular) value in a distribution and passes through the peak of the relative distribution curve, i.e. it is the value at which the frequency is maximum (Figure 5-40).

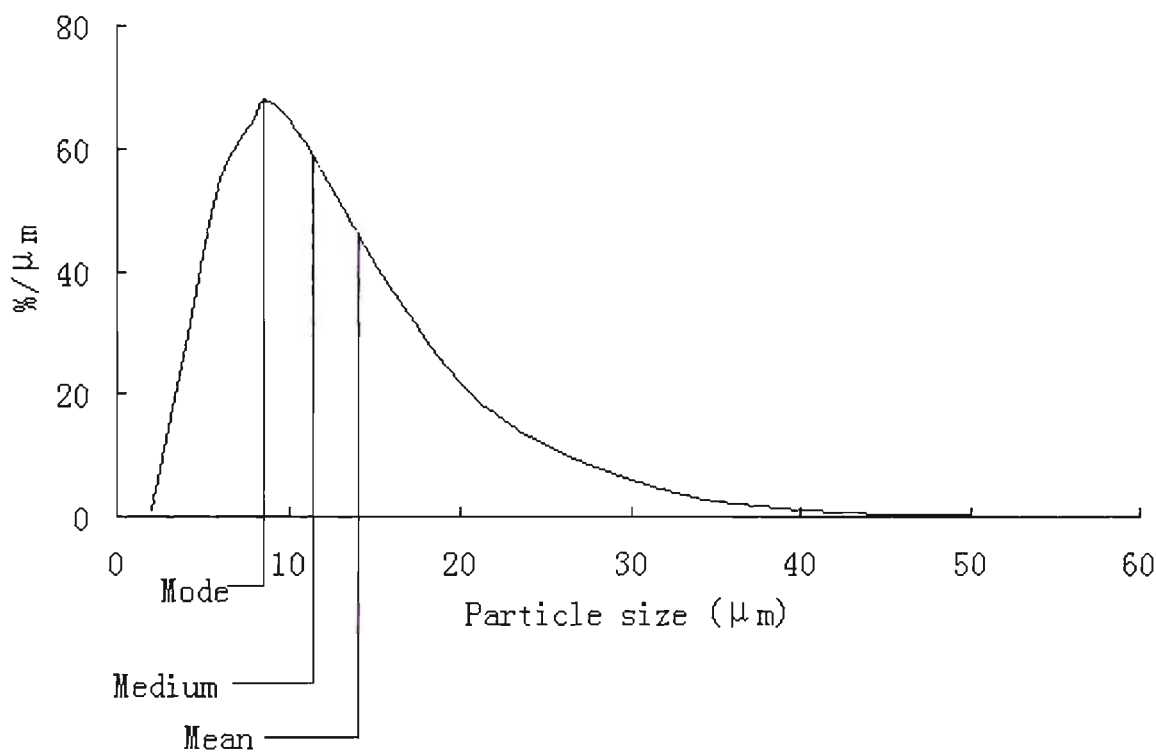


Figure 5-40 Definitions of the most popular values in a distribution curve (Adapted from Allen, 1997)

There are 7 definitions of mean particle size, as these mean diameters are defined in Table 5-7. Based on these definitions, shown in Table 5-7, the values of some experimental results are given in Table 5-8. Particles in sludge vary in size, constituency, and shape which make it difficult to characterise sludge by particle size. Sludge is composed of many different sized particles which change with time and experimental conditions, including the current applied, pH solution, mixing rate and

Chapter 5- Fluoride removal by a batch monopolar electrocoagulation reactor

temperature of solution. The experiments have been conducted in different current values and electrolysis time when pH of solution and temperature was 6 and 25°C, respectively.

Table 5-7 Definitions of mean diameters of particles (Allen, 1997)

Number, length	$x_{NL} = \frac{\sum dL}{\sum dN} = \frac{\sum xdN}{\sum dN}$
Number, surface	$x_{NS} = \sqrt{\frac{\sum dS}{\sum dN}} = \sqrt{\frac{\sum x^2 dN}{\sum dN}}$
Number, volume	$x_{NV} = \left(\frac{\sum dV}{\sum dN}\right)^{\frac{1}{3}} = \left(\frac{\sum x^3 dN}{\sum dN}\right)^{\frac{1}{3}}$
Length, surface	$x_{LS} = \frac{\sum dS}{\sum dL} = \frac{\sum x^2 dN}{\sum xdN}$
Length, volume	$x_{LV} = \sqrt{\frac{\sum dV}{\sum dL}} = \sqrt{\frac{\sum x^3 dN}{\sum xdN}}$
Surface, volume	$x_{SV} = \frac{\sum dV}{\sum dS} = \frac{\sum x^3 dN}{\sum x^2 dN}$
Volume moment	$x_{VM} = \frac{\sum dM}{\sum dV} = \frac{\sum x^4 dN}{\sum x^3 dN}$

Table 5-8 Calculated values of mean diameters for selection of particles in the different electrolysis time by EC process (I=1.5A, C_o=10 mg/L, pH=6, d=5mm, and T=25°C)

Time (min)	15	30	45	60
Mean diameter (μm)				
X _{NL}	1.02	1.59	1.89	1.39
X _{NS}	1.21	2.07	2.5	2.16
X _{NV}	1.53	2.99	3.99	4.38
X _{LS}	1.43	2.68	3.29	3.36
X _{LV}	1.87	4.11	5.8	7.77
X _{SV}	2.45	6.28	10.20	14.58
X _{VM}	4.01	15.95	31.49	45.33

From Table 5-7 the mean diameters can be defined with various ratios. The surface to volume ratio was examined and is reported here, as this ratio “is of fundamental importance”, controlling reaction rates between the particle and its surroundings (Allen 1997).

5.3.8.1 Effect of the charge on the aggregate size

The size of particles in the solution during 60 min electrocoagulation/flotation was measured to investigate the ECF process. The ratio of surface to volume, which controls the reaction rate, was selected in the experiments to define the mean diameter of particle size. Figure 5-41 illustrates the effect of electrolysis time on floc size in the ECF process.

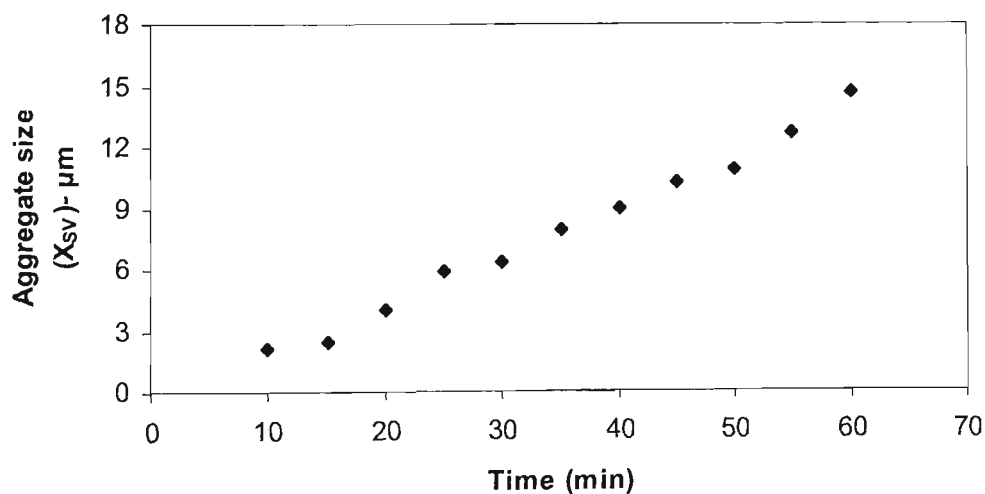


Figure 5-41 Effect of electrolysis time on the floc size in the ECF process ($I=1.5A$, $C_o=10\text{ mg/L}$, $pH=6$, $d=5mm$, and $T=25^{\circ}C$)

As seen, flocs grow bigger when the electrolysis time is increased in EC system for a given current. It is because when the electrolysis time is increased the molar

concentration of aluminium increases in the solution. Obviously the coagulant dosage has a significant effect on the size of the floc formed. The larger the floc formed by electrocoagulation the more easily the particles would be settled that would increase the efficiency of the treatment. The experimental results showed that the different initial fluoride concentrations had no significant effect on floc size while a complete table of results together the volume distribution particle sizes are shown in Appendix C. It seems that the mean diameter of floc size increases with increasing of current values. As noted in sections 5.3.1 and 5.3.2 defluoridation is increased when the current values and electrolysis time increase in ECF system. As seen in Figure 5-42, the combination of electrolysis time and current value (charge) have significant effects on the size of floc formed in ECF process.

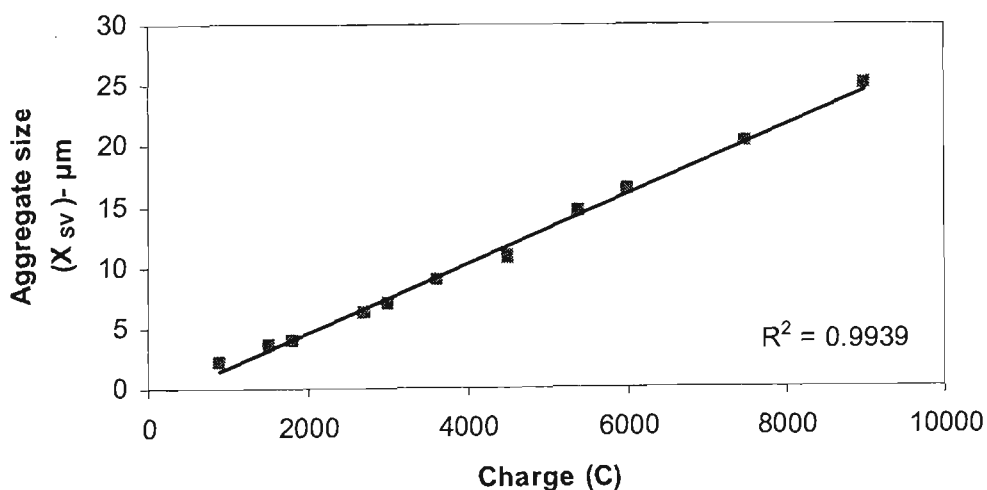


Figure 5-42 Effect of current value and electrolysis time on the floc size in the ECF process ($C_0=10$ mg/L, pH =6, d=5mm, t= 5-60 min, I=1.5-2.5A, and T=25°C)

Chapter 5- Fluoride removal by a batch monopolar electrocoagulation reactor

As seen, the aggregate sizes become bigger when the charge value is increased in EC system. The ratio of surface to volume (mean particle size) increases from 2 to 25 μm when charge value is increased from 900 to 9000 C. This increase might be attributed to the formation of aluminium hydroxide or oxide (Holt et al., 2002). Thus the greater the amount of coagulant, the more pollutant particles bind to form aggregates which are then removed by decantation or flotation. As noted in section 5.3.6, the optimum charge was found to be 5000 -5400 C when initial fluoride concentration was 10 mg/L. At this charge range, the mean particle size was found 13-15 μm and the residual aluminium concentrations on the effluent were less than 0.2 mg/L.

5.3.9 Zeta potential for electrocoagulation

The stability of particle suspensions, colloidal dispersions, emulsions and other similar systems is strongly influenced by the electrical charges that exist at the particle-liquid interface. Most fine particles suspended in fresh water have a net negative charge. Positive ions reduce the net negative charge and make flocculation more likely. The development of a net charge at the surface of a particle affects the distribution of ions in the surrounding interfacial region, and then a double electrical layer exists around each particle. The liquid layer surrounding the particle may be considered as an inner region that includes ions bound relatively to the surface and an outer or diffused region in which ion distribution is determined by a balance of electrostatic forces. Overall, an individual particle and its most closely associated ions move through the solution as a unit, and the potential at the boundary of this unit is known as the zeta potential. Zeta

potential thus provides a measure of the level of the surface charge and serves as an indicator of the relative magnitude of the repulsion force between colloidal particles in aqueous suspension. When colloidal particles are sufficiently low in surface charge or the electrolyte content of the water is elevated, colloidal particles may be pulled together by van der Waals attraction in what we recognise as flocculation (Benefield, 1982). As discussed above, the zeta potential provides an effective measurement of the charge on the particle. Generally, the zeta potential decreased with increasing pH (Letterman et al., 1999). So the pH in each experiment is kept constant around 8. The zeta potential was measured using a Malvern Zetasizer 1000/3000 in this research. Figure 5-43 presents the zeta potential measurements for the electrocoagulation reactor as a function of electrocoagulation time for a current value of 2.5 A along with residual fluoride concentration relative to the initial fluoride of 10 mg/L.

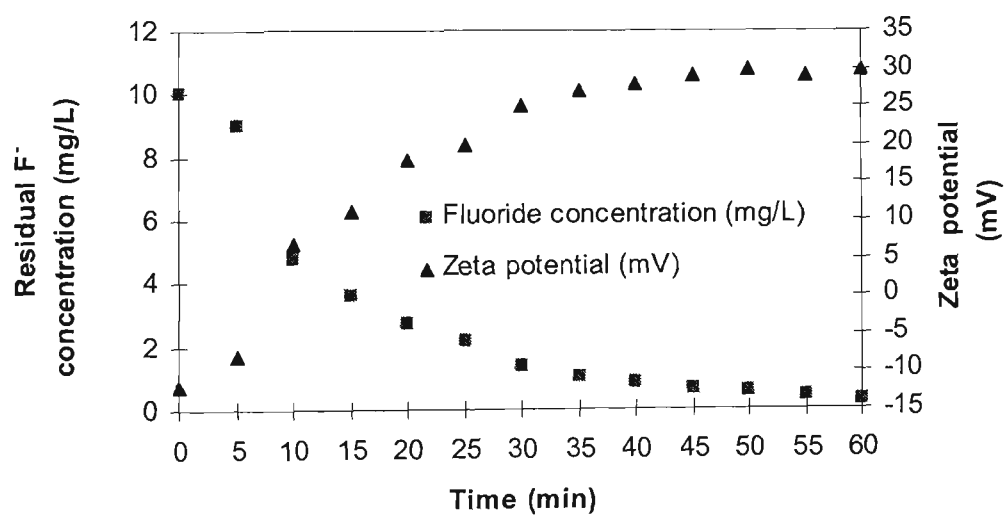


Figure 5-43 Effect on Electrocoagulation reactor’s zeta potential and residual fluoride concentration with electrolysis time on defluoridation (I=2.5A, pH = 8, C₀=10 mg/L)

Chapter 5- Fluoride removal by a batch monopolar electrocoagulation reactor

At beginning of the EC process (5 min electrolysis time), there was no very significant change observed in the zeta potential because in low ionic concentrations limits the possible coagulation mechanisms. As a result, increasing the electrolysis time will increase the Al concentration into solution. Addition of aluminium coagulant could contain the electric double layer around the colloidal particles, decreasing repulsion and encouraging aggregation of the pollutant. Cationic coagulants provide positive electric charges to reduce the negative charge (zeta potential) of the colloids (Holt, 2003). Since the amount of coagulant dissolved at the anode increases, the residual fluoride concentration is decreased and the zeta potential increases. As the system moved into the more electrolysis time (i.e. $t > 35$ min), the rate of fluoride removal continued to decrease from 1 to 0.4 mg/L, while the zeta potential increased from 27 to 30 mV. As noted in section 5.3.6, the optimum detention time was found to 35 min for reducing fluoride concentration from 10 to 1 mg/L when current value was 2.5A. It seems that after 35 min electrolysis time, low increase in zeta potential indicates stabilization of the solution when the fluoride removal rate is very slow in the stable stage.

5.3.10 Sludge production in ECF process

As noted in chapter 4 there are three main mechanisms within an ECF process, including Electrode oxidation, gas bubble generation, and flotation and sedimentation of flocs formed. Electrodes are arranged at the bottom of an ECF tank, which is then filled with waste water containing dispersed solids. Figure 5-44 (a, and b) presents the SEM images of the anode surface before and after defluoridation in the ECF system.

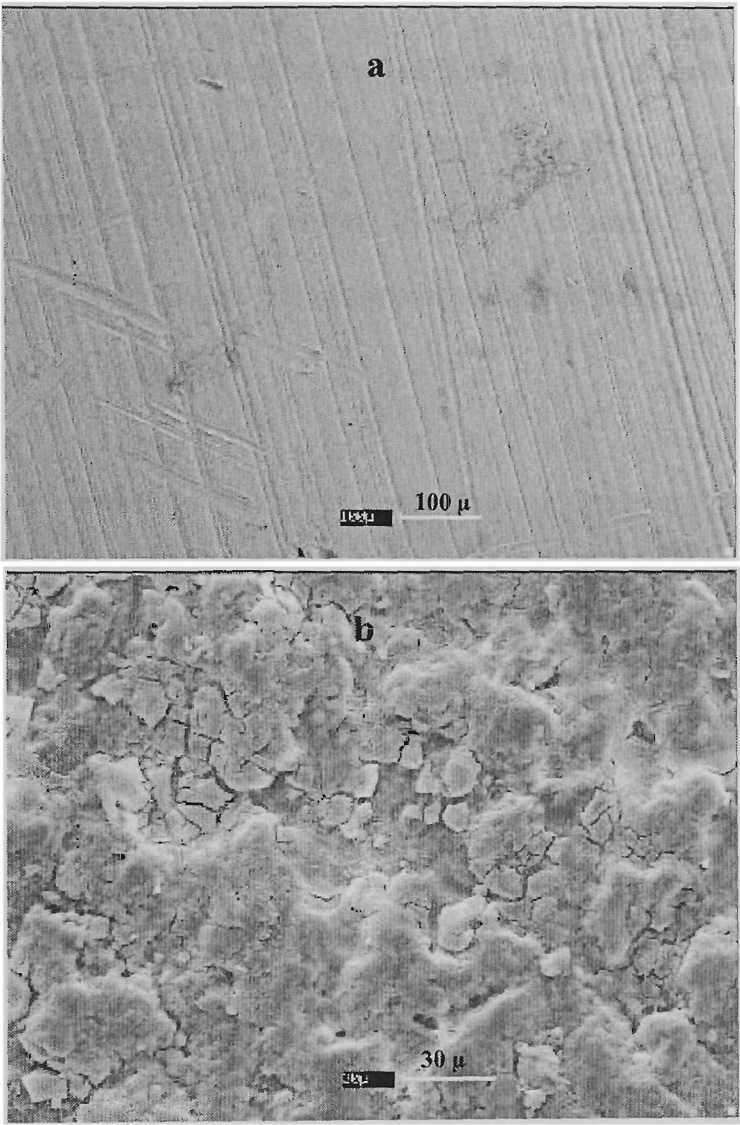


Figure 5-44 SEM images of the anode surface (a) before and (b) after ECF process

As seen, a gelatinous deposition layer is present on the surface of the anode after EC process. This is because the electro-condense effect induces the accumulation of fluoride ions near the anode and leads to surface co-precipitation on the anode. In ECF technology, small bubbles are used to capture contaminant particles and float them to the surface for removal. Bubbles of hydrogen are produced when current is passed through the electrodes and water is broken down through electrolysis. The hydrogen gas bubbles

Chapter 5- Fluoride removal by a batch monopolar electrocoagulation reactor

rise through the waste water attaching to insoluble contaminant particles such as hard to treat metals and organic substances. A foamy layer called floto-sludge, gathers at the surface and is separated from the purified water by mechanical skimming or other means. The sludge is then collected from base and surface of the electrobox for disposal, as shown in Figure 5-45 (a, and b).

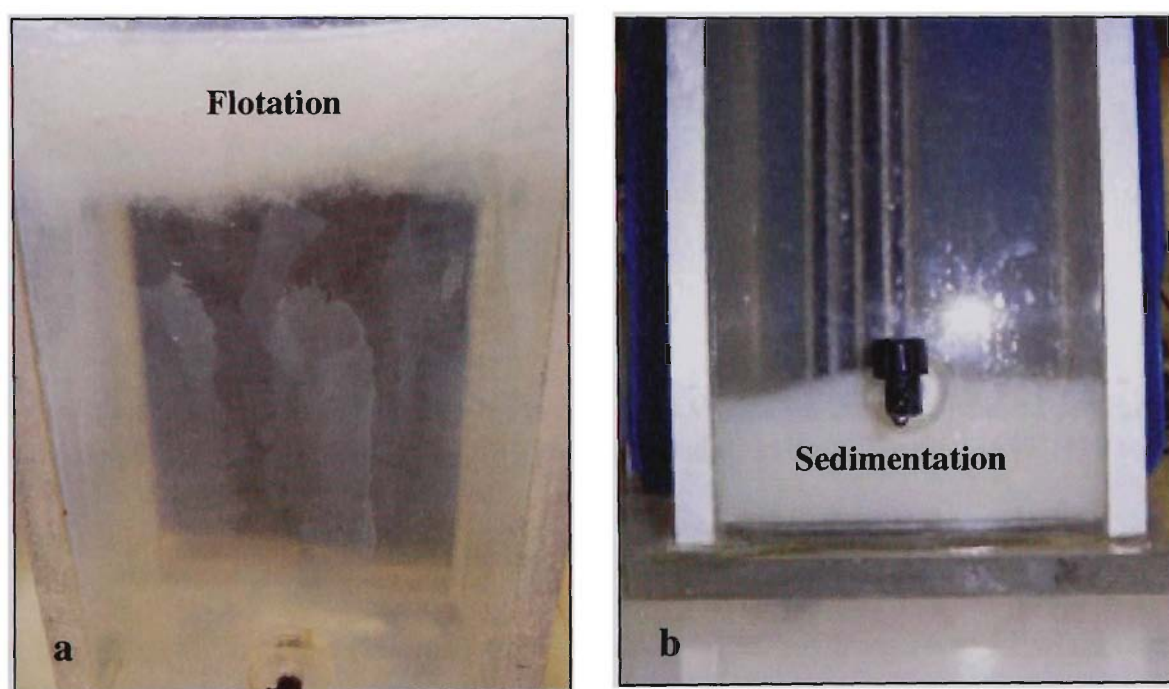


Figure 5-45 Images of the sludge formation on the defluoridation by ECF process (a) flotation of sludge, (b) sedimentation of sludge.

The characterisation of the deposited layer in the surfaces of the electrode and oxide particles in the settled and floated sludge will be explained in chapter 7. The ECF process produced a considerable amount of sludge that was properly collected, volumetrically measured, and analysed. The test is conducted in an Imhoff cone, allowing 1 h settling time. Results are measured and reported in terms of mL of sludge

volume (V_s) to 1 L of sample volume (V). Figure 5-46 shows the ratio of (V_s/V) versus the electrolysis time at different current values. The sludge volume continuously increased in direct proportion to the electrolysis time and applied current values.

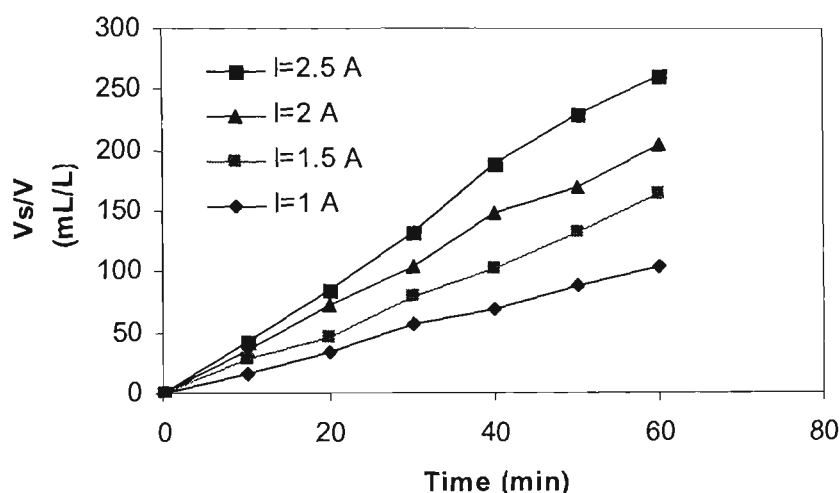


Figure 5-46 Effect of electrolysis time and current values on the ratio of total produced sludge volume/ sample volume (V_s/V) for defluoridation by ECF process ($C_o=10$ mg/L, pH = 8, $d=5$ mm, and $T=25$ °C)

At low electrolysis times (10 min), the ratio of V_s/V ranged from 16 to 42 when current values were increased from 1 to 2.5A respectively. At an electrolysis time of 30 min, this ratio increases from 57 and 132 when the current value is increased from 1 to 2.5A, respectively. It is expected that volume of sludge increases in the electrocoagulator when the current values and time are increased. The collected total sludge mass on the ECF process is also plotted versus the electrolysis time as a function of different current values in Figure 5-47 (a, b, c, and d). At an electrolysis time of 60 min, the collected total sludge mass increased from 1.1 to 2.9 g when the current value increase from 1 to 2.4A.

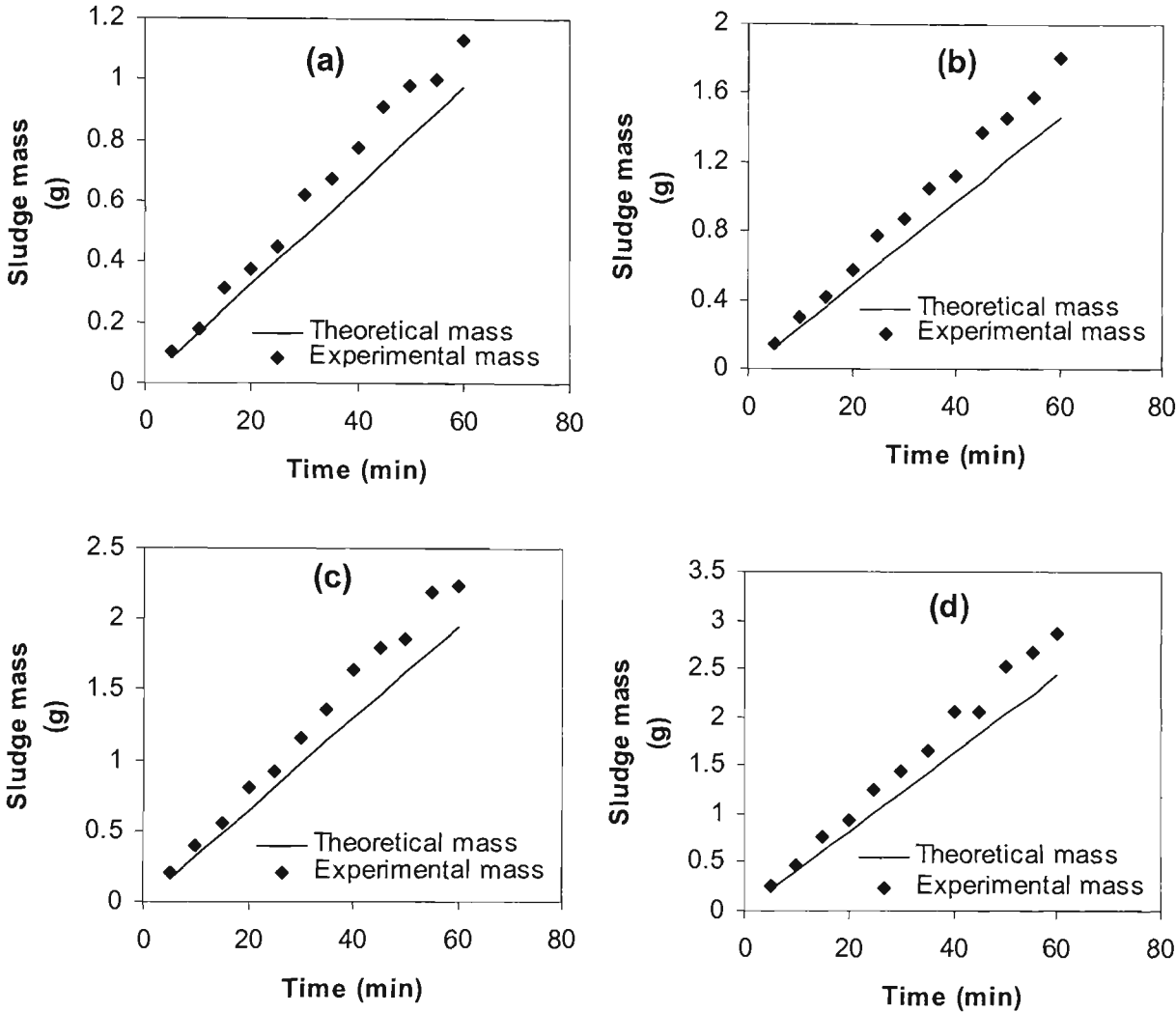


Figure 5-47 Collected total sludge mass versus electrolysis time in different current values for defluoridation by ECF process, [a] $I=1A$, [a] $I=1.5A$, [a] $I=2A$, [a] $I=2.5A$, ($C_o=10\text{ mg/L}$, $pH = 8$, $d=5\text{mm}$, and $T=25\text{ }^{\circ}\text{C}$)

All the curves show a continuous pattern of increasing in direct proportion to the current values and electrolysis time. Theoretically, based on Faraday’s law (Eq. 2-9), charge should affect the quantity of aluminium released to a system using aluminium electrodes. Thus, the amount of experimental sludge volume and mass values that are produced in the cell are higher than the theoretical values. As noted in section 5.3.1, it

could be due to increase the current efficiency which ranging from 100 - 130% for the batch system. It is expected that volume and mass of sludge depends on the charge applied. The collected total sludge volume and mass on the ECF process are respectively plotted versus the charge values in Figures 5-48 and 5-49.

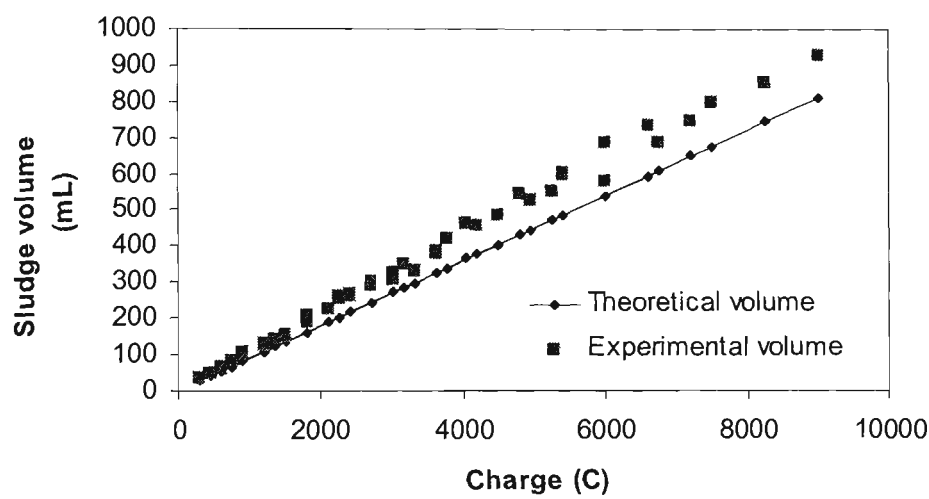


Figure 5-48 Colleted total sludge volume versus charge value for defluoridation by ECF process ($C_o=10$ mg/L, pH = 8, d=5 mm, and T=25 °C)

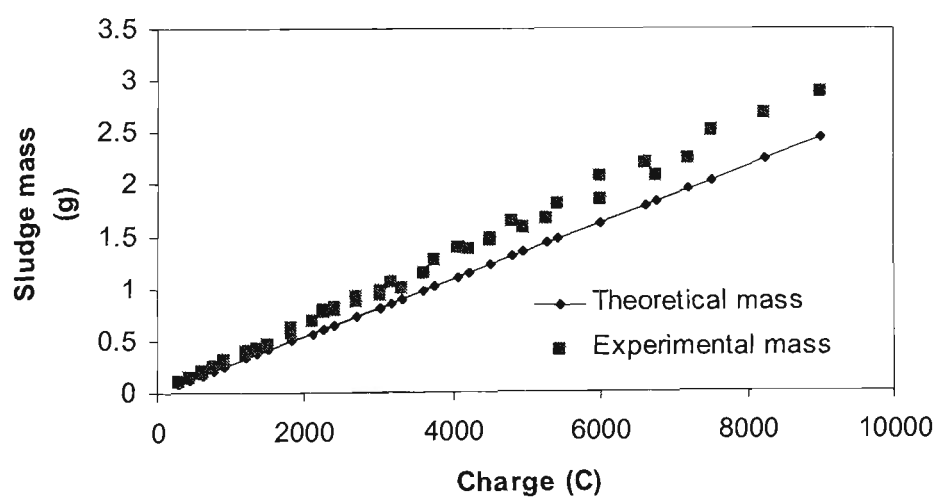


Figure 5-49 Colleted total sludge mass charge value for defluoridation by ECF process ($C_o=10$ mg/L, pH = 8, d=5mm, and T=25 °C)

Chapter 5- Fluoride removal by a batch monopolar electrocoagulation reactor

As seen, the experimental sludge volume and mass values respectively increase to 950 mL and 2.9 g when the charge value is increased to 9000 C. All the curves show a continuous pattern of increasing in direct proportion to the charge values. This is to be expected that a general pattern may be observed from Figures 5-48 and 5-49 that demonstrates higher sludge volume and amounts of sludge mass resulting from an increase in charge values. As noted in above, the amount of experimental sludge volume and mass values are higher than the theoretical values (it was previously explained in section 5.3.1). From results obtained in Table 5-5, the optimum charge value was considered to be 5000-5400 C when the initial fluoride concentration was 10 mg/L, Thus the sludge volume and mass can be decreased while the optimum charge is considered in this range for the batch system and the residual aluminium concentrations on the effluent are found to be less than 0.2 mg/L. More details to determine the sludge composition by XRD spectrum will be explained in chapter 7.

5.4 SUMMARY

Batch experiments were designed to study the effects of parameters such as current density, electrolysis time, solution pH, distance between electrodes, initial concentration of fluoride, electrolyte conductivity, particle size, zeta potential, aluminium concentration ($\text{Al}^{3+}/\text{F}^-$ mass ratio), anion and cations effects (specially Ca^{2+} effect) on the fluoride removal efficiency. The experimental results showed that there is linear relationship between charge value and total aluminium concentration. Since the amount of coagulant dissolved at the anode increases, the residual fluoride concentration is

Chapter 5- Fluoride removal by a batch monopolar electrocoagulation reactor

decreased and the zeta potential increases. The results showed that residual fluoride reached from 10 mg/L to less than 1 mg/L when the optimal electrolysis time was 55, 45 and 35 min at a current range of 1.5, 2 and 2.5 A. Thus the combination of current and time determine the pollutant removal. The residual fluoride concentration reached to 1 mg/L when the total aluminium concentration was between 120-155 mg/L. The optimum charge values were found between 5000 -5400 C and 9500-10500 C for the initial fluoride concentrations 10 and 25 mg/L, respectively. The experimental mass ratio $\text{Al}^{3+}/\text{F}^-$ was found between 13-17.5 in a monopolar ECF process when the residual aluminium concentrations on the effluent were found to be less than 0.2 mg/L which is desirable concentration based on NHMRC and ARMCANZ (2004) guideline. When the distance between the cathodes and the anodes was increased the resistance between electrodes increased hence fluoride removal decreased. The linear relation between $-\ln(C_t/C_o)$ with time confirms the fact that the kinetics of defluoridation follows the exponential law. The F^- removal by ECF follows a simple first order process. The experimental results also showed that defluoridation is more efficient when the pH is constant between 6 and 8 during experiments. The concentration of Cl^- and NO_3^- had no significant effect on defluoridation by the EC process while it was found that Ca^{2+} ion is more efficient for defluoridation process. By adding 250 mg/L of Ca^{2+} ions to the solution, defluoridation increased by approximately 13%. The experimental results showed that the aggregate sizes become bigger when the charge value is increased in EC system. The larger the floc formed by electrocoagulation, the more easily the particles would be settled which would increase the efficiency of the treatment. This is to be expected that a general pattern may be observed from experimental results that

Chapter 5- Fluoride removal by a batch monopolar electrocoagulation reactor

demonstrates higher sludge volume and amounts of sludge mass resulting from an increase in charge values. This chapter has attempted to demystify electrocoagulation by showing that it is possible to classify a wide diversity of reactor systems on a simple basis, to obtain and interpreter detailed dynamic data from a batch reactor system, and to show that the results obtained would be undertaken for designing of continuous flow reactor. The results obtained in batch mode operation showed the merits of this technique and the development for continuous flow operation which is discussed in the next chapter.

CHAPTER 6

CHAPTER 6

FLUORIDE REMOVAL BY A CONTINUOUS FLOW EC REACTOR

6.1 INTRODUCTION

In the previous chapter an explanation of the process of defluoridation process by a batch ECF system was presented. The batch experimental results generally indicated that the electrocoagulation technology using Al electrodes is an effective process for defluoridation. It is expected that outcome of a batch study would be used to design the continuous reactor. This chapter presents results and discussion associated with the design, construction, and operation of a continuous flow reactor for defluoridation based on results from the batch experiments. Several sections in this chapter discuss information related to the effects of operational parameters such as, flowrate, current density, detention time, initial pH, the volume of sludge produced in the sedimentation tank, and initial concentration of fluoride concentration on its removal. Towards the end of this chapter, information regarding the specific electrical energy consumption is also included to provide an estimation of the operational cost of fluoride removal by the EC system.

6.2 MATERIALS AND METHODES

6.2.1 Continuous flow ECF design

A continuous electrocoagulation laboratory reactor, including an EC reactor and sedimentation and flotation sections was designed and constructed. A schematic and

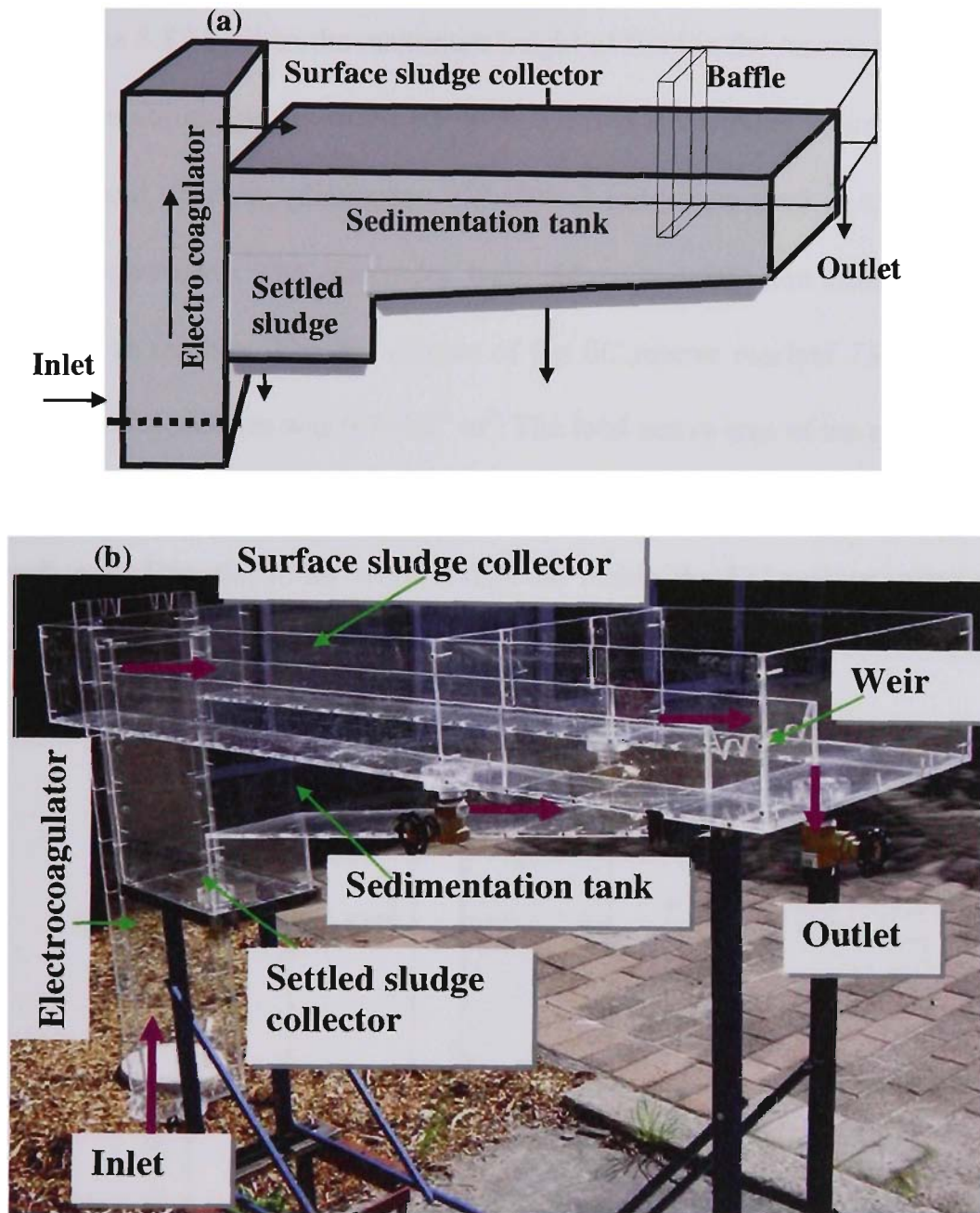


Figure 6-1 [a] Schematic and [b] image of a continuous flow EC reactor

The volume of the continuous flow EC reactor and the area of electrodes were designed according to the A/V ratio on the batch reactor and other literature review data (refer to Table 5-1). The EC reactor, as shown in Figure 6-2, was manufactured from Perspex and is 210 mm long by 48mm wide by 1000 mm high. The total dead volume is 8.87 L when the maximum height of fluid in the reactor was 880 mm. Two

from Perspex and is 210 mm long by 48mm wide by 1000 mm high. The total dead volume is 8.87 L when the maximum height of fluid in the reactor was 880 mm. Two plate aluminium (purity of Al 95–97%, Ullrich Aluminium Company Ltd, Sydney) anodes and cathodes (dimension 950×200×3 mm) were used in the electrochemical cell as electrodes. The electrodes were submerged 800 mm deep into an aqueous solution in the box. The net volume of the EC reactor reached 7.9 L when the total volume of electrodes was $9.7 \times 10^{-4} \text{ m}^3$. The total active area of the anode was 0.16 m^2 . The gap between the two neighbouring electrode plates was kept constant 5 mm for each run. The electrodes were connected inside the EC reactor using monopolar configuration.

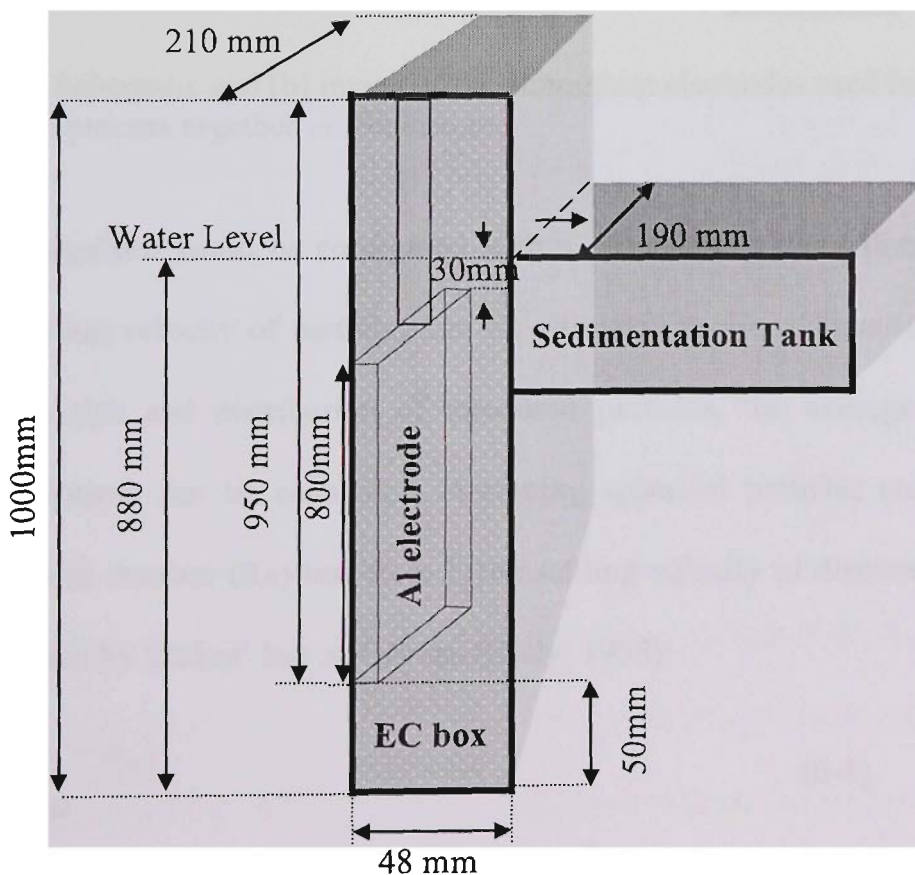


Figure 6-2 Schematic of an electrocoagulator used in continuous EC process including its dimension

Image of the aluminium electrodes used in EC process together its dimensions are shown in Figures 6-3 (a, and b).

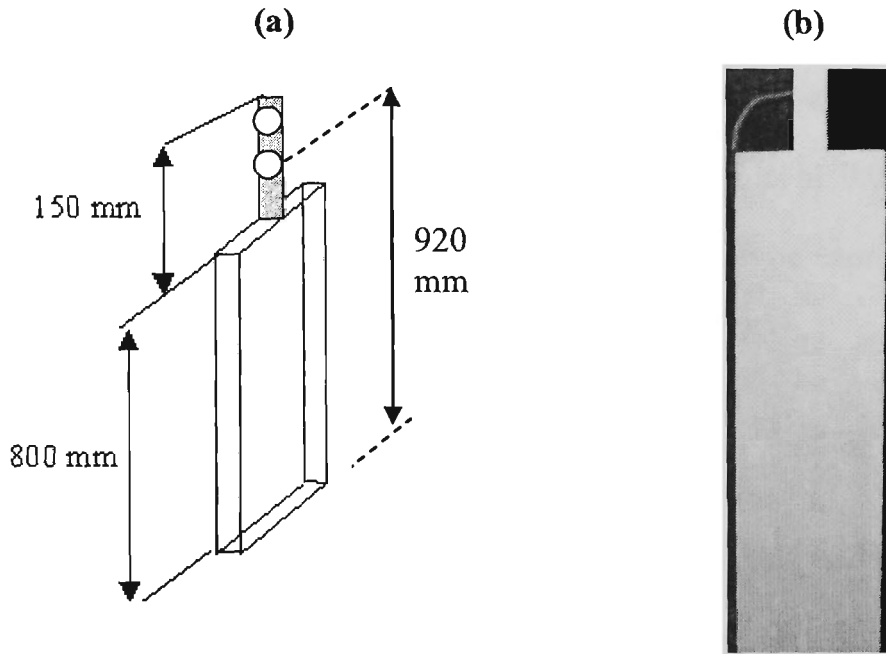


Figure 6-3 [a] Schematic and [b] image of the aluminium electrodes used in continuous EC process together its dimensions

The electrocoagulator could be configured with a sedimentation and flotation tank where the settling velocity of particles can be estimated in the sedimentation tank. Based on the size and distribution of measured particles, the average time for removing pollutants can be calculated. Assuming spherical particles and laminar flow, a Reynolds number (Re) less than 1, the settling velocity of discrete particles can be calculated by Stokes' law as follows (Kiely, 1998):

$$V_s = \frac{g d_p^2 (\rho_s - \rho_w)}{18 \mu} \quad (6-1)$$

where V_s is the Stokes' settling velocity (m/s), d_p is the particle diameter (m), ρ_s particle density, ρ_w density of water, μ viscosity of water and g is the gravitational constant. The XRD spectroscopy of the dried sludge obtained by EC process showed that the composition of the powder may be due to the formation of $Al_nF_m(OH)_{3n-m}$,

and $\text{Al}(\text{OH})_3$. The calculated density obtained for $\text{Al}(\text{OH})_{3-x}\text{F}_x$ was found to be 2500 kg/m^3 for wet state (Jambor et al., 1990). This particle density is similar to that of aluminium hydroxide (2400 kg/m^3). From Eq. 6-1, when the diameter of pollutant particles increases, the settling velocity increases. For particles with minimum size of $0.5 \text{ }\mu\text{m}$, the settling velocity was calculated from Stokes' law to be 0.0013 m/min . The retention time (t_0) for a rectangular sedimentation tank can be expressed by the following equation (Kiely, 1998):

$$t_0 = \frac{H}{V_s} = \frac{L}{V_h} = \frac{WHL}{Q} \quad (6-2)$$

where V_h , Q , H , W , and L are horizontal velocity, flow rate, height, width and length of the sedimentation tank, respectively. Note that $L \geq 2W$ and $L \gg H$. However, all particles will be removed when the settling velocity is equal to or more than the surface overflow rate (V_0) for a rectangular tank ($V_s \geq V_0$). Therefore, where the surface overflow rate (SOR), which is numerically equal to flow divided by the plan area of the basin, is defined as overflow rate ($\text{m}^3/\text{m}^2\text{-min}$) and A_p is the plan area of the settling zone, V_0 is shown to be:

$$V_0 = \frac{Q}{A_p} \quad (6-3)$$

Basic design criteria for a horizontal flow sedimentation tank including overflow rate (V_0) of $0.001 \text{ m}^3/\text{m}^2\text{-min}$ for particle size of $0.5 \text{ }\mu\text{m}$, horizontal velocity of 0.011 m/min , and detention time of 120 min were used to determine the tank dimensions. From equations 6-2 and 6-3, the dimensions $1320 \times 190 \times 120 \text{ mm}$ are calculated for a flow rate of 250 mL/min , as it is schematically shown in Figure 6-4. The electrolytic gas produce at the cathode creates a source of bubbles that enables some of the pollutants to float to the surface. Thus a surface floc collector ($1470 \times 100 \times$

170 mm) is included in the sedimentation tank and so is a 300 × 190 ×140 mm settled sludge collector.

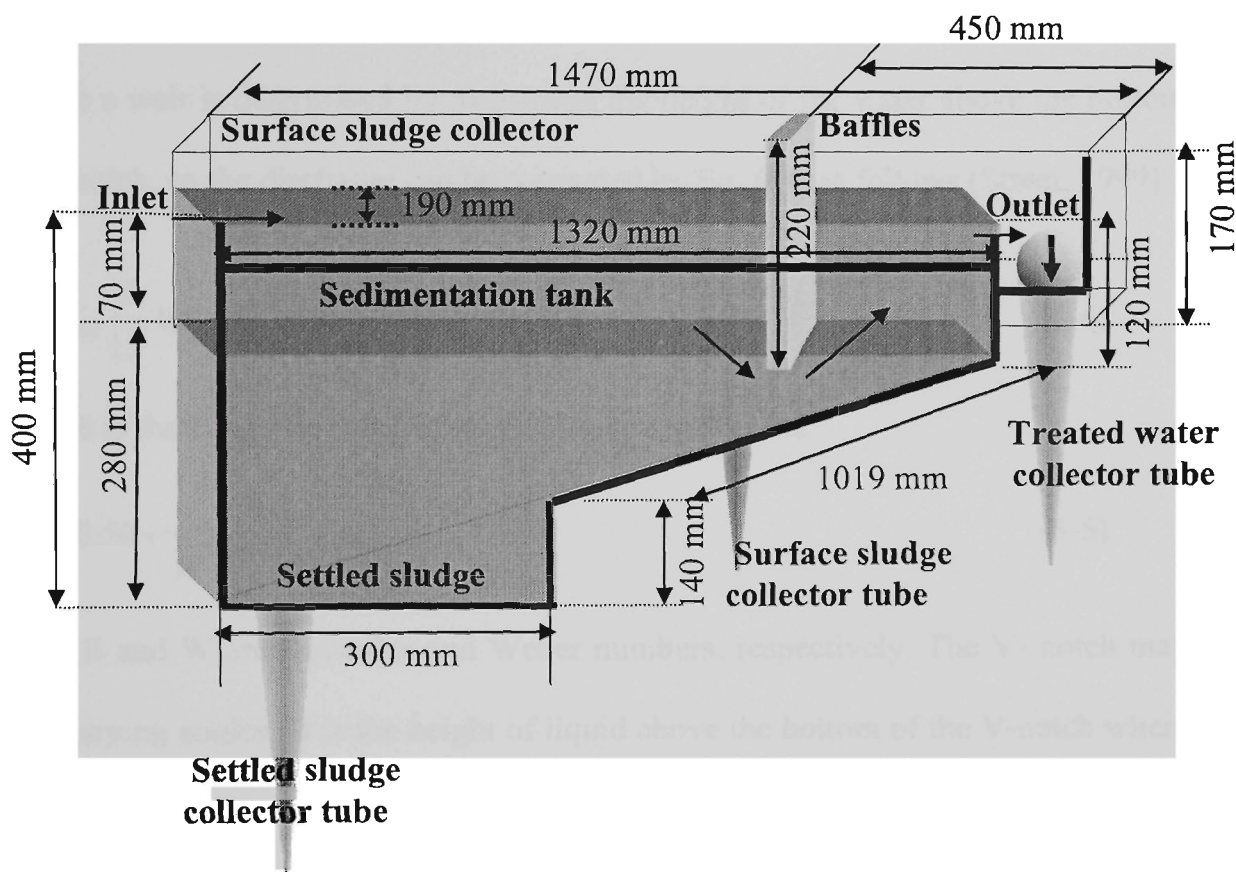


Figure 6-4 Schematic of sedimentation tank and surface sludge collector

The plan area (A_p) and net volume of the sedimentation tank were calculated to be 0.25 m² and 49.5 L, respectively. A plan view of the electrocoagulator, sedimentation, and flotation sections has been shown in Figure 6-5.

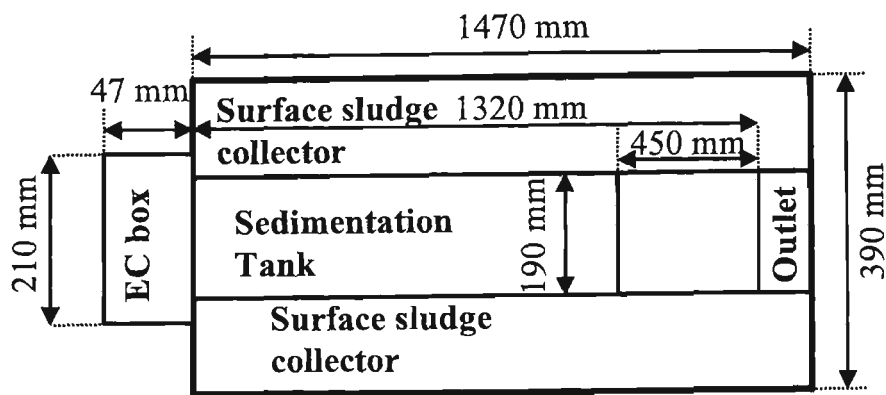


Figure 6- 5 Plan views of the electrocoagulation box

Weirs are often used to measure flows and control artificial channels. The two most common shapes are a rectangle and a V –notch. A V-shape weir was constructed in the sedimentation tank at the outlet zone, as shown in Figure 6-6. The flow rate through a weir is determined by measuring the height of the water above the bottom of the notch, so the discharge can be computed by Eq. 6-4, as follows (Street, 1999):

$$Q = C_w \frac{8}{15} \tan \frac{\theta}{2} \sqrt{2g} H^{\frac{5}{2}} \quad 20^\circ < \theta < 100^\circ \quad (6-4)$$

where θ is the inside weir angle and C_w is weir coefficient.

$$C_w = 0.56 + \frac{0.7}{R^{0.165} W^{0.17}} \quad (6-5)$$

where R and W are Reynolds and Weber numbers, respectively. The V- notch may have varying angles. H is the height of liquid above the bottom of the V-notch where the flow is proportional to $H^{2.5}$.

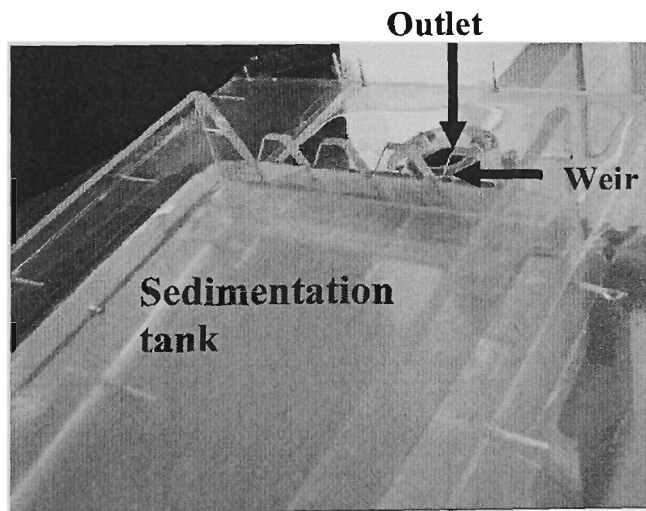


Figure 6-6 Image of a V-shape weir conducted in the sedimentation tank

An end view of the V-shape weir, EC box, and sedimentation/flotation sections, is shown in Figure 6-7.

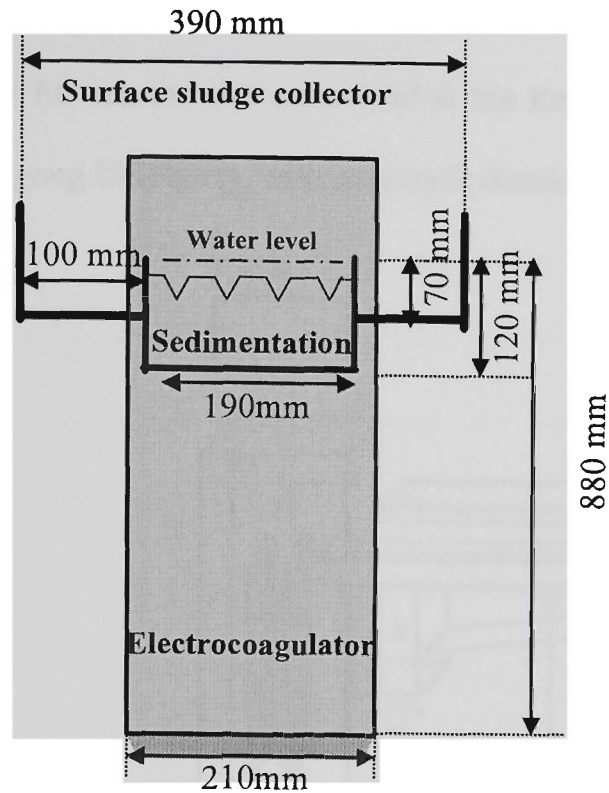


Figure 6-7 End view of the V-shape weir, EC box, and sedimentation and flotation sections

From Eq. 6-4, since $\theta = 60^\circ$, $C_w = 0.62$ and $H = 5$ mm the flow rate can be computed as $1.5 \times 10^{-6} \text{ m}^3/\text{s}$. Thus the estimated number of weirs is 5 when the maximum flow rate is $6.67 \times 10^{-6} \text{ m}^3/\text{s}$ (400 mL/min). A schematic of the weirs is shown in Figure 6-8, together its dimensions.

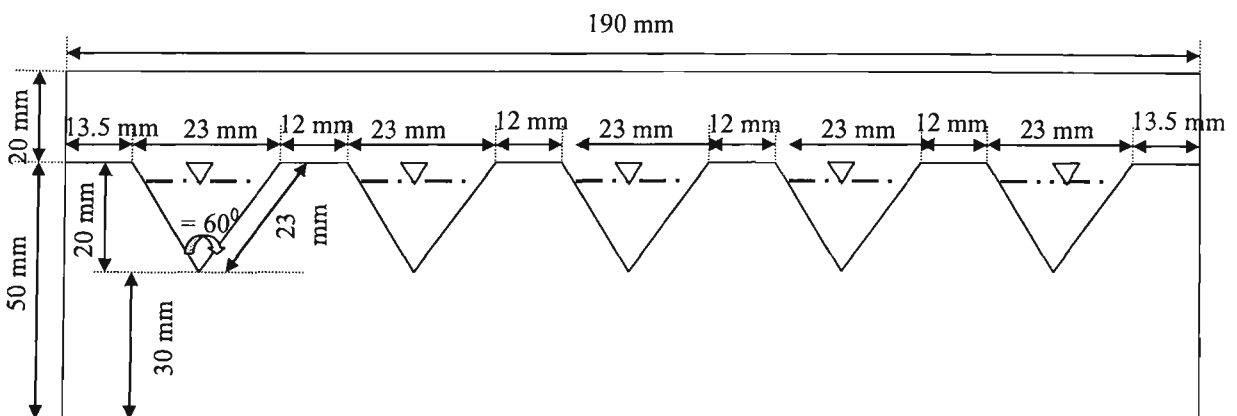
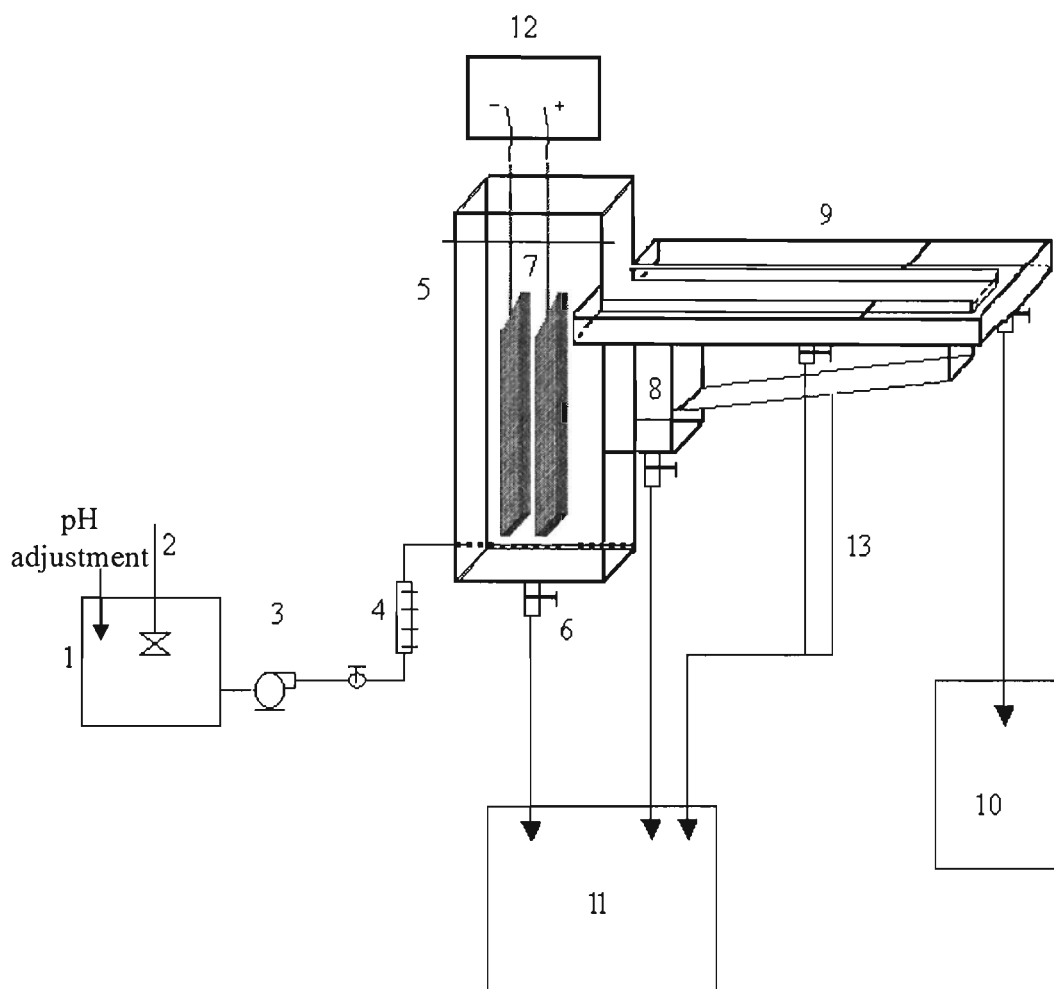


Figure 6-8 End view of flow out of the V-shape weir at sedimentation tank

6.2.2 Experimental procedures

The continuous flow EC reactor was assembled at the Environmental Engineering laboratory of Wollongong University, with schematic details shown in Figure 6-9.



- | | |
|---------------------------------------|-----------------------------|
| 1 Inlet reservoir (180 L) | 8 Separator (49.5 L) |
| 2 Mixer | 9 Surface floc collector |
| 3 Peristaltic pump (10 – 1000 mL/min) | 10 Outlet reservoir (200 L) |
| 4 Flow meter (100-1000 mL/min) | 11 Sludge reservoir (20L) |
| 5 Electrocoagulation box (10 L) | 12 DC power supply |
| 6 Drain tube | 13 Sludge collector tube |
| 7 Aluminium electrodes | |

Figure 6-9 Schematic diagram of a continuous flow electrocoagulation reactor

The influence of the various parameters on the process of defluoridation was achieved using “synthetic” water (Wollongong city tap water + NaF salt + NaCl +

NaHCO₃) in a continuous reactor. The conductivity of the solution was increased with 0.005 M NaCl to 50 mS/m. Sodium bicarbonate (1 mM) was only added in synthetic samples to maintain alkalinity. Fluoride concentration was determined using the ionometric standard method (refer to section 5.2.2.1). The initial pH of the water was varied within the range of 4-8 for each experiment. Conductivity and pH were measured using a calibrated conductivity and pH Meters. 1 M sodium hydroxide and 1:5 hydrochloric acid solutions were used to adjust the pH between 6 and 8 during experiments in the inlet reservoir. The composition of sludge was analysed by the X-ray diffraction (XRD) technique. The different experimental methods that were used to characterise the continuous flow EC process are the same as for the batch process (refer to analytic techniques in section 5.2.2.2)

Direct current from a DC power supply (0–18 V, 0–20 A, ISO-TECH, IPS-1820D) was passed through the solution via the electrodes. Cell voltage and current inputs were monitored using a digital power display. Current was varied from 2 – 8 A but was held constant for each run. The relationship between the current operating values, current densities, and concentrations (I/V) in the continuous flow EC reactor is shown in Table 6-1, when the total active anode area and net volume of the electrocoagulator are 0.16 m² and 7.9 L, respectively.

Table 6-1 Relationship between current operating value, current density and concentration in the continuous flow EC reactor

Current (A)	Current density (A/m ²)	Current concentration (A/m ³)
2	12.5	253
3	18.75	380
4	25	506
5	31.25	633
6	37.5	760
8	50	1013

Fluoride solutions (5 -25 mg/L as F⁻) were prepared by mixing sodium fluoride, sodium chloride, and sodium bicarbonate in Wollongong city tap water, and then stored in a reservoir (200 L). The water quality characteristics that are used for making synthetic samples are shown in Table 6-2.

Table 6-2 Water quality characteristics of test water used for synthetic samples

Sample	Concentration (mg/L)						
Ions	Ca ²⁺	Mg ²⁺	Alkalinity mg/L CaCO ₃	Cl ⁻	pH	SO ₄ ²⁻	Ec (mS/m)
Synthetic sample	15	1.7	100-200	15-55	6-8	2	12-50

The feed water pH was between 7.5 and 8, which was later decreased to 4 in order to investigate the initial pH effect on the performance of the EC reactor. The performance of the continuous flow EC reactor was assessed in terms of the contents of fluoride concentration before and after treatment. Water samples were collected from the effluent after EC reactor and sedimentation tank. The quality parameters were analysed according to the Standard Methods (AWWA and WEF, 1998). The important experimental variables measured in the continuous flow EC reactor were summarised in Table 6-3.

Table 6-3 Important experimental variables measured in the continuous flow EC reactor

Operational parameters		Electrode distance and connection (mm)	Initial pH	Initial fluoride concentration (mg/L)	Flow rate (mL/min)
Current density (A/m ²)	Current concentration (A/m ³)				
12.5	253	5-monpoar	(4– 8)	5-25	150-400
18.75	380	5-monpoar	(4– 8)	5-25	150-400
25	506	5-monpoar	(4– 8)	5-25	150-400
31.25	633	5-monpoar	(4– 8)	5-25	150-400
37.5	760	5-monpoar	(4– 8)	5-25	150-400
50	1013	5-monpoar	(4– 8)	5-25	150-400

6.2.3 Experimental set up

The electrocoagulator was designed to provide various hydraulic and electrolytic configurations. The EC reactor was fed by a peristaltic pump (Master flex-L/S, model 77200-52) from a raw water reservoir. The influent flow rate was varied from 150 mL/min to 400 mL/min that corresponds to a residence time of 53 to 20 min respectively at the electrocoagulation compartment. Settled solids were separated at the bottom of the sedimentation tank and floated solids were collected at the surface sludge collector. Floated solids were separated by an over flow weir in the horizontal separation chamber of the reactor. The treated water was connected to an outlet reservoir (200 L). The continuous flow EC reactor was operated for 8 hours per day during the test period (from February to June 2005). The electrode locations were cleaned every day by diluted hydrochloric acid and then washed in water. The total electrolysis time obtained was 800 hours during the test period (100 days) when the polarity of the electrodes was reversed every day. At the different flow rates, detention times and loading rates are summarised in Table 6-4.

Table 6-4 Summarised design parameters for continuous flow EC reactor

Flow rate (mL/min)	Detention time		Loading rate ($\text{m}^3/\text{m}^2 \cdot \text{min}$)			
	EC reactor		Sedimentation Tank (h)	Area of plates (m^2)	Area of EC box (m^2)	Area of sedimentation tank (m^2)
	min	h				
150	53	0.88	5.50	9.37×10^{-4}	1.5×10^{-3}	6×10^{-4}
200	40	0.66	4.13	1.25×10^{-3}	2×10^{-3}	8×10^{-4}
250	32	0.53	3.30	1.56×10^{-3}	2.5×10^{-3}	1×10^{-3}
300	26	0.44	2.75	1.87×10^{-3}	3×10^{-3}	1.2×10^{-3}
350	23	0.38	2.36	2.19×10^{-3}	3.5×10^{-3}	1.4×10^{-3}
400	20	0.33	2.06	2.5×10^{-3}	4×10^{-3}	1.6×10^{-3}

Detention time on the electrocoagulator and sedimentation tank could be calculated when the net volume of both was found to be 7.9 and 49.5 L, respectively. Different loading rates could be also calculated when the plan area of the aluminium plates, EC box, and sedimentation tank were 0.16, 0.01, and 0.25 m², respectively were used. Sedimentation tanks should be designed on the basis of surface overflow rates (surface loading rates) with due consideration given to the type of floc generated. Concerning the basic design criteria for horizontal flow sedimentation rectangular tanks in the conventional primary clarification, Surface loading rates is considered to be 0.014-0.024 m³/m².min when detention time is between 2-4 h (Kiely, 1998). From results obtained in Table 6-4, the loading rates are calculated to be between 6×10^{-4} - 1.6×10^{-3} m³/m².min for sedimentation rectangular tank when detention time is found between 2-5.5 h. As seen, the surface overflow rates are approximately 15-23 times smaller than the conventional primary clarification. This is because the area of sedimentation tank is designed concerning the maximum flow rate of water going in sedimentation tank (400 mL/min) and the design parameters, which are summarized in Table 6-4, are considered as a lab pilot plant study. Also, there is a gap between electrodes and electrocoagulator when the EC box was designed for more number of electrodes and more flow rates for future research work. Experimental set up of a continuous flow electrocoagulation reactor including inlet reservoir, mixer, peristaltic pump, DC power supply, electrocoagulator together with the aluminium electrodes, sedimentation tank, surface sludge collector, and outlet section, is shown in Figure 6-10.



Figure 6-10 Experimental set up of a continuous flow electrocoagulation reactor

6.3 RESULTS AND DISCUSSION

6.3.1 Effects of surface charge density

As noted in chapter 5, charge is the most important parameter for controlling the reaction rate in most electrochemical processes because charge or surface charge density (a product of current density and time) determines the dosage of coagulant within electrocoagulation, in either a batch or continuous flow model. It is important to determine the Al^{3+} dose achieved within the ECF process, and Faraday's law can be used to describe the relationship between current density, detention time in the EC box, and the amount of concentrated aluminium (refer to Eq. 2-9). At the constant initial fluoride concentration and flow rate, the experiments were conducted to show the effect of different values of the surface charge density on the residual fluoride concentrations in the electrocoagulator. At initial fluoride concentration 10 mg/L and constant flow rate of 150 mL/min, the amount of experimental aluminium released during the electrolysis process at different charge densities (charge per unit area) from 40000 – 160000 C/m^2 is shown in Figure 6-11.

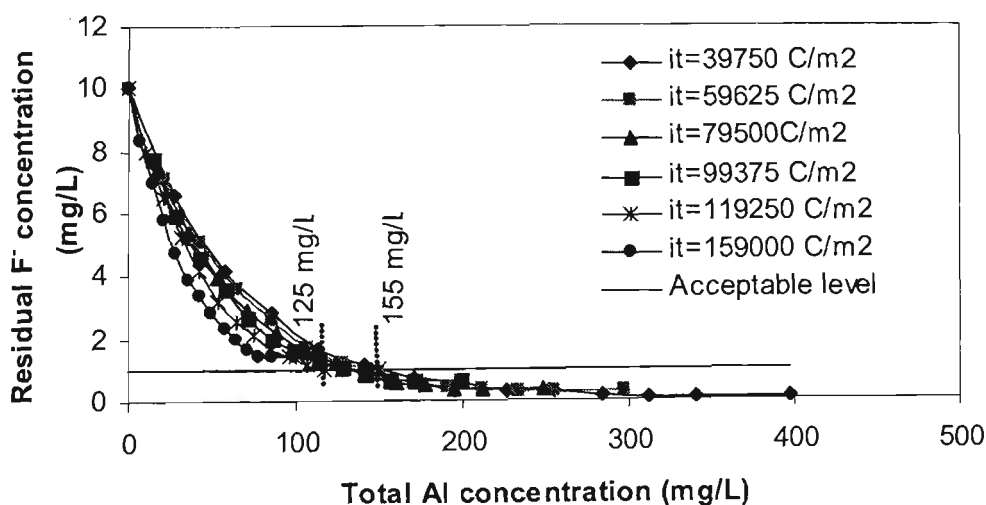


Figure 6-11 Effect of total aluminium concentration on residual fluoride concentration in ECF process ($C_0 = 10 \text{ mg/L}$, $\text{pH}_{\text{in}} = 6$, $E_c = 50 \text{ mS/m}$, $Q = 150 \text{ mL/min}$, $i = 12.5 - 50 \text{ A/m}^2$)

The residual fluoride concentration reaches to 1 mg/L when the total aluminium concentration is between 120-155 mg/L. Increasing of the amount of aluminium released to 400 mg/L in EC reactor not only are not increased fluoride removal efficiency but also the residual of aluminium in the effluent needs to be controlled. This emphasizes that the amount of aluminium released to the system by electrocoagulation is affected by both the current input and time in the electrocoagulator. From results obtained in Figure 6-11, the experimental mass ratio Al^{3+}/F^{-} was found between 13-17.5 in the ECF process when the residual aluminium concentrations on the effluent were found to be less than 0.2 mg/L which is desirable based on NHMRC and ARMCANZ (2004) guidelines. As seen in Figure 6-12, the optimum surface charge density is found between 60000- 70000 C/m^2 to reduce the fluoride concentration from 10 to 1 mg/L.

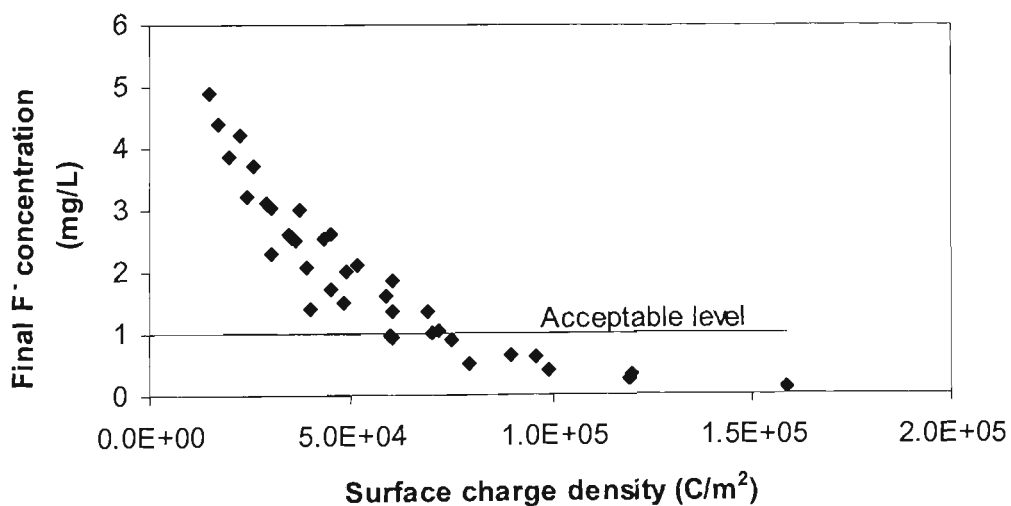


Figure 6-12 Effete of surface charge density on the final fluoride concentration for defluoridation by ECF process ($C_o= 10$ mg/L, $pH_{in} = 6$, $E_c=50$ mS/m, $Q=150-400$ mL/min, $i =12.5 -50$ A/m²)

The residual fluoride concentration is decreased from 1 mg/L at 60000 C/m^2 to 0.1 mg/L at 160000 C/m^2 when the flow rate and initial concentration of fluoride are

kept at 150 mL/min and 10 mg/L respectively. As noted in above, the surface charge density determines the rate of dissolution of Al^{3+} concentration. Since the optimum surface charge density was found to be 60000- 70000 C/m^2 to achieve the desirable fluoride concentration range in the electrocoagulator section, do not need more charge for reducing of fluoride concentration from 1 to 0.1 mg/L. For given flow rate of 150 mL/min, the surface charge density of 60000 C/m^2 is obtained when current density is 18.75 A/m^2 . It can be concluded that the maximum current density is found to be 18.75 A/m^2 to reduce the fluoride concentration from 10 to 1 mg/L when flow rate is kept constant at 150 mL/min.

At a flow rate of 250 mL/min, the effect of surface charge density on defluoridation at an initial fluoride concentration of 5 to 25 mg/L is shown in Figure 6-13.

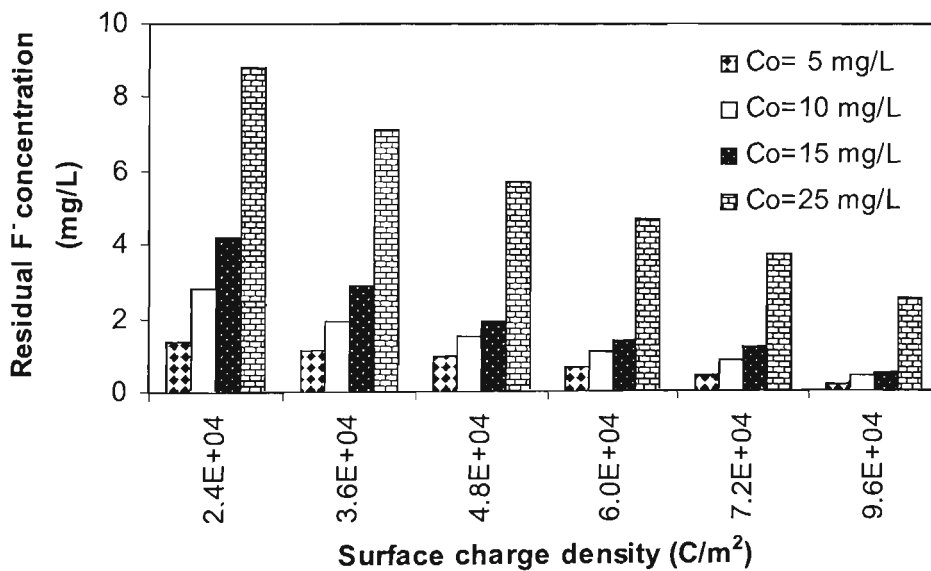


Figure 6-13 Effect of surface charge density on the residual fluoride concentration at different initial fluoride concentration in a continuous flow electrocoagulation ($Q = 250$ mL/min, $i = 12.5 - 50$ A/m^2 , $pH_{in} = 6$, $Ec = 50$ mS/m)

The residual concentration of fluoride was decreased from 2.82 mg/L at 24000 C/m^2 to 0.42 mg/L at 96000 C/m^2 when the flow rate and initial concentration were kept at

250 mL/min and 10 mg/L, respectively. It can be seen that at initial fluoride concentration of 25 mg/L, the residual concentration of fluoride decreased from 8.8 to 2.5 mg/L when the surface charge density was increased from 24000 to 96000 C/m² in a continuous EC system. As seen, the values of residual fluoride concentrations increase when the initial fluoride concentrations increase at a constant surface charge density, because the highest pollutant loading (25 mg/L) needs to a higher current or longer electrolysis time for more treatment.

6.3.2 Effect of flow rate

The effect of flow rate on defluoridation was studied by varying the flow rates in the ranges 150 to 400 mL/min at different initial concentrations of fluoride and current densities, as is shown in Figure 6-14. It can be seen that when the flow rates are increased, less fluoride is removed for the same current densities.

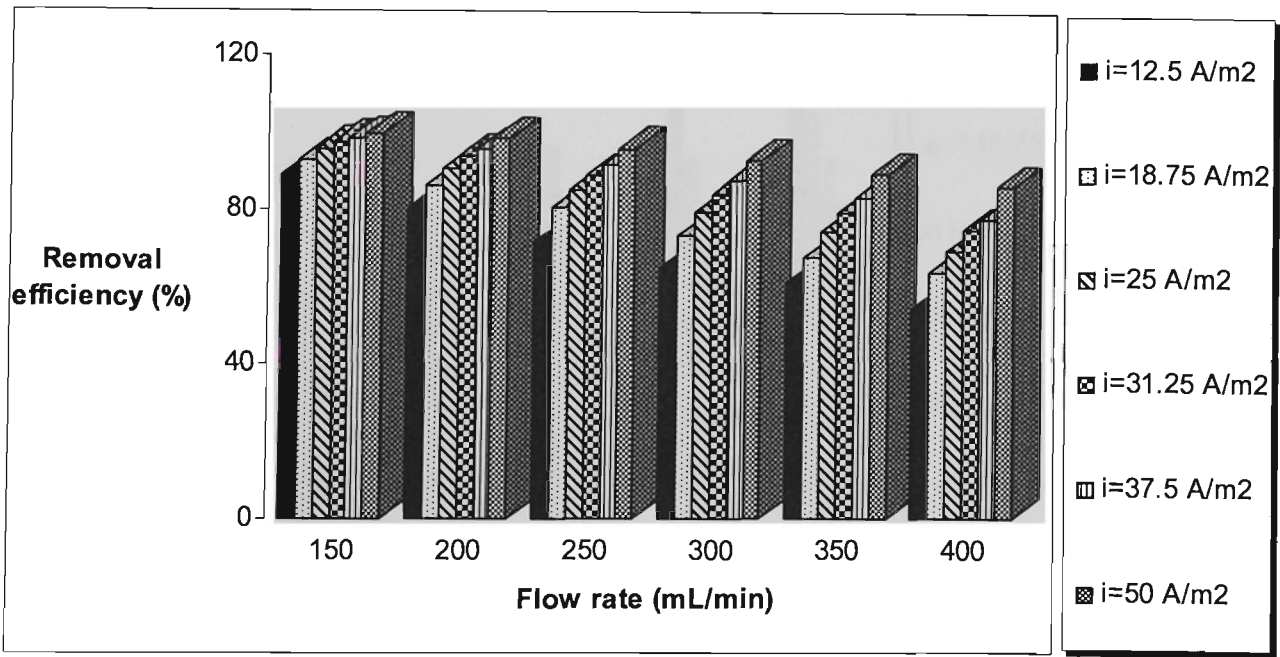


Figure 6-14 Effect of flow rate on the defluoridation efficiency at different current densities from 12.5 to 50 A/m² in a continuous flow electrocoagulation (C₀= 15 mg/L, pH_{in} = 6, Ec=50 mS/m)

As seen in Figure 6-14, for a flow rate of 250 mL/min and initial fluoride concentration of 15 mg/L, the removal of fluoride was increased from 72 % at 12.5 A/m² to 96.5 % at 50 A/m². The fluoride removal rate varies from 55 to 99 % within the flow rate and the different current densities. As expected, at high flow rate (400 mL/min), detention time is shorter.

The effect of flow rate on the residual concentration of fluoride for different current densities is illustrated in Figure 6-15. As seen, for a constant current density of 50 A/m² and initial fluoride concentration of 25 mg/L, the residual fluoride concentration is increased from 0.5 mg/L at 150 mL/min to 5.9 mg/L at 400 mL/min. At low current density (12.5 A/m²), the residual fluoride concentration is increased from 4.2 mg/L at 150 mL/min to 13 mg/L at 400 mL/min when the initial fluoride concentration is 25 mg/L.

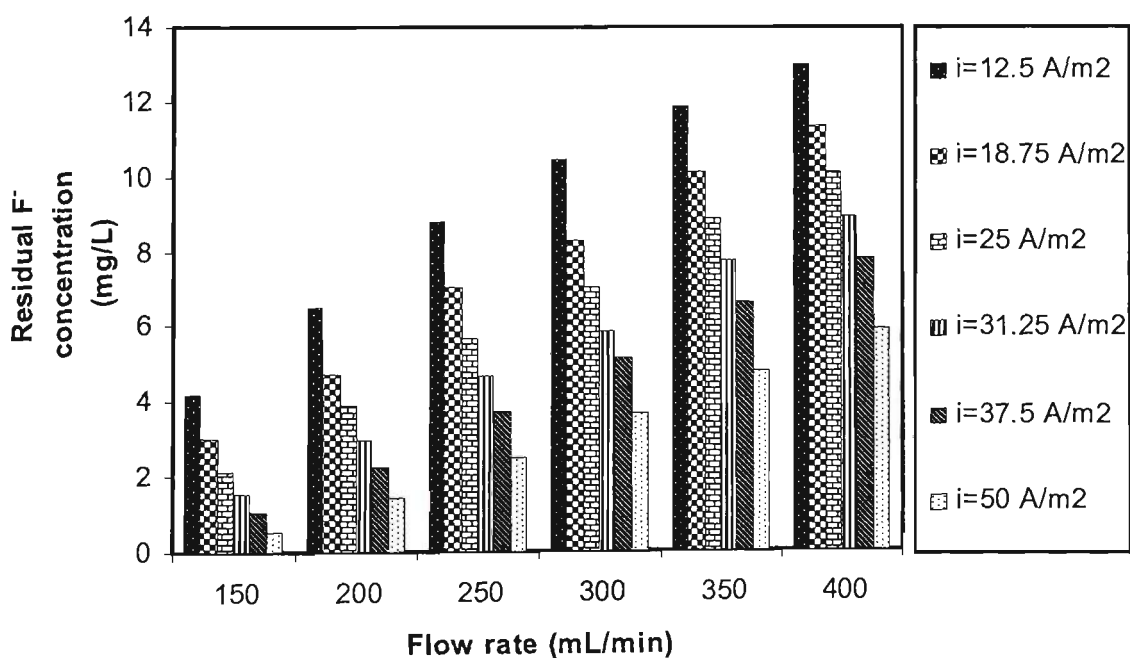


Figure 6-15 Effect of flow rate on the residual fluoride concentration at the different current densities in a continuous flow electrocoagulation ($pH_{in}=6$, $E_c=50$ mS/m, $C_o=25$ mg/L)

For a given constant flow rate, there is a linear relationship between the residual fluoride concentrations and the different current densities. However, the relationship between the residual fluoride concentrations and flow rates is slightly non-linear for a given constant current density. As noted before, this could be due to experimental error when all flow has not passed well through the electrodes in the EC box. As expected, at low flow rate (150 mL/min), detention time was longer than high flow rate (400 mL/min) when the current density was constant. Thus the combination of current and detention time determines the removal of pollutant. It agrees with the results obtained on defluoridation by the batch model which has already been considered in chapter 5, when the electrolysis time in a batch system is equal to the residence time in a continuous flow EC reactor. This will be discussed in the following chapter.

6.3.3 Effect of initial fluoride concentration

In order to find out the effect of initial fluoride concentration on defluoridation, experiments changing the initial fluoride concentration from 5 to 15 mg/L at the same current densities and flow rates were conducted. The effect of initial fluoride concentrations on defluoridation at different current densities from 12.5 to 50 A/m² is shown in Figures 6-16 (a, b, and c). In this experiment the flow rates were increased from 150 to 400 mL/min. The residual fluoride concentrations decreased from 1.94 mg/L at 12.5 A/m² to 0.47 mg/L at 50 A/m² when the flow rate and initial fluoride concentration are kept at 400 mL/min and 5 mg/L respectively. It can be seen that at the same current density (12.5 A/m²) and flow rate (150 mL/min), the residual

fluoride concentration increases from 1.1 to 1.6 mg/L when initial fluoride concentration is increased from 10 to 15 mg/L, respectively.

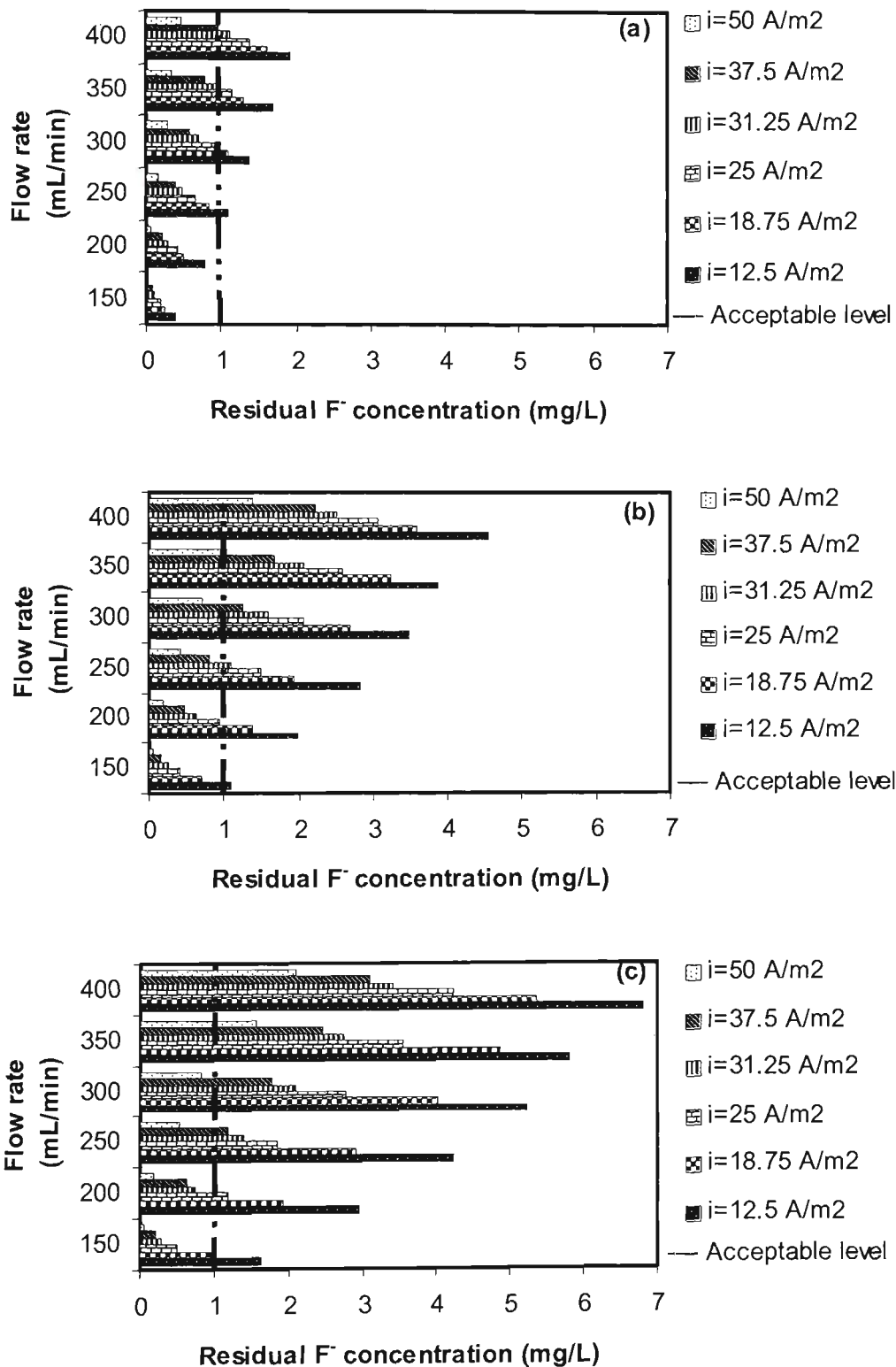


Figure 6-16 Effect of initial fluoride concentration on the residual fluoride concentration at the different current densities in a continuous flow EC reactor ($pH_{in} = 6$, $E_c = 50$ mS/m), [a] $C_0 = 5$ mg/L, [b] $C_0 = 10$ mg/L, [c] $C_0 = 15$ mg/L

It is clear that when the initial fluoride concentration is low, removal is highest. At higher flow rates (400 mL/min) and current densities (50 A/m²), the residual fluoride concentration also increases from 1.39 to 2.1 mg/L when initial fluoride concentration is increased from 10 to 15 mg/L, respectively. This is possibly due to an insufficient amount of aluminium hydroxide complexes forming. The amounts of aluminium ions produced are proportional to the flow rate and current applied in the EC process. The highest amount of fluoride removed occurred at the lowest flowrate (150 mL/min) and highest current density (50 A/m²). It appears that a higher initial fluoride concentration needs a higher current input to improve defluoridation for a given constant flow rate. For high fluoride concentration (25 mg/L), the effete of surface charge density on the final fluoride concentration is shown in Figure 6-17.

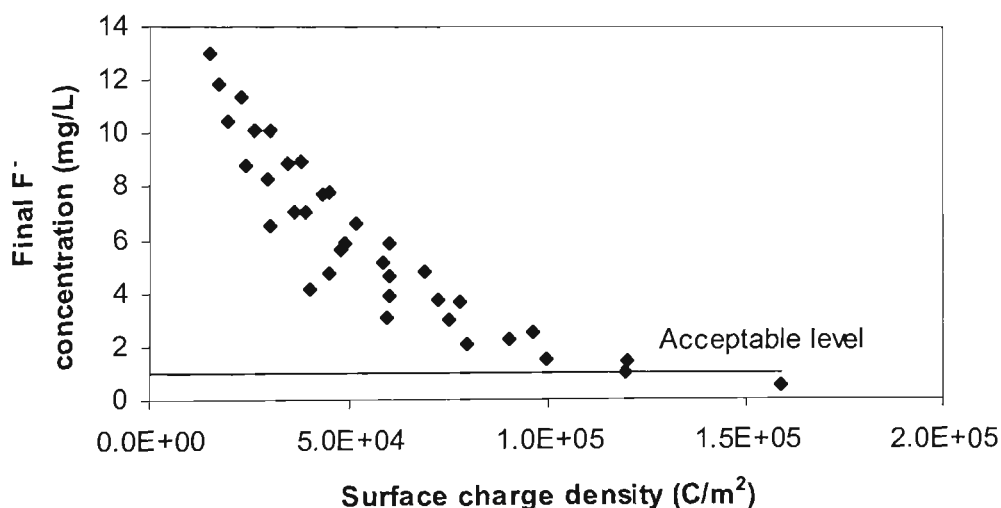


Figure 6-17 Effete of surface charge density on the final fluoride concentration for defluoridation by ECF process ($C_o = 25$ mg/L, $pH_{in} = 6$, $E_c = 50$ mS/m, $Q = 150$ -400 mL/min, $i = 12.5$ -50 A/m²)

As seen, the optimum surface charge density is found between 119000- 120000 C/m² to reduce the fluoride concentration from 25 to 1 mg/L. For given flow rate of 150 mL/min, the surface charge density of 120000 C/m² is obtained when current density is 37.5 A/m². More details will be discussed following the chapter.

6.3.4 Effect of pH

The electrocoagulation process is highly dependent on the pH of the solution (Mameri *et al.*, 1998; Ming *et al.*, 1983). The initial pH is not only one of the important factors in solution chemistry in terms of raw water but also as a potential operational variable. It will affect the speciation of Al and have a significant influence on defluoridation. Since aluminium hydroxide is an amphoteric hydroxide, pH is a sensitive factor for the formation of $\text{Al}(\text{OH})_3$ flocs. The solubility of aluminium in equilibrium with a solid phase $\text{Al}(\text{OH})_3$ depends on the surrounding pH, as the predominant hydrolysis products are $\text{Al}(\text{OH})^{2+}$ and $\text{Al}(\text{OH})_2^+$ between pH 5 and 6. The solid $\text{Al}(\text{OH})_3$ is most prevalent between pH 6 and 8, and above pH 9, the soluble species $\text{Al}(\text{OH})_4^-$ is the predominant species. MINEQL⁺ model (Environmental Research Software, 1999) is utilised in the next chapter (solution speciation) to show how a different pH would influence the solubility of Gibbsite [$\text{Al}(\text{OH})_3$].

Effect of influent pH on fluoride removal by the EC process is shown in Figure 6-18. When the influent pH value increased from 4 and 6 the final pH was increased in the end of EC box (electrocoagulator) from 6 to 8 respectively, and the residual fluoride concentration reached an equilibrium value of 0.74 mg/L. By increasing the initial pH from 6 to 8 the residual fluoride concentration increased from 0.74 to 1.05 mg/L and the final pH reached to 9 in the EC box. It is clear that defluoridation decreases when the final pH is more than 8 because AlO_2^- forms at high pH, which is soluble and not suitable for defluoridation.

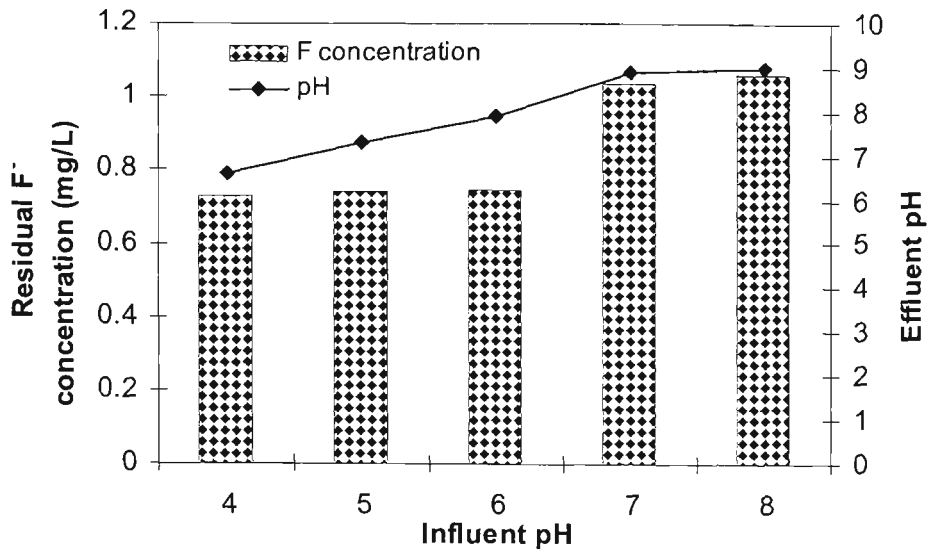


Figure 6-18 Effect of influent pH on the fluoride removal in a continuous flow electrocoagulation ($C_o = 10$ mg/L, $i = 18.75$ A/m², $Q = 150$ mL/min, $E_c = 50$ mS/m)

The results obtained from Figure 6-18 show that defluoridation is more efficient with a final pH ranging between 6 and 8, which agrees with the results obtained from a batch EC reactor. Therefore it can be concluded that during experiments, at a pH range of 6 –8, the majority of aluminium complexes (coagulants) are formed and it is the optimum pH range for carrying out electrocoagulation.

6.3.5 Effect of total detention time

The effect of detention time on defluoridation was investigated separately in the EC system (EC box + sedimentation tank) and electrocoagulator (EC box). Figures 6-19 (a, b, c, d, e, f, g, h, i, k, m, and n) show the effect of detention time in the both electrocoagulator and EC system at the different current densities and flow rates when the initial fluoride concentration is 10 mg/L. The effect of detention time in the EC box and EC system is also shown in Figures 6-20 and 6-21 (a, b, c, d, e, f, g, h, i, k, m, and n) at various flow rates and current densities, when the initial fluoride concentrations are 15 and 25 mg/L, respectively.

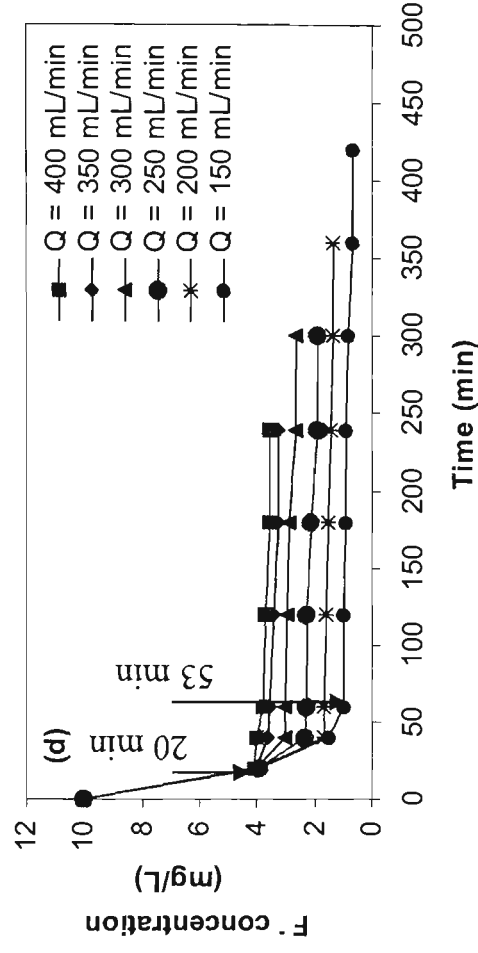
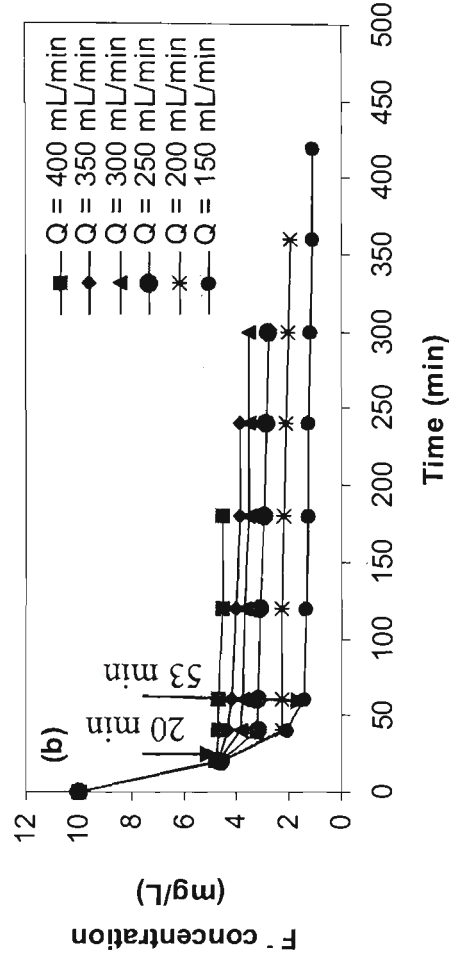
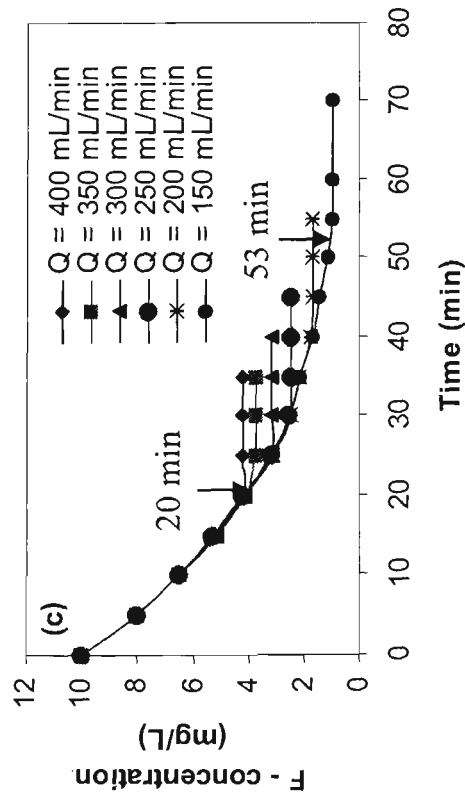
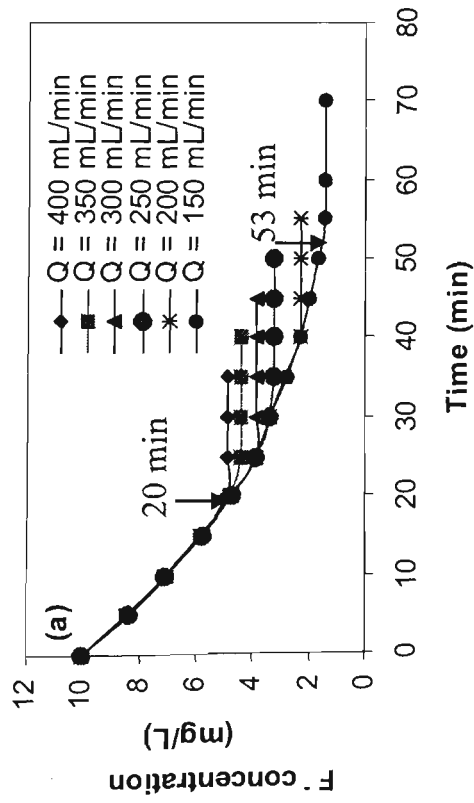


Figure 6-19 Effect of detention time on the residual fluoride concentration at different flow rate values and current densities in a continuous flow electrocoagulation reactor ($C_o = 10 \text{ mg/L}$, $\text{pH}_{in} = 6$, $E_c = 50 \text{ mS/m}$), [a] Electrocoagulator - $i = 12.5 \text{ A/m}^2$, [b] EC system- $i = 12.5 \text{ A/m}^2$, [c] Electrocoagulator - $i = 18.75 \text{ A/m}^2$, [d] EC system- $i = 18.75 \text{ A/m}^2$

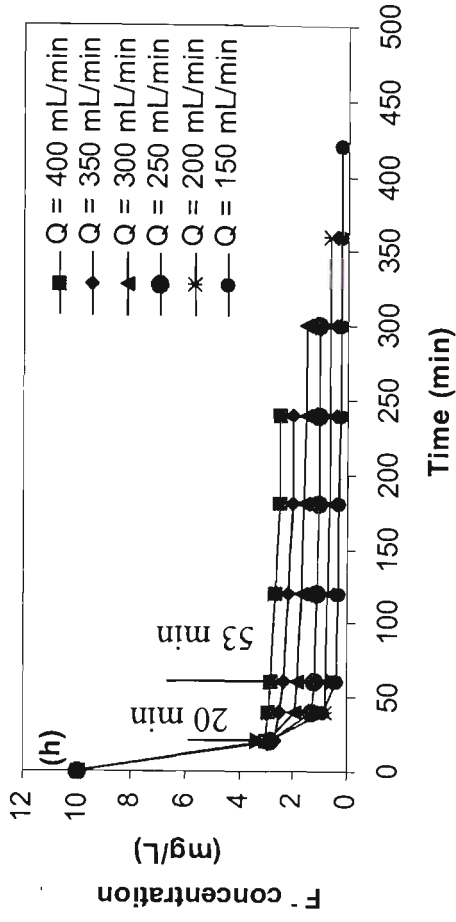
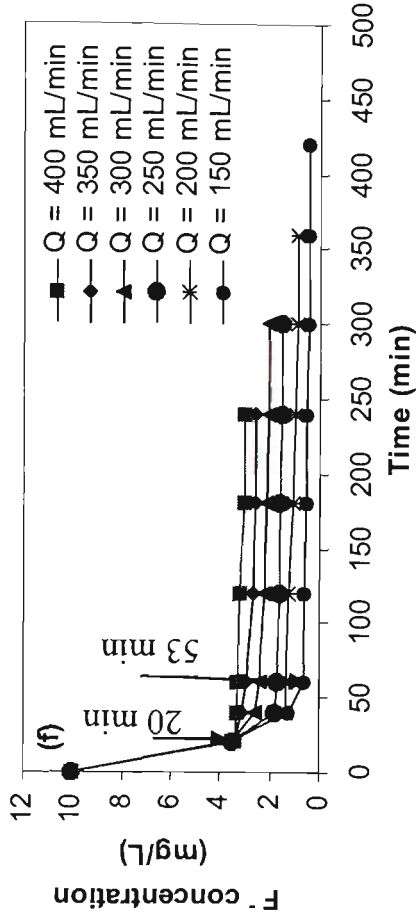
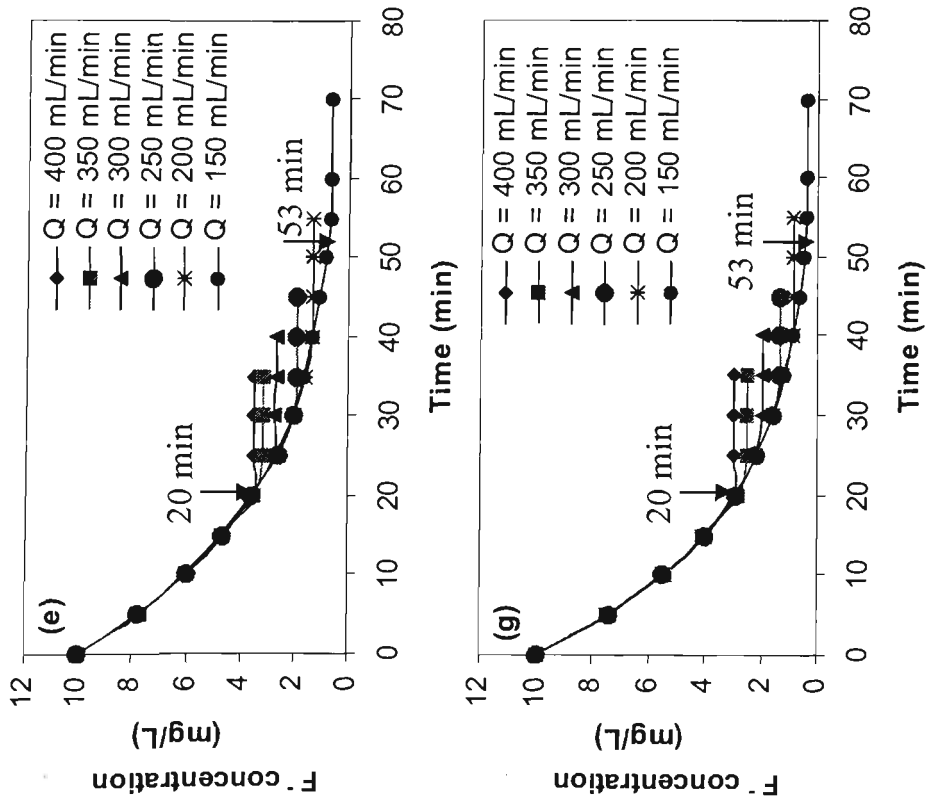


Figure 6-19 (Continued)- Effect of detention time on the residual fluoride concentration at different flow rate values and current densities in a continuous flow electrocoagulation reactor ($C_o = 10$ mg/L, $pH_{in} = 6$, $E_c = 50$ mS/m), [e] Electrocoagulator - $i = 25$ A/m², [f] EC system - $i = 25$ A/m², [g] Electrocoagulator - $i = 31.25$ A/m², [h] EC system - $i = 31.25$ A/m²

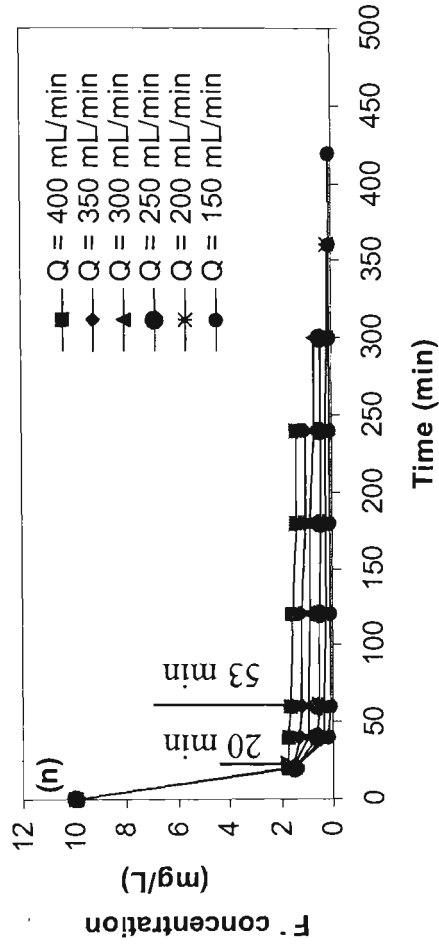
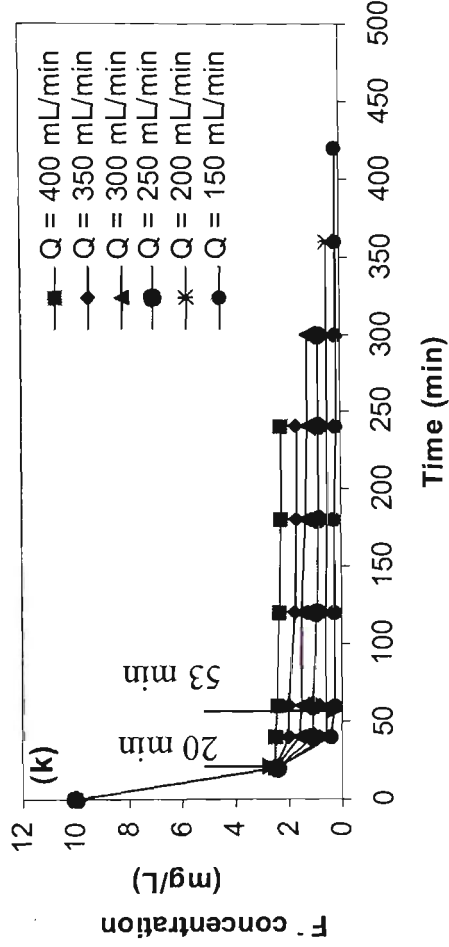
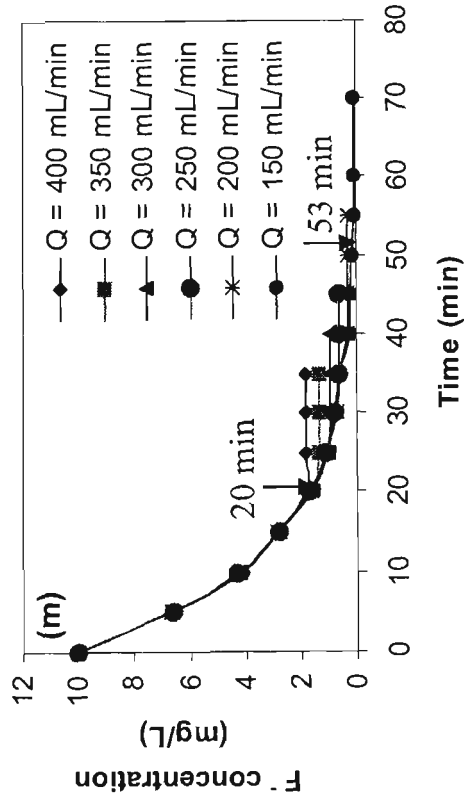
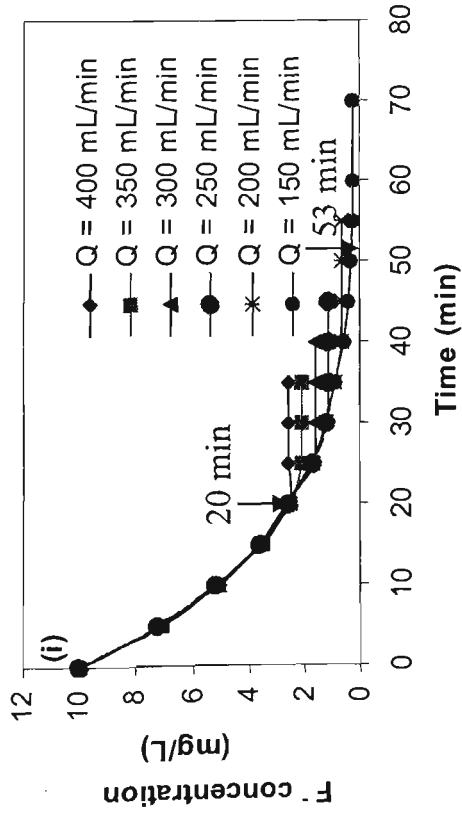


Figure 6-19 (Continued)- Effect of detention time on the residual fluoride concentration at different flow rate values and current densities in a continuous flow electrocoagulation reactor ($C_o = 10$ mg/L, $pH_{in} = 6$, $E_c = 50$ mS/m), [i] Electrocoagulator - $i = 37.5$ A/m², $i = 37.5$ A/m², [m] Electrocoagulator - $i = 50$ A/m², [n] EC system- $i = 50$ A/m²

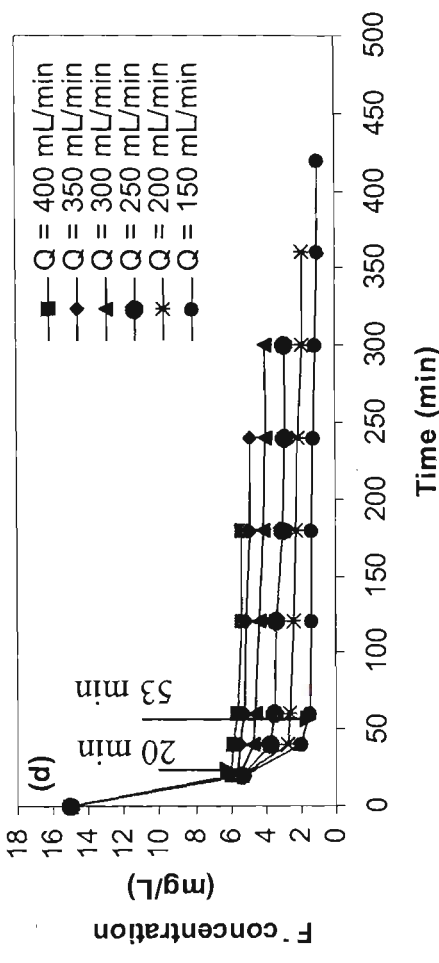
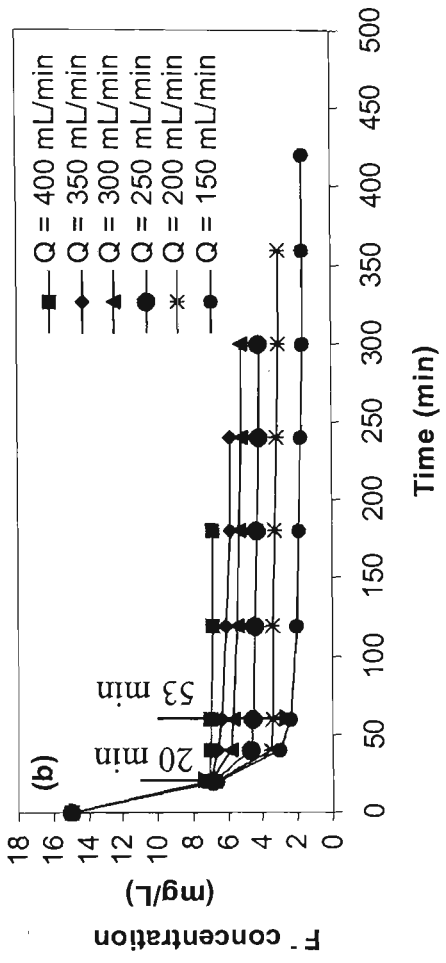
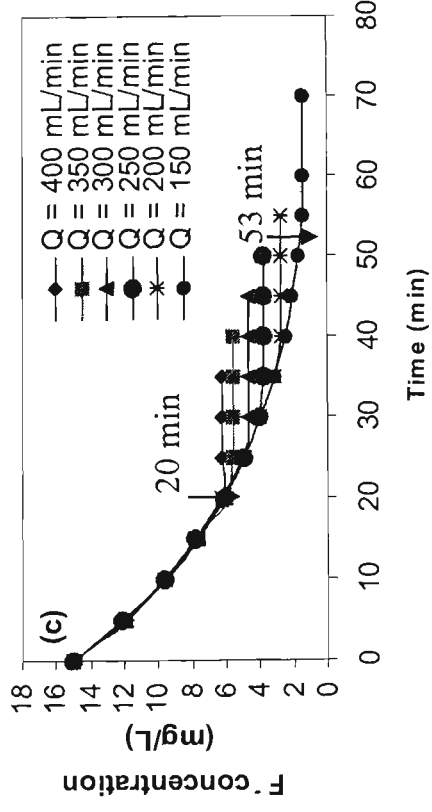
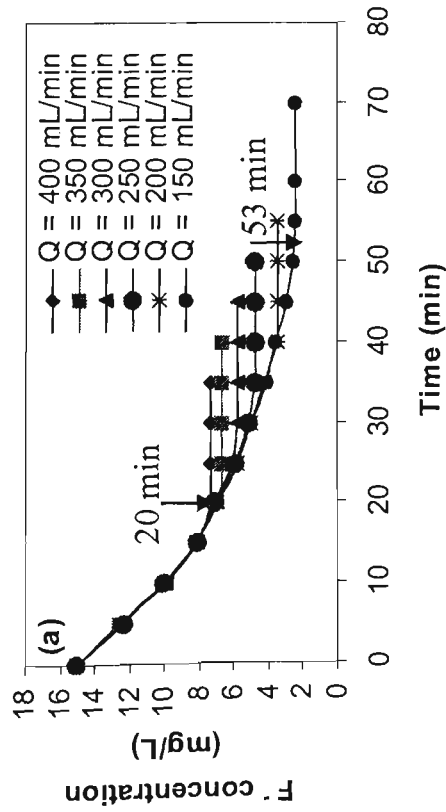


Figure 6-20 Effect of detention time on the residual fluoride concentration at different flow rate values and current densities in a continuous flow electrocoagulation reactor ($C_o = 15 \text{ mg/L}$, $\text{pH}_{i,m} = 6$, $E_c = 50 \text{ mS/m}$), [a] Electrocoagulator - $i = 12.5 \text{ A/m}^2$, [b] EC system- $i = 12.5 \text{ A/m}^2$, [c] Electrocoagulator - $i = 18.75 \text{ A/m}^2$, [d] EC system- $i = 18.75 \text{ A/m}^2$

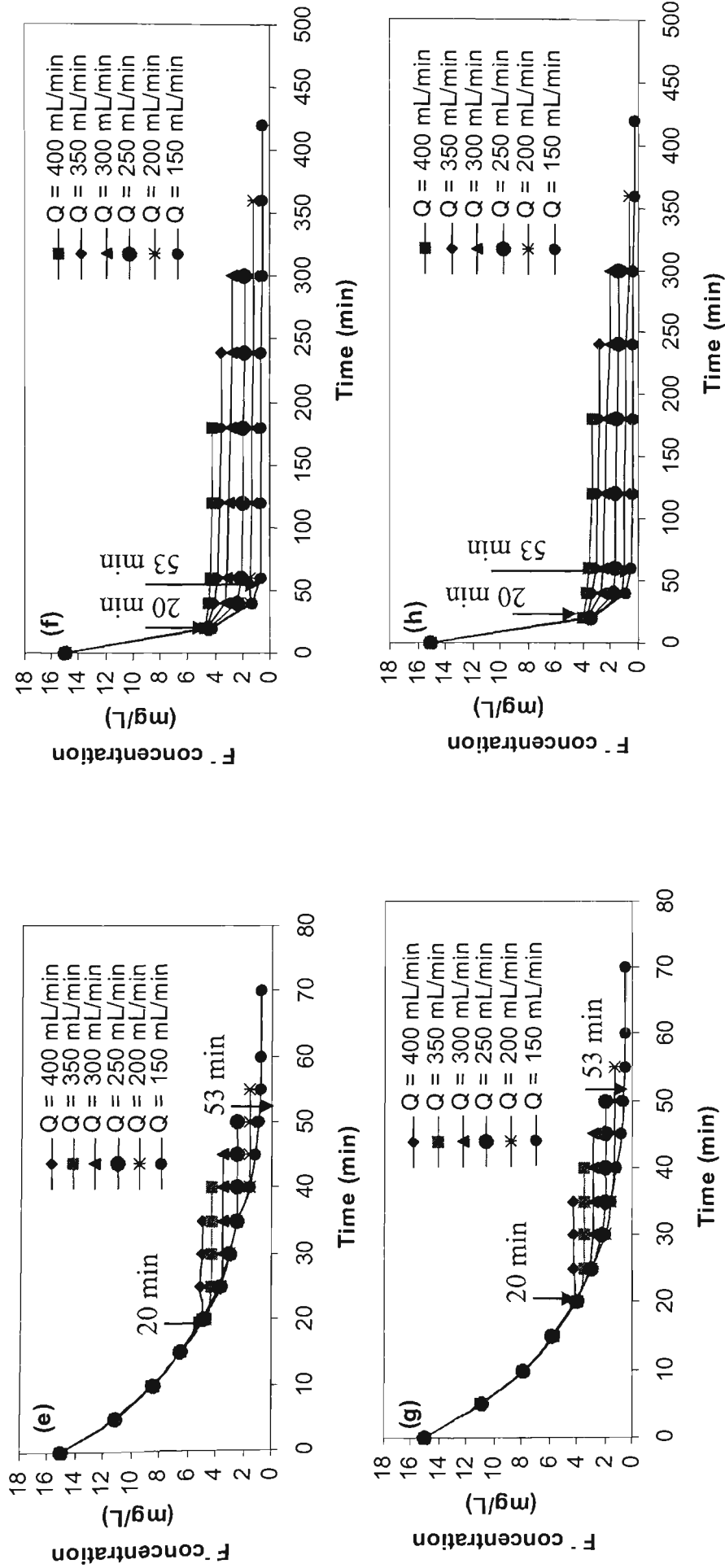


Figure 6-20 (Continued) - Effect of detention time on the residual fluoride concentration at different flow rate values and current densities in a continuous flow electrocoagulation reactor ($C_o = 15$ mg/L, $pH_{in} = 6$, $E_c = 50$ mS/m), [e] Electrocoagulator - $i = 25$ A/m², [f] EC system - $i = 25$ A/m², [g] Electrocoagulator - $i = 31.25$ A/m², [h] EC system - $i = 31.25$ A/m²

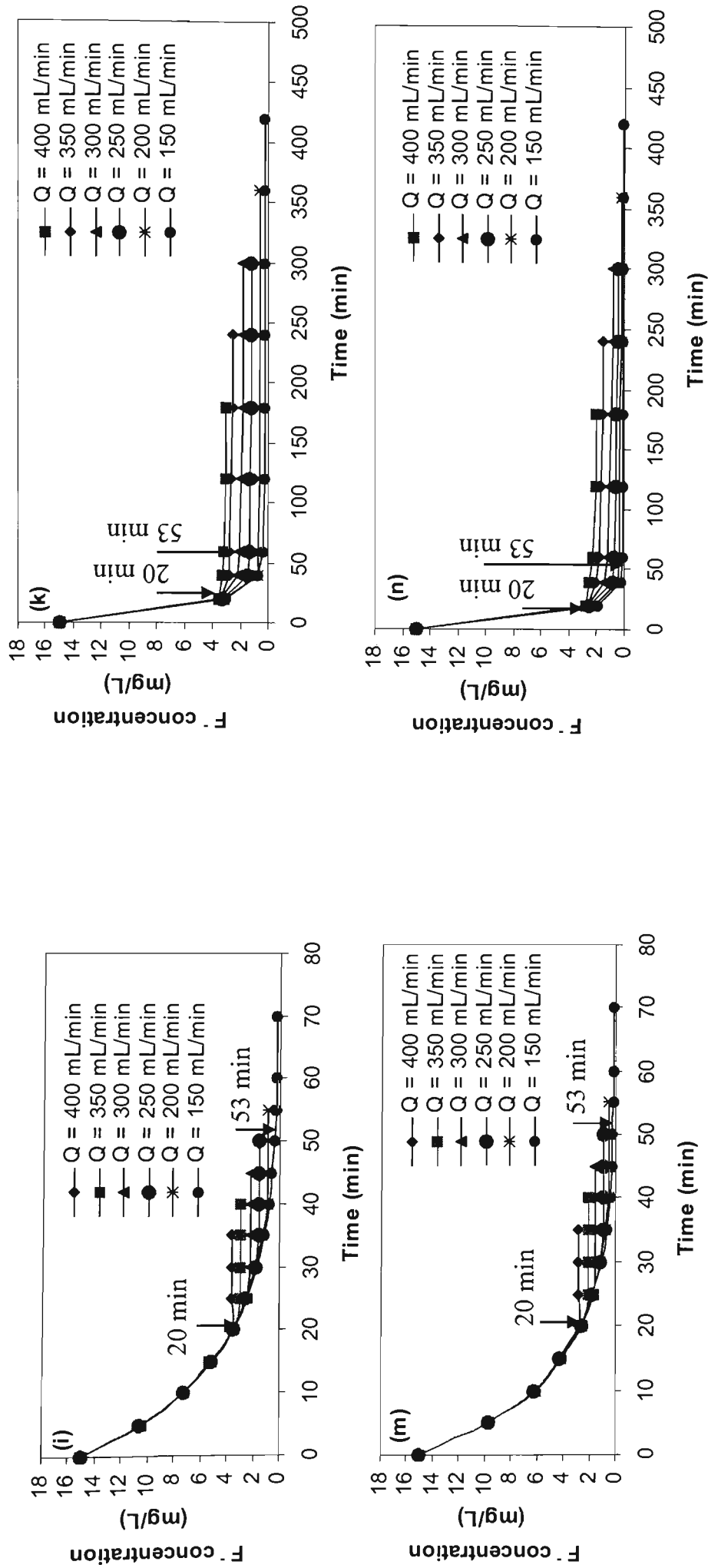


Figure 6-20 (Continued) - Effect of detention time on the residual fluoride concentration at different flow rate values and current densities in a continuous flow electrocoagulation reactor ($C_o = 15 \text{ mg/L}$, $\text{pH}_{in} = 6$, $E_c = 50 \text{ mS/m}$), [i] Electrocoagulator - $i = 37.5 \text{ A/m}^2$, [k] EC system - $i = 37.5 \text{ A/m}^2$, [m] Electrocoagulator - $i = 50 \text{ A/m}^2$, [n] EC system - $i = 50 \text{ A/m}^2$

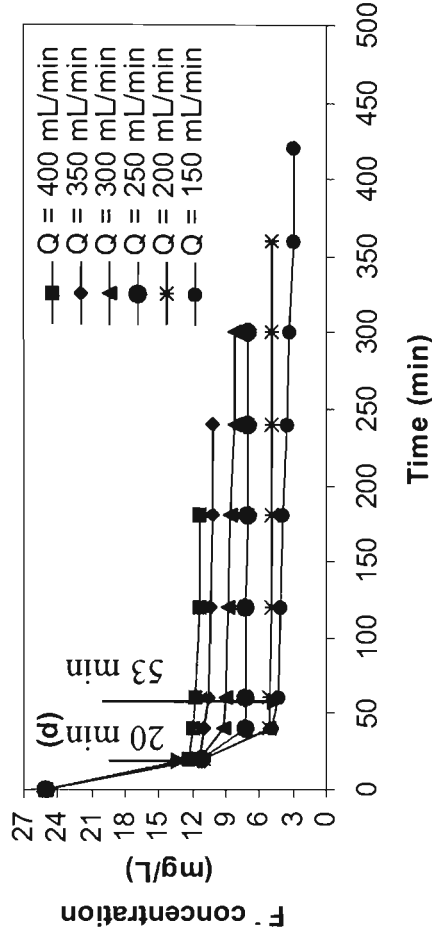
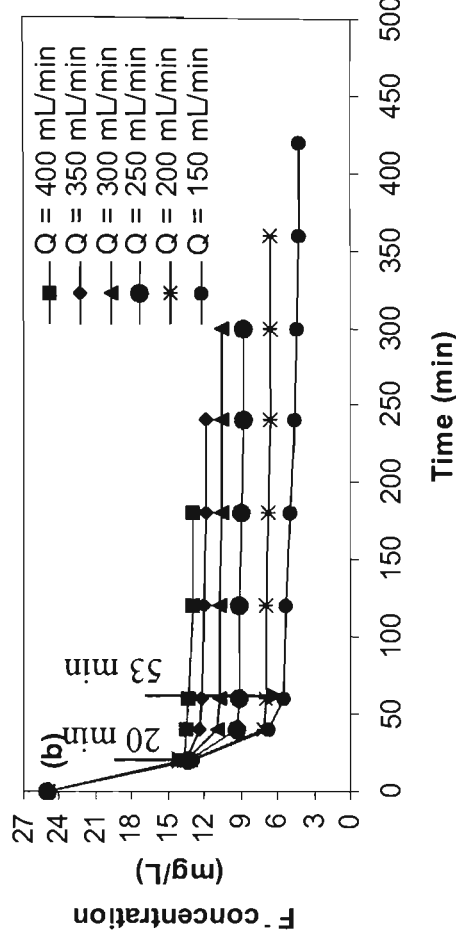
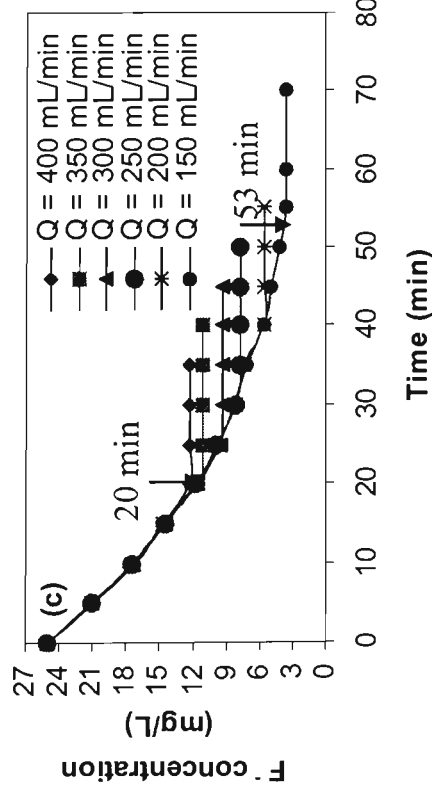
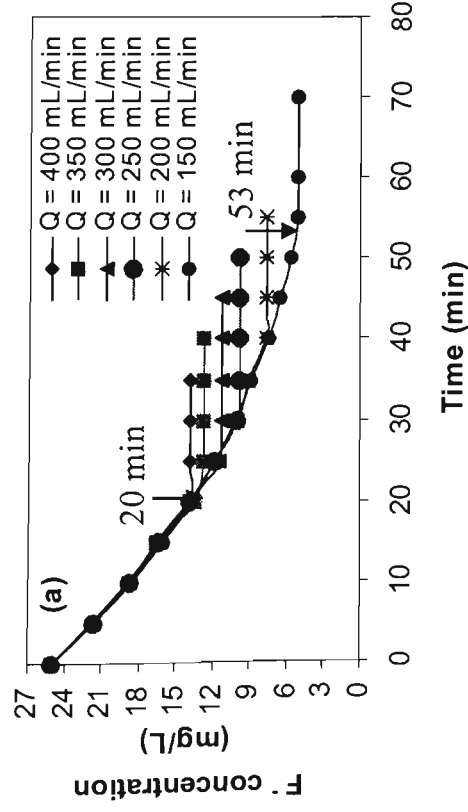


Figure 6-21 Effect of detention time on the residual fluoride concentration at different flow rate values and current densities in a continuous flow electrocoagulation reactor ($C_o = 25$ mg/L, $pH_{in} = 6$, $E_c = 50$ mS/m), [a] Electrocoagulator - $i = 12.5$ A/m², [b] EC system- $i = 12.5$ A/m², [c] Electrocoagulator - $i = 18.75$ A/m², EC system- $i = 18.75$ A/m²

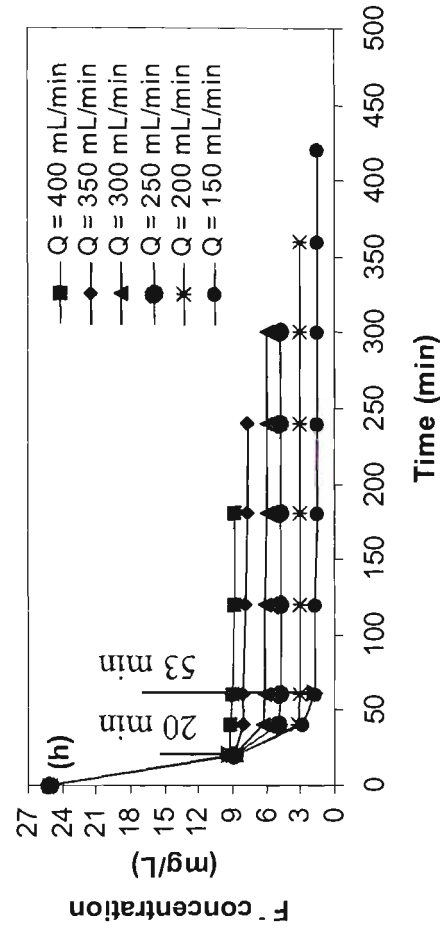
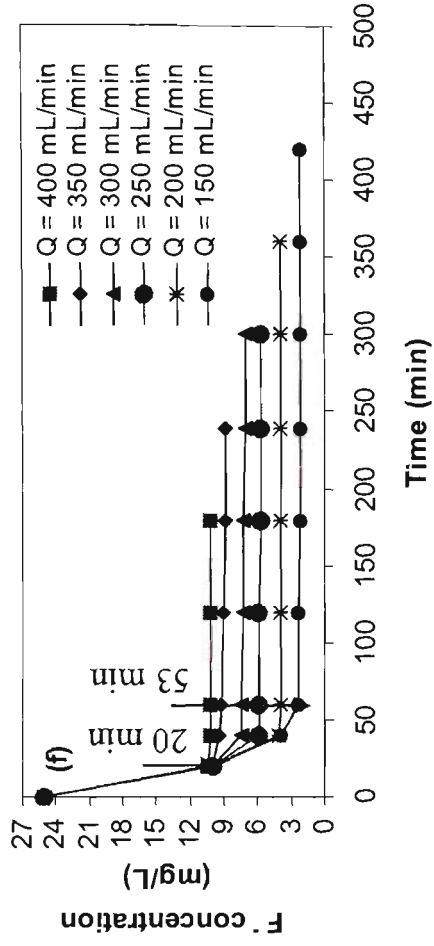
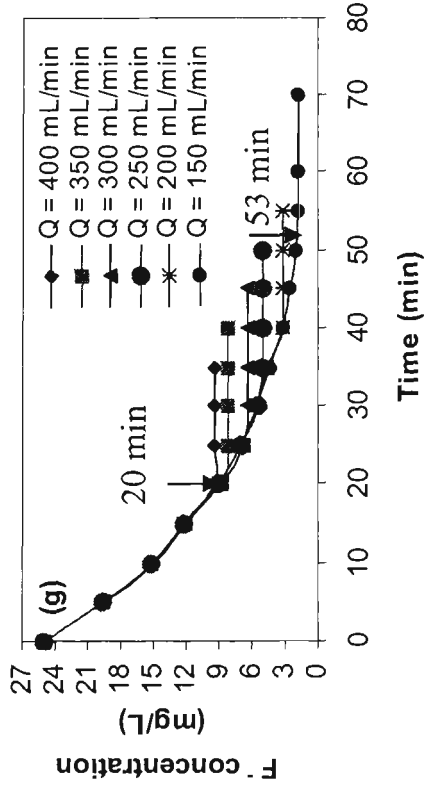
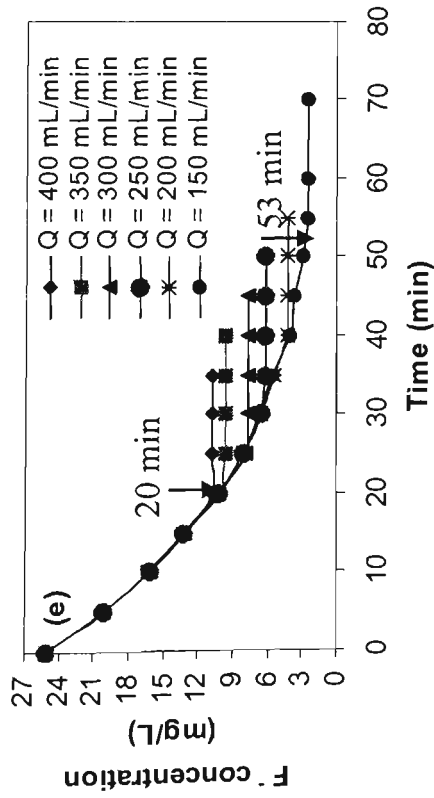


Figure 6-21 (Continued) - Effect of detention time on the residual fluoride concentration at different flow rate values and current densities in a continuous flow electrocoagulation reactor ($C_0 = 25$ mg/L, $pH_{in} = 6$, $E_c = 50$ mS/m), [e] Electrocoagulator - $i = 25$ A/m², [f] EC system - $i = 25$ A/m², [g] Electrocoagulator - $i = 31.25$ A/m², [h] EC system - $i = 31.25$ A/m²

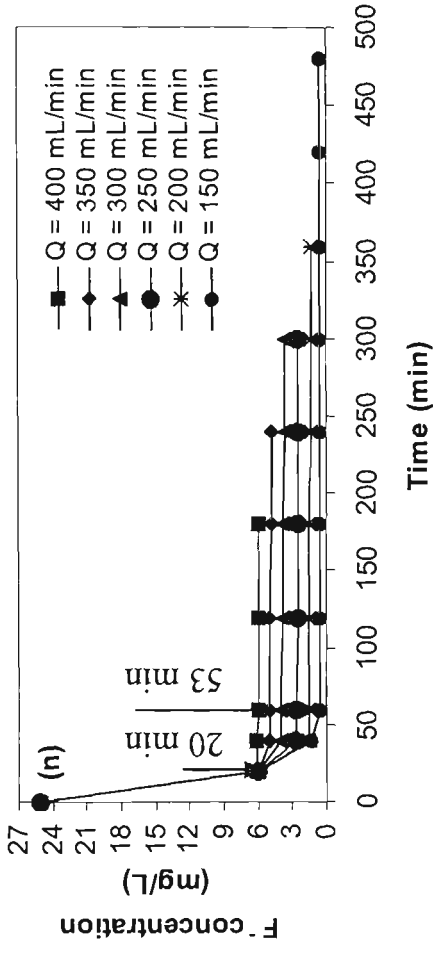
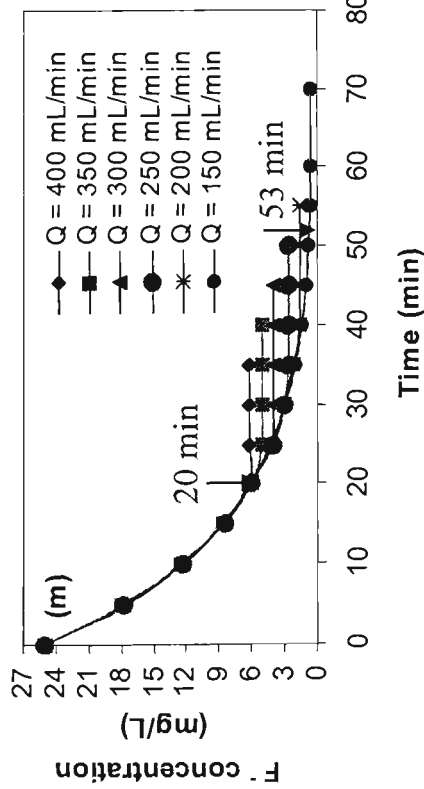
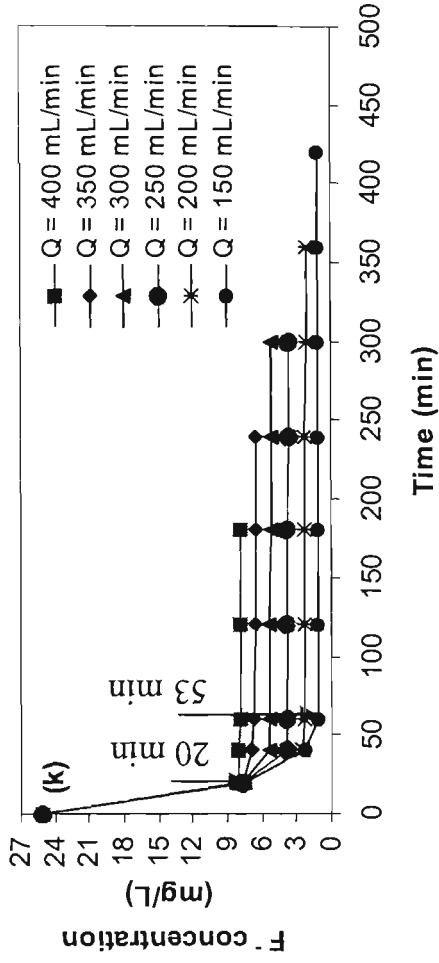
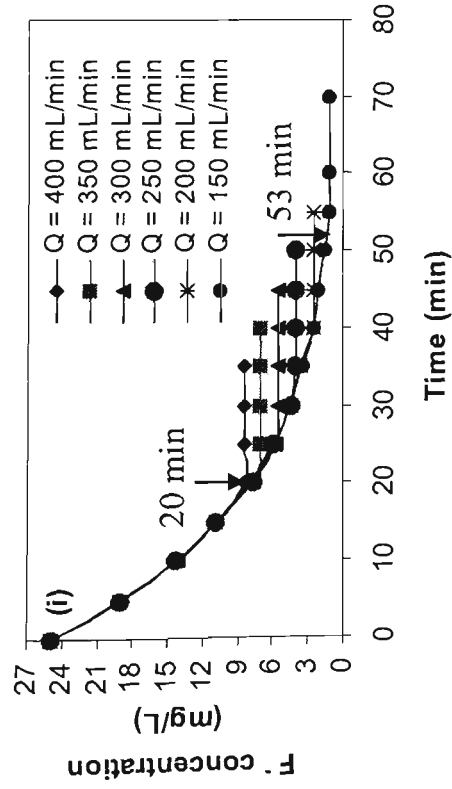


Figure 6-21 (Continued) - Effect of detention time on the residual fluoride concentration at different flow rate values and current densities in a continuous flow electrocoagulation reactor ($C_o = 25$ mg/L, $pH_{in} = 6$, $E_c = 50$ mS/m), [i] Electrocoagulator - $i = 37.5$ A/m², [k] EC system- $i = 37.5$ A/m², [m] Electrocoagulator - $i = 50$ A/m², [n] EC system- $i = 50$ A/m²

As seen, at a constant initial concentration of fluoride the residual concentrations are affected by varying the current density and flow rates in the electrocoagulator. As noted in EC fundamentals in chapter 2, current values and treatment time were important variables for releasing aluminium to the solution in the batch EC process. The theoretical detention time (t_d) within a continuous flow EC system is sometimes called the hydraulic residence time (volume divided by flow rate). Thus flow rate will affect detention time in the electrocoagulator and EC system. It can be seen that the residual fluoride has decreased more in the electrocoagulator when the sedimentation tank is more effective for sludge sedimentation. The experimental results showed that the highest current (8 A) produced the quickest fluoride removal due to the ready availability of Al^{3+} ions in the solution. However at higher currents, more coagulant (aluminium) is available per unit time, which may be unnecessary, because not only is excess residual Al unsafe for drinking water but at a high current is also uneconomic in terms of energy consumption. In this continuous flow EC reactor, the minimum residence time required to reduce the final fluorine concentration to a desirable concentration ($F^- = 1 \text{ mg/L}$) is defined as the optimum residence time (t_{ro}). The residence time was experimentally determined to achieve a desirable concentration range of fluoride in the electrocoagulator section when the residual aluminium concentrations on the effluent were found to be less than 0.2 mg/L which is desirable concentration based on NHMRC and ARMCANZ (2004) guidelines. The optimum residence times and optimum surface charge density have been summarised in Table 6-5 for different flow rates, current densities, and initial fluoride concentrations at the initial pH of 6 when final pH reached to 8 in the electrocoagulator. Chapter 8 will be discussed whether continuous flow EC reactor operations may be subjected to an optimal flow rate.

Table 6-5 The experimentally determined optimum residence time and surface charge density to achieve the desirable fluoride concentration range in the electrocoagulator for different flow rates, current densities, and initial fluoride concentrations

Initial Fluoride concentration (mg/L)	Flow rate (mL/min)	Optimum residence time (min)	Current density (A/m ²)	Optimum surface charge density (C/m ²)	Fluoride removal efficiency (%)
5	200	40	12.5	30000	95
5	250	32	18.75	36000	93
5	300	26	25	39000	92
5	350	23	31.25	43125	91
5	400	20	37.5	45000	90
10	150	53	18.75	59625	93
10	200	40	25	60000	91
10	250	32	37.5	72000	92
10	350	23	50	69000	93
15	150	53	25	79500	90
15	200	40	37.5	90000	92
15	250	32	50	96000	92
25	150	53	37.5	119250	91

As seen, the optimum charge densities were found to be range of 30000-45000 C/m² for 5 mg/L, 60000-70000 C/m² for 10 mg/L, 80000- 96000 for 15 mg/L, and near to 120000 C/m² for 25 mg/L initial fluoride concentrations. The residual Al concentrations on the effluent were found to be less than 0.2 mg/L which is desirable concentration, as is shown in Appendix D.

6.3.6 Sludge quantity

The sludge produced in the continuous flow EC reactor, which is schematically shown in Figures 6-22 (a, and b), was collected from the top and bottom of the sedimentation tank. The effect of the different flow rates and current densities on the total volume of sludge produced is illustrated in Figure 6-23.

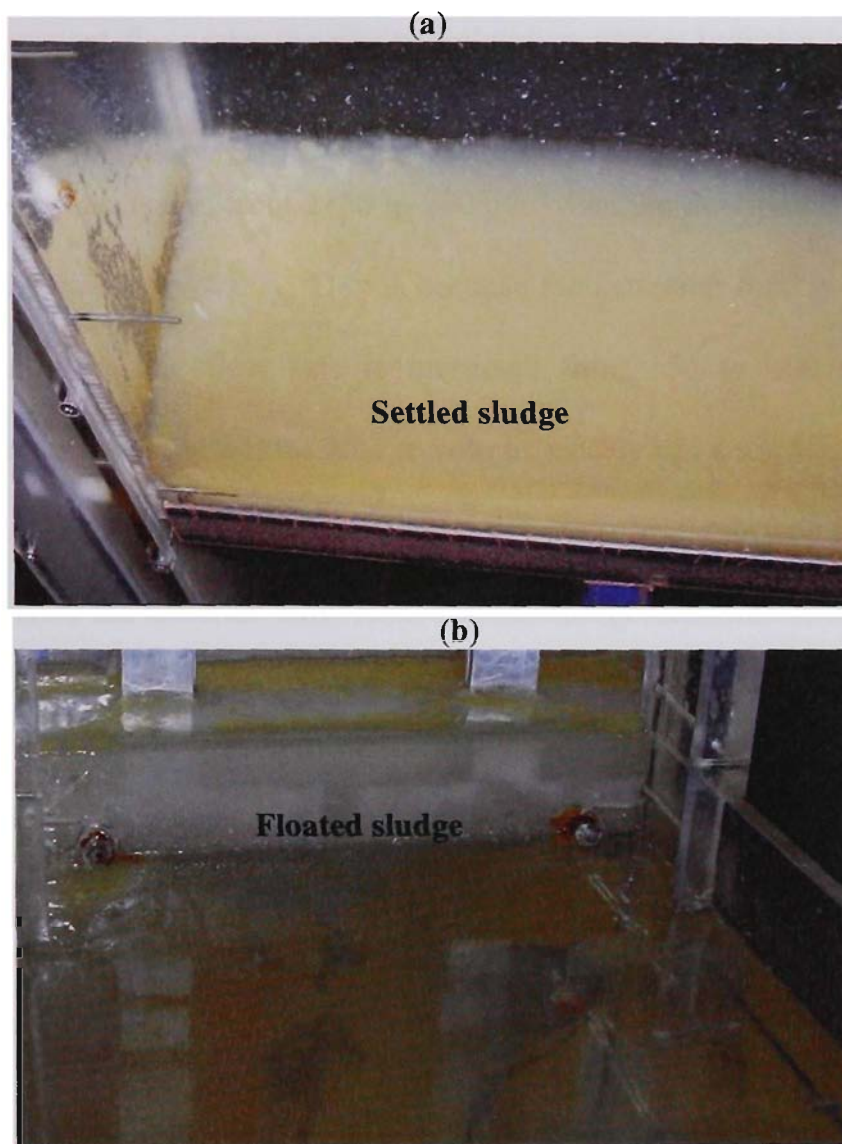


Figure 6-22 Images of the (a) settled sludge and (b) floated sludge in a continuous flow electrocoagulation system

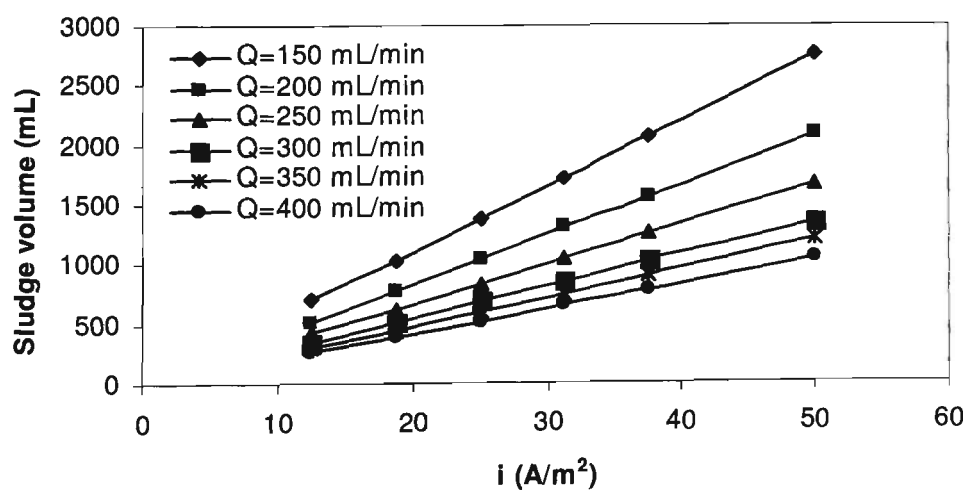


Figure 6-23 Total sludge volume versus flow rate in different current density and flow rates in a continuous flow electrocoagulation reactor ($C_o=10$ mg/L, $pH_{in} = 6$, $d=5$ mm, operational time = 8 h)

For a given constant flow rate, the sludge volume increases linearly by increasing of current density. At a constant current density of 50 A/m^2 and 8 hour operational time the volume of sludge decreases from 2750 to 700 mL when the flow rate is increased from 150 to 400 mL/min, respectively. This is because the detention time is decreased from 53 to 20 min when the flow rate is increased from 150 to 400 mL/min in the electrocoagulator. As expected, the sludge volume clearly has a significant dependency on the production of current density and the detention time (surface charge density). Thus, the effect of the different flow rates and the charge densities on the total volume of sludge production is illustrated in Figure 6-24. As expected, the volume of sludge depends entirely on the surface charge density.

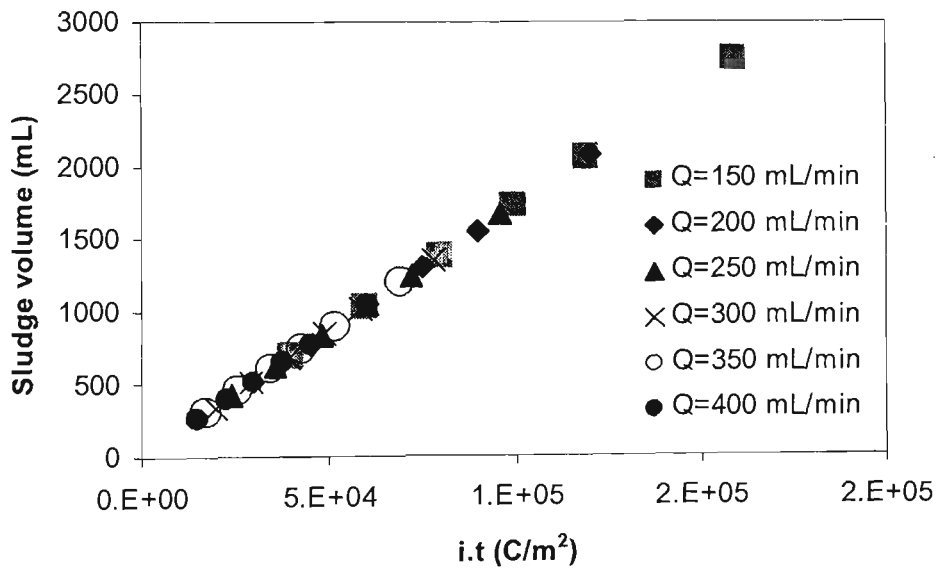


Figure 6-24 Total sludge volume versus flow rate in different surface charge density in a continuous flow electrocoagulation reactor ($C_o=10 \text{ mg/L}$, $i=12.5 - 50 \text{ A/m}^2$, $\text{pH}_{in} = 6$, $d=5\text{mm}$, operational time = 8 h)

As seen, at high flow rate (400 mL/min) and 8 h operational time, the sludge volume decreases from 1040 to 260 mL when the surface charge density is decreased from 60000 to 15000 C/m^2 , respectively. However, it should be noted that the final fluoride concentration is not reduced to less than 1 mg/L at surface charge density of 15000

C/m^2 when it is considered to have less sludge volume. At low flow rate (150 mL/min) and 8 h operational time, the sludge volume increases from 700 to 2750 mL when the surface charge density is respectively increased from 40000 to 160000 C/m^2 .

The total mass of dried sludge versus the flow rate is presented in Figure 6-25. As seen, a continuously pattern (sludge mass) is increasing in direct proportion to the surface charge density. At a constant flow rate of 150 mL/min and 8 h operational time, the total sludge mass increases from 2.5 to 8.5 g when the surface charge density is increased from 40000 to 160000 C/m^2 . As seen, the higher amounts of sludge mass are resulting by increasing of the surface charge density.

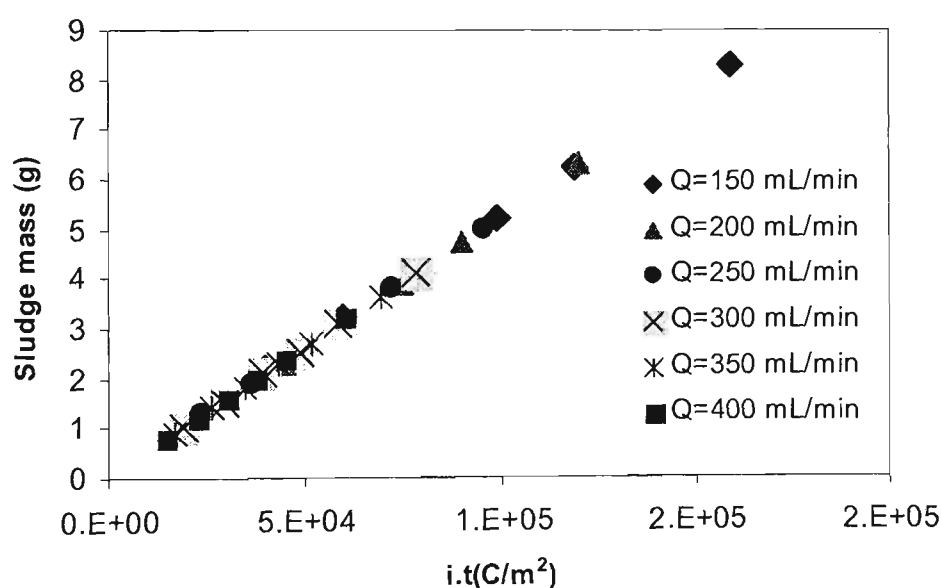


Figure 6-25 Total sludge mass versus flow rate in different surface charge density in a continuous flow electrocoagulation reactor ($C_o=10$ mg/L, $i=12.5-50$ A/m^2 , $pH_{in}=6$, $d=5$ mm, operational time =8 h)

The sludge mass increases linearly by increasing of surface charge density. The final fluoride concentration reaches from 10 to 0.1 mg/L at high charge of 160000 C/m^2 when the residual fluoride concentration is expected to be 1 mg/L in the effluent. It is expected to have high sludge mass when higher coagulation dose are found not to

necessary in a better treatment performance. Concerning an investigation into the mechanism of removing fluoride in a continuous flow electrocoagulation reactor, the composition of dried settled and floated sludge are analysed by XRD spectroscopy, which will be explained in chapter 7.

6.3.7 Total operational costs

The continuous flow EC reactor's total operational cost were estimated from sum of the specific costs of electrical energy, aluminium plate consumption, pH adjustment, and sludge treatment. From optimized results for detention time and surface charge density, which was previously shown in Table 6-5, the energy and aluminium electrode consumptions are calculated. At initial fluoride concentration of 5 mg/L and surface charge density of 30000 C/m², the total estimated operational cost for defluoridation using a pilot-scale continuous flow EC reactor is shown in Table 6-6, while a complete table of results at the different initial fluoride concentrations and charge densities can be found in Appendix E.

Table 6-6 Estimated total operational cost¹ for defluoridation using a pilot-scale continuous flow EC reactor (Q = 200 mL/min, i = 12.5 A/m², U = 4.27 V, C_o = 5 mg/L, and surface charge density = 30000 C/m²)

Item	Cost (AUD/m ³)	Percentage (%)
Energy consumption	0.06	16.7
Aluminium plate consumption	0.19	52.8
pH adjustment	0.03	8.3
Sludge treatment	0.08	22.2
Total	0.36	100

¹ Assuming a depreciation period of 10 years and an interest rate of 5%, the aluminium plate costs AUD 2.8/Kg, electricity cost is AUD 0.085/kWh, the pH adjustment cost is AUD 60/L HCl 1M (50 mL HCl 0.01 M/1m³ is used for each run), the sludge treatment cost was found to be USD 0.06 (adapted from Lin et al., 2005) when 1 USD = 1.327 AUD

Effect of current density on the total operating costs at the different initial fluoride concentration in the continuous flow EC reactor is shown in Figure 6-26. As seen, the total operating cost is increased when the current density increases.

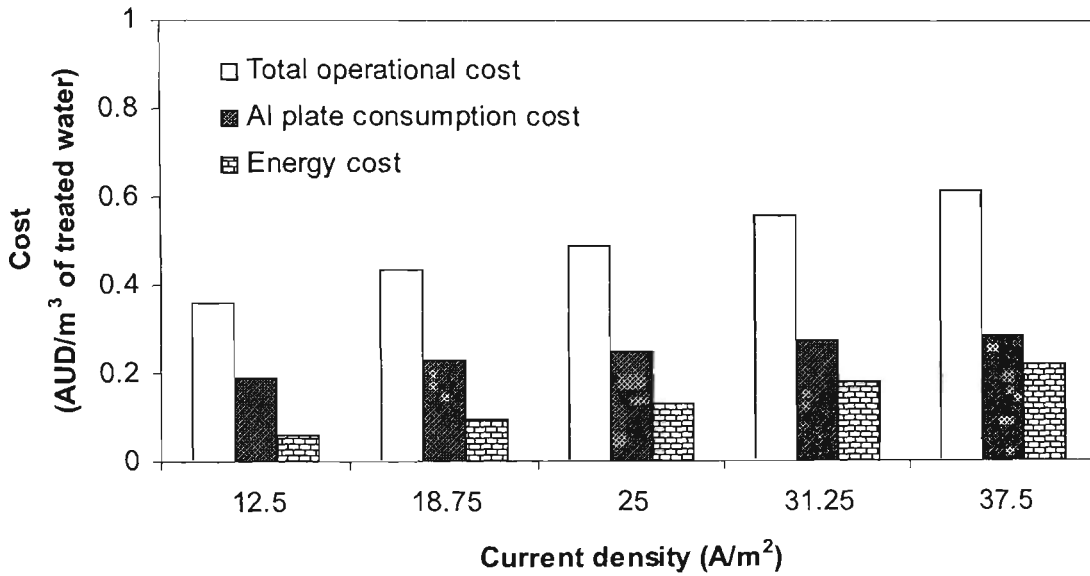


Figure 6-26 Effect of current density on the total operating, energy and the Al materials costs at the different initial fluoride concentration in the continuous flow EC reactor ($pH_{in}=6$, $E_c=50\text{ mS/m}$, $d=5\text{ mm}$)

The specific electrical energy consumption was proportional to the current values and the flow rate. From the different current densities and flow rates, the total operational cost is found between AUD 0.36 -0.61 per m^3 of treated water when initial fluoride concentration is 5 mg/L. The experimental results show that the energy cost increases from AUD 0.061 to 0.22 per m^3 of treated water when the current density is increased from 12.5 to 37.5 A/m^2 . At these current densities, the Al plate consumption cost ranges between AUD 0.19 - 0.29 per m^3 of treated water. As expected, at high current more Al released in to electrocoagulator.

The total operating cost is also increased when initial concentration of fluoride increases in the continuous flow EC reactor, as shown in Figure 6-27, For the current density of

18.75 A/m², the total operational cost is increased from AUD 0.43 to 0.63 per m³ of treated water when the initial concentration of fluoride increases from 5 to 10 mg/L.

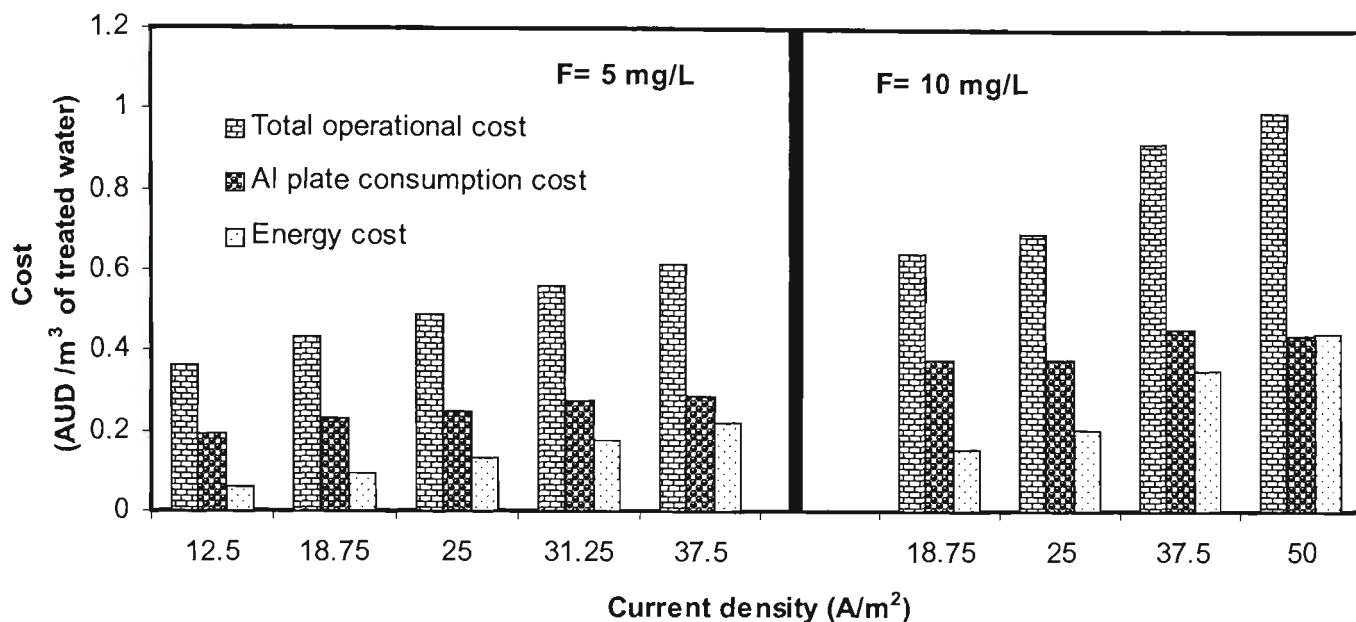


Figure 6-27 Effect of current density on the different operating costs at the different initial fluoride concentration in the continuous flow EC reactor ($pH_{in}=6$, $E_c=50$ mS/m, $d=5$ mm)

The total operational cost increases from AUD 0.64 to 0.99 per m³ of treated water when the current density is increased from 18.75 to 50 A/m² and the initial fluoride concentration is decreased 10 to 1 mg/L. For the same initial concentration of fluoride a lower operating cost is achieved with a lower flow rate. This is because the residence time is increased when the flow rate decreases. Higher coagulant doses do not necessarily improve performance.

The maximum total operational cost for defluoridation by Nalgonda process (NA) was reported to be In RS 33.70/m³ (AUD 1/m³)² of treated water (TNWSDB, 2005) when initial fluoride concentration was 5 mg/L. At the same initial fluoride concentration, the

² 1 AUD = 33 In RS

maximum total operational cost for EC process, as is shown in Figure 6-28, is found to be AUD 0.6 per m³ of treated water.

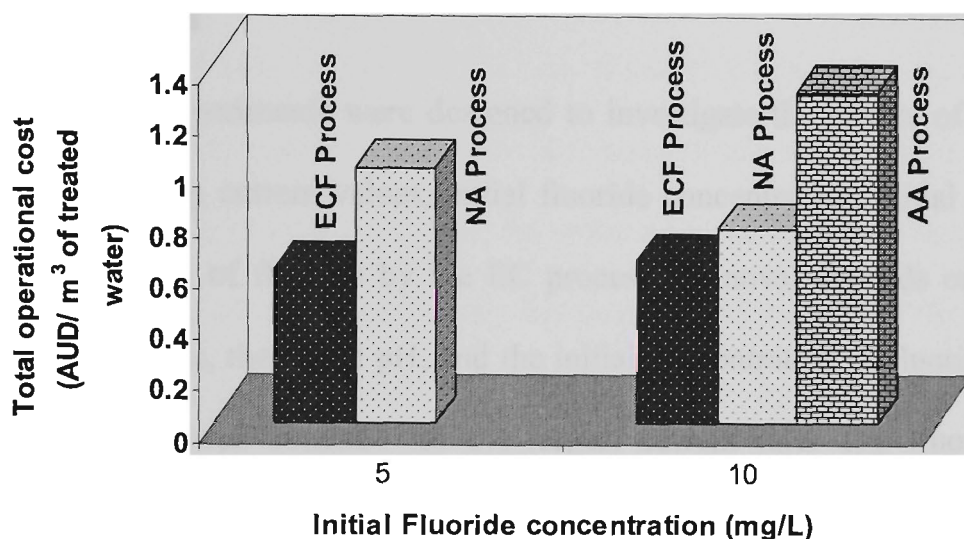


Figure 6-28 Cost comparison on the aluminium electrode consumption for ECF process and the coagulant consumption for CC process

From results obtained in Figure 6-28, it can be concluded that the maximum total operational cost for EC process is accounted to be less than (40 %) that of the NA process when initial fluoride concentration is 5 mg/L. The calculated total operational cost for AA (activated alumina) and NA techniques were found to be RS 43 (AUD1.3) and RS 25 (AUD 0.76) per m³ of treated water, respectively when initial fluoride concentration was at near 10 mg/L (Agarwal et al., 1999). The minimum total operational cost for ECF process was found to be AUD 0.64 per m³ of treated water that was equivalent to that of the NA technique but less than that through the AA methods. From results, the defluoridation by ECF process was found operational cost effective. A cost comparison of all options such as capital cost or total unit cost was not possible; due to the variation in ultimate removal costs per volume of treated water which would greatly affect the cost of each option. The maximum flow rate that is passed to the pilot-

scale continuous flow EC reactor is 400 mL/min when the plant capacity of other defluoridation plants is considered to be very higher than the ECF process.

6.4 SUMMARY

Continuous flow experiments were designed to investigate the effects of the different parameters including current values, initial fluoride concentration, initial pH and flow rate on the removal of fluoride by the EC process. Removal depends on the applied current, the flow rate, the initial pH, and the initial concentration of fluoride. The most efficient treatment was obtained for the largest current rate. The fluoride removal efficiency is increased to 99% at 50 A/m² when the flow rate and initial fluoride concentration are respectively kept at 150 mL/min and 10 mg/L. However, in order to avoid excessive energy consumption it is advisable to limit the current rate when a desirable concentration range of fluoride effluent is achieved. Higher coagulant doses would not necessarily give a better performance. It can be concluded that to reduce fluoride concentration to the NHMRC and ARMCANZ, and WHO drinking water guidelines, the optimum flow rate depends on the flow rate and the initial concentration of fluoride. For a given constant flow rate, it appears that higher initial fluoride concentration needs higher current input for more treatment. the experimental mass ratio Al³⁺/F⁻ was found between 13-17.5 in the ECF process when the residual aluminium concentrations on the effluent were found to be less than 0.2 mg/L. the residual fluoride concentration reaches from 10 to 1 mg/L when the total aluminium concentration is found between 120-155 mg/L and the optimum surface charge density is found between 60000- 70000 C/m². The optimum flow rate can be increased if the current value is increased in the EC continuous flow reactor. The experimental results showed that defluoridation is more efficient for a pH ranging between 6 and 8. The electrical energy

consumption increased specifically with a rising concentration of aluminium, which was proportional to the current values and initial concentration of fluoride. For the same operational conditions the total operating cost was lowest when the flow rate was lower. The total operational cost for EC process was found to be less than 40 % of the NA (Nalgonda process) process when initial fluoride concentration was 5 mg/L.

The results from this project will assist the water and wastewater treatment plants in developing the most attractive technology for treatment of the excess fluoride in water supplies. In the water industry, excess fluoride may exist in three different ways. Firstly, the natural groundwater may have high F^- level that is not acceptable for drinking water standard. The methods developed in this thesis can be successfully applied to reduced F^- level to internationally acceptable drinking water standard. Secondly, fluoride can be found from wastewaters derived from semiconductor, metal processing, fertilizers, and glass-manufacturing industries. The discharge of these wastewaters without treatment into the natural environment would contaminate groundwater and other sources. If the F^- levels can be very high, some form of pre-treatment such as using $CaSO_4$ salts may be necessary before the methods developed in this thesis can be accepted. To treat concentrated groundwater from industries, pre-treatment may be done to bring F^- levels down to below 20 mg/L. The third way in which the research work may be useful is in the application of ECF technologies to existing fluoridated water supplies. There is a growing concern among professionally that the addition of F^- to water supplies may not benefit all population and if should be discontinued in developed countries. Fluoride can be ingested via food, drinks and etc. If this in the case, the methods developed in this thesis can be successfully used to reduce F^- concentration from 1 to 0.1 mg/L which is significantly lower.

CHAPTER 7

CHAPTER 7

SOLUTION SPECIATION AND REMOVAL MECHANISMS

7.1 INTRODUCTION

The results obtained from chapters 5 and 6 showed that electrocoagulation technology is an effective technology for the defluoridation of water in a batch and continuous flow reactor. As noted the electrolytic dissolution of aluminium anodes in water produced aqueous Al^{3+} species in electrocoagulation and it became necessary to study the kinetics of the complexation of aluminium ions in solution with soluble ligands (such as fluoride) that affect its speciation. To assess these effects, a better understanding of the chemistry and speciation of Al and Al-F complexes is essential. The hydrolysis of aluminium ions and the solubility of aluminium hydroxide, as well as the aluminium hydroxide solid phase, are considered by this chapter. The solubility of aluminium in equilibrium with solid phase $\text{Al}(\text{OH})_3$ depends on the surrounding pH. MINEQL⁺ model (Environmental Research Software, 1999) is utilised to illustrate the relative chemical speciation of Al-F complexes in solution and how different pH values would influence the solubility of aluminium hydroxide $[\text{Al}(\text{OH})_3]$. The chemical composition of the system at equilibrium is computed in the MINEQL⁺ model from the analytical data and thermodynamic database. Thus an understanding of the chemical speciation of Al and other species with fluoride ions is the main interest of this chapter. The mechanism for removing fluoride is explained in more detail in the following sections where the composition of dried sludge is analysed using the XRD spectrum.

7.2 BASIC PRINCIPLES

7.2.1 Chemical speciation

The chemistry of water based processes is traditionally understood from a basic knowledge of relatively simple chemical reactions and practical experience. The ability to model speciation quantitatively and the interaction of the aqueous phase with solid phases are key steps towards understanding and controlling the processes. Methods based on thermodynamics can be very useful for understanding processes such as dissolution and precipitation, which govern the chemical composition of aqueous chemical systems. Typically, these models require the computation of equilibrium compositions for systems containing numerous species distributed among an aqueous phase and several solid phases. For this reason, data is required for aqueous species and pure substance compounds when modelling applications for aqueous systems. Most aqueous databases include a small sub-set of pure substance data to enable such calculations to be performed (Snoeyin & Jenkins, 1980).

An important consideration in the use of the data is a reference or standard state for the elements. Although the data in a database should be self consistent, in general, care should be taken when mixing data from different databases. This is particularly important if critically assessed data is combined with estimated data, for which there is a limited experimental basis, and when considering data for pure substances which may not have the same reference state as the aqueous species (Butler, 1998).

7.2.2 A chemical equilibrium modelling system

Applying chemical equilibrium models to natural systems has always had subtle difficulties. Certainly limitations in thermodynamic data and interference from the

dependent reactions are major restrictions, but the equilibrium approach provides a technique for understanding potential chemical interactions and simplifying complex mechanisms. The presence of uncertainty in input data or underlying system processes should not deter anyone from using equilibrium programmes. Interesting information often come from the differences between a system and equilibrium rather than the answer from equilibrium itself. The numerical engine for the MINEQL⁺ model was developed to solve expressions of mass balance using equilibrium constants by Environmental Research Software (1996). The uses of Gibb's free energy or equilibrium constants are both valid approaches. MINEQL⁺ is an interactive data management system for modelling chemical equilibrium which uses the original MINEQL⁺ programme as an integrated software package with a solid theoretical foundation superimposed on advanced data management tools. MINEQL⁺ allows the speciation of any type of aqueous chemical system to be investigated. Key features include the ability to:

- Compose a system from choices of chemical components
- Calculate the equilibrium conditions for any system
- Calculate, manage, view, and extract output data from any perspective
- Graph any output data versus any independent variable, for log C-pH or distribution diagrams (total concentration %)
- Extract the pH and alkalinity of the system for any number of calculations
- Extract the ion balance for an unlimited number of runs
- Extract the saturation indexes for all solids
- Compile all species output into a single report for easy comparison

The process of solving chemical equilibrium problems, which schematically is shown in Figure 7-1, can be broken down into the following 5 simple steps:

1. Selection of the chemical components that will define the system
2. Creation of chemical species from these components, including scanning a database for the thermodynamic constants
3. Setting the total concentration of individual components
4. Running the calculation together with setting the ionic strength and temperature
5. Viewing and extracting output data (may include creating graphic plots, specialised reports, and saving data)

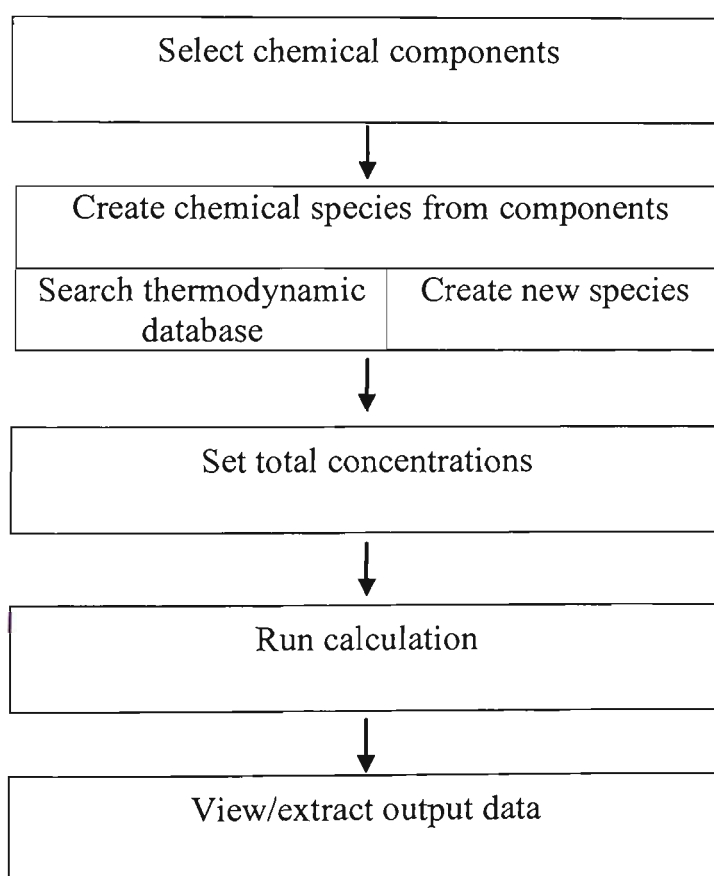


Figure 7-1 Chemical equilibrium problem solving process (from Environmental Research Software, 1996)

7.3 SPECIATION RESULTS

7.3.1 Speciation of Al in water

The aquo aluminium ion is the hardest of the trivalent metal ions, with an effective ionic radius of 0.5\AA , which is smaller than other commonly encountered trivalent metal ions. Aluminium has a strong tendency to hydrolyse in an aqueous solution (Martell et al, 1996). Aluminium can exist in surface and ground water in a number of different forms, which depend on pH, temperature, ionic strength, and the type of organic and inorganic elements in the raw water (Srinivasan and Viraraghavan, 2002). In a basic and acidic solution Al ion will be found in anionic $[\text{Al}(\text{OH})_4^-]$ and cationic $[\text{Al}(\text{OH})_2^+]$ forms, respectively. The aqueous Al, in cationic form, can react with anions such as: OH^- , F^- , SO_4^{2-} , and HCO_3^- to form various Al complexes. However, the Al complexes formation with anions of OH^- and F^- are the most significant in natural waters (Driscoll and Schecher, 1990). The aquo complex $\text{Al}(\text{H}_2\text{O})_6^{3+}$ predominates at $\text{pH} < 4$ when the aluminium hydroxide complexes are formed at $\text{pH} > 4$. There are many different complexes about the products of hydrolysis of aluminium ions in the aqueous solution. With regard to the general formula $\text{Al}_q(\text{OH})_{3q-p}^{p+}$ for hydrolysed species the values 1, 2, 3, 4, 5, 7, 8, 13 for q , and 1+, 2+, 3+, 4+, 5+, 0, 1-, 3-, 4-, 6-, for charge p have been suggested (Dezelic et al, 1971). In the absence of significant concentrations of other anions the aqueous Al will form various hydroxyl complexes, the relative amounts of which will depend on pH and on the initial concentration of the Al in solution (Smith, 1996). The total aluminium content in water can be subdivided into three fractions (Srinivasan et al, 1999):

1. Acid-soluble aluminium, which includes forms of aluminium that require acid digestion before analysis (polymeric, colloidal, and extremely stable organic and hydroxy organic complexes)
2. Non-labile (organic) monomeric aluminium
3. Labile (inorganic) monomeric aluminium.

Concerning the aluminium ionic species in an aqueous solution, the relationships of aluminium solubility are considered by use of the thermodynamic properties of the aluminium aqueous species. One way of showing the relationships of aluminium solubility in water is through the use of equilibrium relationships. The thermodynamic equilibrium constant (K^0) at standard temperature and pressure (STP) is defined by Sposito (1996). Thermodynamic properties are used to determine the stable aqueous species. The mononuclear complexes are initially formed as summarised in Table 7-1.

Table 7-1 Predominant aluminium species in drinking water (Sposito, 1996)

Reaction	Log K^0
$Al^{3+} + H_2O \longleftrightarrow Al(OH)^{2+} + H^+$	-5
$Al^{3+} + 2H_2O \longleftrightarrow Al(OH)_2^+ + 2H^+$	-10
$Al^{3+} + 3H_2O \longleftrightarrow Al(OH)_3^0 + 3H^+$	-16.8
$Al^{3+} + 4H_2O \longleftrightarrow Al(OH)_4^- + 4H^+$	-22.7

7.3.1.1 Dependence of aluminium solubility on the pH

The solubility of aluminium in equilibrium with solid phase $Al(OH)_3$ depends on the surrounding pH. Considering only mononuclear speciation, the hydroxyl aluminium species are forming such as $Al(OH)^{2+}$, $Al(OH)_2^+$, $Al(OH)_3_{(aq)}$, and $Al(OH)_4^-$. As seen

in Figure 7-2, in the pH range of 5 and 6, the predominant hydrolysis products are found to be $\text{Al}(\text{OH})_2^+$ and $\text{Al}(\text{OH})_3^0$.

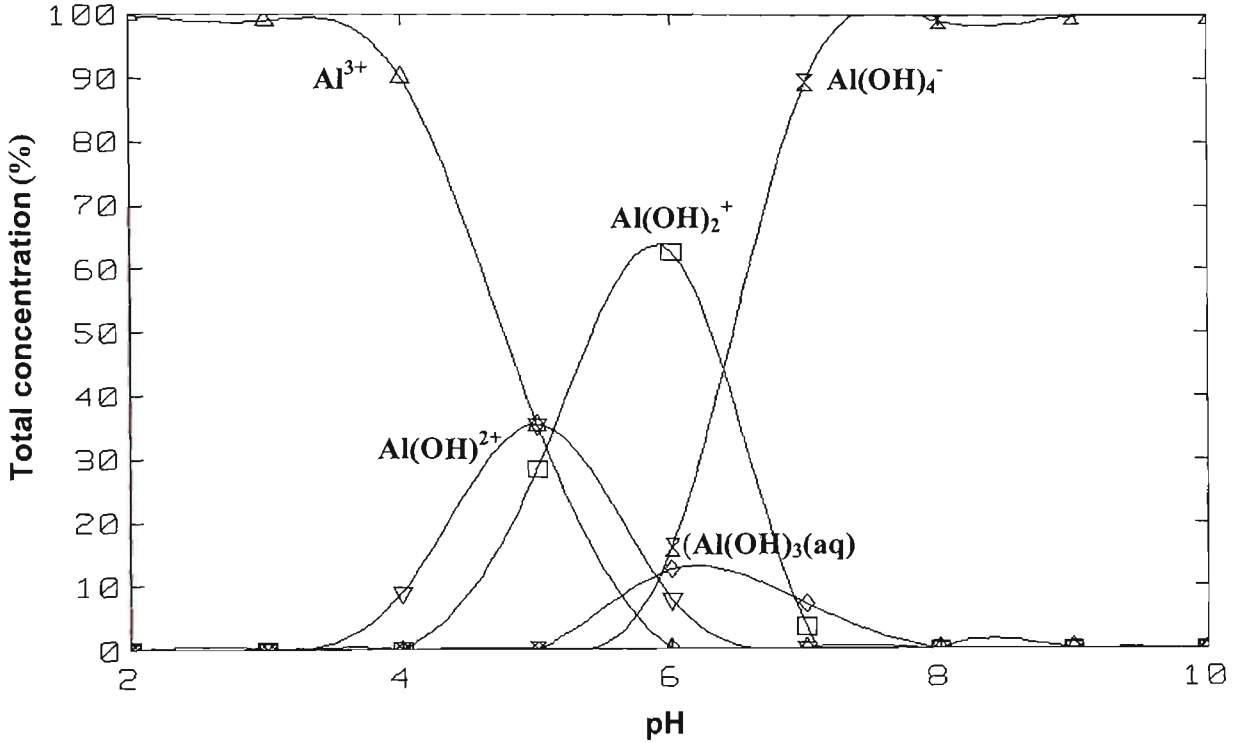


Figure 7-2 Distribution diagram of mononuclear species for Al-H₂O as a function of pH ($\text{Al}_T = 1 \times 10^{-6} \text{ M}$, $T=25^\circ\text{C}$; Ionic strength = 0.001 M)

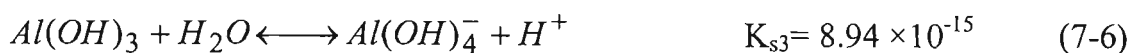
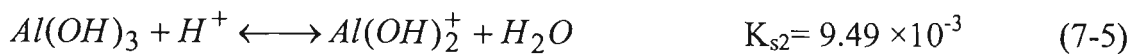
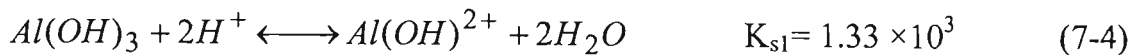
The analytical total concentration of aluminium (C_{Al}) in aqueous acidic solution is given by:

$$C_{\text{Al}} = [\text{Al}^{3+}] + [\text{Al}(\text{OH})^{2+}] + [\text{Al}(\text{OH})_2^+] + [\text{Al}(\text{OH})_3^0] + [\text{Al}(\text{OH})_4^-] \quad (7-1)$$

The concentration of $\text{Al}(\text{OH})_3^0$ species remained unchanged in the solution and may be omitted in an alternative speciation model. So Eq. 7-1 can be arranged to Eq. 7-2:

$$C_{\text{Al}} = [\text{Al}^{3+}] + [\text{Al}(\text{OH})^{2+}] + [\text{Al}(\text{OH})_2^+] + [\text{Al}(\text{OH})_4^-] \quad (7-2)$$

Equations 7-3 to 7-6 are used to evaluate the thermodynamic properties of the most probable ion species to aluminium hydroxide through appropriate ion activity products, or solubility products, for the following reaction (May et al., 1979).



From Eq. 7-2, by doing correlation analysis of the relationships between $[Al_T]$ and H^+ activity, the Eq. 7-7 can be developed:

$$[Al_T] = \frac{K_{s0}(H^+)^3}{\gamma Al^{3+}} + \frac{K_{s1}(H^+)^2}{\gamma Al(OH)^{2+}} + \frac{K_{s2}(H^+)}{\gamma Al(OH)_2^+} + \frac{K_{s3}(H^+)^{-1}}{\gamma Al(OH)_4^-} \quad (7-7)$$

where γ is activity coefficient. Additional relations can be also obtained from mass balances on each of the components in the system. Each element or group that appears in a number of species can be the subject of a mass balance. The total amount of Al concentration $[Al_T]$ is calculated by the MINEQL⁺ model and the results are shown in Table 7-2. The total amount of Al concentration must equal to the sum of all the various species.

The aqueous of aluminium is dominated by the interaction of Al^{3+} with water to form hydrolytic species via the following reaction (Eq. 7-8):

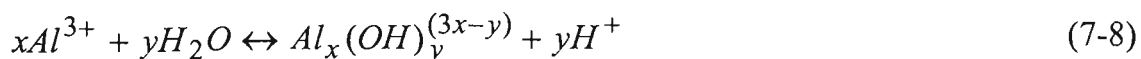
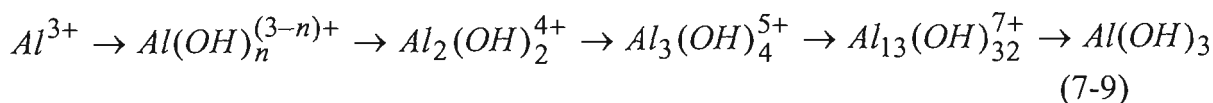


Table 7-2 Total molar concentration of the mononuclear Al ion species at different pH ($Al_T = 1 \times 10^{-6}$ M, $T=25^\circ\text{C}$; Ionic strength = 0.001 M)

pH	$[H^+]$ M	$[Al^{3+}]$ M	$[Al(OH)^{2+}]$ M	$[Al(OH)_2^+]$ M	$[Al(OH)_4^-]$ M	$[Al_T]$ M
3	1.04E-03	2.70E-01	1.63E-05	2.27E-03	4.15E-12	2.72E-01
4	1.04E-04	2.70E-04	1.63E-06	2.27E-05	4.15E-11	2.94E-04
5	1.04E-05	2.70E-07	1.63E-07	2.27E-07	4.15E-10	6.64E-07
6	1.04E-06	2.70E-10	1.63E-08	2.27E-09	4.15E-09	2.62E-08
7	1.04E-07	2.70E-13	1.63E-09	2.27E-11	4.15E-08	4.64E-08
8	1.04E-08	2.70E-16	1.63E-10	2.27E-13	4.15E-07	4.19E-07
9	1.04E-09	2.70E-19	1.63E-11	2.27E-15	4.15E-06	4.16E-06
10	1.04E-10	2.70E-22	1.63E-12	2.27E-17	4.15E-05	4.16E-05

Polynuclear species with x values up to 13 have been reported in concentrated solutions at intermediate pH. Although in natural waters, only monomeric $[Al(OH)_y^{3-x-y}]$ species (y=0-4) are important. Since the aluminium concentration increases, polynuclear species or aluminium complexes are formed and aluminium hydroxide precipitates, as shown in Eq. 7-9.



Throughout the pH of 4.7 and 10.5, polymeric aluminium hydroxides can be found. As polymers come together, aluminium hydroxide becomes large enough to precipitate from solution. Additionally, at pH>7.0 the aluminium hydroxide complexes dominate when the content of dissolved organic matter is low.

Thermodynamic modelling packages assist in the calculation of equilibrium speciation. The equilibrium concentrations of the soluble complexes are calculated from the data in the MINEQL⁺ software. At a low concentration of Al there are no polymeric species. Solid $Al(OH)_3$ precipitates at pH 5 and predominates over soluble complexes between pH 5 and 8.5. At a higher pH the soluble aluminate species

$[Al(OH)_4^-]$ predominates. MINEQL⁺ software was utilised to illustrate in Figure 7-3 how different pH values would influence on the solubility of aluminium hydroxide (see Appendix F). The solubility boundary denotes the thermodynamic equilibrium that exists between the dominant aluminium species in solution at a given pH, and solid aluminium hydroxide. Minimum solubility (0.03 mg-Al/L) occurs between pH ranges of 6.3-6.5. Since the solution becomes either more acidic or alkaline, solubility is increased. As seen, solid $Al(OH)_3$ is most prevalent in the pH range of 6 and 8.5. When the pH is above 9 the soluble $Al(OH)_4^-$ is the predominant species.

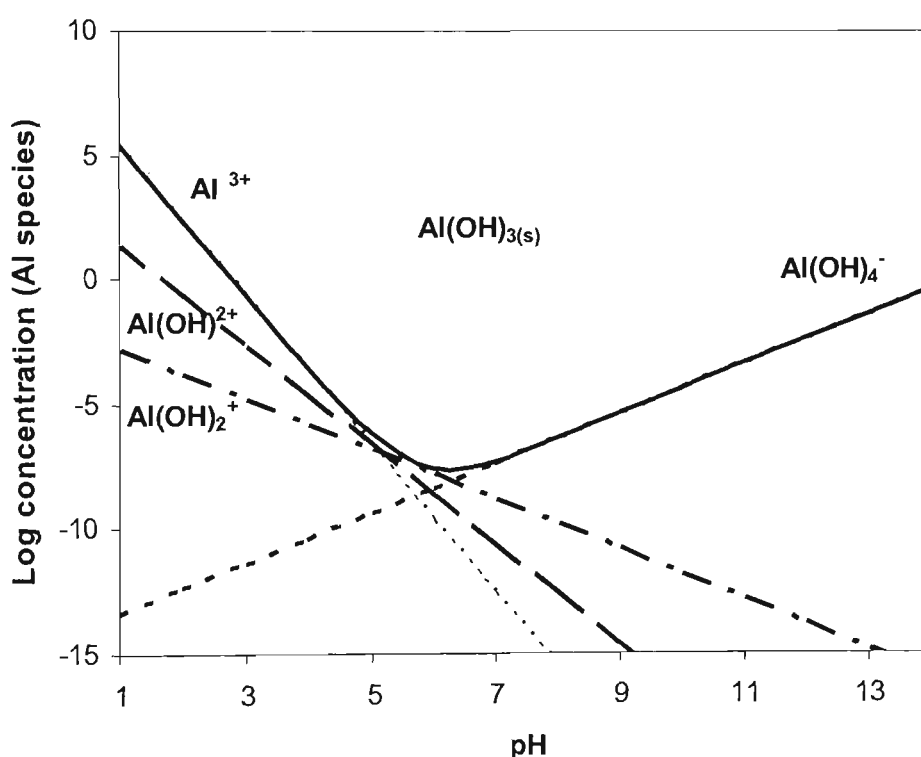


Figure 7-3 Solubility of aluminium hydroxide at various pH values by using MINEQL⁺ software

7.3.2 Speciation of Al-F Complexes

In natural water the most likely forms of soluble fluoride are the free anion F^- , the non-dissociated hydrofluoric acid HF , and complexes with aluminium or others. In a

theoretical study of the forms of fluoride ions in drinking water after coagulation with alum artificial fluoridation (optimum free fluoride concentration of 1 mg/L), fluoro-aluminates were nearly all converted to hydroxy-aluminates in neutral and alkaline solution ($\text{pH} \geq 7$), and the concentration of free F^- equalled that of the total concentration of fluoride. At a pH of 6 only three complexes, AlF^{2+} , AlF_2^+ , and AlF_3 were thought to be significant. At an operational pH more than 7 the amount of dissolved aluminium was observed to be a simple function of pH, primarily composed of $\text{Al}(\text{OH})_4^-$.

The thermodynamic analysis of chemical equilibrium was performed to predict the optimal conditions for the selective release of free fluoride ions. Thermodynamic calculations indicate that aluminium fluoride complexes are generally the dominant inorganic aluminium species. The predominant Al-F species in aqueous solution are summarised in Table 7-3.

Table 7-3 Predominant aluminium-fluoride species in aqueous solution (Sposito, 1996; and from MINEQL⁺ data base, 1996)

Reaction	Log K ^o
$\text{Al}^{3+} + \text{F}^- \longleftrightarrow \text{AlF}^{2+}$	6.98
$\text{Al}^{3+} + 2\text{F}^- \longleftrightarrow \text{AlF}_2^+$	12.60
$\text{Al}^{3+} + 3\text{F}^- \longleftrightarrow \text{AlF}_3^0$	16.65
$\text{Al}^{3+} + 4\text{F}^- \longleftrightarrow \text{AlF}_4^-$	19.03
$\text{Al}^{3+} + 5\text{F}^- \longleftrightarrow \text{AlF}_5^{2-}$	20.8*
$\text{Al}^{3+} + 6\text{F}^- \longleftrightarrow \text{AlF}_6^{3-}$	20.5*

*(Were adapted from the MINEQL⁺ data base program)

7.3.2.1 Effect of pH on speciation of Al-F complexes

The rate of complex aluminium - fluoride formation is generally dependent on the pH values of the solution. The presence of fluoride can produce comprehensible

changes in the progress of Al in water. Since fluoride ion forms strong complexes with aluminium it can increase the solubility of Al considerably. MINEQL⁺ software was utilised to show how a different pH would influence the speciation of Al – F complexes. With 1×10^{-5} M fluoride present, the distribution curves in Figure 7-4 show that the fluoride complexes AlF^{2+} , and AlF_2^+ predominate in an acid solution. In the alkaline solution the complex formed is the $Al(OH)_4^-$ anion. It can be seen that the fluoride complexes account for a substantial amount of the dissolved aluminium at pH values less than 7.

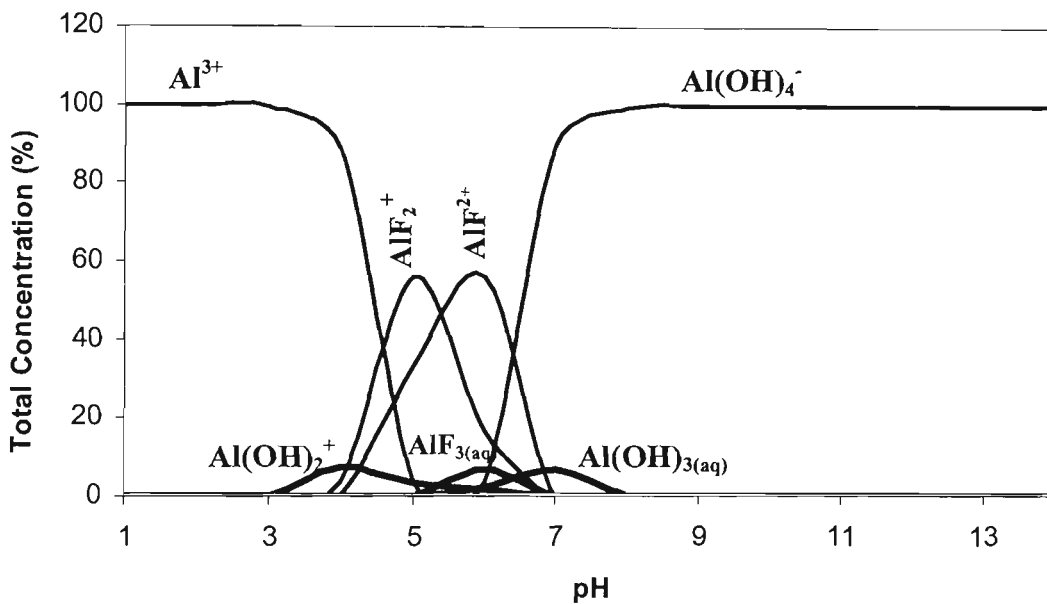


Figure 7-4 Distribution diagram of chemical species formed from 1×10^{-6} M aquo Al^{3+} ion; 1×10^{-5} M fluoride ion as a function of pH

In order to emphasise the aluminium chemical reaction the total concentration of aluminium can be written as:

$$C_{Al} = [Al^{3+}] + [Al - OH] + [Al - F] \quad (7-10)$$

where $[Al-OH]$ and $[Al-F]$ are the total concentration of aluminium hydroxy-complexes and aluminium fluoro-complexes, respectively. The expressions can be written as:

$$[Al-OH] = [Al(OH)^{2+}] + [Al(OH)_2^+] + [Al(OH)_3^0] + [Al(OH)_4^-] \quad (7-11)$$

$$[Al-F] = [AlF^{2+}] + [AlF_2^+] + [AlF_3] + [AlF_4^-] + [AlF_5^{2-}] + [AlF_6^{3-}] \quad (7-12)$$

From Eq. 7-12, the total amount of Al concentration must equal the sum of all the various species between aluminium and fluoride ions. The total amount of Al concentration (C_A) is calculated by MINEQL⁺ model at a different pH. The temperature within this calculation is set at a constant 25°C. The results for aluminium solubility and speciation are given in Table 7-4. The chemical species of both AlF_5^{2-} and AlF_6^{3-} are insignificant when their concentrations are very low. Under acidic conditions F^- has a strong affinity for Al. For acidic and neutral solutions the formation of various Al-F complexes is predominant, while the presence of a free fluoride ion and aluminium hydroxide complexes predominates where the pH solution values are greater than 8. At high pH values (>7), the concentration of OH^- is elevated and it becomes difficult for F^- to compete with OH^- for aqueous Al. As seen in Table 7-4, the concentration of the soluble $Al(OH)_3$ complex in aqueous solution (at saturation) is about 4.65×10^{-8} M ($\log C = -7.3$) at pH 7. The solubility of aluminium is calculated to be 0.001 mg/L when the fluoride concentration is low (0.01 mM). This result indicates that fluoride could dissolve aluminium deposits within the distribution.

Table 7-4 Total molar concentrations of aluminium speciation in the presence of 0.01mM F (from MINEQL⁺ model)

pH	Al ³⁺ (M)	Al(OH) ²⁺ (M)	Al(OH) _{3(aq)} (M)	Al(OH) ⁴⁻ (M)	Al(OH) ₂ ⁺ (M)	AlF ²⁺ (M)	AlF _{3(aq)} (M)	AlF ₂ ⁺ (M)	AlF ₄ ⁻ (M)	Total Al ³⁺ (M)
1	2.70E+05	1.63E-03	3.16E-09	4.15E-14	2.27E+01	1.59E-17	8.54E-31	1.00E-05	1.97E-45	2.70E+05
2	2.70E+02	1.63E-04	3.16E-09	4.15E-13	2.27E-01	1.59E-14	8.54E-25	1.00E-05	1.97E-36	2.70E+02
3	2.70E-01	1.63E-05	3.16E-09	4.15E-12	2.27E-03	1.59E-11	8.54E-19	1.00E-05	1.97E-27	2.72E-01
4	2.70E-04	1.63E-06	3.16E-09	4.15E-11	2.27E-05	1.57E-08	8.44E-13	9.96E-06	1.94E-18	3.04E-04
5	2.70E-07	1.63E-07	3.16E-09	4.15E-10	2.27E-07	2.20E-06	4.42E-08	3.73E-06	3.79E-11	6.64E-06
6	2.70E-10	1.63E-08	3.16E-09	4.15E-09	2.27E-09	7.20E-08	8.27E-09	2.13E-08	4.06E-11	1.28E-07
7	2.70E-13	1.63E-09	3.16E-09	4.15E-08	2.27E-11	7.50E-11	8.79E-12	2.18E-11	4.41E-14	4.65E-08
8	2.70E-16	1.63E-10	3.16E-09	4.15E-07	2.27E-13	7.51E-14	8.80E-15	2.18E-14	4.41E-17	4.19E-07
9	2.70E-19	1.63E-11	3.16E-09	4.15E-06	2.27E-15	7.51E-17	8.80E-18	2.18E-17	4.41E-20	4.16E-06
10	2.70E-22	1.63E-12	3.16E-09	4.15E-05	2.27E-17	7.51E-20	8.80E-21	2.18E-20	4.41E-23	4.16E-05
11	2.70E-25	1.63E-13	3.16E-09	4.15E-04	2.27E-19	7.51E-23	8.80E-24	2.18E-23	4.41E-26	4.15E-04
12	2.70E-28	1.63E-14	3.16E-09	4.15E-03	2.27E-21	7.51E-26	8.80E-27	2.18E-26	4.41E-29	4.15E-03
13	2.70E-31	1.63E-15	3.16E-09	4.15E-02	2.27E-23	7.51E-29	8.80E-30	2.18E-29	4.41E-32	4.15E-02
14	2.70E-34	1.63E-16	3.16E-09	4.15E-01	2.27E-25	7.51E-32	8.80E-33	2.18E-32	4.41E-35	4.15E-01

7.3.2.2 Effect of fluoride concentration on speciation of Al-F complexes

In the absence of fluoride ions, hydrolysis of Al^{3+} solutions yields a series of hydroxy compounds. The least soluble hydrolysis product $\text{Al}(\text{OH})_3$, forms when equilibrium levels of Al^{3+} and OH^- exceed the products solubility requirements ($\text{pK}_{\text{so}}=33$) (Snoeyink and Jenkins, 1980). In the presence of fluoride, competing equilibrium relationships define the pH and the regions in which fluoride sorption by $\text{Al}(\text{OH})_3$ can occur. Fluoride is similar in size and therefore readily substitutes for OH^- in metallic complexes. The stoichiometry of Al-F complexes varies with the total F^- concentration. At pH values below 5.5, molar concentrations of dissolved Al generally exceed concentrations of F^- , and low ligand Al-F complexes in natural acidic solutions is therefore generally limited by total concentration of F^- available for complexation. From the different equilibrium reactions listed in Table 7-3, total concentration of the fluoride component (C_F) can easily be obtained by the following equation of mass balance:

$$C_F = [\text{F}^-] + [\text{AlF}^{2+}] + 2[\text{AlF}_2^+] + 3[\text{AlF}_3] + 4[\text{AlF}_4^-] + 5[\text{AlF}_5^{2-}] + 6[\text{AlF}_6^{3-}]$$

(7-13)

MINEQL⁺ software was used in Figure 7-5 to illustrate how different values of fluoride concentration would influence the solubility of aluminium hydroxide $[\text{Al}(\text{OH})_3]$. This plot shows a series of solubility lines corresponding to the various total concentrations of F^- in the system. It is clear that the solubility of aluminium is affected by the presence of total F^- in the pH range of 4-8. The total concentration of fluoride has little effect outside this pH range. It was found that increasing the concentration of fluoride will increase the dissolved aluminium in the solution.

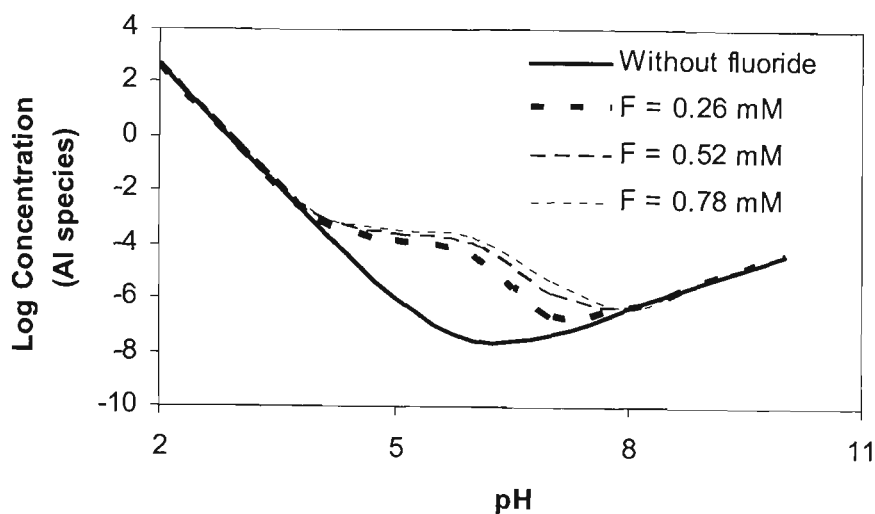


Figure 7-5 Solubility of aluminium hydroxide as a function of pH at various concentrations of total F^-

For example, in the presence of 5.2×10^{-4} M fluoride, the distribution curves in Figure 7-6 show that the species of AlF^{2+} , AlF_2^+ , AlF_3 , and AlF_4^- are the main form of Al-F complexes in acid solution until $Al(OH)_3$ precipitates. The total molar concentration of the soluble Al-F complex species in aqueous solution with high concentration of fluoride (0.52 mM F^-) is shown in Table 7-5.

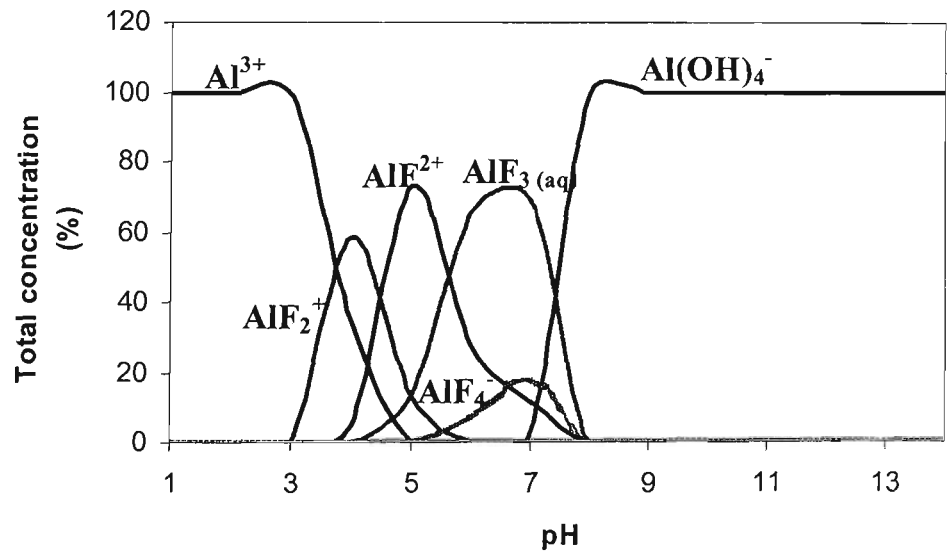


Figure 7-6 Distribution diagram of Al-F complex species formed in a solution with 0.52 mM F^- as a function of pH ($T=25^\circ C$)

Table 7-5 Total molar concentrations of aluminium speciation in the presence of 0.52mM F (from MINEQL⁺ model)

pH	Al ³⁺ (M)	Al(OH) ²⁺ (M)	Al(OH) _{3(aq)} (M)	Al(OH) ⁴⁻ (M)	Al(OH) ₂ ⁺ (M)	AlF ²⁺ (M)	AlF _{3(aq)} (M)	AlF ₂ ⁺ (M)	AlF ₄ ⁻ (M)	Total Al ³⁺ (M)
1	2.70E+05	1.63E-03	3.16E-09	4.15E-14	2.27E+01	4.39E-14	1.24E-25	5.26E-04	1.51E-38	2.70E+05
2	2.70E+02	1.63E-04	3.16E-09	4.15E-13	2.27E-01	4.39E-11	1.24E-19	5.26E-04	1.51E-29	2.70E+02
3	2.70E-01	1.63E-05	3.16E-09	4.15E-12	2.27E-03	4.38E-08	1.24E-13	5.26E-04	1.50E-20	2.73E-01
4	2.70E-04	1.63E-06	3.16E-09	4.15E-11	2.27E-05	3.34E-05	8.24E-08	4.59E-04	8.71E-12	7.86E-04
5	2.70E-07	1.63E-07	3.16E-09	4.15E-10	2.27E-07	1.86E-04	3.43E-05	3.42E-05	2.70E-07	2.55E-04
6	2.70E-10	1.63E-08	3.16E-09	4.15E-09	2.27E-09	3.15E-05	7.55E-05	4.46E-07	7.75E-06	1.15E-04
7	2.70E-13	1.63E-09	3.16E-09	4.15E-08	2.27E-11	2.03E-07	1.24E-06	1.13E-09	3.24E-07	1.81E-06
8	2.70E-16	1.63E-10	3.16E-09	4.15E-07	2.27E-13	2.08E-10	1.28E-09	1.14E-12	3.37E-10	4.21E-07
9	2.70E-19	1.63E-11	3.16E-09	4.15E-06	2.27E-15	2.08E-13	1.28E-12	1.14E-15	3.37E-13	4.16E-06
10	2.70E-22	1.63E-12	3.16E-09	4.15E-05	2.27E-17	2.08E-16	1.28E-15	1.14E-18	3.37E-16	4.16E-05
11	2.70E-25	1.63E-13	3.16E-09	4.15E-04	2.27E-19	2.08E-19	1.28E-18	1.14E-21	3.37E-19	4.15E-04
12	2.70E-28	1.63E-14	3.16E-09	4.15E-03	2.27E-21	2.08E-22	1.28E-21	1.14E-24	3.37E-22	4.15E-03
13	2.70E-31	1.63E-15	3.16E-09	4.15E-02	2.27E-23	2.08E-25	1.28E-24	1.14E-27	3.37E-25	4.15E-02
14	2.70E-34	1.63E-16	3.16E-09	4.15E-01	2.27E-25	2.08E-28	1.28E-27	1.14E-30	3.37E-28	4.15E-01

From a comparison between Table 7-4 and Table 7-5, it can be seen that at high fluoride concentration, concentration of the soluble $\text{Al}(\text{OH})_3$ complex in aqueous solution was $4.21 \times 10^{-7} \text{ M}$ at pH 8 when it was found to be $4.65 \times 10^{-8} \text{ M}$ in low fluoride concentration solutions at pH 7. This result indicates that Al is free to move in an aqueous solution in the environment, and in the absence of more effective precipitating agents.

7.3.3 Aluminium hydroxide precipitation

As noted in section 7.3.2, the speciation of Al is pH-dependent. In the absence of fluoride ions, Al undergoes hydrolysis, resulting in a series of OH^- complexes such as $\text{Al}(\text{OH})^{2+}$ and $\text{Al}(\text{OH})_2^+$ in acidic solution. The solubility of Al is minimum near pH 6.5 and increases at higher pH values due to the formation of $\text{Al}(\text{OH})_4^-$. In the presence of fluoride the complexes of Al-F species appear. The chemical form of soluble Al species depends on the system pH and concentration of fluoride. Thus where the F^- concentration at equilibrium was $1 \times 10^{-5} \text{ M}$, the complexes formed should have been mainly AlF^{2+} and AlF_2^+ . At high fluoride concentration the amounts of Al-F complexes formed increased. These complexes should have been mainly AlF^{2+} , AlF_2^+ , and AlF_3 . By increasing the concentration of fluoride the amount of AlF_3 is increased, in which this species predominates with $[\text{F}^-]_{\text{eq}} > 5 \times 10^{-4} \text{ M}$. These results suggest that at pH between 5 and 6, AlF^{2+} and AlF_2^+ species predominates until $\text{Al}(\text{OH})_3$ precipitates. These complexes of Al prevent it from precipitating as a hydroxide until pH 6 is reached. The excess solid $\text{Al}(\text{OH})_3$ maintains a constant concentration of complex $\text{Al}(\text{OH})_3$. It is believed that the fluoride ion interacts with a solid $\text{Al}(\text{OH})_3$ precipitate over a range of pH values

Chapter 7-Solution speciation and removal mechanisms

between 4-8. At low pH this uptake decreased due to an AlF_x soluble species forming. The solubility boundary denotes the thermodynamic equilibrium that exists between the dominant Al-F species in solution at a given pH and solid aluminium hydroxide. The solubility boundary of the dominant Al-F species are shown in Figure 7-7 and Figure 7-8 in the presence of high and low concentrations of fluoride at different pH values.

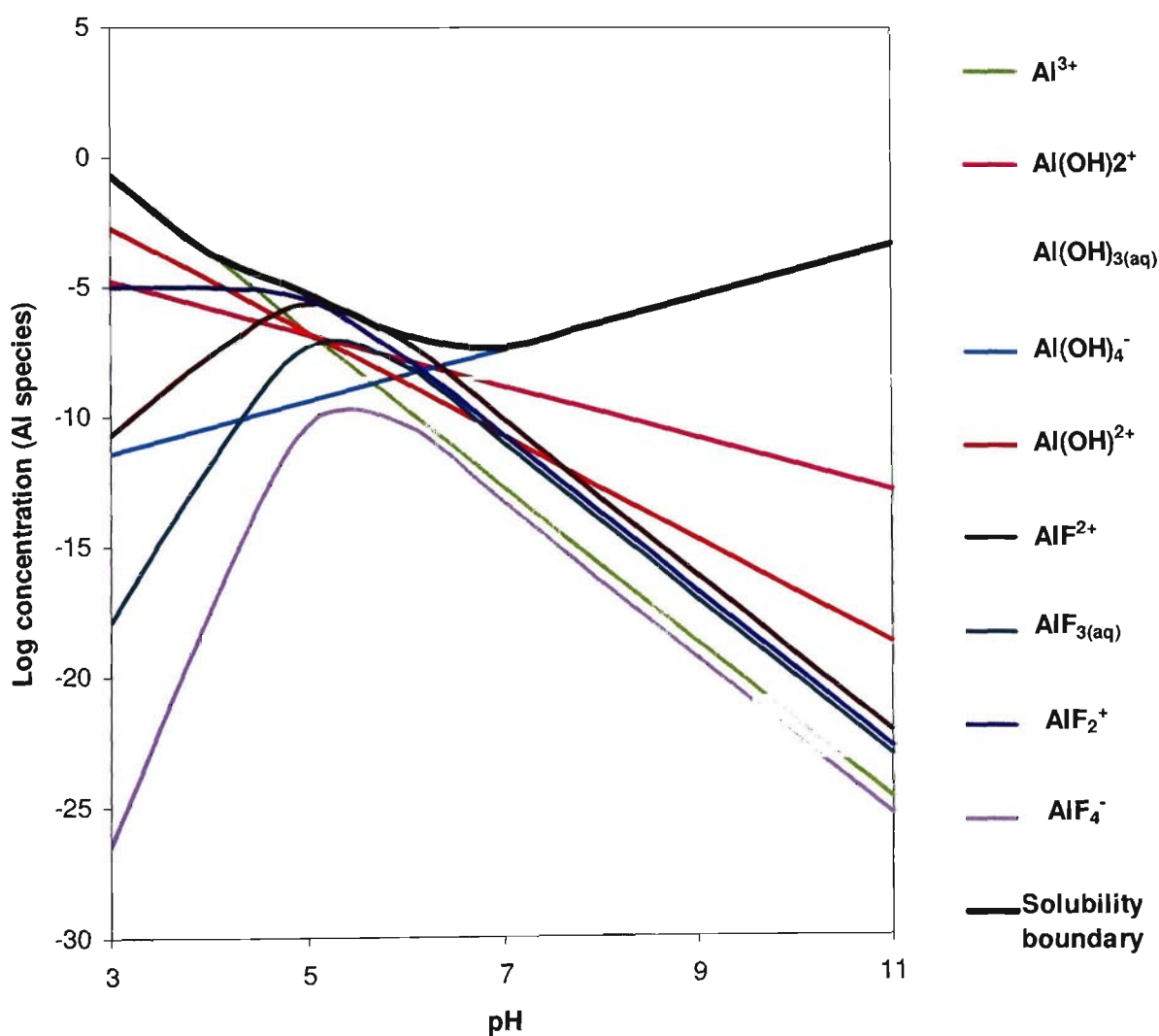


Figure 7-7 Equilibrium concentrations of Al-F complexes in a solution with 0.01 mM F⁻ at various pH values (T=25°C)

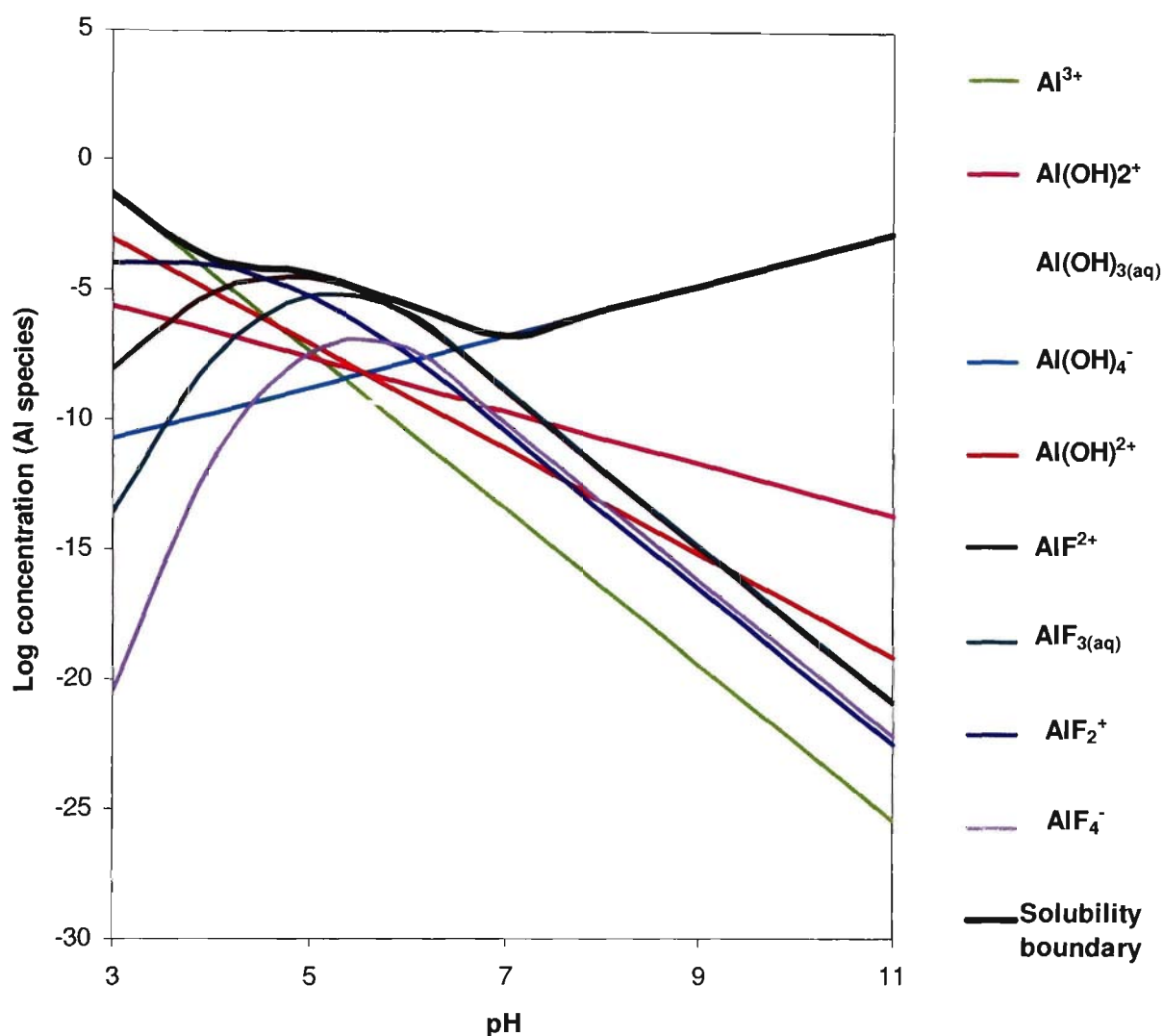


Figure 7-8 Equilibrium concentrations of Al-F complexes in a solution with 0.52 mM F⁻ at various pH values (T=25°C)

From a comparison between Figure 7-7 and Figure 7-8, it appeared that the concentration and mobility of Al³⁺ in natural waters are increased by increasing the concentration of fluoride. At high fluoride concentration (0.52 mM), the solubility of aluminium is calculated to be 0.01 mg/L when it decreases to 0.001 mg/L in low fluoride concentration (0.01mM). The amount of soluble aluminium may be increased by the addition of concentrated fluoride in the solution.

7.3.4 Calcium precipitation

Effect of Ca^{2+} ions on defluoridation by the ECF process has already been explained in section 5.3.8.3. The experimental results showed that defluoridation is significant when the concentration of Ca^{2+} in the solution is increased. Most of the fluoride ion included in the water or waste water is treated by the addition of a Ca^{2+} salt such as $\text{Ca}(\text{OH})_2$, to form CaF_2 granula, through the following reaction:



Sediment consisting of CaF_2 separates from the water and settles at the bottom. In the absence of Al the solubility of fluorite (CaF_2) is theoretically decreased when concentrations of Ca^{2+} increase in the solution, as shown in Figure 7-9. It is considered that two aspects on the formation of fluorite are affected when there is no $\text{Al}(\text{OH})_3$ in the solution. Firstly, the kinetic effect which means a slow formation of the solid phase. Secondly, the particle size effect, which means the settling down of the flocs formed in the solution is incomplete.

Therefore, to solve these problems another defluoridation process should be used after fluorite has formed to remove residual fluoride. Aluminium coagulant has been used as a useful absorbent for removing fluoride (Hara et al., 2001; Sujana et al., 1998). Sediments consisting of the CaF_2 and $\text{Al}(\text{OH})_3$ separates from the water and settles at the bottom of the tank. From Figure 7-10 it can be seen that the solubility of aluminium hydroxide is decreased between pH ranges of 5 and 8 when calcium concentrations increase in the solution. The minimum solubility of aluminium hydroxide is found to be around pH 7.

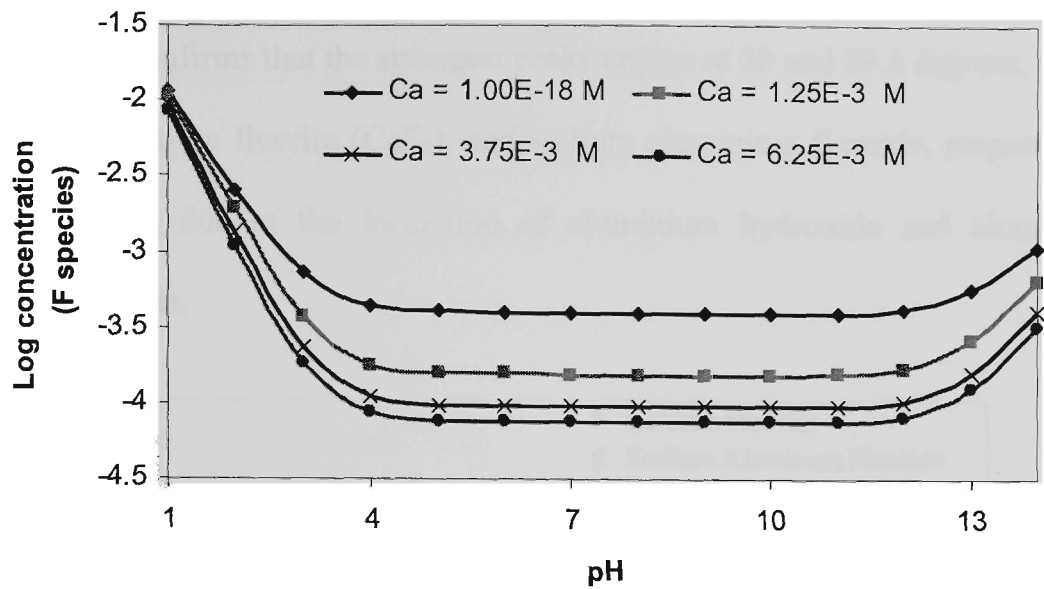


Figure 7-9 Solubility of fluorite in the presence of different Ca^{2+} ions and without aluminium concentration in the solution at different pH by using MINEQL⁺ software ($C_0=15\text{ mg/L}$, and $T=25\text{ }^{\circ}\text{C}$)

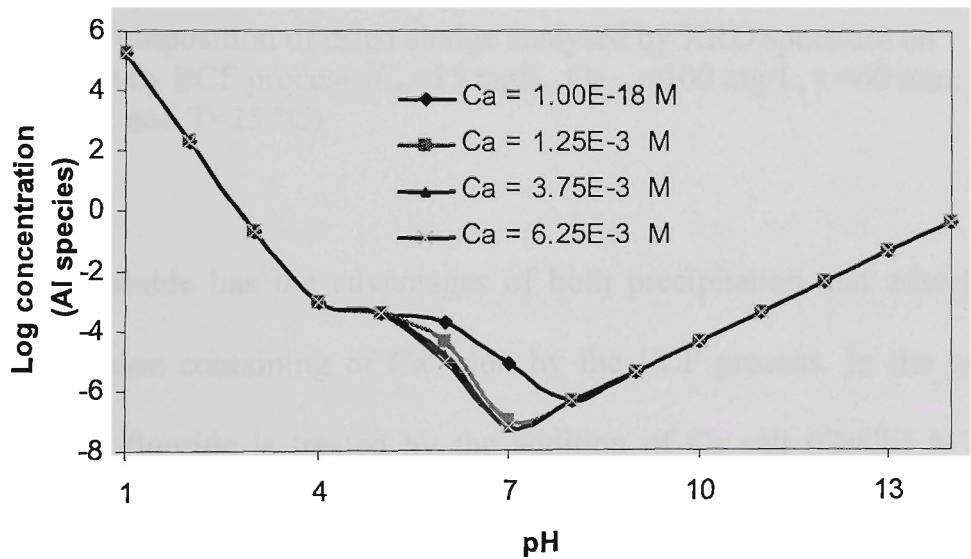


Figure 7-10 Solubility of aluminium hydroxide at different Ca^{2+} ions at different pH by using MINEQL⁺ software ($C_0=15\text{ mg/L}$, and $T=25\text{ }^{\circ}\text{C}$)

In order to further explore the mechanism of removing fluoride by the ECF process in the presence of concentrations of calcium, the composition of dried sludge was

studied using XRD spectroscopy. The XRD traces of the sludge shown schematically in Figure 7-11 confirms that the strongest peaks appear at 28 and 29.5 degrees, which were identified to be fluorite (CaF_2), and sodium aluminium fluoride, respectively. Other peaks are due to the formation of aluminium hydroxide and aluminium fluoride hydroxide.

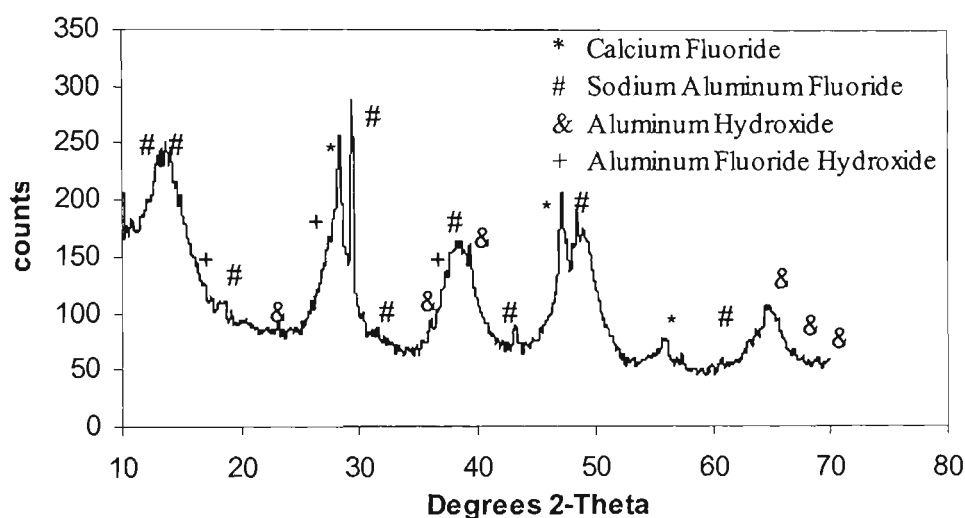


Figure 7-11 Composition of dried sludge analysed by XRD spectrum on defluoridation by ECF process ($C_o=15$ mg/L, $Ca_{in}=100$ mg/L, $t=60$ min, $I=1.5$ A, $d=5$ mm, $pH=7$, and $T=25$ °C)

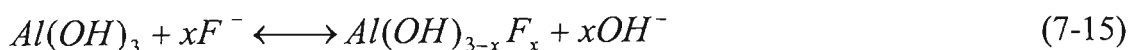
Removing fluoride has the advantages of both precipitation and adsorption in an aqueous solution containing of Ca^{2+} ion by the ECF process. In the precipitation process most fluoride is treated by the addition of Ca salt (CaCl_2) to form CaF_2 granules and then settle at the bottom of the electro-box. In the adsorption method, by increasing the concentration of Al, $\text{Al}(\text{OH})_3$ floc is formed and residual fluoride is adsorbed by the $\text{Al}(\text{OH})_3$. By adding a large amount of Al, $\text{Al}(\text{OH})_3$ gel is formed and residual fluoride is adsorbed by the $\text{Al}(\text{OH})_3$. It is separated by both sedimentation and flotation in the ECF process.

7.4 REMOVAL MECHANISMS

To understand the chemical speciation of Al and other species with fluoride ions, the mechanism for removing fluoride is explained in more detail in the following sections, when the composition of sludge produced was analysed using XRD spectrum.

7.4.1 Mechanism and speciation

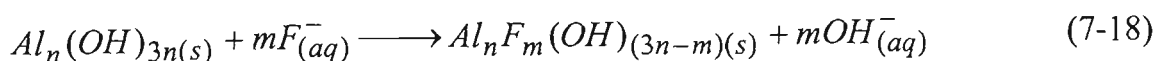
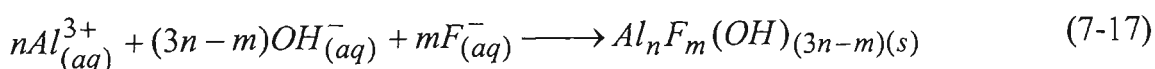
As explained in chapter 4, in the ECF process Al electrodes are used instead of Al salts for removing fluoride. The electrolytic dissolution of Al anodes by oxidation in water produces aqueous Al^{3+} species and the Al^{3+} ions further react to form solid $Al(OH)_3$ precipitate. These coagulants destabilise and aggregate suspended particles or precipitate and adsorb dissolved contaminants. For example, the $Al(OH)_3$ floc is believed to adsorb F^- strongly, as shown by Eq. 7-15.



Freshly formed amorphous $Al(OH)_3$ precipitates that are required for “sweep coagulation” have large surface areas, which is beneficial for a rapid adsorption of soluble compounds and trapping of colloidal particles. These flocs usually polymerise at high concentrations of Al as:



Co-precipitation (Eq.7-17) or adsorption (Eq. 7-18) reaction may occur when aluminium salt is used to remove fluoride.



Also, fluoride may be segregated in water as Na_3AlF_6 (cryolite) or other compounds that contain the complex ion AlF_6^{3-} , as the process is highly dependent on the pH of solution. The following reactions may occur by complexation of F and Al^{3+} , AlF^{2+} , AlF_3 and subsequent precipitation of Cryolite (Na_3AlF_6).



The aluminium oxidation mechanisms and various species between aluminium and fluoride component is illustrated in Figure 7-12.

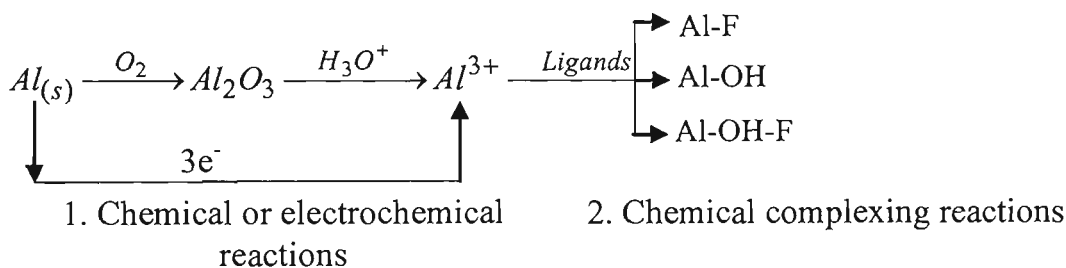
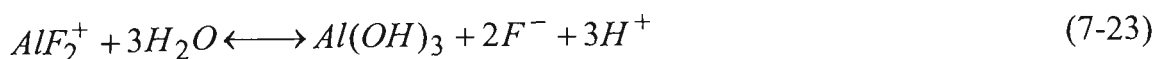
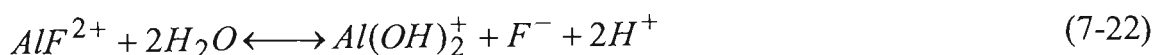
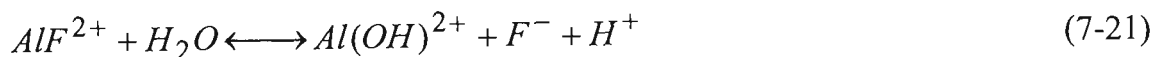
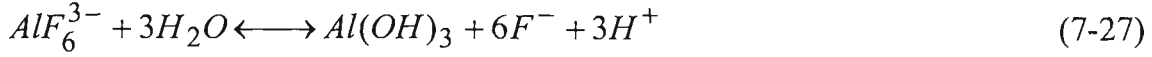
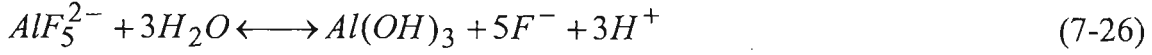
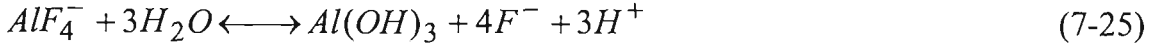
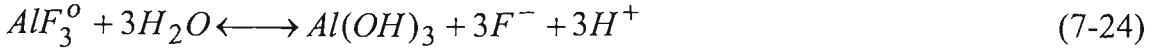


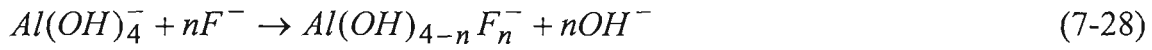
Figure 7-12 Aluminium oxidation process and complexing reactions

The relationships between the total activity of the fluoride or aluminium ions and pH under standard equilibrium conditions were calculated for each reaction based on the thermodynamic data of the standard free energies and reaction constants. The hydrolysis of aluminium fluoride complexes, including the formation of a solid phase, is described by the equations:





Also, increase of concentrations of Al with fluoride can contribute to the formation of $Al(OH)_{4-n}F_n^-$ complexes according to:



Coagulation with aluminium salts occurs at a wide range of pH due to different mechanisms. In the ECF process, the pH of the coagulation cell increases with liberation of H_2 at the cathode. This increase is mainly dependent on the current for all cases. When $pH < 4$, aluminium remains in the form of Al^{3+} , and no precipitation occurs, so the fluoride concentration cannot be reduced. When $4 < pH < 5.5$, the hydrogen ion concentration remains relatively high. Consequently, a high zeta potential and strong repulsive force between the aluminium hydroxide colloidal flocs that is not conducive to flocculation and precipitation is maintained. More formation of Al-F species (AlF_n^{3-n}) such as AlF^{2+} , AlF_2^+ , AlF_3 , AlF_4^- can be seen between the pH range of 5 -7. When $pH > 7$, OH^- ions increase in water. In the anodic adsorption layer, the concentration of OH^- ions is higher than the concentration of F^- , so the production of the AlF_n^{3-n} species becomes difficult; therefore, the reduction of fluoride from water and waste water at a range of $pH > 7$ is affected by the formation of aluminium hydroxide floc.

In the earlier sections, the experimental results showed that defluoridation is more efficient for a pH ranging between 6 and 8. At this pH range the residual fluoride in such a solution may occur in different dissolved forms (F^- , AlF^{2+} , AlF^{4-}) or finely formed to solid aluminium fluoride hydroxide $[Al_nF_m(OH)_{3n-m}]$.

7.4.2 Characterisation of sludge

The composition of the sludge produced in the batch and continuous flow reactor was analysed using an X-ray diffraction (XRD) spectrum at the adjusted pH range of 6-8. The compositions of the sludge were studied in two steps, first by XRD spectroscopy and then by a trace analysis software. As seen in Figures 7-13 and 7-14, the strongest peaks appeared at degree 18 and 20, which were identified to be the aluminium fluoride hydroxide and aluminium hydroxide, respectively. From a comparison between Figure 7-13 and Figure 7-14, the characteristics of the dried sludge collected from both batch and continuous flow reactor were found to be same.

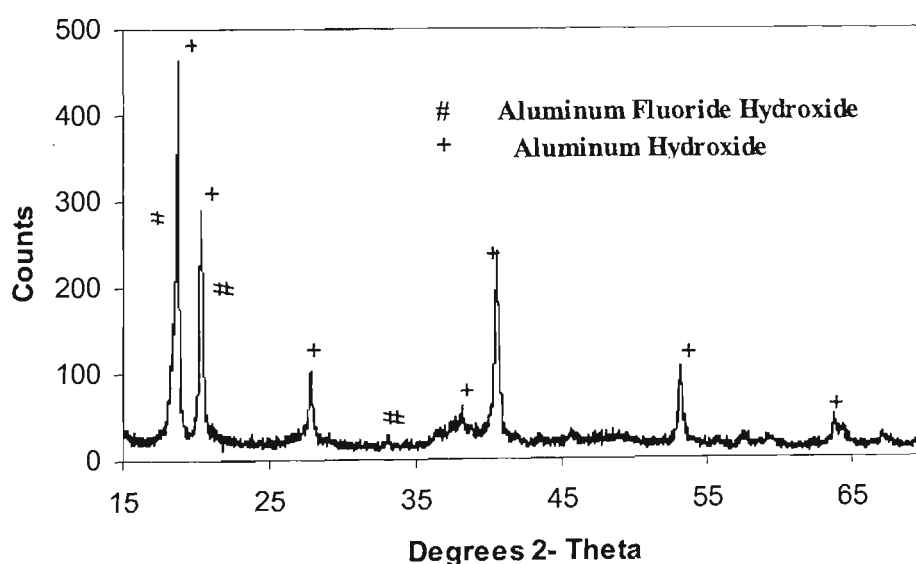


Figure 7-13 Composition of dried settled sludge in batch reactor analysed by XRD spectrum ($C_0 = 10 \text{ mg/L}$, $i = 25 \text{ A/m}^2$, $t = 60 \text{ min}$, $pH_{in} = 6$, $Ec_{in} = 15 \text{ mS/m}$)

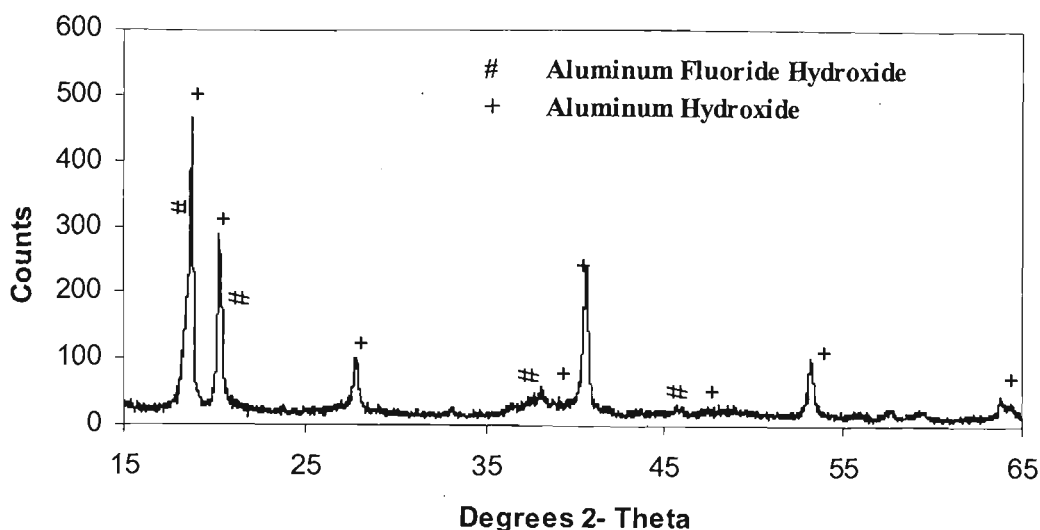


Figure 7-14 Composition of dried settled sludge for continuous flow reactor analysed by XRD spectrum ($C_o = 10 \text{ mg/L}$, $i = 25 \text{ A/m}^2$, $Q = 200 \text{ mL/min}$, $\text{pH}_{\text{in}} = 6$, $E_{\text{cin}} = 15 \text{ mS/m}$)

The characterisation of the deposited layer and oxide particles in the electrode surfaces was investigated by XRD spectroscopy. As seen in Figure 7-15, the strongest peaks appeared to be the aluminium fluoride hydroxide and aluminium hydroxide. It has the same characterisation as sludge settled in the EC process.

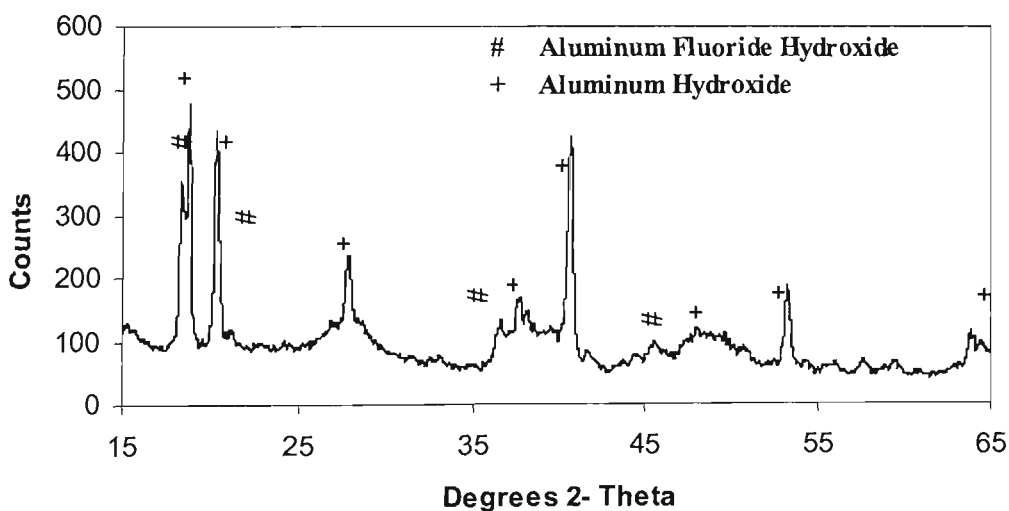


Figure 7-15 Composition of dried collected sludge from surface of the electrodes analysed by XRD spectrum ($C_o = 10 \text{ mg/L}$, $i = 18.75 \text{ A/m}^2$, $t = 60 \text{ min}$, $\text{pH}_{\text{in}} = 6$, $E_{\text{cin}} = 15 \text{ mS/m}$)

The XRD spectrums reported in Figures 7-16, and 7-17 were obtained at different current densities and values of fluoride concentration. As seen, increasing the current range from 2A to 2.5A and fluoride concentration from 10mg/L to 25 mg/L had no significant difference between their sludge characteristics. It can be seen that the strongest peaks appeared at 18 and 20 degrees, which were identified to be aluminium fluoride hydroxide and aluminium hydroxide. In order to explore the mechanism of fluoride removal, the results from the XRD spectrum showed that competitive adsorption between the hydroxide ion OH^- and F^- may exist. Thus, the reduction of fluoride from water between the pH range of 6 and 8 is affected by the formation of aluminium hydroxide floc. In this pH range, the sludge characterisation results showed that residual fluoride in such a solution may occur in precipitated solid particles such as $[\text{Al}_n\text{F}_m(\text{OH})_{3n-m}]$.

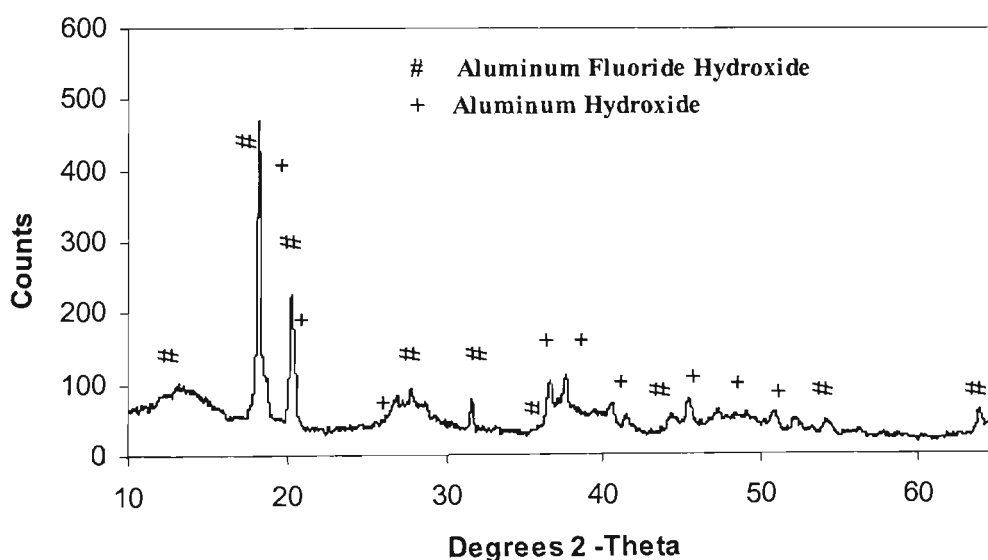


Figure 7-16 Composition of dried settled sludge analysed by XRD spectrum ($C_o = 10$ mg/L, $i = 25 \text{ A/m}^2$, $t = 60 \text{ min}$, $\text{pH}_{\text{in}} = 6$, $E_{\text{cin}} = 15 \text{ mS/m}$)

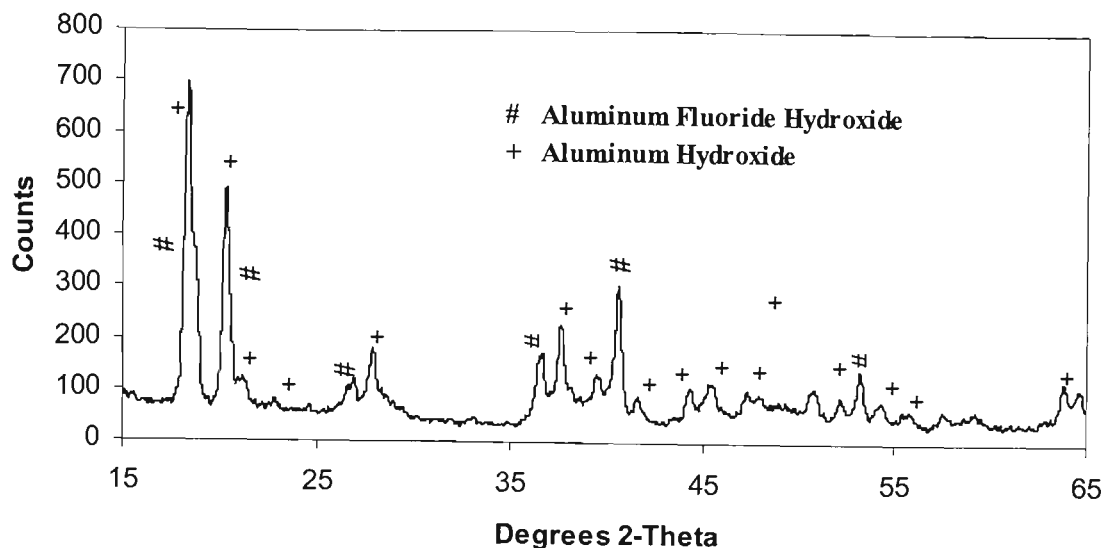


Figure 7-17 Composition of dried settled sludge analysed by XRD spectrum ($C_o = 25$ mg/L, $i = 31.25$ A/m², $t = 60$ min, $pH_{in} = 6$, $Ec_{in} = 15$ mS/m)

Also, the dried sludge from surface of electrocoagulator was also analysed by XRD spectrum. As seen in Figure 7-18, the strongest peaks are due to formation of aluminium hydroxide and aluminium fluoride hydroxide, which are similar to peaks obtained by XRS spectroscopy of the dried settled sledges (e.g. Figure 7-13).

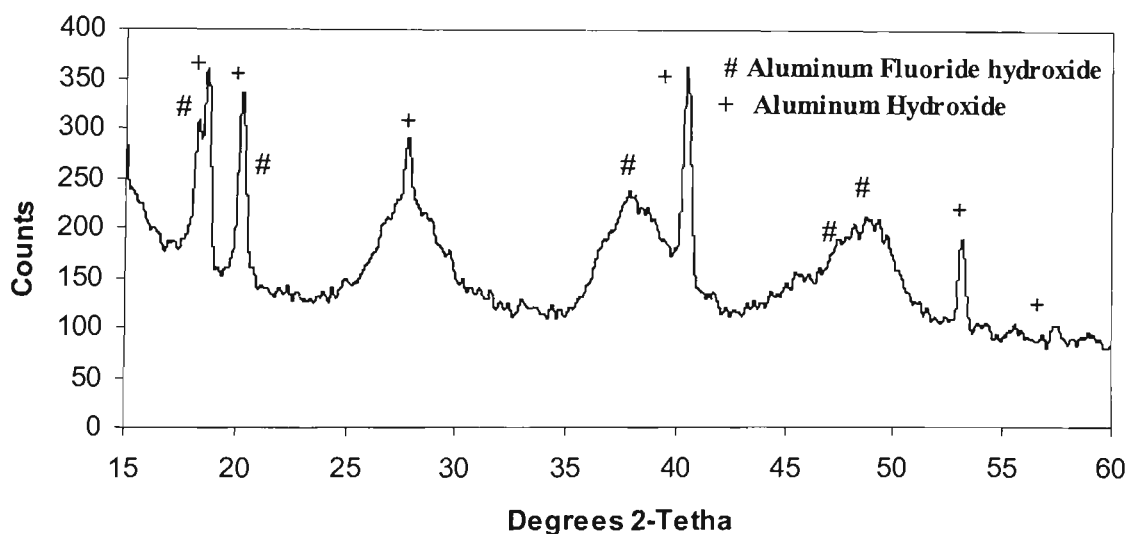


Figure 7-18 Composition of dried floating sludge analysed by XRD spectrum ($C_o = 10$ mg/L, $i = 25$ A/m², $t = 60$ min, $pH_{in} = 6$, $Ec_{in} = 15$ mS/m)

As seen, there is no difference between floc characteristics collected from the top and bottom of the electrocoagulator. In summary, XRD analysis of the composition of the dried sludge obtained by EC shows the formation of $[Al_nF_m(OH)_{3n-m}]$ and provides confirmation for the main mechanism for removing fluoride.

7.5 SUMMARY

A clear understanding of various interconnected processes including measurement, speciation, and mechanisms, is required to successfully increase the scale of defluoridation by the electrochemical method. MINEQL⁺ model was utilised to illustrate the relative chemical speciation of Al-F complexes in solution and how different pH values would influence the solubility of aluminium hydroxide $[Al(OH)_3]$. The experimental results showed that the pH of a solution is an important factor for removing fluoride. When $pH < 5$, dissolved aluminium (Al^{3+}) is predominant and aluminium hydroxide tends to be soluble. For the pH range of 5 and 6, the predominant hydrolysis products are found to be $Al(OH)^{2+}$ and $Al(OH)_2^+$ and the solid $Al(OH)_3$ is most prevalent in the pH range of 6 and 8.5. When pH is > 9 , the soluble $Al(OH)_4^-$ is the predominant species. The results showed that removing fluoride efficiently is the highest, and remains unchanged between the adjusted pH range of 6 –8, and then decreases when the adjusted pH value is increased from 8 to 10. Thus a weakly acidic condition is favoured for this treatment. The mechanism of the removal process was confirmed to be a competitive adsorption between OH^- and F^- at adjusted pH range of 6 and 8. XRD analysis of the composition of the dried sludge obtained by electrocoagulation shows the formation of aluminium fluoride hydroxide complexes $[Al_nF_m(OH)_{3n-m}]$ and provides confirmation for the main mechanism for removing fluoride.

CHAPTER 8

CHAPTER 8

EC MODELLING

8.1 INTRODUCTION

A theoretical model is developed with the assistance of appropriate mass balance and reaction kinetics describing the overall fluoride removal process. This chapter presents the output results for removing fluoride using the empirical models and theory explained earlier in chapter 4. The chemical batch reactor theory is used as the basis for the development of the semi-empirical model. Results from the plotted experimental data showed a first order behaviour for removing fluoride by the ECF reactor. The experimental results from batch and the continuous flow EC reactor are used to evaluate the empirical model. The main aim of this chapter is firstly to present a empirical model using critical parameters including current concentration (I/V), distance between electrodes (d), ion competition effects (Ca^{2+}), pH of the solution, and initial concentration of fluoride (C_0) on evaluation of the rate constant (K) for removing fluoride using a monopolar ECF process. Secondly, to determine the optimal time required for detention to achieve a desirable concentration of fluoride. A multiple regression analysis can be used to summarise data as well as to study relations among variables. An empirical model is developed by a statistical tool known as “SPSS pack for windows”. Towards the end of this chapter the semi-empirical model is calibrated with experimental data gathered during this research and then the independent data set is used for its verification. It is shown that the semi- empirical model will match the continuous flow data very well.

8.2 RESULTS: DETERMINATION OF EXPERIMENTAL RATE CONSTANTS

The effects of some operational parameters including, current value, electrolysis time, solution pH, distance of electrode, initial concentration of fluoride, and the effects of ionic competition (especially Ca^{2+}) on the removal of fluoride by the ECF process at batch model were explained in chapter 5. Based on Faraday's formula it is clear that electrolysis time and current concentration (I/V) are two important parameters that determine Al dissolution in water. One of the most important reasons that the current concentration was used to develop the empirical model is to compare the results obtained from batch and continues flow EC reactors.

Development of the theoretical and empirical models was thoroughly explained in chapter 4. The analytical procedure that was used to present the results depicted in the following figures and tables was described in chapters 4 and 5. One of the first steps taken to analyse the experimental data collected was to plot the logarithm of the measured concentration of fluoride against the time for electrolysis. The slope of the individual equations obtained for each current applied corresponds to the experimentally determined rate constant (K_{exp}) at that particular value. It appeared that the points may be fitted by a linear regression. The plots were developed as a first step to examine whether the ECF process follows a first order behaviour. This fact was corroborated by a linear alignment of all points on the graph. The results obtained, which were previously shown in Appendix B. demonstrated that lower rate constants were obtained for lower currents when a linear trend was plotted to correlate all the data points. In the procedure, the slope of each line represents an experimentally determined rate constant (K_{exp}) for the process. The results for

obtaining of the different experimental rate constants (K_{exp}) have been summarised in Appendix G. It is clear that the experimental rate constant (K_{exp}) depends on the independent variables, including the concentration of current (I/V), pH of the solution, initial concentration of pollutant (C_o), distance between electrodes(d), and initial concentration of Ca^{2+} . The next step was to find the appropriate correlation between experimentally determined constants with their separate, corresponding independent values.

8.3 DISCUSSION OF RESULTS: (DATA MODELLING AND ANALYSIS)

8.3.1 The multiple regression analysis

One of the most common problems in statistics is to fit an equation to the dependent or independent data. The problem might be as simple as fitting a straight line calibration curve between dependent and independent variables, or it might be to fit an unsteady state non-linear model. The simplest regression problem is that pairs of data are to be described by a simple fitted function $Y=f(x)$. The models to be fitted can be simple functions of a single independent variable, or have many independent variables. Multiple regression analysis is similar to simple linear regression models except that multiple regressions contain more terms and can be used to represent more complex relationships. The model can be expressed as:

$$Y_i = b_o + b_1X_1 + b_2X_2 + \dots + b_pX_p + e_i \quad (8-1)$$

where X_1, X_2, \dots , and X_p are a vector of independent variables, b_o, b_1, b_2, \dots , and b_p are parameters of the model that will be estimated by carrying out the multiple regression analysis, and the term “ e_i ” that is usually called the residual (or residuals)

from the regression, is the difference between the observed (Y_i) and the predicted values of Y (\hat{Y}_i) [$e_i = Y_i - \hat{Y}_i$]. A positive residual means the value of Y for that case is being under predicted while a negative residual indicates over prediction. Across the whole sample the mean residual is always zero. The values of e_i are assumed to be independent, normally distributed, and random variables with a mean of 0 and variance of σ^2 .

In this research a multiple regression analysis is used by the SPSS package to estimate the coefficients of the linear equation involving one or more independent variables. In fact the model is developed to predict the rate constants (refer to Figure 4-6 in chapter 4). Based on the experimental results presented in Table 8-1, the rate constant (K_{exp}) may depend on the parameters such as, I/V , Ca^{2+} , d , pH , and C_o . The data files were analysed by SPSS package. After pre-forming the appropriate software and running the SPSS multiple linear regression analysis, an equation was developed with the corresponding coefficients. A summary of the statistical output is shown in the following chapter.

Table 8-1 Descriptive statistics of sampled data

Variable	Mean	Std. Deviation	N
$K_{\text{(exp)}}$	4.7E-02	1.4E-02	300
I/V	478	152.98	300
Ca^{2+}	120	118.52	300
d	10	4.7	300
pH	7.5	1.41	300
C_o	16.67	6.25	300

Table 8-1 shows the descriptive statistics of all the data used to feed the computer package. This table shows the mean values, standard deviations, and number of the sampled points for the dependent variable (K_{exp}), and the independent variables (I/V ,

Ca²⁺, d, pH, and C_o). The standard deviation (SD) is the square root of the variance and is described by the equation:

$$SD = \sqrt{\frac{\sum_{i=1}^N (X_i - \bar{X})^2}{(N-1)}}$$

(8-2)

where N is the number of cases, N-1 is degree of freedom for a sample or number of independent variables in a dataset, X_i is the value of the variable for ith case, and \bar{X} is the mean of values of X. The correlation between the dependent and the independent variables are presented in Table 8-2.

Table 8-2 Correlation between all the variables included in the SPSS statistical tool

Variable		K _(exp)	I/V	C _o	d	Ca ²⁺	pH
Pearson correlation	K _(exp)	1.000	0.644	-0.159	-0.268	0.638	-0.264
	I/V	0.644	1.000	0.000	0.000	0.000	0.000
	Ca ²⁺	0.638	0.000	0.000	0.000	1.000	0.000
	d	-0.268	0.000	0.000	1.000	0.000	0.000
	pH	-0.264	0.000	0.000	0.000	0.000	1.000
	C _o	-0.159	0.000	1.000	0.000	0.000	0.000

N= 300

The Pearson correlation coefficient for most of the variables is well below 1 which means that independent variables have a high or low effect upon the dependent variable. The correlation coefficient, R, can be calculated using the following equation:

$$R = \frac{\sum_{i=1}^N (X_i - \bar{X})(Y_i - \bar{Y})}{(N-1)S_x S_y}$$

(8-3)

where S_x and S_y are the standard deviations of the two independents and dependent variables. The absolute value of R indicates the strength of the linear relationship. As can be seen the high correlation coefficients may be respectively observed for the independent variables of I/V , Ca^{2+} , d , pH , and C_o . The great effect that the parameters of I/V and Ca^{2+} have on whole defluoridation process is confirmed.

8.3.1.1 Estimating parameters using the method of least squares:

Since the variables of I/V , Ca^{2+} , d , pH , and C_o are unknown population parameters, they must be estimated from the sample. The least squared coefficients “b” are used to estimate the population parameters. In fact “b” is the regression coefficient for each independent variable in the equation. The best estimates of the parameters are obtained by the method of least squares. A summary of the statistical results for estimating of the parameters is presented in Table 8-3.

Table 8-3 Summary of statistical results for the predictive equation

Variable	b	Std. Error (SE)	Beta	t	Sig t	Lower 95%	Upper 95%
I/V	5.9E-05	5.82E-07	0.644	102.01	0.0000	0.000	0.000
Ca ²⁺	7.6E-05	7.51E-07	0.638	100.95	0.0000	0.000	0.000
d	-82.0E-05	1.89E-05	-0.268	-42.38	0.0000	-0.001	-0.001
pH	263.6E-05	6.3E-05	-0.264	-41.74	0.0000	-0.003	-0.003
C _o	-37.0E-05	1.42E-05	-0.159	-25.16	0.0000	0.000	0.000
Constant	4356.8E-05	64E-05		68.03	0.0000	0.042	0.045

R²=0.99

For multi- regression models, R is the correlation between the observed and predicted values of the dependent variables. The accuracy of the prediction is directly

related to the correlation coefficient. After running the SPSS software with the input data, the output shows a calculated R^2 equivalent to 0.99. The regression coefficients (b) tell us how much the dependent variable can be expected to change when there is a change in the independent variable. Usually a t -test is applied to each of the b coefficients to test if it is significantly different from zero. To calculate t , SPSS generates the standard error of b (S_b on the printout), and divides b by its standard error to give a value of t . If t is significantly greater than 0.05, then there is insufficient evidence to warrant the conclusion that an independent variable is predictive of the dependent variable. These t -test results and their significant levels are displayed in the last two columns of Table 8-3. The small but significant levels observed (less than 0.05) show that the slope the population regression line is not 0, which means there is a linear relationship between the dependent and independent variables. The standard error of a random variable is a measure of how far it is likely to be from its expected value that will be explained in the following chapter.

8.3.1.2 The precision of estimated parameters

The slope and intercept (regression coefficients) estimated from a single sample typically differ from the population values and vary from sample to sample. To use these estimates for inference about the population values, the sampling distributions are needed. When the assumptions of linear regression are met, the sample distributions of the regression coefficient (b) for each independent variable are normal. The standard error (SE) of constant value (b_0) is given by (Spiegel, 1988):

$$SE_{b_0} = \sigma \left(\sqrt{\frac{1}{N} + \frac{\bar{X}^2}{\sum (X_i - \bar{X})^2}} \right) \quad (8-4)$$

And the standard error of each independent variable is:

$$SE_{b_1} = \sigma \left(\sqrt{\frac{1}{\sum (X_i - \bar{X})^2}} \right) \quad (8-5)$$

The difference between our estimate of some parameter of interest and its true value will be due only to random variation. The size of this random variation is measured by a quantity called standard error. The magnitude of the standard error is known as precision. The smaller the standard error, the more precise are our estimates. One statement of the precision of b would be to simply report the interval bounded by $b \pm S(b)$. An improvement on this would be to determine a confidence interval on estimated parameters using the t distribution. The $(1-\alpha)100$ % confidence limits are given by:

$$b \pm t_{(1-\alpha/2, N-2)} \cdot S(b) \quad (8-6)$$

One way to make regression coefficients somewhat more comparable is to calculate beta weight, which are the coefficients of the independent variables when all variables are expressed in standardised form, or are converted into Z scores (i.e. standardized to have means of 0 and standard deviations of 1). The size of beta indicates the underlying linear relationship between independent and dependent variables regardless of the units of measurement. The beta coefficients can be calculated directly from the regression coefficients using the following equation:

$$Beta_1 = b_1 \left(\frac{S_{X_1}}{S_{Y_1}} \right) \quad (8-7)$$

Multiplying the regression coefficient (b_1) by the ratio of the standard deviation of the independent variable (S_X), to the standard deviation of the dependent variable

(S_Y) results in a dimensionless coefficient. In fact the beta coefficient is an indicator of the relative importance of variables. The results obtained from Tables 8-2 and 8-3 show the significant effect of the current concentrations and initial concentrations of Ca^{2+} on the entire process.

8.3.1.3 Precision of the estimated model

The best estimates of the model parameters are those that minimise the sum of the squared (SS) residuals:

$$SS = \sum_{i=1}^n (e_i)^2 = \sum_{i=1}^n (Y_i - \hat{Y}_i)^2 \quad (8-8)$$

The total variability observed in the dependent variable is subdivided into component, regression and residual. The distance from Y_i to \bar{Y} (the mean of the Y) can be subdivided into two parts,

$$Y_i - \bar{Y} = (Y_i - \hat{Y}_i) + (\hat{Y}_i - \bar{Y}) \quad (8-9)$$

The distance from Y_i (the observed value) to \hat{Y}_i (the value predicted by the regression line), is called the residual from the regression. The second component is the distance from the regression line to the mean of Y ($\hat{Y}_i - \bar{Y}$). The analysis of variance (ANOVA) is summarised in Table 8-4. It displays the two sums of squares under the heading of residual sum of squares $[\sum (Y_i - \hat{Y}_i)^2]$ and regression sum of squares $[\sum (\hat{Y}_i - \bar{Y})^2]$.

The mean square (MS) for each entry is the sum of squares divided by degrees of freedom (df). The ratio of the mean square regression to the mean square residual is

distributed as an F statistic. F test serves to test how well the regression model fits the data. The observed significant level (Sig F) is less than 0.00005 (Norusis, 1993), thus the F statistics is small and the hypothesis that $R^2 = 0$ (no linear relationship between independent and dependent variables) is rejected.

Table 8-4 Summary of analysis of variance (ANOVA) results

Model	Sum of squares (SS)	df	Mean square (MS)	F	Sig.
Regression	5.87E-02	5	1.17E-02	4953.84	0.00000 ^a
Residual	6.97E-04	294	2.37E-06		
Total	5.94E-02	299			

a. Independent variables (I/V, Ca^{2+} , d, pH, and C_0)
Dependent variable $K_{(\text{exp})}$

Therefore either t or F values can be computed to test the hypothesis for rejection or acceptance. Another useful statistical summary is the standard error of the estimate $SE_{\hat{Y}}$, which can be also calculated as the square root of the residual mean square. It can be expressed as:

$$SE_{\hat{Y}} = \sqrt{\frac{\sum (Y_i - \hat{Y}_i)^2}{N - p - 1}} = \sqrt{MS_{\text{residual}}} \tag{8-10}$$

p is number of values estimated on the basis of the sample. From results obtained in Table 8-4 and Eq. 8-10, the standard error of the model estimated is calculated to be 1.54×10^{-3} . A way to include the true value of the mean by relating it to an expression of the sample mean is by expressing the estimated value as a range (eg. $\hat{Y} \pm 10$). Therefore, the confidence interval (CI) of the true population mean estimated by the value of the sample mean is presented by the following equation:

$$CI = \hat{Y} \pm t_{(1-\alpha/2, N-2)} \cdot SE_{\hat{Y}} \tag{8-11}$$

Where $t_{(1-\alpha/2)}$ is the chosen for $N-2$ degrees of freedom. When calculating the CI, the t -values are chosen for the desired level of significance. Typically, prediction intervals for the predicted model are expressed in the standard way of a 95 % confidence interval ($\alpha = 0.05$). Regarding the statistical table (probability points of the t distribution with degrees of freedom), $t_{(1-\alpha/2, N-2)}$ is calculated to be 1.98 (Spiegel, 1988). Thus, the confidence interval for the predicted model is calculated to be $\hat{Y} \pm (3.05 \times 10^{-3})$ that will be discussed in the next section.

8.3.1.4 Searching for residuals and linearity

In model building, a residual is what is left after the model is fit. It is the difference between an observed value and the value predicted by the model. For judging how well a straight line fits the data, one convenient method is to plot the residuals against predicted values. If the assumptions of the homogeneity of variance are met, there should be no relationship between the predicted values and residuals. Systematic patterns between the predicted values and residuals suggest a possible violation of the assumption of linearity. If the assumption were met, the residuals would be randomly distributed in a band clustered around the horizontal line through zero, as shown in Figure 8-1 (a).

The relative magnitude of residuals is easier to judge when they are divided by estimates of their standard deviations. As seen in Figure 8-1 (b), the residuals and standardised residuals are calculated to aid in assessing how the regression line fits. Thus it allows us to obtain data which may be plotted using a graphic, to examine the fit of the regression line in the original units.

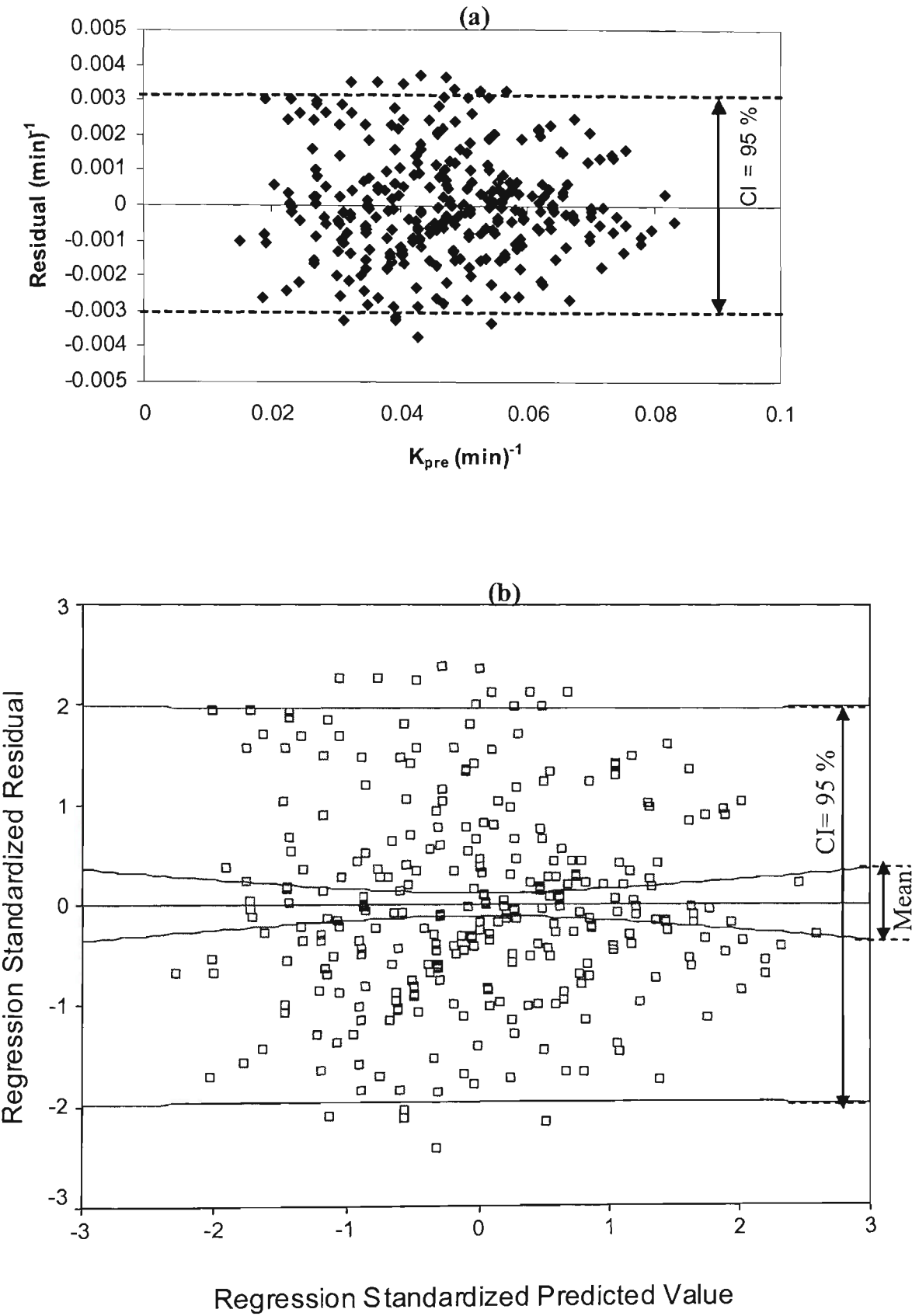


Figure 8-1 Randomly distributed residuals (a) non- standardised (b) standardised

To calculate the standardised residuals (std. residuals), each observed residual is divided by the estimated standard deviation of all the residuals. Like z scores, standardised residuals tell us how many standard deviation units they lie from the mean. The standardisation of residuals is important in that it shifts the median to 0 and the scale to 1, thus the residuals can be compared to standard normal distribution. They should show no pattern when plotted against the predicted values, as successive residuals should be approximately independent. If the distribution of residuals is approximately normal, then about 95% of the standardized residuals should fall between -2 and $+2$ (Norusis, 1997). The results obtained from Figure 8 -1 (a, and b) show that the residual values fall within ± 0.003 for the non-standardised residuals and lie between ± 2 for standardized residuals, which indicates the model fit the data well. For the multi regression analysis, a scatter plot is a good means of judging how well a straight line fits the data.

It is important to investigate the residuals after fitting the regression line to determine whether or not they appear to fit the assumption of a normal distribution. Thus one way to compare the observed distribution of the residuals to the expected distribution under an assumption of normality is to plot the two cumulative distributions against each other for a series of points. If the two distributions are identical, a straight line can be expected, because by observing how points scatter about the straight line expected, the two distributions may be compared. A plot of the cumulative probability of the residuals is shown in Figure 8-2. The observed residuals are above the normal line because there are smaller numbers of large negative residuals than expected. The observed points are below the normal line because the cumulative percentage exceeds that expected.

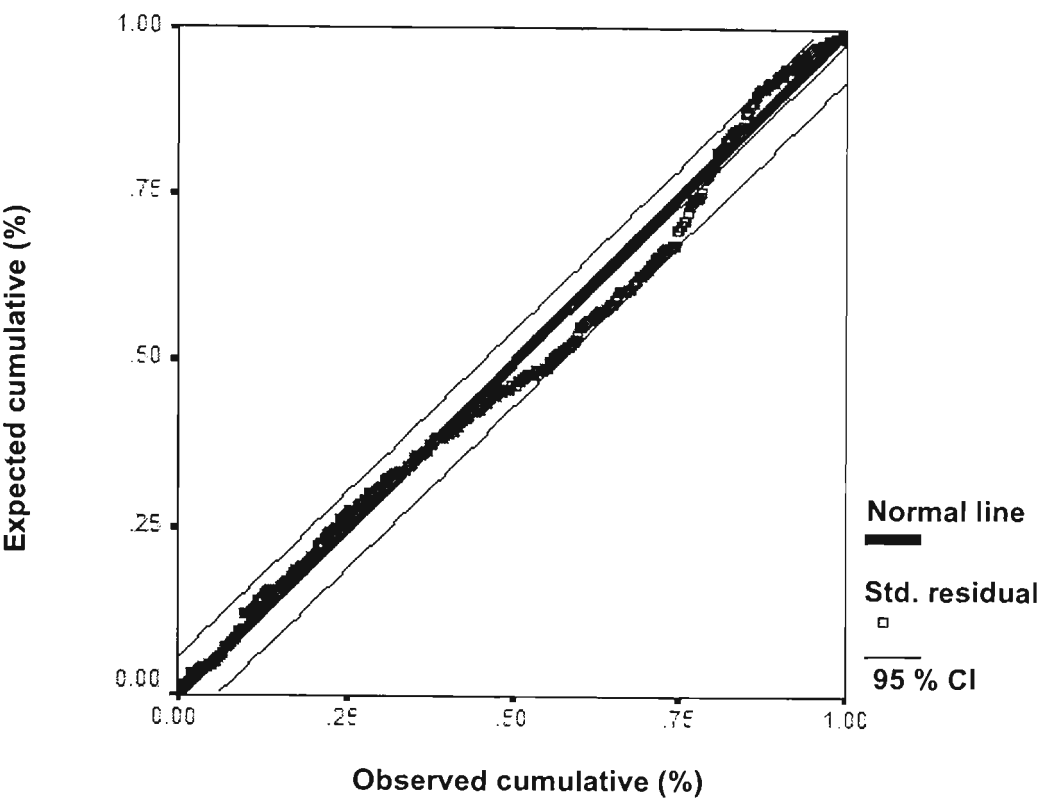


Figure 8-2 Normal probability plot between expected and observed cumulative data with interval confidential of 95 %

Normal distribution plays an important role in statistical analysis. As seen in Figure 8-2, distribution of the residuals (points) is approximately normal when the points are clustered around a straight line. This means the distribution of the residuals is almost normal when a statistical model is fitted to the data.

8.3.2 Empirical model

Development of the empirical model including an analysis of experimental data was performed using the computer package “SPSS”. As noted in the previous section the multiple regression analysis involves incorporating multiple independent variables. The equation being fitted to the data is an empirical model, expressed as,

$$\hat{Y}_i = b_o + b_1X_1 + b_2X_2 + + b_iX_i \tag{8-12}$$

Based on the experimental results presented in Table 8-1, it was found that the experimental rate constant (K_{exp}) depends on the independent variables, including concentration of current (I/V), solution pH, initial concentration of pollutant (C_o), distance between electrode (d), and initial concentration of Ca^{2+} (refer to Eq. 4-34 in section 4.2.4). A multiple regression analysis of the results shown in Table 8-3 presented a high degree of correlation ($R^2=0.99$) for the following equation:

$$K_{pre} = 10^{-5} [5.9 \left(\frac{I}{V} \right) + 7.6(Ca^{2+}) - 82.0(d) - 263.6(pH) - 37.0(C_o) + 4356.8] \quad (8-13)$$

A linear relation between K_{exp} and K_{pre} , is illustrated in Figure 8-3 showing that there is no significant difference between measured and predicted values.

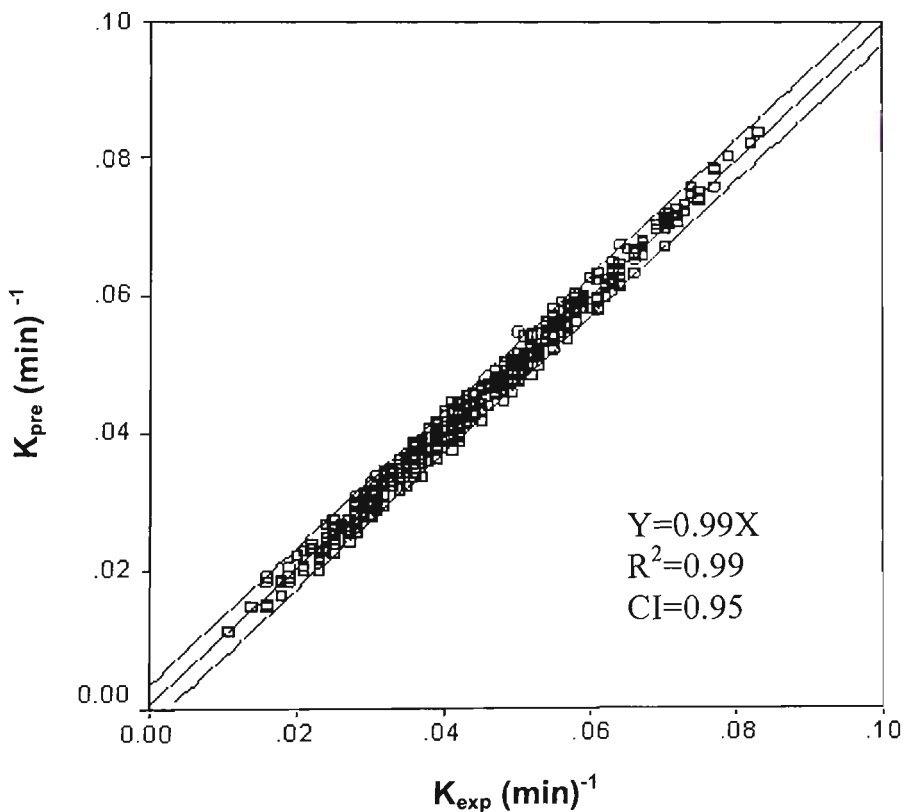


Figure 8-3 Relationship between the experimental and predicted rate constants for the ECF process at different operational parameters ($I=1-2.5$ A, $V=3.66$ L, $C_o=10-25$ mg/L, $d=5-15$ mm, $E_{cin}=10-50$ mS/m, $Ca^{2+}=50-300$ mg/L, $pH=6-8$, and $T=25$ °C)

As seen, good agreement between the experimental and predicted rate constants was confirmed with confidence interval (CI) 95 % when the range of the rate constants are considered to be between 0.01-0.09 min⁻¹. A summary of the statistical results at the different predicted rate constants (K_{pre}) in confidence intervals (95 %) is shown in Appendix H.

The chemical batch reactor theory was used as the basis for developing the empirical model and the experimental data gathered, which were explained in detail in chapter 4. The equation 8-13 can now be substituted into Eq.4-18 to provide Eq. 8-14 as:

$$C_t = C_o \cdot e^{-10^{-5} [5.9 (\frac{I}{V}) + 7.6(Ca^{2+}) - 82.0(d) - 263.6(pH) - 37.0(C_o) + 4356.8] t} \quad (8-14)$$

As noted in chapter 4, it was found that the fluoride removal efficiency (R_{ef}) may be obtained by Eq. 4-22. Thus it can be rearranged to provide an equation for removal as,

$$R_{ef} = 1 - e^{-10^{-5} [5.9 (\frac{I}{V}) + 7.6(Ca^{2+}) - 82.0(d) - 263.6(pH) - 37.0(C_o) + 4356.8] t} \quad (8-15)$$

The efficiency calculated by the empirical equation is plotted against the experimental fluoride removal efficiency in Figure 8-4. As expected the match is very good, with a high confidence interval 95 % when plotting theoretical fluoride removal efficiency against the experimental fluoride removal efficiency was considered between 15 to 100 %.

Concerning the theoretical considerations, as noted in chapter 4, the optimal detention time (d_{10}) was determined to achieve the desired fluoride concentration

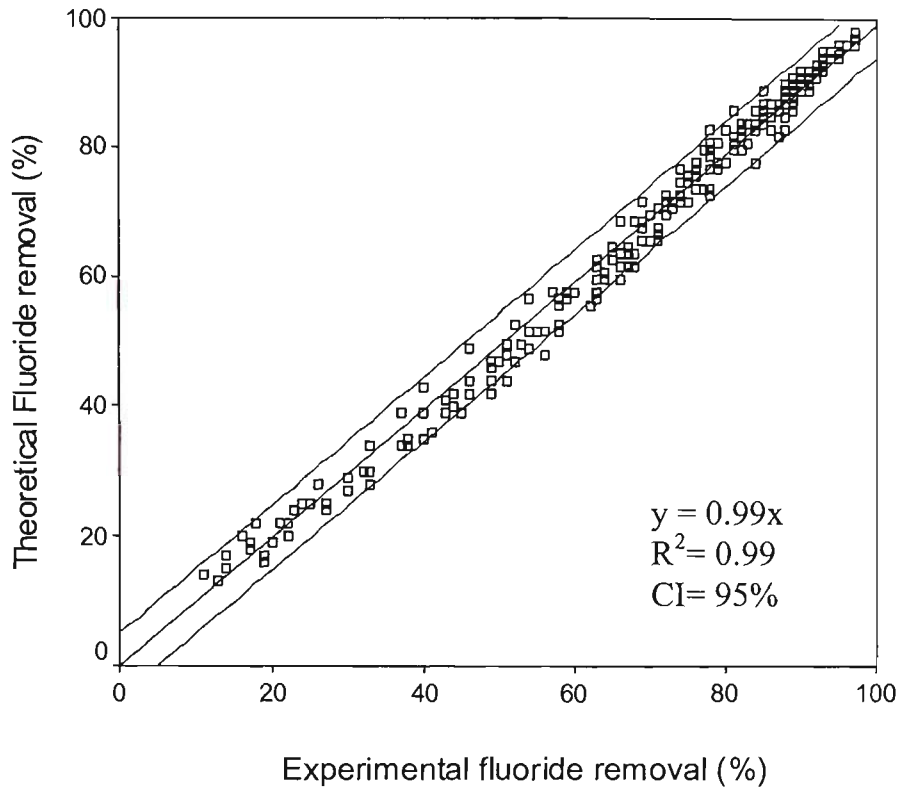


Figure 8-4 Relationship between theoretical fluoride removal efficiency and the experimental defluoridation efficiency by ECF process at different operational parameters ($I=1-2.5$ A, $V=3.66$ L, $C_o=10-25$ mg/L, $d= 5-15$ mm, $Ca^{2+}=50-300$ mg/L $Ec_{in}=10-50$ mS/m, $pH=6-8$, and $T=25$ °C)

range in the electrocoagulator (refer to Eq. 4-20 in chapter 4). Eq. 8-13 can be substituted into Eq. 4-20 to provide:

$$d_{to} = \frac{1}{10^{-5} \left[5.9 \left(\frac{I}{V} \right) + 7.6(Ca^{2+}) - 82.0(d) - 263.6(pH) - 37.0(C_o) + 4356.8 \right]} \ln(C_o) \quad (8-16)$$

From Eq.8-16, the optimal detention time for removing fluoride using the monopolar ECF process is calculated for various operational parameters including current concentration ($270-700$ A/m²), distance between electrodes ($5-15$ mm), solution pH ($6-9$), initial concentration of Ca^{2+} ($50-300$ mg/L), and initial concentrations of fluoride ($10-25$ mg/L).

8.3.3 Monopolar and bipolar processes

The influences of selected parameters on defluoridation by the monopolar ECF process are compared with results obtained by other researchers in the bipolar electrocoagulation process. Earlier monopolar ECF experiments in chapter 5 showed that the Al^{3+}/F^- mass ratio was between 13 and 17.5 for various initial concentrations of fluoride from 10 to 25 mg/L. This result agrees with the results obtained by Mameri et al. (1998) observation in the bipolar electrocoagulation process. It can be concluded that the difference in Al^{3+}/F^- mass ratio between monopolar and bipolar ECF system is insignificant.

Previous results presented in chapter 5, showed that the Ca^{2+} ion competition effect on defluoridation is very significant. Thus a comparison is also made on the residual concentration of fluoride between the authors' data and Mameri data (Mameri et al., 1998), as shown in Figure 8-5.

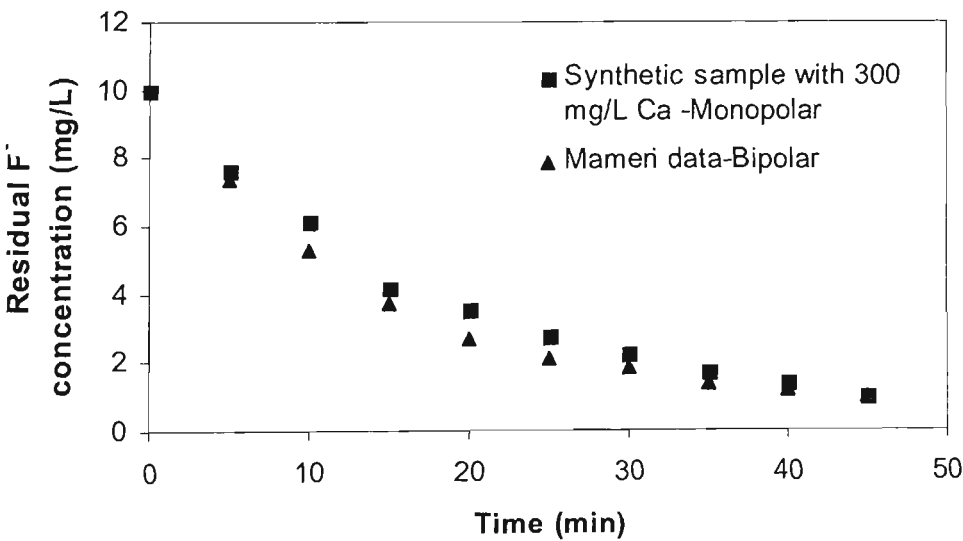


Figure 8-5 Comparison between monopolar and bipolar systems for defluoridation by ECF process for the same concentration of Ca^{2+} and the same operational parameters ($i=10.2\text{ A/m}^2$, $C_o=10\text{ mg/l}$, $d=20\text{ mm}$, and $pH=6-8$)

It is clear that there is no significant difference between the residual concentration of fluoride in monopolar and bipolar systems when the same water quality was conducted.

8.3.4 Model verification

Defluoridation experiments were also conducted using bore water sample taken from Central Australia (results was shown in chapter 5). This bore is currently not used for human consumption. For the same operational conditions, Figure 8-6 presents a comparison between the predicted and measured residual fluoride concentration for the Central Australian bore sample by the monopolar ECF system. The result shows good agreement between the experimentally measured data (independent data) and the predictive equation 8-14.

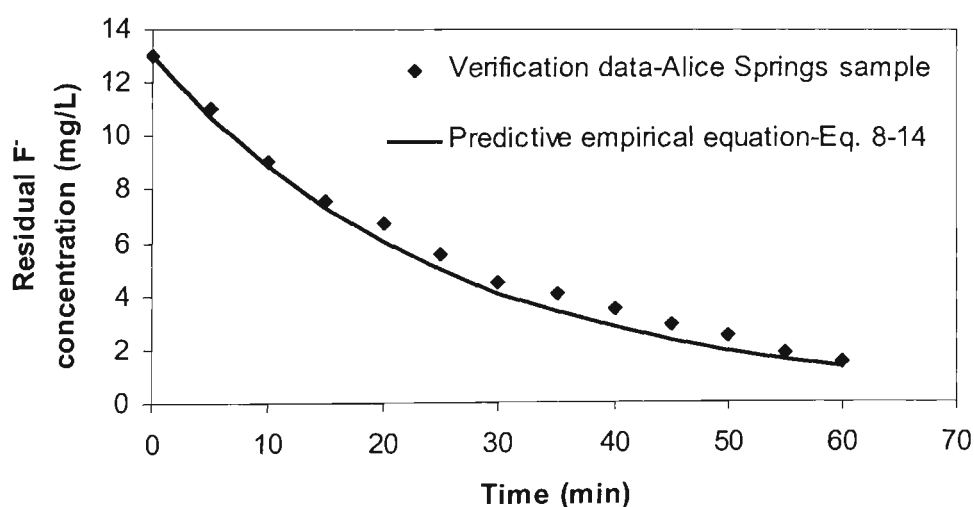


Figure 8-6 Comparison between predicted and experimental residual fluoride concentrations with electrolysis time for bore water data ($I=1.3$ A, $V=3.66$ L, $C_0=13$ mg/L, $d=7$ mm, $pH=7.8$)

A regression analysis based on ratios of sum of squares, is used to test equality of means in analysis of variance and significance of estimated parameters; which is called a variance ratio test or F- test. As described in section 8.3.1.3, F -test applies to test how well the model fits the data. The analysis of variance (ANOVA) is performed using the Microsoft Excel for the predicted and measured residual fluoride concentrations for bore sample. The summary of the statistical output results for the comparison is shown in Table AI-1 in Appendix I. This indicates that the observed significant level of F (Sig F) is less than 0.00005, when R^2 is found to be 0.99. Thus the hypothesis that $R^2 = 0$ (no linear relationship between variables) is rejected.

Figure 8-7 illustrates a comparison between the predicted residual concentrations of fluoride and Mameri data (Mameri et al., 1998). The results agree with the other experimentally measured data for a bipolar ECF system and the predictive equation 8-14, with similar water quality and operational conditions.

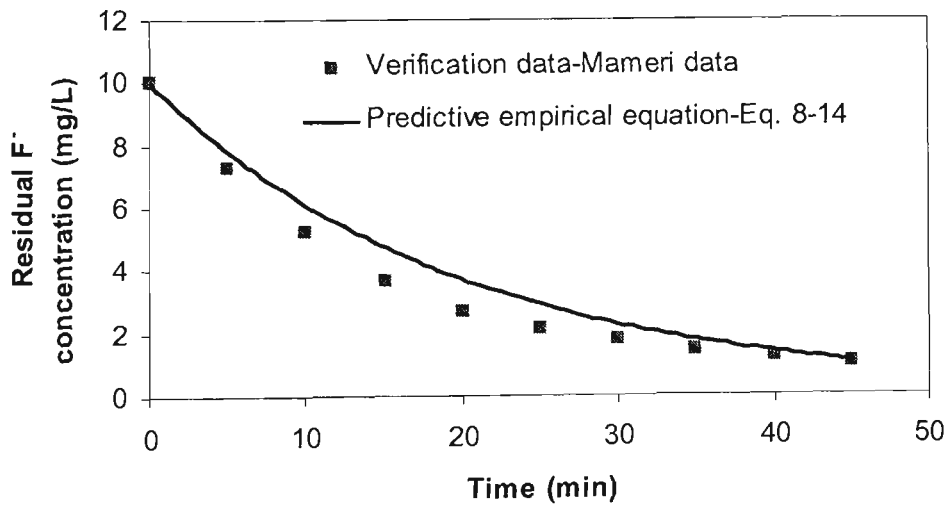


Figure 8-7 Comparison between predicted and experimental residual fluoride concentrations with electrolysis time for Mameri’s data ($I/V=353\text{ A/m}^3$, $C_o=10\text{ mg/L}$, $d=20\text{ mm}$, $\text{pH}=6$, $\text{Ca}^{2+}=280\text{ mg/L}$)

The results shows that there is an over prediction in Figure 8-7, which may be caused by high Ca^{2+} presence. As explained at above, the ratio of the mean square regression to the mean square residual is explained to elucidate goodness of fit. The analysis of variance results for the predicted residual concentrations of fluoride and Mameri data is summarized in Table AI-2 in Appendix I. This indicates that F –value is very small ($2.5 \times 10^{-9} < 0.00005$) when R^2 is found to be 0.99. The P-value is also found to be less than the conventional 0.05, as indicates that the null hypothesis is rejected ($R^2 = 0$) and good agreement between the experimentally measured data and the predictive equation 8-14 is indicated.

Another comparison between the predicted final concentrations of fluoride and Shen data (Shen et al., 2003) with similar water quality is shown in Figure 8-8. The effect of electrolysis time for defluoridation by ECF process was not considered by the authors. However, the final concentration of fluoride was only identified at 32 min electrolysis time for the different initial fluoride concentrations from 10 to 25 mg/L.

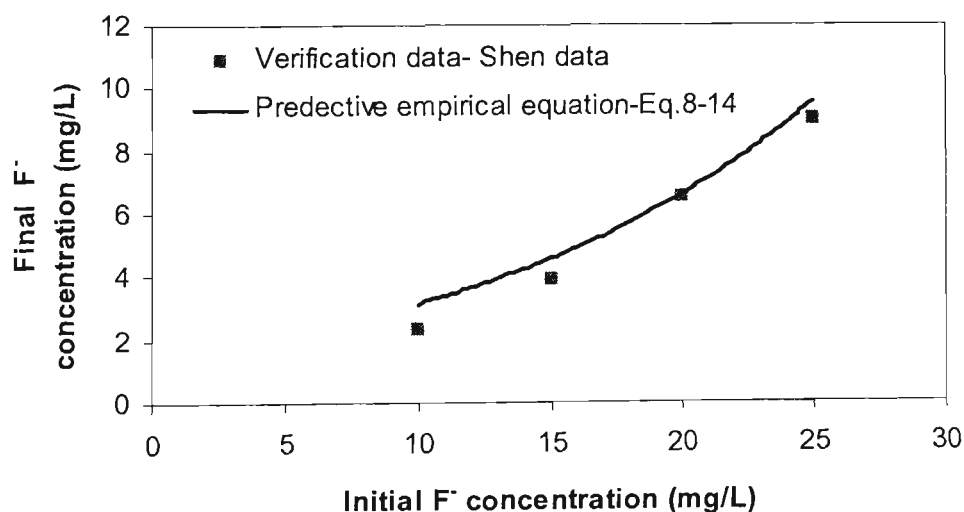


Figure 8-8 Comparison between predicted and experimental final fluoride concentrations with initial fluoride concentration for Shen's data ($I/V=278 \text{ A/m}^3$, $d=4 \text{ mm}$, $\text{pH}=6$, $\text{Ca}^{2+}=0 \text{ mg/L}$)

The regression analysis is performed for the predicted and measured final fluoride concentrations for Shen data to show goodness of fit. The summary of the statistical output results for the comparison is shown in Table AI-3 in Appendix I. Typically, prediction intervals for the predicted model are expressed in the standard way of a 95 % confidence interval ($\alpha = 0.05$). The P-value is also found to be less than the conventional 0.05 when R^2 is found to be 0.99. This indicates that the null hypothesis ($R^2 = 0$) is rejected and good agreement between the experimentally measured data (independent data) and the predictive equation 8-14 is indicated.

8.3.5 Empirical model and continuous flow data

Mixing in the continuous flow reactor is a function of reactor geometry, residence time and flow rate. A continuous flow reactor has a fixed feed flow rate rather than fixed volume as in a batch processes. As noted in chapter 4, Plug flow reaction time is theoretically equivalent to a batch reaction system (Huck & Averill, 1983). From Eq. 4-30 (presented in chapter 4), the model of continuous flow reactors may be evaluated by the following equation,

$$\frac{C_o}{C_e} = \exp\left(\frac{V.K}{Q}\right) \quad (8-17)$$

The flow rate can be expressed as:

$$Q = \frac{V.K}{\ln \frac{C_o}{C_e}} \quad (8-18)$$

If defluoridation process is take placed to achieve the desirable residual fluoride concentration 1 mg/L, the design flow rate (Q_o) can be expressed as:

$$Q_o = \frac{V.K}{\ln C_o}$$

(8-19)

Eq. 8-14 can be substituted to Eq. 8-19 to provide Eq. 8-20, when it is expected to match the analytical model with continuous flow data.

$$Q_o = \frac{V \times 10^{-5} [5.9 (\frac{I}{V}) + 7.6(Ca^{2+}) - 82.0(d) - 263.6(pH) - 37.0(C_o) + 4356.8]}{\ln C_o}$$

(8-20)

It is clear that the flow rate depends on the volume of the electrocoagulator, the concentration of current, pH of the solution, the concentration of calcium ions, the initial concentration of fluoride, and distance between electrodes. From Eq. 8-20, the design (optimal) flow rate can be calculated for various operational parameters including current concentrations from 380 to 1000 A/m³, and initial concentrations of fluoride from 10-25 mg/L for removing fluoride in a continuous flow EC reactor, as is shown in Table 8-5. The optimum residence time can be predicted by divided the optimum flow rate to the total net volume of EC box (7.9 L).

Table 8-5 Prediction of the optimal flow rate and residence time for various current concentrations and initial fluoride concentrations in the continuous flow EC reactor (pH_{in}=6, Ca²⁺=15 mg/L, and d=5mm)

C _o (mg/L)	I (A/)	i (A/m ²)	I/V (A/m ³)	Q _{o(pre)} (mL/min)	t _{ro(pre)} (min)
10	3	18.75	380	149	53
10	5	31.25	633	200	40
10	6	37.5	759	230	34
10	8	50	1013	280	28
15	4	25	506	145	54
15	6	37.5	759	190	42
15	8	50	1013	230	34
25	6	37.5	759	150	53

As noted in chapter 6, for a given constant current density, less fluoride is removed when the flow rates are increased in the continuous flow EC reactor. As expected, at high flow rate (400 mL/min), detention time is shorter when the current density was kept constant. It agrees with the results obtained on defluoridation by the batch model which has already been considered in chapter 5, when the electrolysis time in a batch system is equal to the residence time in a continuous flow EC reactor. Thus, the design (optimal) flow rate is needed to consider for continuous flow EC reactor (see Table 8-5). The optimum residence times and the experimental flow rate for different operational parameters such as: flow rates, current densities, and initial fluoride concentrations were previously summarized in Table 6-5 in chapter 6. From results obtained in Tables 6-5 and 8-5, the relationship between the experimental and predicted flow rates and also comparison between the experimental and predicted optimum residence times are shown in Figures 8-9 and 8-10.

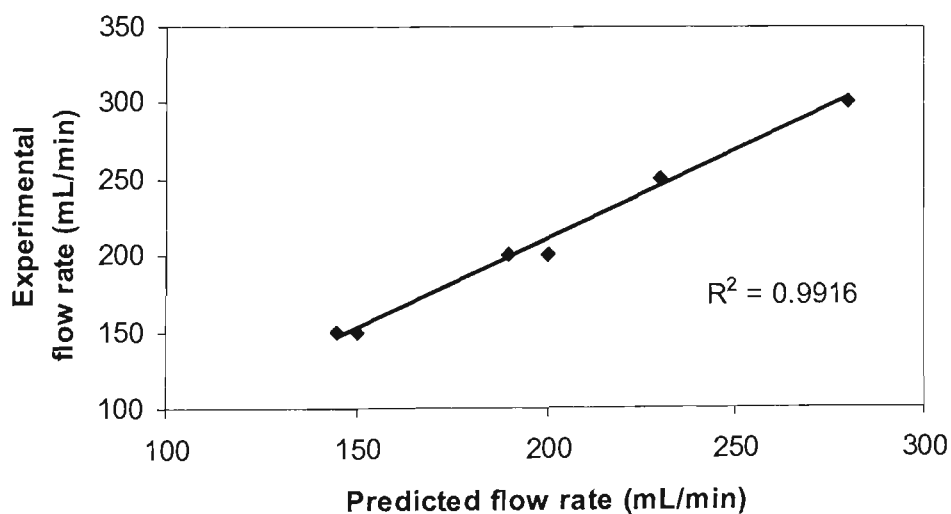


Figure 8-9 Relationship between the experimental and predicted flow rate for defluoridation by the continuous flow EC reactor at different operational parameters ($I/V=380-1000 \text{ A/m}^3$, $C_o=10-25 \text{ mg/L}$, $t_{ro}=26-53 \text{ min}$, $d=5 \text{ mm}$, $Ec_{in}=10-50 \text{ mS/m}$, $Ca^{2+}=15 \text{ mg/L}$, final pH=6-8, and $T=25 \text{ }^\circ\text{C}$)

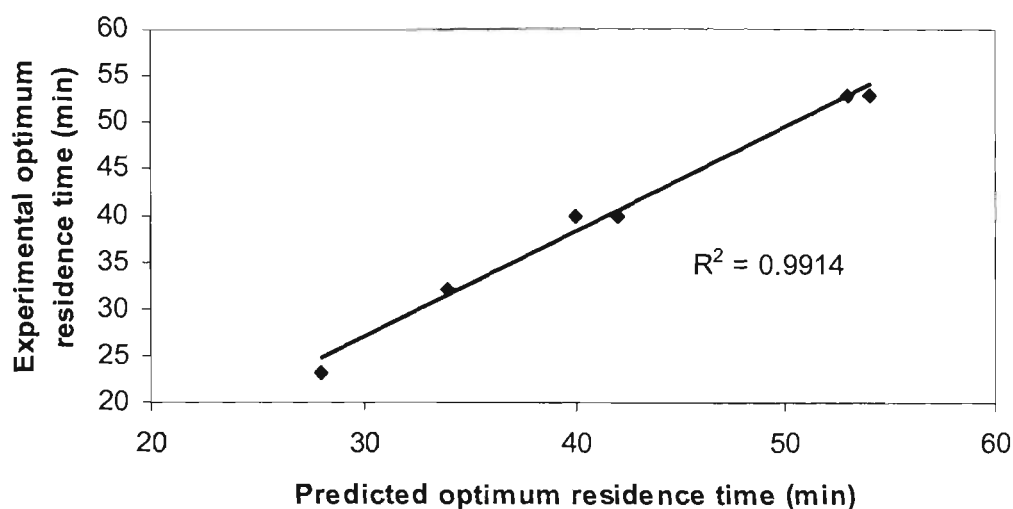


Figure 8-10 Relationship between the experimental and predicted optimum residence time for defluoridation by the continuous flow EC reactor at different operational parameters ($I/V=380-1000 \text{ A/m}^3$, $Q=150-300 \text{ mL/min}$, $C_o=10-25 \text{ mg/L}$, $d=5 \text{ mm}$, $E_{c_{in}}=10-50 \text{ mS/m}$, $Ca^{2+}=15 \text{ mg/L}$, final $pH=6-8$, and $T=25 \text{ }^\circ\text{C}$)

From results obtained in Figures 8-9 and 8-10, it can be concluded that there is no significant difference between the experimental flow rate and the predicted flow rates and also the experimental and predicted optimum residence times for various operational parameters including current concentrations from 380 to 1000 A/m^3 , initial concentrations of fluoride from 10-25 mg/L , final pH 6-8, distance between electrodes 5 mm, and Ca^{2+} concentration 15 mg/L for removing fluoride in a continuous flow EC reactor. The linear relationship between the experimental and predicted flow rates with good fitness shows that the empirical model could be used to match with continuous flow data when the steady state was reached. For the same operational conditions in a continuous flow EC reactor, Figure 8-11 presents a comparison between the predicted and measured flow rates with different initial concentrations of fluoride.

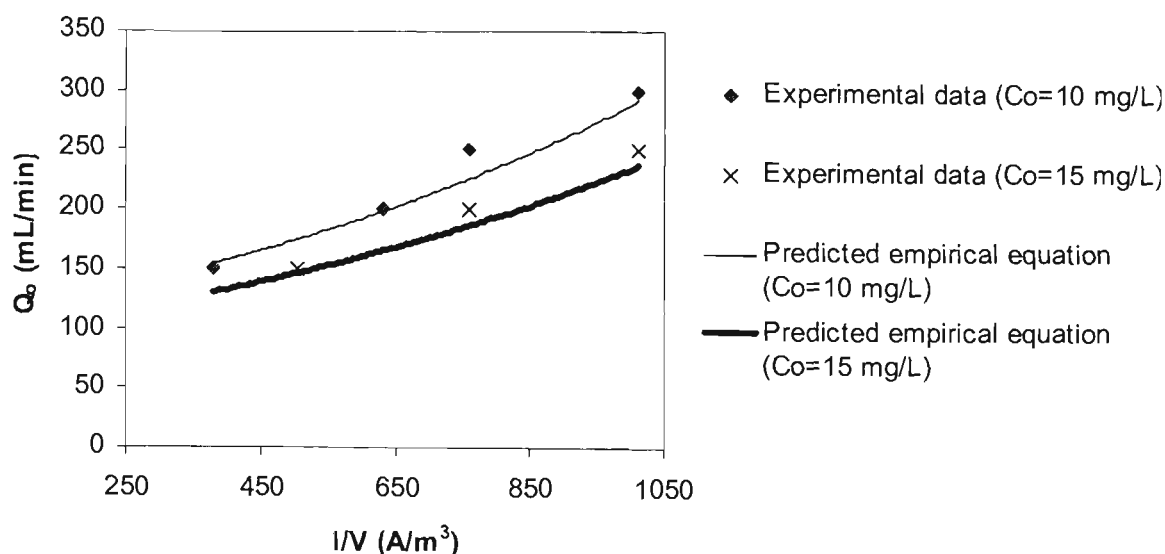


Figure 8-11 Comparison between the predicted and experimental optimum flow rates with the different current concentrations at the different initial fluoride concentrations for defluoridation by the continuous flow EC reactor ($d=5$ mm, $pH_{in}=6$, $Ca^{2+}=15$ mg/L, $Ec_{in}=20-35$ mS/m)

The result shows good agreement between the data measured experimentally from a continuous flow EC reactor and the predictive equation 8-20. As noted in section 8.3.4, a statistical F-test based on ratios of sums of squares and other statistics is used to test equality of means in analysis of variance and goodness of fit. The regression is performed using the Microsoft Excel for the predicted and measured optimum flow rate for the different initial fluoride concentration and current concentration. The summaries of the statistical output results for the comparison are shown in Tables AI-4 and AI-5 in Appendix I. This indicates that the P-value are also found to be less than the conventional 0.05 when the prediction intervals for the predicted model are expressed in the standard way of a 95 % confidence interval ($\alpha = 0.05$). The correlation coefficient is found to be 0.99. This indicates that the null hypothesis ($R^2=0$) is rejected and good agreement between the experimentally measured data and the predictive equation 8-20 is indicated.

As noted in section 8.3.2, an empirical model was developed to relate the critical parameters such as the current concentration from 270 to 700 A/m³, the Ca²⁺ concentration from 0 to 300 mg/L, the electrodes distance from 5 to 15 mm, the constant pH range from 6 to 9, and initial fluoride concentration from 10 to 25 mg/L in the batch EC reactor. From Eq. 8-20, this model could be used to match with continuous flow data when the same operational parameters are used. However, the effect of the Ca²⁺ concentration and distance between electrodes were not considered for the various values for defluoridation by the continuous flow EC reactor. Thus this model is calibrated for the different operational parameters including the different initial fluoride concentration from 10 -25 mg/L, final pH of 6-8, current concentration of 270 -1000 A/m², constant distance between electrodes of 5 mm, and the constant Ca²⁺ concentration of 15 mg/L. Figure 8-12 presents a comparison between the predicted and measured flow rates when the initial concentration of fluoride is 5 mg/L.

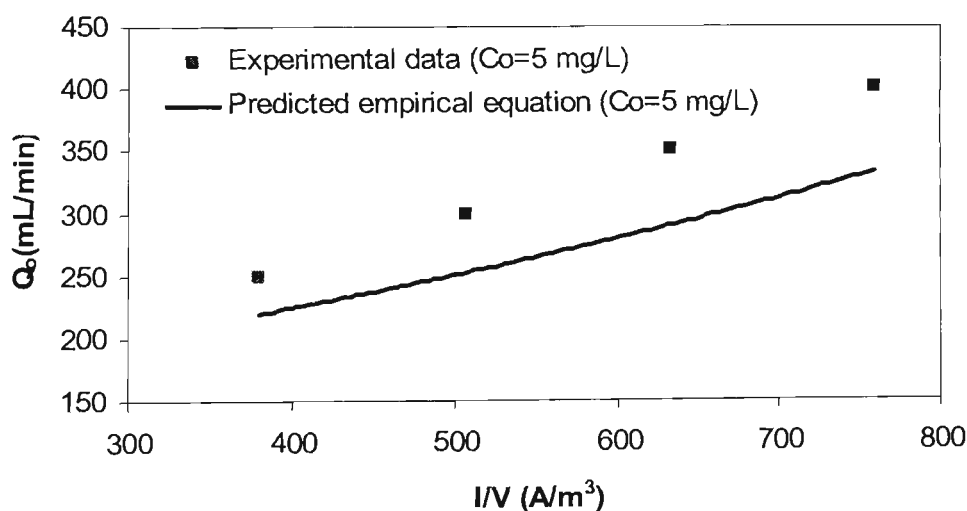


Figure 8-12 Comparison between the predicted and experimental optimum flow rates with the different current concentrations for defluoridation by continuous flow EC reactor ($d = 5$ mm, $pH_{in} = 6$, $Ca^{2+} = 15$ mg/L, $Ec_{in} = 10$ mS/m)

As seen, there is not good agreement between the optimum flow rates measured experimentally from a continuous flow EC reactor and the predictive equation 8-20 when the initial fluoride concentration is 5 mg/L. The results indicated that the model is valid to the initial fluoride concentration between 10 and 25 mg/L for defluoridation by continuous flow EC reactor.

8.4 SUMMARY

The chemical batch reactor theory was used as the basis for developing the empirical model. Several plots were developed to corroborate the first order behaviour of the ECF process for removing fluoride. The slope of the individual equations for each current applied, corresponds to the experimentally determined rate constant (K_{exp}) at that particular value. A log linear trend was confirmed for the data. A regression of the plotted data confirmed the first order behaviour and helped to determine the rate constant. It was also used to present the agreement between the independent data and predictive equation. The SPSS package was used as the statistical tool for the multiple correlation approximation of all data by regression analysis. An empirical model was developed to relate critical parameters such as concentration of current, distance between electrode, effects of Ca^{2+} ion competition, solution pH, and initial concentration of fluoride, with a constant rate of fluoride removal using the batch monopolar ECF process. The results demonstrated that the high correlation coefficients may be respectively observed for the independent variables of I/V , Ca^{2+} , d , pH, and C_0 . The great effect that the parameters of I/V and Ca^{2+} have on whole defluoridation process was confirmed. On the other hand the mathematical expression developed for studying the removal of fluoride showed positive

coefficient values for the independent variables of current and calcium concentration where a negative coefficient was obtained for the variables representing the pH of the solution, the initial concentration of fluoride, and the distance between electrodes. An empirical equation based on the operational parameters is given to calculate the optimal detention time for removing fluoride. The results show agreement between the experimental data and the predictive equation when defluoridation experiments were conducted using bore water sample. Also, comparison between the predicted residual concentrations of fluoride with Mameri and Shen data indicated that the results agree with the experimentally measured data and the predictive equation 8-14, with similar water quality and operational conditions. There was no significant difference in Al^{3+}/F^{-} mass ratio and residual concentration of fluoride between the monopolar and bipolar ECF systems when the same operational parameters are used. The results also showed that the empirical model could be used to match with continuous flow data when the steady state was reached. There are no significant differences between the predicted and measured design (optimal) flow rates and values of optimum residence time in the continuous flow monopolar EC reactor for the different operational parameters such as the current concentration between 270 - 1000 A/m², the Ca^{2+} concentration of 15 mg/L, the distance between electrodes of 5 mm, adjusted pH of 6-8, and the different initial fluoride concentration from 10 -25 mg/L. As expected the match was very good. However, it was indicated that Eq. 8-20 was limited to the initial fluoride concentration while there is not good agreement between the optimum flow rates measured experimentally and the predictive equation for the initial fluoride concentration of 5 mg/L.

CHAPTER 9

CHAPTER 9

CONCLUSIONS AND RECOMMENDATIONS FOR FURTHER RESEARCH

9.1 CONCLUSIONS

9.1.1 Electrocoagulation fundamental

This research work was carried out to show that fluoride may be removed from water or wastewater by electrocoagulation technology. Electrocoagulation is an electrochemical technique in which a variety of unwanted dissolved particles and suspended matter can be removed from an aqueous solution by electrolysis. When aluminium electrodes are used the aluminium dissolves at the anode and hydrogen gas is released at the cathode, and dissolution of Al anodes produces aqueous aluminium species. The coagulating agent combines with the pollutants to form large size flocs. The bubbles also float to the top of the tank, collide with particles suspended in the water on the way up, adhere to them, and float them to the surface. The EC process involves three successive stages including, formation of coagulants by electrolytic oxidation of the ‘sacrificial electrode’, destabilisation of the contaminants, and aggregation of the destabilised phases to form flocs. In fact a conceptual framework of the over all electrocoagulation process was linked to the generation of coagulant, coagulant hydrolysis, and aggregation and removal of pollutant, (by flotation and settling). This research work has focused on the key foundation sciences including electrochemistry, coagulation, and flotation for all electrocoagulation/flotation processes.

9.1.2 Batch and continuous flow EC reactor experiments

Batch experiments with monopolar aluminium electrodes were conducted to study different parameters such as, current values, electrolysis time, pH of the solution, distance between electrodes, initial concentration of fluoride, electrolyte conductivity, particle size, zeta potential, mass ratio of concentration of aluminium and fluoride ($\text{Al}^{3+}/\text{F}^-$ mass ratio), and the effects of ionic competition (especially the Ca^{2+} effect) on the removal of fluoride. Continuous flow experiments were also conducted to investigate different parameters including, current values, initial concentration of fluoride, initial pH and flow rate on the efficient removal of fluoride by the EC process. The general conclusions from the experimental results are summarised below:

- The amount of aluminium ion produced is proportional to combination of the current supplied and electrolysis time; charge (I.t), which affects fluoride removal significantly. Thus charge value determines the removal rate of pollutant. The optimum charge values were found between 5000 -5400 C and 9500-10500 C for the initial fluoride concentrations 10 and 25 mg/L, respectively when the residual aluminium concentrations on the effluent were found to be less than 0.2 mg/L which is desirable concentration based on NHMRC and ARMCANZ (2004) guideline.
- At higher currents the removal time was shorter due to a faster addition of coagulant. Settling can be increased with larger flocs.
- Fluoride removal by the electrocoagulation/flotation process was obtained by sedimentation and flotation in the electrocoagulator. As the characteristics of the sludge in both processes were similar.

- When the distance between the electrodes was increased the resistance between them increased and the removal of fluoride decreased.
- The optimal electrolysis time and design (optimum) flow rate depends on the current concentration (I/V), the effect of Ca^{2+} concentration, distance of the electrodes (d), pH of the solution, and the initial concentration of fluoride (C_0) in the batch and continuous flow EC reactor.
- The F^- removal by ECF follows a simple first order process.
- The experimental results showed that the $\text{Al}^{3+}/\text{F}^-$ mass ratio was between 13 and 17.5 when the residual aluminium concentrations on the effluent were found to be less than 0.2 mg/L.
- The results showed that defluoridation process is more efficient when pH is kept constant between 6 and 8 during experiments in the batch ECF reactor.
- The residual fluoride concentration reaches from 10 to 1 mg/L when the optimum charge density is found between 60000- 70000 C/m^2 .
- The affect of the Ca^{2+} ion competition on defluoridation was very significant.
- The anion of Cl^- had no significant effect on defluoridation. However, adjustment of conductivity (by Cl^-) was appropriate to reduce energy consumption without affecting EC efficiency.
- There was no significant effect on floc size when the initial concentration of fluoride was increased. It seems that the mean diameter of floc size increases as the electrolysis time and current inputs are increased.
- The volume of sludge produced had depended on the current values and treatment time in the electrocoagulator.

- Efficient fluoride removal on the continuous flow EC reactor depends on the current inputs, flow rate, and the initial concentration of fluoride for the adjusted pH between 6 and 8.
- The total operational costs in the ECF process are found between AUD 0.36 - 0.61 and AUD 0.64 to 0.99 per m³ of water treated when initial fluoride concentration are 5 and 10 mg/L, respectively. For a given 5 mg/L initial fluoride concentration, it was found that the total operational cost in the ECF process is less than (40 %) that of the NA (Nalgonda) process.

The methods developed in this thesis can be successfully by industries in three different ways to reduce excess F⁻ levels. Firstly, it can be used to reduce excess F⁻ in natural groundwater. Secondly, F⁻ can be reduced from industrially contaminated groundwater with a suitable pre-treatment. Thirdly, if there is a need to reduce F⁻ from fluorinated water supplies, the method can be successfully used to reduce F⁻ levels from 1 to 0.1 mg/L.

9.1.3 Solution speciation and removal mechanisms

A better understanding of the chemistry and speciation of Al and Al-F complexes were essential to verify the mechanisms for the defluoridation process. The solubility of aluminium in equilibrium with solid phase Al(OH)₃ depended on the surrounding pH. The chemical composition of the system at equilibrium was computed using the MINEQL⁺ model using the analytical data and thermodynamic database. To investigate the mechanism of removing fluoride in the EC process, the composition of the dried sludge was analysed using XRD spectrum, and the speciation of Al-F

complexes were studied by the MINEQL⁺ model. The following are the summary of the conclusions:

- When the pH < 5 dissolved aluminium (Al^{3+}) is predominant and aluminium hydroxide tends to be soluble. In the pH range of 5 and 6 the predominant hydrolysis products are $\text{Al}(\text{OH})^{2+}$ and $\text{Al}(\text{OH})_2^+$ when the solid $\text{Al}(\text{OH})_3$ is most prevalent in the adjusted pH range of 6 and 8. When the pH is > 9, soluble $\text{Al}(\text{OH})_4^-$ is the predominant species.
- For acidic and neutral solutions the formation of various Al-F complexes is predominant while the presence of free fluoride ion predominates at solution pH values greater than 7.5. So there is no Al-F complex in the effluent when the pH > 7.5.
- The chemical species of both AlF_5^{2-} and AlF_6^{3-} are insignificant when their concentrations are very low.
- The solubility of aluminium is affected by different initial concentrations of fluoride and pH of the solution.
- An XRD analysis of the composition of dried sludge obtained by EC shows the formation of $\text{Al}_n\text{F}_m(\text{OH})_{3n-m}$ and provides confirmation of the main mechanism for removing fluoride at an adjusted pH range of 6–8. However, it is important to keep in mind that discharging of this sludge into environment is needed to consider when it contains the removed fluoride.

9.1.4 EC modelling of design

The theory of chemical batch reactor was used as the basis for development of the semi-empirical model. Results from the experimental data showed that the

defluoridation process follows a first order behaviour within the ECF reactor. The experimental results from batch and continuous flow electrocoagulation reactor were used to evaluate the empirical model developed. This model was developed to relate critical parameters such as the current concentration from 270 to 700A/m³, the Ca²⁺ concentration from 0 to 300 mg/L, the electrodes distance from 5 to 15 mm, the constant pH range from 6 to 9, and initial fluoride concentration from 10 to 25 mg/L, with the constant rate for removing fluoride using batch monopolar ECF process. The SPSS package was used as the statistical tool for the multiple correlation approximation of all data by regression analysis, and the conclusions are summarised as follows:

- One of the first steps taken to analyse the experimental data collected, was to plot the logarithm of the measured concentration of fluoride against the time for electrolysis. The slope of the individual equations obtained for each current applied, corresponds to the experimentally determined rate constant (K_{exp}) at that particular value
- A regression of the plotted data confirmed the first order behaviour and helped determine the rate constant.
- An empirical equation is developed to calculate the optimal detention time for removing fluoride. The results show good agreement between the experimental data (independent data from the literature and case study) with predictive equation.
- There is no significant difference in the Al³⁺/F⁻ mass ratio and residual concentration of fluoride between monopolar and bipolar ECF systems when the same operational parameters are used.

- The results demonstrated that the high correlation coefficients may be respectively observed for the independent variables of I/V , Ca^{2+} , d , pH , and C_o . The great effect that the parameters of I/V and Ca^{2+} have on whole defluoridation process was confirmed.
- The results showed that the empirical model could be used to match with the continuous flow data, as there are no significant differences between the predicted and measured design (optimal) flow rates and values of optimum residence time in the continuous flow monopolar EC reactor for the different operational parameters such as the current concentration between 270 -1000 A/m^2 , the Ca^{2+} concentration of 15 mg/L, the distance between electrodes of 5 mm, adjusted pH of 6-8, and the different initial fluoride concentration from 10 -25 mg/L. As expected the match was very good
- It was indicated that the predictive equation was limited to the initial fluoride concentration while that the model is valid to the initial fluoride concentration between 10 and 25 mg/L for defluoridation by continuous flow EC reactor.

9.2 RECOMMENDATIONS FOR FURTHER RESEARCH

The literature review and experimental results confirmed that EC or ECF technology is a very sensitive and advanced process for removing excess fluoride from water supplies. The EC is an electrochemical technique with many applications, as it has many advantages and the quality of treated water can be improved significantly. To understand how the EC process works it is important to discuss the mechanism of water electrolysis and other related chemical reactions. So, understanding of EC fundamentals together pollutant removal mechanisms and the speciation of Al-F

complexes are vitally important. To improve this understanding, modification and development of a conceptual model is required. Also, the scientific framework of reactor designing has become more difficult to build upon. A greater understanding of the contact patterns is required to develop more complicated reactor design. This can be also undertaken by study computational fluid dynamic where complex flow patterns can be quantified. There is still scope for further research in this area and the following recommendations may help to improve the treatment:

- The experimental results obtained from this research showed that EC technology is an efficient process for defluoridation when it can be used and applied to assess the suitability of electrocoagulation to other pollutants such as COD, BOD, turbidity, oil, dye, cadmium, arsenic, nitrate, pesticides, TOC, organic compounds, boron, bacteria and E.coli.
- Efficient removal of pollutants by flotation is affected by the density of the bubble. The size of the bubble may influence the flotation mechanism. A detailed knowledge of the bubble characteristics will enable a better evaluation of the role of the electrolytic bubbles in removing pollutants and enable the design of a more effective electrocoagulation reactor.
- Different electrode material (dissolved and undissolved) can be used to assess different coagulant types for specific pollutants. Different electrode material can be used to assess different coagulant types for specific pollutants. For example, the use of iron will produce ferric ions that are used in water and wastewater treatment processes. The use of inert electrodes such as titanium, platinum or other non-corrosive metals requires further investigation, as they may affect the amount of residuals produced, which could increase the

treatment efficient in a solution that already contains significant amounts of coagulating materials.

- The rate of mixing on the electrocoagulator may affect performance, which was not noted too much in this research but further discussion on the basis of flocculation and their interactions is required for a better understanding. However, rising bubbles create disturbances in the fluid in EC batch reactor when mixing in continuous system is determined by the residence time and flow path. Concerning the aggregation principles, the transportation and collisions between pollutant particles, coagulant and bubbles are determined by the important fundamentals including the transport mechanism, mass diffusion, contact pattern, reaction kinetics, and fluid regime that should be more investigated.
- Different ways of connecting the electrodes might be conducted in future experiments. Bipolar electrodes connected in series can be tried to optimise performance. However, a higher potentials difference is required for a given current to flow in a series arrangement, because the cells connected in series have higher resistance. And alternating current EC instead of direct current EC process could also be studied in the future. The direct current electrocoagulation technology is inherent with the formation of an impermeable oxide layer on the cathode as well as deterioration of the anode due to oxidation. These limitations of the direct current EC process have been minimized to some extent by the addition of parallel plate sacrificial electrodes in the cell configuration. However, further researches need to be investigated.

- The EC process consumes electricity treating water and waste water but in some places using and generating may be expensive using EC to treat water. Solar energy could be considered as a source of power, knowing that it would save more than directly consuming electricity.

REFERENCES

- Abuzaid, N. S., Bukhari, A. A. & Hamouz, Z. M. (2002), Ground water coagulation using soluble stainless steel electrodes, *Advances in Environmental Research*, 6 (3), pp. 325-333.
- Agarwal, K. C., Gupta, S. K. & Gupta, A. B. (1999), Development of new low cost defluoridation technology (KRASS), *J. Wat. Sci. Tech*, 40(2), pp. 167-173.
- Agarwal, M., Rai, K., Shrivastav, R. & Dass, S. (2003), Defluoridation of water using amended clay, *Journal of cleaner production*, 11 (4), pp. 439-444
- Alfafara, C. G., Nakano, K., Nomura, N., Igarashi, T. & Matsumura, M. (2002), Operating and scale-up factors for the electrolytic removal of algae from eutrophied lake water, *Journal of Chemical Technology and Biotechnology*, 77, pp. 871-876.
- Allen, T. (1997), *Particle size measurement, powder sampling and particle size measurement*, Vol 1, London: Chapman and Hall, 525 p.
- Amor, Z., Bariou, B., Mameri, N., Taky, M., Nicolas, S. & Elmidaoui, A. (2001), Fluoride removal from brackish water by electrodialysis, *Desalination*, 133, pp. 215-223.
- Angers, J. (1998), Small utility network Qom: What are the best methods for fluoride removal? *American Water Works Association*, Accessed on 15 July 2004, Available: www.awwa.org/science/sun/qom/qom0498.cfm
- AWWA & WEF (1998), *Standard methods for the examination of water and wastewater*, American Water Works Association and Water Environment Federation, 20th ed, Washington, D. C, USA.
- Baklan, V. Y. & Kolesnikova, I. P. (1996), Influence of electrode material on the electrocoagulation, *Journal of Aerosol Science*, 27 (1), pp. S209-S210.

- Balasubramanian, N. & Madhavan, K. (2001), Arsenic removal from industrial effluent through electrocoagulation, *Chem.Eng. Technol*, 24 (5), pp. 519-521.
- Balmer, L. M. & Foulds, A. W. (1986), Separation oil from oil-in- water emulsions by electroflocculation/electroflotation, *Filtration and Separation*, pp. 366-370.
- Bard, A. J. & Faulkner, L. R. (2001), *Electrochemical methods: fundamentals and applications*, New York: John Wiley, 833 p.
- Bayramoglu, M., Kobya, M., Can, O. T. & Sozbir, M. (2004), Operating cost analysis of electrocoagulation of textile dye wastewater, *Separation and Purification Technology*, 37 (2), pp. 117-125.
- Bebeshko, G. I. (2004), Therodynamic analysis of fluorine-metal-water systems for improving the selectivity of the potentiometric determination of fluorine in raw minerals, *Journal of Analytical Chemistry*, 59 (6), pp. 528-531.
- Bektas, N., Oncel, S., Akbulut, H. Y. & Dimoglo, A. (2004), Removal of boron by electrocoagulation, *Environ Chem Lett*, 2, pp. 51-54.
- Belongia, B. M., Haworth, P. D., Baygents, J. C. & Raghavan, S. (1999), Treatment of alumina and silica chemical mechanical polishing waste by electrodecantation and electrocoagulation, *Journal of Electrochemical Society*, 146 (11), pp. 4124-4130.
- Benefield, L. D., Judkins, J. F., Weand, B. L. & (1982), *Process chemistry for water and wastewater treatment*, Englewood Cliffs, N.J.: Prentice-Hall, 510 p.
- Binnie, C., Kimber, M. & Smethurst, G. (2002), *Basic water treatment*, London, Thomas Telford Publishing, 291 p.
- Bonilla, C. F. (1947), Possibilities of the electronic coagulator for water treatment, *Water and sewage*, (March), pp. 21-22.
- British Geological Survey (1995), Water quality fact sheet: Fluoride, *Geological Survey Technical Report*, accessed on 20 June 2003, Available:www.wateraid.org/other/startdownload.

- Buffle, J. & Parthasarathy, N. (1985), Importance of speciation methods in analytical control of water treatment processes with application to fluoride removal from waste waters, *Water Research*, 19 (1), pp. 7-23.
- Butler, J. N. (1998), *Ionic Equilibrium, Solubility and pH calculations*. Canada, John Wiley & Sons, 559 p.
- Calvo, L. S., Leclerc, J.P., Tanguy, G., Cames, M. C., Paternotte, G., Valentin, G., Rostan, A. & Lapique, F. (2003), An electrocoagulation unit for the purification of soluble oil wastes of high COD, *Environmental Progress*, 22 (1), pp.57-65.
- Can, O. T., Bayramoglu, M. & Kobya, M. (2003), Decolourization of reactive dye solutions by electrocoagulation using aluminium electrodes, *Ind. Eng. Chem. Res*, 42, pp. 3391-3396.
- Can, O. T., Kobya, M., Demirbas, E. & Bayramoglu, M. (2006), Treatment of the textile wastewater by combined electrocoagulation, *Chemosphere*, 62 (2), pp.181-187.
- Carmona, M., Khemis, M., Leclerc, J.P. & Lapique, F. A. (2006), Simple model to predict the removal of oil suspensions from water using the electrocoagulation technique, *Chemical Engineering Science*, 61 (4), pp. 1237-1246.
- Chen.W. J, Chen. T. N & Cheng, Y. C. (2002), Polyelectrolyte conditioning for iron-hydroxide- containing sludge produced from electroflocculation of fermentation wastewater, *Journal of Environmental Science and health, part A: toxic/hazardous substances and environmental engineering.*, A37 (7), pp. 1277-1293.
- Chen, G. (2004), Electrochemical technologies in wastewater treatment, *Separation and Purification Technology*, 38 (1), pp. 11-41.
- Chen, X., Chen, G. & Yue, P. L. (2000), Separation of pollutants from restaurant wastewater by electrocoagulation, *Separation and Purification Technology*, 19 (1-2), pp. 65-76.

- Chen, X., Chen, G. & Yue, P. L. (2002a), Investigation on the electrolysis voltage of electrocoagulation, *Chemical Engineering Science*, 57 (13), pp. 2449-2455.
- Chen, X., Chen, G. & Yue, P. L. (2002b), Novel electrode system for electroflotation of wastewater, *Environ.Sci. Technol*, 36, pp. 778-783.
- Chidambaram, S., Ramanathan, A. L. & Vasudevan, S. (2003), Fluoride removal studies in water using natural materials, *Water SA*, 29 (3), pp. 339-343.
- Choi, W.W. & Chen, K. Y. (1979), The removal of fluoride from waters by adsorption, *Journal AWWA*, (october), pp. 562-570.
- Ciardelli, G. & Ranieri, N. (2001), The treatment and reuse of wastewater in the textile industry by means of ozonation and electroflocculation, *Water Research*, 35 (2), pp. 567-572.
- Ciorba, G. A., Radovan, C., Vlaicu, I. & Masu, S. (2002), Removal of nonylphenol ethoxylates by electrochemically-generated coagulants, *Journal of Applied Electrochemistry*, 32, pp. 561-567.
- Clemens, O. A. (1981), Purifying oily wasteawter by electrocoagulation, *Plant Engineering*, (September 17), pp. 124-125.
- Coetzee, P. P., Coetzee, L. L. & Mubenga, S. (2003), Characterisation of selected South african clays for defluoridation of natural waters, *Water SA*, 29 (3), pp. 331-338.
- Daneshvar, N., Sorkhabi, A.H. & Tizpar, A. (2003), Decolorization of orange II by electrocoagulation method, *Separation and Purification Technology*, 31 (2), pp. 153-162.
- Daneshvar, N., Sorkhabi, A. H. & Kasiri, M. B. (2004), Decolorization of dye solution containing Acid Red 14 by electrocoagulation with a comparative investigation of different electrode connections, *Journal of Hazardous Materials*, B112 (1-2), pp. 55-62.

Daneshvar, N., Oladegaragoze, A. & Djafarzadeh, N. (2005), Decolorization of basic dye solutions by electrocoagulation: An investigation of the effect of operational parameters, *Journal of Hazardous Materials*, In press, pp.

Daw, R. K. (2004), People-centred approaches to water and environmental sanitation: Experiences with domestic defluoridation in India. *30 th WEDC international Conference*. Vientiane, Lao PDR, pp.467-473.

Den, W. & Huang, C. (2005), Electrocoagulation for removal of silica nano-particles from chemical-mechanical-planarization wastewater, *Colloids and Surfaces A: Physicochemical and Engineering Aspects*, 254 (1-3), pp. 81.

Dezelic, N., Bilinski, H. & Wolf, R. H. H. (1971), Precipitation and hydrolysis of metallic ions-IV, Studies on the solubility of aluminum hydroxide in aqueous solution, *J. inorg. nucl. chem*, 33, pp. 791-798.

Dimoglo, A., Akbulut, H. Y., Cihan, F. & Karpuzcu, M. (2004), Petrochemical wastewater treatment by means of clean electrochemical technologies, *Clean Techn Environ Policy*, 6, pp. 288-295.

Donini, J. C., Kan, J. & Szynekarczuk, J. (1994), The operating cost of electrocoagulation, *The canadian journal of chemical Engineering*, 72, pp. 1007-1012.

Driscoll, C. T. & Schecher, W. D. (1990), The chemistry of aluminium in the environment, *Environmental Geochemistry and Health*, 12 (1/2), pp. 28-49.

Drondina, R. V. & Drako, I. V. (1994), Electrochemical technology of fluorine removal from underground and wastewaters, *Journal of Hazardous Materials*, 37 (1), pp. 91-100.

Drondina, R. V., Romanov, A. M., Matveevich, V. A., Motspan, V. P. & Shafranskij, V. N. (1989), Electrochemical method to remove fluorine from waters. The study of its mechanism, *Journal of Fluorine Chemistry*, 45 (1), pp. 58.

Emamjomeh, M. M. and Sivakumar, M. (2005), Electrocoagulation technology for nitrate removal, *9th Annual Environmental Research Event (ERE) Conference*, 29th November - 2nd December, Hobart, Tasmania, Australia, Published in the Conference proceeding

Environmental Research Software (1999), *MINEQL⁺ computer program, The first choice in chemical equilibrium modeling*. 4.5 ed., Environmental Research Software, Hallowell, USA. 220p.

Fan, L., Yang, F. & Yang, W. (2004), Performance of the decolorization of an Azo dye with bipolar packed bed cell, *Separation and Purification Technology*, 34, pp. 89-96.

Fang, L., Ghimire, K. N., Kuriyama, M., Inoue, K. & Makino, K. (2003), Removal of fluoride using some ianthanum(III)-loaded adsorbents with different functional groups and polymer matrices, *Journal of Chemical Technology and Biotechnology*, 78, pp. 1038-1047.

Fanning, J. C. (2000), The chemical reduction of nitrate in aqueous solution, *Coordination Chemistry Reviews*, 199 (1), pp. 159-179.

Farrah, H., Slavek, J. & Pickering, W. F. (1987), Fluoride interactions with hydrous aluminium oxides and alumina, *Aust. J. Soil. Res*, 25, pp. 55-69.

Feng, C., Sugiura, N., Shimada, S. & Maekawa, T. (2003), Development of a high performance electrochemical wastewater treatment system, *Journal of Hazardous Materials*, 103 (1-2), pp. 65-78.

Fitzgerald, J., David. C, Stephan.R, Sandy. D, & Stephen. H (1999), *Groundwater quality and environmental health implications, Anangu Pitjantjatjara Lands, South Australia*, in Bureau of Rural Sciences. Avaialable:

[Http://Www.Affa.Gov.Au/Corporate_Docs/Publications/Pdf/Rural_Science/Landwater/Aridzone/Report.Pdf](http://Www.Affa.Gov.Au/Corporate_Docs/Publications/Pdf/Rural_Science/Landwater/Aridzone/Report.Pdf)>.

- Fukui, Y. & Yuu, S. (1984), Development of apparatus for electro-flotation, *Chemical Engineering Science*, 39 (6), pp. 939-945.
- Gao, P., Chen, X., Shen, F. & Chen, G. (2005), Removal of chromium(VI) from wastewater by combined electrocoagulation-electroflotation without a filter, *Separation and Purification Technology*, 43 (2), pp. 117.
- Ge, J., Qu, J., Lei, P. & Liu, H. (2004), New bipolar electrocoagulation-electroflotation process for the treatment of laundry wastewater, *Separation and Purification Technology*, 36 (1), pp. 33-39.
- Gnusin, N. P., Zabolotskaya, L. I. & Vitulskaya, N. V. (1986), Effect of pH, electrical and hydrodynamic regimes on electrocoagulation treatment of solutions containing Cd^{2+} , *Soviet Journal of Water Chemistry and Technology*, 7 (4), pp. 32-35.
- Golder, A. K., Hridaya, N., Samanta, A. N. & Ray, S. (2005), Electrocoagulation of methylene blue and eosin yellowish using mild steel electrodes, *Journal of Hazardous Materials*, 127 (1-3), pp. 134-140.
- Grechko, A. V., Marchenko, P. V. & Shevchenko, M. A. (1982), Removal of pesticides from greenhouse drainage wastewater. *Soviet Journal of water Chemistry and Technology*, 4(1), pp. 56-58.
- Gurses, A., Yalcin, M. & Dogar, C. (2002), Electrocoagulation of some reactive dyes: a statistical investigation of some electrochemical variables, *Waste Management*, 22 (5), pp. 491-499.
- Habib, K., Riad, W., Muhanna, K. & Al-Sumait, H. (2002), Electrochemical behavior of Al-brass in polluted natural seawater, *Desalination*, 142 (1), pp. 5-9.
- Han, M, S. J., and Kwon. A (2002), Preliminary investigation of electrocoagulation as a substitute for chemical coagulation, *Water Science and Technology: Water Supply*, 2 (5-6), pp. 73-76.

- Hansen, H. K., Nunez, P. & Grandon, R. (2005), Electrocoagulation as a remediation tool for wastewaters containing arsenic, *Minerals Engineering*, In Press, Corrected Proof.
- Hao, O. J, and Huang, C. P. (1986), Adsorption characteristics of fluoride onto hydrous alumina, *Journal of Environmental Engineering*, 112 (6), pp. 1054-1069.
- Hara, H., Kobayashi, H., Maeda, M., Ueno, A. & Kobayashi, Y. (2001), Speciation of aluminium in rainwater using a fluoride ion selective electrode and ion-exchange chromatography with fluorometric detection of the aluminium-lumogallion complex, *Anal. Chem*, 73, pp. 5590-5595.
- Heidweiller, V. M. L. (1990), Fluoride removal methods, *Proc. Symposium on endemic fluorosis in developing countries: causes, effects and possible solutions*, ed: Frencke, J. E. Chapter 6, NIPGTNO, leiden, pp. 51-58 (as cited in British Geological Survey, 1995),
- Hernlem, B. J. & Tsai, L. S. (2000), Chlorine generation and disinfection by electroflotation, *Food Engineering and Physical Properties*, 65 (5), pp. 834-837.
- Hicyilmaz, C., Bilgen, S. & Ozbas, K. E. (1997), The effect of dissolved species on hydrophobic aggregation of fluorite, *Colloids and Surfaces A: Physicochemical and Engineering Aspects*, 121, pp. 15-21.
- Holt, P. K., Barton, G. W. & Mitchell, C. A. (1999), Electrocoagulation as a wastewater treatment. *The third Annual Australian Environmental Engineering Research Event*. 23-26 November Castlemaine, Victoria.
- Holt, P. K. (2003) Electrocoagulation: unravelling and synthesising the mechanisms behind a water treatment process. Thesis (PhD), Dept. of Chemical Engineering, University of Sydney, NSW, Australia. 228p.
- Holt, P. K., Barton, G. W. & Mitchell, C. A. (2004), Deciphering the science behind electrocoagulation to remove clay particles from water, *Water Science & Technology*, 50 (12), pp. 177-184.

- Holt, P. K., Barton, G. W. & Mitchell, C. A. (2005), The future for electrocoagulation as a localised water treatment technology, *Chemosphere*, 59 (3), pp. 355-367.
- Holt, P. K., Barton, G. W., Wark, M. & Mitchell, C. A. (2002), A quantitative comparison between chemical dosing and electrocoagulation, *Colloids and Surfaces A: Physicochemical and Engineering Aspects*, 211 (2-3), pp. 233-248.
- Hosny, A. Y. (1992), Separation of oil from oil/water emulsions using an electroflotation cell with insoluble electrodes, *Filtration & Separation*, 29 (5), pp. 419-423.
- Hosny, A. Y. (1996), Separating oil from oil-water emulsions by electroflotation technique, *Separations Technology*, 6 (1), pp. 9-17.
- Hu, C. Y., Lo, S. L. & Kuan, W. H. (2003), Effects of co-existing anions on fluoride removal in electrocoagulation (EC) process using aluminum electrodes, *Water Research*, 37 (18), pp. 4513-4523.
- Hu, C. Y., Lo, S. L. & Kuan, W. H. (2005a), Effects of the molar ratio of hydroxide and fluoride to Al(III) on fluoride removal by coagulation and electrocoagulation, *Journal of Colloid and Interface Science*, 283 (2), pp. 472.
- Hu, C. Y., Lo, S. L., Kuan, W. H. & Lee, Y. D. (2005b), Removal of fluoride from semiconductor wastewater by electrocoagulation-flotation, *Water Research*, 39 (5), pp. 895.
- Huang, C. J. & Liu, J. C. (1999), Precipitate flotation of fluoride-containing wastewater from a semiconductor manufacturer, *Water Research*, 33 (16), pp. 3403-3412.
- Huck, P. M. & Averill, D. W. (1983), Scale-up of a Radium -226 removal process. in Schmidtke, N. W. And Smith, D. W (ed.) *Scale-up of water and wastewater treatment processes*. USA, Butterworth. 430p.

- Hutnan, M., Drtil, M. & Kalina, A. (2005), Anaerobic stabilisation of sludge produced during municipal wastewater treatment by electrocoagulation, *Journal of Hazardous Materials*, In Press, Corrected Proof.
- Ibanez, J., Singh, M. M. & Szafran, Z. (1998), Laboratory experiments on electrochemical remediation of the environment. Part 4: Color removal of simulated wastewater by electrocoagulation-electroflotation, *Journal of chemical education*, 75 (8), pp. 1040-1041.
- Ibanez, J. G., Takimoto, M. M. & Vasquez, R. C. (1995), laboratory experiments on electrochemical remediation of the Environment: electrocoagulation of oily wastewater, *Journal of chemical education*, 72 (11), pp. 1050-1051.
- Inan, H., Dimoglo, A., Simsek, H. & Karpuzcu, M. (2004), Olive oil mill wastewater treatment by means of electro-coagulation, *Separation and Purification Technology*, 36 (1), pp. 23-31.
- Jambor, J. L., Sabina, A. P., Ramik, R. A. & Sturman, B. D. (1990), A fluorine-bearing gibbsite-like mineral from the Francon quarry, Montreal, Quebec, *Canadian Mineralogist*, 28, pp. 147-153.
- Jiang, J.Q., Graham, N., Andre, C., Kelsall, G. H. & Brandon, N. (2002), Laboratory study of electro-coagulation-flotation for water treatment, *Water Research*, 36 (16), pp. 4064-4078.
- Jiang, J.Q. (1988), An anodic passivation of electrocoagulator in the process of water treatment, *Water treatment*, 3, pp. 344-352.
- Jiang, J.Q., Graham, N., Andre, C., Kelsall, G. H., Brandon, N. P., and Chipps, M. J. (2002), Comparative performance of an electrocoagulation/flotation system with chemical coagulation-dissolved air flotation: a pilot-scale trial, *Water Science and Technology: Water Supply*, 2 (1), pp. 289-297.

- Jinadasa, K. B. P. N., Weerasooriya, S. & Dissanayake, C. B. (1988), A rapid method for the defluoridation of fluoride-rich drinking waters at village level, *Intern.J. Environmental studies*, 31, pp. 305-312.
- Joffe, L. & Knieper, L. (2000), Electrocoagulation technology quickly removes barium, total suspended solids from a water-retention pond for fractions of a cent per gallon, *Industrial wastewater*, January /February, pp. 1-5.
- Juttner, K., Galla, U. & Schmieder, H. (2000), Electrochemical approaches to environmental problems in the process industry, *Electrochimica Acta*, 45 (15-16), pp. 2575-2594.
- Kaliniichuk, E. M., Vasilenko, I. I., Shchepanyuk, V. Y., Sukhoverkhova, N. A. & Makarov, I. A. (1976), Treating refinery wastewaters to remove emulsified oils by electrocoagulation and electroflotation, *International Chemical Engineering*, 16 (3), pp. 434-435.
- Kauffman, J. M. (2005), Water fluoridation: a review of recent research and actions, *Journal of American Physicians and Surgeons*, 10 (2), pp. 38-44
- Khachaturian, Z. S. & Radebaugh, T. S. (1996), *Alzheimer's disease: cause(s), diagnosis, treatment, and care*, Boca Raton: CRC Press, 351p.
- Kiely, G. (1997), *Environmental engineering*, New York: McGraw-Hill, 979p.
- Kim, T.H., Park, C., Shin, E.B. & Kim, S. (2002), Decolorization of disperse and reactive dyes by continuous electrocoagulation process, *Desalination*, 150 (2), pp. 165-175.
- King, R. P. (1982), *Principal of flotation*, Republic of South Africa, Cap and Transvaal Printers, 352p.
- Kobya, M., Can, O. T. & Bayramoglu, M. (2003), Treatment of textile wastewaters by electrocoagulation using iron and aluminum electrodes, *Journal of Hazardous Materials*, 100 (1-3), pp. 163-178.

- Kobyas, M., Demirbas, E., Can, O. T. & Bayramoglu, M. (2005), Treatment of levafix orange textile dye solution by electrocoagulation, *Journal of Hazardous Materials*, In Press, Corrected Proof.
- Kobyas, M., Senturk, E. & Bayramoglu, M. (2005), Treatment of poultry slaughterhouse wastewaters by electrocoagulation, *Journal of Hazardous Materials*, In Press, Corrected Proof.
- Koparal, A. S. & Ogutveren, U. B. (2002), Removal of nitrate from water by electroreduction and electrocoagulation, *Journal of Hazardous Materials*, 89 (1), pp. 83-94.
- Koren, J. P. F. & Syversen, U. (1995), State-of-the-Art Electroflocculation, *Filtration & Separation*, 32 (4), pp. 336.
- Ku, Y. & Chiou, H. M. (2002), The adsorption of fluoride ion from aqueous solution by activated alumina, *Water, Air, and Soil Pollution*, 133, pp. 349-360.
- Kumar, P. R., Chaudhari, S., Khilar, K. C. & Mahajan, S. P. (2004), Removal of arsenic from water by electrocoagulation, *Chemosphere*, 55 (9), pp. 1245-1252.
- Lai, C. L. & Lin, S. H. (2003), Electrocoagulation of chemical mechanical polishing (CMP) wastewater from semiconductor fabrication, *Chemical Engineering Journal*, 95 (1-3), pp. 205-211.
- Lai, C. L. & Lin, S. H. (2004), Treatment of chemical mechanical polishing wastewater by electrocoagulation: system performances and sludge settling characteristics, *Chemosphere*, 54 (3), pp. 235-242.
- Lalumandier, J. & Jones, J. (1999), Fluoride concentrations in drinking water, *American Water Works Association Journal*, 91 (10), pp. 42-51.
- Larue, O. & Vorobiev, E. (2003), Floc size estimation in iron induced electrocoagulation and coagulation using sedimentation data, *International Journal of Mineral Processing*, 71 (1-4), pp. 1-15.

- Larue, O., Vorobiev, E., Vu, C. & Durand, B. (2003), Electrocoagulation and coagulation by iron of latex particles in aqueous suspensions, *Separation and Purification Technology*, 31 (2), pp. 177-192.
- Lesney, M. S. (2002), It is not eV being green? In fact, electrochemistry does make it easier to treat environmental problems, from wastewater cleanup to computer recycling, *Today's Chemist at work*, American Chemical Society, July, pp. 33-38.
- Letterman, R. D., Amirtharajah, A. & O'melia, C. R. (1999), Coagulation and flocculation. in Letterman, R. D (ed.) *Water quality and treatment: A handbook of community water supplies*, AWWA, U.S.A, McGraw-Hill. 1194p.
- Li-Cheng, S. (1985), Electro-chemical method to remove fluoride from drinking water, *Water Supply*, 3, pp. 177-186.
- Lin, S. H. & Peng, C. (1994), Treatment of textile wastewater by electrochemical method, *Wat. Res*, 28 (2), pp. 277-282.
- Lin, S. H. & Wu, C. L. (1996), Electrochemical removal of nitrite and ammonia for aquaculture, *Water Research*, 30 (3), pp. 715-721.
- Lounici, H., Addour, L., Belhocine, D., Grib, H., Nicolas, S., Bariou, B. & Mameri, N. (1997), Study of a new technique for fluoride removal from water, *Desalination*, 114 (3), pp. 241-251.
- Mahramanlioglu, M., Kizilcikli, I. & Bicer, I. O. (2002), Adsorption of fluoride from aqueous solution by acid treated spent bleaching earth, *Journal of Fluorine Chemistry*, 115 (1), pp. 41-47.
- Mamatha, P. & Rao, S. M. (2005), A sustainable option for de-fluoridation of water using using magnesium oxide. *International Conference on Energy, Environment and Disasters - INCEED*, July 24-30, Chalotte, NC, USA.
- Mameri, N., Yeddou, A. R., Lounici, H., Belhocine, D., Grib, H. & Bariou, B. (1998), Defluoridation of septentrional Sahara water of North Africa by

- electrocoagulation process using bipolar aluminium electrodes, *Water Research*, 32 (5), pp. 1604-1612.
- Martell, E. A., Hancock, R. D., Smith, R. M. & Motekaitis, R. J. (1996), Coordination of Al(III) in the environment and in biological systems, *Coordination Chemistry Reviews*, 149, pp. 311-328.
- Matis, K. A. & Mavros, P. (1991), Recovery of metals by ion flotation from dilute aqueous solutions, *Separation and purification methods*, 20, pp. 1-48.
- Matis, K. A. & Zouboulis, A. I. (1995) Electrolytic flotation: An unconventional technique, In Matis, K. A (ed.), *Flotation science and engineering*, New York, Marcel Dekker, 450 p.
- Matteson, M. J., Dobson, R. L., Glenn, J., Robert W., Kukunoor, N. S., Waits, I., William H. & Clayfield, E. J. (1995), Electrocoagulation and separation of aqueous suspensions of ultrafine particles, *Colloids and Surfaces A: Physicochemical and Engineering Aspects*, 104 (1), pp. 101-109.
- May, H. M., Helmke, P. A. & Jackson, M. L. (1979), Gibbsite solubility and thermodynamic properties of hydroxy-aluminium ions in aqueous solution at 25 °C, *Geochim. Cosmochim. Acta*, 43, pp. 861-868.
- Meeussen, J. C. L., Scheidegger, A., Hiematra, T., Riemsdijk, W. H. V., & Borkovec, M. (1996), Predicting multicomponent adsorption and transport of fluoride at variable pH in a Goethite-Silica sand system, *Environ. Sci. Technol*, 30, pp. 481-488.
- Miramontes, M. P., Margulis, R. G. B., & Hernandez, A. P. (2003), Removal of arsenic and fluoride from drinking water with cake alum and a polymeric anionic flocculent, *Fluoride*, 36 (2), pp. 122-128.
- Mills, D. (2000), A new process for electrocoagulation, *American Water Works Association. Journal*, 92 (6), pp. 34-43.

- Ming, L., Yi, S. R., Hua, Z. J., Lei, B. Y. W., Ping, L. & Fuwa, K. C. (1987), Elimination of excess fluoride in potable water with coacervation by electrolysis using aluminium anode, *Fluoride*, 20, pp. 54-63.
- Mollah, M. Y. A., Morkovsky, P., Gomes, J. A. G., Kesmez, M., Parga, J. & Cocke, D. L. (2004a), Fundamentals, present and future perspectives of electrocoagulation, *Journal of Hazardous Materials*, 114 (1-3), pp. 199-210.
- Mollah, M. Y. A., Pathak, S. R., Patil, P. K., Vayuvegula, M., Agrawal, T. S., Gomes, J. A. G., Kesmez, M. & Cocke, D. L. (2004b), Treatment of orange II azo-dye by electrocoagulation (EC) technique in a continuous flow cell using sacrificial iron electrodes, *Journal of Hazardous Materials*, 109 (1-3), pp. 165-171.
- Mollah, M. Y. A., Schennach, R., Parga, J. R. & Cocke, D. L. (2001), Electrocoagulation (EC) -- science and applications, *Journal of Hazardous Materials*, 84 (1), pp. 29-41.
- Mostefa, N. M. & Tir, M. (2004), Coupling flocculation with electroflotation for waste oil/water emulsion treatment: Optimization of the operating conditions, *Desalination*, 161, pp. 115-121.
- Murphy, A. P. (1991), Chemical removal of nitrate from water, *Nature*, 350 (21), pp. 223-225.
- Musquere, P. & Ellingsen, F. (1983), Electro-technics in drinking and wastewater, *Water Supply*, 1 (2/3), pp. 1-8.
- Naumczyk, J., Szpyrkowicz, L. & Zilio-Grandi, F. (1996), Electrochemical treatment of textile wastewater, *Water Science and Technology*, 34 (11), pp. 17-24.
- Nawlakhe, W. G. & Paramasivam, R. (1993), Defluoridation of potable water by Nalgonda technique, *Current science*, 65 (10), pp. 743-748.

- Ndiaye, P. I., Moulin, P., Dominguez, L., Millet, J. C. & Charbit, F. (2005), Removal of fluoride from electronic industrial effluent by RO membrane separation, *Desalination*, 173 (1), pp. 25-36.
- NHMRC & ARMCANZ. (2004), *Australian Drinking Water Guidelines*, National Health and Medical Research Council and the Agriculture and Resource Management Council of Australia and New Zealand, accessed on 29 June 2005
<http://www.nhmrc.gov.au/publications/synopses/eh19syn.htm>
- Nikolaev, N. V., Kozlovskii, A. S. & Utkin, I. I. (1982), Treating natural waters in small water systems by filtration with electrocoagulation, *Khimiya i Tekhnologiya Vody (Soviet journal of water chemistry and technology)*, 4 (3), pp. 70-73.
- Ninova, V. K. (2003), Electrochemical treatment of mine wastewaters containing heavy metal ions, *Annual Mining and mineral processing (part II)*, Sofia, 46, pp. 215-220
- Nirmalakhandan, N. (2002), Modelling tools for environmental engineers and scientists, USA, CRC Press. 307 p.
- Norusis, M. J. (1993), *SPSS for Windows: base system user's guide, release 6.0*, Chicago, SPSS Inc., 828p.
- Norusis, M. J. (1997), *SPSS 7.5 guide to data analysis*, Upper Saddle River, N.J., Prentice Hall, 553p.
- Ogutveren, U. B., Gonen, N. & Koparal, S. (1992), Removal of dye stuffs from wastewater: Electrocoagulation of Acilan Blau using soluble anode, *J. Environ. Sci. Health*, A27 (5), pp.1237-1247.
- Ogutveren. U.B & Koparal, S. (1997), Electrocoagulation for oil-water emulsion treatment, *J. Environ. Sci. Health*, A32 (9&10), pp. 2507-2520.
- Osipenko, V. D. & Pogorelyi, P. I. (1977), Electrocoagulation neutralization of chromium containing effluent, *Metallurgist*, 21 (9-10), pp. 44-45.

- Paidar, M., Rousar, I. & Bousek, K. (1999), Electrochemical removal of nitrate ions in waste solutions after regeneration of ion exchange columns, *Journal of Applied Electrochemistry*, 29, pp. 611-617.
- Parga, J. R., Cocke, D. L., Valenzuela, J. L., Gomes, J. A., Kesmez, M., Irwin, G., Moreno, H. and Weir, M. (2005), Arsenic removal via electrocoagulation from heavy metal contaminated groundwater in La Comarca Lagunera Mexico, *Journal of Hazardous Materials*, 124 (1-3), pp. 247-254.
- Park, J., Jung, Y., Han, M. & Lee, S. (2002), Simultaneous removal of cadmium and turbidity in contaminated soil-washing water by DAF and electroflotation, *Water Science & Technology*, 46 (11-12), pp. 225-230.
- Parthasarathy, N., Buffle. J & Haerdi.W (1986), Combined use of calcium salts and polymeric aluminum hydroxide for defluoridation of waste waters, *Water Research*, 20 (4), pp. 443-448.
- Phutdhawong, W., Chowwanapoonpohn, S. & Buddhasukh, D. (2000), electrocoagulation and subsequent recovery of phenolic compounds, *analytical Sciences*, 16, pp. 1083-1084.
- Poon, C. P. C. (1997), Electroflotation for groundwater decontamination, *Journal of Hazardous Materials*, 55 (1-3), pp. 159-170.
- Population Reference Bureau (2005), 2005 world population data sheet, accessed on 29 June 2005, Available: <http://www.prb.org/wpds/>
- Pouet, M.F. & Grasmick, A. (1994), Electrocoagulation and flotation: Applications in crossflow microfiltration, *Filtration & Separation*, 31 (3), pp. 269-272.
- Pouet, M.F. & Grasmick, A. (1995), Urban wastewater treatment by electrocoagulation and flotation, *Water Science and Technology*, 31 (3-4), pp. 275-283.

- Pouet, M. F., Persin.F (1992), Intensive treatment by electrocoagulation- flotation-tangential flow microfiltration in areas of high seasonal population, *water science and technology*, 25 (12), pp. 247-253.
- Pozhidaeva, E. Y., Sinitsyna, L. G., Akul'shina, V. D. & Reznikova, S. S. (1989), Thorough purification of electroplating plant effluent by electrocoagulation, *Soviet Journal of Water Chemistry and Technology*, 11 (7), pp. 659-661.
- Przhegorlinskii, V. I., Ivanishvili, A. I. & Grebenyuk, V. D. (1987), Dissolution of aluminium electrodes in the electrocoagulation treatment of water, *Khimiya i Tekhnologiya Vody (Soviet journal of water chemistry and technology)*, 9 (2), pp. 181-182.
- Qian, J., Susheela A.K., Mudgal A. & Keast G. (1999), Fluoride in water: An overview, *A UNICEF Publication on Water, Environment, Sanitation and Hygiene*, (13), pp. 11-13.
- Radic, N. & Bralic, M. (1995), Aluminum fluoride complexation and its ecological importance in the aquatic environment, *The Science of the Total Environment*, 172, pp. 237-243.
- Radosevic. J, Mentus. Z, Djordjevic.A & R, D. A. (1985), The effect offluoride ions on the electrochemical activity of aluminium, *J. Electroanalytical Chemistry*, 193, pp. 241-254.
- Raichur, A. M. & Basu, M. J. (2001), Adsorption of fluoride onto mixed rare earth oxides, *Separation and Purification Technology*, 24, pp. 121-127.
- Rajeshwar, K. & Ibanez, J. (1997), Environmental Electrochemistry: Fundamentals and Applications in Pollution Abatement. in Matthew, A. Tarr (ed.) *Chemical Degradation Methods for Wastes and Pollutants*. U.S.A: Academic Press. 720p.
- Rajeshwar.K (1994), Electrochemistry and the environment, *Journal of Applied Electrochemistry*, 24, pp. 1077-1091.

- Rao, N. C. R. (2003), Fluoride and environment- A review, *Proceedings of the Third International Conference on Environment and Health*, 15-17 December, Chennai, India, pp. 386-399.
- Rao, S. M. & Mamatha, P. (2004), Water quality in sustainable water management, *Current science*, 87 (7), pp. 942-947.
- Reardon, E. J. & Wang, Y. (2000), A limestone reactor for fluoride removal from wastewatrs, *Environ.Sci. Technol*, 34, pp. 3247-3253.
- Rieger, P. H. (1994), *Electrochemistry*, New York, Chapman &Hall, 483p.
- Rubach, S. & Saur, I. F. (1997), Onshore Testing of Produced Water by Electroflocculation, *Filtration & Separation*, 34 (8), pp. 877-882.
- Rubio, J., Souza, M. L. & Smith, R. W. (2002), Overview of flotation as a wastewater treatment technique, *Minerals Engineering*, 15, pp. 139-155.
- Saha.S (1993), Treatment of aqueous effluent for fluoride removal, *J.water Research*, 27 (8), pp. 1347-1350.
- Sandbank, E., Shelef, G. & Wachs, A. M. (1973), Improved electroflotation for the removal of suspended solids from algal pond effluents, *Water Research*, 8, pp. 587-592.
- Sanfan, W. (1991), Studies on economic property of pretreatment process of brackish water using electrocoagulation (EC) method, *Desalination*, 82 (1-3), pp. 359-363.
- Sanfan, W. & Qinlai, W. (1987), Experimental studies on pretreatment process of brackish water using electrocoagulation (EC) method, *Desalination*, 66, pp. 353-364.
- Sawyer, C. N. & McCarty, P. L. (1994), *Chemistry for environmental engineering*, London, McGraw-Hill, 544p.
- Scott, K. (1995), *Electrochemical processes for clean technology*, UK, The Royal society of Chemistry, 688 p.

- Shen, F., Chen, X., Gao, P. & Chen, G. (2003), Electrochemical removal of fluoride ions from industrial wastewater, *Chemical Engineering Science*, 58, pp. 987-993.
- Shin, M. S, Lee, K. H, Kim, D. J. & Han, M. Y. (2001), Treatment characteristics of livestock wastewater by electroflotation (EF), *Proceeding of IWA Water World Congress*, 15-19 October, Berlin.
- Simonsson, D. (1979), Reduction of fluoride by reaction with limestone particles in a fixed bed, *Ind. Eng. Chem. Process Des. Dev*, 18 (2), pp. 288-292.
- Sinha, S., Pandey, K., Mohan, D. & Singh, K. P. (2003), Removal of fluoride from aqueous solutions by eichhornia crassipes biomass and its carbonized form, *Ind. Eng. Chem. Res*, 42, pp. 6911-6918.
- Sivakumar, M., Emamjomeh, M. M. & Chen, M. (2004), Use of electrocoagulation (EC) as an alternative method to chemical coagulation in water treatment. *8th Annual Environmental Engineering Research Event (EERE) Conference*, 6th – 9th December, Wollongong, New South Wales, Australia, PP. 320-332
- Sivasamy, A., Singh, K. P., Mohan, D. & Maruthamuthu, M. (2001), Studies on defluoridation of water by coal-based sorbents, *Journal of Chemical Technology and Biotechnology*, 76, pp. 717-722.
- Smith, R. W. (1996), Kinetic aspects of aqueous aluminum chemistry: environmental implications, *Coordination Chemistry Reviews*, 149, pp. 81-93.
- Snoeyink, V. L. & Jenkins, D. (1980) *Water chemistry*, Canada, John Wiley & Sons, 463p.
- Solsona, F. (1985), Water defluoridation in the Rift vally, Ethiopia, *UNICEF technical report*, pp. 27(as cited in British Geological Survey, 1995),
- Spiegel, M. R. (1988), *Schaum's outline of theory and problems of statistics*, New York: McGraw-Hill, 504p.

- Sposito, G. (1996), *The environmental chemistry of aluminum*, U.S.A, Lewis (CRC press), 464p.
- Srinivasan, P. T. & Viraraghavan, T. (2002), Characterisation and concentration profile of aluminum during drinking-water treatment, *Water SA*, 28 (1), pp. 99-106.
- Srinivasan, P. T., Viraraghavan, T. & Subramanian, K. S. (1999), Aluminum in drinking water: An overview, *Water SA*, 25 (1), pp. 47-56.
- Street, R. L., Watters, G. Z., Vennard, J. K. (1996), *Elementary fluid mechanics*, U.S.A, John Wiley & Sons. 755 p.
- Stuart, F. E. (1946), Electronic water purification, *Water and sewage*, May, pp. 24-43.
- Sujana, M. G., Thakur. R. S & Rao, S. B. (1998), Removal of fluoride from aqueous solution by using alum sludge, *Journal of Colloid and Interface Science*, 206, pp. 94-101.
- Susheela, A. K. (1992), Defluoridation of drinking water: Merits of alternative technologies, *NFI Bulletin*, 13 (3), pp. 6-7.
- Syrbu, V. K., Botoshan, N. I. & Rabko, A. E. (1989), Optimization of fluorine extraction process by electroflotation of aluminum hydroxofluoride complexes, *Journal of Fluorine Chemistry*, 45 (1), pp. 57.
- Szpyrkowicz, L., Zilio-Grandi, F., Kaul, S. N. & Rigoni-Stern, S. (1998), Electrochemical treatment of copper cyanide wastewaters using stainless steel electrodes, *Water Science and Technology*, 38 (6), pp. 261-268.
- Tamil Nadu Water Supply and Drainage Board, TNWSDB, (2005), Technical notes for defluoridation treatment techniques with cost analysis. Accessed on 19 December, 2005, Available;
http://www.twadboard.com/photos/nletjune02_11.pdf
- Townsend, G. S. & Bache, B. W. (1992), Kinetics of aluminum fluoride complexation in single- and mixed ligand systems, *Talanta*, 39 (11), pp. 1531-1535.

- Toyoda, A. & Taira, T. (2000), A new method for treating fluorine wastewater to reduce sludge and running costs, *IEEE Transactions on semiconductor manufacturing*, 13 (3), pp. 305-309.
- Tsai, C. T., Lin, S. T., Shue, Y. C. & Su, P. L. (1997), Electrolysis of soluble organic matter in leachate from landfills, *Water Research*, 31 (12), pp. 3073-3081.
- Tsouris, C., Depaoli, D. W., Shor, J. T., Hu, M. Z.-C. & Ying, T.-Y. (2000), Electrocoagulation for magnetic seeding of colloidal particles, *Colloids and Surfaces A: Physicochemical and Engineering Aspects*, 177 (2-3), pp. 223-233.
- Ugurlu, M. (2004), The removal of some inorganic compounds from paper mill effluents by the electrocoagulation method, *G.U.Journal of Science*, 17 (3), pp. 85-99.
- UNESCO (2003), *United Nations Educational, Scientific and Cultural Organization*, Political inertia exacerbates water crisis, World Water Development Report, First UN system-wide evaluation of global water resources. In Unesco Press, accessed on 28 November 2005, Available:
[Http://Portal.Unesco.Org/Ev.Php?Url_Id=10064&Url](http://Portal.Unesco.Org/Ev.Php?Url_Id=10064&Url)
- Veressinina, Y., Trapido, M., Ahelik, V. & Munter, R. (2001), Fluoride in drinking water: The problem and its possible solutions, *Proc. Estonian Acad. Sci. Chem*, 50 (2), pp. 81-88.
- Vik, E. A., Carlson, D. A., Eikum, A. S. & Gjessing, E. T. (1984), Electrocoagulation of potable water, *Water Research*, 18 (11), pp. 1355-1360.
- Wang, S. & Wang, Q. (1987), Experimental studies on pretreatment process of brackish water using electrocoagulation (EC) method, *Desalination*, 66, pp. 353-364.
- Wasay, S. A., Haron, M., J & Tokunaga, S. (1996), Adsorption of fluoride, phosphate, and arsenate ions on lanthanum-impregnated silica gel, *Water Environment Research*, 68 (3), pp. 295-300.

- Weintraub, M. H., Golovoy, R. L. & Dzieciuch, M. A. (1983), Development of electrolytic treatment of oily wastewater, *Environmental Progress*, 2 (1), pp. 32-37.
- WHO (2002), Water, sanitation and health, Water, sanitation and hygiene links to health, accessed on 18 November 2005, Available:
http://www.who.int/water_sanitation_health/publications/facts2004/en/index.html
- WHO (2004), Water, sanitation and health: Guidline for drinknig- water quality, Third edition, accssed on 2 December 2005, Available:
http://www.who.int/water_sanitation_health/dwq/gdwq3/en/index.html
- WHO (2005), Report: Water Sanitation and Health -Fluoride, accessed on 2 March 2005, Aвалиable:
http://www.who.int/water_sanitation_health/naturalhazards/en/index2.html>
- Yang, C.L. & Dluhy, R. (2002), Electrochemical generation of aluminum sorbent for fluoride adsorption, *Journal of Hazardous Materials*, 94 (3), pp. 239-252.
- Yilmaz, A. E., Boncukcuoglu, R., Kocakerim, M. M. & Keskinler, B. (2005), The investigation of parameters affecting boron removal by electrocoagulation method, *Journal of Hazardous Materials*, 125 (1-3), pp. 160 -172.
- Zaroual, Z., Azzi, M., Saib, N. & Chainet, E. (2005), Contribution to the study of electrocoagulation mechanism in basic textile effluent, *Journal of Hazardous Materials*, In Press, Corrected Proof.
- Zhu, B., Clifford, D. A. & Chellam, S. (2005), Comparison of electrocoagulation and chemical coagulation pretreatment for enhanced virus removal using microfiltration membranes, *Water Research*, 39 (13), pp. 3098.
- Zolotukhin, I. A. (1989), A pilot-scale system for treatment of mine water by electrocoagulation-flotation, *khimiya i Tekhnologiya Vody (Soviet journal of water chemistry and technology)*, 11 (2), pp. 147-151.

APPENDIXES

APPENDIX A: Summary of results for defluoridation by batch EC process at the different operational parameters

Table AA-1 Summarised the residual fluoride concentration, the total aluminium concentration, and the removal efficiency using the batch EC reactor at the different electrolysis time and current densities ($C_0=10$ mg/L, Adjusted pH= 6-8 during experiments, $E_c=12$ mS/m)

I=1A

Sampling number	Time	Current density	Voltage	F ⁻ concentration	Al concentration		Removal efficiency
					Total	Residual	
	min	A/m ²	V	mg/L	mg/L		(%)
	0	12.5	12.2	10			
1	5	12.5	10.2	8.1	9.56	0.05	19
2	10	12.5	10.1	6.7	21.85	0.1	33
3	15	12.5	10.1	5.58	30.62	0.08	44.2
4	20	12.5	10.1	4.2	39.86	0.12	58
5	25	12.5	10.1	3.6	44.52	0.06	64
6	30	12.5	10.1	2.9	47.24	0.08	71
7	35	12.5	10.1	2.65	59.62	0.15	73.5
8	40	12.5	10.1	2.22	70.52	0.18	77.8
9	45	12.5	10.1	1.92	77.71	0.1	80.8
10	50	12.5	10.1	1.85	82.64	0.09	81.5
11	55	12.5	10.1	1.75	90.56	0.12	82.5
12	60	12.5	10	1.7	100.43	0.14	83

I=1.5A

Sampling number	Time	Current density	Voltage	F ⁻ concentration	Al concentration		Removal efficiency
					Total	Residual	
	min	A/m ²	V	mg/L	mg/L		(%)
	0	18.75	16.1	10			
1	5	18.75	14.9	7.8	18.18	0.06	22
2	10	18.75	14.8	5.9	32.17	0.08	41
3	15	18.75	14.8	4.6	45.46	0.08	54
4	20	18.75	14.8	3.45	61.55	0.07	65.5
5	25	18.75	14.7	2.92	75.19	0.11	70.8
6	30	18.75	14.7	2.25	88.83	0.1	77.5
7	35	18.75	14.7	1.83	102	0.18	81.7
8	40	18.75	14.8	1.62	111.92	0.16	83.8
9	45	18.75	14.8	1.44	123.81	0.17	85.6
10	50	18.75	14.8	1.12	129.4	0.14	88.8
11	55	18.75	14.8	0.91	138.5	0.18	90.9
12	60	18.75	14.8	0.73	146.89	0.14	92.7

I=2A							
Sampling number	Time	Current density	Voltage	F ⁻ concentration	Al concentration		Removal efficiency
					Total	Residual	
	min	A/m ²	V	mg/L	mg/L		(%)
	0	25	21.23	10			
1	5	25	19.8	7.3	21.25	0.06	27
2	10	25	19.8	5.1	35.26	0.08	49
3	15	25	19.7	4.2	48.76	0.08	58
4	20	25	19.7	3.05	63.82	0.08	69.5
5	25	25	19.8	2.45	77.51	0.1	75.5
6	30	25	19.8	1.87	95.48	0.12	81.3
7	35	25	19.8	1.52	122.57	0.17	84.8
8	40	25	19.8	1.02	130.68	0.14	89.8
9	45	25	19.9	0.96	142.95	0.15	90.4
10	50	25	19.9	0.84	155.62	0.15	91.6
11	55	25	19.9	0.72	182.46	0.14	92.8
12	60	25	19.9	0.5	195.56	0.2	95
I=2.5A							
Sampling number	Time	Current density	Voltage	F ⁻ concentration	Al concentration		Removal efficiency
					Total	Residual	
	min	A/m ²	V	mg/L	mg/L		(%)
	0	31.25	27.9	10			
1	5	31.25	25.6	7	23.51	0.08	30
2	10	31.25	25.5	4.8	45.86	0.08	52
3	15	25.5	25.5	3.6	60.59	0.09	64
4	20	25.6	25.5	2.7	71.43	0.11	73
5	25	25.5	25.4	2.2	98.57	0.15	78
6	30	25.4	25.4	1.05	120.41	0.12	89.5
7	35	25.4	25.4	0.95	141.52	0.11	90.5
8	40	25.4	25.4	0.72	160.59	0.1	92.8
9	45	31.25	25.5	0.54	198.88	0.18	94.6
10	50	31.25	25.5	0.44	224.71	0.15	95.6
11	55	31.25	25.5	0.35	246.24	0.2	96.5
12	60	31.25	25.6	0.28	260.67	0.2	97.2

APPENDIX B: Determination of the kinetic constants for the defluoridation by electrocoagulation process at the different operational parameters

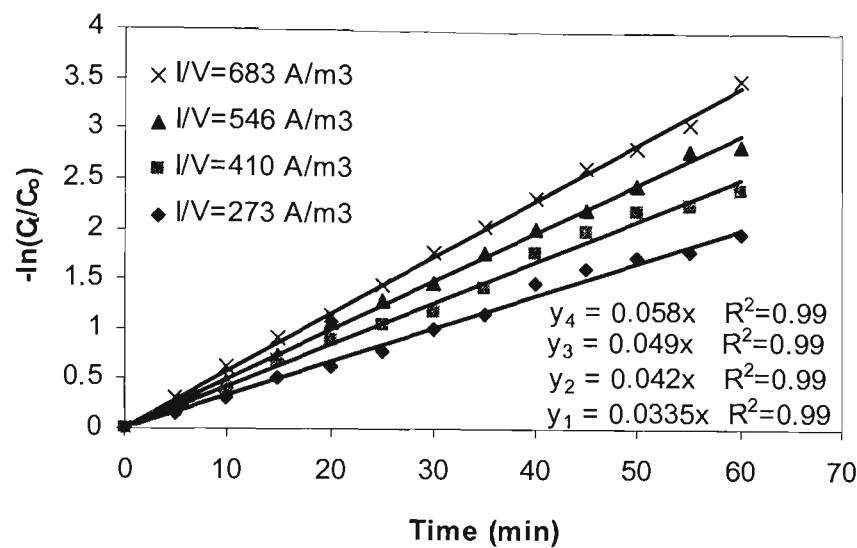


Figure AB-1 Determination of the kinetic constants for the defluoridation by ECF process at different current concentrations ($C_0= 15 \text{ mg/L}$, $d=5\text{mm}$, adjusted $\text{pH}=6\text{-}8$, and $\text{Ca}^{2+}=0 \text{ mg/L}$)

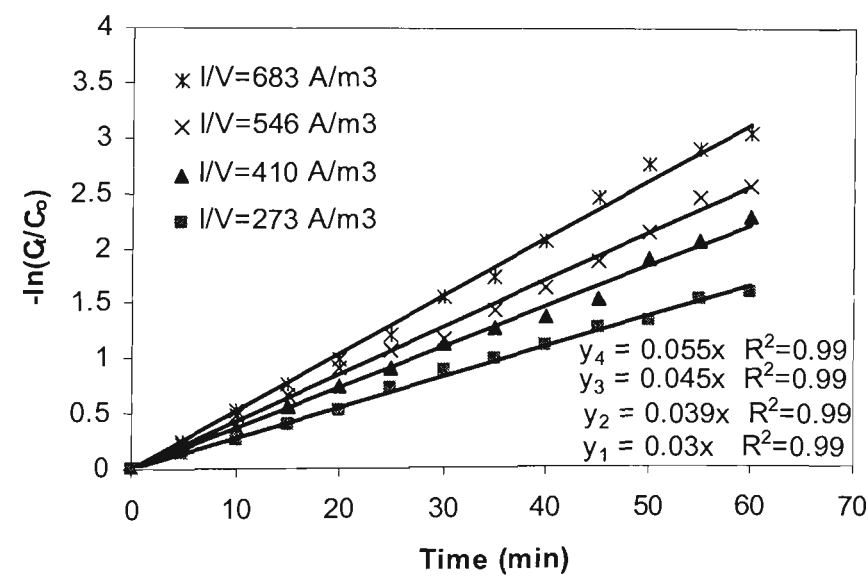


Figure AB-2 Determination of the kinetic constants for the defluoridation by ECF process at different current concentrations ($C_0= 25 \text{ mg/L}$, $d=5\text{mm}$, adjusted $\text{pH}=6\text{-}8$, and $\text{Ca}^{2+}=0 \text{ mg/L}$)

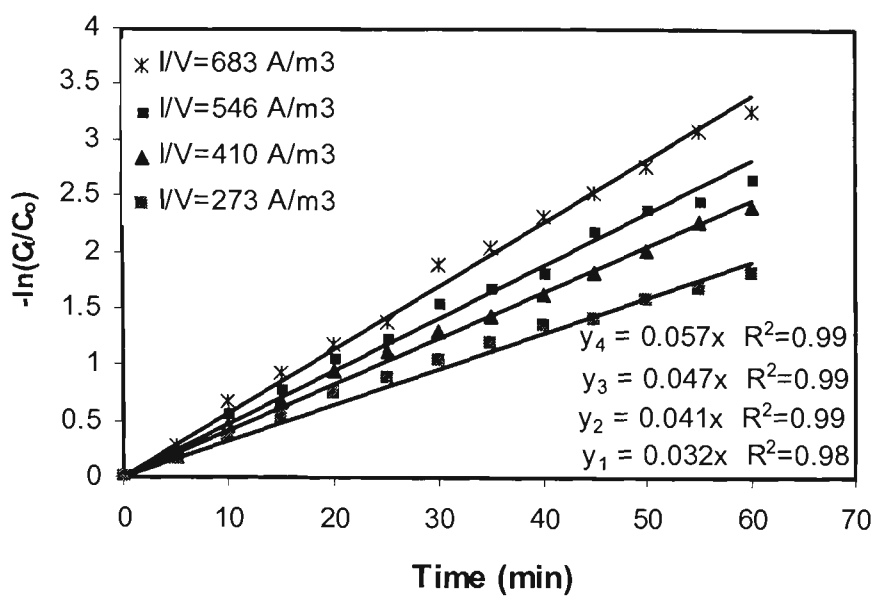


Figure AB-3 Determination of the kinetic constants for the defluoridation by ECF process at different current concentrations ($C_0= 10 \text{ mg/L}$, $d=10 \text{ mm}$, adjusted $\text{pH}=6-8$, and $\text{Ca}^{2+}=0 \text{ mg/L}$)

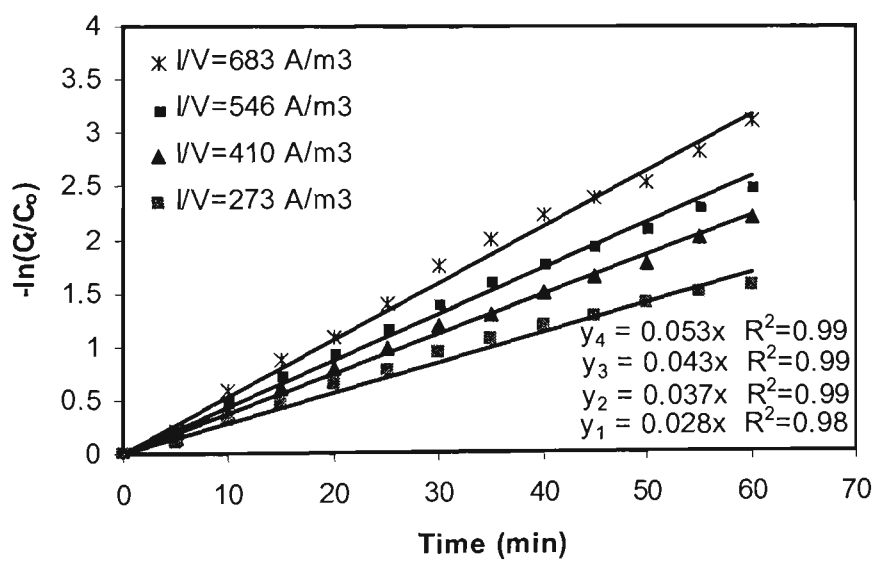


Figure AB-4 Determination of the kinetic constants for the defluoridation by ECF process at different current concentrations ($C_0= 10 \text{ mg/L}$, $d=15\text{mm}$, adjusted $\text{pH}=6-8$, and $\text{Ca}^{2+}=0 \text{ mg/L}$)

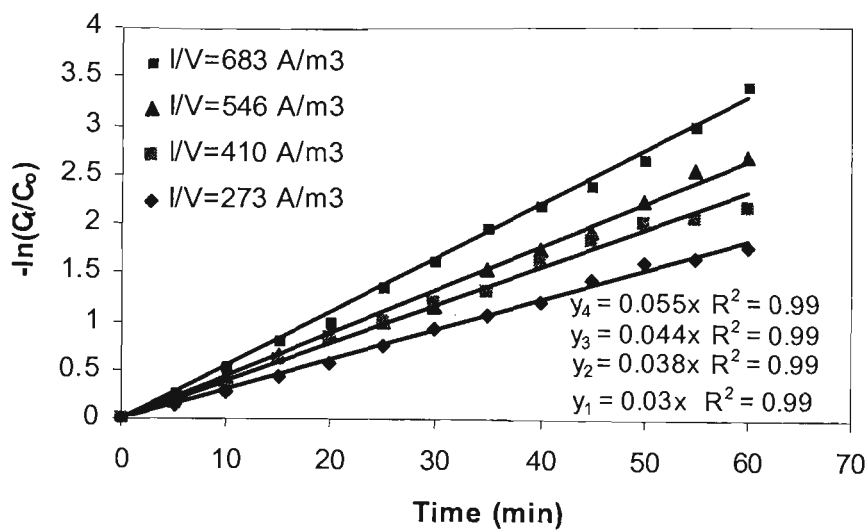


Figure AB-5 Determination of the kinetic constants for the defluoridation by ECF process at different current concentrations ($C_0= 15 \text{ mg/L}$, $d=10 \text{ mm}$, adjusted $\text{pH}=6-8$, and $\text{Ca}^{2+}=0 \text{ mg/L}$)

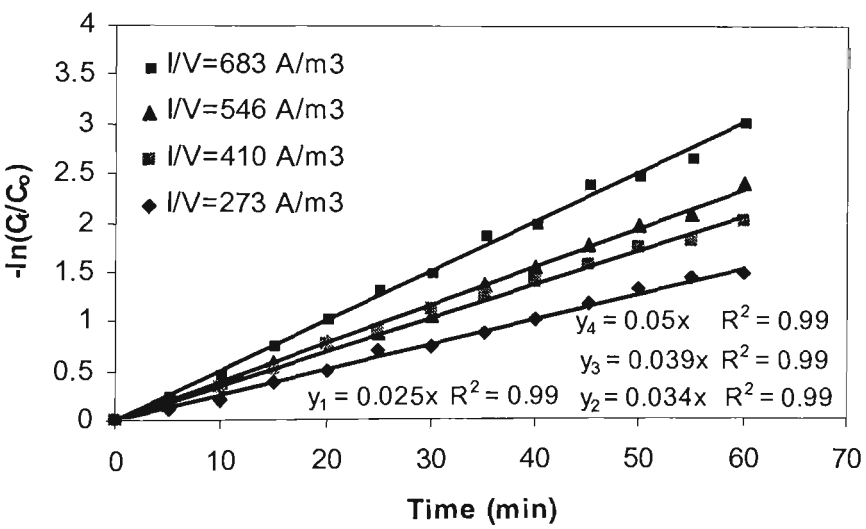


Figure AB-6 Determination of the kinetic constants for the defluoridation by ECF process at different current concentrations ($C_0= 15 \text{ mg/L}$, $d=15 \text{ mm}$, adjusted $\text{pH}=6-8$, and $\text{Ca}^{2+}=0 \text{ mg/L}$)

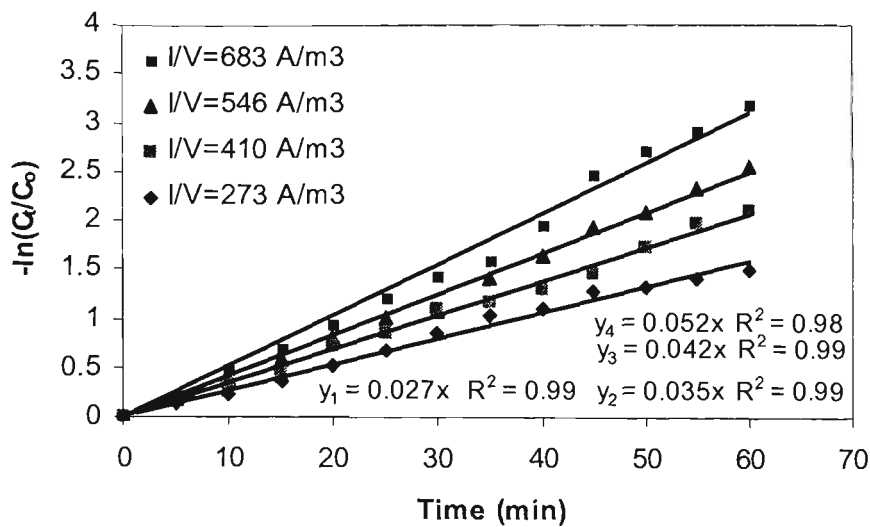


Figure AB-7 Determination of the kinetic constants for the defluoridation by ECF process at different current concentrations ($C_0= 25$ mg/L, $d=10$ mm, adjusted pH=6-8, and $Ca^{2+}=0$ mg/L)

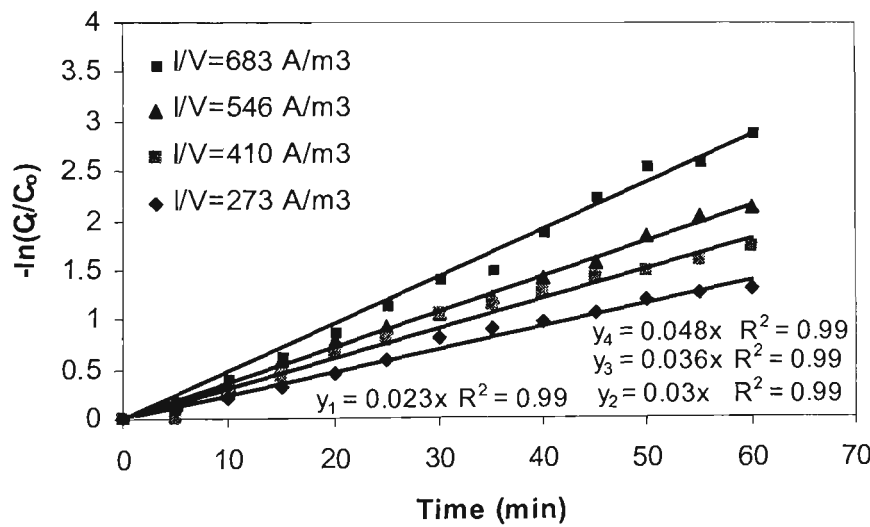


Figure AB-8 Determination of the kinetic constants for the defluoridation by ECF process at different current concentrations ($C_0= 25$ mg/L, $d=15$ mm, adjusted pH=6-8, and $Ca^{2+}=0$ mg/L)

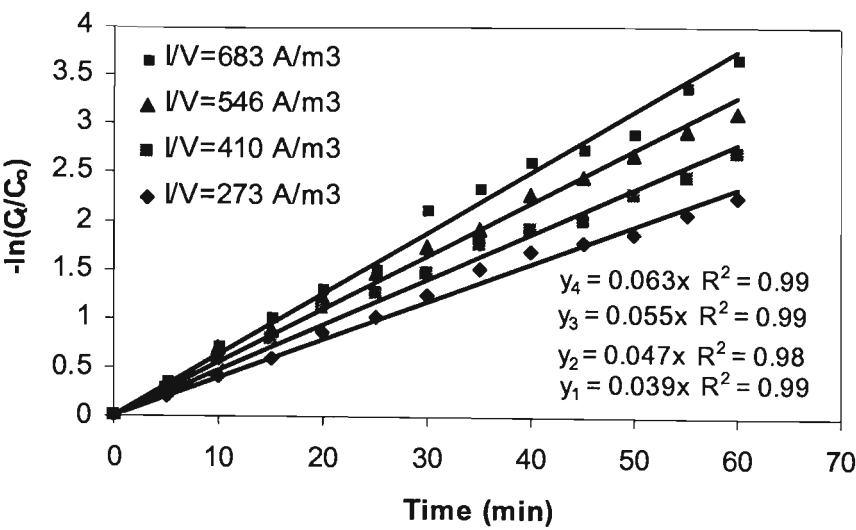


Figure AB-9 Determination of the kinetic constants for the defluoridation by ECF process at different current concentrations ($C_0= 10 \text{ mg/L}$, $d=5 \text{ mm}$, adjusted $\text{pH}=6-8$, and $\text{Ca}^{2+}=50 \text{ mg/L}$)

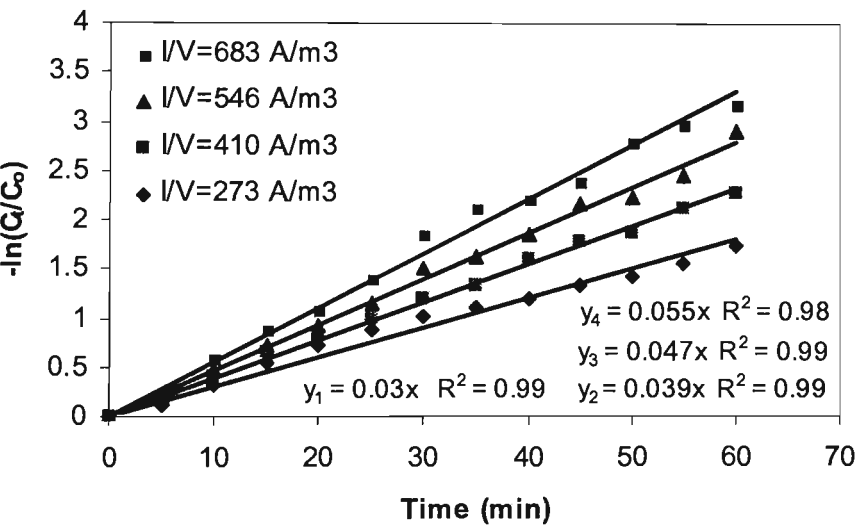


Figure AB-10 Determination of the kinetic constants for the defluoridation by ECF process at different current concentrations ($C_0= 10 \text{ mg/L}$, $d=15 \text{ mm}$, adjusted $\text{pH}=6-8$, and $\text{Ca}^{2+}=50\text{mg/L}$)

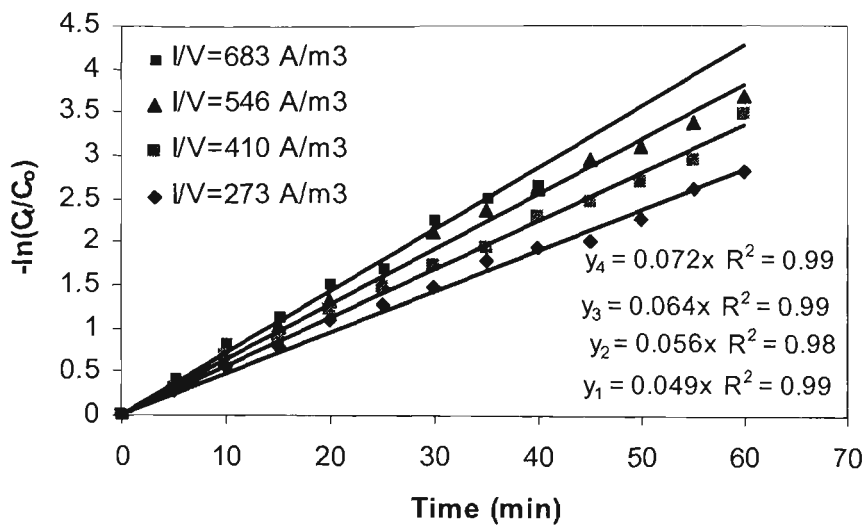


Figure AB-11 Determination of the kinetic constants for the defluoridation by ECF process at different current concentrations ($C_0= 10 \text{ mg/L}$, $d=5 \text{ mm}$, adjusted $\text{pH}=6-8$, and $\text{Ca}^{2+}=150\text{mg/L}$)

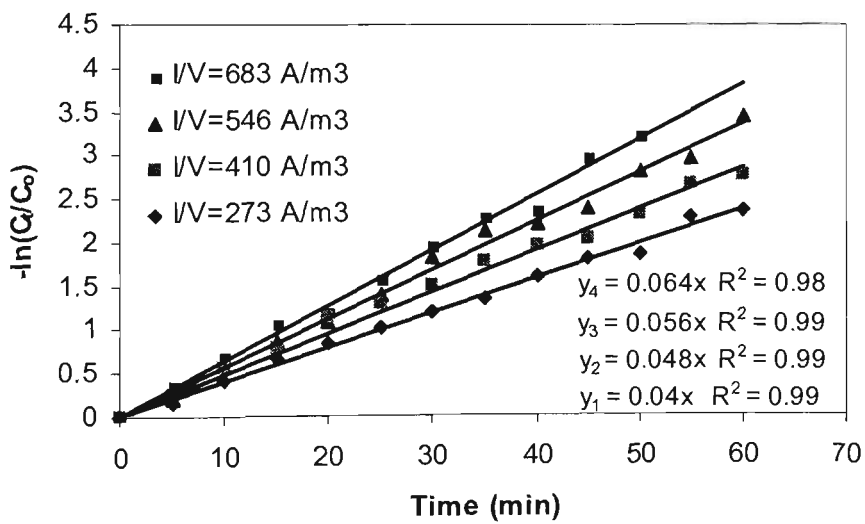


Figure AB-12 Determination of the kinetic constants for the defluoridation by ECF process at different current concentrations ($C_0= 10 \text{ mg/L}$, $d=15 \text{ mm}$, adjusted $\text{pH}=6-8$, and $\text{Ca}^{2+}=150\text{mg/L}$)

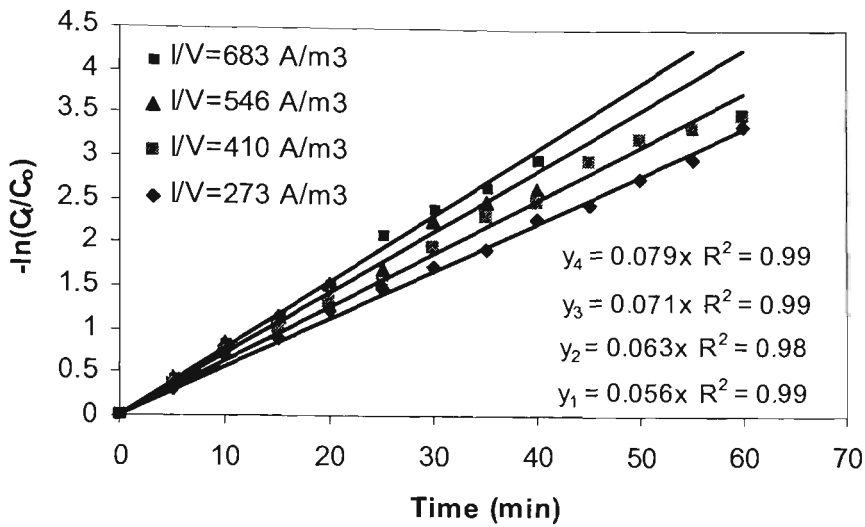


Figure AB-13 Determination of the kinetic constants for the defluoridation by ECF process at different current concentrations ($C_0= 10 \text{ mg/L}$, $d=5 \text{ mm}$, adjusted $\text{pH}=6-8$, and $\text{Ca}^{2+}=250\text{mg/L}$)

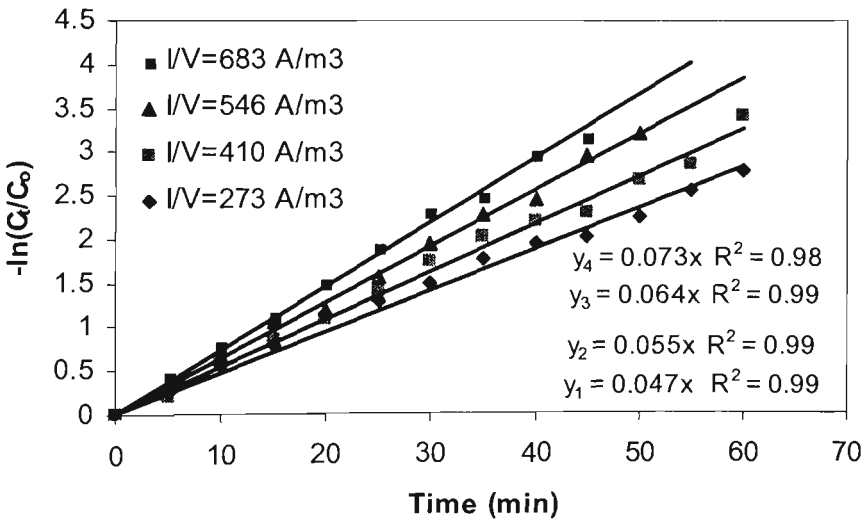


Figure AB-14 Determination of the kinetic constants for the defluoridation by ECF process at different current concentrations ($C_0= 10 \text{ mg/L}$, $d=15 \text{ mm}$, adjusted $\text{pH}=6-8$, and $\text{Ca}^{2+}=250\text{mg/L}$)

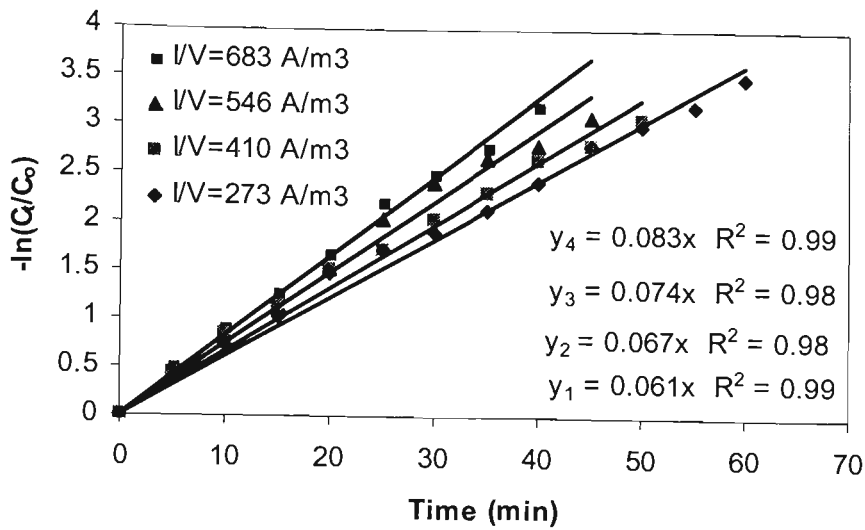


Figure AB-15 Determination of the kinetic constants for the defluoridation by ECF process at different current concentrations ($C_0= 10 \text{ mg/L}$, $d=5 \text{ mm}$, adjusted $\text{pH}=6-8$, and $\text{Ca}^{2+}=300\text{mg/L}$)

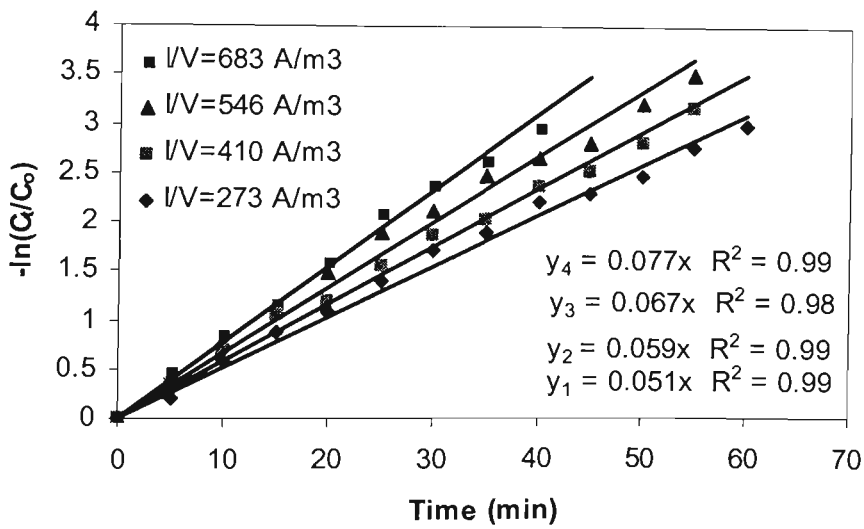


Figure AB-16 Determination of the kinetic constants for the defluoridation by ECF process at different current concentrations ($C_0= 10 \text{ mg/L}$, $d=15 \text{ mm}$, adjusted $\text{pH}=6-8$, and $\text{Ca}^{2+}=300\text{mg/L}$)

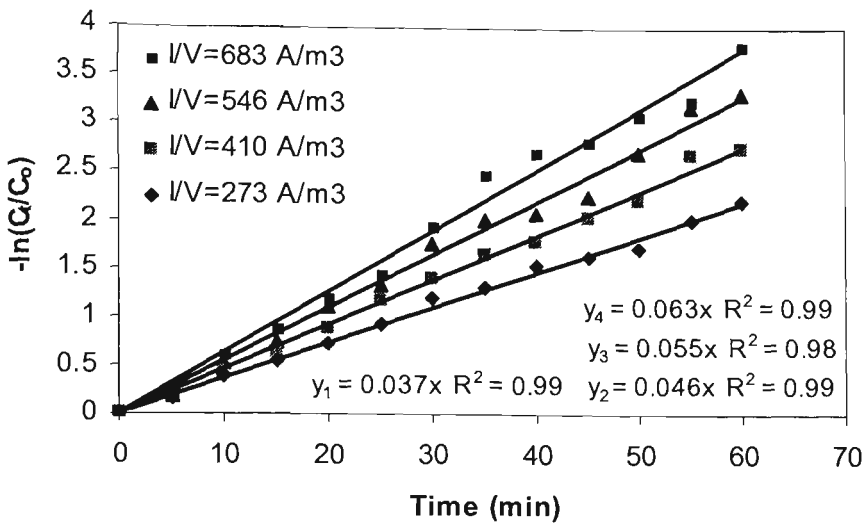


Figure AB-17 Determination of the kinetic constants for the defluoridation by ECF process at different current concentrations ($C_0= 15 \text{ mg/L}$, $d=5 \text{ mm}$, adjusted $\text{pH}=6-8$, and $\text{Ca}^{2+}=50 \text{ mg/L}$)

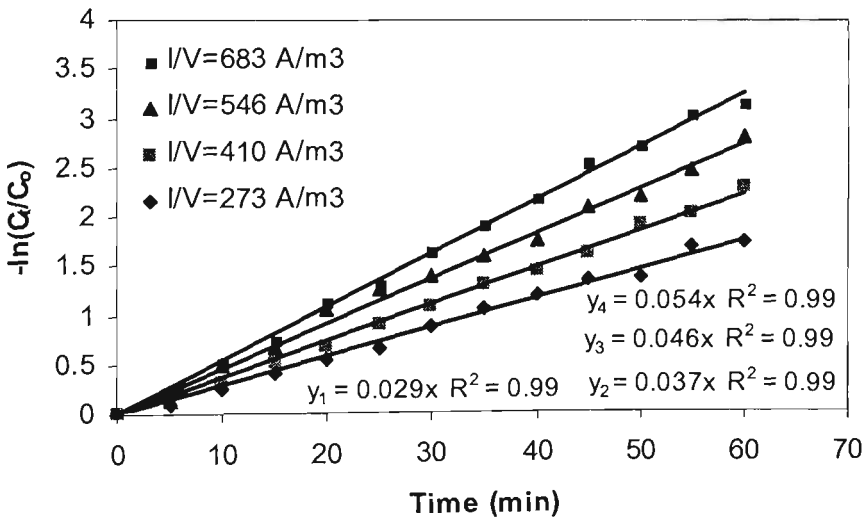


Figure AB-18 Determination of the kinetic constants for the defluoridation by ECF process at different current concentrations ($C_0= 15 \text{ mg/L}$, $d=15 \text{ mm}$, adjusted $\text{pH}=6-8$, and $\text{Ca}^{2+}=50 \text{ mg/L}$)

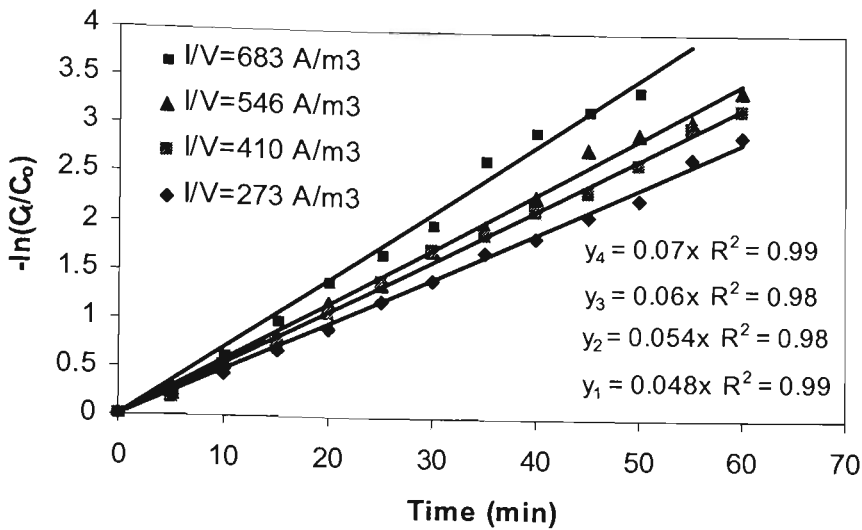


Figure AB-19 Determination of the kinetic constants for the defluoridation by ECF process at different current concentrations ($C_0= 15 \text{ mg/L}$, $d=5 \text{ mm}$, adjusted $\text{pH}=6-8$, and $\text{Ca}^{2+}=150 \text{ mg/L}$)

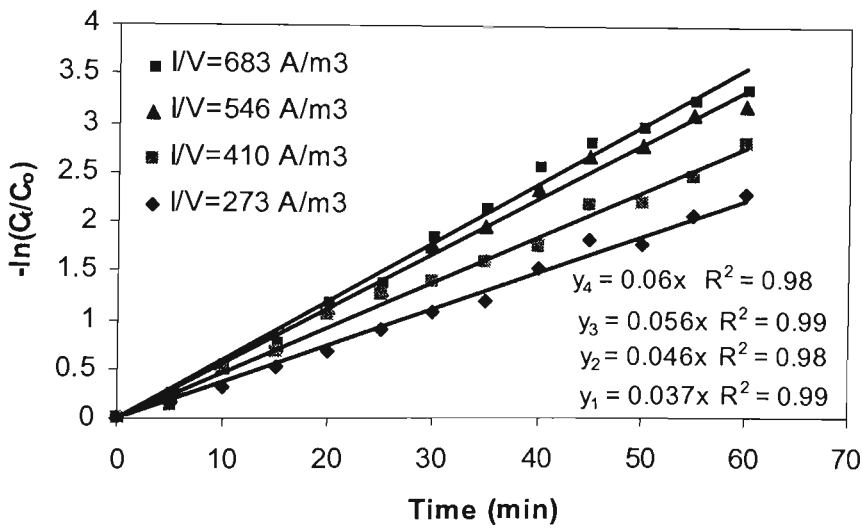


Figure AB-20 Determination of the kinetic constants for the defluoridation by ECF process at different current concentrations ($C_0= 15 \text{ mg/L}$, $d=15 \text{ mm}$, adjusted $\text{pH}=6-8$, and $\text{Ca}^{2+}=150 \text{ mg/L}$)

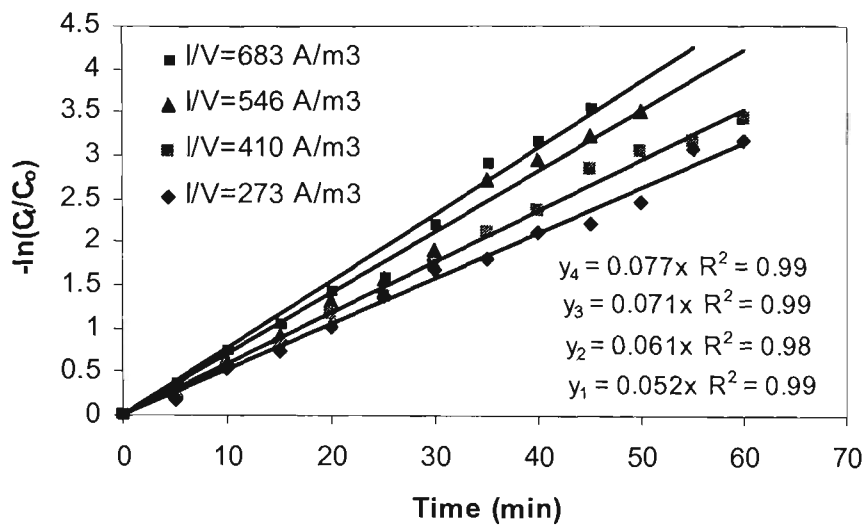


Figure AB-21 Determination of the kinetic constants for the defluoridation by ECF process at different current concentrations ($C_0 = 15 \text{ mg/L}$, $d=5 \text{ mm}$, adjusted $\text{pH}=6-8$, and $\text{Ca}^{2+}=250 \text{ mg/L}$)

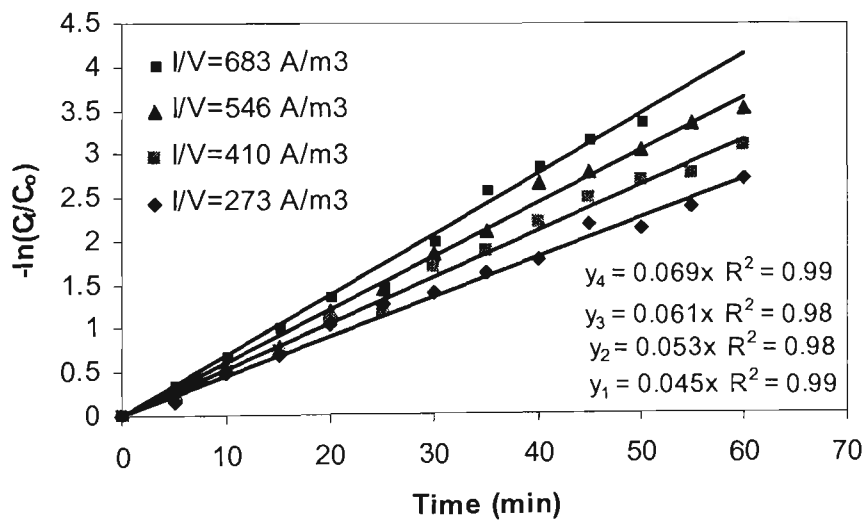


Figure AB-22 Determination of the kinetic constants for the defluoridation by ECF process at different current concentrations ($C_0 = 15 \text{ mg/L}$, $d=15 \text{ mm}$, adjusted $\text{pH}=6-8$, and $\text{Ca}^{2+}=250 \text{ mg/L}$)

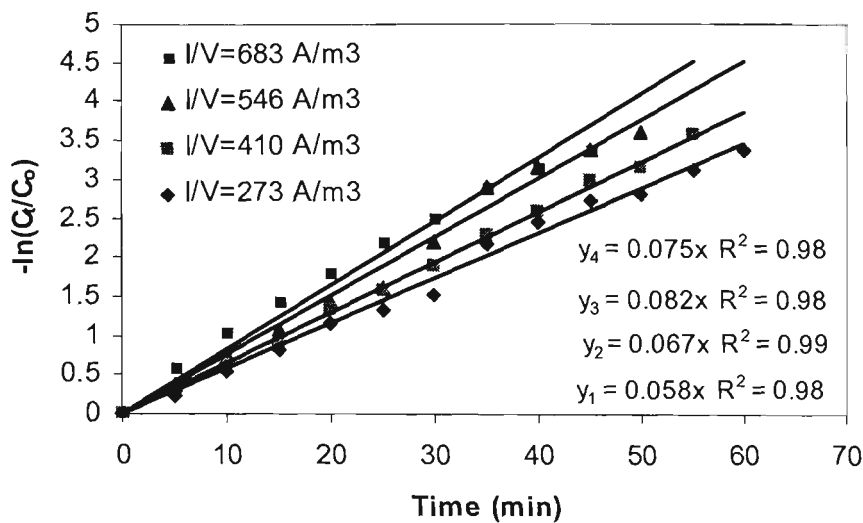


Figure AB-23 Determination of the kinetic constants for the defluoridation by ECF process at different current concentrations ($C_0= 15 \text{ mg/L}$, $d=5 \text{ mm}$, adjusted $\text{pH}=6-8$, and $\text{Ca}^{2+}=300 \text{ mg/L}$)

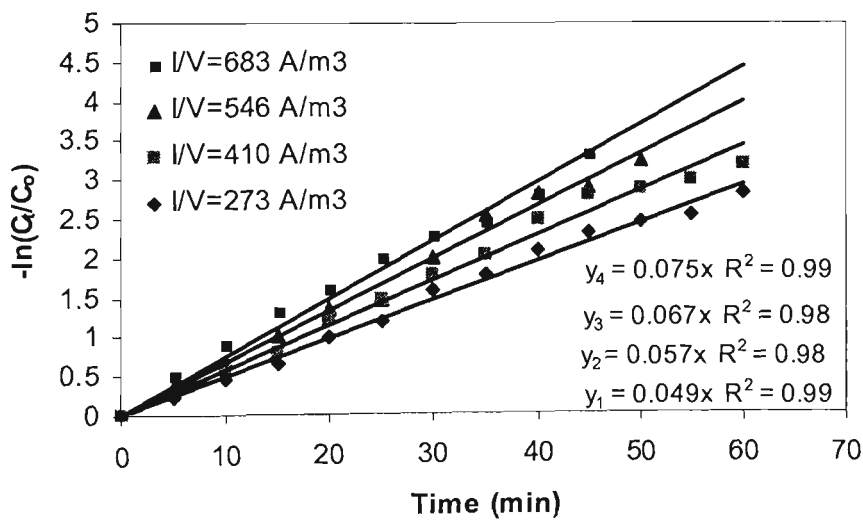


Figure AB-24 Determination of the kinetic constants for the defluoridation by ECF process at different current concentrations ($C_0= 15 \text{ mg/L}$, $d=15 \text{ mm}$, adjusted $\text{pH}=6-8$, and $\text{Ca}^{2+}=300 \text{ mg/L}$)

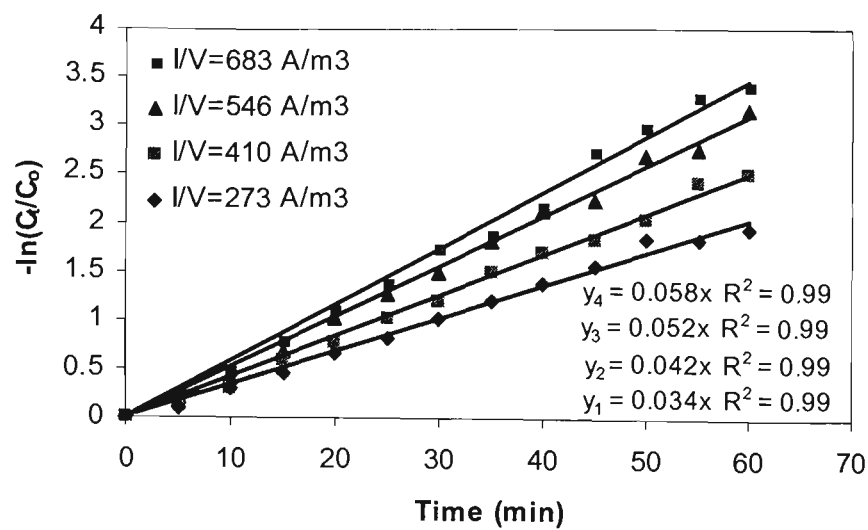


Figure AB-25 Determination of the kinetic constants for the defluoridation by ECF process at different current concentrations ($C_0= 25 \text{ mg/L}$, $d=5 \text{ mm}$, adjusted $\text{pH}=6-8$, and $\text{Ca}^{2+}=50 \text{ mg/L}$)

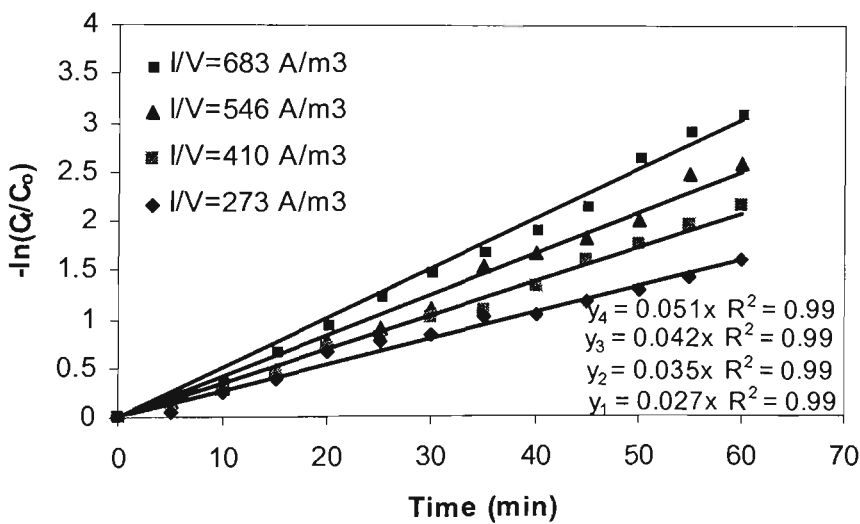


Figure AB-26 Determination of the kinetic constants for the defluoridation by ECF process at different current concentrations ($C_0= 25 \text{ mg/L}$, $d=15 \text{ mm}$, adjusted $\text{pH}=6-8$, and $\text{Ca}^{2+}=50 \text{ mg/L}$)

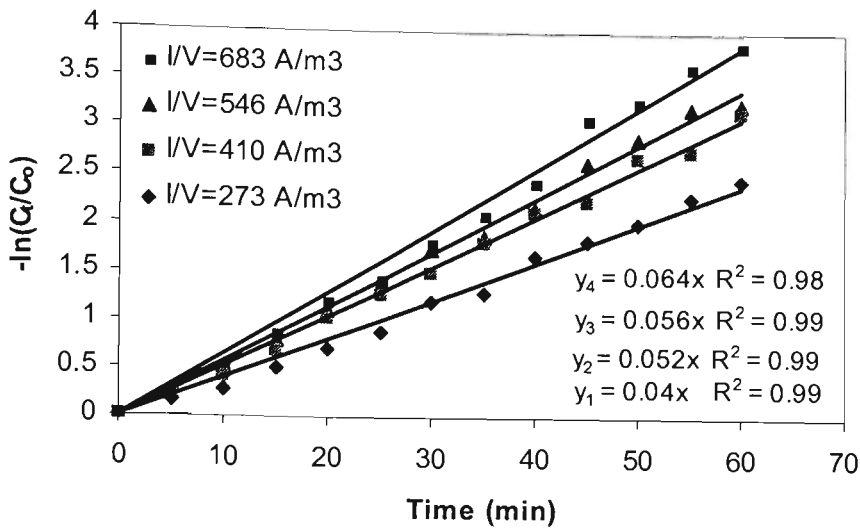


Figure AB-27 Determination of the kinetic constants for the defluoridation by ECF process at different current concentrations ($C_0= 25 \text{ mg/L}$, $d=5 \text{ mm}$, adjusted $\text{pH}=6-8$, and $\text{Ca}^{2+}=150 \text{ mg/L}$)

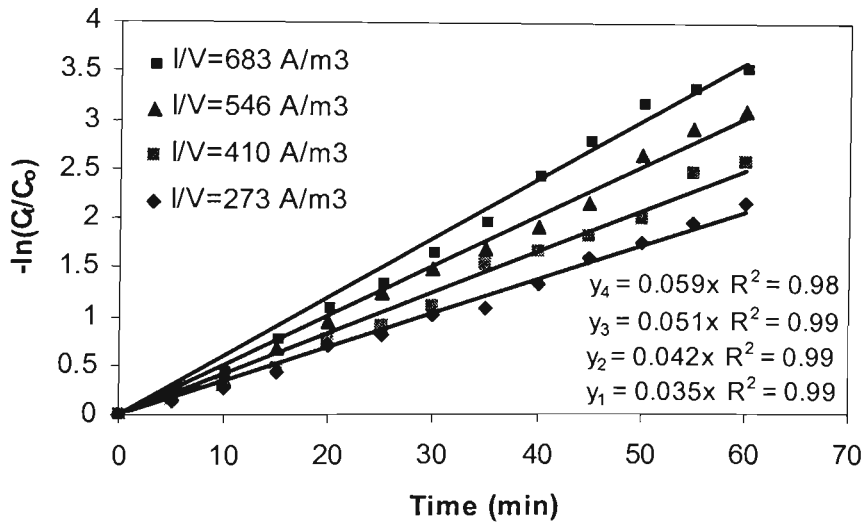


Figure AB-28 Determination of the kinetic constants for the defluoridation by ECF process at different current concentrations ($C_0= 25 \text{ mg/L}$, $d=15 \text{ mm}$, adjusted $\text{pH}=6-8$, and $\text{Ca}^{2+}=150 \text{ mg/L}$)

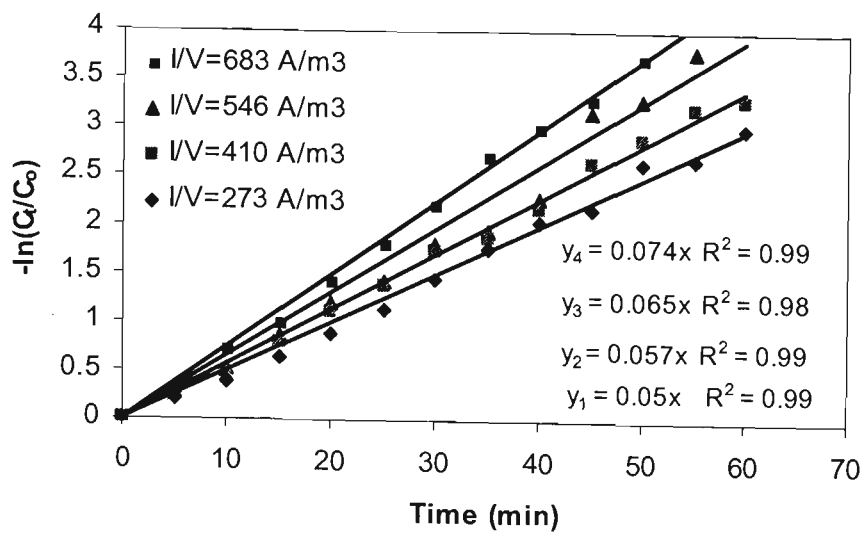


Figure AB-29 Determination of the kinetic constants for the defluoridation by ECF process at different current concentrations ($C_0=25 \text{ mg/L}$, $d=5 \text{ mm}$, adjusted $\text{pH}=6-8$, and $\text{Ca}^{2+}=250 \text{ mg/L}$)

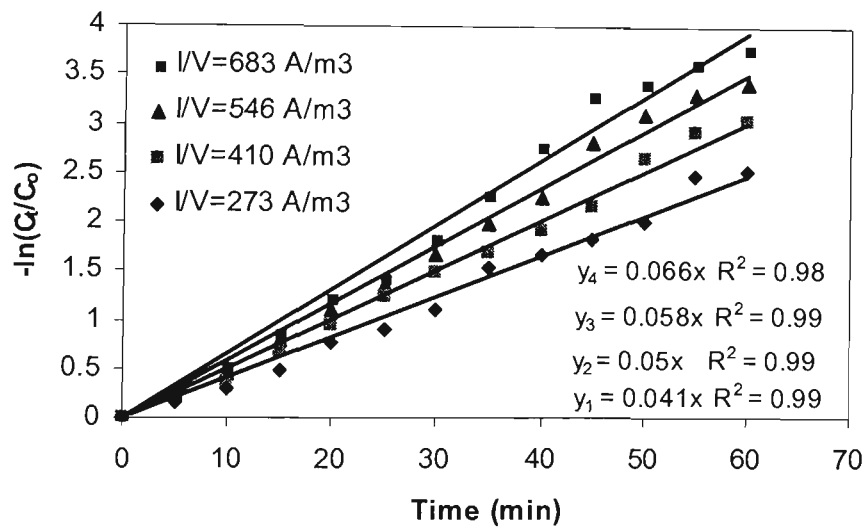


Figure AB-30 Determination of the kinetic constants for the defluoridation by ECF process at different current concentrations ($C_0=25 \text{ mg/L}$, $d=15 \text{ mm}$, adjusted $\text{pH}=6-8$, and $\text{Ca}^{2+}=250 \text{ mg/L}$)

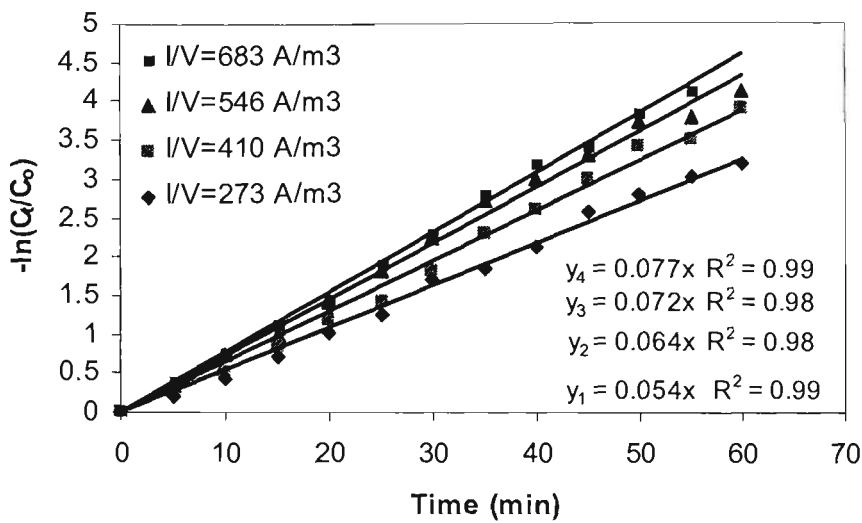


Figure AB-31 Determination of the kinetic constants for the defluoridation by ECF process at different current concentrations ($C_0= 25 \text{ mg/L}$, $d=5 \text{ mm}$, adjusted $\text{pH}=6-8$, and $\text{Ca}^{2+}=300 \text{ mg/L}$)

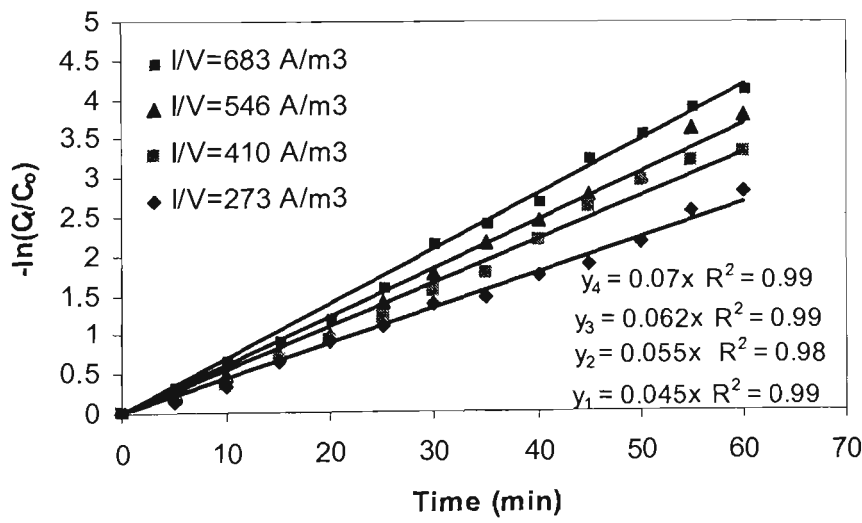


Figure AB-32 Determination of the kinetic constants for the defluoridation by ECF process at different current concentrations ($C_0= 25 \text{ mg/L}$, $d=15 \text{ mm}$, adjusted $\text{pH}=6-8$, and $\text{Ca}^{2+}=300 \text{ mg/L}$)

APPENDIX C: Data for Particle Size Analysis

Tables AC-1 Calculated values of mean diameters of particles in the different initial fluoride concentration and current inputs by EC process

	I=1A, pH=6, C _o =10 mg/L Ca ²⁺ =0 mg/L		I=1A, pH=6, C _o =15 mg/L, Ca ²⁺ =0 mg/L		I=1 A, pH=6, C _o =25 mg/L, Ca ²⁺ =0 mg/L	
	Mean Diam. (μm)	Std Dev	Mean Diam. (μm)	Std Dev	Mean Diam. (μm)	Std Dev
Number, length	1.84	1.49	1.98	1.94	2.06	2.34
Number, surface	2.37	1.58	2.77	2.09	3.11	2.57
Number, volume	3.44	2.18	3.58	2.84	3.45	3.35
Length, surface	3.04	3.59	3.27	4.32	3.71	4.56
Length, volume	4.7	3.95	4.8	4.73	4.9	4.91
Surface, volume	7.27	11.2	7.6	8.48	7.92	6.30
Volume moment	24.47	20.7	16.96	11.1	13.47	6.58

	I=1.5A,pH=6 C _o =10 mg/L Ca ²⁺ =0 mg/L		I=2A, pH=6, C _o =10 mg/L, Ca ²⁺ =0 mg/L		I=2.5 A, pH=6, C _o =10 mg/L, Ca ²⁺ =0 mg/L	
	Mean Diam. (μm)	Std Dev	Mean Diam. (μm)	Std Dev	Mean Diam. (μm)	Std Dev
Number, length	1.39	1.29	2.15	2.1	2.56	2.39
Number, surface	2.16	1.98	3.28	3.11	4.26	3.22
Number, volume	4.38	3.58	6.16	5.56	8.34	7.32
Length, surface	3.36	3.98	5.46	5.11	9.06	12.5
Length, volume	7.77	6.88	9.04	8.47	10.58	13.1
Surface, volume	14.58	16.2	20.45	22.1	24.8	22.1
Volume moment	45.33	25.6	42.18	29.5	41.26	34.3

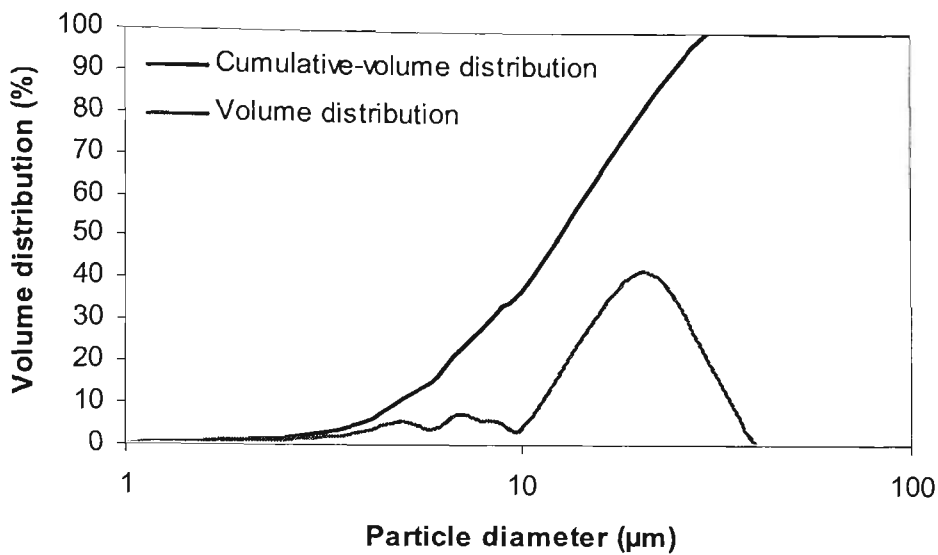


Figure AC-1 The volume distribution particle sizes in different current values, initial fluoride concentrations, and initial Ca^{2+} concentrations by EC process ($I=1\text{ A}$, $\text{pH}=6$, $C_0=10\text{ mg/L}$)

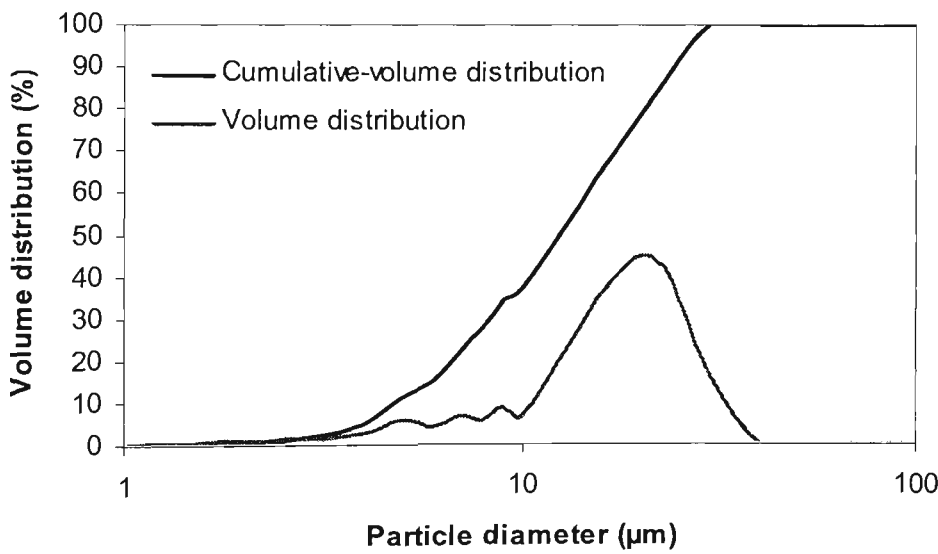


Figure AC-2 The volume distribution particle sizes in different current values, initial fluoride concentrations, and initial Ca^{2+} concentrations by EC process ($I=1\text{ A}$, $\text{pH}=6$, $C_0=15\text{ mg/L}$)

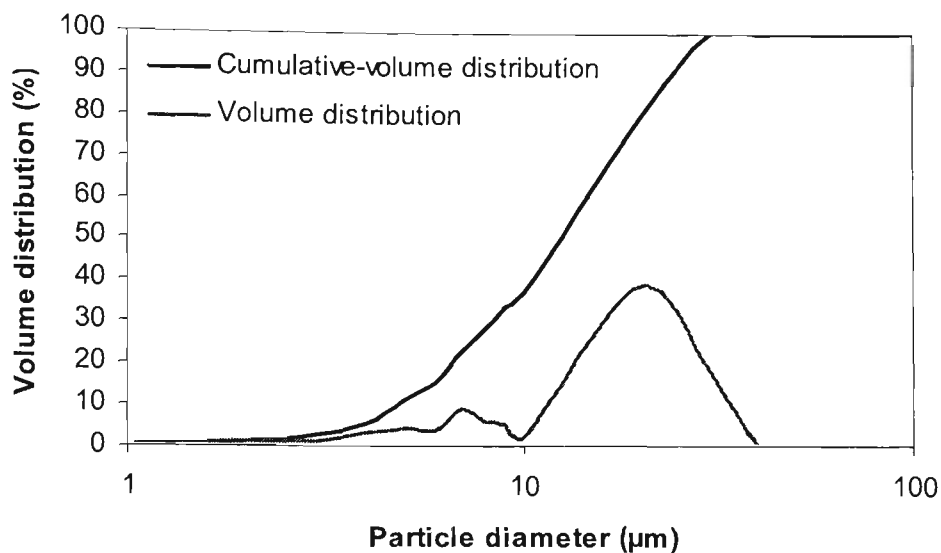


Figure AC-3 The volume distribution particle sizes in different current values, initial fluoride concentrations, and initial Ca^{2+} concentrations by EC process ($I=1\text{A}$, $\text{pH}=6$, $C_0=25\text{ mg/L}$)

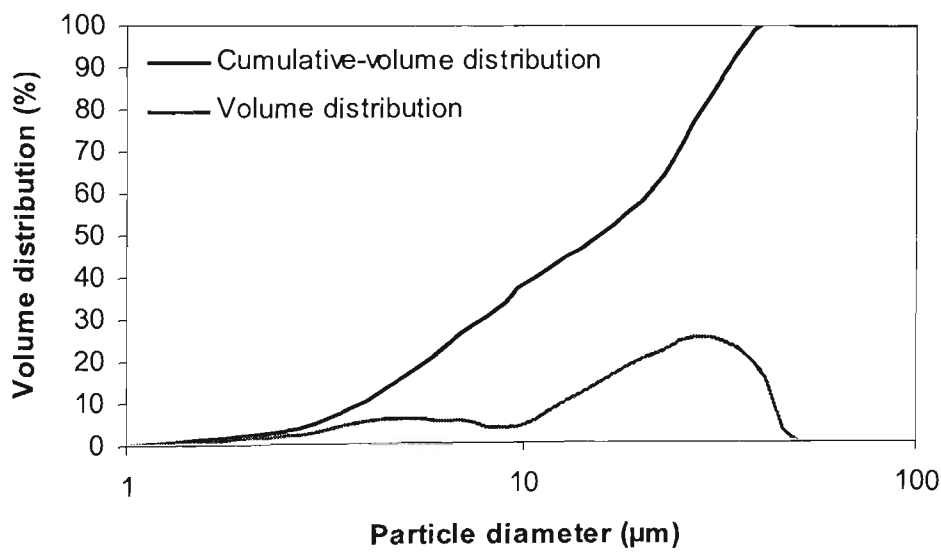


Figure AC-4 The volume distribution particle sizes in different current values, initial fluoride concentrations, and initial Ca^{2+} concentrations by EC process ($I=2.5\text{A}$, $\text{pH}=6$, $C_0=10\text{ mg/L}$)

APPENDIX D: Summary of results for the defluoridation by continuous flow EC reactor

Table AD-1: Summary of results for the defluoridation by continuous flow EC reactor at different operational parameters

Initial F ⁻ concentration (mg/L)	Flow rate (L/min)	Current density (A/m ²)	Charge Density (C/m ²)	Final fluoride concentration (mg/L)			Residence time (min)			Residual Al concentration (mg/L)
				EC reactor	EC system	EC reactor	Sedimentation tank	EC system		
10	0.15	12.5	39750	1.42	1.09	53	330	383	0.1	
10	0.2	12.5	30000	2.32	1.98	40	248	287	0.15	
10	0.25	12.5	24000	3.20	2.82	32	198	230	0.13	
10	0.3	12.5	19500	3.87	3.49	26	165	191	0.06	
10	0.35	12.5	17250	4.43	3.87	23	141	164	0.12	
10	0.4	12.5	15000	4.91	4.54	20	124	144	0.01	
10	0.15	18.75	59625	0.98	0.72	53	330	383	0.01	
10	0.2	18.75	45000	1.76	1.39	40	248	287	0.05	
10	0.25	18.75	36000	2.49	1.93	32	198	230	0.01	
10	0.3	18.75	29250	3.14	2.68	26	165	191	0.18	
10	0.35	18.75	25875	3.70	3.23	23	141	164	0.12	
10	0.4	18.75	22500	4.19	3.58	20	124	144	0.13	
10	0.15	25	79500	0.65	0.42	53	330	383	0.20	
10	0.2	25	60000	1.33	0.93	40	248	287	0.01	
10	0.25	25	48000	1.87	1.50	32	198	230	0.01	
10	0.3	25	39000	2.61	2.06	26	165	191	0.01	
10	0.35	25	34500	3.16	2.58	23	141	164	0.03	
10	0.4	25	30000	3.51	3.06	20	124	144	0.05	
10	0.15	31.25	99375	0.38	0.25	53	330	383	0.20	
10	0.2	31.25	75000	0.86	0.63	40	248	287	0.04	
10	0.25	31.25	60000	1.36	1.09	32	198	230	0.001	

10	0.3	31.25	48750	2.00	1.58	26	165	191	0.05
10	0.35	31.25	43125	2.52	2.06	23	141	164	0.09
10	0.4	31.25	37500	3.00	2.51	20	124	144	0.01
10	0.15	37.5	119250	0.26	0.16	53	330	383	0.06
10	0.2	37.5	90000	0.65	0.46	40	248	287	0.01
10	0.25	37.5	72000	1.13	0.82	32	198	230	0.03
10	0.3	37.5	58500	1.62	1.25	26	165	191	0.01
10	0.35	37.5	51750	2.10	1.68	23	141	164	0.01
10	0.4	37.5	45000	2.56	2.23	20	124	144	0.02
10	0.15	50	159000	0.10	0.05	53	330	383	0.32
10	0.2	50	120000	0.32	0.19	40	248	287	0.09
10	0.25	50	96000	0.62	0.42	32	198	230	0.01
10	0.3	50	78000	0.98	0.72	26	165	191	0.08
10	0.35	50	69000	1.37	1.04	23	141	164	0.06
10	0.4	50	60000	1.86	1.39	20	124	144	0.03
15	0.15	12.5	39750	2.37	1.6	53	330	383	0.05
15	0.2	12.5	30000	3.48	3.0	40	248	287	0.08
15	0.25	12.5	24000	4.81	4.2	32	198	230	0.11
15	0.3	12.5	19500	5.81	5.2	26	165	191	0.06
15	0.35	12.5	17250	6.65	5.8	23	141	164	0.01
15	0.4	12.5	15000	7.36	6.8	20	124	144	0.08
15	0.15	18.75	59625	1.48	1.0	53	330	383	0.18
15	0.2	18.75	45000	2.74	1.9	40	248	287	0.12
15	0.25	18.75	36000	3.73	2.9	32	198	230	0.13
15	0.3	18.75	29250	4.71	4.0	26	165	191	0.18
15	0.35	18.75	25875	5.55	4.8	23	141	164	0.05
15	0.4	18.75	22500	6.29	5.4	20	124	144	0.13
15	0.15	25	79500	0.74	0.5	53	330	383	0.21
15	0.2	25	60000	1.52	1.2	40	248	287	0.04
15	0.25	25	48000	2.47	1.9	32	198	230	0.16

15	0.3	25	39000	3.43	2.8	26	165	191	0.09
15	0.35	25	34500	4.23	3.5	23	141	164	0.18
15	0.4	25	30000	4.96	4.2	20	124	144	0.04
15	0.15	31.25	99375	0.49	0.3	53	330	383	0.32
15	0.2	31.25	75000	1.24	0.7	40	248	287	0.11
15	0.25	31.25	60000	1.92	1.4	32	198	230	0.018
15	0.3	31.25	48750	2.85	2.1	26	165	191	0.05
15	0.35	31.25	43125	3.53	2.8	23	141	164	0.20
15	0.4	31.25	37500	4.23	3.4	20	124	144	0.018
15	0.15	37.5	119250	0.32	0.2	53	330	383	0.3
15	0.2	37.5	90000	0.87	0.6	40	248	287	0.08
15	0.25	37.5	72000	1.54	1.2	32	198	230	0.06
15	0.3	37.5	58500	2.25	1.8	26	165	191	0.06
15	0.35	37.5	51750	2.95	2.5	23	141	164	0.12
15	0.4	37.5	45000	3.62	3.1	20	124	144	0.16
15	0.15	50	159000	0.14	0.1	53	330	383	0.34
15	0.2	50	120000	0.48	0.2	40	248	287	0.45
15	0.25	50	96000	0.93	0.5	32	198	230	0.47
15	0.3	50	78000	1.48	0.8	26	165	191	0.16
15	0.35	50	69000	2.06	1.6	23	141	164	0.18
15	0.4	50	60000	2.80	2.1	20	124	144	0.12
25	0.15	12.5	39750	5.1	4.2	53	330	383	0.25
25	0.2	12.5	30000	7.6	6.5	40	248	287	0.16
25	0.25	12.5	24000	9.7	8.8	32	198	230	0.08
25	0.3	12.5	19500	11.3	10.5	26	165	191	0.03
25	0.35	12.5	17250	12.7	11.9	23	141	164	0.12
25	0.4	12.5	15000	13.8	13.0	20	124	144	0.08
25	0.15	18.75	59625	3.6	3.0	53	330	383	0.14
25	0.2	18.75	45000	5.6	4.8	40	248	287	0.03
25	0.25	18.75	36000	7.8	7.1	32	198	230	0.11

25	0.3	18.75	29250	9.4	8.3	26	165	191	0.03
25	0.35	18.75	25875	11.1	10.1	23	141	164	0.13
25	0.4	18.75	22500	12.3	11.3	20	124	144	0.18
25	0.15	25	79500	2.5	2.1	53	330	383	0.22
25	0.2	25	60000	4.2	3.9	40	248	287	0.18
25	0.25	25	48000	6.2	5.7	32	198	230	0.11
25	0.3	25	39000	7.6	7.1	26	165	191	0.13
25	0.35	25	34500	9.5	8.8	23	141	164	0.13
25	0.4	25	30000	10.7	10.1	20	124	144	0.18
25	0.15	31.25	99375	1.8	1.5	53	330	383	0.15
25	0.2	31.25	75000	3.3	3.0	40	248	287	0.09
25	0.25	31.25	60000	5.1	4.7	32	198	230	0.02
25	0.3	31.25	48750	6.5	5.9	26	165	191	0.20
25	0.35	31.25	43125	8.3	7.7	23	141	164	0.15
25	0.4	31.25	37500	9.5	8.9	20	124	144	0.11
25	0.15	37.5	119250	1.2	1.1	53	330	383	0.13
25	0.2	37.5	90000	2.5	2.2	40	248	287	0.18
25	0.25	37.5	72000	4.0	3.7	32	198	230	0.16
25	0.3	37.5	58500	5.6	5.1	26	165	191	0.14
25	0.35	37.5	51750	7.1	6.6	23	141	164	0.11
25	0.4	37.5	45000	8.3	7.8	20	124	144	0.13
25	0.15	50	159000	0.6	0.5	53	330	383	0.20
25	0.2	50	120000	1.6	1.4	40	248	287	0.18
25	0.25	50	96000	2.7	2.5	32	198	230	0.11
25	0.3	50	78000	4.0	3.7	26	165	191	0.16
25	0.35	50	69000	5.1	4.8	23	141	164	0.12
25	0.4	50	60000	6.3	5.9	20	124	144	0.16

Appendix E: Total operational cost estimation for the pilot -scale continuous flow EC reactor

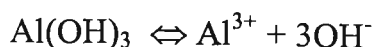
Estimated cost for the pilot -scale continuous flow EC reactor at the different initial fluoride concentrations and charge density ($pH_{i,m}=6$, $Ec=50$ mS/m, $d=5$ mm)

C_o	Q	t_d	I	i	i.t/A	U	SEEC	Energy cost	Al plate consumption cost	pH adjustment cost	Sludge treatment cost	Total operational cost ¹
mg/L	mL/min	min	A	A/m ²	C/m ²	V	kWh/m ³	AUD/m ³	AUD/m ³	AUD/m ³	AUD/m ³	AUD/m ³
5	200	40	2	12.5	30000	4.27	0.721	0.061	0.19	0.03	0.08	0.36
5	250	32	3	18.75	36000	5.49	1.112	0.095	0.23	0.03	0.08	0.43
5	300	26	4	25	39000	7.06	1.549	0.132	0.25	0.03	0.08	0.49
5	350	23	5	31.25	43125	8.64	2.096	0.178	0.27	0.03	0.08	0.56
5	400	20	6	37.5	45000	10.22	2.587	0.220	0.29	0.03	0.08	0.62
10	150	53	3	18.75	59625	5.49	1.842	0.157	0.38	0.03	0.08	0.64
10	200	40	4	25	60000	7.06	2.383	0.203	0.38	0.03	0.08	0.69
10	250	32	6	37.5	72000	10.22	4.140	0.352	0.46	0.03	0.08	0.92
10	350	23	8	50	69000	13.53	5.252	0.446	0.44	0.03	0.08	0.99
15	150	53	4	25	79500	6.8	3.041	0.259	0.50	0.03	0.08	0.87
15	200	40	6	37.5	90000	10.1	5.114	0.435	0.57	0.03	0.08	1.12
15	250	32	8	50	96000	13.2	7.129	0.606	0.61	0.03	0.08	1.33
25	150	53	6	37.5	119250	10.2	6.843	0.582	0.76	0.03	0.08	1.45

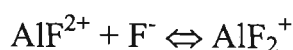
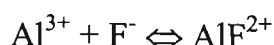
¹ Assuming a depreciation period of 10 years and an interest rate of 5%, the aluminium plate costs AUD 2.8/Kg, and electricity cost is AUD 0.085/kWh, the pH adjustment cost is AUD 60/L HCl 1M (50 mL HCl 0.01 M/1m³ is used for each run), the sludge treatment cost was found to be US \$ 0.06 (adapted from Lin et al., 2005) when 1 USD=1.327 AUD

APPENDIX F: How pH and F⁻ concentration will influence the solubility of aluminium hydroxide (MINEQL⁺ model)

The solubility of aluminium hydroxide is often used as the control of Al³⁺ concentrations in soil water.



F⁻ forms very stable complexes with Al³⁺,

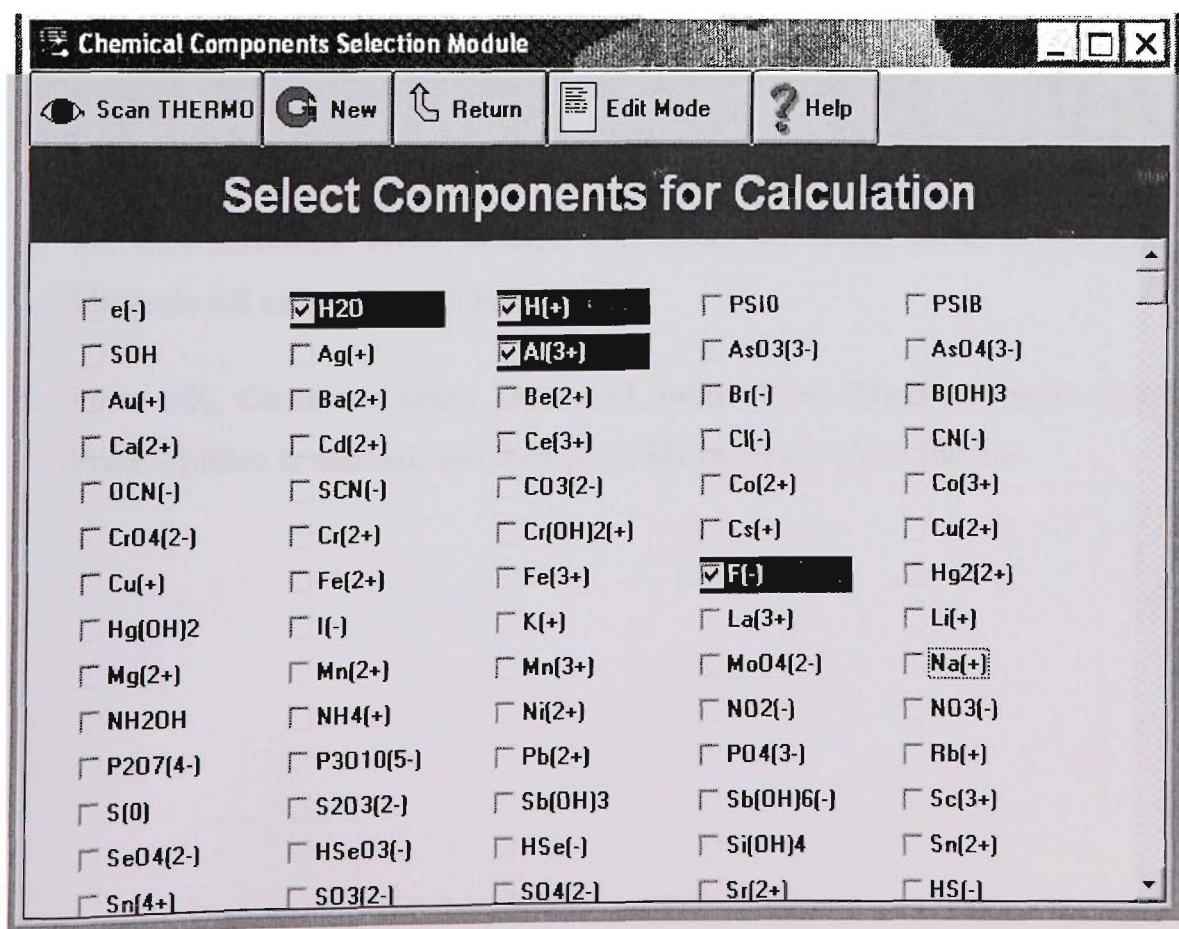


etc...

We can use MINEQL⁺ to show how different concentrations of F⁻ will influence the solubility of gibbsite [Al(OH)₃] at various pH values.

Procedure:

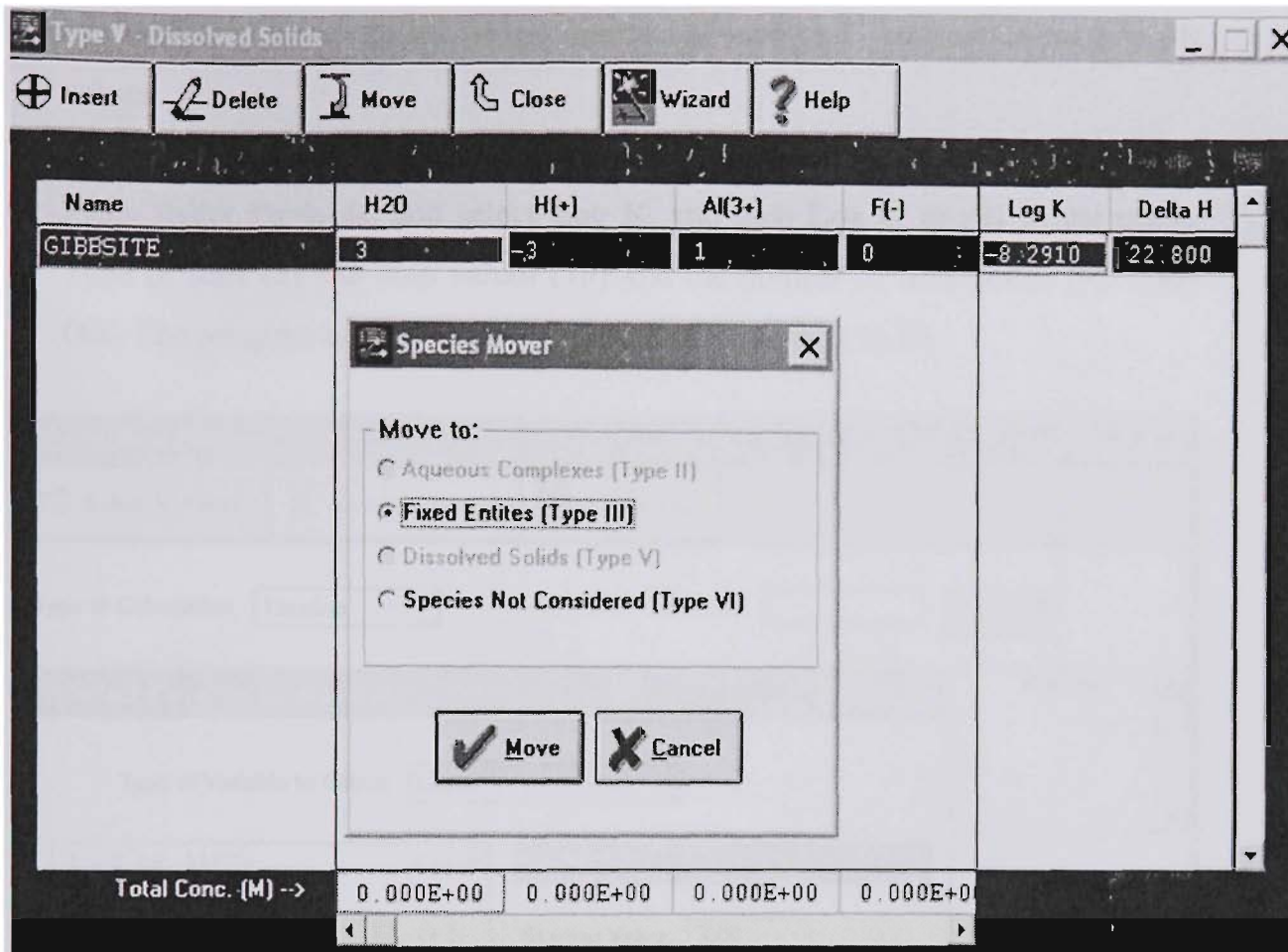
1. Start MINEQL+
2. Select the following elements: (H₂O, H⁺), Al³⁺, F⁻



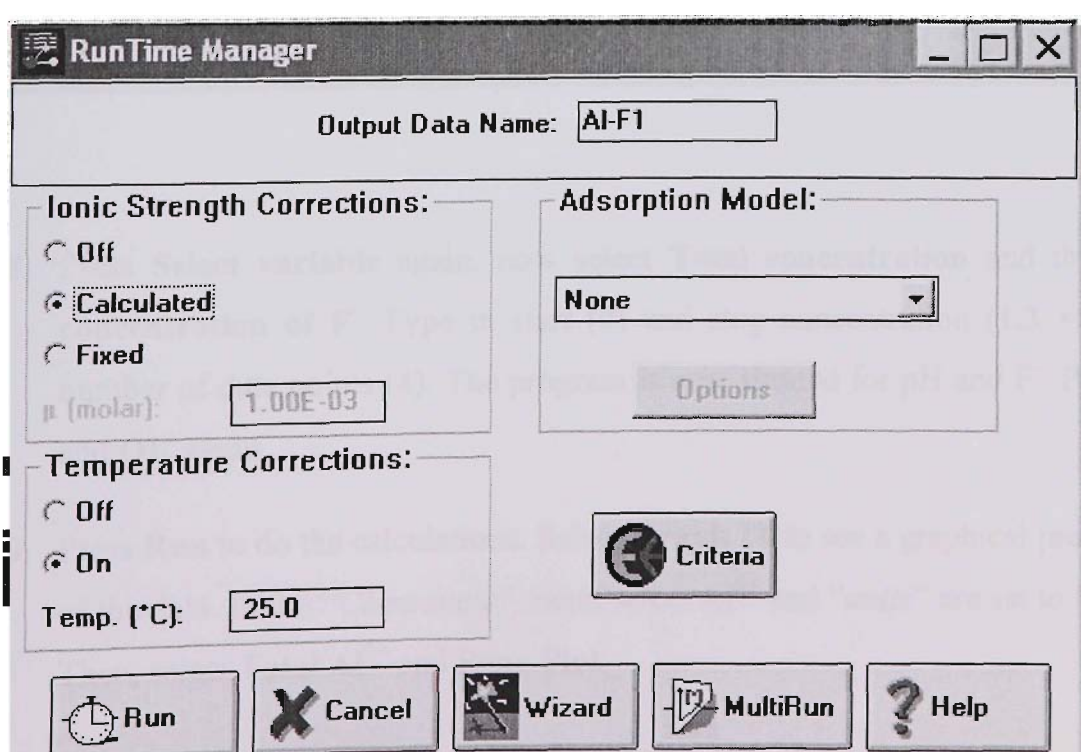
3. Press **Scan thermo**

Type II - Aqueous Species						
<div> <div>+</div> Insert <div></div> Delete <div></div> Move <div></div> Close <div></div> Wizard <div></div> Help </div>						
Name	H ₂ O	H(+)	Al(3+)	F(-)	Log K	Delta H
OH- (-1)	1	-1	0	0	-13.997	13.339
Al(OH)2+ (+1)	2	-2	1	0	-10.094	0.0000
Al(OH)3 (aq)	3	-3	1	0	-16.791	0.0000
Al(OH)4- (-1)	4	-4	1	0	-22.688	41.405
AlOH+2 (+2)	1	-1	1	0	-4.9970	11.427
H2F2 (aq)	0	2	0	2	6.7680	0.0000
HF2- (-1)	0	1	0	2	3.7500	4.1590
HF (aq)	0	1	0	1	3.1700	3.1790
AlF2+ (+1)	0	0	1	2	12.600	1.9840
AlF3 (aq)	0	0	1	3	16.700	2.0790
AlF+2 (+2)	0	0	1	1	7.0000	1.0990
AlF4- (-1)	0	0	1	4	19.400	2.0790
Total Conc. (M) -->						
	0.000E+00	0.000E+00	0.000E+00	0.000E+00		

4. We now have got up a list of all the species that can be formed and the K values for their reactions. Press **Wizard** and select the folder **Solid mover** and set Minerals **All off**, except Gibbsite
5. Press **OK**, **Close** and select **Dissolved Solids**. Press **Move** and make sure that Fixed Entities is marked, and then press **Move**. Press Close and **No**

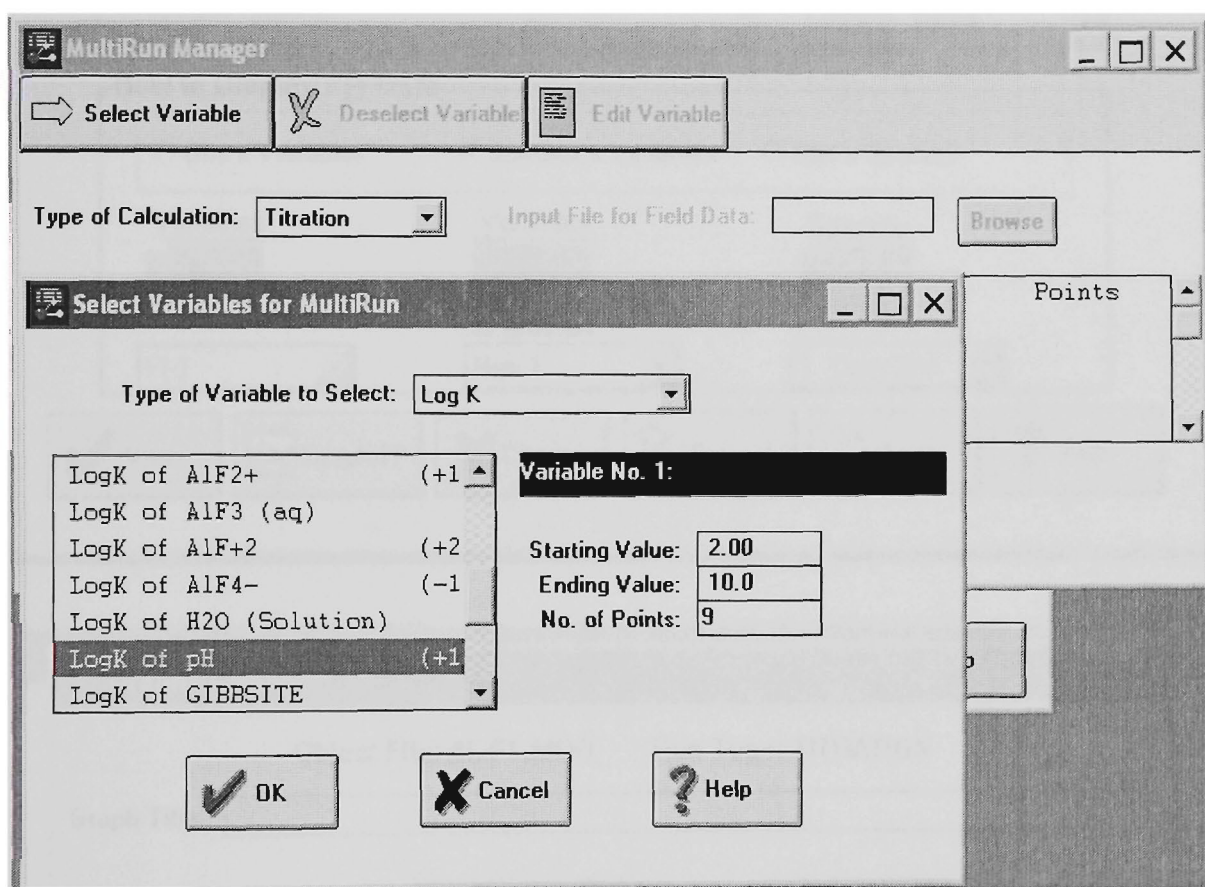


6. Type the filename for the "Output Data Name" (e.g. Al-F1)



7. We will now do a number of calculations at various F^- concentrations and pH values.

Press **Multi run**. In the "type of calculations" menu select "**2-way analysis**". Press *Select Variable*, and select **Log K**, and then **Log K of pH** in the menu. Type in start (**2**) and stop values (**10**) and the number of data points (**9**). Press **OK**. The program is now titrated the solution from pH 2 to 10.



8. Press **Select variable** again, now select **Total concentration** and then **Total concentration of F^-** . Type in start (**0**) and stop concentration (**1.3×10^{-3}**) and number of data points (**4**). The program is now titrated for pH and F^- . Press **OK**, and **OK** again
9. Press **Run** to do the calculations. Select **Graph IT** to see a graphical presentation of the data. In the "*Component*" menu select **Al^{3+}** and "*units*" are set to "**Log C**". Then, select **Total Al^{3+}** and Press **Plot**.

Output Manager

Component: F(-)

Output Type:

☐ Header

☐ Log

☐ MultiRun Variables

☒ **Component Groups**

☐ Special Reports

Data Object:

AL-F1.MD0

F(-)
Al(3+)
H2O
H(+)

Directory:

D:\MINWIN45

D:\
MINWIN45

D: DATA

How to Display F(-) Data

☐ Obs x Variables ☒ **Species x Variables** ☐ Obs x Species

Variables

OBS

F(-)

Variables

SPECIES

Run 1

Species

OBS

1. Conc (M)

View Graph IT Close Copy Delete Help

Graphics Manager

Object File: AL-F1.MD0 Run Type: TITRATION

Graph Title:

Graph Type: X-Y Plot

Component: Al(3+)

Observation: Run 1

Units: Log C

X Axis: L:pH

Y Axis:

☐ 3: GIBBSITE

☐ 6: DIASPORE

☐ 6: Al2O3

☐ 6: BOEHMITE

☐ 6: Al(OH)3 (am)

☒ 7: TOTAL Al(3+)

Plot Cancel Help

View Graph IT Close Copy Delete Help

APPENDIX G: Summary of the results for the determined experimental rate constants (K_{exp}) by batch EC process at the different operational parameters

Table AG-1 Summary of the results for the determined the experimental rate constants (K_{exp}) by batch EC process at the different operational parameters

I	I/V	C_0	d	Ca^{2+}	pH	$K_{\text{(exp)}}$	R^2
(A)	(A/m ³)	(mg/L)	(mm)	(mg/L)		(min) ⁻¹	
1	273	10	5	0	6	0.036	0.99
1.5	410	10	5	0	6	0.045	0.99
2	546	10	5	0	6	0.051	0.99
2.5	683	10	5	0	6	0.061	0.99
1	273	10	10	0	6	0.032	0.98
1.5	410	10	10	0	6	0.041	0.99
2	546	10	10	0	6	0.047	0.99
2.5	683	10	10	0	6	0.057	0.99
1	273	10	15	0	6	0.028	0.98
1.5	410	10	15	0	6	0.037	0.99
2	546	10	15	0	6	0.043	0.99
2.5	683	10	15	0	6	0.053	0.99
1	273	15	5	0	6	0.034	0.99
1.5	410	15	5	0	6	0.042	0.99
2	546	15	5	0	6	0.049	0.99
2.5	683	15	5	0	6	0.058	0.99
1	273	15	10	0	6	0.03	0.99
1.5	410	15	10	0	6	0.038	0.99
2	546	15	10	0	6	0.044	0.99
2.5	683	15	10	0	6	0.055	0.99
1	273	15	15	0	6	0.025	0.99
1.5	410	15	15	0	6	0.034	0.99
2	546	15	15	0	6	0.039	0.99
2.5	683	15	15	0	6	0.05	0.99
1	273	25	5	0	6	0.03	0.99
1.5	410	25	5	0	6	0.039	0.99
2	546	25	5	0	6	0.045	0.99
2.5	683	25	5	0	6	0.055	0.99
1	273	25	10	0	6	0.027	0.98
1.5	410	25	10	0	6	0.035	0.99
2	546	25	10	0	6	0.042	0.99

2.5	683	25	10	0	6	0.052	0.99
1	273	25	15	0	6	0.023	0.99
1.5	410	25	15	0	6	0.03	0.99
2	546	25	15	0	6	0.036	0.99
2.5	683	25	15	0	6	0.048	0.99
1	273	10	5	0	7.5	.035	0.99
1.5	410	10	5	0	7.5	.044	0.99
2	546	10	5	0	7.5	.051	0.99
2.5	683	10	5	0	7.5	.060	0.98
1	273	10	10	0	7.5	.031	0.99
1.5	410	10	10	0	7.5	.040	0.98
2	546	10	10	0	7.5	.047	0.99
2.5	683	10	10	0	7.5	.056	0.99
1	273	10	15	0	7.5	.027	0.98
1.5	410	10	15	0	7.5	.036	0.99
2	546	10	15	0	7.5	.043	0.99
2.5	683	10	15	0	7.5	.052	0.99
1	273	15	5	0	7.5	.032	0.98
1.5	410	15	5	0	7.5	.041	0.99
2	546	15	5	0	7.5	.049	0.99
2.5	683	15	5	0	7.5	.057	0.99
1	273	15	10	0	7.5	.029	0.99
1.5	410	15	10	0	7.5	.037	0.98
2	546	15	10	0	7.5	.044	0.99
2.5	683	15	10	0	7.5	.054	0.99
1	273	15	15	0	7.5	.025	0.99
1.5	410	15	15	0	7.5	.033	0.99
2	546	15	15	0	7.5	.039	0.99
2.5	683	15	15	0	7.5	.050	0.99
1	273	25	5	0	7.5	.030	0.99
1.5	410	25	5	0	7.5	.037	0.98
2	546	25	5	0	7.5	.045	0.99
2.5	683	25	5	0	7.5	.054	0.99
1	273	25	10	0	7.5	.026	0.99
1.5	410	25	10	0	7.5	.034	0.98
2	546	25	10	0	7.5	.042	0.99
2.5	683	25	10	0	7.5	.051	0.99
1	273	25	15	0	7.5	.022	0.98
1.5	410	25	15	0	7.5	.030	0.99
2	546	25	15	0	7.5	.036	0.99
2.5	683	25	15	0	7.5	.047	0.98

1	273	10	5	0	9	0.029	0.99
1.5	410	10	5	0	9	0.037	0.98
2	546	10	5	0	9	0.044	0.99
2.5	683	10	5	0	9	0.052	0.99
1	273	10	10	0	9	0.024	0.98
1.5	410	10	10	0	9	0.033	0.99
2	546	10	10	0	9	0.039	0.99
2.5	683	10	10	0	9	0.05	0.98
1	273	10	15	0	9	0.021	0.99
1.5	410	10	15	0	9	0.028	0.99
2	546	10	15	0	9	0.034	0.99
2.5	683	10	15	0	9	0.044	0.99
1	273	15	5	0	9	0.025	0.98
1.5	410	15	5	0	9	0.033	0.99
2	546	15	5	0	9	0.04	0.99
2.5	683	15	5	0	9	0.049	0.99
1	273	15	10	0	9	0.023	0.99
1.5	410	15	10	0	9	0.031	0.98
2	546	15	10	0	9	0.036	0.99
2.5	683	15	10	0	9	0.048	0.99
1	273	15	15	0	9	0.016	0.99
1.5	410	15	15	0	9	0.027	0.98
2	546	15	15	0	9	0.032	0.99
2.5	683	15	15	0	9	0.042	0.99
1	273	25	5	0	9	0.023	0.99
1.5	410	25	5	0	9	0.031	0.98
2	546	25	5	0	9	0.036	0.99
2.5	683	25	5	0	9	0.047	0.99
1	273	25	10	0	9	0.018	0.99
1.5	410	25	10	0	9	0.028	0.99
2	546	25	10	0	9	0.034	0.98
2.5	683	25	10	0	9	0.045	0.99
1	273	25	15	0	9	0.014	0.99
1.5	410	25	15	0	9	0.023	0.99
2	546	25	15	0	9	0.028	0.98
2.5	683	25	15	0	9	0.041	0.99
1	273	10	5	50	6	0.039	0.99
1.5	410	10	5	50	6	0.047	0.98
2	546	10	5	50	6	0.055	0.99
2.5	683	10	5	50	6	0.063	0.99
1	273	10	15	50	6	0.03	0.99

1.5	410	10	15	50	6	0.039	0.99
2	546	10	15	50	6	0.047	0.99
2.5	683	10	15	50	6	0.055	0.98
1	273	15	5	50	6	0.037	0.99
1.5	410	15	5	50	6	0.046	0.99
2	546	15	5	50	6	0.055	0.99
2.5	683	15	5	50	6	0.063	0.99
1	273	15	15	50	6	0.029	0.99
1.5	410	15	15	50	6	0.037	0.99
2	546	15	15	50	6	0.046	0.99
2.5	683	15	15	50	6	0.054	0.99
1	273	25	5	50	6	0.034	0.99
1.5	410	25	5	50	6	0.042	0.99
2	546	25	5	50	6	0.052	0.99
2.5	683	25	5	50	6	0.058	0.99
1	273	25	15	50	6	0.027	0.99
1.5	410	25	15	50	6	0.035	0.99
2	546	25	15	50	6	0.042	0.99
2.5	683	25	15	50	6	0.051	0.99
1	273	10	5	150	6	0.049	0.99
1.5	410	10	5	150	6	0.056	0.98
2	546	10	5	150	6	0.064	0.99
2.5	683	10	5	150	6	0.072	0.99
1	273	10	15	150	6	0.04	0.99
1.5	410	10	15	150	6	0.048	0.99
2	546	10	15	150	6	0.056	0.99
2.5	683	10	15	150	6	0.064	0.98
1	273	15	5	150	6	0.048	0.99
1.5	410	15	5	150	6	0.054	0.99
2	546	15	5	150	6	0.06	0.99
2.5	683	15	5	150	6	0.07	0.99
1	273	15	15	150	6	0.037	0.99
1.5	410	15	15	150	6	0.046	0.99
2	546	15	15	150	6	0.056	0.99
2.5	683	15	15	150	6	0.06	0.99
1	273	25	5	150	6	0.04	0.99
1.5	410	25	5	150	6	0.052	0.99
2	546	25	5	150	6	0.056	0.99
2.5	683	25	5	150	6	0.064	0.98
1	273	25	15	150	6	0.035	0.99
1.5	410	25	15	150	6	0.042	0.99

2	546	25	15	150	6	0.051	0.99
2.5	683	25	15	150	6	0.059	0.98
1	273	10	5	250	6	0.056	0.99
1.5	410	10	5	250	6	0.063	0.98
2	546	10	5	250	6	0.071	0.99
2.5	683	10	5	250	6	0.079	0.99
1	273	10	15	250	6	0.047	0.99
1.5	410	10	15	250	6	0.055	0.99
2	546	10	15	250	6	0.064	0.99
2.5	683	10	15	250	6	0.073	0.98
1	273	15	5	250	6	0.052	0.99
1.5	410	15	5	250	6	0.061	0.99
2	546	15	5	250	6	0.071	0.99
2.5	683	15	5	250	6	0.077	0.99
1	273	15	15	250	6	0.045	0.99
1.5	410	15	15	250	6	0.053	0.99
2	546	15	15	250	6	0.061	0.99
2.5	683	15	15	250	6	0.069	0.99
1	273	25	5	250	6	0.05	0.99
1.5	410	25	5	250	6	0.057	0.99
2	546	25	5	250	6	0.065	0.98
2.5	683	25	5	250	6	0.074	0.99
1	273	25	15	250	6	0.041	0.99
1.5	410	25	15	250	6	0.05	0.99
2	546	25	15	250	6	0.058	0.99
2.5	683	25	15	250	6	0.066	0.98
1	273	10	5	300	6	0.061	0.99
1.5	410	10	5	300	6	0.067	0.98
2	546	10	5	300	6	0.074	0.98
2.5	683	10	5	300	6	0.083	0.99
1	273	10	15	300	6	0.051	0.99
1.5	410	10	15	300	6	0.059	0.99
2	546	10	15	300	6	0.067	0.98
2.5	683	10	15	300	6	0.077	0.99
1	273	15	5	300	6	0.058	0.99
1.5	410	15	5	300	6	0.067	0.99
2	546	15	5	300	6	0.075	0.99
2.5	683	15	5	300	6	0.082	0.99
1	273	15	15	300	6	0.049	0.99
1.5	410	15	15	300	6	0.057	0.99
2	546	15	15	300	6	0.067	0.99

2.5	683	15	15	300	6	0.075	0.99
1	273	25	5	300	6	0.054	0.99
1.5	410	25	5	300	6	0.064	0.98
2	546	25	5	300	6	0.072	0.98
2.5	683	25	5	300	6	0.077	0.99
1	273	25	15	300	6	0.045	0.99
1.5	410	25	15	300	6	0.055	0.99
2	546	25	15	300	6	0.062	0.98
2.5	683	25	15	300	6	0.07	0.99
1	273	10	5	50	9	0.032	0.99
1.5	410	10	5	50	9	0.039	0.99
2	546	10	5	50	9	0.048	0.99
2.5	683	10	5	50	9	0.054	0.99
1	273	10	15	50	9	0.022	0.99
1.5	410	10	15	50	9	0.031	0.99
2	546	10	15	50	9	0.039	0.99
2.5	683	10	15	50	9	0.048	0.99
1	273	15	5	50	9	0.03	0.99
1.5	410	15	5	50	9	0.037	0.99
2	546	15	5	50	9	0.046	0.98
2.5	683	15	5	50	9	0.054	0.99
1	273	15	15	50	9	0.02	0.99
1.5	410	15	15	50	9	0.028	0.98
2	546	15	15	50	9	0.037	0.99
2.5	683	15	15	50	9	0.047	0.99
1	273	25	5	50	9	0.026	0.99
1.5	410	25	5	50	9	0.035	0.98
2	546	25	5	50	9	0.044	0.99
2.5	683	25	5	50	9	0.051	0.99
1	273	25	15	50	9	0.018	0.99
1.5	410	25	15	50	9	0.028	0.99
2	546	25	15	50	9	0.035	0.99
2.5	683	25	15	50	9	0.043	0.99
1	273	10	5	150	9	0.042	0.98
1.5	410	10	5	150	9	0.048	0.99
2	546	10	5	150	9	0.056	0.99
2.5	683	10	5	150	9	0.064	0.99
1	273	10	15	150	9	0.031	0.99
1.5	410	10	15	150	9	0.041	0.98
2	546	10	15	150	9	0.048	0.99
2.5	683	10	15	150	9	0.057	0.99

1	273	15	5	150	9	0.039	0.99
1.5	410	15	5	150	9	0.047	0.99
2	546	15	5	150	9	0.052	0.98
2.5	683	15	5	150	9	0.063	0.98
1	273	15	15	150	9	0.028	0.99
1.5	410	15	15	150	9	0.038	0.98
2	546	15	15	150	9	0.049	0.99
2.5	683	15	15	150	9	0.051	0.98
1	273	25	5	150	9	0.032	0.99
1.5	410	25	5	150	9	0.044	0.99
2	546	25	5	150	9	0.048	0.99
2.5	683	25	5	150	9	0.057	0.99
1	273	25	15	150	9	0.028	0.99
1.5	410	25	15	150	9	0.033	0.99
2	546	25	15	150	9	0.042	0.99
2.5	683	25	15	150	9	0.05	0.99
1	273	10	5	250	9	0.048	0.99
1.5	410	10	5	250	9	0.054	0.99
2	546	10	5	250	9	0.063	0.98
2.5	683	10	5	250	9	0.07	0.99
1	273	10	15	250	9	0.04	0.99
1.5	410	10	15	250	9	0.048	0.99
2	546	10	15	250	9	0.056	0.99
2.5	683	10	15	250	9	0.066	0.98
1	273	15	5	250	9	0.043	0.99
1.5	410	15	5	250	9	0.054	0.98
2	546	15	5	250	9	0.064	0.99
2.5	683	15	5	250	9	0.069	0.99
1	273	15	15	250	9	0.038	0.99
1.5	410	15	15	250	9	0.044	0.98
2	546	15	15	250	9	0.054	0.98
2.5	683	15	15	250	9	0.062	0.99
1	273	25	5	250	9	0.041	0.99
1.5	410	25	5	250	9	0.05	0.99
2	546	25	5	250	9	0.057	0.99
2.5	683	25	5	250	9	0.067	0.99
1	273	25	15	250	9	0.032	0.99
1.5	410	25	15	250	9	0.043	0.99
2	546	25	15	250	9	0.05	0.99
2.5	683	25	15	250	9	0.059	0.99
1	273	10	5	300	9	0.053	0.99

1.5	410	10	5	300	9	0.059	0.99
2	546	10	5	300	9	0.067	0.99
2.5	683	10	5	300	9	0.075	0.99
1	273	10	15	300	9	0.043	0.99
1.5	410	10	15	300	9	0.052	0.99
2	546	10	15	300	9	0.059	0.99
2.5	683	10	15	300	9	0.07	0.99
1	273	15	5	300	9	0.051	0.98
1.5	410	15	5	300	9	0.058	0.99
2	546	15	5	300	9	0.066	0.98
2.5	683	15	5	300	9	0.073	0.98
1	273	15	15	300	9	0.041	0.99
1.5	410	15	15	300	9	0.048	0.98
2	546	15	15	300	9	0.058	0.98
2.5	683	15	15	300	9	0.066	0.99
1	273	25	5	300	9	0.047	0.99
1.5	410	25	5	300	9	0.057	0.99
2	546	25	5	300	9	0.064	0.99
2.5	683	25	5	300	9	0.07	0.99
1	273	25	15	300	9	0.036	0.99
1.5	410	25	15	300	9	0.048	0.99
2	546	25	15	300	9	0.055	0.99
2.5	683	25	15	300	9	0.062	0.99

APPENDIX H: Summary of the statistical results for comparison between the experimental and predicted rate constants

Table AH-1 Summary of output results, analysis of variance, and estimation of parameters and residuals between the experimental and predicted rate constants

Summary output						
Regression Statistics						
Multiple R	0.999					
R Square	0.999					
Adjusted R Square	0.997					
Standard Error	0.001					
Observations	432					
ANOVA						
	<i>df</i>	<i>SS</i>	<i>MS</i>	<i>F</i>	<i>Sig. F</i>	<i>Sig. F</i>
Regression	1	0.971	0.971	423.048	0	0
Residual	431	0.0009	2.29E-06			
Total	432	0.972				
	<i>Coefficients</i>	<i>Standard Error</i>	<i>t Stat</i>	<i>P-value</i>	<i>Lower 95%</i>	<i>Lower 95%</i>
Intercept	0	#N/A	#N/A	#N/A	#N/A	#N/A
X Variable	1.000	0.001	650.542	0.000	0.997	0.997
Residual output						
<i>Observation</i>	<i>Predicted Y</i>	<i>Residuals</i>	Lower 95%	<i>Upper 95%</i>		
1	0.041	-0.002	0.038	0.044		
2	0.049	-0.002	0.046	0.052		
3	0.057	-0.002	0.054	0.060		
4	0.065	-0.002	0.062	0.068		
5	0.033	-0.003	0.030	0.036		
6	0.041	-0.002	0.038	0.044		
7	0.049	-0.002	0.046	0.052		
8	0.057	-0.002	0.054	0.060		
9	0.039	-0.002	0.036	0.042		
10	0.047	-0.001	0.044	0.050		
11	0.055	0.000	0.052	0.058		
12	0.063	0.000	0.060	0.066		
13	0.031	-0.002	0.028	0.034		
14	0.039	-0.002	0.036	0.042		
15	0.047	-0.001	0.044	0.050		
16	0.055	-0.001	0.052	0.058		
17	0.035	-0.001	0.032	0.039		
18	0.044	-0.002	0.040	0.047		
19	0.052	0.000	0.048	0.055		

20	0.060	-0.002	0.057	0.063
21	0.027	0.000	0.024	0.030
22	0.036	-0.001	0.032	0.039
23	0.044	-0.002	0.040	0.047
24	0.052	-0.001	0.049	0.055
25	0.048	0.001	0.045	0.051
26	0.056	0.000	0.053	0.059
27	0.064	0.000	0.061	0.068
28	0.073	-0.001	0.069	0.076
29	0.040	0.000	0.037	0.043
30	0.048	0.000	0.045	0.051
31	0.056	0.000	0.053	0.059
32	0.064	0.000	0.061	0.068
33	0.047	0.001	0.044	0.050
34	0.055	-0.001	0.052	0.058
35	0.063	-0.003	0.060	0.066
36	0.071	-0.001	0.068	0.074
37	0.039	-0.002	0.036	0.042
38	0.047	-0.001	0.044	0.050
39	0.055	0.001	0.052	0.058
40	0.063	-0.003	0.060	0.066
41	0.043	-0.003	0.040	0.046
42	0.051	0.001	0.048	0.054
43	0.059	-0.003	0.056	0.062
44	0.067	-0.003	0.064	0.070
45	0.035	0.000	0.032	0.038
46	0.043	-0.001	0.040	0.046
47	0.051	0.000	0.048	0.054
48	0.059	0.000	0.056	0.062
49	0.056	0.000	0.053	0.059
50	0.064	-0.001	0.061	0.067
51	0.072	-0.001	0.069	0.075
52	0.080	-0.001	0.077	0.083
53	0.048	-0.001	0.045	0.051
54	0.056	-0.001	0.053	0.059
55	0.064	0.000	0.061	0.067
56	0.072	0.001	0.069	0.075
57	0.054	-0.002	0.051	0.057
58	0.062	-0.001	0.059	0.065
59	0.070	0.001	0.067	0.073
60	0.078	-0.001	0.075	0.081
61	0.046	-0.001	0.043	0.049
62	0.054	-0.001	0.051	0.057
63	0.062	-0.001	0.059	0.065
64	0.070	-0.001	0.067	0.073
65	0.051	-0.001	0.048	0.054

66	0.059	-0.002	0.056	0.062
67	0.067	-0.002	0.064	0.070
68	0.075	-0.001	0.072	0.078
69	0.043	-0.002	0.040	0.046
70	0.051	-0.001	0.048	0.054
71	0.059	-0.001	0.056	0.062
72	0.067	-0.001	0.064	0.070
73	0.060	0.001	0.057	0.063
74	0.068	-0.001	0.065	0.071
75	0.076	-0.002	0.073	0.079
76	0.084	-0.001	0.081	0.087
77	0.052	-0.001	0.049	0.055
78	0.060	-0.001	0.057	0.063
79	0.068	-0.001	0.065	0.071
80	0.076	0.001	0.073	0.079
81	0.058	0.000	0.055	0.061
82	0.066	0.001	0.063	0.069
83	0.074	0.001	0.071	0.077
84	0.082	0.000	0.079	0.085
85	0.050	-0.001	0.047	0.053
86	0.058	-0.001	0.055	0.061
87	0.066	0.001	0.063	0.069
88	0.074	0.001	0.071	0.077
89	0.054	0.000	0.051	0.057
90	0.062	0.002	0.059	0.065
91	0.070	0.002	0.067	0.073
92	0.078	-0.001	0.075	0.082
93	0.046	-0.001	0.043	0.049
94	0.054	0.001	0.051	0.057
95	0.062	0.000	0.059	0.065
96	0.070	0.000	0.067	0.074
97	0.034	0.002	0.030	0.037
98	0.042	0.003	0.039	0.045
99	0.050	0.001	0.047	0.053
100	0.058	0.003	0.055	0.061
101	0.029	0.003	0.026	0.033
102	0.038	0.003	0.035	0.041
103	0.046	0.001	0.043	0.049
104	0.054	0.003	0.051	0.057
105	0.025	0.003	0.022	0.029
106	0.034	0.003	0.030	0.037
107	0.042	0.001	0.039	0.045
108	0.050	0.003	0.047	0.053
109	0.032	0.002	0.029	0.035
110	0.040	0.002	0.037	0.043
111	0.048	0.001	0.045	0.051

112	0.056	0.002	0.053	0.059
113	0.028	0.002	0.025	0.031
114	0.036	0.002	0.033	0.039
115	0.044	0.000	0.041	0.047
116	0.052	0.003	0.049	0.055
117	0.024	0.001	0.021	0.027
118	0.032	0.002	0.029	0.035
119	0.040	-0.001	0.037	0.043
120	0.048	0.002	0.045	0.051
121	0.028	0.002	0.025	0.031
122	0.036	0.003	0.033	0.039
123	0.044	0.001	0.041	0.047
124	0.052	0.003	0.049	0.055
125	0.024	0.003	0.021	0.027
126	0.032	0.003	0.029	0.035
127	0.040	0.002	0.037	0.043
128	0.048	0.004	0.045	0.051
129	0.020	0.003	0.017	0.023
130	0.028	0.002	0.025	0.031
131	0.036	0.000	0.033	0.039
132	0.044	0.004	0.041	0.047
133	0.035	0.001	0.032	0.038
134	0.043	0.002	0.040	0.046
135	0.051	0.000	0.048	0.054
136	0.059	0.002	0.056	0.062
137	0.031	0.001	0.028	0.034
138	0.039	0.002	0.036	0.042
139	0.047	0.000	0.044	0.050
140	0.055	0.002	0.052	0.058
141	0.027	0.001	0.024	0.030
142	0.035	0.002	0.032	0.038
143	0.043	0.000	0.040	0.046
144	0.051	0.002	0.048	0.054
145	0.033	0.001	0.030	0.037
146	0.042	0.000	0.038	0.045
147	0.050	-0.001	0.047	0.053
148	0.058	0.000	0.055	0.061
149	0.029	0.001	0.026	0.033
150	0.038	0.000	0.034	0.041
151	0.046	-0.002	0.042	0.049
152	0.054	0.001	0.051	0.057
153	0.025	0.000	0.022	0.029
154	0.034	0.000	0.030	0.037
155	0.042	-0.003	0.038	0.045
156	0.050	0.000	0.047	0.053
157	0.030	0.000	0.027	0.033

158	0.038	0.001	0.035	0.041
159	0.046	-0.001	0.043	0.049
160	0.054	0.001	0.051	0.057
161	0.026	0.001	0.023	0.029
162	0.034	0.001	0.031	0.037
163	0.042	0.000	0.039	0.045
164	0.050	0.002	0.047	0.053
165	0.022	0.001	0.019	0.025
166	0.030	0.000	0.027	0.033
167	0.038	-0.002	0.035	0.041
168	0.046	0.002	0.043	0.049
169	0.025	0.000	0.022	0.028
170	0.033	0.000	0.030	0.036
171	0.041	-0.003	0.038	0.044
172	0.049	0.001	0.046	0.052
173	0.021	0.000	0.018	0.024
174	0.029	0.002	0.026	0.032
175	0.037	-0.001	0.034	0.040
176	0.045	-0.002	0.042	0.048
177	0.017	0.001	0.014	0.020
178	0.025	-0.001	0.022	0.028
179	0.033	-0.001	0.030	0.036
180	0.041	0.000	0.038	0.044
181	0.023	0.001	0.020	0.026
182	0.031	-0.002	0.028	0.034
183	0.039	-0.002	0.036	0.042
184	0.047	-0.001	0.044	0.050
185	0.019	-0.001	0.016	0.022
186	0.027	-0.001	0.024	0.030
187	0.035	-0.002	0.032	0.038
188	0.043	0.001	0.040	0.046
189	0.015	-0.001	0.012	0.018
190	0.023	-0.002	0.020	0.026
191	0.031	-0.003	0.028	0.034
192	0.039	0.000	0.036	0.042
193	0.019	-0.003	0.016	0.022
194	0.027	-0.002	0.024	0.030
195	0.035	-0.001	0.032	0.038
196	0.043	-0.002	0.040	0.046
197	0.015	0.001	0.012	0.018
198	0.023	0.001	0.020	0.026
199	0.031	0.000	0.028	0.034
200	0.039	0.002	0.036	0.042
201	0.011	0.000	0.008	0.014
202	0.019	0.000	0.016	0.022
203	0.027	-0.002	0.024	0.030

204	0.035	0.000	0.032	0.038
205	0.028	0.001	0.025	0.031
206	0.036	0.001	0.033	0.039
207	0.044	0.000	0.041	0.047
208	0.052	0.000	0.049	0.055
209	0.024	0.000	0.021	0.027
210	0.032	0.001	0.029	0.035
211	0.040	-0.001	0.037	0.043
212	0.048	0.002	0.045	0.051
213	0.020	0.001	0.017	0.023
214	0.028	0.000	0.025	0.031
215	0.036	-0.002	0.033	0.039
216	0.044	0.000	0.041	0.047
217	0.026	-0.001	0.023	0.029
218	0.034	-0.001	0.031	0.038
219	0.042	-0.002	0.039	0.046
220	0.051	-0.002	0.047	0.054
221	0.022	0.001	0.019	0.025
222	0.030	0.001	0.027	0.034
223	0.038	-0.002	0.035	0.042
224	0.047	0.001	0.043	0.050
225	0.018	-0.002	0.015	0.021
226	0.026	0.001	0.023	0.030
227	0.034	-0.002	0.031	0.038
228	0.043	-0.001	0.039	0.046
229	0.023	0.000	0.020	0.026
230	0.031	0.000	0.028	0.034
231	0.039	-0.003	0.036	0.042
232	0.047	0.000	0.044	0.050
233	0.019	-0.001	0.016	0.022
234	0.027	0.001	0.024	0.030
235	0.035	-0.001	0.032	0.038
236	0.043	0.002	0.040	0.046
237	0.015	-0.001	0.012	0.018
238	0.023	0.000	0.020	0.026
239	0.031	-0.003	0.028	0.034
240	0.039	0.002	0.036	0.042
241	0.032	0.000	0.029	0.035
242	0.040	-0.001	0.037	0.043
243	0.048	0.000	0.045	0.051
244	0.056	-0.002	0.053	0.059
245	0.024	-0.002	0.021	0.027
246	0.032	-0.001	0.029	0.035
247	0.040	-0.001	0.037	0.043
248	0.048	0.000	0.045	0.051
249	0.030	0.000	0.027	0.033

250	0.038	-0.001	0.035	0.041
251	0.046	0.000	0.043	0.049
252	0.054	0.000	0.051	0.057
253	0.022	-0.002	0.019	0.025
254	0.030	-0.002	0.027	0.033
255	0.038	-0.001	0.035	0.041
256	0.046	0.001	0.043	0.049
257	0.027	-0.001	0.024	0.030
258	0.035	0.000	0.032	0.038
259	0.043	0.001	0.040	0.046
260	0.051	0.000	0.048	0.054
261	0.019	-0.001	0.016	0.022
262	0.027	0.001	0.024	0.030
263	0.035	0.000	0.032	0.038
264	0.043	0.000	0.040	0.046
265	0.040	0.002	0.036	0.043
266	0.048	0.000	0.045	0.051
267	0.056	0.000	0.053	0.059
268	0.064	0.000	0.061	0.067
269	0.032	-0.001	0.028	0.035
270	0.040	0.001	0.037	0.043
271	0.048	0.000	0.045	0.051
272	0.056	0.001	0.053	0.059
273	0.038	0.001	0.035	0.041
274	0.046	0.001	0.043	0.049
275	0.054	-0.002	0.051	0.057
276	0.062	0.001	0.059	0.065
277	0.030	-0.002	0.027	0.033
278	0.038	0.000	0.035	0.041
279	0.046	0.003	0.043	0.049
280	0.054	-0.003	0.051	0.057
281	0.034	-0.002	0.031	0.037
282	0.042	0.002	0.039	0.045
283	0.050	-0.002	0.047	0.053
284	0.058	-0.001	0.055	0.061
285	0.026	0.002	0.023	0.029
286	0.034	-0.001	0.031	0.037
287	0.042	0.000	0.039	0.045
288	0.050	0.000	0.047	0.053
289	0.047	0.001	0.044	0.050
290	0.055	-0.001	0.052	0.058
291	0.063	0.000	0.060	0.066
292	0.071	-0.001	0.068	0.074
293	0.039	0.001	0.036	0.042
294	0.047	0.001	0.044	0.050
295	0.055	0.001	0.052	0.058

296	0.063	0.003	0.060	0.066
297	0.045	-0.002	0.042	0.048
298	0.053	0.001	0.050	0.056
299	0.061	0.003	0.058	0.064
300	0.069	0.000	0.066	0.072
301	0.037	0.001	0.034	0.040
302	0.045	-0.001	0.042	0.048
303	0.053	0.001	0.050	0.056
304	0.061	0.001	0.058	0.064
305	0.042	-0.001	0.039	0.045
306	0.050	0.000	0.047	0.053
307	0.058	-0.001	0.055	0.061
308	0.066	0.001	0.063	0.069
309	0.034	-0.002	0.031	0.037
310	0.042	0.001	0.039	0.045
311	0.050	0.000	0.047	0.053
312	0.058	0.001	0.055	0.061
313	0.051	0.002	0.048	0.054
314	0.059	0.000	0.056	0.062
315	0.067	0.000	0.064	0.070
316	0.075	0.000	0.072	0.078
317	0.043	0.000	0.040	0.046
318	0.051	0.001	0.048	0.054
319	0.059	0.000	0.056	0.062
320	0.067	0.003	0.064	0.070
321	0.049	0.002	0.046	0.052
322	0.057	0.001	0.054	0.060
323	0.065	0.001	0.062	0.068
324	0.073	0.000	0.070	0.076
325	0.041	0.000	0.038	0.044
326	0.049	-0.001	0.046	0.052
327	0.057	0.001	0.054	0.060
328	0.065	0.001	0.062	0.068
329	0.046	0.001	0.042	0.049
330	0.054	0.003	0.051	0.057
331	0.062	0.002	0.059	0.065
332	0.070	0.000	0.067	0.073
333	0.038	-0.002	0.034	0.041
334	0.046	0.002	0.043	0.049
335	0.054	0.001	0.051	0.057
336	0.062	0.000	0.059	0.065
337	0.028	0.000	0.025	0.031
338	0.036	-0.001	0.033	0.040
339	0.044	-0.002	0.041	0.048
340	0.053	-0.001	0.050	0.056
341	0.020	-0.001	0.017	0.023

342	0.028	0.001	0.025	0.032
343	0.036	0.000	0.033	0.040
344	0.045	-0.004	0.041	0.048
345	0.027	0.000	0.024	0.030
346	0.035	-0.002	0.032	0.038
347	0.043	0.001	0.040	0.046
348	0.051	0.000	0.048	0.054
349	0.019	0.000	0.016	0.022
350	0.027	-0.003	0.024	0.030
351	0.035	-0.001	0.032	0.038
352	0.043	-0.001	0.040	0.046
353	0.023	-0.001	0.020	0.026
354	0.031	-0.001	0.028	0.034
355	0.039	0.002	0.036	0.042
356	0.047	0.000	0.044	0.050
357	0.015	0.001	0.012	0.018
358	0.023	-0.001	0.020	0.026
359	0.031	0.000	0.028	0.034
360	0.039	0.001	0.036	0.042
361	0.036	-0.001	0.033	0.039
362	0.044	-0.002	0.041	0.047
363	0.052	0.001	0.049	0.055
364	0.060	-0.002	0.057	0.063
365	0.028	0.001	0.025	0.031
366	0.036	0.001	0.033	0.039
367	0.044	0.001	0.041	0.047
368	0.052	0.001	0.049	0.055
369	0.034	0.002	0.031	0.037
370	0.042	0.001	0.039	0.045
371	0.050	-0.001	0.047	0.053
372	0.058	-0.001	0.055	0.061
373	0.026	0.000	0.023	0.029
374	0.034	0.000	0.031	0.037
375	0.042	0.001	0.039	0.045
376	0.050	-0.001	0.047	0.053
377	0.031	-0.002	0.028	0.034
378	0.039	0.003	0.036	0.042
379	0.047	-0.002	0.044	0.050
380	0.055	-0.003	0.052	0.058
381	0.023	0.002	0.020	0.026
382	0.031	-0.002	0.028	0.034
383	0.039	0.001	0.036	0.042
384	0.047	0.000	0.044	0.050
385	0.044	0.002	0.041	0.047
386	0.052	-0.002	0.049	0.055
387	0.060	-0.001	0.057	0.063

388	0.068	-0.001	0.065	0.071
389	0.036	-0.001	0.032	0.039
390	0.044	-0.001	0.041	0.047
391	0.052	0.001	0.049	0.055
392	0.060	0.002	0.057	0.063
393	0.042	-0.001	0.039	0.045
394	0.050	-0.002	0.047	0.053
395	0.058	0.002	0.055	0.061
396	0.066	0.000	0.063	0.069
397	0.034	-0.003	0.031	0.037
398	0.042	-0.003	0.039	0.045
399	0.050	0.000	0.047	0.053
400	0.058	-0.003	0.055	0.061
401	0.038	0.001	0.035	0.041
402	0.046	0.000	0.043	0.049
403	0.054	0.000	0.051	0.057
404	0.062	0.001	0.059	0.065
405	0.030	-0.001	0.027	0.033
406	0.038	0.001	0.035	0.041
407	0.046	0.001	0.043	0.049
408	0.054	-0.001	0.051	0.057
409	0.047	0.003	0.044	0.050
410	0.055	0.000	0.052	0.058
411	0.063	-0.002	0.060	0.066
412	0.071	0.001	0.068	0.075
413	0.039	0.001	0.036	0.042
414	0.047	0.002	0.044	0.050
415	0.055	0.001	0.052	0.058
416	0.063	0.000	0.060	0.066
417	0.046	0.002	0.042	0.049
418	0.054	0.000	0.051	0.057
419	0.062	0.002	0.059	0.065
420	0.070	0.000	0.067	0.073
421	0.038	0.001	0.034	0.041
422	0.046	-0.002	0.043	0.049
423	0.054	0.001	0.051	0.057
424	0.062	0.001	0.059	0.065
425	0.042	0.000	0.039	0.045
426	0.050	0.002	0.047	0.053
427	0.058	0.003	0.055	0.061
428	0.066	0.000	0.063	0.069
429	0.034	0.000	0.031	0.037
430	0.042	0.000	0.039	0.045
431	0.050	0.001	0.047	0.053
432	0.058	0.001	0.055	0.061

Appendix I: Summary of the statistical output results
between predicted and experimental data

Table AI-1 Summary of output results between predicted and experimental residual fluoride concentrations with electrolysis time for bore water data

SUMMARY OUTPUT

Regression Statistics						
Multiple R	0.998271285					
R Square	0.996545558					
Adjusted R Square	0.913212225					
Standard Error	0.405720105					
Observations	13					
ANOVA						
	df	SS	MS	F	Significance F	
Regression	1	569.8408944	569.8409	3461.789	4.2257E-15	
Residual	12	1.975305643	0.164609			
Total	13	571.8162				
	Coefficients	Standard Error	t Stat	P-value	Lower 95%	Upper 95%
Intercept	0	#N/A	#N/A	#N/A	#N/A	#N/A
X Variable 1	1.041767926	0.01770601	58.83697	3.84E-16	1.003189844	1.080346

Table AI-2 Summary of output results between predicted and experimental residual fluoride concentrations with electrolysis time for Mameri’s data

SUMMARY OUTPUT

Regression Statistics						
Multiple R	0.997144464					
R Square	0.994297083					
Adjusted R Square	0.869297083					
Standard Error	0.228971257					
Observations	9					
ANOVA						
	df	SS	MS	F	Significance F	
Regression	1	73.1258637	73.12586	1394.791	2.56584E-09	
Residual	8	0.419422692	0.052428			
Total	9	73.54528639				
	Coefficients	Standard Error	t Stat	P-value	Lower 95%	Upper 95%
Intercept	0	#N/A	#N/A	#N/A	#N/A	#N/A
X Variable 1	0.904653255	0.024222982	37.3469	2.9E-10	0.848794958	0.9605116

Table AI-3 Summary of output results between predicted and experimental final fluoride concentrations with initial fluoride concentration for Shen’s data

SUMMARY OUTPUT

Regression Statistics						
Multiple R	0.99735874					
R Square	0.99472445					
Adjusted R	0.79472445					
Standard E	0.43083036					
Observatio	4					

ANOVA						
	df	SS	MS	F	Significance F	
Regressior	1	174.991926	174.9919	942.7692	6.7031E-06	
Residual	3	0.928074003	0.185615			
Total	4	175.92				

	Coefficients	Standard Error	t Stat	P-value	Lower 95%	Upper 95%
Intercept	0	#N/A	#N/A	#N/A	#N/A	#N/A
X Variable	1.05658692	0.034411415	30.70455	6.88E-07	0.968129564	1.145044

Table AI-4 Summary of output results between the predicted and experimental optimum flow rates with the different current concentrations for initial fluoride concentrations of 10 mg/L

Multiple R	0.999562427
R Square	0.999125046
Adjusted R Square	0.749125046
Standard Error	7.207661291
Observations	4

ANOVA						
	df	SS	MS	F	Significance F	
Regression	1	237292.1985	237292.2	4567.67	7.13816E-06	
Residual	3	207.8015252	51.95038			
Total	4	237500				

	Coefficients	Standard Error	t Stat	P-value	Lower 95%	Upper 95%
Intercept	0	#N/A	#N/A	#N/A	#N/A	#N/A
X Variable 1	1.036423832	0.015335221	67.58454	2.87E-07	0.993846433	1.079001

Table AI-5 Summary of output results between the predicted and experimental optimum flow rates with the different current concentrations for initial fluoride concentrations of 15 mg/L

SUMMARY OUTPUT

Regression Statistics						
Multiple R	0.999645951					
R Square	0.999292027					
Adjusted R Square	0.749292027					
Standard Error	5.277300914					
Observations	3					
ANOVA						
	df	SS	MS	F	Significance F	
Regression	1	157238.6004	157238.6	5645.93	5.19506E-06	
Residual	2	111.3996198	27.8499			
Total	3	157350				
	Coefficients	Standard Error	t Stat	P-value	Lower 95%	Upper 95%
Intercept	0	#N/A	#N/A	#N/A	#N/A	#N/A
X Variable 1	0.96245197	0.012808885	75.1394	1.88E-07	0.926888803	0.998015